Five Steps to Start Your REFRACTIVE SURGERY

A Case-Based Systematic Approach

Mazen M Sinjab

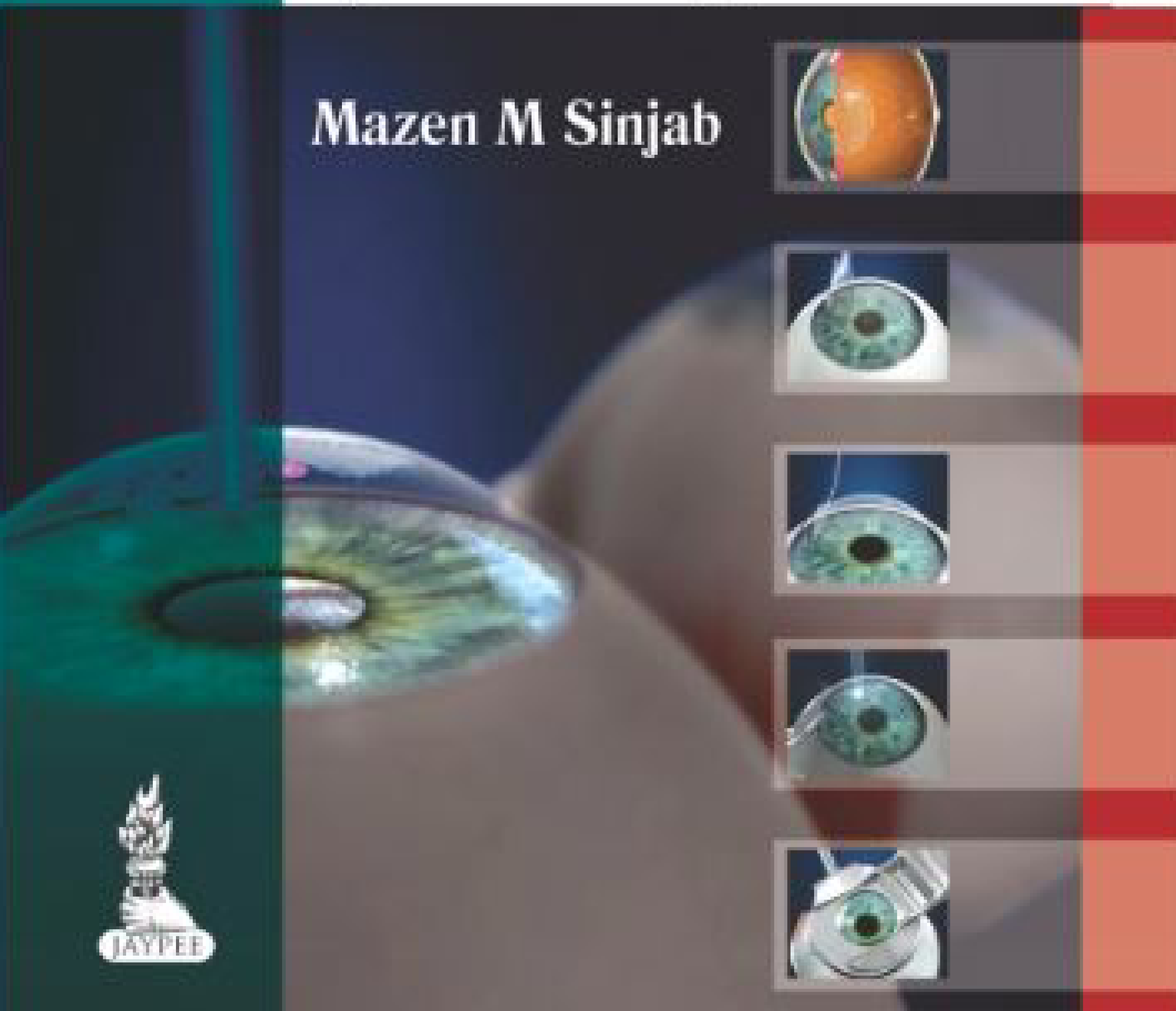

JAYPEE

Five Steps to Start Your

REFRACTIVE SURGERY

Notification

1. The information provided via this book is intended for general information purposes.
2. The information provided via this book is published to assist you, but it is not to be relied upon as authoritative.
3. The author accepts no liability whatsoever for any direct or consequential loss arising from any use of the information contained in this book.

Five Steps to Start Your REFRACTIVE SURGERY

A Case-Based Systematic Approach

Mazen M Sinjab MD MS CAB (Ophth) PhD
Professor of Ophthalmology in Damascus University Damascus, Syria
Senior Consultant in Anterior Segment and Refractive Surgery
Senior Consultant in Oculoplastic Surgery

JAYPEE

JAYPEE BROTHERS MEDICAL PUBLISHERS (P) LTD
New Delhi • London • Philadelphia • Panama

Jaypee Brothers Medical Publishers (P) Ltd

Headquarters

Jaypee Brothers Medical Publishers (P) Ltd
4838/24, Ansari Road, Daryaganj
New Delhi 110 002, India
Phone: +91-11-43574357
Fax: +91-11-43574314
Email: jaypee@jaypeebrothers.com

Overseas Offices

J.P. Medical Ltd
83 Victoria Street, London
SW1H 0HW (UK)
Phone: +44-2031708910
Fax: +02-03-0086180
Email: info@jpmedpub.com

Jaypee Medical Inc
The Bourse
111 South Independence Mall East
Suite 835, Philadelphia, PA 19106, USA
Phone: + 267-519-9789
Email: joe.rusko@jaypeebrothers.com

Jaypee Brothers Medical Publishers (P) Ltd
Bhotahity, Kathmandu,
Nepal
Phone: +977-9741283608
Email: Kathmandu@jaypeebrothers.com

Jaypee-Highlights Medical Publishers Inc
City of Knowledge, Bld. 237, Clayton
Panama City, Panama
Phone: +507-301-0496
Fax: +507-301-0499
Email: cservice@jphmedical.com

Jaypee Brothers Medical Publishers (P) Ltd
17/1-B Babar Road, Block-B, Shaymali
Mohammadpur, Dhaka-1207
Bangladesh
Mobile: +08801912003485
Email: jaypeedhaka@gmail.com

Website: www.jaypeebrothers.com
Website: www.jaypeedigital.com

Inquiries for bulk sales may be solicited at: jaypee@jaypeebrothers.com

Five Steps to Start Your Refractive Surgery: A Case-Based Systematic Approach

First Edition: **2014**

ISBN 978-93-5090-987-4

Printed at

Dedicated to

My wounded country, Syria
All the rebellious people who are seeking freedom in this biased world
The martyrs who irrigate homeland by their blood for us to live free.

My dear Father Mahamed (may God rest his soul),
who planted in my soul the love of excellence.
I will mention his name with my name all my life.

My Mother Almasah (may God rest her soul),
who planted in my heart the love of poor and helping others

My Wife Ruba (may God save her),
whose unwavering support was critical for this book

Preface

Refractive surgery is one of the major fields in ophthalmology. It is a rapidly growing and developing field. A better understanding of corneal biomechanics, etiology of complications and pathophysiology has added a lot to this field in terms of improving diagnostic devices, laser profiles, surgical techniques and IOL technology; but above all, a better approach of the candidate.

The reader will find in this book a modern perspective on this field. A five-step systematic approach is applied in this book.

Step one consists of chapters 1 to 4 dealing with corneal imaging and its clinical application in refractive surgery. It deals with corneal topography, tomography, wavefront science and anterior OCT. What is new and unique in this regard is that any information is presented in relation to its clinical application in terms of diagnostic, avoiding complications or management purposes. To achieve this purpose, abundant images of high quality are included.

Step two consists of chapter 5, which deals with major refractive procedures. Laser procedures, phakic IOL implantation and refractive lens exchange were discussed in terms of new technologies, new laser ablation profiles, surgical techniques, indications, conditions, contraindications, advantages, pitfalls in addition to clinical hints and pearls. This chapter is supported with a high number of tables that compare between refractive options and aid the reader to take the right decision.

Step three consists of chapter 6. This step was designed to be a step before approaching the candidate. All rules, laws and recommendations in the refractive field were assembled, supported with examples and presented in a manner that is easy to access and easy to apply.

Step four is the start-off step. It includes chapters 7 and 8. Chapter 7 presents a thorough detailed approach of the candidate in relation to refractive applications, clinical and surgical aspects, and avoiding complications. Chapter 8 presents complications that can be avoidable. It discusses every complication in terms of etiology, predisposing factors, symptoms and signs, and management. This chapter is supported with high quality and informative images.

Finally, step five that consists of chapter 9 is a clinical case study. Nine clinical examples were carefully selected. They are presented in a practical method, and discussed in a systematic critical thinking in order to build in readers the skills that are necessary in their practice.

It is my hope that readers will find in this book the requisite links between the science and practice of refractive surgery. The surgical outcomes and quality of life of patients undergoing refractive surgery has steadily improved. The promise of refractive surgery rests in our singular focus on our patients' quality of life and quality of vision. Continued improvements in our field are dependent on enhanced technologies and superior training. To this end, I offer this book as a complement in order to assist ophthalmologists in becoming better educated about the ever-developing field.

Although this book is aimed at all those who need some initial assistance in starting their refractive surgery, this book is also aimed at providing current and future refractive surgeons with up-to-date information.

There are sure to be some errors, as the ophthalmology editor, I take full responsibility for these and look forward to being further educated.

Mazen M Sinjab

Acknowledgments

I would like to acknowledge ophthalmology residents in Damascus University who encouraged me to write this book and have had a great role in selecting some of the topics that have been written in this book.

I would like to acknowledge Al Zahra Medical Center in Damascus, for providing me with most figures included in the book.

Contents

Step One: Corneal Imaging

Step Two: Main Refractive Options

Step Three: Rules and Guidelines in Refractive Surgery

Step Four: Start Off

Step Five: Case Study

Abbreviations

AB: Asymmetric bowtie
ACA: Anterior chamber angle
ACD: Anterior chamber depth
ACV: Anterior chamber volume
AD: Ablation depth
AM: Acuity map
AMD: Age-related macular degeneration
AOD: Angle opening distance
ArF: Argon-fluoride
Astig.: Astigmatism
ATR: Against-the-rule
BCL: Bandage contact lens
BFS: Best fit sphere
BFTE: Best fit toric ellipsoid
BSS: Balanced salt solution
CA: Cycloplegic astigmatism
CAM: Correction all aberration map
CCT: Central corneal thickness
CDVA: Corrected distance visual acuity
CET: Central epithelial thickness
CH: Corneal hysteresis
CHOM: Correction high order aberration map
CL: Contact lens
CNV: Choroidal neovascularization
CR: Cycloplegic refraction
CRF: Corneal resistance factor
CS: Cycloplegic sphere
CT: Computed tomography
CTK: Central toxic keratitis
CWF: Corneal wavefront
CXL: Corneal crosslinking
D: Diopter
DALK: Deep anterior lamellar keratoplasty
DCC: Dynamic cyclotorsion compensation
DES: Dry eye syndrome
DOF: Depth of focus
EffRP: Effective refractive power
Epi-LASIK: Epipolis LASIK
FFKC: Forme Fruste keratoconus
HCL: Hard contact lens
HOA: High order aberration
ICR: Intra corneal ring
Irr: Irregular
I-S: Inferior–Superior
IS: Inferior steep
IT-SN: Inferiotemporal–Superionasal
IWF: Internal wavefront
K1: flat K
K2: Steep K
K-avg: Average K
KC: Keratoconus
Kf: Flat K reading
Km: Mean K
K-max: Maximum K
Ks: Steep K reading
LA: Lamellar ablation
LASEK: Laser sub epithelial keratomileusis
LASIK: Laser in situ keratomileusis
LOA: Low order aberration
MA: Manifest astigmatism
MD: Macular degeneration
MFIOL: Multifocal intraocular lens
MMC: Mitomycin C
MMK: Mechanical microkeratome
MR: Manifest refraction
MRI: Magnetic resonance imaging
MRSE: Manifest refractive spherical equivalent
MS: Manifest sphere
MTF: Modulation transfer function
NSAID: Non-steroidal anti-inflammatory drugs
O: Oval
OCT: Optical coherence tomography
ORA: Ocular response analyzer
OWF: Ocular wavefront
OZ: Optical zone
PCI: Partial coherence interferometry
PCO: Posterior capsule opacification
PET: Peripheral epithelial thickness
PIOL: Phakic intraocular lens
PISK: Pressure induced interface stromal keratitis
PMD: Pellucid marginal degeneration

PMT: Post mydriatic test
PRK: Photo refractive keratectomy
PRT: Photo refractive treatment
PSF: Point spread function
PTK: Photo therapeutic keratectomy
R: Round
RD: Retinal detachment
RGP: Rigid gas permeable
RLE: Refractive lens exchange
RK: Radial keratotomy
RMS: Root mean square
RSB: Residual stromal bed
SA: Surface ablation
SB: Symmetric bowtie
SBCs: Sub-Bowman calcifications
SBK: Sub-Bowman keratomileusis
SCC: Static cyclotorsion compensation
SCL: Soft contact lens
SLA: Surface lamellar ablation
SND: Salzman's nodular degeneration
SR: Strehl ratio
SRAX: Skewed radial axis
SS: Superior steep
TA: Topographic astigmatism
TBUT: Tear film break up time test
TE-PRK: Transepithelial photorefractive keratectomy
TISA: Trabecular iris space area
UBM: Ultrasound biomicroscopy
UDVA: Uncorrected distance visual acuity
VA: Visual acuity
WFGT: Wavefront guided treatment
WHOM: Wavefront high order aberrations map
WTR: With-the-rule
ZC: Zernike coefficient

Step One

Corneal Imaging

CHAPTER 1

Topography and Tomography Science

CORE MESSAGE

- Study parameters and maps
- K-readings are important for qualification, quantification and flap measurements
- Q-value is important for qualification and treatment planning
- Pupil center co-ordinates are important for angle Kappa assessment and for decentration
- Pupil diameter is important for optical zone (OZ)
- Thinnest location is important for qualification and quantification
- Anterior chamber depth and angle are necessary when phakic IOLs are considered
- Anterior chamber angle and volume are important for glaucoma assessment

Corneal tomography is a new term addressed today to the maps and images given by Scheimpflug-based machines, while corneal topography is an old term kept now for maps given by Placido-based machines consisting of two maps: anterior sagittal (axial) and anterior tangential (instantaneous) curvature maps. Corneal tomography includes the mentioned topographic maps beside more maps and profiles of both corneal surface in addition to corneal pachymetry map.

Corneal tomography is the most important screening test for refractive surgery to detect abnormalities, diagnose early cases of ectatic corneal diseases and classify these diseases, diagnose post keratorefractive ectasia and put the plan for the best choice in refractive surgery. In spite of this, it should be complimented by other investigations.

MAIN TOMOGRAPHIC MAPS AND PROFILES

Figure 1.1 represents corneal tomography consisting of two parts: corneal parameters on the left side and four composite colored maps on the right side.

Corneal Parameters

Figure 1.2 represents corneal parameters; the followings are the abbreviations and what they stand for:

- **Qs**: Quality specification. It specifies the quality of the tomographic capture; it should be "OK," otherwise there is some missed information which was virtually reproduced (extrapolated) by the computer and the capture should preferably be repeated.
- **Q-val**: Value of Q, which represents the asphericity of the anterior surface of the cornea. The ideal value is measured within the central 6 mm zone as shown between two brackets. Normal value is

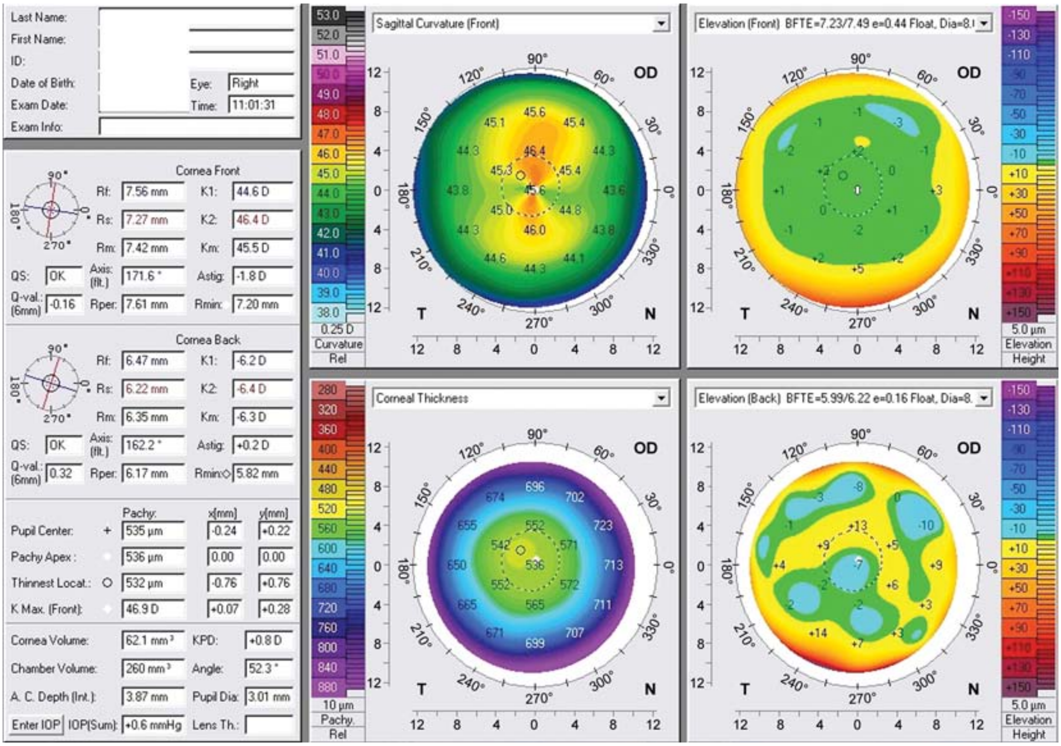

Fig. 1.1 Corneal tomography. On the left: Corneal parameters; on the right: the four composite maps.

(–1 to 0). Plus Q (>0) is found in oblate corneas (e.g. after > – 4D myopic photoablation and after radial keratotomy (RK). Extra minus Q (< –1) is found in hyperprolate corneas (e.g. after >+3 D hyperopic photoablation and in keratoconus (KC). Both oblate and hyperprolate corneas produce spherical aberrations. Refer to Q-value law in chapter 6.

- **K_1**: Curvature power of the flat meridian of the anterior surface of the cornea measured within the central 3 mm zone and expressed in diopters (D). Normal K_1 is >34 D. It is important for myopic ablations: each –1 D correction reduces flat K by 0.75 D, final flat K should be >34 D. Refer to K-reading rules in chapter 6.
- **K_2**: Curvature power of the steep meridian of the anterior surface of the cornea measured within the central 3 mm zone and expressed in diopters (D). Normal K_2 is <47 D. It is important for hyperopic ablations: each +1 D correction will add 1.2 D to steep K, final steep K should be <49 D. Refer to K-reading rules in chapter 6.
- **Km**: Mean curvature power of the anterior surface of the cornea within the central 3 mm zone expressed in diopters (D). In some machines, Km is displayed as average K (K-avg). It is important for flap measurements: Km <40 D may result in free flap, Km >46 D may result in button hole. Refer to K-reading rules in chapter 6.
- **K-max**: Maximum curvature power of the whole anterior surface of the cornea expressed in diopters (D). Normal K-max is <48 D. Normal difference in K-max between both eyes is <2 D. Normal (K-max-K_2) difference is <1 D. K-max is important to avoid post photorefractive irregularities and for hyperopic ablations. Refer to K-reading rules in chapter 6.

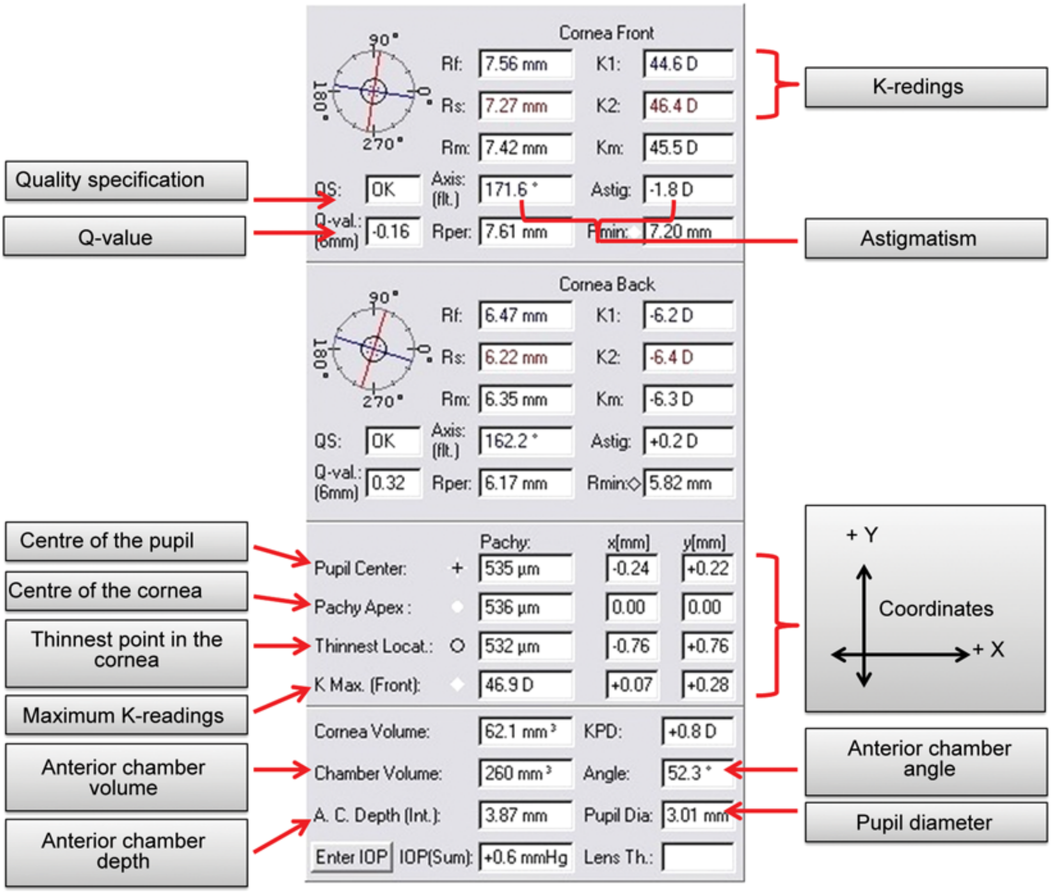

Fig. 1.2 Corneal parameters

- **Astig**: Amount of corneal (topographic) astigmatism (TA) on the anterior surface of the cornea, i.e. the amount of difference between the two curvature radii (K_2 - K_1) within the central 3 mm zone. The normal amount is <6 D. Compare with manifest astigmatism (MA). Refer to astigmatism rules in chapter 6.
- **Axis**: The axis of anterior corneal astigmatism within the central 3 mm zone. Compare with manifest axis. Refer to astigmatism rules in chapter 6.
- **Pachy Apex**: It represents thickness at the apex of the cornea. The computer considers the apex as the origin of the coordinates, where *X* is the horizontal and *Y* is the vertical. Therefore, zero is displayed in both squares of pachy apex coordinates. The direction of axis *X* is from the patient's right to his/her left when the patient is seated opposite to the physician. The direction of axis *Y* is from the bottom up. Example: a point "e" in the left cornea is located at "+0.3, –0.5" position, i.e. this point is located 0.3 mm temporal to and 0.5 mm inferior to corneal apex.
- **Pupil Center**: Corneal thickness corresponding to pupil center location is displayed in addition to the coordinates of pupil center. These coordinates are important for angle kappa and decentration. Normal pupil center *x*-coordinate is ≤200 µm, *x* >200 µm indicates

decentered pupil and a significant angle Kappa, hence, the need for decentration. Refer to pupil center and angle kappa rule in chapter 6.

- **Pupil diameter**: It is the diameter of pupil in the circumstance of capture (photopic, mesopic or scotopic according to the amount of illumination). Pupil size is important for adjusting optical zone (OZ) diameter; it should be adjusted at least 0.5 mm larger than the scotopic size. Refer to pupil diameter considerations in chapter 6.
- **Thinnest location**: Thickness and location of the thinnest point of the cornea. Thickness of >500 µm, 450-500 µm, or <450 µm is usually normal, suspected or abnormal respectively. A difference in thickness of >25 µm at the thinnest location between both eyes is found in <5% of normals and a difference of >34 µm is found in only <0.5% of normals; therefore, a normal difference is <30 µm in average. The difference in thickness between thinnest location and pachy apex is normally ≤10 µm. *Y*-coordinate is most often normal, suspected or abnormal when it is <0.500 mm, 0.500 to 1.000 mm, or >1.000 mm respectively; the important algebraic sign is the minus indicating inferior displacement of the thinnest location. Refer to thickness rules in chapter 6.
- **Anterior Chamber Volume (ACV), Angle (ACA) and Depth (ACD)**: ACV of <100 mm^3, ACA of <24°, or ACD of <2.1 mm may indicate the risk of angle closure glaucoma. On the other hand, if phakic IOL (PIOL) is indicated, ACD should be >3.0 mm and ACA should be >30°.

TAKE-HOME MESSAGE

- Look at flat K for myopic treatment: each –1D correction reduces flat K by 0.75 D, final flat K should be >34 D
- Look at steep K for hyperopic treatment: each +1 D correction will add 1.2 D to steep K, final steep K should be <49 D
- Look at Km (K-avg) for flap measurement: Km <40 D may result in free flap, Km >46 D may result in button hole
- K-max >47 D is abnormal, a difference of >1 D between K-max and steep K is abnormal and a difference of >2 D in K-max between both eyes is abnormal
- Normal TA is <6 D, compare TA with MA, there are 9 probabilities of TA~MA relationship
- Normal Q-value within the central 6 mm zone of anterior corneal surface is (–1 to 0), correcting beyond –4 D and +3 D necessitates special profiles to avoid corruption in Q-value and production of spherical aberrations
- Normal pupil center x-coordinate is ≤200 µm, x >200 µm indicates decentered pupil and a significant angle Kappa, hence the need for decentration
- Normal corneal thickness at the thinnest location is >500 µm, 450–500 µm is suspected, <450 µm is abnormal
- Normal difference in thickness between pachy apex and thinnest location is <10 µm
- Normal difference in thickness at the thinnest location between both eyes is <30 µm
- Normal y-coordinate of thinnest location is <–500 µm, y=(–500 µm to –1000 µm) is suspected, y>–1000 µm is abnormal
- Optical zone (OZ) of refractive surgery should be adjusted at least 0.5 mm larger than the scotopic pupil diameter
- Normal anterior chamber angle is >24°
- Normal anterior chamber volume is >100mm^3
- Normal anterior chamber depth is >2.1mm. PIOLs are contraindicated when anterior chamber depth is <3.0 mm

Maps

CORE MESSAGE

- Study the main four maps: the anterior curvature sagittal map, the anterior and posterior elevation maps and the pachymetry map
- Study the pachymetry profiles
- Study both eyes
- Study the tangential map in case of corneal irregularities, keratoconus and ectatic corneal disorders

Figure 1.3 represents the four composite maps: the anterior curvature sagittal map, the anterior and posterior elevation maps and the pachymetry map. Occasionally, the anterior curvature tangential map should also be studied.

The Anterior Curvature Sagittal Map

CORE MESSAGE

- The sagital curvature map represents patterns of corneal surface power
- The normal pattern is the symmetric bowtie (SB) representing regular astigmatism, but not every SB is necessarily normal
- Study the pattern and study the inferior ~ superior difference on the steep axis at the central 5 mm circle
- Study both eyes for enantiomorphism
- The anterior tangential map describes irregularity, determines cone pattern in keratoconus and ectatic corneal disorders

Figure 1.4 represents anterior surface dioptric power measured with the sagittal method. Steep areas are displayed with hot colors (red and orange), while flat areas are displayed with cold colors (green and blue). On the other hand, red segments are displayed on steep areas, while blue segments are displayed on flat areas. The cross point of this segmentation represents

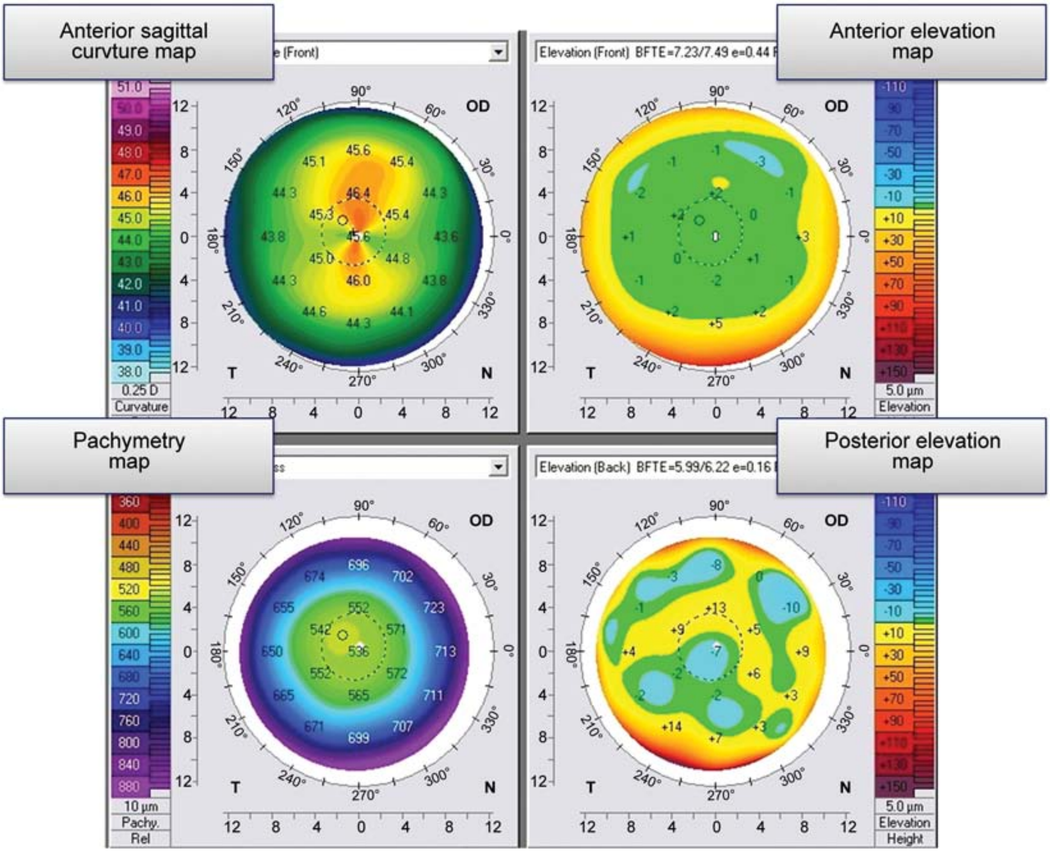

Fig. 1.3 The four composite maps. Anterior curvature sagittal map, anterior and posterior elevation maps and pachymetry map.

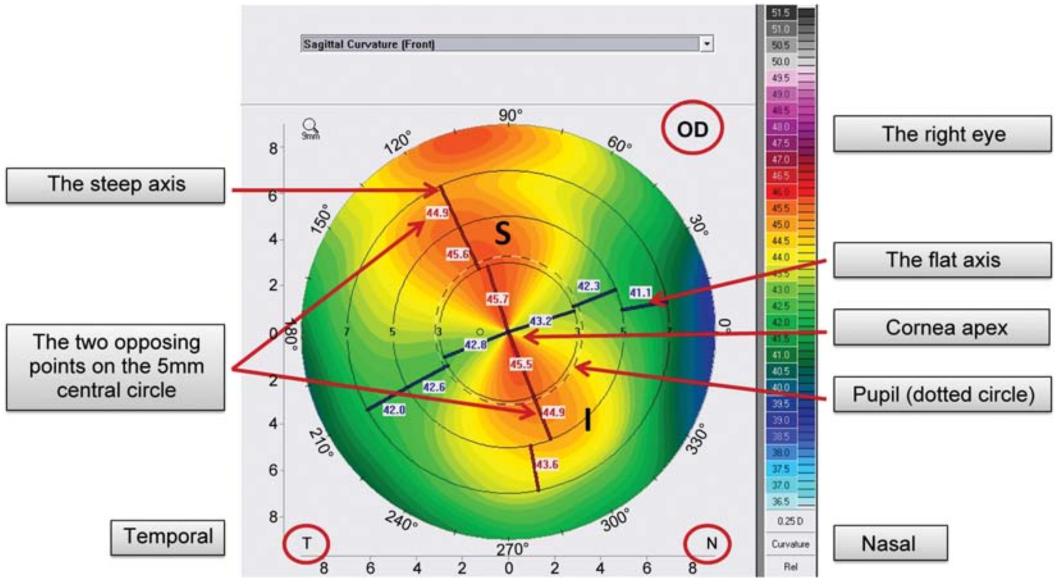

Fig. 1.4 Anterior curvature sagittal map. Notice the steep and flat axes, the two opposing points on the steep axis at central 5 mm circle, cornea apex (center) and image of pupil border on the map.

apex (anatomical center) of the cornea. Beside the shape of the map, values should be studied particularly on the steep axis at the central 5 mm circle.

The normal pattern is the symmetric bowtie (SB), which has the following characteristics:

a. Two lobes "a" and "b" (Fig. 1.5).
b. The axes of the lobes are aligned or there is an angle of < 22° between them.
c. On the steep axis, there are two opposing points at the central 5 mm circle: the superior (S) and the inferior (I) as shown in Figure 1.4. The normal S-I is <2.5 D and the normal I-S is <1.5 D.

The SB pattern represents regular astigmatism, which can be one of three types:

i. Vertical (Fig. 1.5); i.e. the steep axis is on or within ±15° of the vertical meridian of the cornea; it is named "with-the-rule astigmatism (WTR)."
ii. Horizontal (Fig. 1.6); i.e. the steep axis is on or within ±15° of the horizontal meridian of the cornea; it is named "against-the-rule astigmatism (ATR)." This type is considered suspicious.
iii. Oblique (Fig. 1.7); i.e. the steep axis is neither vertical nor horizontal; it is named "oblique astigmatism."

The SB pattern is not always normal, it can occasionally be encountered in KC; therefore, it is not only the shape but also the values which are important.

Figure 1.8 represents the abnormal patterns of this map. Abnormal patterns are better seen when using the tangential map as shown in Figure 1.9. Abnormal patterns include the followings:

1. Round (R) (Fig. 1.10).
2. Oval (O) (Fig. 1.11).
3. Superior Steep (SS) (Fig. 1.12).

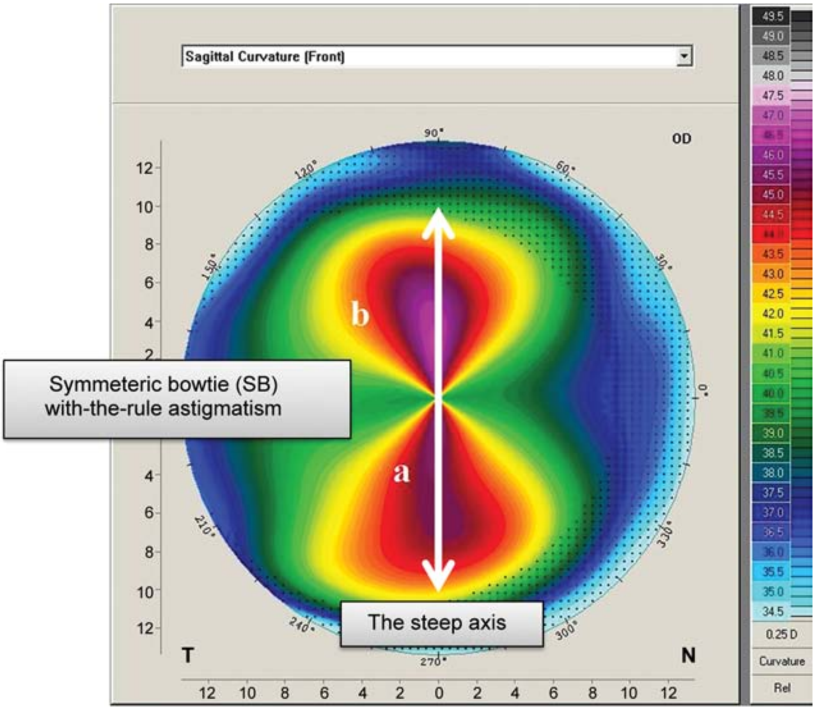

Fig. 1.5 Bowtie pattern consisting of two lobes, "a" and "b." In symmetric bowtie (SB), "a" equals "b" in shape and values. Vertically oriented SB represents with-the-rule (WTR) astigmatism.

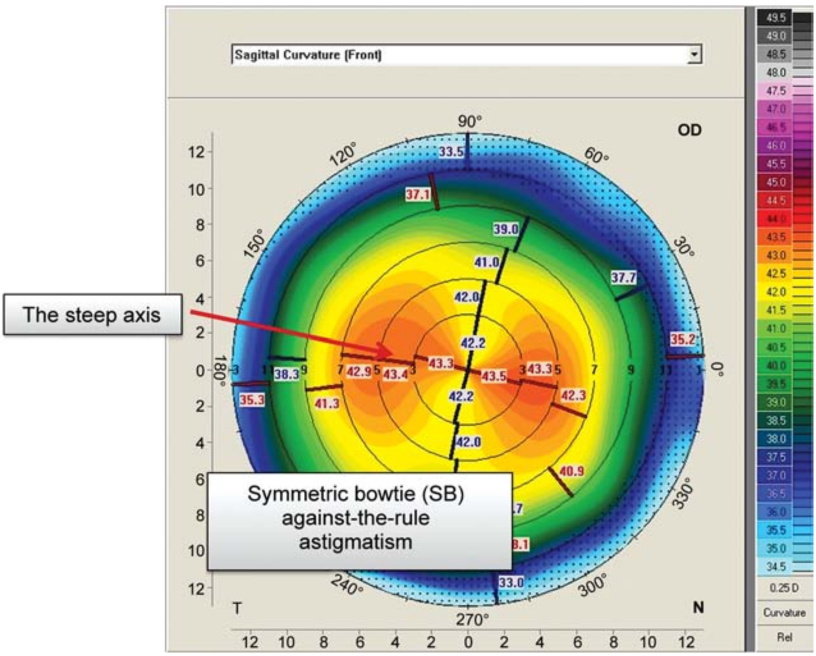

Fig. 1.6 Horizontal symmetric bowtie (SB) representing against-the-rule (ATR) astigmatism.

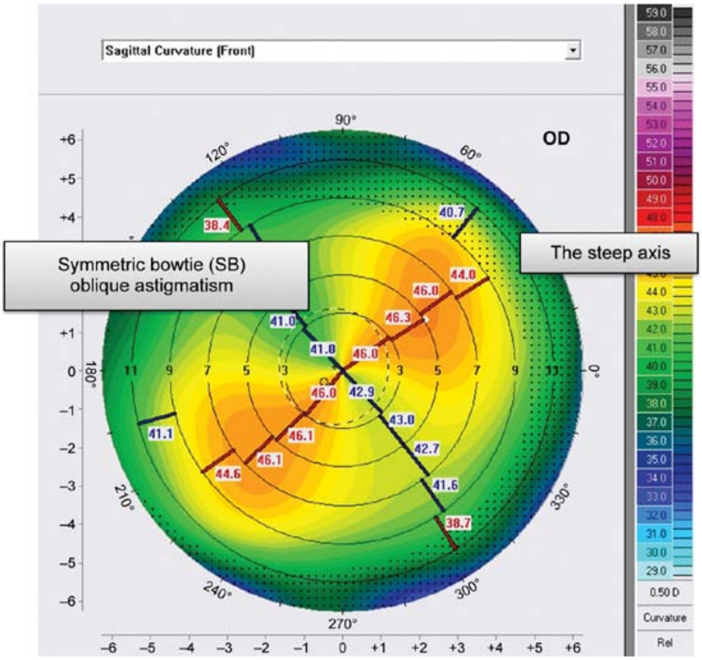

Fig. 1.7 Oblique symmetric bowtie (SB) representing oblique astigmatism.

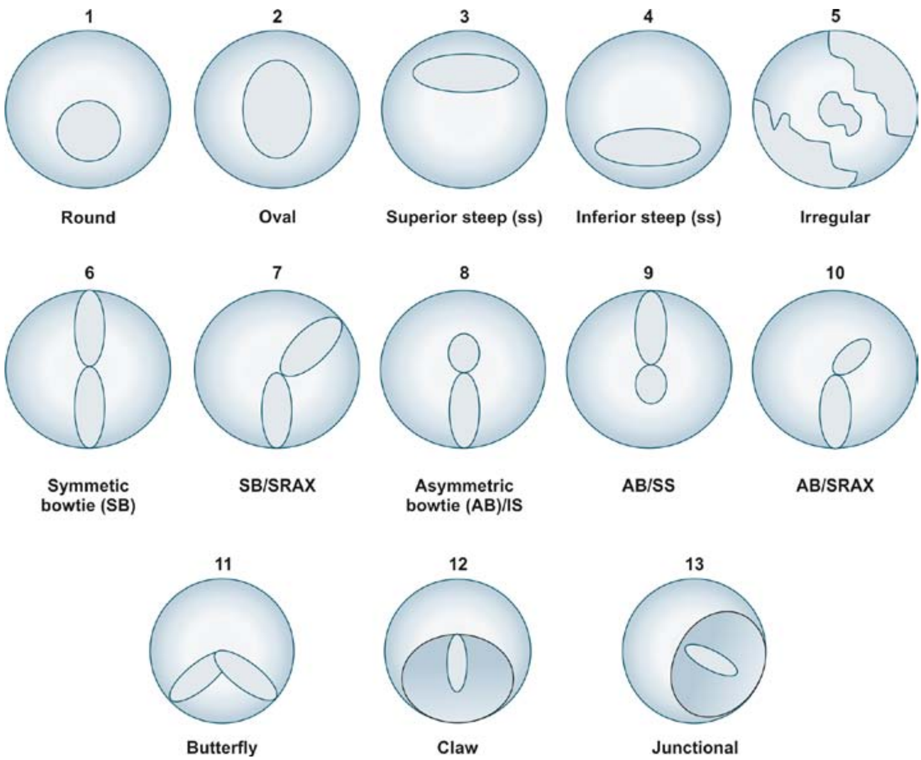

Fig. 1.8 Abnormal patterns of the anterior curvature sagital map.

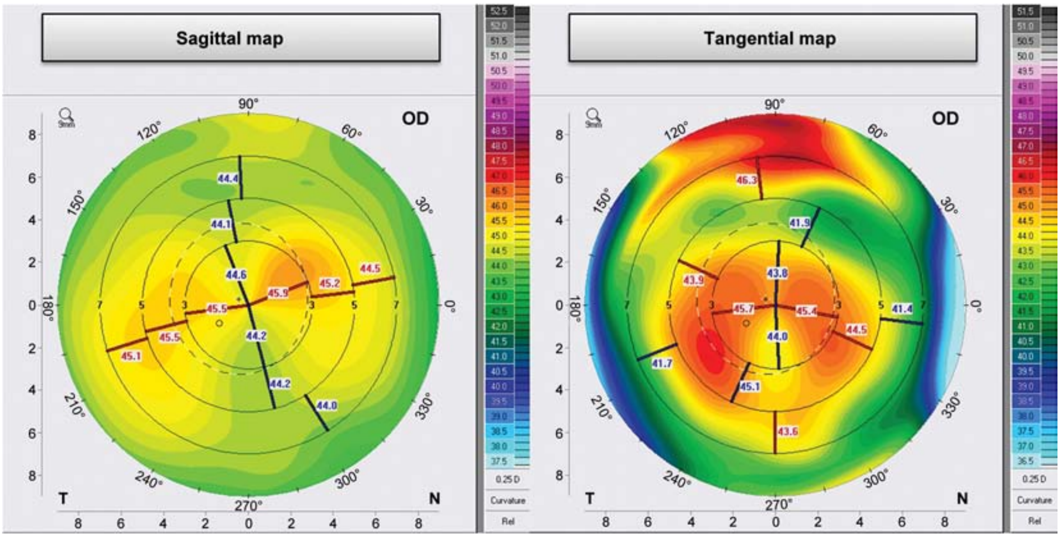

Fig. 1.9 The anterior curvature sagittal and tangential maps of the same cornea. The tangential map is more noisy and bettor to show irregularities. Notice the pattern on both maps; it seems as symmetric bowtie (SB) on left while it is claw pattern on the right.

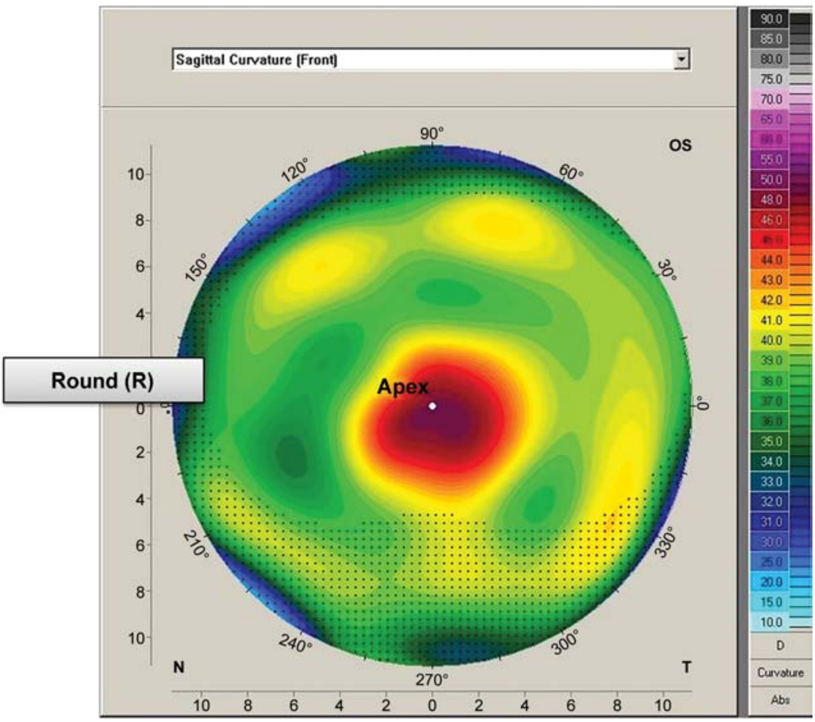

Fig. 1.10 Round hot spot (R). A round area of relatively high K-readings.

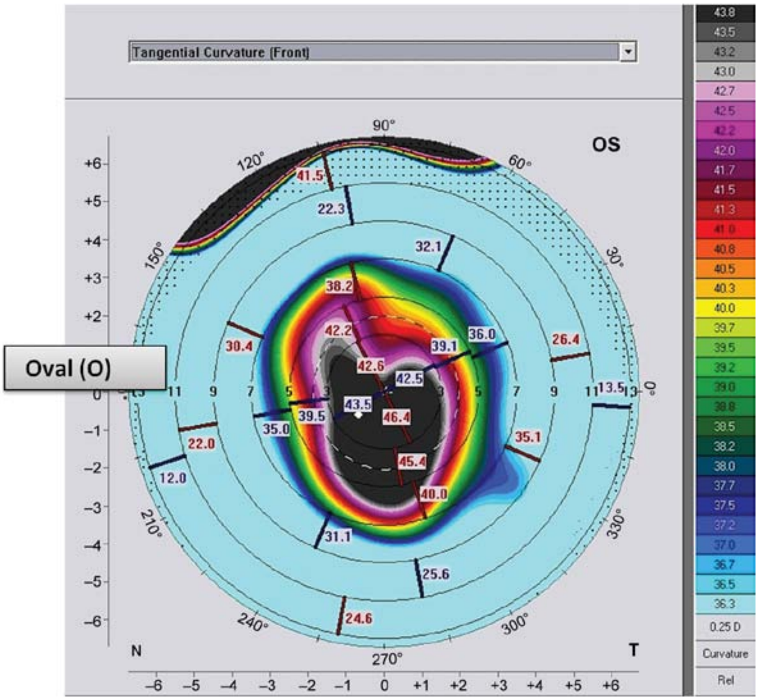

Fig. 1.11 Oval hot spot (O). An oval area of relatively high K-readings.

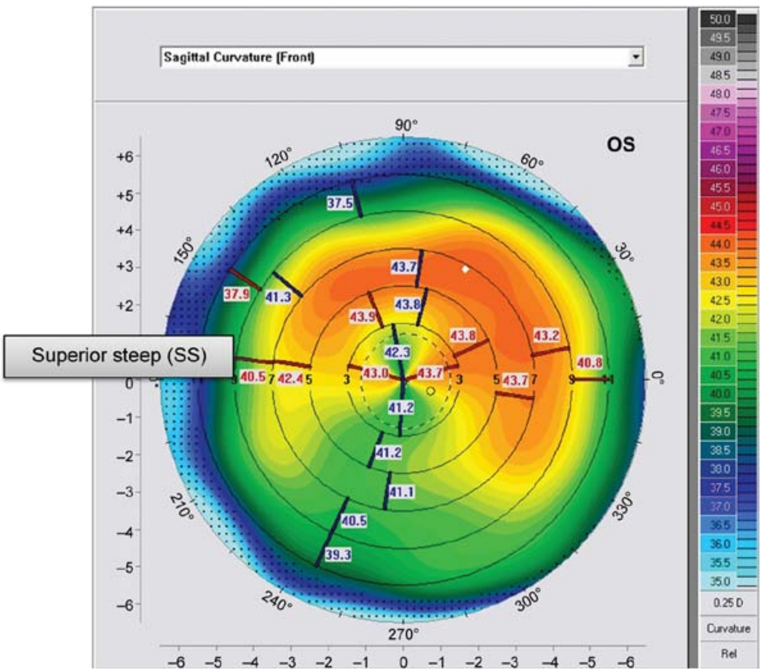

Fig. 1.12 Superior steep pattern (SS). A superior area of relatively high K-readings.

4. Inferior Steep (IS) (Fig. 1.13).
5. Irregular (Irr) (Fig. 1.14).
6. Abnormal Symmetric Bowtie (SB) (Fig. 1.15).
7. Symmetric Bowtie with Skewed Radial Axis >22° (SB/SRAX) (Fig. 1.16).
8. Asymmetric Bowtie/Inferior Steep (AB/IS); the I-S difference is >1.5 D (Fig. 1.17).
9. Asymmetric Bowtie/Superior Steep (AB/SS); the S-I difference is >2.5 D (Fig. 1.18).
10. Asymmetric Bowtie with Skewed Radial Axis >22° (AB/SRAX) (Fig. 1.19).
11. Butterfly (B) (Fig. 1.20).
12. Claw pattern (C) (Fig. 1.21).
13. Junctional (Vertical D) (Fig. 1.22).
14. Smiling face (SF) (Fig. 1.23).
15. Vortex (Fig. 1.24).

Occasionally, some border line irregularities may exist; therefore, it would be helpful to compare between the sagittal maps of both eyes; if almost the same irregularity is found as a mirror shape in the other eye, the border line irregularity can be accepted. This is called "enantiomorphism phenomenon" as shown in Figure 1.25.

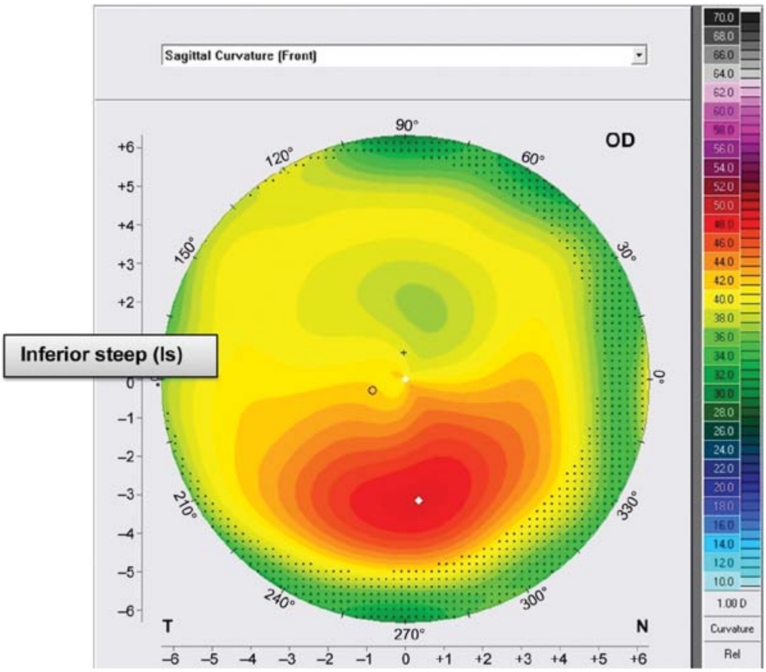

Fig. 1.13 Inferior steep pattern (IS). An inferior area of relatively high K-readings.

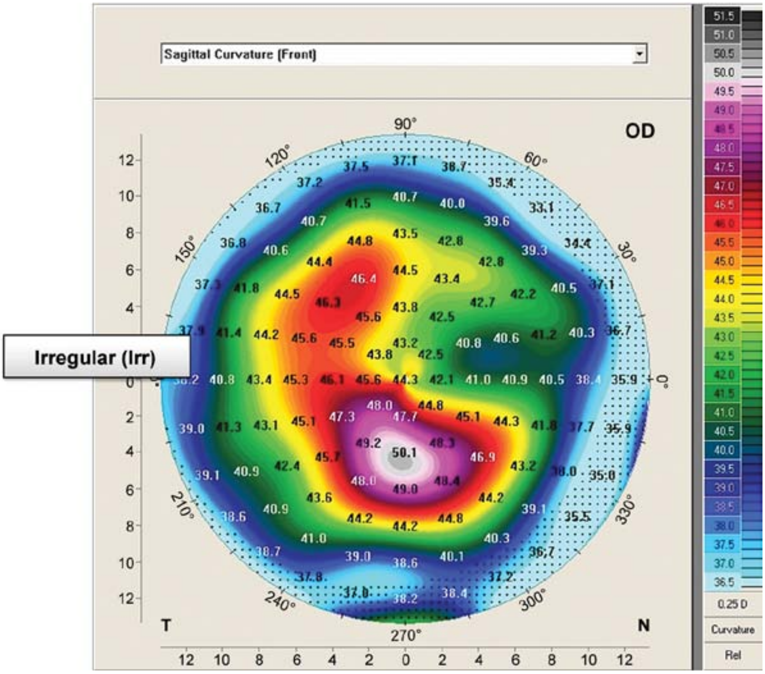

Fig. 1.14 Irregular pattern (Irr). Multiple areas of relatively high K-readings.

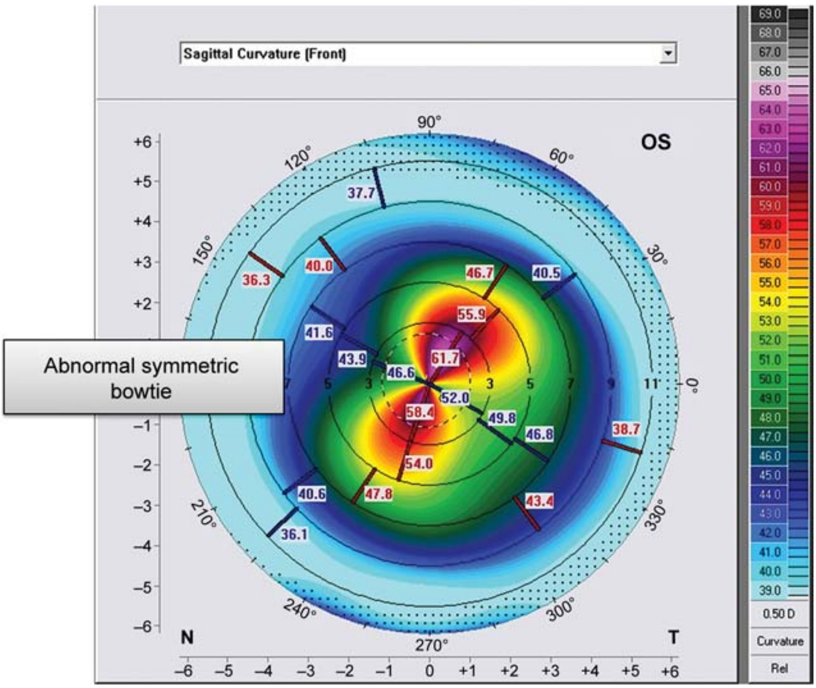

Fig. 1.15 Abnormal symmetric bowtie (SB). It is abnormal due to abnormal high K-readings.

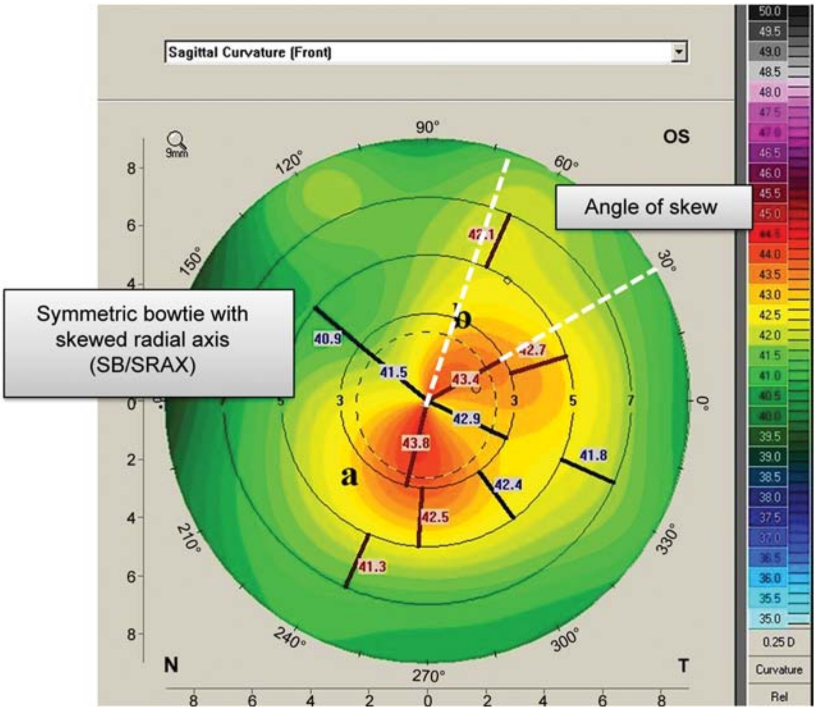

Fig. 1.16 Symmetric bowtie with skewed radial axis (SB/SRAX). A significant skew is >22°.

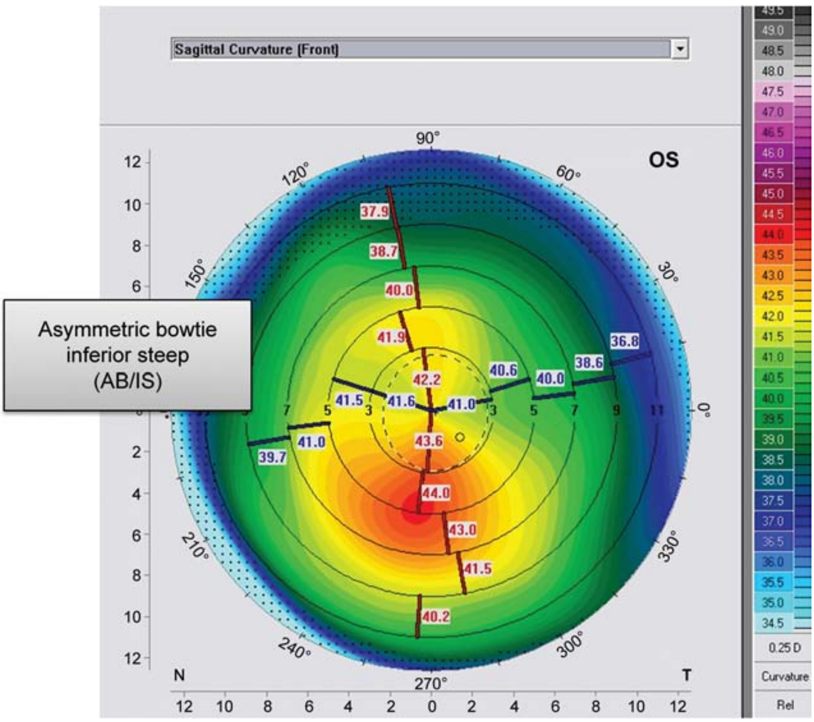

Fig. 1.17 Asymmetric bowtie inferior steep (AB/IS). The inferior lobe is steeper and larger than the superior lobe.

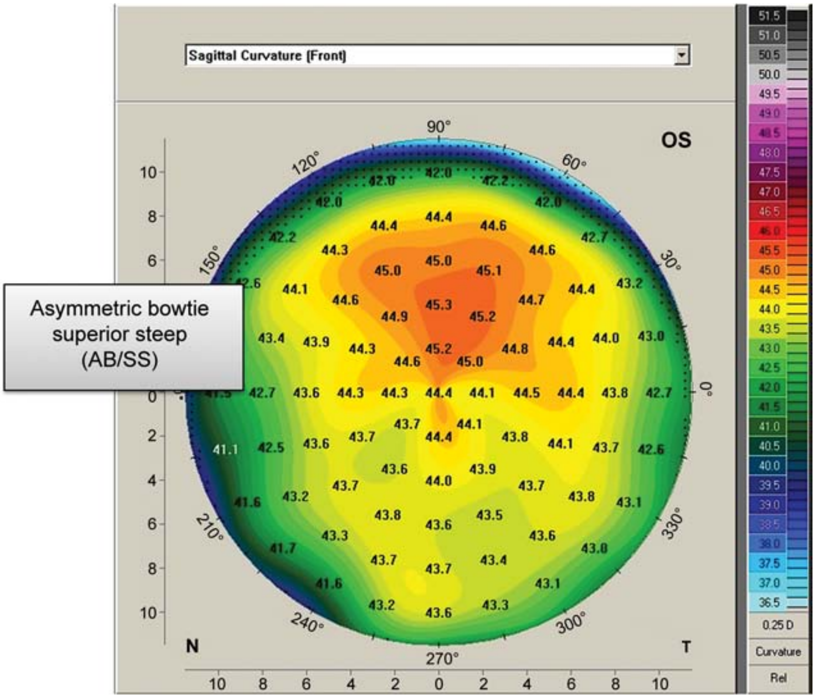

Fig. 1.18 Asymmetric bowtie superior steep (AB/SS). The superior lobe is steeper and larger than the inferior lobe.

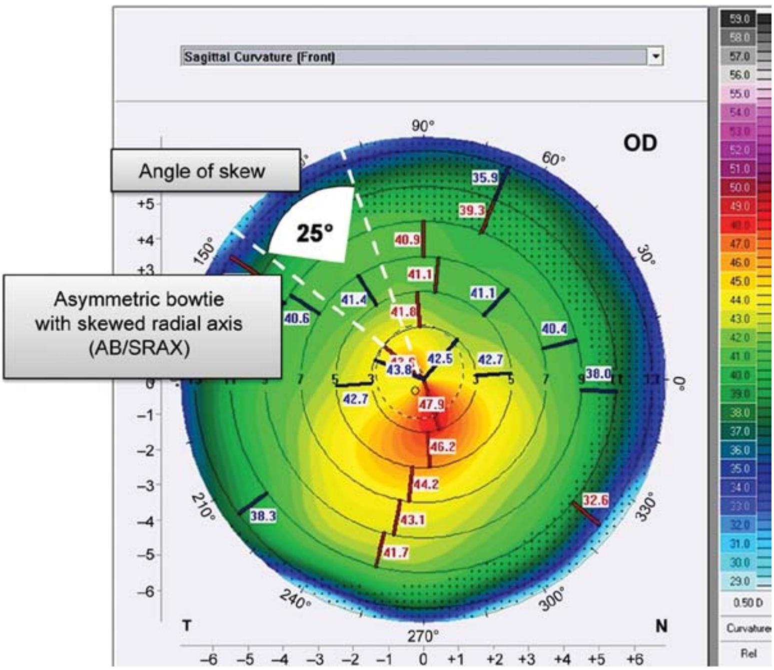

Fig. 1.19 Asymmetric bowtie with skewed radial axis (AB/SRAX). A significant skew is >22°.

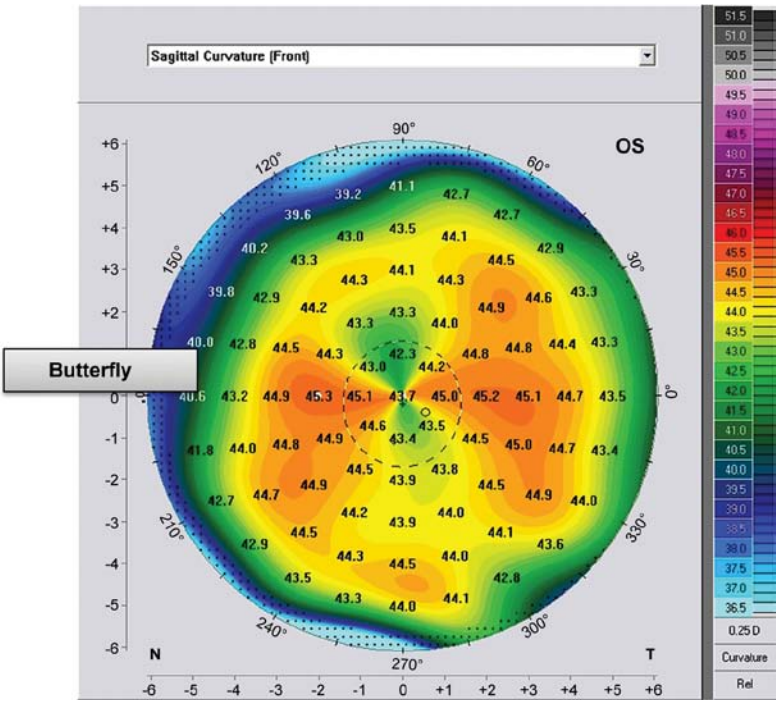

Fig. 1.20 Butterfly pattern (B).

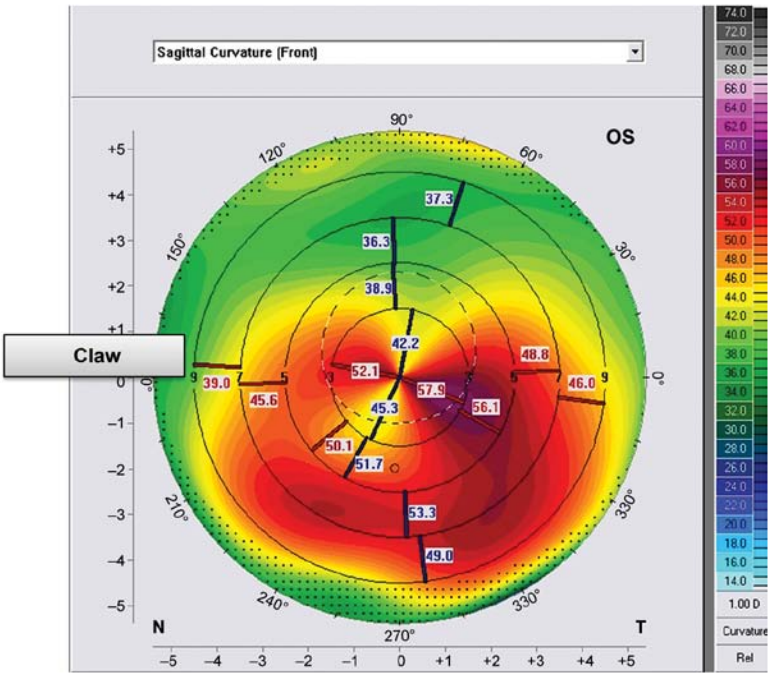

Fig. 1.21 Claw pattern (C). The lobes are joined inferiorly.

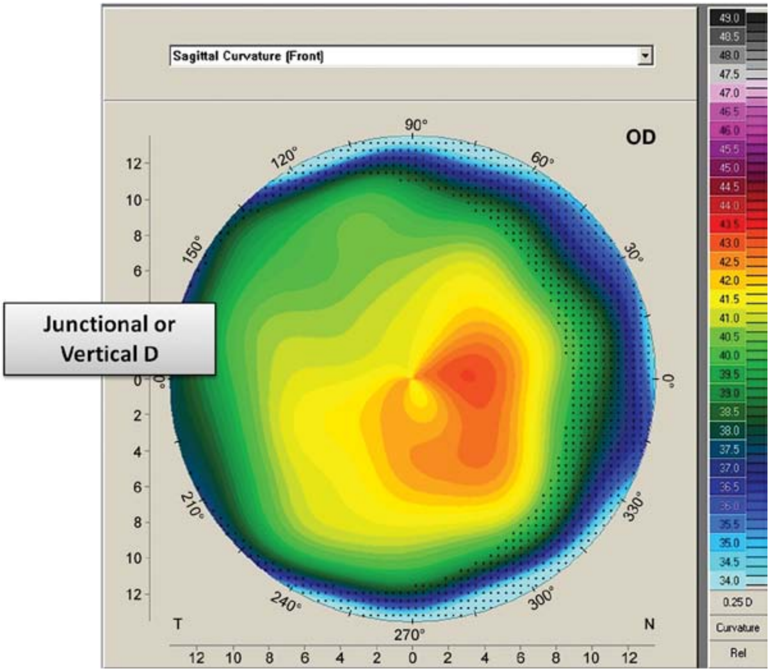

Fig. 1.22 Junctional pattern or vertical D. The lobes are joined laterally.

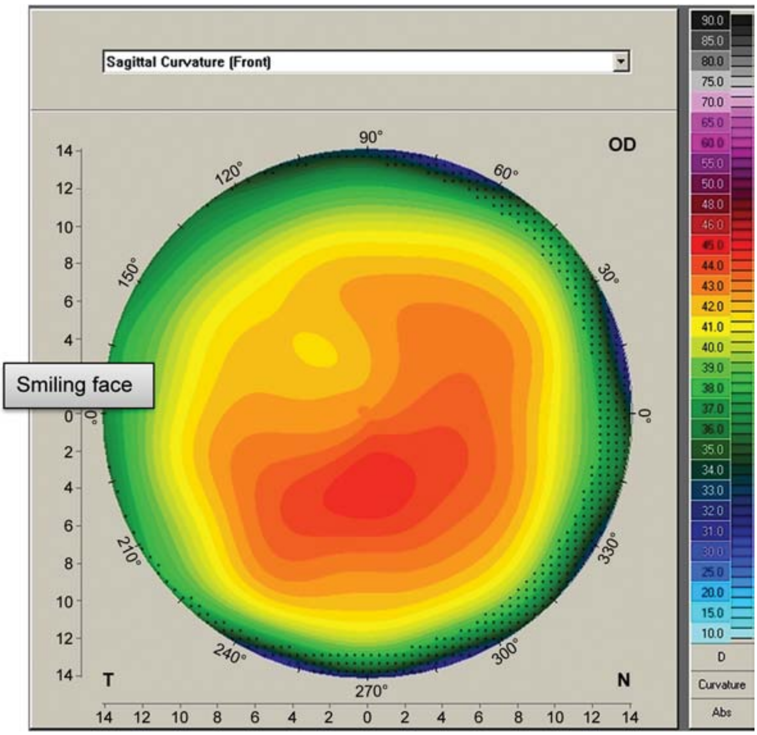

Fig. 1.23 Smiling face.

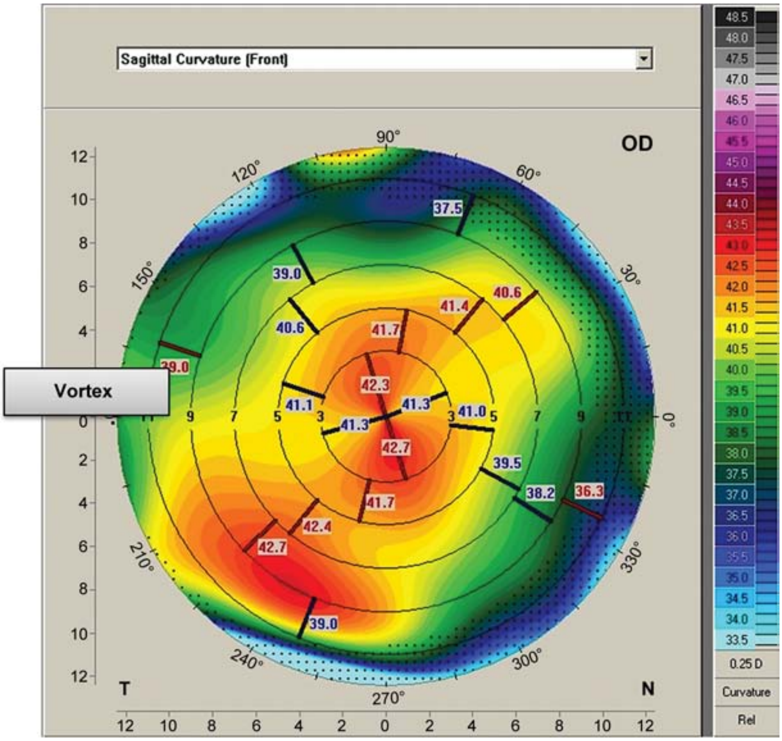

Fig. 1.24 Vortex pattern. Red segments (steep) and blue segments (flat) are distributed in a vortex pattern.

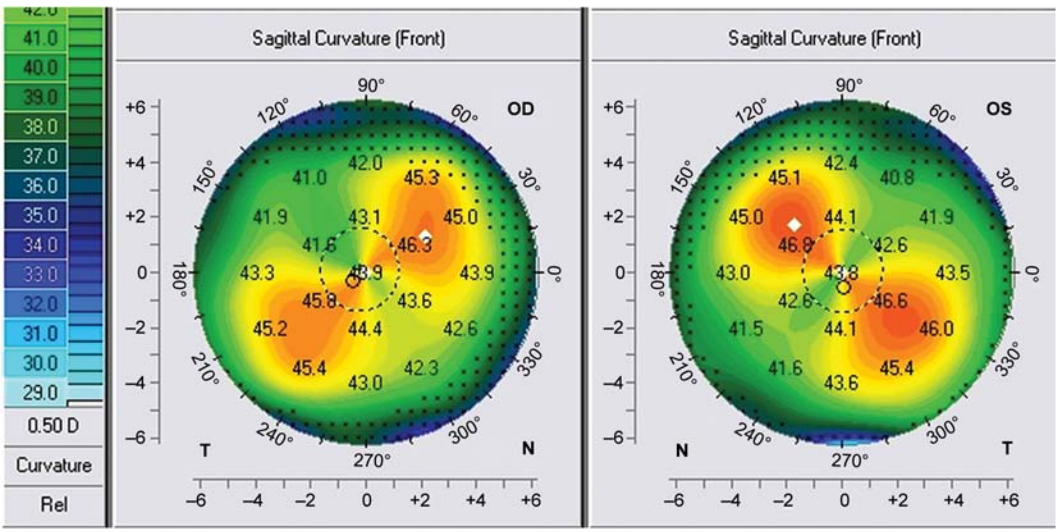

Fig. 1.25 Enantiomorphism. Each cornea is a mirror image of the other cornea in same subject.

The Anterior Curvature Tangential Map

As mentioned before, this map helps in describing corneal irregularities. On the other hand, it is useful for determination of morphologic patterns of the cone in ectatic corneal disorders. Depending on this map, there are three patterns of the cone (Table 1.1):

a. Nipple (Fig. 1.26).
b. Oval (Fig. 1.27).
c. Globus (Fig. 1.28).

TABLE 1.1 Morphological Patterns of Keratoconus and Ectatic Diseases

Morphology	*Cone Size*	*Cone Shape*	*Displacement of Cone Apex*
Nipple	5 mm	steep	inferonasally
Oval	5-6 mm	ellipsoid	inferotemporally
Globus	>6 mm	generalized	generalized

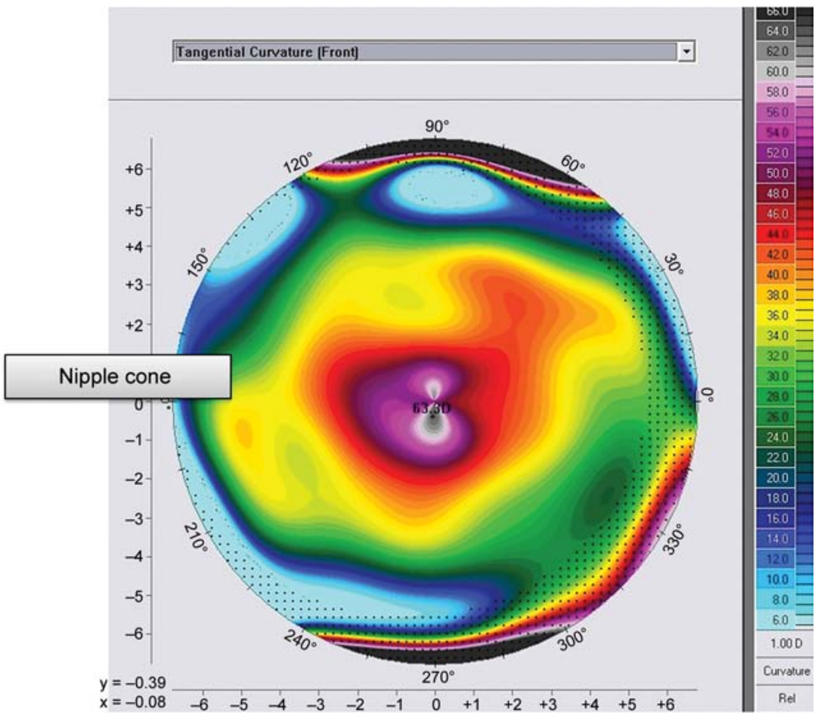

Fig. 1.26 Nipple cone in keratoconus, better seen on the anterior curvature tangential map.

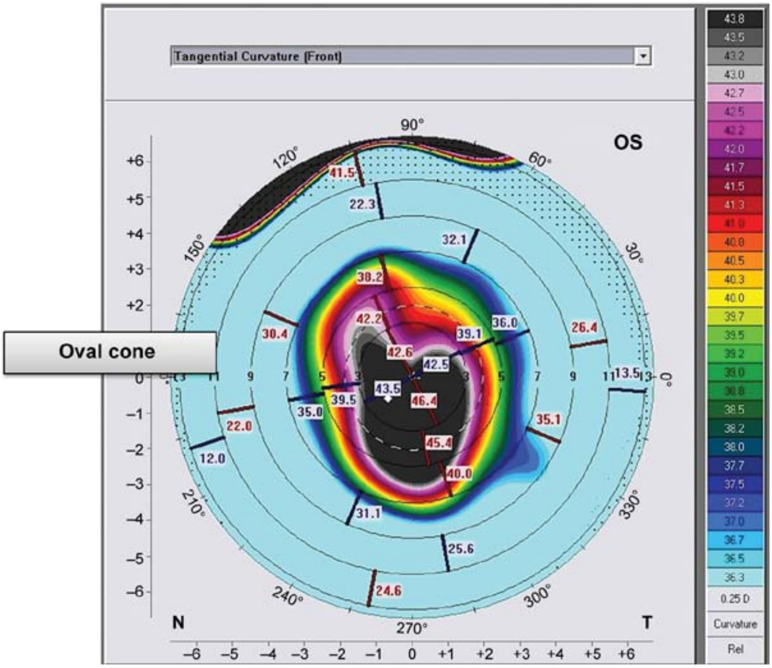

Fig. 1.27 Oval cone in keratoconus, better seen on the anterior curvature tangential map.

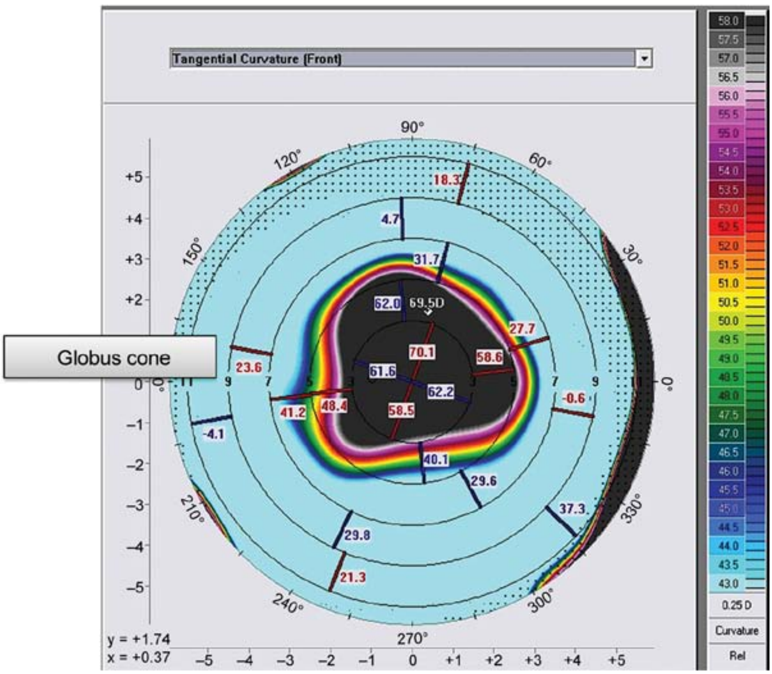

Fig. 1.28 Globus cone in keratoconus, better seen on the anterior curvature tangential map.

TAKE-HOME MESSAGE

- On the anterior sagittal map:
  - Normal corneal pattern is SB, it is usually vertical (WTR astigmatism), sometimes oblique (oblique astigmatism) and not commonly horizontal (ATR astigmatism); the latter is suspicious
  - Not every SB is normal; it may be seen in KC; therefore, values are important
  - I-S >1.5 D or S-I >2.5 D are abnormal.
  - SRAX >22° is abnormal
- On the anterior tangential map:
  - Cone pattern is either nipple, oval or globus
  - Irregularities are better described

The Elevation Maps

CORE MESSAGE

- Study the elevation maps with best fit sphere (BFS) and best fit toric ellipsoid (BFTE) float modes
- Study the shape with BFS float mode
- Study the values with BFTE float mode
- In KC and ectatic corneal disorders, the cone is located with BFS float mode

Elevation maps describe the height details of the measured corneal surface by matching it with a reference surface above which points are considered elevations and expressed in plus values and below which points are considered depressions and expressed in minus values as shown in Figure 1.29. On the other hand, in WTR astigmatism, the vertical meridian is steeper than the horizontal one and lies under the surface of the reference body contrary to the horizontal meridian which lies over the reference surface (Fig. 1.30).

There are several shapes of the reference surface, but the most important are best fit sphere float (BFS) which describes (qualifies) the shape of the measured surface and best fit toric ellipsoid float (BFTE) which estimates (quantifies) values. The ideal diameter of the best fit reference body is 8 mm and the ideal mode is the float mode.

Shape (BFS float mode)

The normal shape of a cornea that has regular WTR astigmatism is the symmetric sandy watch shape as shown in Figure 1.31.

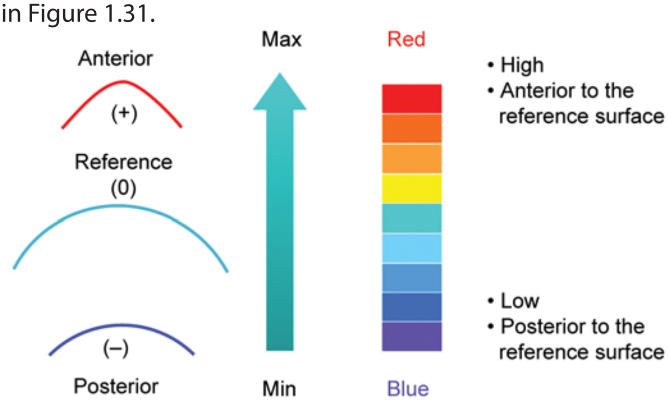

Fig. 1.29 Principle of the elevation map. A reference body is matched to the measured corneal surface. Parts that are above the reference body are considered elevations and plotted with hot colors and plus values, whereas parts that are below the reference body are considered depressions and plotted with cold colors and minus values.

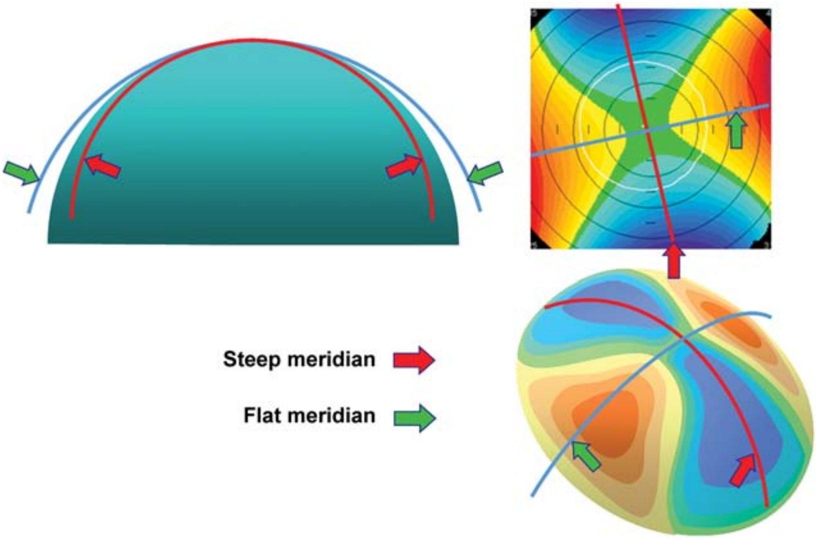

Fig. 1.30 With-the-rule (WTR) astigmatism. The vertical meridian of the cornea is displayed in minus values and cold colors since it lies below the reference surface.

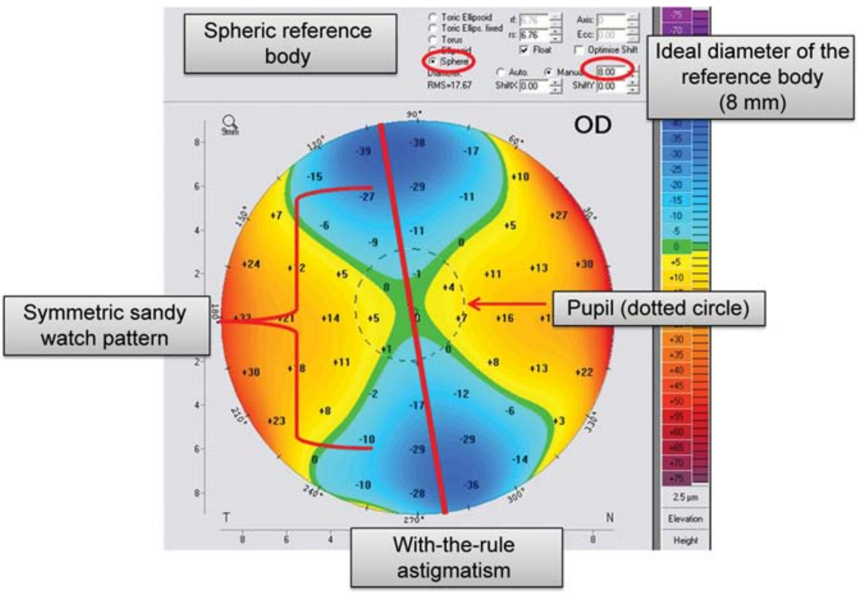

Fig. 1.31 Elevation map with best fit sphere reference body. It describes the shape. The normal shape is the symmetric sandy watch pattern representing WTR astigmatism.

Abnormal shapes include:

a. Skewed sandy watch (Fig. 1.32), it can be normally seen with large angle Kappa, misalignment during capture or in abnormal distorted corneas.
b. Tongue-like extension and irregular sandy watch (Figs 1.33 and 1.34), it is seen in abnormal distorted corneas.
c. Isolated island (Fig. 1.35), it is seen in abnormal distorted corneas with central or paracentral protrusion.

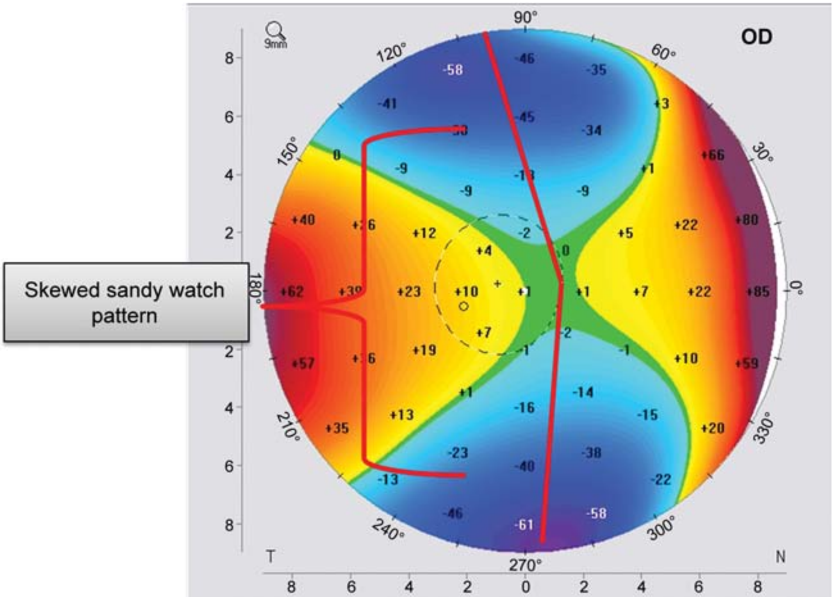

Fig. 1.32 Skewed sandy watch pattern.

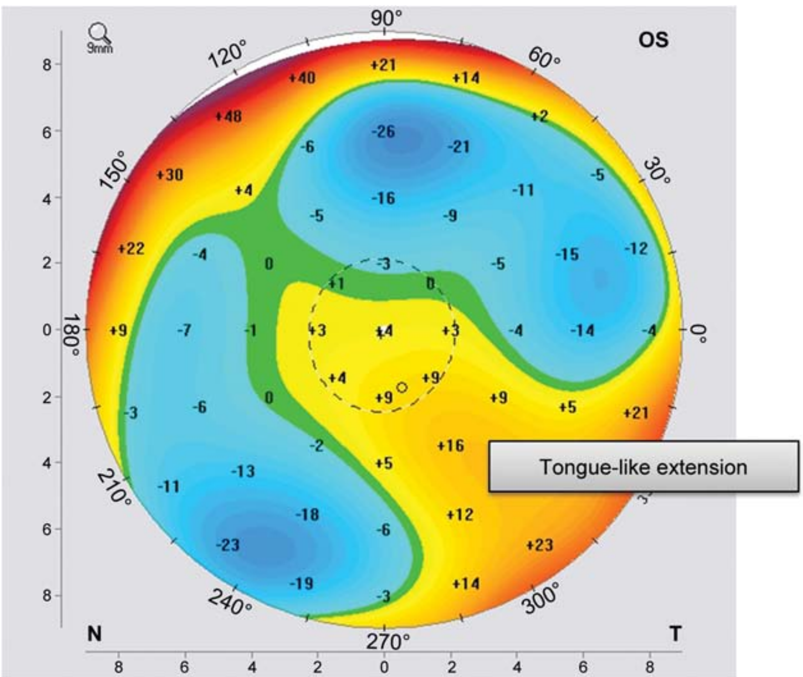

Fig. 1.33 Tongue-like extension. It can be considered as severely skewed sandy watch indicating an abnormal distorted cornea.

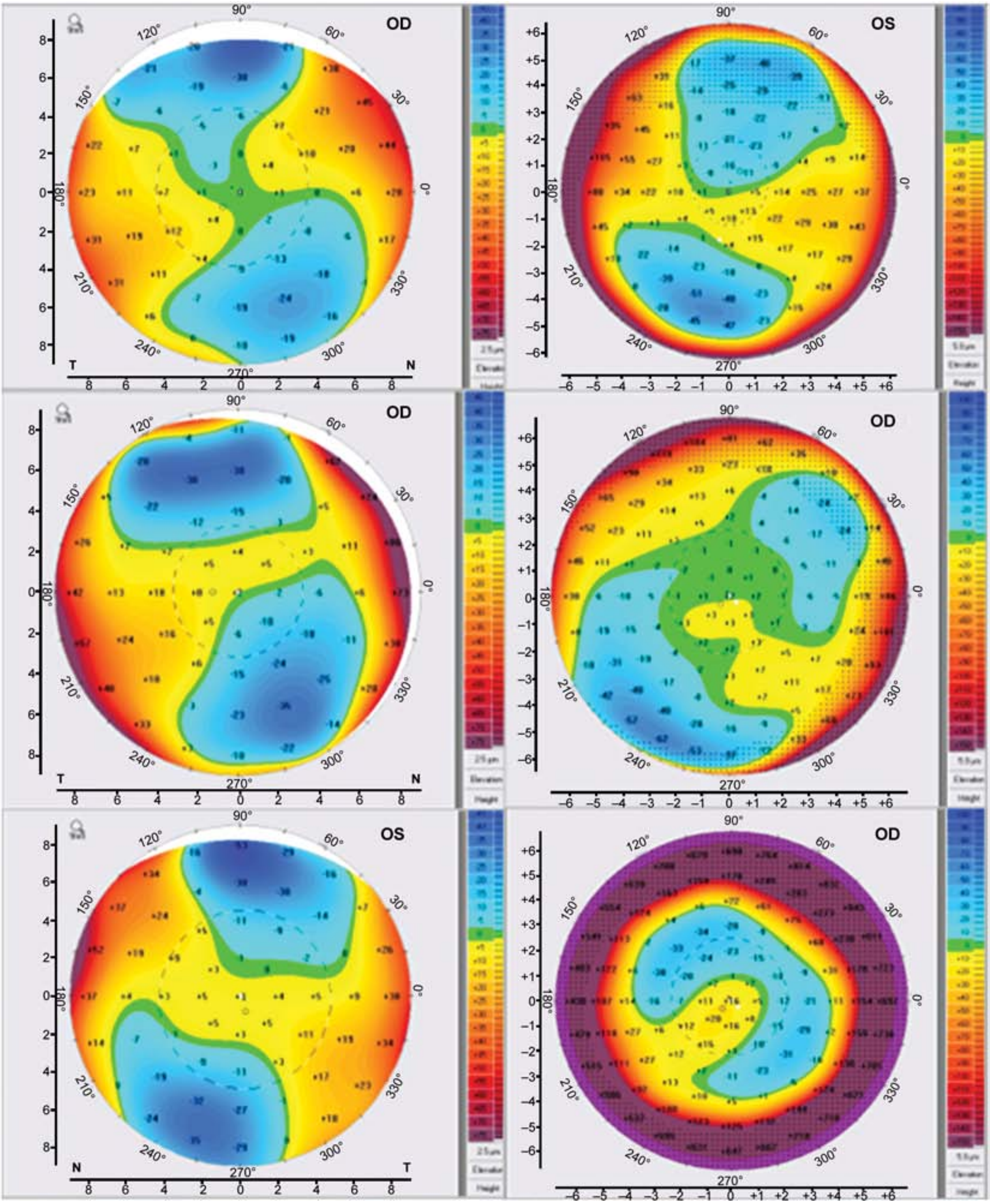

Fig. 1.34 Different patterns of tongue-like extensions.

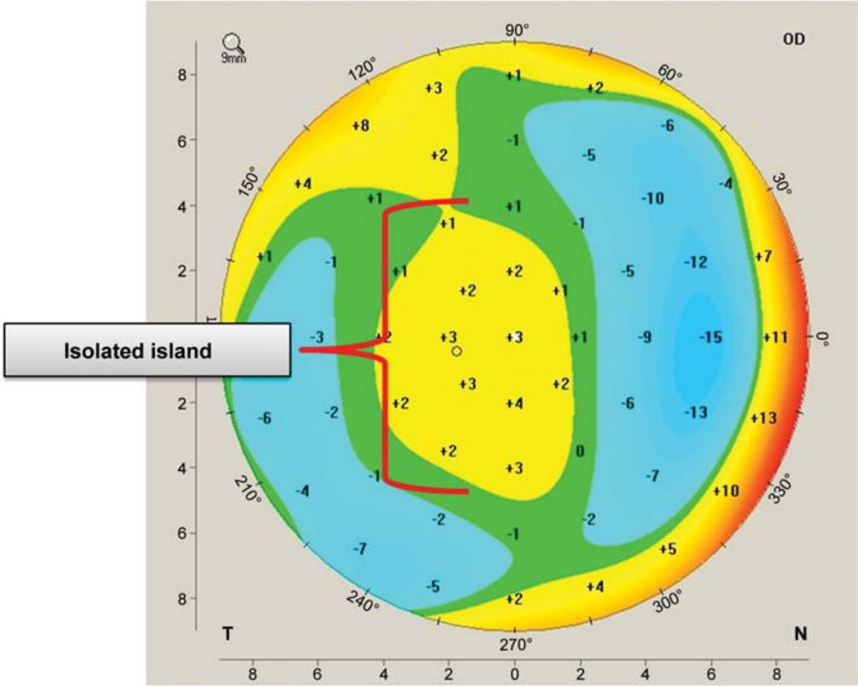

Fig. 1.35 Isolated island. It is an indicator of an abnormal surface with central or paracentral protrusion.

Values (BFTE float mode)

Values are estimated in two ways:

a. Values within the central 5 mm zone on both corneal surfaces (Fig. 1.36). Normal values are <12 μm and <15 μm on the anterior and posterior elevation maps, respectively.
b. Values corresponding to the thinnest location. These values can be seen by pointing with the cursor at the thinnest location symbol on the map and left click on the mouse to see the corresponding anterior and posterior elevation values. Normal values are presented in Table 1.2. It is clear in this table that there is a difference in normal values between myopic and hyperopic eyes.

TABLE 1.2 Values of Elevations Corresponding to Thinnest Location (>95% of normal population)

	Anterior	*Posterior*
Myopia	≤ 6 μm	≤13 μm
Hyperopia	≤4 μm	≤22 μm

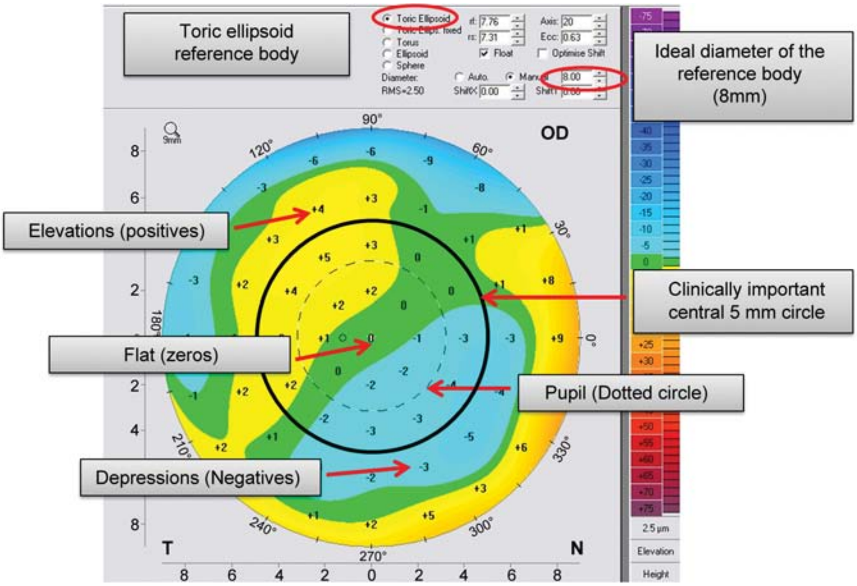

Fig. 1.36 Elevation map with BFTE reference body. It describes values. On this map, elevations take plus values and coded with yellow, whereas depressions take minus values and coded with blue.

Cone Location

It can only be determined by the elevation maps. The best to locate the cone is the BFS and the best to evaluate the height of the cone is the BFTE (Fig. 1.37). On the BFS, the cone can be central, paracentral or peripheral depending on its location in relation with the central 3 mm or 5 mm circles as shown in Figure 1.38. This classification is important for treatment. See ectatic corneal disorders below.

TAKE-HOME MESSAGE

- Normal elevation shape on BFS mode is the sandy watch
- Exclude tongue-like extension and isolated island on BFS mode
- On BFTE mode, normal elevation values within the central 5 mm zone are:
  - ≤ 12 µm on the anterior surface
  - ≤ 15 µm on the posterior surface
- In KC and ectatic corneal disorders use the BFS mode to locate the cone:
  - within 3 mm, it is central
  - between 3 mm and 5 mm, it is paracentral
  - out of 5 mm, it is peripheral

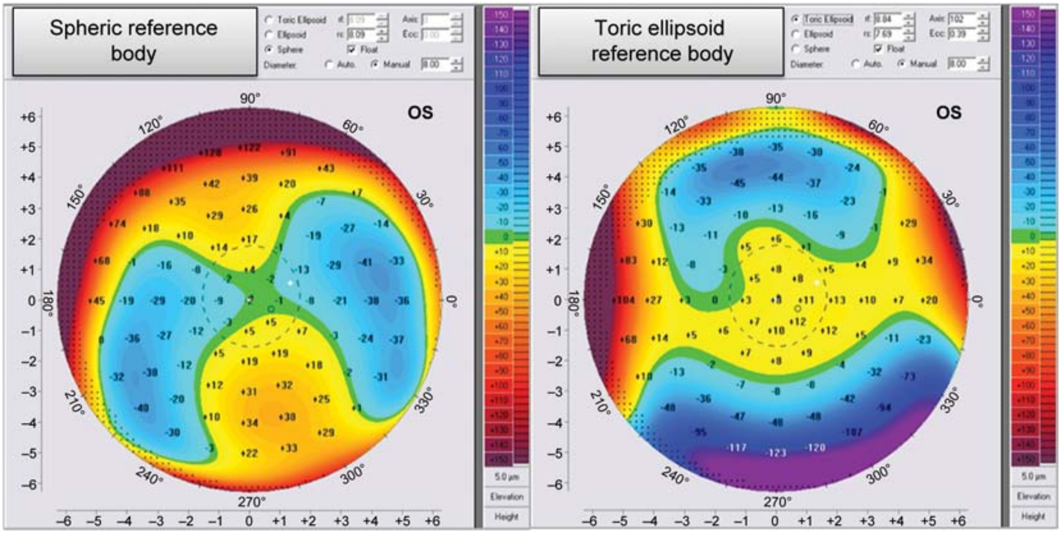

Fig. 1.37 Difference between elevation map with BFS (on the left) and BFTE (on the left). In keratoconus, the former locates the cone and the latter measures its height.

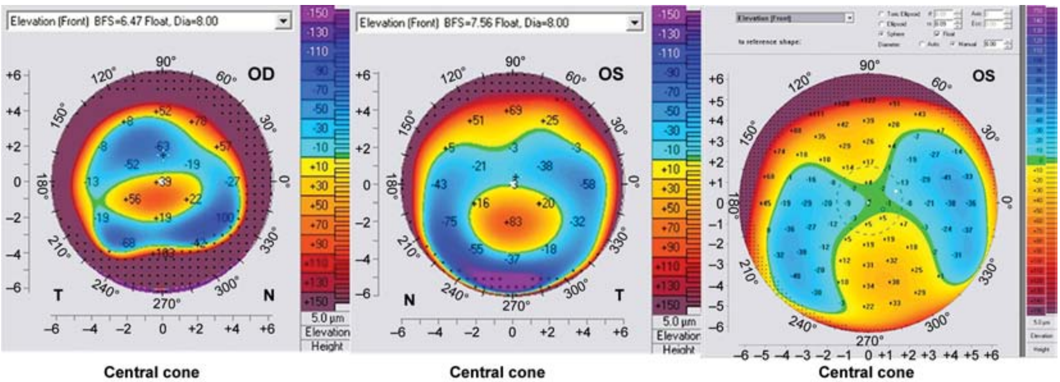

Fig. 1.38 Classification of cone location by elevation map with BFS reference body. The cone is central, paracentral or peripheral when its apex falls within central 3 mm, 3–5 mm or out of 5 mm, respectively.

The Difference between the Curvature and the Elevation Maps

Although, the curvature means power and the elevation means height, it is not that easy to understand the relationship between both maps. The idea can better be explained when studying an illustration of a keratoconus case. Figure 1.39 represents a keratoconus with paracentral cone. The dotted lines in this figure are elevation contours similar to those in the height maps of the earth. A cross section is made through this surface to show the cone and the flat superior area. Unlike the elevation map, the sagittal curvature map depends on a reference axis, which in optimal situations co-insides with the visual axis. The red spot in Figure 1.39 is the fixation point

through which visual axis passes. From this point, the sagittal curvature map starts as shown in Figure 1.40. Figure 1.41 is the sagittal curvature map presented in relation to the cone. Notice that the curvature power over the cone may be low as shown in this figure and the explanation is very simple; both maps are of different concept. On the other hand, the shape of the curvature map differs according to the shape of the elevation map; see Figures 1.42 and 1.43; the cone is central and accordingly the bowtie is more symmetric.

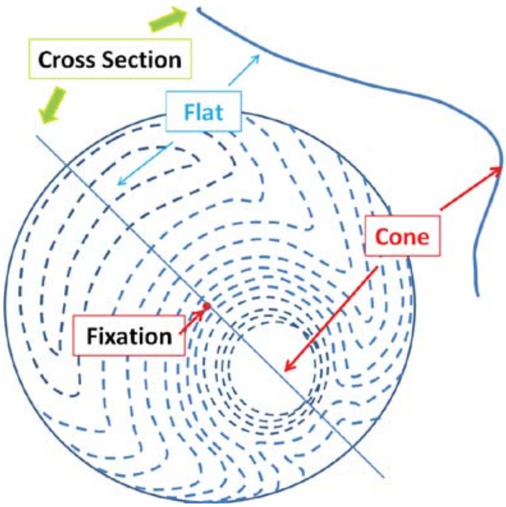

Fig. 1.39 Elevation contours in a keratoconic cornea. Contours are closer to each others in steep areas such as the cone and vice versa in flat areas.

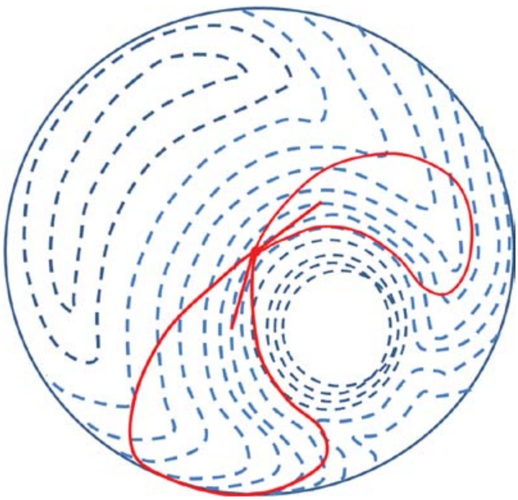

Fig. 1.40 The relationship between elevation contour map and curvature sagittal map. The latter is related to the visual reference axis.

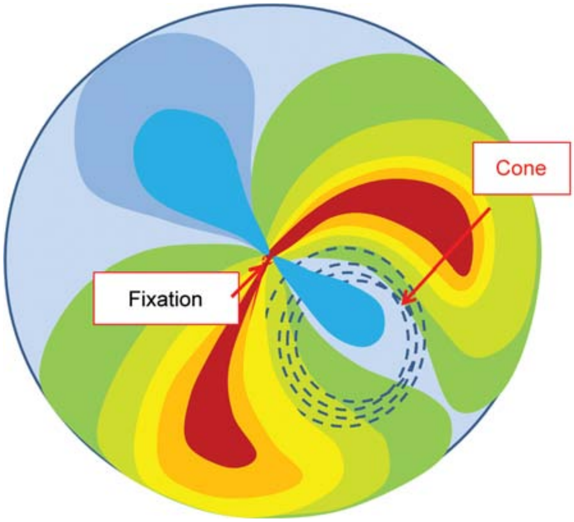

Fig. 1.41 The relationship between elevation contour map and curvature sagital map. Notice that the curvature power may be low over the cone such as in pellucid marginal degeneration.

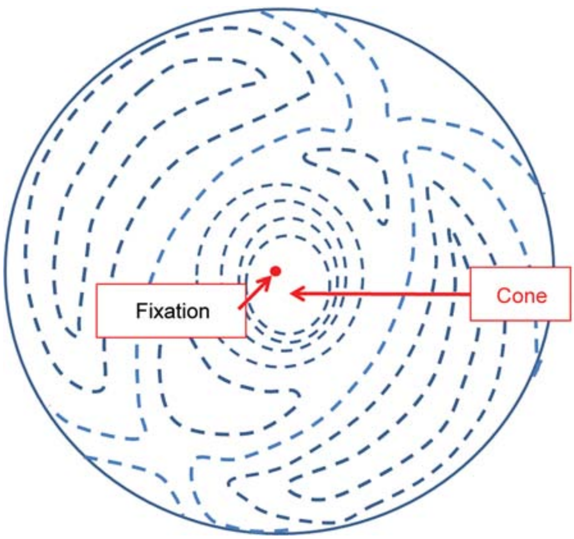

Fig. 1.42 Another example of an elevation contour map.

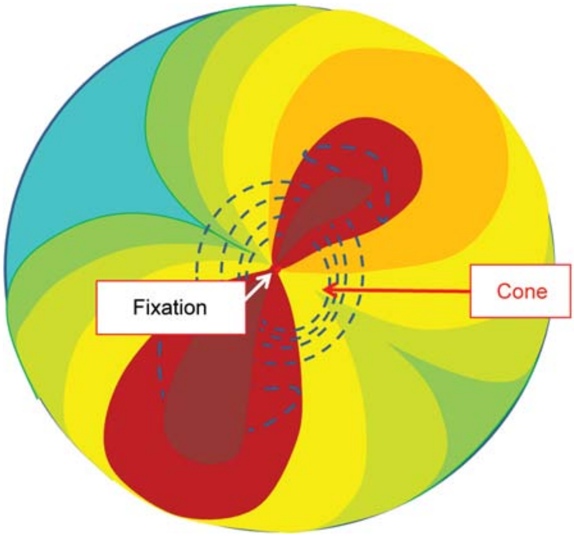

Fig. 1.43 Another example of the relationship between elevation contour map and curvature sagittal map. Since the cone is central, the bowtie is more symmetric.

The Pachymetry Map

CORE MESSAGE

- Study shape of and values of the pachymetry map
- Study the S-I deference on the vertical meridian at the central 5 mm circle
- On the thickness profiles:
  - study the shape
  - see the average

There are three main land marks on the pachymetry map (Fig. 1.44): cornea apex, thinnest location, and the two opposing points on the vertical meridian at the central 5 mm circle. The relationship between the first two landmarks was described previously. The two opposing points are superior (S) and inferior (I); the normal S-I difference is <30 µm.

Abnormal shapes of the pachymetry map are:

a. Horizontal displacement of the thinnest location (Fig. 1.45).
b. Dome shape. The thinnest location is vertically displaced (Fig. 1.46).
c. Bell shape. A thin band in the inferior part of the cornea (Fig. 1.47); it is specific for PMD.
d. Keratoglobus. A generalized thinning reaching the limbus (Fig. 1.48).

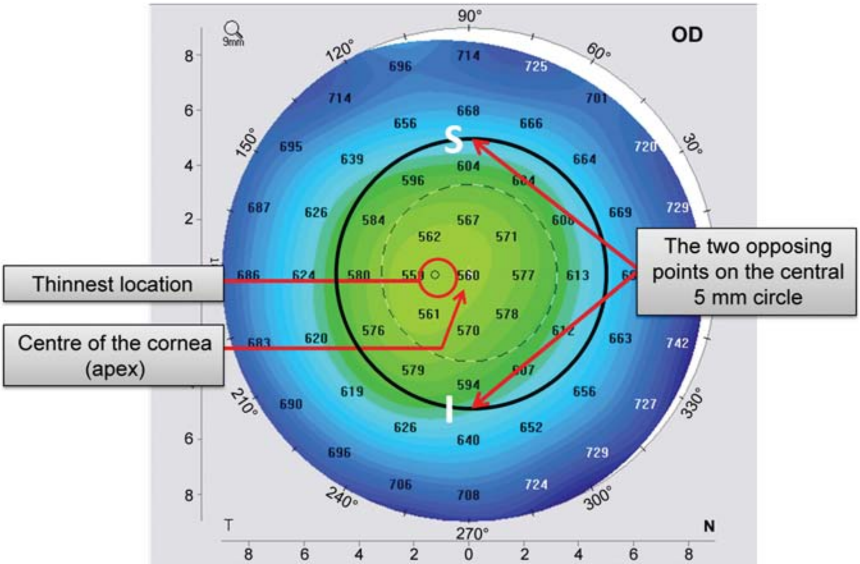

Fig. 1.44 The pachymetry map with the three main landmarks, thinnest location, corneal apex and the two opposing points at the central 5 mm circle.

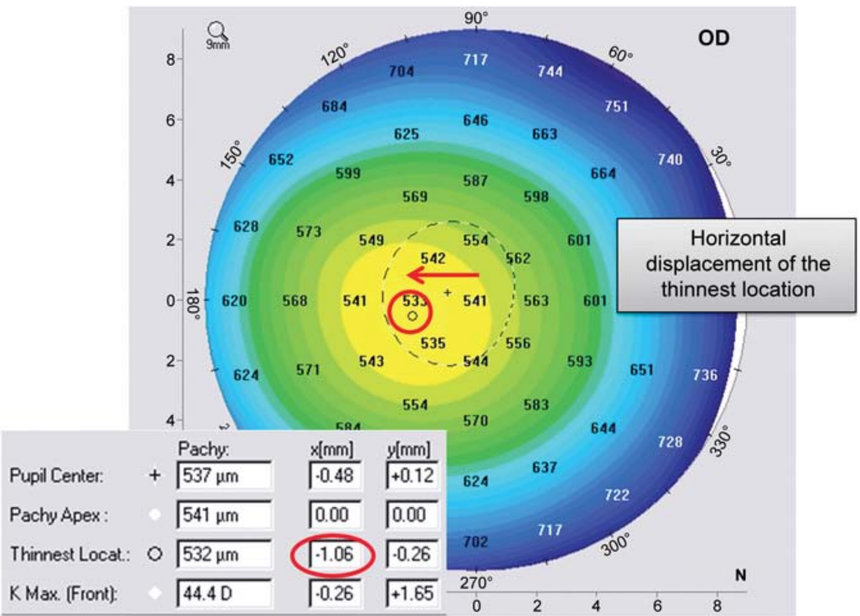

Fig. 1.45 Horizontal displacement of the thinnest location.

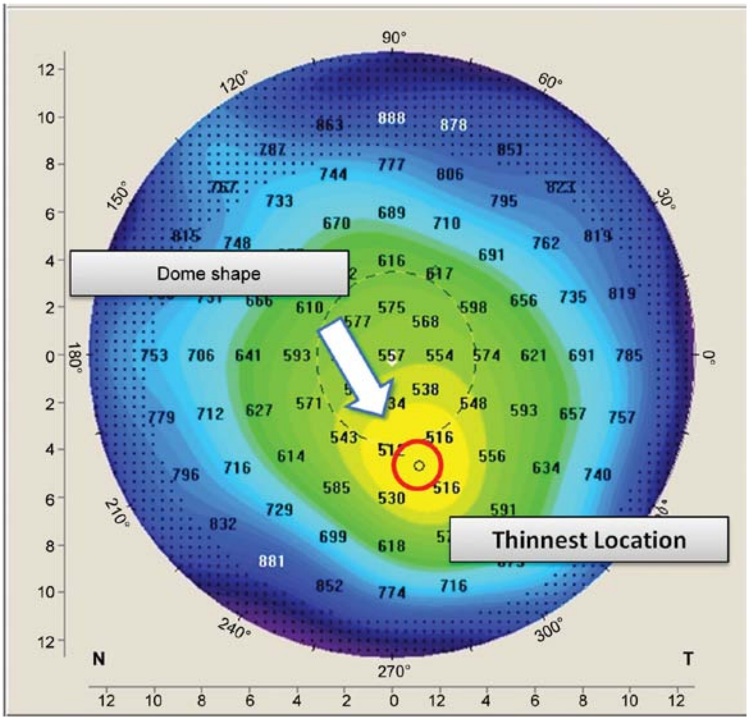

Fig. 1.46 Dome shape of the pachymetry map.

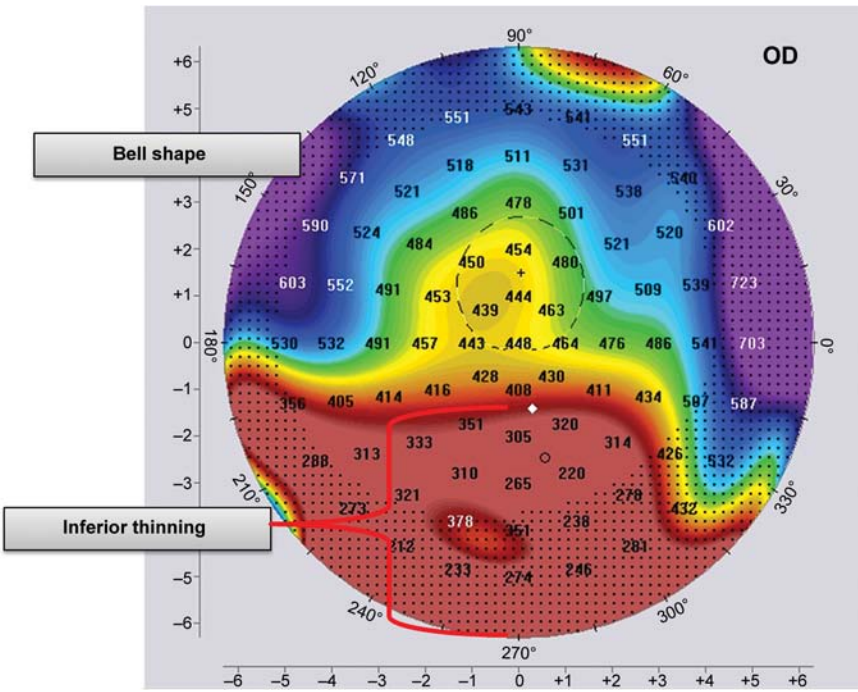

Fig. 1.47 Bell shape of the pachymetry map.

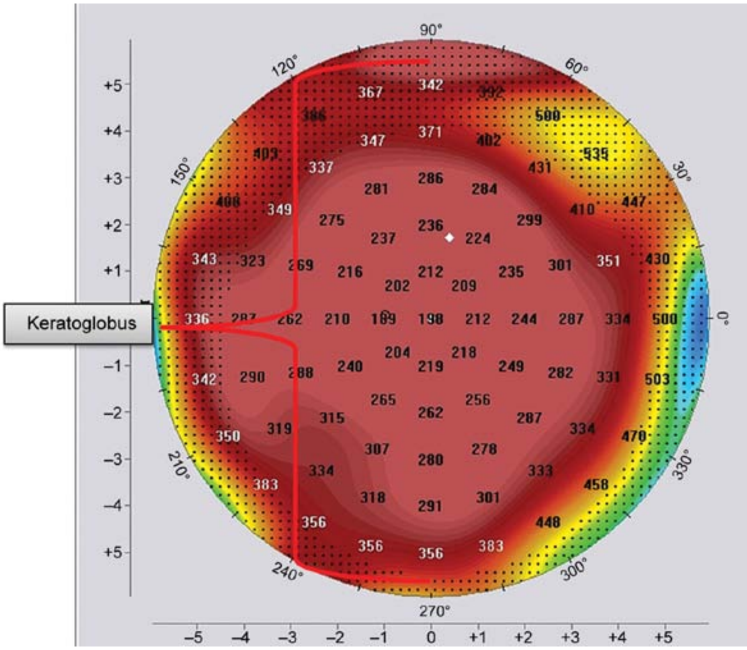

Fig. 148 Globus shape of the pachymetry map.

Thickness Profiles

CORE MESSAGE

- Thickness profiles describe the progression in thickness from the thinnest location to corneal periphery
- These profiles are important in diagnosis of ectatic corneal disorders and corneas with other pathologies such as Guttata and Fuch's

Figure 1.49 shows the two pachymetry profiles: corneal thickness spatial profile (CTSP) and percentage thickness increase (PTI). The former describes the average progression of thickness starting from the thinnest location to corneal periphery in relation to zones concentric with the thinnest location. The latter describes the percentage of progression of the same.

The normal profile is a curved line plotted in red, following (but not necessarily within) the course of the normative black dotted curves, with an average less than 1.2.

Abnormal profiles include:

a. Quick Slope (Fig. 1.50). The red curve leaves its course before the 6 mm zone. It is encountered in forme fruste keratoconus (FFKC) and ectatic disorders.

b. S-shape (Fig. 1.51). The red curve takes the shape of an "S." It is encountered in FFKC and ectatic disorders.
c. Flat shape (Fig. 1.52). The red curve takes a straight course. It is encountered in diseased thickened (oedematous) corneas such as Fuch's dystrophy and cornea Guttata.
d. Inverted (Fig. 1.53). The red curve takes an upward course. It is encountered in PMD.

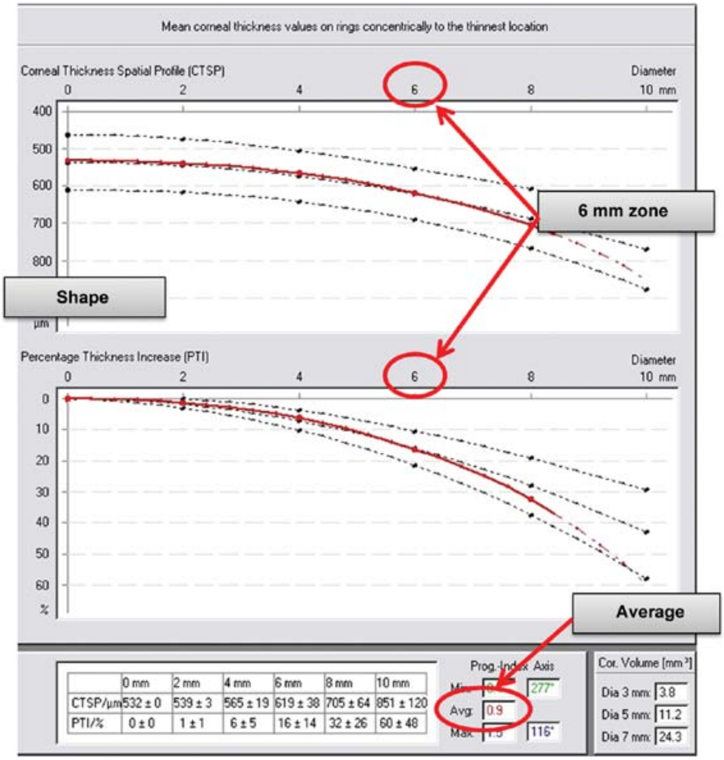

Fig. 1.49 Thickness profiles. Normal profiles (red) follow the course of the standard (dotted black) curves, do not leave the course before the 6 mm central zone and take an average less than 1.2.

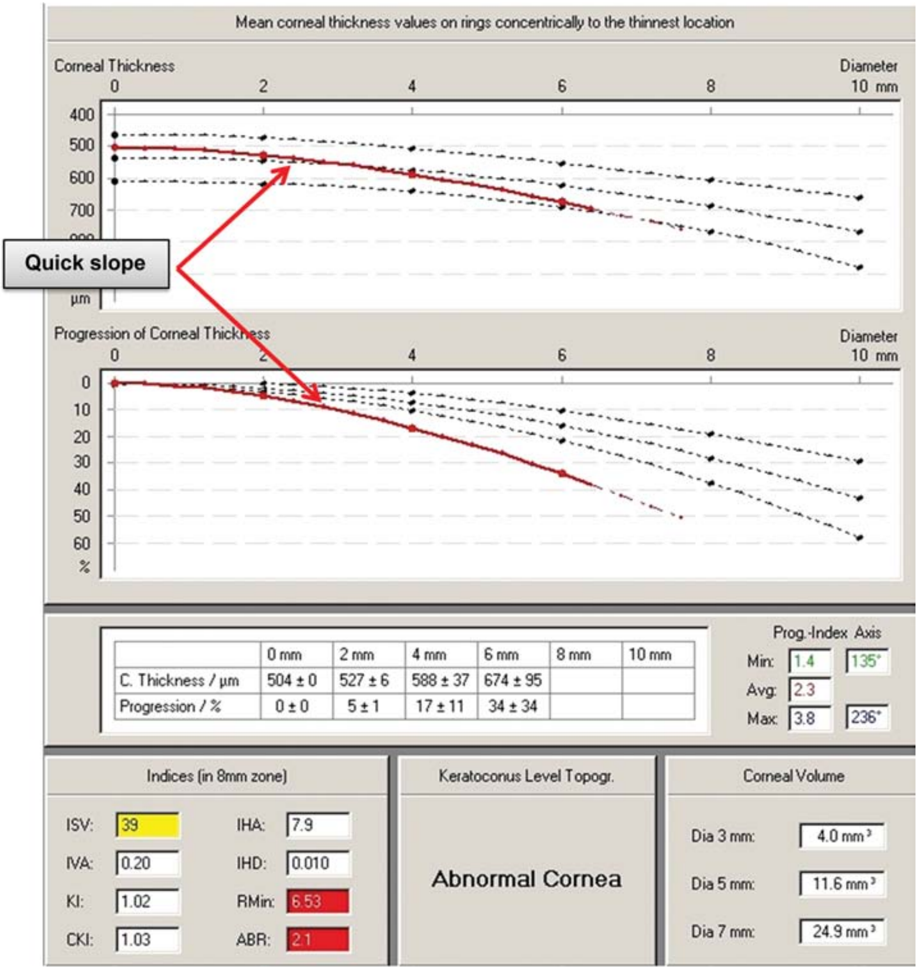

	0 mm	2 mm	4 mm	6 mm	8 mm	10 mm
C. Thickness / µm	504 ± 0	527 ± 6	588 ± 37	674 ± 95		
Progression / %	0 ± 0	5 ± 1	17 ± 11	34 ± 34		

Fig. 1.50 Thickness profiles. Abnormal quick slope.

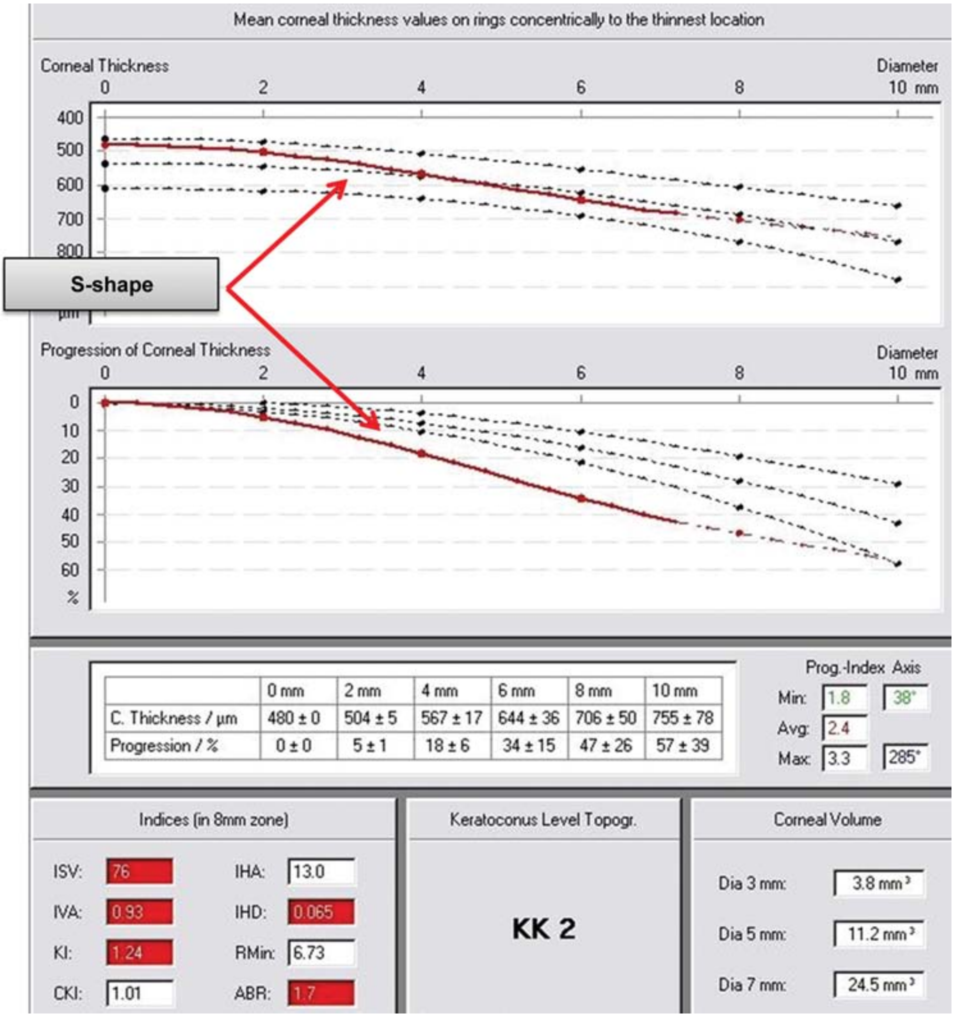

	0 mm	2 mm	4 mm	6 mm	8 mm	10 mm
C. Thickness / µm	480 ± 0	504 ± 5	567 ± 17	644 ± 36	706 ± 50	755 ± 78
Progression / %	0 ± 0	5 ± 1	18 ± 6	34 ± 15	47 ± 26	57 ± 39

Fig. 1.51 Thickness profiles. Abnormal S-shape slope.

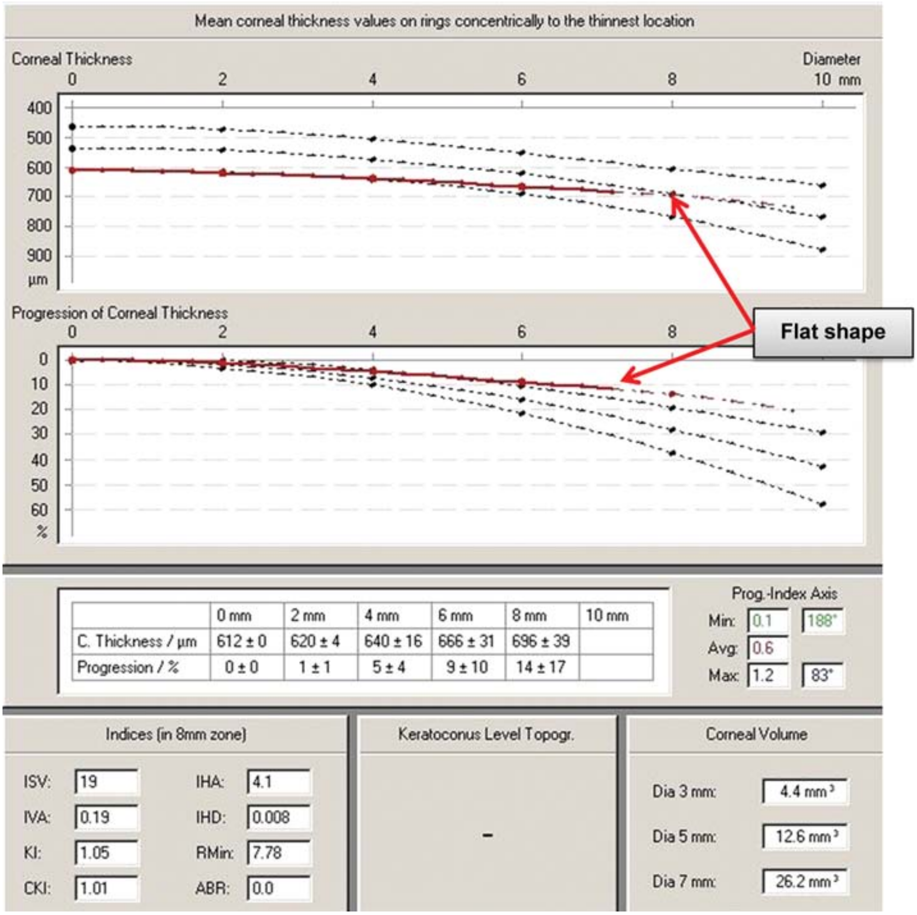

Fig. 1.52 Thickness profiles. Abnormal flat shape.

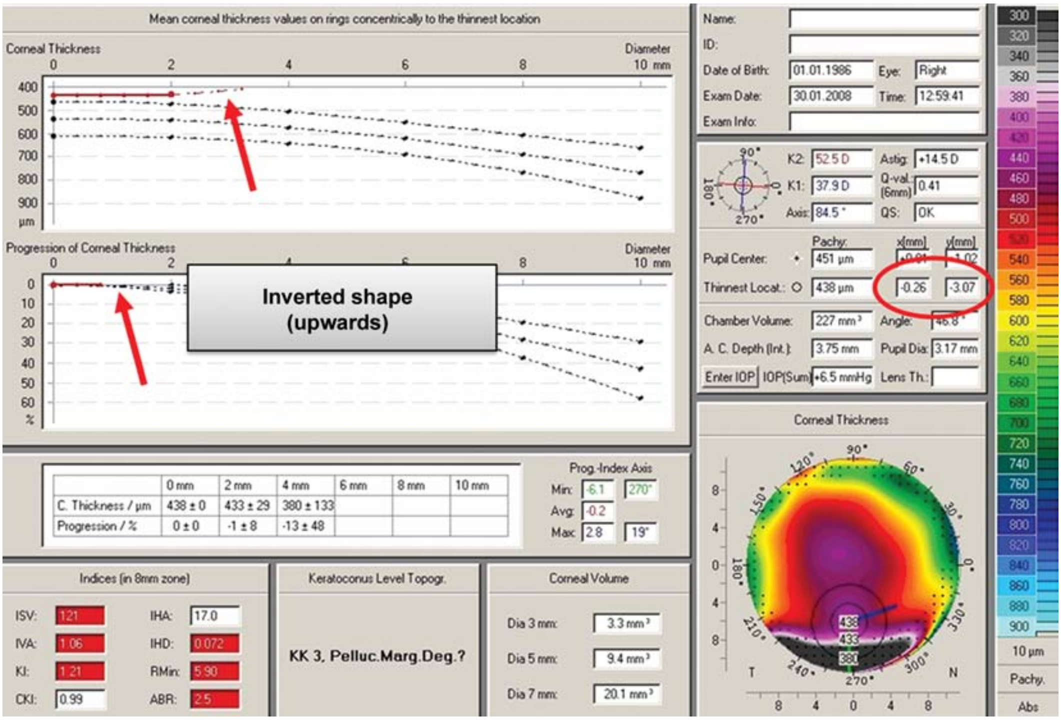

Fig. 1.53 Thickness profiles. Abnormal inverted shape.

TAKE-HOME MESSAGE

- Abnormal shapes of pachymetry map are dome, bell and globus shapes
- Normal S-I difference is <30 µm
- Abnormal shapes of thickness profiles are S-shape, quick slope, inverted and flat shapes
- Normal average is <1.2

Corneal Topometry

CORE MESSAGE

- Corneal topometry describes the slope of the cornea
- Corneal topometry is affected by keratorefractive surgery
- Abnormal corneal topometry is the main cause of spherical aberrations

Corneal topometry measures the slope of the cornea. Corneal surface may take one of four main shapes: spheric, aspheric oblate, aspheric prolate or aspheric hyperprolate.

In the spheric refractive surface (Fig. 1.54), the incident rays are focused in multifocal points since the peripheral incident and refractive angles are larger than the paracentral ones. This is called eccentricity where the surface acts as a multifocal lens.

In the aspheric oblate refractive surface (Fig. 1.55), the eccentricity is more severe since the peripheral part is steeper than the central part, which exaggerates the incident and refractive angles.

In aspheric prolate surface (Fig. 1.56), the peripheral part is flatter than the central part, which compensates for the peripheral angles of incidence and refraction, resulting in one focal point for the incident rays.

In aspheric hyperprolate surface (Fig. 1.57), eccentricity appears again but with a different type known as depth of focus (DOF). This is the principle of a type of presbyopic management known as Q-adjustment.

To give the slope of the cornea a value, Q-value was calculated. Q-value is positive (>0) when the cornea is oblate, negative (<0) when the cornea is prolate or hyperprolate and = 0 when the cornea is spheric. The normal value is [–1 , 0]. In KC, Q-value is highly negative; and after high myopic photoablation, Q-value is positive.

Spherical aberrations resulting from abnormal Q-value:

When the cornea is hyperprolate, the peripheral rays will be focused behind the central rays, leaving an amount of aberration on the retinal surface (ab) measured in microns and named "negative spherical aberration" as shown in Figure 1.58.

When the cornea is spheric or oblate, the peripheral rays will be focused in front of the central rays, leaving an amount of aberration on the retinal surface (ab) measured in microns and named "positive spherical aberration" as shown in Figure 1.59. Figure 1.60 is a simulation of what a patient with spherical aberrations sees.

The least spherical aberrations are found when Q-value = –0.4.

TAKE-HOME MESSAGE

- Corneal topometry is expressed by Q-value
- Normal Q-value = [–1 , 0]
- Q-value is positive (>0) in oblate cornea
- Q-value is negative (<0) in prolate and hyperprolate cornea
- Q-value is plano (=0) in spherical cornea
- Abnormal Q-value results in spherical aberrations

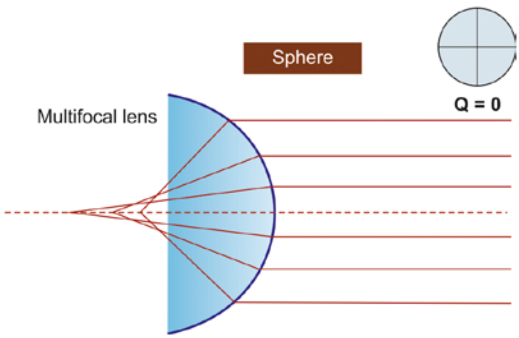

Fig. 1.54 Spherical refractive surface. It acts as a multifocal lens. Q-value = 0.

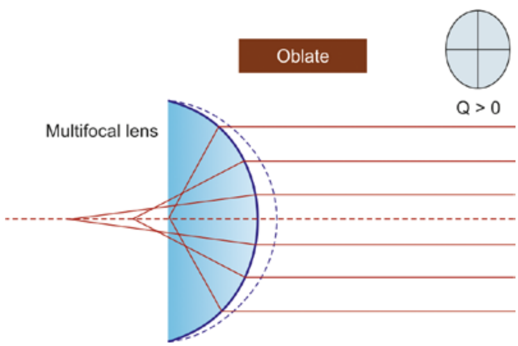

Fig. 1.55 Aspheric oblate refractive surface. It acts as a multifocal lens. Q-value > 0.

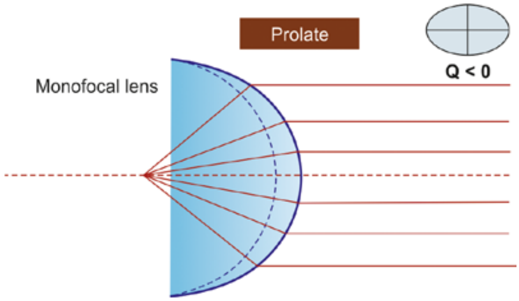

Fig. 1.56 Aspheric prolate refractive surface. It acts as a monofocal lens. Q-value < 0.

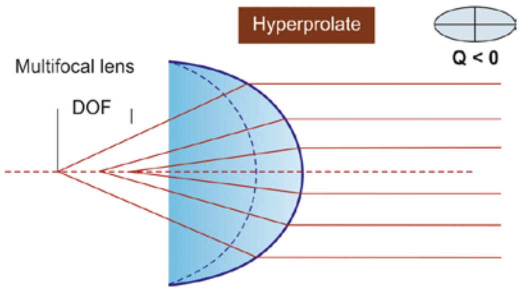

Fig. 1.57 Aspheric hyperprolate refractive surface. It acts as a multifocal lens with depth of focus (DOF). Q-value < 0.

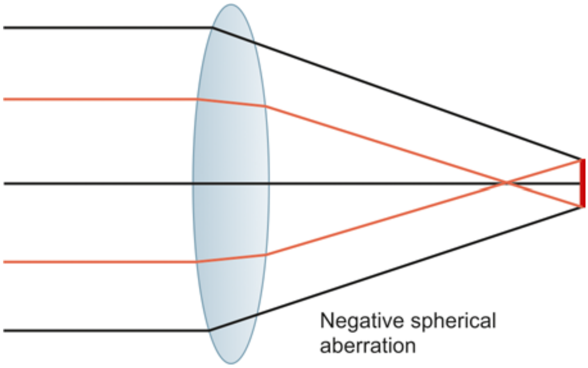

Fig. 1.58 Negative spherical aberration induced by prolate cornea. The red line represents the amount of aberrations measured in microns (see Fig. 1.60).

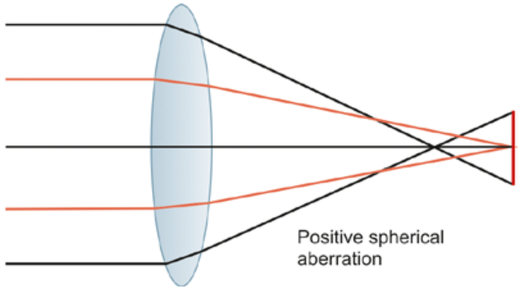

Fig. 1.59 Positive spherical aberration induced by spheric or oblate cornea. The red line represents the amount of aberrations measured in microns (see Fig. 1.60).

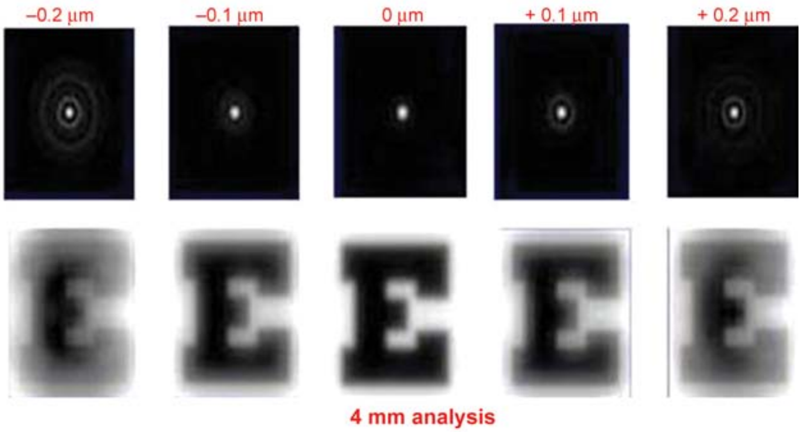

Fig. 1.60 Simulation of spherical aberrations in a 4 mm pupil analysis. Numbers written in red represent the amount of aberrations.

TOPOGRAPHIC AND TOMOGRAPHIC FEATURES IN ECTATIC CORNEAL DISORDERS

Ectatic corneal disorders mainly consist of 4 major entities, KC, Pellucid Marginal Degeneration (PMD), Forme Fruste Keratoconus (FFKC) and Pellucid-Like Keratoconus (PLK).

Morphologic Classification

Morphologically, KC has three patterns of cones (Table 1.3):

a. Nipple cone (see Fig. 1.26).
b. Oval cone (see Fig. 1.27).
c. Globus cone (see Fig. 1.28).

The best map to evaluate the shape of the cone is the tangential map since it is the best to highlight corneal irregularities. In mild cases, cone morphology may be indeterminate.

Tomographic Classifications

Tomographically, abnormal cornea can be classified according to elevation maps, pachymetry map or curvature map. Table 1.4 summarizes tomographic classification.

When more than one of the following criteria is found, any of the above mentioned patterns is considered as frank KC, FFKC, early stage KC, or at least a case of suspicion according to the severity and amount of the following signs.

On the Sagittal Map

a. Steep K > 48 D.
b. K-max > Steep K by more than 1 D.
c. SRAX > 22°.

TABLE 1.3 Morphological Patterns of Keratoconus and Ectatic Diseases

Morphology	*Cone Size*	*Cone Shape*	*Displacement of Cone Apex*
Nipple	5 mm	steep	inferonasally
Oval	5–6 mm	ellipsoid	inferotemporally
Globus	>6 mm	generalized	generalized

TABLE 1.4 Tomographic Patterns of Keratoconus and Ectatic Diseases

Curvature-Based (see Figs 1.10-1.24)	
Pattern	*Specifications*
R	Round hot spot
O	Oval hot spot
SS	Superior steep
IS	Inferior steep
Irr	Irregular shape
SB	Symmetric bowtie
SB/SRAX	Symmetric bowtie with skewed radial axis
AB/IS	Asymmetric bowtie inferior steep
AB/SS	Asymmetric bowtie superior steep
AB/SRAX	Asymmetric bowtie with skewed radial axis
B	Butterfly
Claw	Claw
Junctional (vertical D)	Junctional (vertical D)
SF	Smiling face
Vortex	Vortex (Nazi logo)

Contd...

Contd...

Elevation-based (see Fig. 1.38)	
Pattern	Specification
Central cone	Apex within 3 mm
Paracentral cone	Apex within 3-5 mm
Peripheral cone	Apex out of 5 mm
Pachymetry-based (see Figs 1.46-1.48)	
Pattern	Specifications
Dome-like	Conic shape (protrusion)
Bell-Shaped	Shape of a bell (inferior thinning)
Globus	Generalized thinning

d. S-I on the 5 mm circle > 2.5 D.
e. I-S > 1.5 D.
f. TA > 6 D.
g. ATR astigmatism.

On the Elevation Maps

a. Isolated island or tongue-like extension (BFS mode) on either surface.
b. Values >12 µm within the central 5 mm on the anterior elevation map (BFTE mode).
c. Values >15 µm within the central 5mm on the posterior elevation map (BFTE mode).

On the Pachymetry Map

a. Dome-shape, Bell-shape or Globus.
b. Superior – inferior @ 5 mm circle >30 µm.
c. Thinnest location <470 µm.
d. Thickness @ pachy apex – thickness @ thinnest location >10 µm.
e. *Y* coordinate value of the thinnest location >–500 µm.
f. Difference in thickness between both eyes @ thinnest locations >30 µm.

On Thickness Profiles

a. Average >1.1.
b. Quick slope.
c. S-shape.
d. Flat shape.
e. Inverted.

Forme Fruste Keratoconus

Forme Fruste Keratoconus (FFKC) is a subclinical disease and is not a variant of KC. Although clinicians use many other terms such as mild KC, early KC and subclinical KC, their exact meanings

and applications are less certain. These terms are not universally accepted. The diagnosis of KC is a clinical one that is aided by tomography, while the diagnosis of FFKC is only tomographic.

Recently, there are two opinions regarding the definition of this disease:

1. FFKC is a completely normal cornea with neither clinical nor tomographic risk factors, but this cornea is able to develop KC when treated by photoablation. The fellow eye may be keratoconic or there may be a family history of KC.
2. FFKC is an abnormal cornea. Corneal tomography or corneal hysteresis (see chapter 4) or both are abnormal; i.e. there are risk factors but the case is still not a clinically obvious KC.

Pellucid Marginal Degeneration (PMD) and Pellucid-Like Keratoconus (PLK)

Pellucid marginal degeneration (PMD) is an ectatic corneal disorder characterized by peripheral inferior corneal thinning observed with slitlamp biomicroscopy and on Scheimpflug image. Pellucid-like keratoconus (PLK) is a different entity; it is KC that has some features of PMD as will be discussed bellow. Differentiation between these two entities is important for the plan of management.

Clinical Findings

In PMD, results of slitlamp biomicroscopy are characterized by:

1. A peripheral band of thinning of the inferior cornea from the 4-o'clock position to the 8-o'clock position. This thinning is accompanied by 1–2 mm of normal cornea between the limbus and the area of thinning.
2. Corneal ectasia is most marked just central to the band of thinning. The central cornea is usually of normal thickness and the epithelium overlying the area of thinning is intact.
3. The light slit becomes very narrow abruptly in the inferior part of the cornea which is the hallmark of the disease (Fig. 1.61, white arrow).
4. Flourescein pattern with the RGP lens. There is an inferior touch between the cornea and the contact lens (CL) as shown in Figure 1.62. In the same figure, the Placido rings are distributed in an oval shape which is vertically oriented due to ATR astigmatism. Notice that the rings become very thin and close to each others in the inferior cornea while they are relatively broader and not crowded in the superior part of the cornea.

Tomographic Findings

Identifying features of PMD on corneal tomography is very important; there is some similarity between PMD and PLK on corneal tomography especially in early stages of PMD. This similarity leads doctors to misinterpret PLK as PMD. Careful studying of the tomography reveals many differences between these two entities. Features are mainly seen on the curvature, elevation and pachymetry maps and on thickness profiles.

- Curvature map. The anterior sagittal curvature map takes a claw pattern (see Fig. 1.21). This feature is seen in both PMD and PLK.
- Elevation maps: There are two important things related to each others that can be identified on the elevation maps, mainly the anterior elevation map, the location of the cone and the "kissing birds" sign. Neither the kissing birds sign nor the peripheral cone is a hallmark of

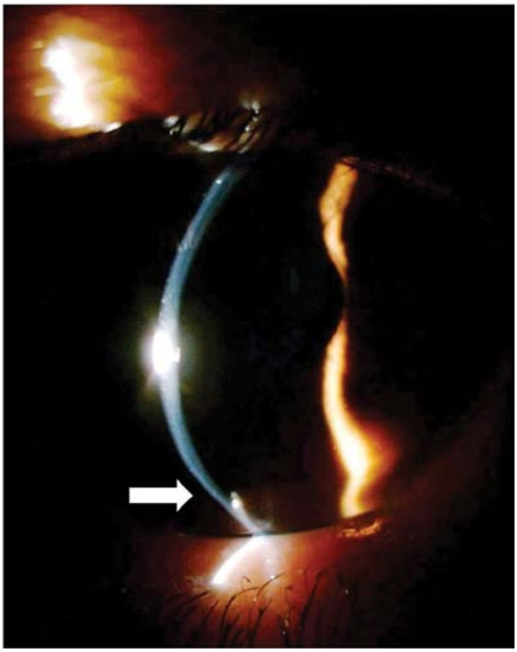

Fig. 1.61 PMD. Inferior thinning of the cornea (white arrow).

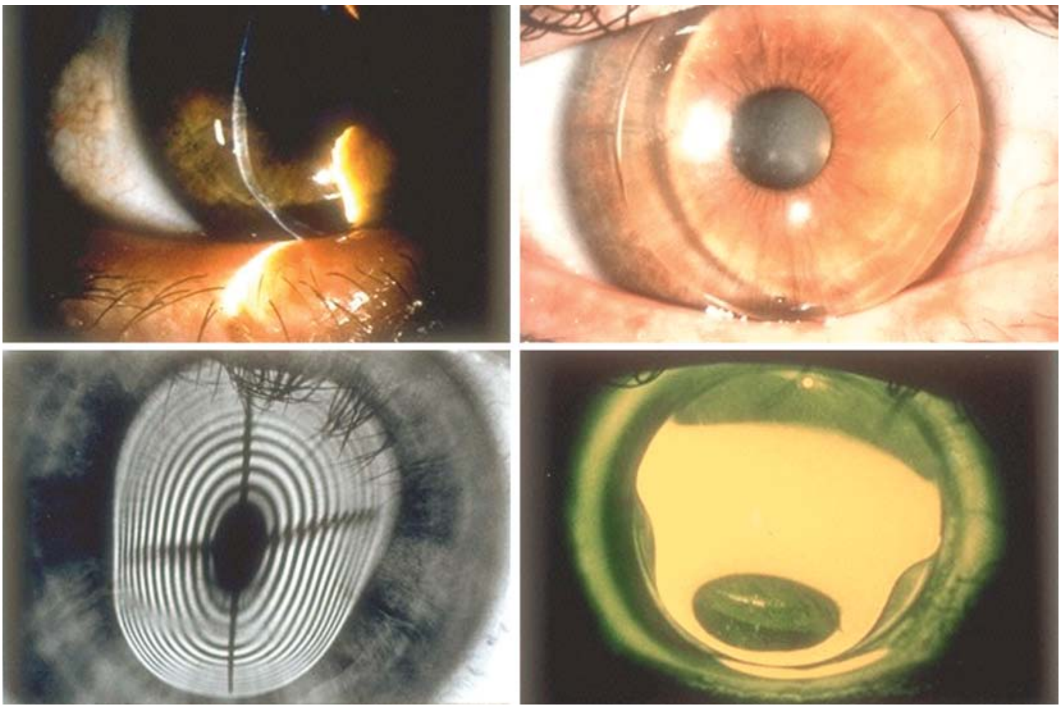

Fig. 1.62 PMD. Upper left: inferior corneal thinning; lower left: Placido ring pattern (notice the vertical distribution due to ATR astigmatism); upper right: RGP contact lens; lower right: flourescein pattern (notice the inferior touch with the cone which is just above the inferior thinning).

PMD or PLK. Figure 1.63 is a PMD case without the kissing birds sign; Figure 1.64 is a PLK case with this sign.

- Corneal thickness map: In PMD, the corneal thickness map reveals a thinning of the inferior cornea. This thinning is characterized by a special sign that can be called "bell" shape (see Fig. 1.47). This sign is a hallmark of PMD; it is absent in PLK.
- The Pachymetry Profiles: In KC, PLK and in PMD, this curve deviates from the normal range rapidly and usually before the 6 mm zone (see Fig. 1.50). S-shape is one of the indicators of ectatic disorders or at least abnormal cornea (see Fig. 1.51). In advanced cases of PMD, the curve usually takes an inverted passage (see Fig. 1.53).

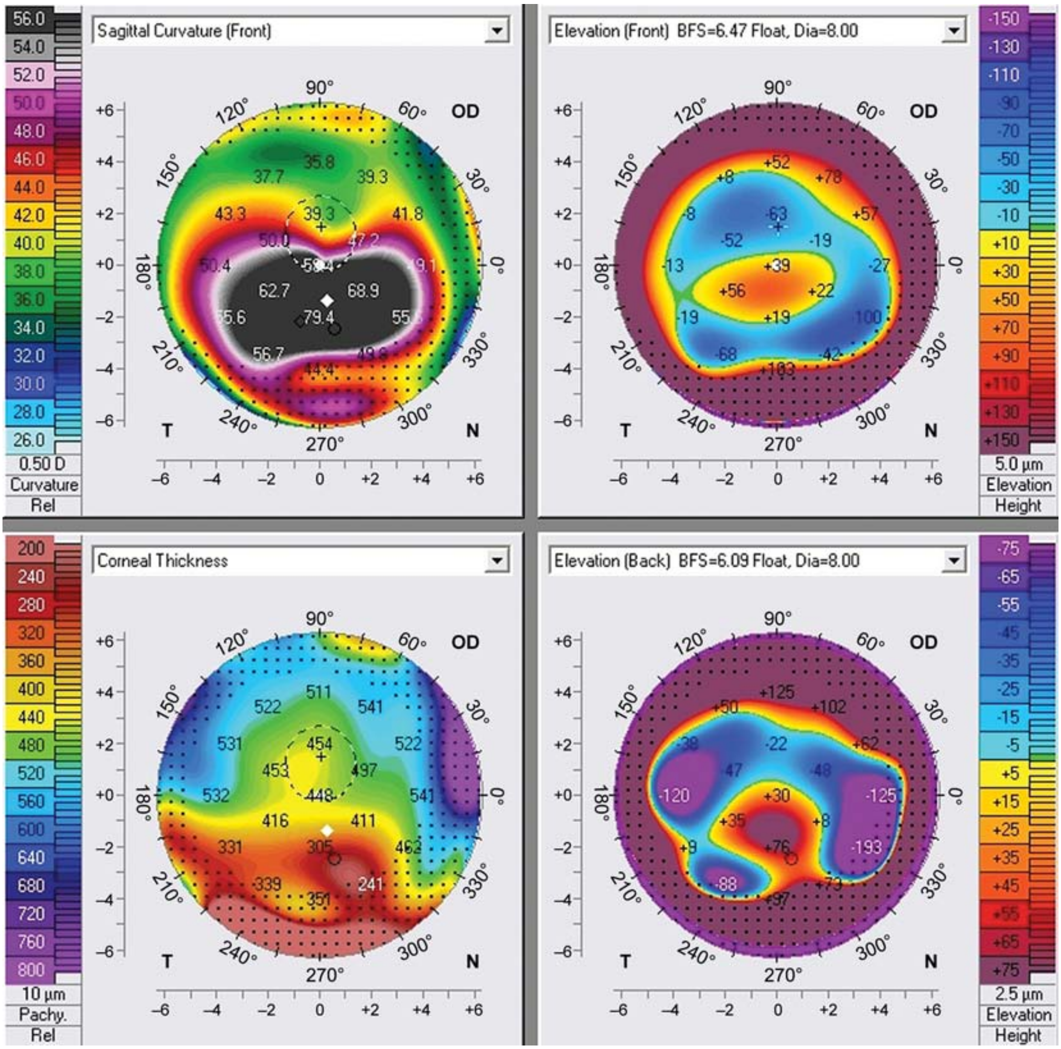

Fig. 1.63 Corneal tomography of PMD. Notice the bell shape of the pachymetry map and the absence of the kissing birds sign on the elevation maps due to central cone. The claw pattern is not clear on the curvature map because of the severity of the case, yet still can be identified by changing the color scale.

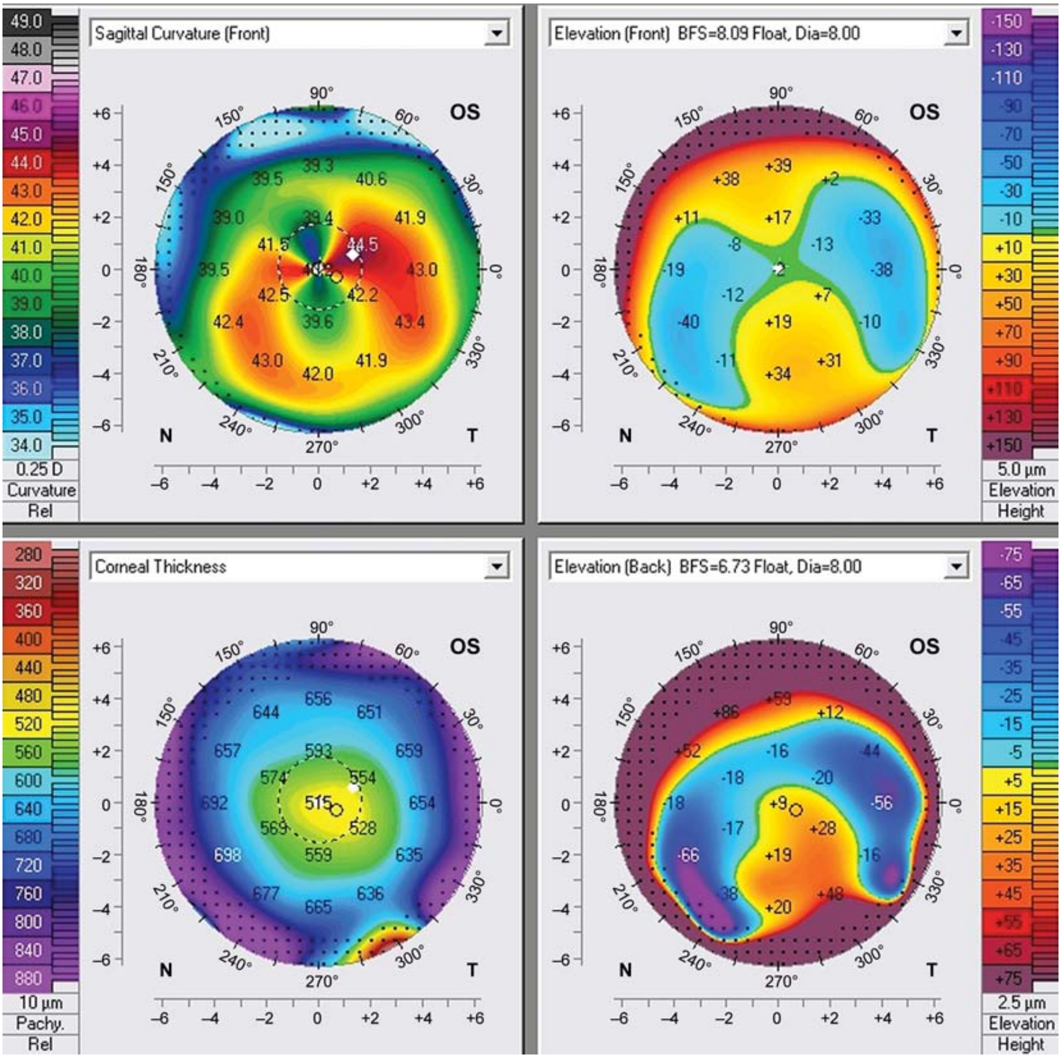

Fig. 1.64 Corneal tomography of PLK. Notice the claw pattern on the curvature map and the kissing birds sign on the anterior elevation map due to peripheral cone. The bell shape is absent in the pachymetry map.

Table 1.5 summarizes the difference between PLK and PMD.

For more details about corneal topography and tomography, please refer to the second edition of my book (Corneal Topography in Clinical Practice) by Jaypee Highlight 2012.

For more details about abnormal corneas, KC and ectatic corneal disorders, please refer to my book (Keratoconus: When, Why and Why Not) by Jaypee Highlight 2012.

TABLE 1.5 Comparison between PLK and PMD

		PLK	*PMD*
Nature		central or para-central ectasia	peripheral ectasia
Age of presentation		early teens	usually 20–40
Slitlamp and Scheimpflug image		central or paracentral thinning	inferior peripheral thinning
Curvature map		claw	claw
Elevation maps	Cone	central or paracentral cone	central, paracentral or inferior peripheral cone
	Kissing birds	present occasionally	present in early and moderate cases
Thickness map	"Bell" sign	absent	present in moderate and advanced cases
	Thinnest location	may be displaced	usually largely displaced
Thickness profiles		deviated	deviated and usually inverted in advanced cases

BIBLIOGRAPHY

1. Ambrosio R Jr, Alonso RS, Luz A, et al. Corneal-thickness spatial profile and corneal-volume distribution: tomographic indices to detect keratoconus. J Cataract Refract Surg. 2006;32:1851-9.
2. Ambrósio R Jr and Belin MW. Imaging of the Cornea: Topography vs. Tomography. J Refract Surg. 2010;26(11):847-9.
3. Azar DT, Gatinel D and Hoang-Xuan T. Refractive surgery. Philadelphia: Mosby Elsevier; 2007.
4. Buhren J, Kook D, Yoon G, et al. Invest. Ophthalmol. Vis. Sci. 2010;51(7):3424-32.
5. Gills JP et al. Corneal Topography: The State of the Art. Thorofare, NJ: Slack Incorporated. 1995;1-328.
6. Goins KM and Wagoner MD. Focal points: Imaging the anterior segment. American academy of ophthalmology. 2009;27(11):1-17.
7. Holladay JT. Corneal topography using the Holladay Diagnostic Summary. J Cataract Refract Surg. 1997;23(2):209-21.
8. Holladay JT. Detecting Forme Fruste Keratoconus with the Pentacam. Supplement to Cataract & Refractive Surgery Today. 2008;11-2.
9. Karimian F et al. Tomographic evaluation of relatives of patients with keratoconus. Cornea. 2008;27:874-8.
10. Kaufman HE, Barron BA, McDonald M, et al. Companion Handbook to the Cornea. Butterworth Heinemann. 2000;947-59.
11. Khachikian SS, Belin MW and Ciolino JB. Intrasubject corneal thickness asymmetry. J Refract Surg. 2008;24(6):606-9.
12. Klyce SD. Chasing the suspect: keratoconus. Br J Ophthalmol. 2009;93:845-7.
13. Lee BW, Jurkunas UV, Harissi-Dagher M, et al. Ectatic disorders associated with a claw shaped pattern on corneal topography. J Ophthalmol. 2007;144:154-6.
14. Li X, Yang H and Rabinowitz YS. Keratoconus: classification scheme based on videokeratography and clinical signs. J Cataract Refract Surg. 2009;35:1597-603.
15. Luz A, Ursulio M, Castaneda D, et al. Corneal thickness progression from the thinnest point to the limbus: study based on a normal and a keratoconus population to create reference values (in Portuguese). Arq Bras Oftalmol. 2006;69:579-83.

16. Michel WB, Khachikian SS and Ambrosio Jr R. Elevation Based Corneal Tomography. Jaypee-Highlights Medical Publishers, Inc. 2012.
17. Nilforoushan MR, Speaker M, Marmor M, et al. Comparative evaluation of refractive surgery candidates with Placido topography, Orbscan II, Pentacam, and wavefront analysis. J Cataract Refract Surg. 2008;34:623-31.
18. Rabbetts RB. Clinical Visual Optics. Butterworth Heinemann. 998;378-420.
19. Rabinowitz YS. Keratoconus. Surv Ophthalmol. 1998;42:297-319.
20. Rabinowitz YS. Diagnosing Keratoconus and Patients at Risk. J Cataract Refract Surg Today. 2007;85-7.
21. Saad A and Gatinel D. Topographic and Tomographic Properties of Forme Fruste Keratoconus Corneas. Invest. Ophthalmol. Vis. Sci. 2010;51(11):5546-55.
22. Schlegel Z, Hoang-Xuan T and Gatinel D. Comparison of and correlation between anterior and posterior corneal elevation maps in normal eyes and keratoconus-suspect eyes. J Cataract Refract Surg. 2008;34:789-95.
23. Schuman JS. Ophthalmic imaging and diagnostics. Ophthalmology Clinics of North America. 1998;11:1-490.
24. Shirayama-Suzuki M, Amano S, Honda N, et al. Longitudinal analysis of corneal topography in suspected keratoconus. Br J Ophthalmol. 2009;93:815-9.
25. Sinjab MM. Step by Step Reading Pentacam Topography (Basics and Case Study Series). Jaypee - Highlights Medical Publishers, New Delhi; 2010.
26. Sinjab MM. A guide to interpreting corneal tomography. J Cataract Refract Surg Today. 2012;20-4.
27. Sinjab MM. Corneal Topography in Clinical Practice (Pentacam System): Basics and Clinical Interpretation. Jaypee-Highlights Medical Publishers, Inc. 2012.
28. Sinjab MM. Keratoconus: When, Why and Why Not: A Step by Step Systematic Approach. Jaypee-Highlights Medical Publishers Inc. 2012.
29. Sinjab MM. Management Modalities for Keratoconus. J Cataract Refract Surg Today Europe. 2012;40-7.
30. Tomidokoro A, Oshika T, Amano S, et al. Changes in anterior and posterior corneal curvatures in keratoconus. Ophthalmology. 2000;107:1328-32.

CHAPTER 2

Wavefront Science

PRINCIPLES OF WAVEFRONT AND WAVEFRONT ANALYSIS

CORE MESSAGE

- A wavefront is the locus of points having the same phase
- A wavefront reflects the quality of an optical system
- Zernike analysis describes orders and shapes of aberrations

The incident light rays coming from infinity are parallel. Every light ray consists of a sinusoidal oscillation (Fig. 2.1). Locations of equal phase within the total array of sinusoidal oscillations form planar wavefronts, which are parallel and perpendicular to the direction of the incident light rays as shown in the same figure. When the parallel light rays pass through a perfect refractive surface, they (and the wavefronts) meet precisely at a point known as the focal point F. But the ideal case is virtually never encountered in practice because real wavefronts show deviations from a perfect plane or spherical wave after passing through the refractive surface leading to the aberrations (Fig. 2.2). The shape of a wavefront passing through a theoretically perfect eye with no aberrations is a flat plane known, for reference, as piston (see below).

The measure of difference between the actual wavefront shape and the ideal flat shape represents the amount of aberration in the wavefront (as shown in Fig. 2.2). The smaller the deviation (aberration), the higher the quality of the refractive system, be it a telescope, a microscope, the cornea or the entirety of refractive media comprised by the human eye. The Dutch physician and Nobel Prize winner Fritz Zernike (1888–1966) succeeded in mathematically

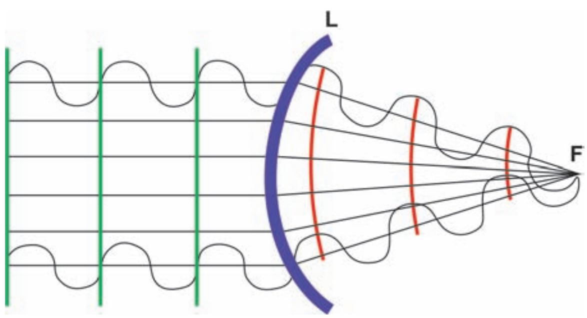

Fig. 2.1 Wavefront principle. In perfect refractive surface, the produced wavefronts are symmetric, parallel and take the shape of the refractive surface.

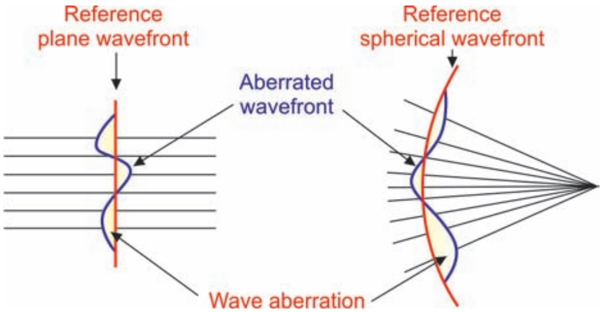

Fig. 2.2 Aberrated wavefront. Imperfect wavefronts are deviated from ideal reference wavefront.

representing the deviations of a real wavefront from an ideal one expressed as symbols depending on the analysis of the scientist Fourier.

Zernike analysis describes wavefront analysis of ocular refractive surfaces in circle polynomials in the radial (n) and angular (m) directions by using an equation, depending on which, Zernike polynomials are calculated, given indexes and expressed as low order aberrations (LOAs) and high order aberrations (HOAs) as shown. Figure 2.3 is Zernike pyramid representing order and shapes of HOAs and LOAs. Table 2.1 shows Zernike description of aberrations.

However, whatever the order of the aberrations is, above 70% of the refractive power of the eye is owed to the cornea. Even if the crystalline lens is responsible for some ocular aberrations, corneal distortion has a higher impact than any other component.

TABLE 2.1 Zernike Description of Aberrations

Coefficient	*Index Z(n, m)*	*Order*	*Description*
0	Z(0, 0)	Zero	Piston
1	Z(1, -1)	First	Vertical Tilt
2	Z(1, 1)	First	Horizontal Tilt
3	Z(2, -2)	Second	Vertical Astigmatism
4	Z(2, 0)	Second	Defocus
5	Z(2, 2)	Second	Horizontal Astigmatism
6	Z(3, -3)	Third	Vertical Trefoil
7	Z(3, -1)	Third	Vertical Coma
8	Z(3, 1)	Third	Horizontal Coma
9	Z(3, 3)	Third	Horizontal Trefoil
10	Z(4, -4)	Fourth	Vertical Tetrafoil
11	Z(4, -2)	Fourth	Secondary Vertical Astigmatism
12	Z(4, 0)	Fourth	Spherical Aberration
13	Z(4, 2)	Fourth	Secondary Horizontal Astigmatism
14	Z(4, 4)	Fourth	Horizontal Tetrafoil
15	Z(5, -5)	Fifth	Vertical Pentafoil
16	Z(5, -3)	Fifth	Secondary Vertical Trefoil

Contd...

Contd...

Coefficient	*Index Z(n, m)*	*Order*	*Description*
17	Z(5, -1)	Fifth	Secondary Vertical Coma
18	Z(5, 1)	Fifth	Secondary Horizontal Coma
19	Z(5, 3)	Fifth	Secondary Horizontal Trefoil
20	Z(5, 5)	Fifth	Horizontal Pentafoil
21	Z(6, -6)	Sixth	Vertical Hexafoil
22	Z(6, -4)	Sixth	Secondary Vertical Tetrafoil
23	Z(6, -2)	Sixth	Tertiary Vertical Astigmatism
24	Z(6, 0)	Sixth	Secondary Spherical Aberration
25	Z(6, 2)	Sixth	Tertiary Horizontal Astigmatism
26	Z(6, 4)	Sixth	Secondary Horizontal Tetrafoil
27	Z(6, 6)	Sixth	Horizontal Hexafoil

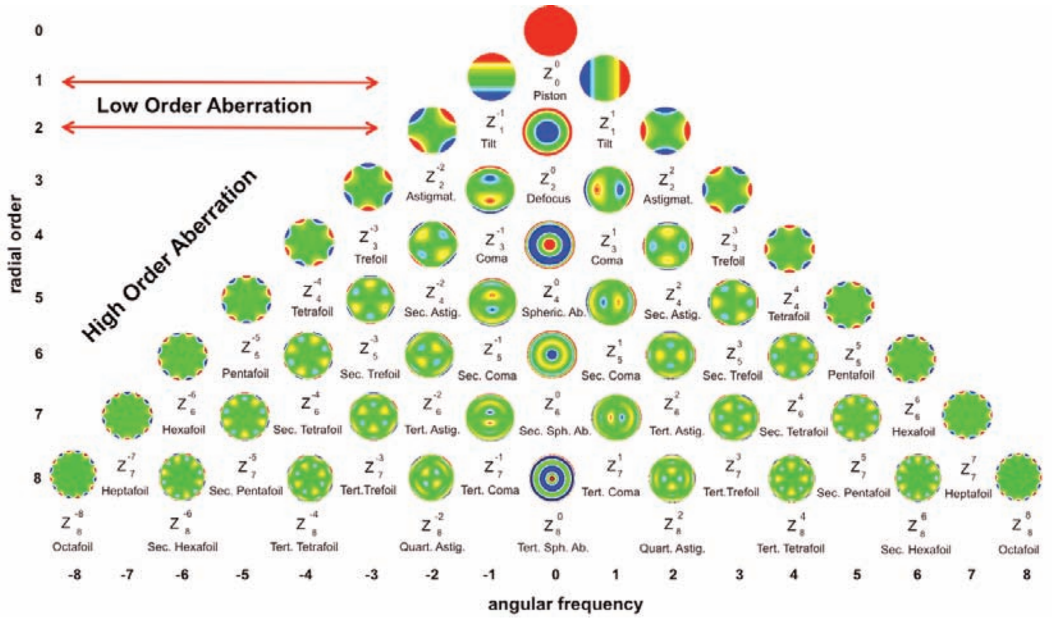

Fig. 2.3 Zernike pyramid. Orders and shapes of LOAs and HOAs.

TYPES OF ABERRATIONS

Low Order Aberrations (LOAs)

CORE MESSAGE

- Low order aberrations (LOAs) are aberrations associated with the spherocylindrical refractive errors
- LOAs constitute 85% of aberrations
- There are three types of LOAs, tilt, defocus and astigmatic aberrations

Low order aberrations (LOAs) are aberrations associated with the spherocylindrical refractive errors and can be corrected with glasses. In general population, LOAs constitute approximately 85% of all aberrations. There are 3 types of LOAs:

a. **Tilt or prism (Fig. 2.4):** It is a deviation in the direction that a beam of light propagates. It is caused by decentred optics. In Zernike polynomials, vertical tilt takes the symbol (1,–1) and horizontal tilt takes the symbol (1,1) as shown in Figure 2.3 and Table 2.1.
b. **Defocus (Fig. 2.5):** In optics, defocus is the aberration in which an image is simply out of focus. This aberration is familiar to anyone who has used a camera, video camera, microscope, telescope, or binoculars. Optically, defocus refers to a translation along the optical axis away from the plane or surface of best focus (Fig. 2.6). In general, defocus reduces the sharpness and contrast of the image. What should be sharp, high-contrast edges in a scene become gradual transitions. Fine detail in the scene is blurred or even becomes invisible. Nearly all image-forming optical devices incorporate some form of focus adjustment to minimize defocus and maximize image quality.
   In human eye, spherical refractive errors are associated with defocus; in myopia the focal point lies in front of the retina, whereas in hyperopia it lies behind it causing blurring of vision. Defocus increases with larger pupil size as shown in Figure 2.7.
   In Zernike polynomials, defocus is given the symbol (2,0) as shown in Figure 2.3 and Table 2.1.
c. **Astigmatic aberration (Fig. 2.8):** An optical system with regular astigmatism is one where rays that propagate in two perpendicular planes have different foci. If an optical system with regular astigmatism is used to form an image of a cross, the vertical and horizontal lines will be in sharp focus at two different distances (Fig. 2.9). According to which focal point is nearer to or on the retina, the image will be blurred horizontally if it is vertically focused (the horizontal is out of focus), blurred vertically if it is horizontally focused (the vertical is out of focus) or compromised (both are out of focus) as shown in Figure 2.10.
   In human eye, low order astigmatic aberration is associated with regular astigmatism.
   In Zernike polynomials, vertical astigmatism is given the symbol (2,–2) and the horizontal astigmatism is given the symbol (2,2) as shown in Figure 2.3 and Table 2.1.

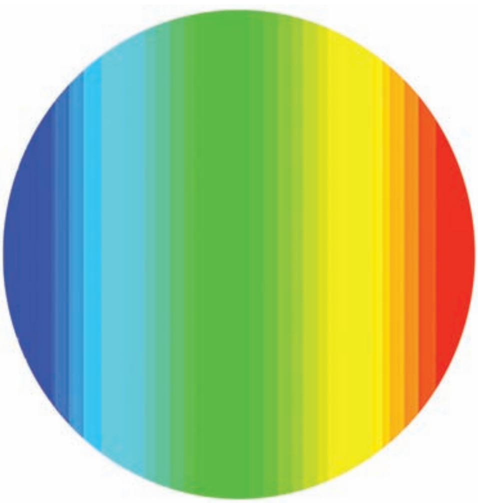

Fig. 2.4 Tilt. It is a LOA due to decentered optics causing a prismatic effect.

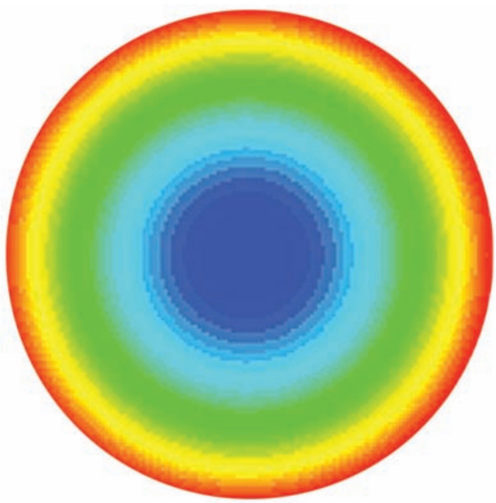

Fig. 2.5 Defocus. It is a LOA associated with sphere refractive errors (myopia and hyperopia).

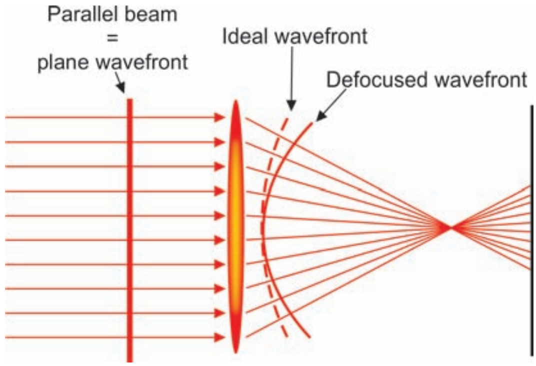

Fig. 2.6 Wavefront principle in defocus. The produced wavefront is defocused in relation to ideal reference wavefront.

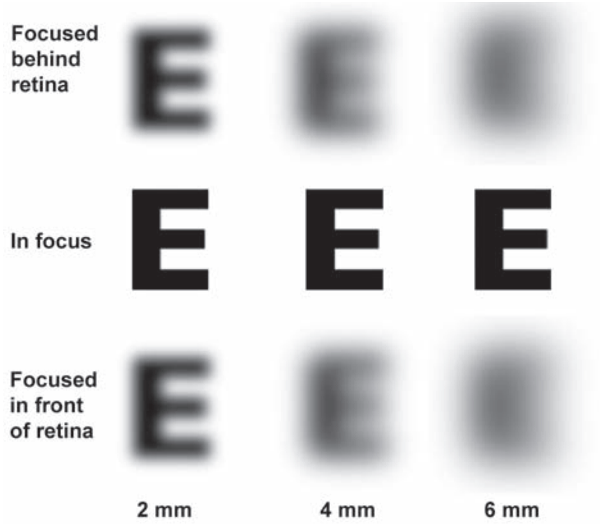

Fig. 2.7 Images in defocus in relation with pupil size. In hyperopia, images are focused behind the retina and vice versa in myopia. The larger the pupil the more prominent the defocus.

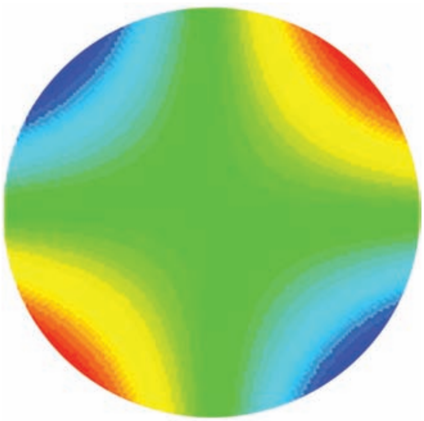

Fig. 2.8 Astigmatic aberration. It is a LOA associated with astigmatism.

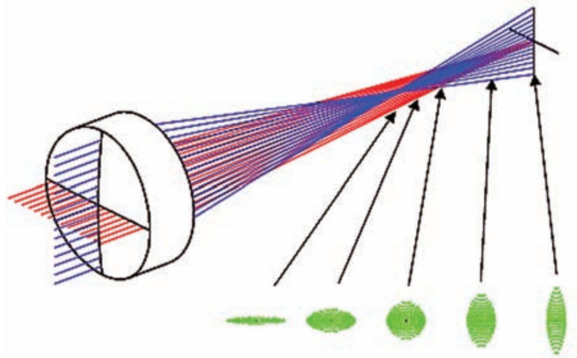

Fig. 2.9 Principle of Sturm Cone due to astigmatism. In this example, the vertical meridian (in blue) is steeper than the horizontal one (in red). Green shapes represent the shape of the image according to the location of the perception plane.

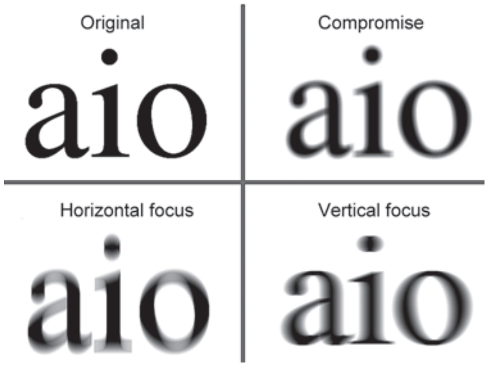

Fig. 2.10 Images in astigmatic aberration. Upper left: original focused image; upper right: defocused image; lower left: horizontally focused that is vertically compromised; lower right: vertically focused that is horizontally compromised.

TAKE-HOME MESSAGE

- LOAs can be corrected with glasses
- There are three types of LOAs, tilt, defocus and astigmatic aberrations: tilt produced by decentered optics, defocus produced by spherical component of the refractive error and astigmatic aberration produced by astigmatic component of the refractive error

High Order Aberrations (HOAs)

CORE MESSAGE

- High order aberrations (HOAs) are aberrations that may or may not be associated with refractive errors
- HOAs result from media irregularities or opacities
- Although there is a wide range and types of HOAs, the main types are coma, trefoil and spherical aberrations
- HOAs impact vision more severe than LOAs
- Coma is a central aberration and affects central vision, whereas trefoils and spherical are peripheral aberrations

High order aberrations (HOAs) start at the third level in Zernike polynomials (see Fig. 2.3 and Table 2.1). They may or may not be associated with refractive errors but cannot be corrected with

classic optics; they need special designs of contact lenses (CLs) or glasses, or can be treated by photorefractive surgery or special designs of phakic IOLs.

HOAs result from any disturbance, scar, haziness, opacity or irregularity in one or more of the refractive components of the ocular optical system including tear film, cornea, aqueous humor, crystalline lens and vitreous humor.

The impact of HOAs on vision quality depends on various factors, including the underlying cause of the aberration. People with larger pupil sizes generally may have more visual symptoms related to HOAs, particularly in low lighting conditions. But even people with small or moderate pupils can have significant visual symptoms when HOAs are caused by conditions such as corneal scars or cataracts. Also, specific types and orientation of HOAs have been found in some studies to affect vision quality of eyes with smaller pupils. Large amounts of certain HOAs can have a severe, even disabling, impact on vision quality.

Some of the HOAs have names such as coma, trefoil and spherical aberration, but many more of them are identified only by mathematical expressions (Zernike polynomials) to have an order. Order refers to the complexity of the shape of the wavefront emerging through the pupil; the more complex the shape, the higher the order of aberration.

The most common HOAs are:

a. **Coma (Fig. 2.11):** Coma is defined as a variation of magnification (refractive power) over the entrance pupil (Fig. 2.12). Coma causes the eye to see a point of light sort like a comet (has a tail) as shown in Figure 2.13. Figure 2.14 represents the wavefront of a coma. The coma results from central and paracentral asymmetry in ocular optical components, which affects central vision. Figure 2.15 is an asymmetric corneal surface due to decentered ablation zone causing asymmetric refractive power along the entrance pupil which induces coma.

   In Zernike polynomials (Fig. 2.3 and Table 2.1), coma takes odd order (3, 5, 7…etc.); e.g. 1st coma is given the symbol (3,–1) for the vertical and (3,1) for the horizontal; 2nd coma is given the symbol (5,–1) for the vertical and (5,1) for the horizontal and so on.

b. **Spherical aberrations (Fig. 2.16):** As mentioned in chapter 1, spherical aberrations result from abnormal Q value. Figure 2.17 is an illustration of an optical system with a positive spherical aberration; the shape of the image differs according to the location of the perception plane (retina in the eye). Figure 2.18 is a simulation of the scene of a light point seen by an eye with spherical aberrations. Spherical aberrations affect peripheral vision and result in halos around oncoming lights.

   In Zernike polynomials (Fig. 2.3 and Table 2.1), spherical aberrations take an even order (4, 6, 8…etc.); e.g. 1st spherical aberration is given the symbol (4,0), 2nd spherical aberration is given the symbol (6,0) and so on.

c. **Trefoil (Fig. 2.19):** The name came from the Trifolium plant (Clover) that has compound trifoliate leaflets as shown in Figure 2.20. Trefoil aberration results from regular alternating variation in magnification along meridians in corneal periphery.

   The eye with a Trefoil aberration sees a point of light like a Mercedes-Benz symbol.

   In Zernike polynomials (Fig. 2.3 and Table 2.1), trefoil starts at the 3rd order and takes the symbols (3,–3) for vertical and (3,3) for horizontal. In orders higher than the 3rd, the aberration is no longer named trefoil; the leaflets increase in number in the name follows; e.g. quadrafoil (4 leaflets), pentafoil (5 leaflets) and so on.

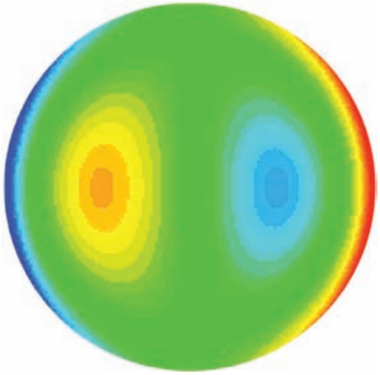

Fig. 2.11 Coma.

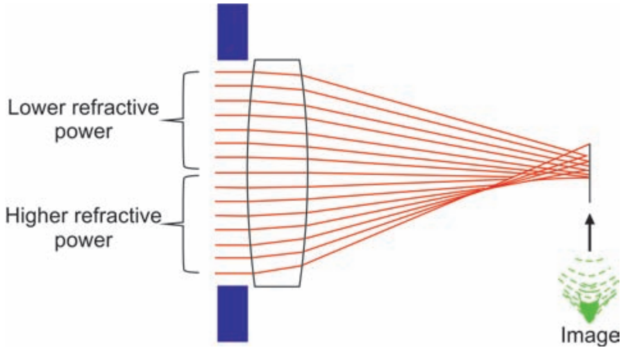

Fig. 2.12 Coma. It is a HOA produced by a refractive surface with a variation of magnification over the entrance pupil.

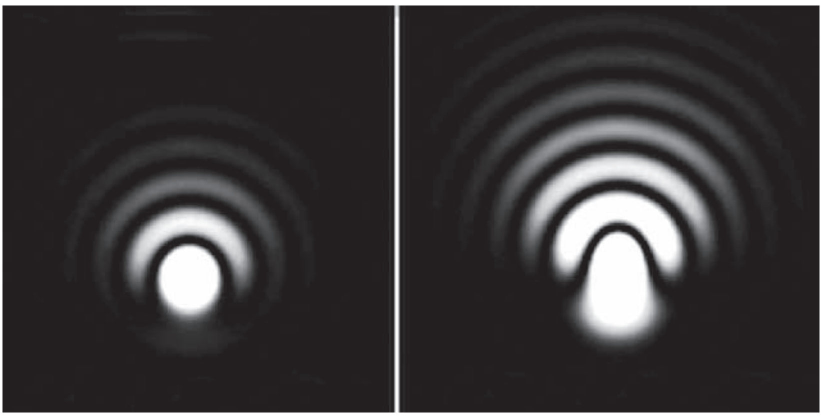

Fig. 2.13 Comet image of a spot light in case of coma.

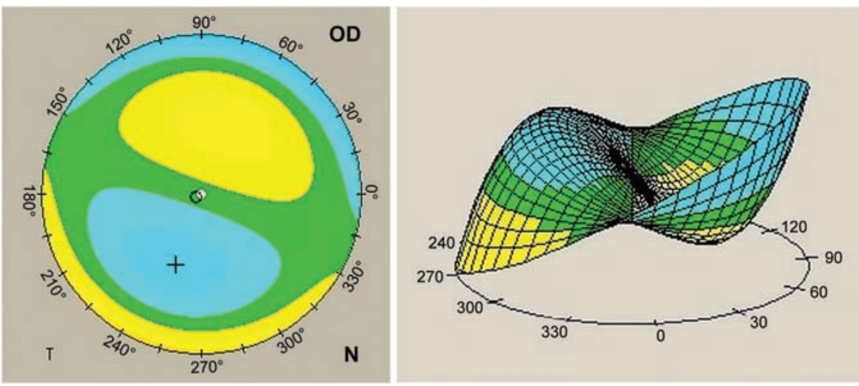

Fig. 2.14 Coma shape in 2D (left) and 3D (right) dimensions.

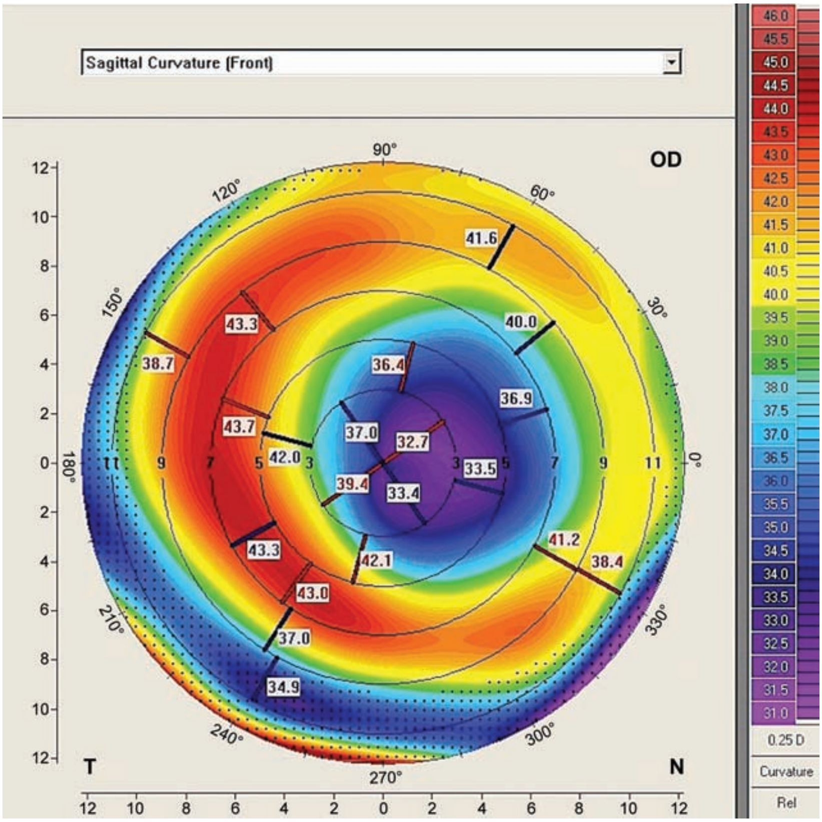

Fig. 2.15 Decentered ablation zone. One of the major causes of coma.

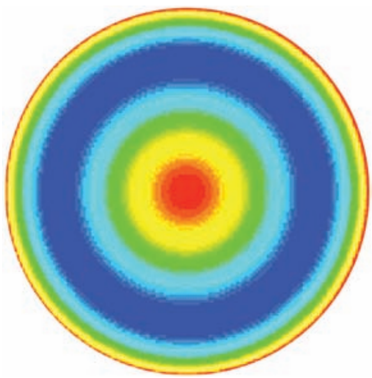

Fig. 2.16 Spherical aberration. It is a HOA produced by difference in curvature between corneal central zone and peripheral zone; such as in oblate and hyperprolate corneas.

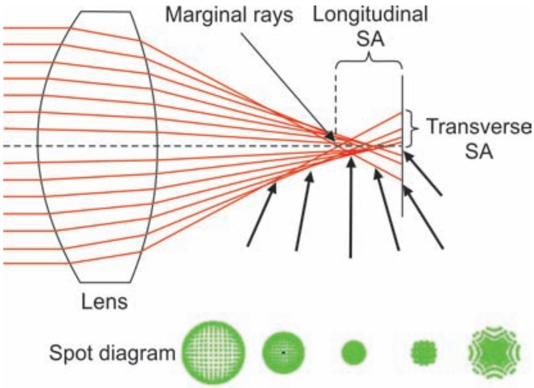

Fig. 2.17 Principle of spherical aberration. In this figure, positive spherical aberration was taken as an example. Green shapes represent shapes of the image in relation to the location of the perception plane. Images closer to the refractive surface are convex and vice versa.

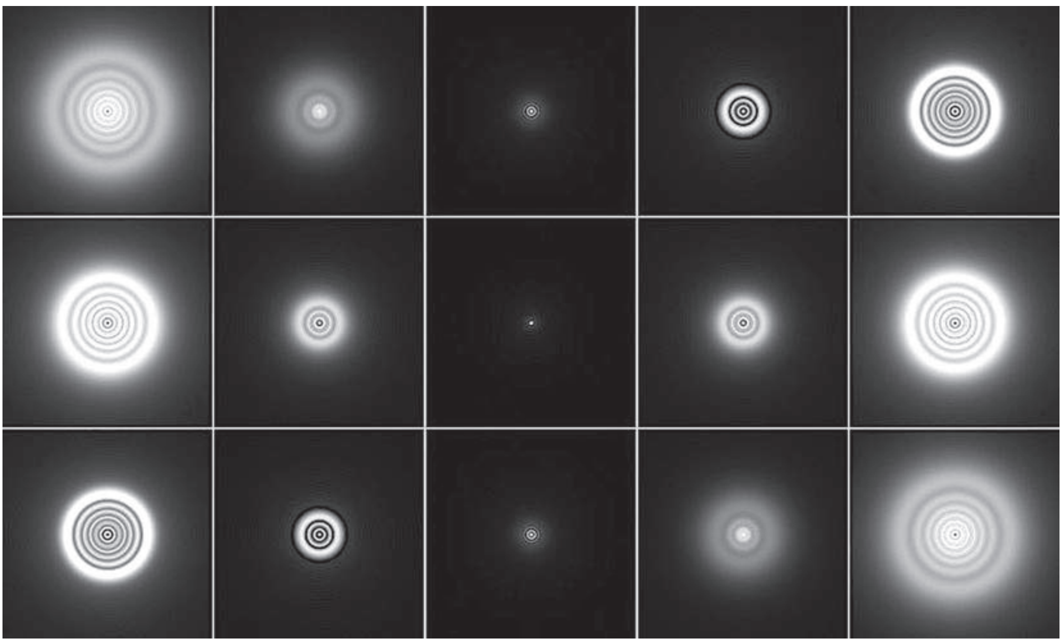

Fig. 2.18 Images of a light spot in spherical aberrations. Spherical aberrations are responsible for halos around oncoming lights. The amount and shape of halos differ according to severity of aberrations and pupil size; the larger the pupil the bigger the amount of halos and the larger the number of halo rings.

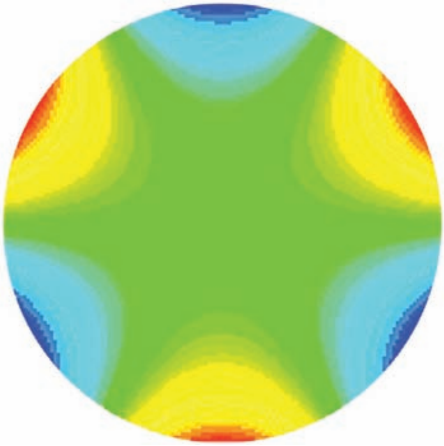

Fig. 2.19 Trefoil. It is a HOA resulting from regular alternating variation in magnification along meridians in corneal periphery.

Fig. 2.20 Trifolium plant. Three leaves in each petal.

TAKE-HOME MESSAGE

- HOAs cannot be corrected with classic optics
- Although there is a wide range and types of HOAs, the main types are coma, trefoil and spherical aberrations
- Coma results from a variation of magnification (refractive power) over the entrance pupil. It affects central vision
- Trefoil aberration results from regular alternating variation in magnification along the meridians in corneal periphery. It affects peripheral vision
- Spherical aberration results from abnormal Q value. It affects peripheral vision.

MEASUREMENT OF ABERRATIONS

CORE MESSAGE

- Aberrations are measured by points spread function (PSF), Strehl Ratio (SR), modulation transfer function (MTF), root mean square (RMS) and Zernike coefficients (ZCs)
- PSF describes the shape of an image in an optical system
- SR describes the percentage of perfection in the shape of an image in an optical system
- MTF measures the reduction of contrast from an object to image in an optical system
- RMS is a thorough expression of the magnitude of deviation in a wavefront regardless from types of aberrations
- ZCs measure the amount of each type of aberrations
- All measurements are affected by two main factors, severity of irregularities and pupil diameter

There are several means for measuring aberrations; each one of them serves for a definite function and application.

Point Spread Function (PSF)

It describes the response of an imaging system to a point source or point object. By definition: PSF is the image that an optical system forms of a point source, where the point source is the most fundamental object, and forms the basics for any complex object. If an optical system were perfect, the image of a point would be a point (Fig. 2.21A), but because the optical system of the human eye is not usually perfect, the point is imaged as a spread image. In aberration, free

optics, the image of a point takes a special shape called "Airy disc," which is a phenomenon of light diffraction (Fig. 2.21B) and, in human eye, it is the Fraunhofer diffraction pattern of a circular pupil.

In optics, the Airy disk (or Airy disc) and Airy pattern are descriptions of the best focused spot of light that a perfect lens with a circular aperture can make, limited by the diffraction of light (Fig. 2.22). The diffraction pattern resulting from a uniformly-illuminated circular aperture, has a bright region in the centre, known as the Airy disk which together with the series of concentric bright rings around is called the Airy pattern. Both are named after G. B. Airy. Figure 2.23 shows the PSF in a perfect eye, as shown in this figure, the amount of diffraction (and therefore the diameter of the Airy disk) enlarges when the diameter of the pupil gets smaller; the ideal pupil diameter is 6–7 mm.

In typical eye (with HOAs), the image of a point is not simply an Airy disk; it takes several shapes according to the type, severity and complexity of HOAs as shown in Figure 2.24. Pupil diameter has an impact on the amount of spread and shape of image as shown in the same figure; therefore, PSF and other measurements are usually taken for a standard pupil diameter of 6 mm.

Measuring PSF helps the physician to see what the patient sees as shown in Figure 2.25, to simulate potential treatments and to predict how those treatments would alter patient's PSF.

On the other hand, PSF of the total wavefront can give an approximation of the real spherical equivalent refractive error by the expression "Eff. Blur," which stands for efficient blur as shown in Figure 2.26. In this figure, the amount of total blur (LOAs and HOAs) equals 3.27 D as shown in the upper left corner of the figure (blue arrow); and the amount of the efficient blur of only HOAs equals 0.41 D as shown in the upper right corner (red arrow).

Nevertheless, the PSF is displayed on a minutes-of-arc scale, the wider the spread on this scale the higher the aberrations. Compare Figure 2.27 with Figure 2.28; the PSF in the former is spread over 40 minutes of arc, whereas it is spread in the latter over 4 minutes of arc. This corresponds to the Eff. Blur, which is 3.27 D in the former and 0.20 D in the latter.

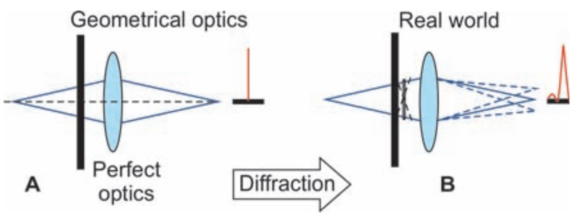

Fig. 2.21 Principle of point spread function (PSF). In geometric optics (A), the image of a point is a point. In real optics (B), the image of a point is not a point.

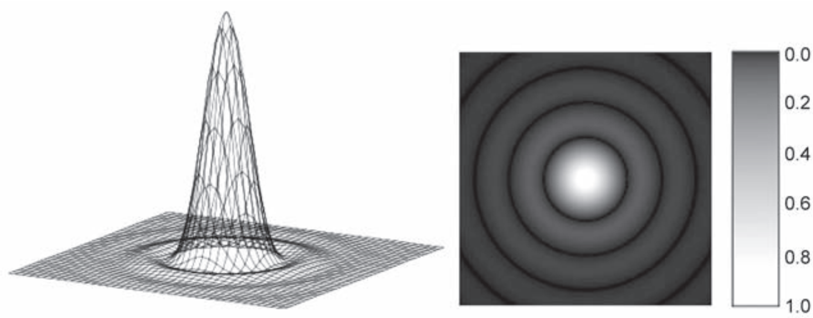

Fig. 2.22 Airy disk. It is a phenomenon of diffraction.

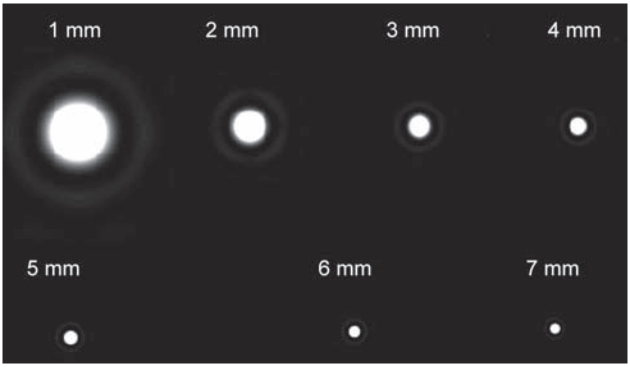

Fig. 2.23 Point spread function vs. pupil size in perfect eye where there are no HOAs.

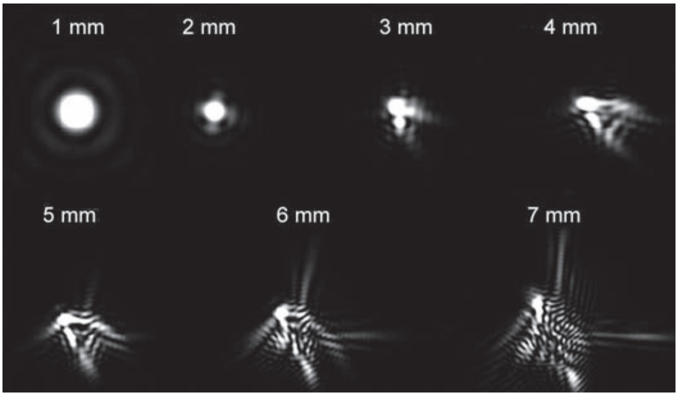

Fig. 2.24 Point spread function vs. pupil size in a typical eye.

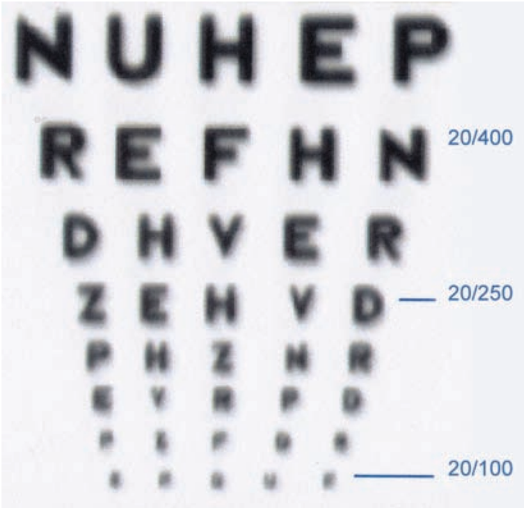

Fig. 2.25 Simulation of a visual acuity chart blurred by diffraction in a perfect eye.

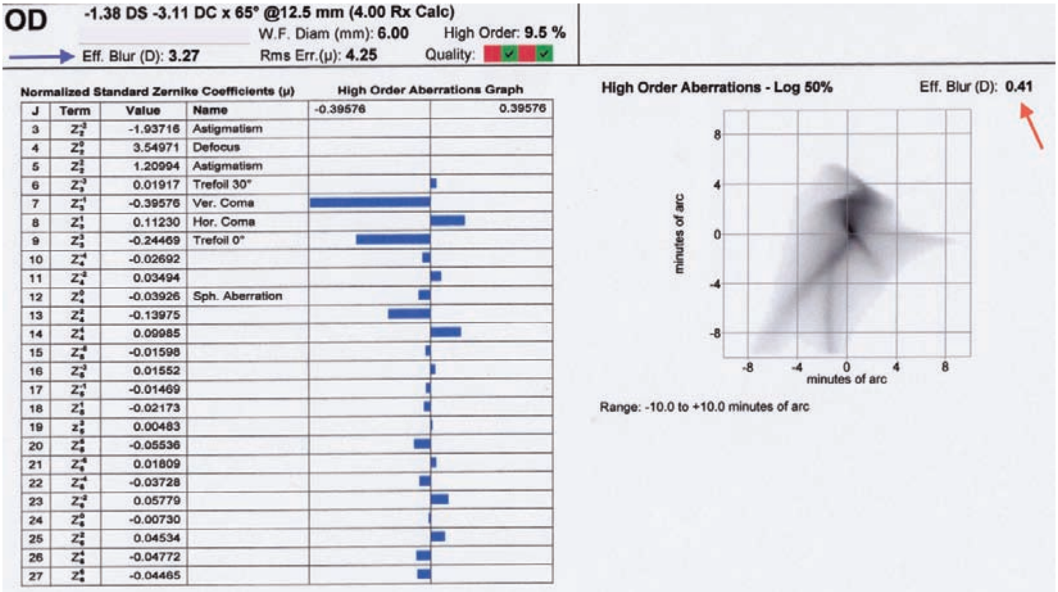

J	Term	Value	Name
3	Z_2^{-2}	-1.93716	Astigmatism
4	Z_2^0	3.54971	Defocus
5	Z_2^2	1.20994	Astigmatism
6	Z_3^{-3}	0.01917	Trefoil 30°
7	Z_3^{-1}	-0.39576	Ver. Coma
8	Z_3^1	0.11230	Hor. Coma
9	Z_3^3	-0.24469	Trefoil 0°
10	Z_4^{-4}	-0.02692	
11	Z_4^{-2}	0.03494	
12	Z_4^0	-0.03926	Sph. Aberration
13	Z_4^2	-0.13975	
14	Z_4^4	0.09985	
15	Z_5^{-5}	-0.01598	
16	Z_5^{-3}	0.01552	
17	Z_5^{-1}	-0.01469	
18	Z_5^1	-0.02173	
19	Z_5^3	0.00483	
20	Z_5^5	-0.05536	
21	Z_6^{-6}	0.01809	
22	Z_6^{-4}	-0.03728	
23	Z_6^{-2}	0.05779	
24	Z_6^0	-0.00730	
25	Z_6^2	0.04534	
26	Z_6^4	-0.04772	
27	Z_6^6	-0.04465	

Fig. 2.26 Aberration analysis display. Upper left: subjective refraction; lower left: table of measured aberrations; right: PSF of HOAs (shape of the image of a point distorted by HOAs). The blue arrow points at efficient blur of total aberrations (HOAs + LOAs). The red arrow points at the efficient blur of HOAs.

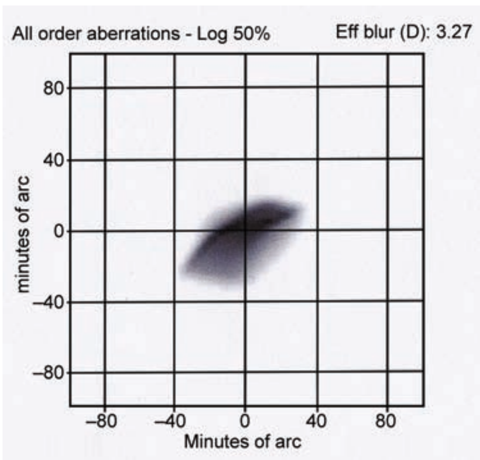

Fig. 2.27 PSF display. It gives the shape of the image of a point along minutes of arc. The wider the display on minutes of arc the higher the PSF. In this example, PSF is high (±40 min of arc).

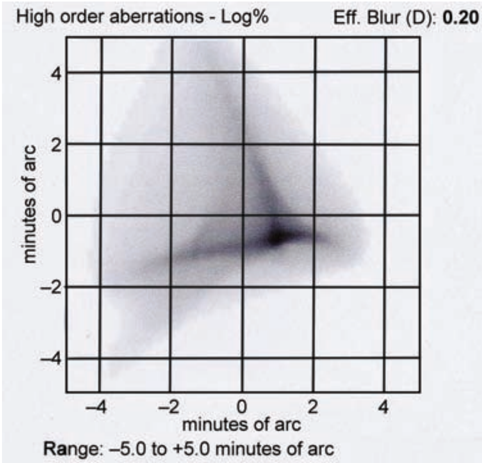

Fig. 2.28 PSF display. It gives the shape of the image of a point along minutes of arc. The wider the display on minutes of arc the higher the PSF. In this example, PSF is almost insignificant (±4 min of arc).

Strehl Ratio (SR)

It is the simplest meaningful way of expressing the effect of wavefront aberrations on image quality. Not like the root mean square (RMS), Strehl ratio (SR) is a measure of optical excellence in terms of theoretical performance results rather than an expression of the physical surface or the shape of the wavefront.

In other words, this ratio is an expression of the amount of light contained within the Airy disk as a percentage of the theoretical maximum that would be contained within the disk with a perfect optical system (Fig. 2.29). It is the measure of the fractional drop in the peak of the Airy disk as a function of wavefront error with a 1 Strehl being perfection and anything less than 1 less than perfection. Roughly saying, 1 is perfection, 0.8 is okay, 0.9 is good and 0.95 is extremely good.

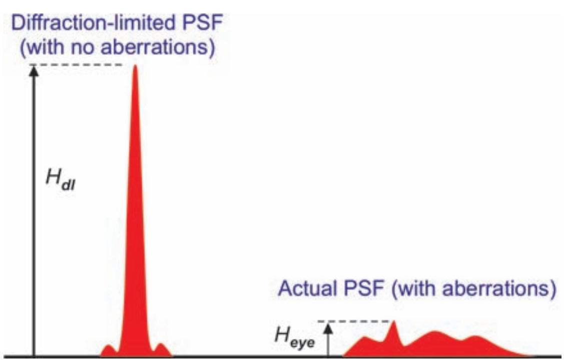

Fig. 2.29 Strehl ratio. It is a measure of the fractional drop in the peak of the Airy disk as a function of wavefront error.

Modulation Transfer Function (MTF)

It is the most widely used scientific method for describing optical system performance. The MTF is a measure of the reduction in contrast from object to image. In other words, it measures how faithfully the optical system reproduces (or transfers) detail from the object to the image produced by the optical system.

To understand MTF, spatial frequency should be understood first. Spatial frequency can be defined as: a) number of lines per 1mm (lp/mm), where "line" here means the pair of black and white shown in Figure 2.30; b) or it can be defined as cycles of waves per 1mm (cy/mm), which is exactly the same as lp/mm; c) or can be defined as cycles of waves per 1° of arc as shown in Figure 2.31. In the last case, spatial frequency represents visual acuity; e.g. spatial frequency of 300cyl/1° equals 20/20 (1.0 Snellen) and 30cy/1° equals 20/200 (0.1 Snellen).

To understand the relationship between MTF and spatial frequency, see Figure 2.32. Line (A) represents an object with alternating black and white bars. Those bars become narrower and closer to each others as the spatial frequency increases from left (low spatial frequency) to right (high spatial frequency). Line (B) is the image of line (A) produced by an optical system. Note that the borders of the image bars are blurred (partially resolved) because of diffraction found in any optical system.

Since the MTF is the ratio of the image modulation to the object modulation in all spatial frequencies, it takes a value ranging from 0 to 1, where 0 stands for imperfection and 1 stands for full perfection. If an optical system were perfect, MTF would be 1, which means that image B would be as sharp as object A; if an optical system is imperfect and MTF = 0, image B will be totally grey (totally resolved: no modulation in the image).

The relationship between MTF and spatial frequency is inverse; the higher the spatial frequency the lower the MTF as shown in Figure 2.33. That is because in high spatial frequency recognition of black-and-white structure is less and the structure will be resolved to be gray, which means low MTF. The same can be said about visual acuity; the higher the spatial frequency

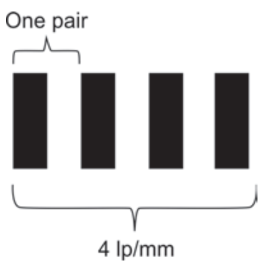

Fig. 2.30 Spatial Frequency. It is defined as number of paired lines per 1mm.

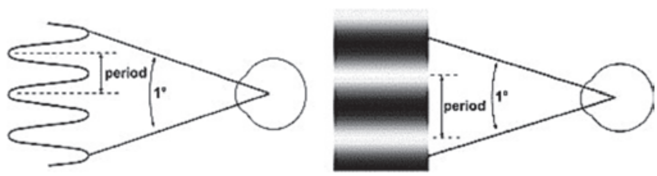

Fig. 2.31 Spatial Frequency. It is defined as number of cycles per 1° of arc.

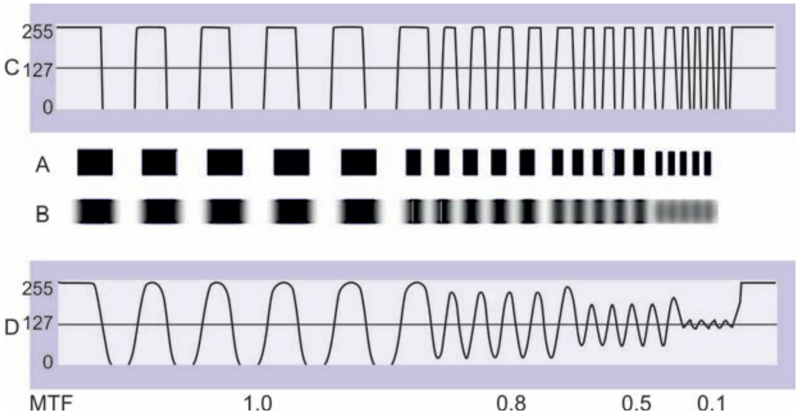

Fig. 2.32 Relationship between MTF (contrast sensitivity) and spatial frequency.

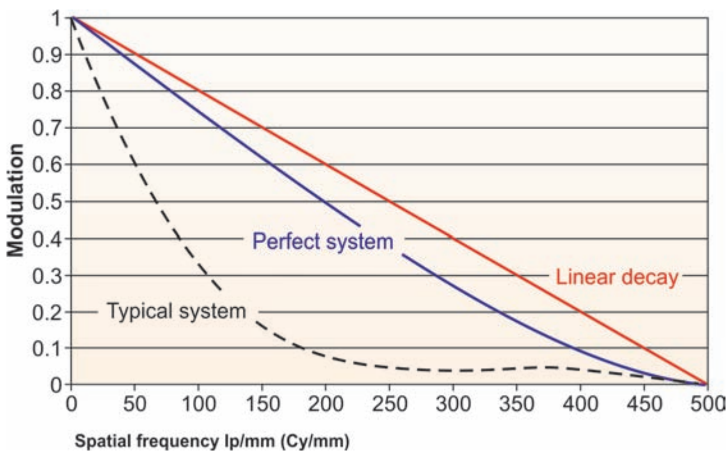

Fig. 2.33 Relationship between MTF (contrast sensitivity) and spatial frequency. In ideal geometric optics, the relationship is linear inverse, whereas it is curved inverse in perfect and typical optics. In typical optics, the MTF falls down quickly with higher spatial frequency. In perfect optics, the slope is less concave indicating slower drop of MTF with higher spatial frequency.

the lower the visual acuity and the lower the MTF. Therefore, it can be said that the better the visual acuity the higher the MTF should be. Still in the same figure, the curve of a perfect optical system is presented in blue and the curve of a typical optical system is presented in dashed black. Optical systems of good quality lie between these two curves, whereas those with bad quality lie in the area left to the typical system curve. On the other hand, when spatial frequency gets higher (towards right), MTF gets lower, meaning that the quality of the image becomes lower and vice versa; this is shown in Figure 2.34.

There is also an inverse relationship between MTF and PSF; the narrower the PSF the higher the MTF and the higher the quality of an optical system.

Moreover, the relationship between MTF and pupil size is also inverse; the larger the pupil the lower the MTF and the lower the quality of the image; this is shown in the Figure 2.35.

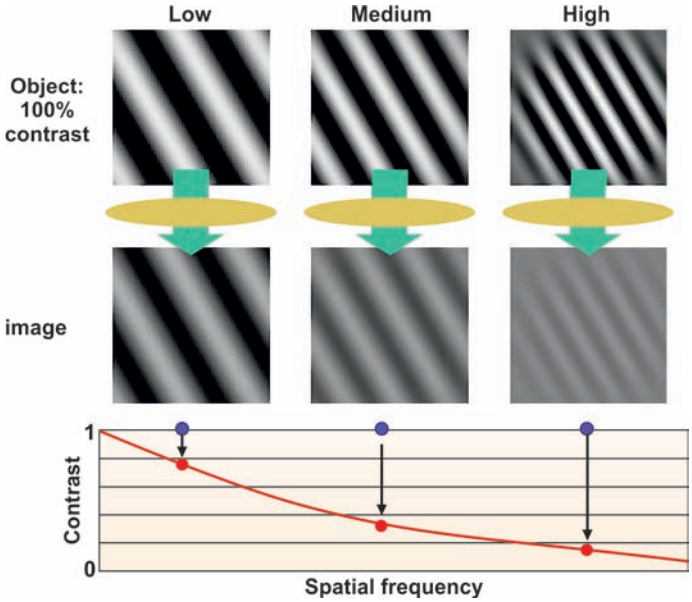

Fig. 2.34 Image quality in relation to spatial frequency. The higher the spatial frequency, the lower the quality of the image.

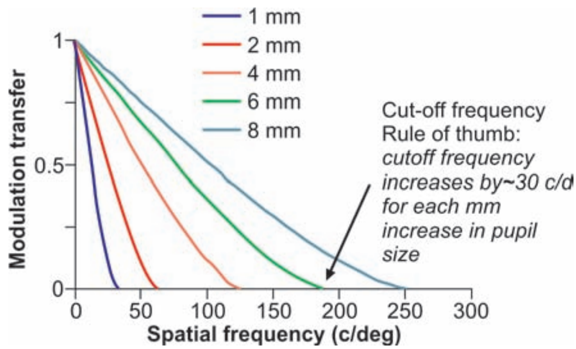

Fig. 2.35 Relationship among MTF, spatial frequency and pupil size. The smaller the pupil the more adverse impact on the MTF/spatial relationship.

Root Mean Square (RMS)

It is an expression of the physical surface or the shape of the wavefront. It expresses the deviation averaged over the entire wavefront in reference to the perfect wavefront as shown in Figure

2.36. The quadratic values are summed and rooted by the following equation (as in the figure example):

$RMS = \sqrt{[(-0.2)^2 + (0.25)^2 + (-0.3)^2]} = 0.438$ µm

RMS error by itself is an accurate representation of the magnitude of wavefront deviation only when it is affecting relatively large wavefront area, which is generally the case with the conic surface aberrations, otherwise it is an approximate representation. Quantitative comparisons between different eyes and conditions are usually made by using RMS.

In order to measure RMS for each type of aberration, the difference between the aberration and mean value is squared and averaged across the pupil area. Different kinds of aberrations may have equal RMS across the pupil but have different effects on vision; therefore, RMS error is unrelated to visual performance. The majority of normal eyes have total RMS values less than 0.3 µm.

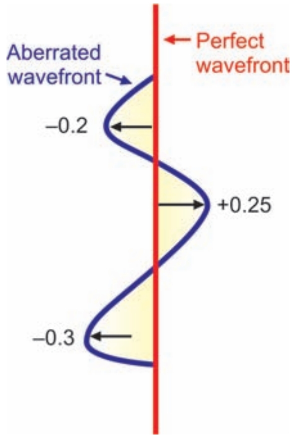

Fig. 2.36 Principle of RMS. It expresses the deviation averaged over the entire wavefront in reference to the perfect wavefront.

In wavefront analysis, the RMS is given in two values, the total RMS of LOAs and HOAs and a HOAs-related RMS. The former is higher than the latter since it reflects the effect of refractive errors on the wavefront, but the latter is the one of interest in decision making.

Zernike Coefficients (ZCs)

Zernike Coefficient (ZC) is an expression of the amount of each individual aberration. Sophisticated equations are used to calculate ZC for each polynomial as shown in Table 2.2. Unlike RMS, ZCs may take either negative or positive values and displayed as shown in Figure 2.37. As shown in this figure, the example eye has high defocus due to the spherical refractive error, whereas HOAs are within the normal limits. Generally speaking, ZCs are normal, suspected or abnormal when they are <0.25 µm, 0.25–0.5 µm or >0.5 µm, respectively.

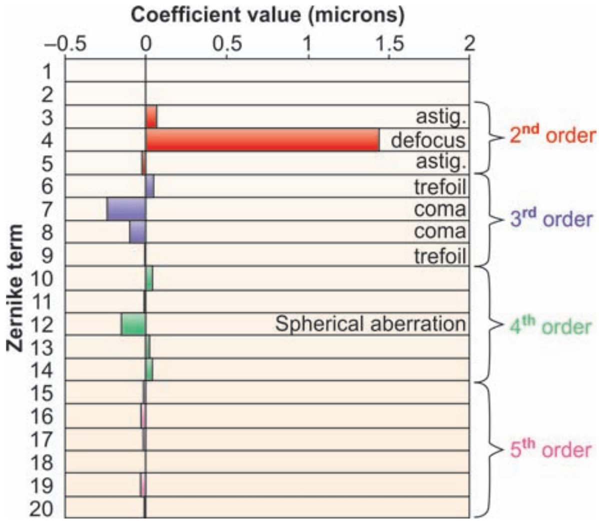

Fig. 2.37 Zernike Coefficients (ZCs). ZC is an expression of the amount of each individual aberration.

TABLE 2.2 Zernike polynomials

n = order	*m = frequency*	$Z^m_n(\rho, \theta)$	
0	0	1	Zero Order (Piston)
1	-1	$2\rho\sin\theta$	First Order (Tilt)
1	1	$2\rho\sin\theta$	
2	-2	$\sqrt{6}\ \rho^2 \sin 2\theta$	Second order aberrations
2	0	$\sqrt{3}\ (2\rho^2 - 1)$	
2	2	$\sqrt{6}\ \rho^2 \cos 2\theta$	
3	-3	$\sqrt{8}\ \rho^3 \sin 3\theta$	Higher order aberrations
3	-1	$\sqrt{8}\ (3\rho^3 - 2\rho) \sin\theta$	
3	1	$\sqrt{8}\ (3\rho^3 - 2\rho) \cos\theta$	
3	3	$\sqrt{8}\ \rho^3 \cos 3\theta$	
4	-4	$\sqrt{10}\ \rho^4 \sin 4\theta$	
4	-2	$\sqrt{10}\ (4\rho^4 - 3\rho^2)\sin 2\theta$	
4	0	$\sqrt{5}\ (6\rho^4 - 6\rho^2 + 1)$	
4	2	$\sqrt{10}\ (4\rho^4 - 3\rho^2) \cos 2\theta$	
4	4	$\sqrt{10}\ \rho^4 \cos 4\theta$	
5	-5	$\sqrt{12}\ \rho^5 \sin 5\theta$	
5	-3	$\sqrt{12}\ (5\rho^5 - 4\rho^3) \sin 3\theta$	
5	-1	$\sqrt{12}\ (10\rho^5 - 12\rho^3 + 3\rho) \sin\theta$	
5	1	$\sqrt{12}\ (10\rho^5 - 12\rho^3 + 3\rho) \cos\theta$	
5	3	$\sqrt{12}\ (5\rho^5 - 4\rho^3) \cos 3\theta$	

TAKE-HOME MESSAGE

- Measurement of aberrations is usually taken for a standard pupil diameter of 6 mm
- The wider the PSF the more distorted the wavefront
- The PSF is a function of diffraction, therefore, the larger the pupil the wider the PSF
- SR ranges from 0 to 1. It is perfect, extremely good, good or accepted when it is 1, 0.95, 0.9 or 0.8, respectively
- The better the visual acuity the higher the MTF
- The larger the pupil the lower the MTF
- Normal RMS related to HOAs is <0.3 μm
- ZC is normal, suspected or abnormal when it is <0.25 μm, 0.25–0.5 μm or >0.5 μm, respectively

WAVEFRONT MAPS

CORE MESSAGE

- There are four main wavefront maps, acuity map, high order aberrations map, high order aberrations correction map and correction all aberrations map
- Acuity map is the wavefront resulting from refractive error(s); in other words, it is low order aberrations (LOAs) map
- High order aberrations map is the wavefront resulting from HOAs
- high order aberrations correction map is the correction profile for HOAs
- Correction all aberrations map is the correction profile for LOAs and HOAs
- Each map is provided with efficient blur value and RMS value
- Efficient blur measures the spherical equivalent that equals the deviation of the wavefront from the perfect wavefront
- RMS of HOAs is the RMS of concern for diagnosis and treatment

There are four wavefront maps which can be either for the cornea known as corneal wavefront (CWF) or for all media known as total or ocular wavefront (OWF).

Figure 2.38 is a four composite wavefront map. In the upper left corner, the efficient blur is 5.05 D, i.e. the spherical equivalent refractive error measured by the total wavefront; the total

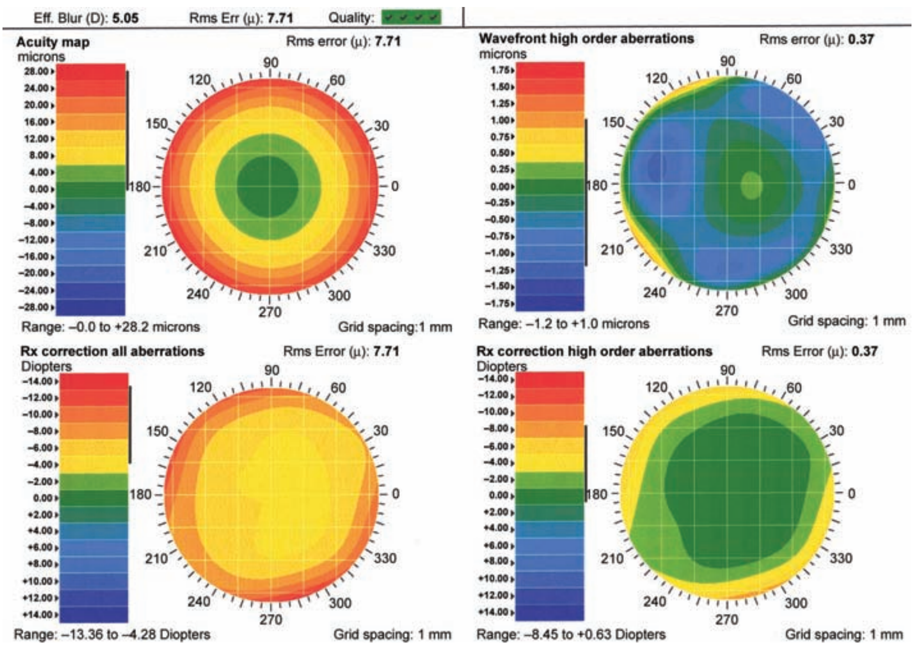

Fig. 2.38 Wavefront maps. A four composite map consists of acuity map (upper left), high order aberrations (upper right), correction all aberrations (lower left) and correction high order aberrations (lower right).

RMS error is 7.71µm and the quality of the capture is very good. This figure shows the wavefront maps: the acuity map, the wavefront high order aberrations map, the Rx correction all aberrations map and the Rx correction high order aberrations map.

The Acuity Map (AM)

It is the wavefront map of the LOAs resulting from refractive errors. Figure 2.39 is an AM of an eye with myopia. Figure 2.40 is an AM of an eye with myopic astigmatism. Figure 2.41 is an AM

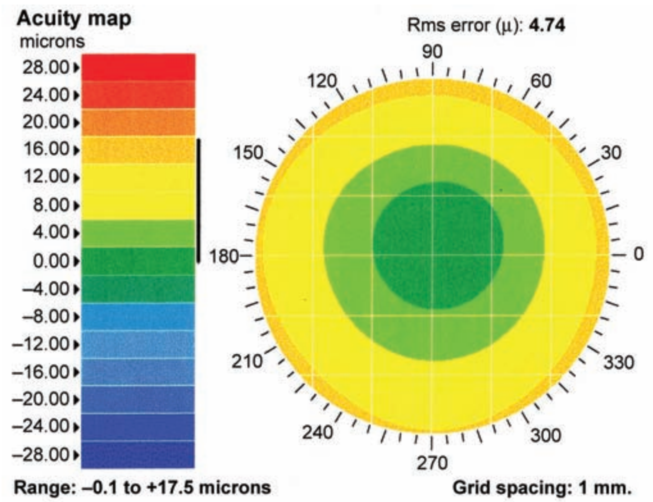

Fig. 2.39 Acuity map. It represents the wavefront of LOAs. In this example, the eye is myopic.

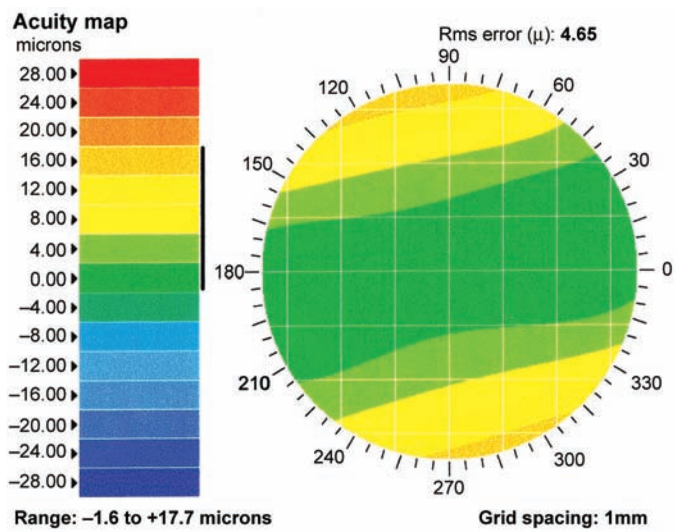

Fig. 2.40 Acuity map in myopic astigmatism.

of an eye with myopia and myopic astigmatism. Figure 2.42 is an AM of an eye with hyperopia. Shown in the upper left corner of the map is the RMS error which describes the deviation of the wavefront due to the refractive error.

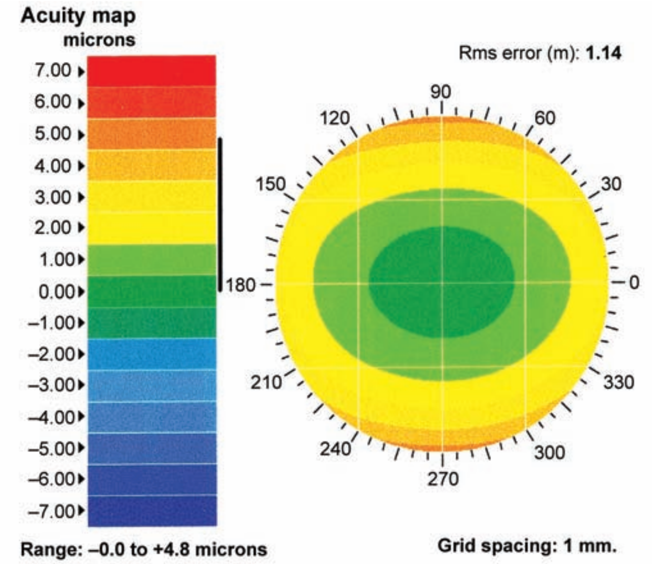

Fig. 2.41 Acuity map in combined myopic astigmatism.

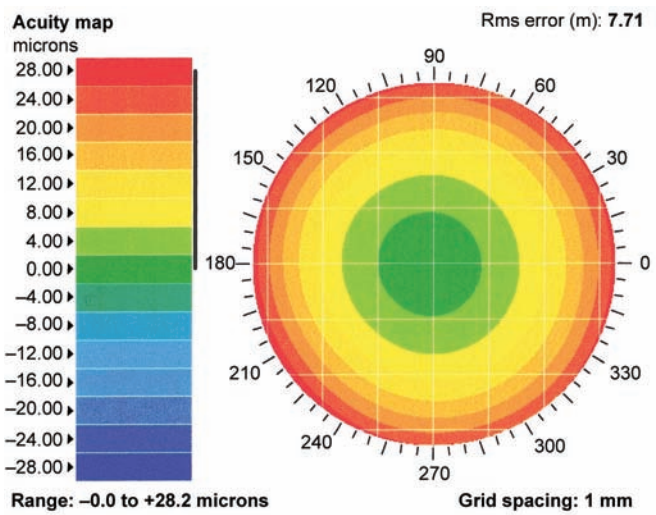

Fig. 2.42 Acuity map in hyperopic eye.

Wavefront High Order Aberrations Map (WHOM) (Fig. 2.43)

It is the wavefront map of the HOAs. Shown in the upper left corner of the map is the RMS error which describes the deviation of the wavefront due to the HOAs.

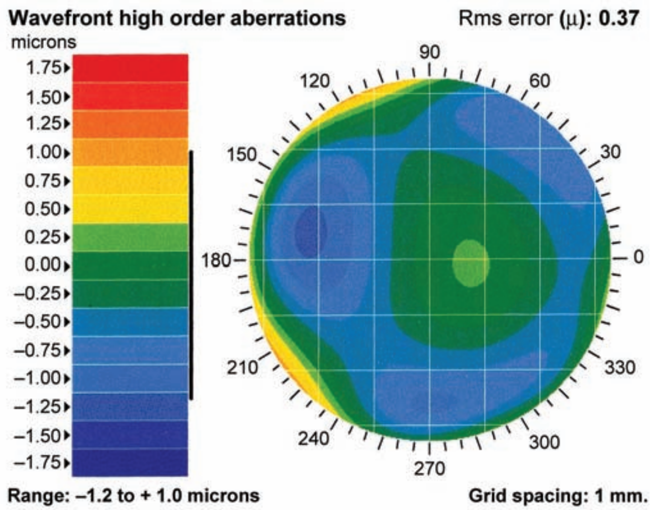

Fig. 2.43 Wavefront high order aberration map. It represents the wavefront of HOAs.

Rx Correction High Order Aberration Map (CHOM) (Fig. 2.44)

This is the correction profile of HOAs. In a way, it can be considered as the negative of the WHOM presented in Figure 2.43.

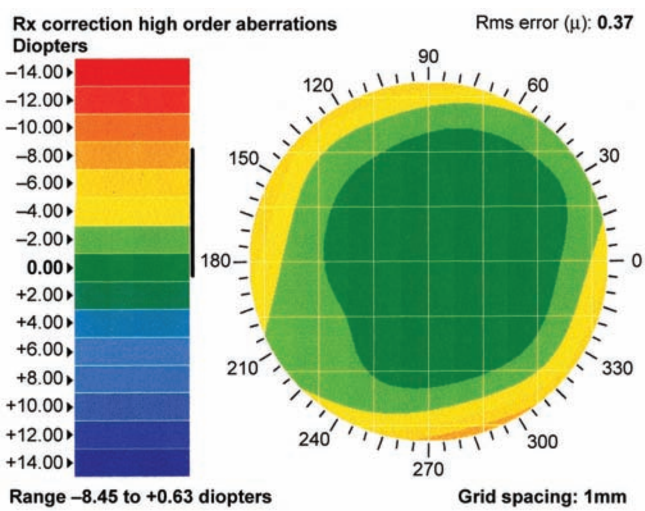

Fig. 2.44 Rx Correction high order aberration map. It is a simulation of the profile of wavefront-guided treatment to correct HOAs.

Rx Correction all Aberrations Map (CAM) (Fig. 2.45)

This is the correction profile of LOAs and HOAs. In a way, it can be considered as the mixture of the AM correction and the CHOM.

CHANGES OF ABERRATIONS WITH AGE

CORE MESSAGE

- Ocular aberrations change with age
- Cornea changes with age
- Crystalline lens changes with age

Ocular aberrations change with age due to changes in the cornea and the crystalline lens.

Corneal Changes with Age

In young eyes, the cornea is typically steeper on the vertical meridian and, therefore, has WTR astigmatism. This tends to reverse with age and, therefore, old cornea has ATR astigmatism.

In general, the cornea tends to be more curved with age. This decrease of radius of curvature is on the account of the anterior corneal surface.

The only significant change in corneal aberration with age is a decrease in the posterior surface asphericity.

Crystalline Lens Changes with Age

Major changes in aberrations are related to aging of the crystalline lens. With age, spherical aberrations change to be less negative or even positive, the RMS increases, contrast sensitivity decreases due to increased scattering.

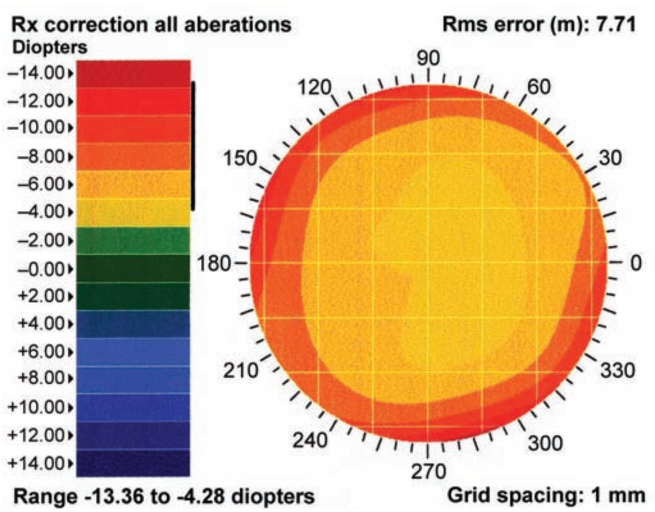

Fig. 2.45 Rx Correction all aberrations. . It is a simulation of the profile of wavefront-guided treatment to correct HOAs and LOAs (refractive error).

Corneal/Internal Aberration Compensation

In young eyes, there is a balance of aberrations between cornea and lens. This balance decreases with age to cause positive total spherical aberrations and an increase in coma-like aberrations. The coma-like changes are unexplainable. Figure 2.46 shows examples of corneal, internal, and total aberrations for a young and an old subject, illustrating the positive addition of aberrations of the ocular components in the older subject, as opposed to the partial balance of aberrations in the young subject.

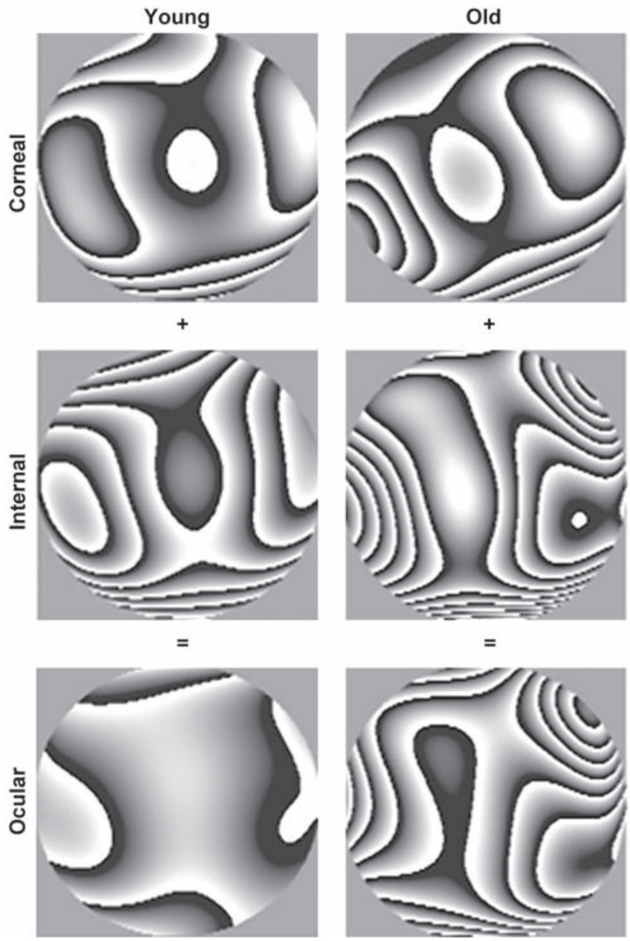

Fig. 2.46 Change of aberrations with age. Left column represents corneal, internal and ocular (total) aberrations in young people; notice that the internal aberrations compensate for corneal aberrations. Right column represents corneal, internal and ocular (total) aberrations in old people; notice that the internal aberrations may slightly compensate for corneal aberrations.

TAKE-HOME MESSAGE

- With age, corneal WTR astigmatism converts into ATR astigmatism
- In aging crystalline lens, spherical aberrations change to be less negative or even positive, the RMS increases and contrast sensitivity decreases
- With age, the cornea/crystalline lens compensation decreases

WAVEFRONT IN FFKC DETECTION

Wavefront HOAs can be used as a diagnostic measure of ectatic corneal disorders in general and the detection of FFKC in particular. Some studies found that HOAs begin to change either before prominent changes appear on corneal topography and tomography.

Main changes can be summarized as follows.

The *corneal* vertical tilt (ZC_1^{-1}), the *corneal* vertical coma (ZC_3^{-1}), and *corneal* horizontal trefoil (ZC_3^3) take significantly more negative values in FFKC.

The *corneal* total coma RMS starts to increase taking higher values than in normal eyes. No such significant change is found in *corneal* total trefoil.

The *ocular* vertical tilt (ZO_1^{-1}), *ocular* vertical coma (ZO_3^{-1}) and *ocular* horizontal trefoil (ZO_3^3) take significantly high values in FFKC.

No significant change is found either in *ocular* total RMS or trefoil. This might partly be due to internal aberrations compensating for the corneal aberrations generated by the FFKC cornea.

Cut-off points differ between studies due to different devices used in measuring HOAs. However, the mentioned HOAs and their values can be monitored in suspected cases to document any significant change.

BIBLIOGRAPHY

1. Alió JL and Shabayek MH. Corneal higher order aberrations: a method to grade keratoconus. J Refract Surg. 2006;22(6):539-45.
2. American Academy of Ophthalmology (2012-2013 edition). Basic and Clinical Science Course, Section 13: Refractive Surgery.
3. American Academy of Ophthalmology (2012-2013 edition). Basic and Clinical Science Course, Section 3: Clinical Optics.
4. Applegate RA, Thibos LN and Hilmantel G. Optics of aberroscopy and super vision. J Cataract Refract Surg. 2001;27(7):1093-107.
5. Atchison DA, Scott DH and Charman WN. Measuring ocular aberrations in the peripheral visual field using Hartmann-Shack aberrometry. J Opt Soc Am A Opt Image Sci Vis. 2007;24(9):2963-73.
6. Azar DT, Gatinel D and Hoang-Xuan T. Refractive surgery. Philadelphia: Mosby Elsevier; 2007.
7. Brightbill FS, McDonnell PJ, McGhee CNJ, et al. Corneal Surgery: Theory, Technique and Tissue. Mosby Elsevier; 2009.
8. Buhren J, Kuhne C and Kohnen T. Wavefront analysis for the diagnosis of subclinical keratoconus (in German). Ophthalmologe. 2006;103:783-90.
9. Buhren J, Kuhne C and Kohnen T. Defining subclinical keratoconus using corneal first-surface higher-order aberrations. Am J Ophthalmol. 2007;143(3):381-9.
10. Campbell C. The effect of tear film on higher order corrections applied to the corneal surface during wavefront-guided refractive surgery. J Refract Surg. 2005;21(5):S519-24.
11. Cerviño A, Hosking, SL, Montes-Mico R, et al. Clinical ocular wavefront analyzers. J Refract Surg. 2007;23(6):603-16.
12. Charman WN. Wavefront technology: past, present and future. Cont Lens Anterior Eye. The journal of the British Contact Lens Association. 2005;28(2):75-92.
13. Diaz-Douton F, Benito A and Pujol J. Comparison of the retinal image quality with a Hartmann-Shack wavefront sensor and a double-pass instrument. Invest Ophthalmol Vis Sci. 2004;47(4):1710-6.
14. Endl MJ, Martinez CE, Klyce SD, et al. Effect of larger ablation zone and transition zone on corneal optical aberrations after photorefractive keratectomy. Archives of ophthalmology. 2001;119(8):1159-64.

15. Feder RS and Rapuano. The lasik handbook: a case-based approach. Lippincott Williams and Wilkins; 2007.
16. Fong CS. Refractive surgery: the future of perfect vision?. Singapore Med J. 2007;48(8):709-18.
17. Gobbe M and Guillon M. Corneal wavefront aberration measurements to detect keratoconus patients. Cont Lens Anterior Eye. 2005;28:57-66.
18. Goins KM and Wagoner MD. Focal points: Imaging the anterior segment. American academy of ophthalmology. 2009;27(11):1-17.
19. Krueger RR, Applegate RA and MacRae SM. Wavefront Customized Visual Correction. Chapter 2 "A Review of Basic Wavefront Optics" by Roorda A. SLACK Inc. 2004.
20. Lawless MA and Hodge C. Wavefront's role in corneal refractive surgery. Clinical and experimental ophthalmology. 2005;33(2):199-209.
21. Lombardo M and Lombardo G. Wave aberration of human eyes and new descriptors of image optical quality and visual performance. J Cataract Refract Surg. 2010;36(2):313-31.
22. Molebny VV, Panagopoulou SI, Molebny SV, et al. Principles of ray tracing aberrometry. J Refract Surg. 2000;16(5):S572-5.
23. Mrochen M, Kaemmerer M, Mierdel P, et al. Principles of Tscherning aberrometry. J Refract Surg. 2000;16(5):S570-1.
24. Nilforoushan MR, Speaker M, Marmor M, et al. Comparative evaluation of refractive surgery candidates with Placido topography, Orbscan II, Pentacam, and wavefront analysis. J Cataract Refract Surg. 2008;34:623-31.
25. Oliveira CM, Ferreira A and Franco S. Wavefront analysis and Zernike polynomial decomposition for evaluation of corneal optical quality. J Cataract Refract Surg. 2012;38(2):343-56.
26. Rabbetts RB. Clinical Visual Optics. Butterworth-Heinemann; 1998.
27. Rozema JJ, Van Dyck DE and Tassignon MJ. Clinical comparison of 6 aberrometers. Part 2: statistical comparison in a test group. J Cataract Refract Surg. 2006;32(1):33-44.
28. Saad A and Gatinel D. Evaluation of Total and Corneal Wavefront High Order Aberrations for the Detection of Forme Fruste Keratoconus. Invest. Ophthalmol. Vis. Sci. 2012;23(6):2978-92.
29. Schallhorn SC. Focal points: Wavefront-Guided LASIK. American Academy of Ophthalmology. 2008;26(1):1-15.
30. Schuman JS. Ophthalmic imaging and diagnostics. Ophthalmology Clinics of North America. 1998;11:1-490.
31. Sinjab MM. Corneal Topography in Clinical Practice (Pentacam System): Basics and Clinical Interpretation. Jaypee-Highlights Medical Publishers, Inc. 2012.
32. Thibos LN. Principles of Hartmann-Shack aberrometry. J Refract Surg. 2000;16(5):S563-5.
33. Thibos LN, Applegate RA, Schwiegerling JT and Webb R. Report from the VSIA taskforce on standards for reporting optical aberrations of the eye. J Refract Surg. 2000;16(5):S654-5.
34. Warden L, Liu Y, Binder PS, Dreher AW and Sverdrup L. Performance of a new binocular wavefront aberrometer based on a self-imaging diffractive sensor. J Refract Surg. 2008;24(2):188-96.
35. Wyant J C. "Zernike Polynomials". Powered by WebMATHEMATICA. http://wyant.optics.arizona.edu/zernikes/zernikes.htm
36. Yanoff M and Duker JS. Ophthalmology. Mosby Elsevier; 2012.

CHAPTER 3

Optical Coherence Tomography (OCT)

INTRODUCTION

CORE MESSAGE

- Optical coherence tomography (OCT) is an important complementary investigation
- It gives optical images with higher resolution than Scheimpflug-based devices
- It measures corneal thickness and gives a pachymetry map that is less affected by corneal opacities
- It can be used in diagnosis and treatment of refractive complications and some corneal pathologies
- It is taking an important role in detecting early KC and other ectatic corneal disorders
- It is taking an important role in diagnosing and planning for management of glaucoma

Optical coherence tomography (OCT) is a fundamentally new type of medical diagnostic imaging technology that performs high-resolution, micron-scale, cross-sectional imaging of the internal microstructure in biological tissues by measuring the intensity and echo time delay of light.

OCT is a powerful imaging modality because it enables the real-time, *in situ* imaging of tissue structure or pathology with resolutions of 1 to 15 μm, which is one to two orders of magnitude finer than conventional clinical imaging technologies such as ultrasound, magnetic resonance imaging (MRI), or computed tomography (CT). The operation of OCT is analogous to ultrasound B-mode imaging or radar except that light is used rather than acoustic or radio waves. OCT is especially suited for diagnostic applications in ophthalmology because of the ease of optical access to the anterior and posterior eye. The physical basis of imaging depends on the contrast in optical reflectivity between different tissue microstructures.

NORMAL ANTERIOR EYE

Anterior Chamber

Figure 3.1 displays an OCT image of a normal anterior chamber obtained from a healthy human eye. Clearly identifiable structures include the cornea, sclera, iris and lens anterior capsule. The strongest reflected signals arise from the epithelial surface of the cornea and the highly scattering sclera and iris. Smaller amounts of backscatter are visible from within the nominally transparent cornea and lens. The backscatter intensity gradually decreases from central to peripheral cornea. This signal fading may be attributed to highly angle-dependent backscattering from the stromal collagen lamellae, which run parallel to the corneal surface. The limbus appears as the angled interface between the cornea and the sclera. The normal "watch glass" insertion of the cornea into the sclera is clearly visible.

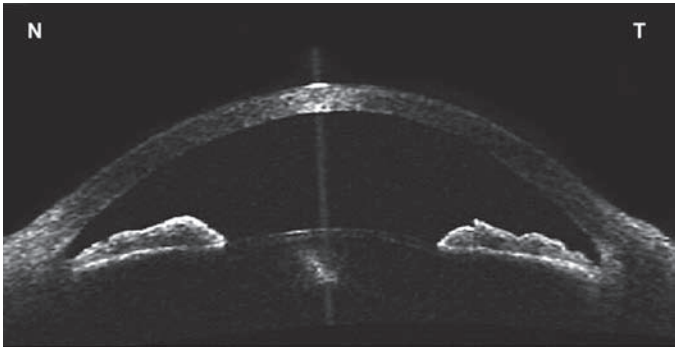

Fig. 3.1 OCT view of anterior chamber obtained from a normal healthy eye.

Cornea and Angle

By narrowing the field-of-view, OCT can be used to obtain high resolution images of corneal microstructure. A magnified OCT image of the cornea appears in Figure 3.2, which differentiates the corneal epithelium, Bowman's layer, stroma, Descemet's membrane and endothelium based on the differences in their optical properties. Normal corneal thickness is 550µm in average (450 – 700 µm) and consists of the followings: 30–80 µm for epithelium, 16µm for Bowman, 380–480 µm for stroma, and 20µm for Descemet and endothelium. A close-up view of the angle region (Fig. 3.3) shows the iris contour and epithelium, the corneoscleral limbus and the ACA. Structures in the angle region such as the trabecular meshwork and canal of Schlemm are not clearly visualized in the tomogram since the incident and backscattered light is highly attenuated after traversing the overlying scleral tissue.

Pachymetry Map

Anterior OCT measures corneal thickness and displays a pachymetry map provided with indices that help in detection of KC and ectatic corneal disorders (Fig. 3.4).

CLINICAL APPLICATION OF ANTERIOR OCT

Anterior OCT is used for diagnosis and planning and guiding treatment.

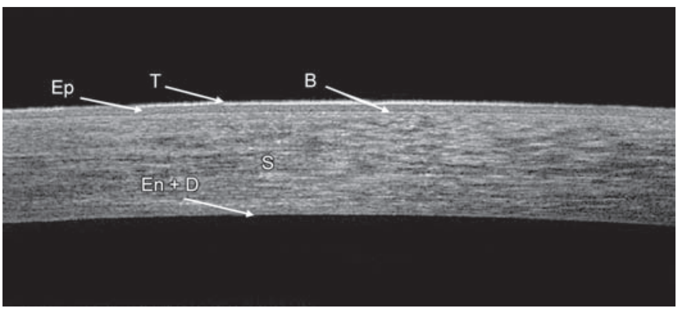

Fig. 3.2 Corneal layers by OCT. T: tear; Ep: epithelium; B: Bowman; S: stromal; En: endothelium; D: Descemet.

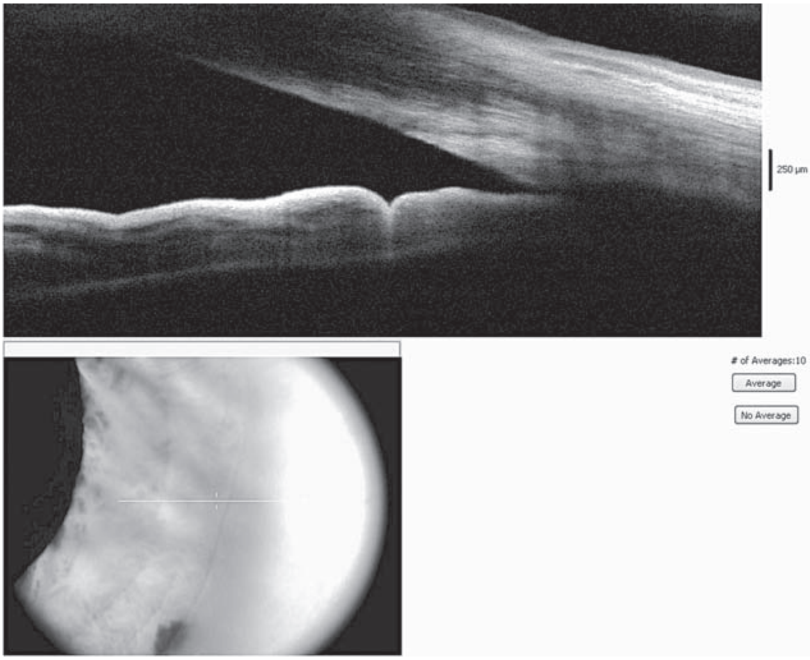

Fig. 3.3 OCT view of anterior chamber angle.

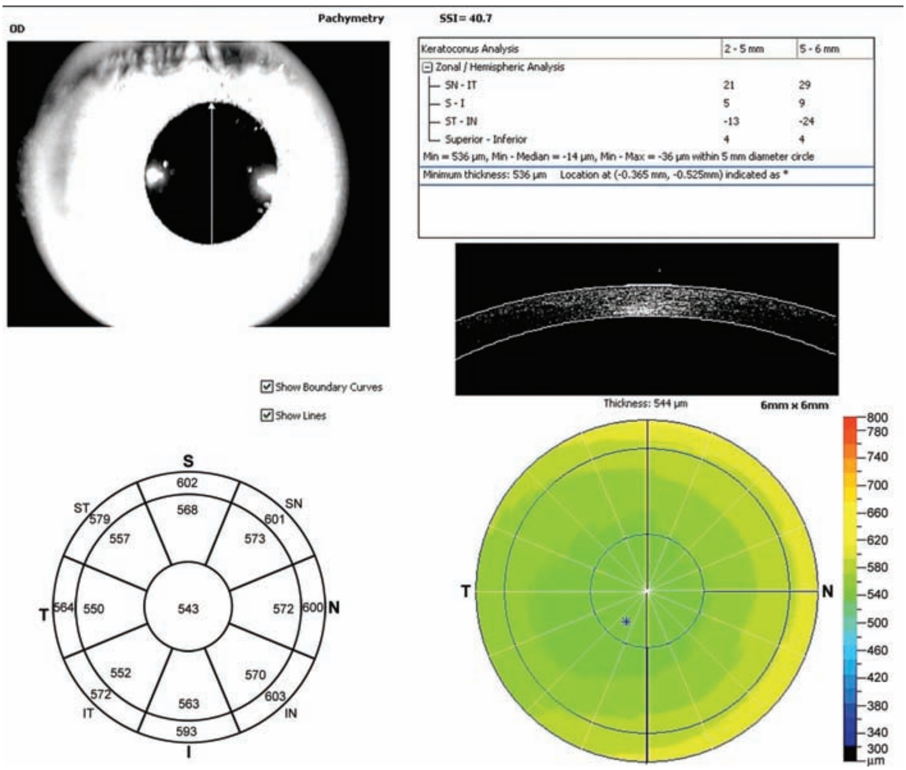

Fig. 3.4 OCT pachymetry map. In the upper right is KC detection indices.

Diagnosis

Anterior OCT is used to aid diagnosis of several pathologies, but we are concerned here in what is related to refractive surgery.

Corneal Lesions

1. Sub Bowman Calcifications (SBCs):
   Case 1: A 32 y/o female.
   Figure 3.5 is her Pentacam tomography showing irregular cornea.
   Figure 3.6 is corneal tomogram 3D image showing corneal calcifications.
   Figure 3.7 is anterior OCT showing the location and depth of the calcifications.
   N.B.: Figures 3.5–3.7 are registered under author's name in "Atlas of Ophthalmology: Online Multimedia Database."
   Case 2: 14 y/o male that has bilateral SBCs. His twin brother has the same disease.
   Figure 3.8 is anterior OCT of the right eye showing the location and depth of the calcifications.
   Figure 3.9 is the OCT pachymetry map showing irregular thickness.
   Figure 3.10 is the same eye after treatment with photo therapeutic keratectomy (PTK).
   Figure 3.11 is the OCT pachymetry map post-PTK; notice the regular pattern.

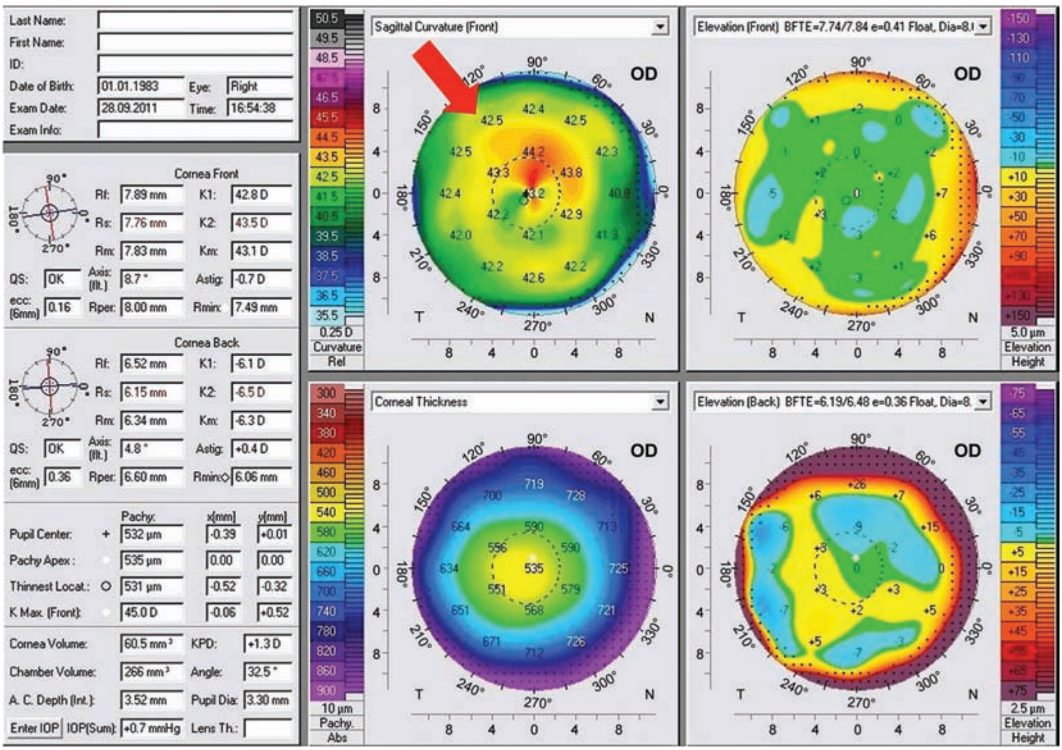

Fig. 3.5 Sun Bowman Calcifications (SBCs). Corneal tomography; notice the AB/SS pattern (red arrow).

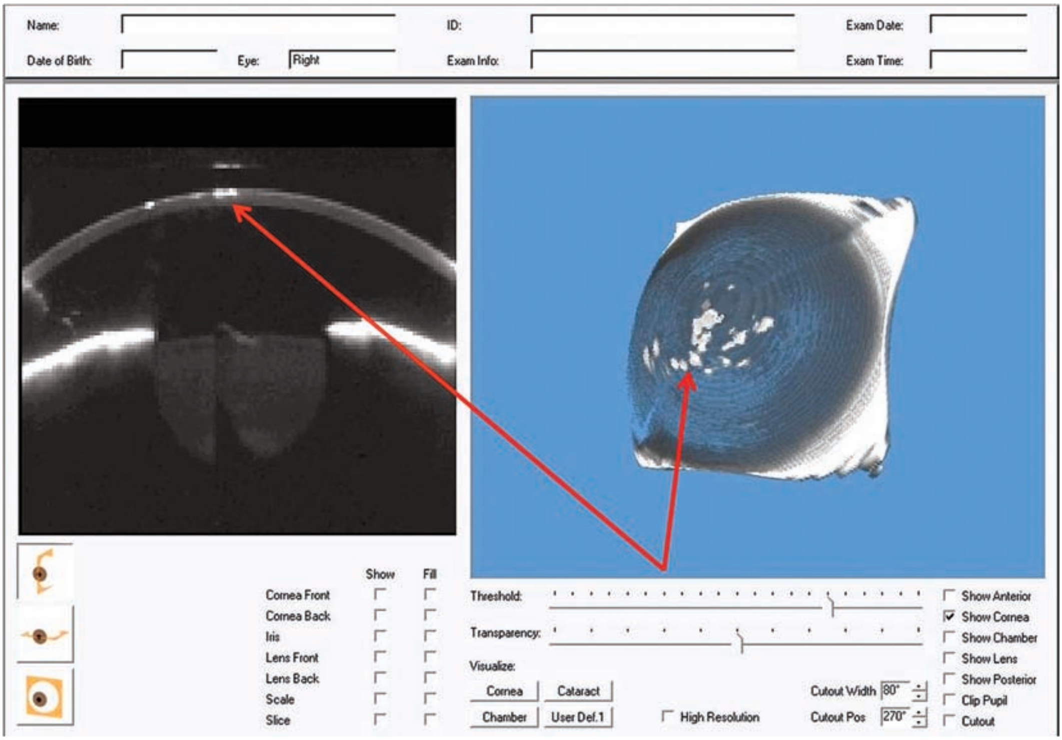

Fig. 3.6 SBCs. Scheimpflug tomogram; red arrows point at the calcifications.

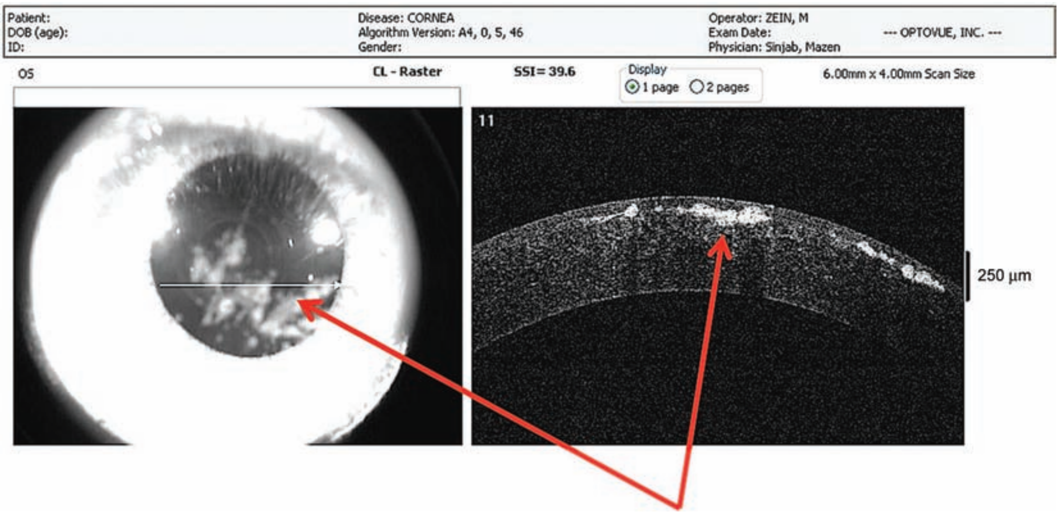

Fig. 3.7 SBCs. OCT view; red arrows point at the calcifications. Thickness and depth of the calcifications can be measured by OCT.

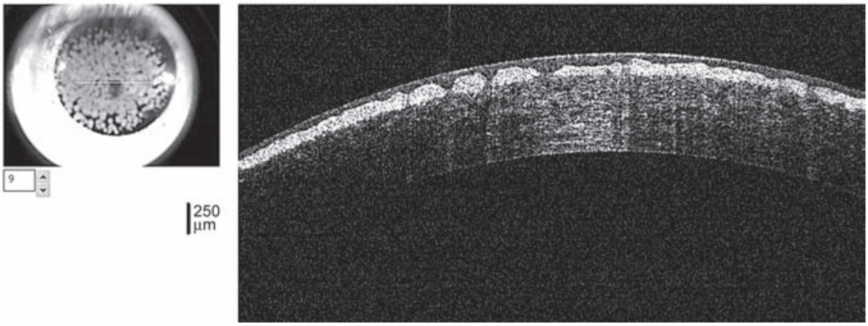

Fig. 3.8 SBCs. OCT view of a cornea with a severe bilateral disease in a twin of males.

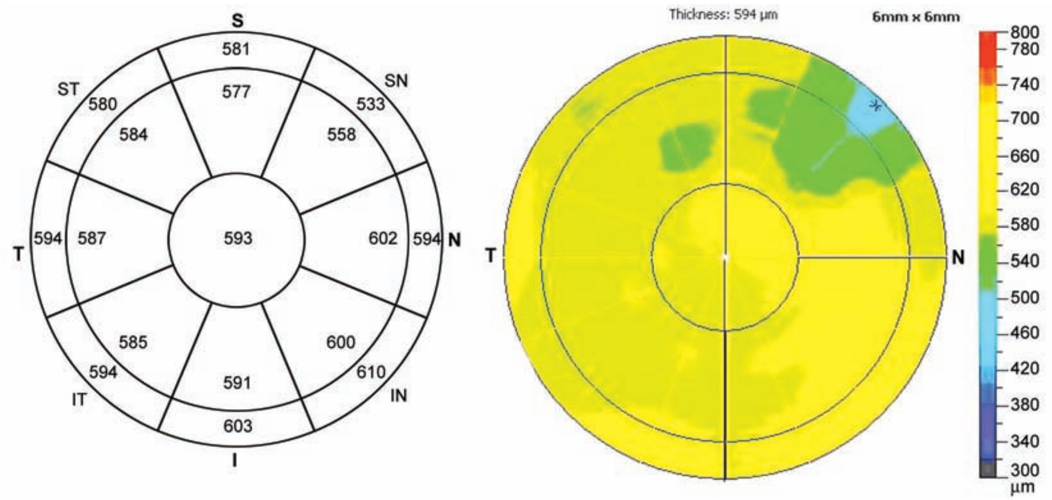

Fig. 3.9 SBCs. OCT pachymetry map; irregular thickness.

Fig. 3.10 SBCs. OCT view after PTK treatment.

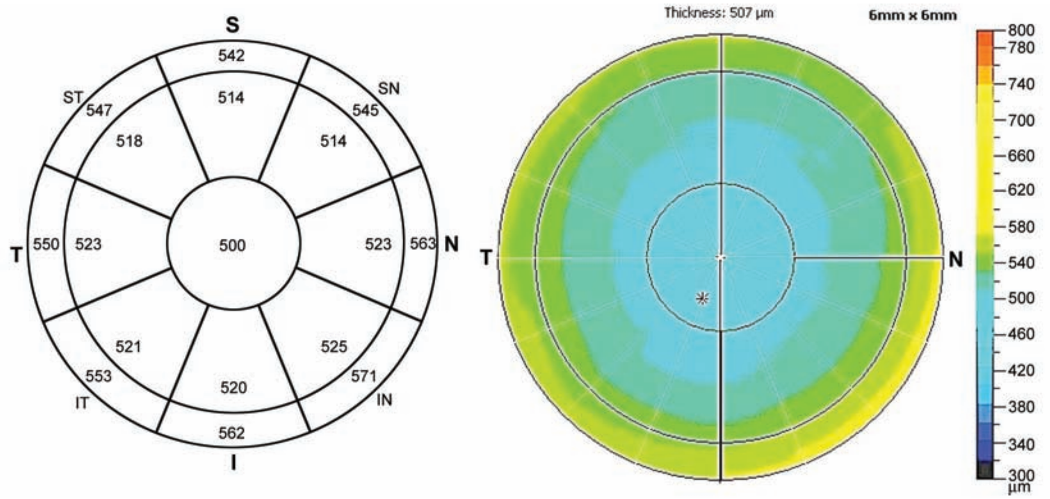

Fig. 3.11 SBCs. OCT pachymetry map after PTK treatment; regular thickness.

2. Salzmann's Nodular Degeneration (SND):
   Salzmann's nodular degeneration (SND) is a lesion located above Bowman layer as shown in Figures 3.12 and 3.13. Figure 3.14 is the OCT pachymetry map showing the thickened part of the cornea, corresponding to the nodule (red arrow).
3. Posterior corneal abnormality:
   Posterior corneal abnormality includes Descemet folds (Fig. 3.15), cornea guttata and Fuch's endothelial dystrophy (Fig. 3.16).

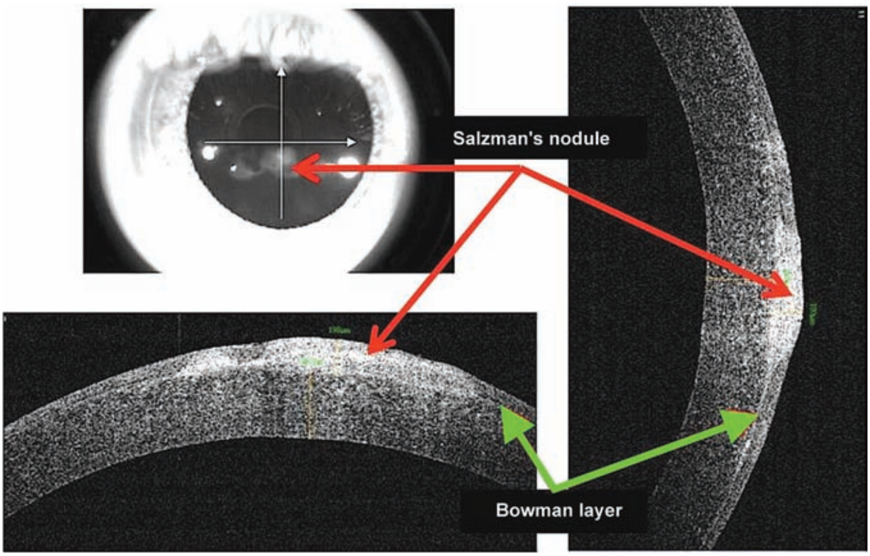

Fig. 3.12 Salzmann's nodular degeneration (SND). OCT view; the red arrows point at the nodules; the green arrows point at Bowman.

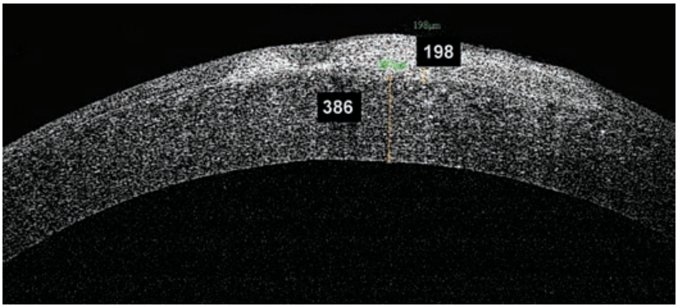

Fig. 3.13 SND. Magnified OCT view; notice the position of the nodule above Bowman layer. The lesion measures about 200 µm, while the cornea measures about 400 µm (apart from lesion).

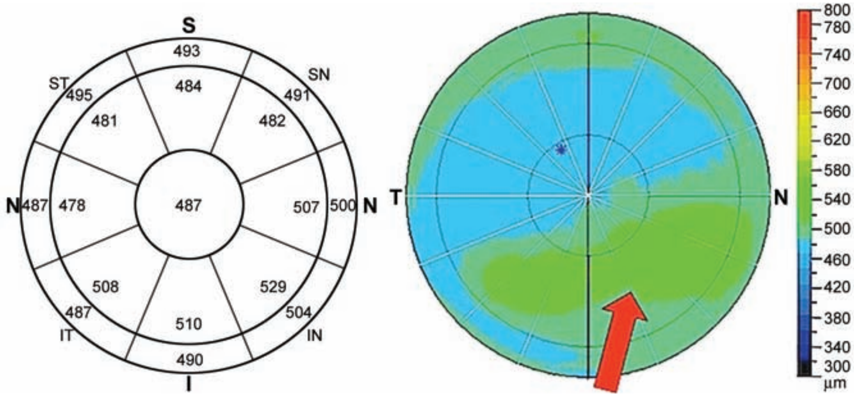

Fig. 3.14 SND. OCT pachymetry map; the red arrow points at the thick area in the map corresponding to the lesion.

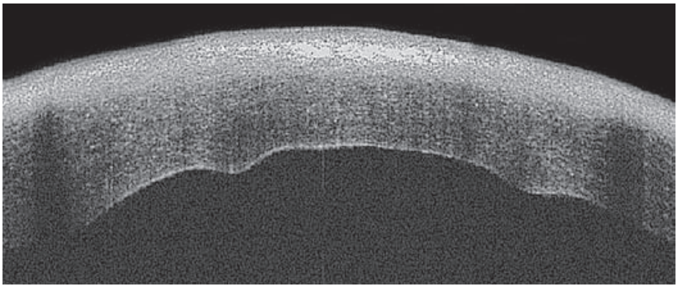

Fig. 3.15 OCT view of posterior corneal abnormality due to Descemet folds. Notice irregularity of the posterior surface.

LASIK Flap Complications

One of the major causes of induced HOAs after LASIK is related to flap cut. OCT provides a good method of measuring flap thickness and shape. Flaps created with femtosecond tend to be more uniform and regular than those created with mechanical microkeratome (MMK). Figures 3.17 to 3.22 show the difference between MMK cut and femtosecond cut by means of central vs. peripheral and right vs. left.

Use of anterior OCT in post LASIK complications will be discussed in chapter 8.

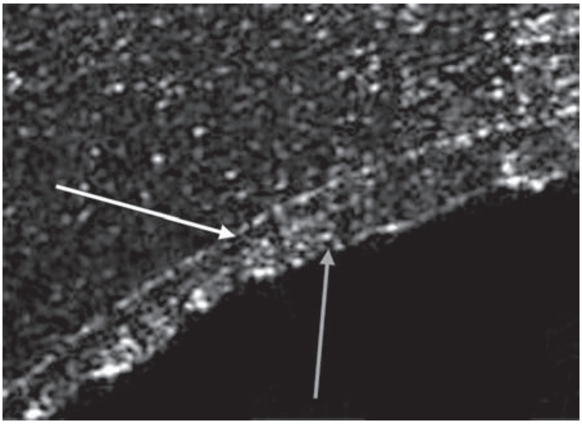

Fig. 3.16 OCT view of posterior corneal abnormality due to Fuch's endothelial dystrophy. The white arrow points at Descemet membrane and the gray arrow points at abnormal endothelial layer.

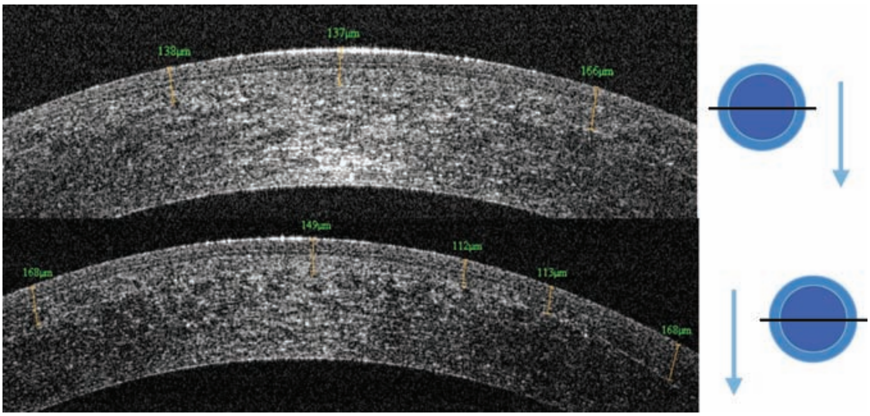

Fig. 3.17 Flap cut with MMK. A comparison between the two eyes. The upper OCT view is for the right eye and the lower is for the left. Notice the difference in thickness; the right flap is thinner than the left flap since the former was performed first.

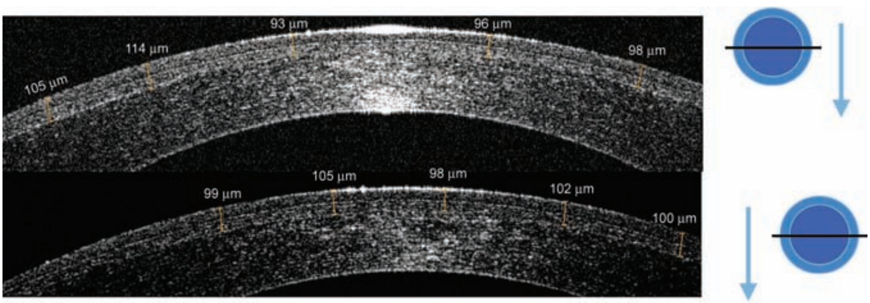

Fig. 3.18 Flap cut with femtosecond laser. A comparison between the two eyes. The upper OCT view is for the right eye and the lower is for the left. There is no significant difference in thickness.

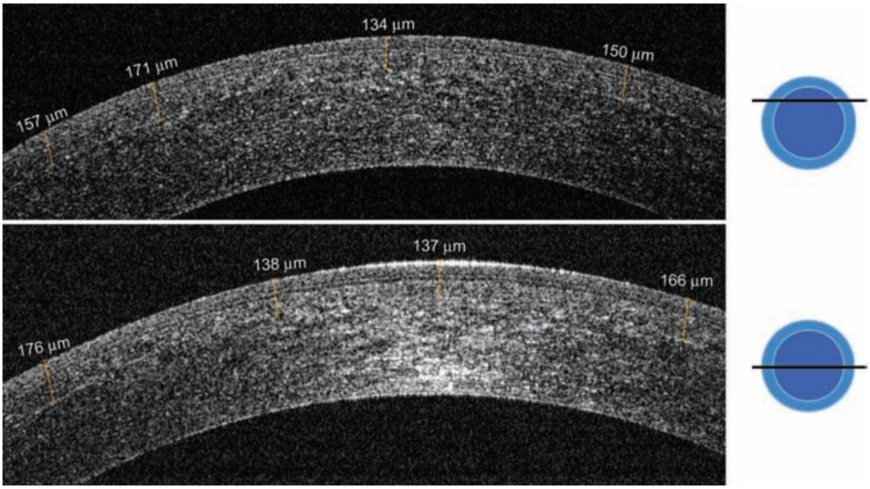

Fig. 3.19 Flap cut with MMK. A comparison between flap periphery (upper OCT view) and flap center (lower OCT view). Both views are comparable but the flap is irregular along both cuts.

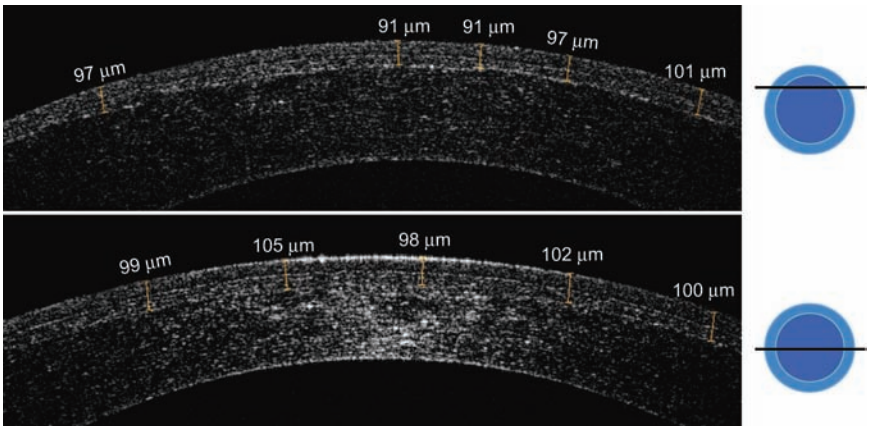

Fig. 3.20 Flap cut with femtosecond laser. A comparison between flap periphery (upper OCT view) and flap center (lower OCT view). Notice the uniform regular cut in both views and along the cuts.

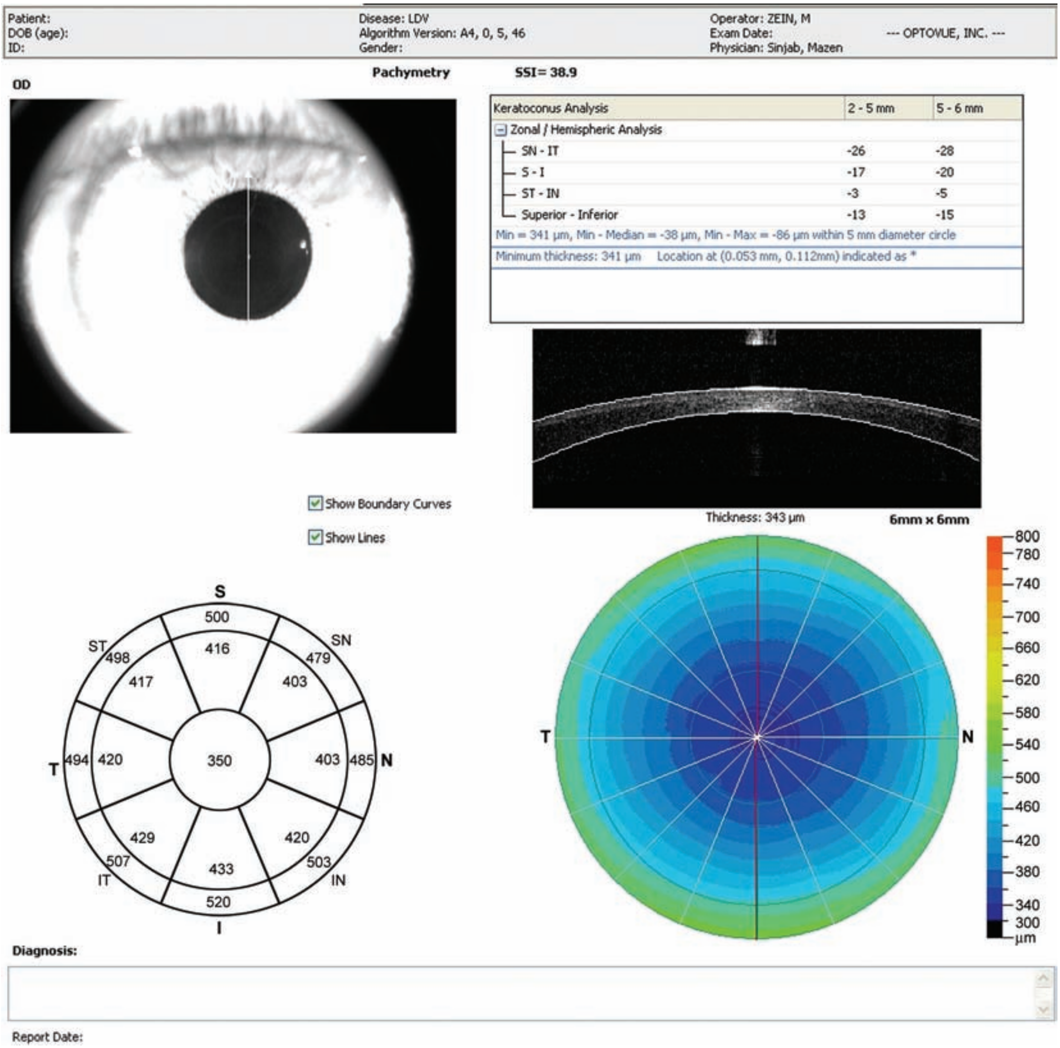

Fig. 3.21 OCT pachymetry after femtosecond flap creation in the right eye. Notice the regular concentric pattern.

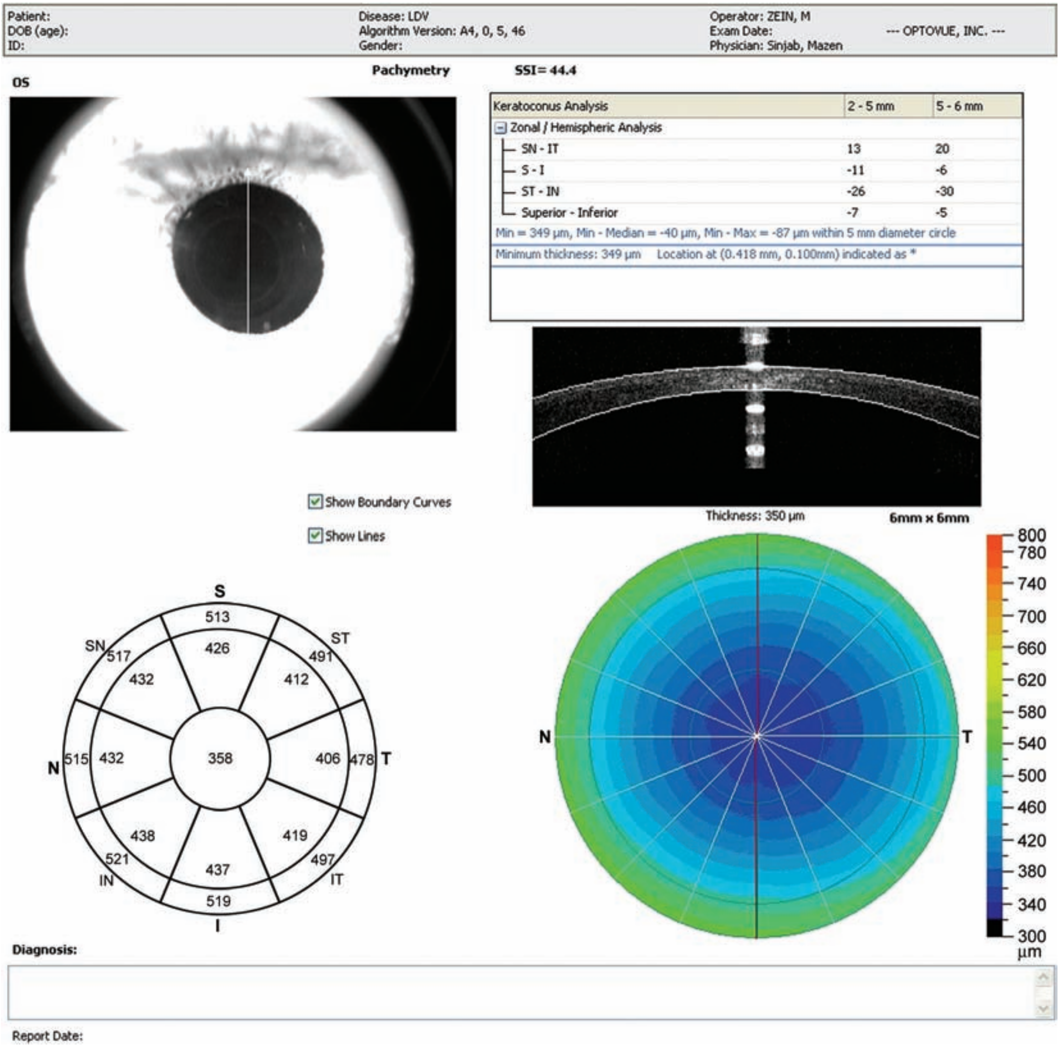

Fig. 3.22 OCT pachymetry after femtosecond flap creation in the left eye. Notice the regular concentric pattern which is quite similar to that in the right eye in the previous figure.

Double Anterior Chamber

One of the causes of graft failure after deep anterior lamellar keratoplasty (DALK) is Descemet membrane dehiscence. The best method to diagnose the problem is to use OCT. Figure 3.23 is an OCT view showing edematous lamellar graft with dehiscent Descemet membrane (red arrow).

OCT is also useful in detecting double Descemet membrane after DALK due to incomplete removal of the membrane from the donor.

Keratoconus Detection

OCT measures corneal thickness and gives a pachymetry map. Figure 3.24 shows a pachymetry map which consists of two parts, indices in the upper part (within red rectangle) and the pachymetry map per se in the lower part.

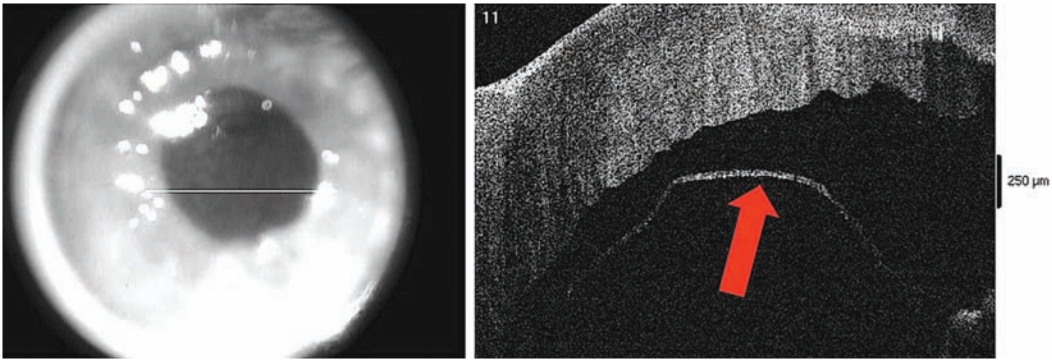

Fig. 3.23 OCT view of a double anterior chamber after DALK due to dehiscent Descemet membrane (red arrow); notice the edematous graft.

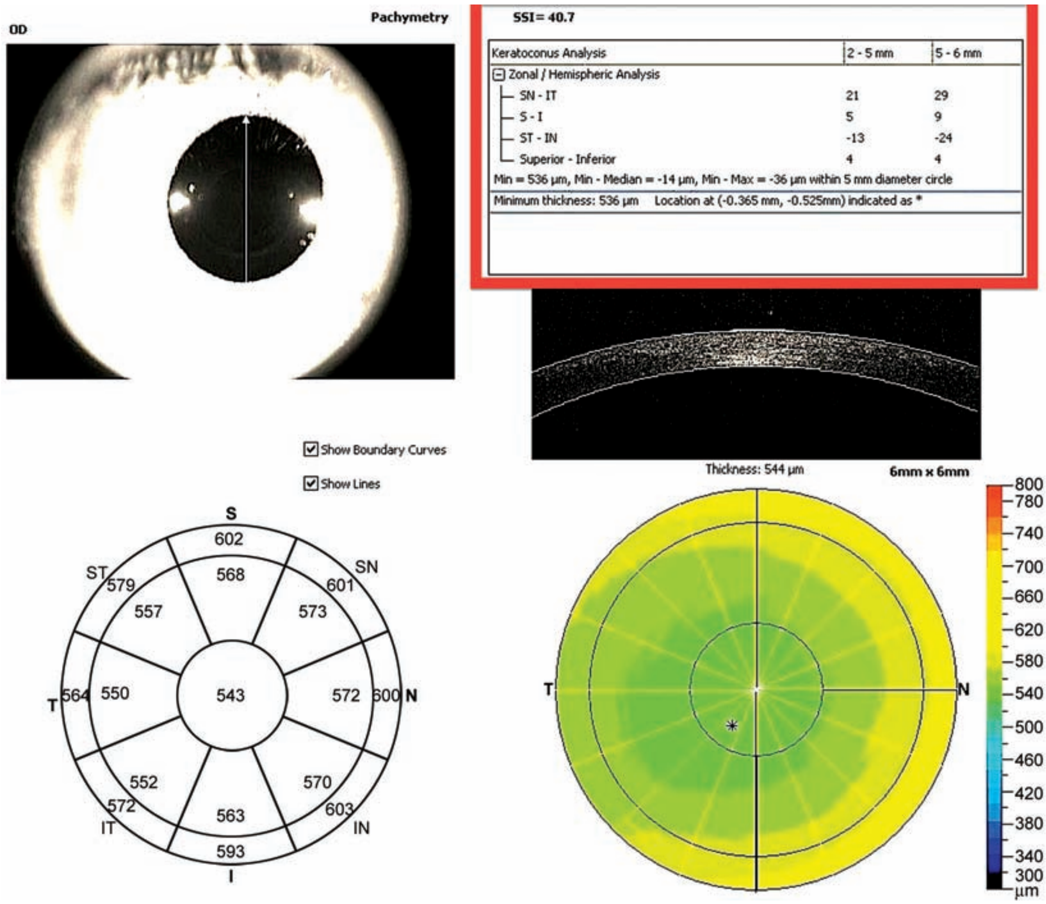

Fig. 3.24 OCT pachymetry map. It consists of two parts: Indices for KC detection (red rectangle), and the map per se.

KC indices are:

1. Thickness at the thinnest location: cut-off value = 470 µm
2. Inferior displacement of thinnest location: cut-off value = –716 µm
3. Focal thinning index: minimum-median: cut-off value = –62.6 µm
4. Inferior-superior (I-S): cutoff value = –31.3 µm
5. Inferotemporal-superionasal (IT-SN): cut-off value = –48.2 µm

Pachymetry Map

The shape of the pachymetry map is also important; in early KC, focal thinning with eccentric pattern can be seen as shown in Figure 3.25 (red arrow). Compare this figure with normal concentric map shown in Figure 3.23.

New epithelial pachymetry map is being developed. This map will be much accurate than the full pachymetry map since in KC and ectatic corneal disorders the epithelium thins over the cone before any irregularity appears either on the full pachymetry map or on corneal tomography.

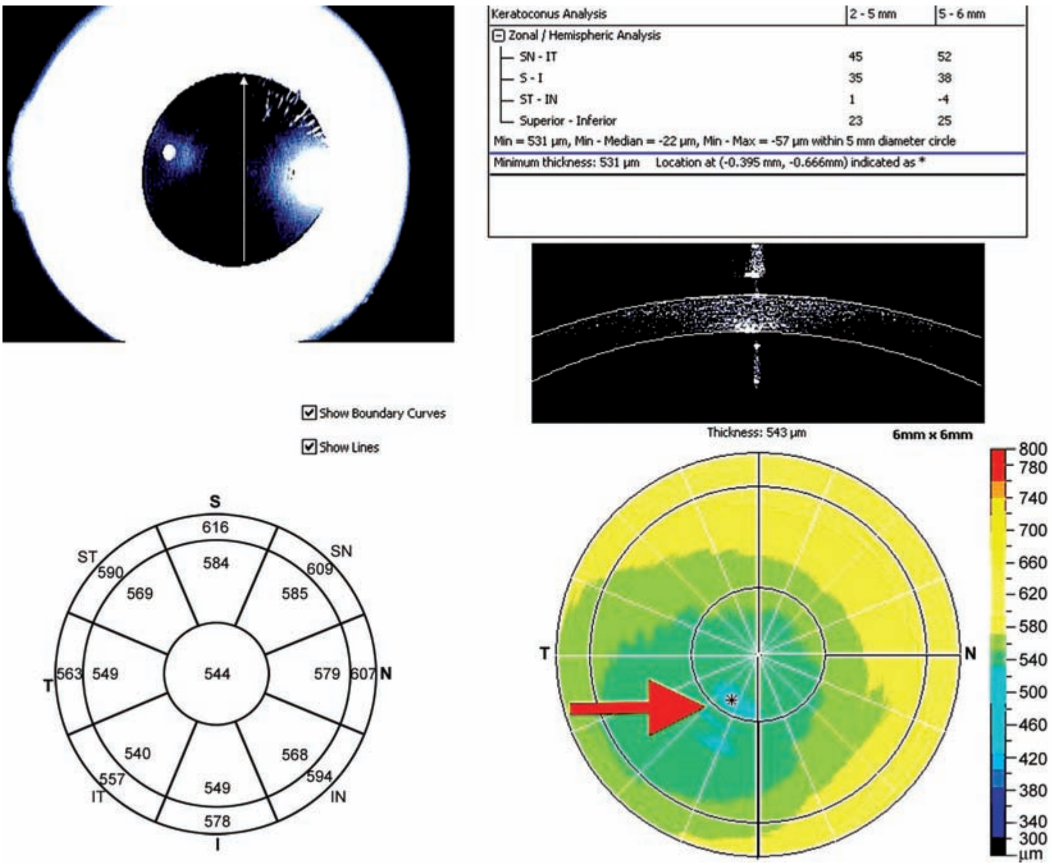

Fig. 3.25 OCT pachymetry map in early KC. Focal thinning with eccentric shape (red arrow). This can be obvious by changing the color scale.

Keratoglobus

In keratoglobus, there is a generalized thinning of the cornea.
Figure 3.26 is the OCT view, Figure 3.27 is the OCT pachymetry map, Figure 3.28 is the Scheimpflug image and Figure 3.29 is corneal tomography. Notice the generalized thinning in all these maps.

Measuring Corneal Power and Pupil Diameter

Treatment

OCT aids in guiding treatment in the following situations:

Guiding PTK

OCT is mandatory before PTK since it gives answers to the following questions:

1. Why PTK?
   OCT measures the depth and the thickness of corneal opacity. When the opacity is very deep, corneal grafting is the solution. When the pathology is above Bowman as in SND, manual

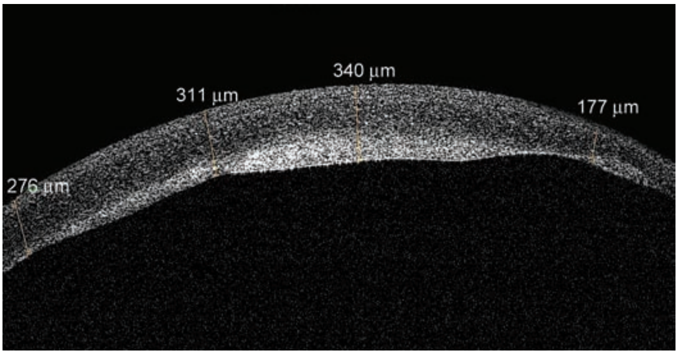

Fig. 3.26 Keratoglobus. OCT view; notice the generalized thinning.

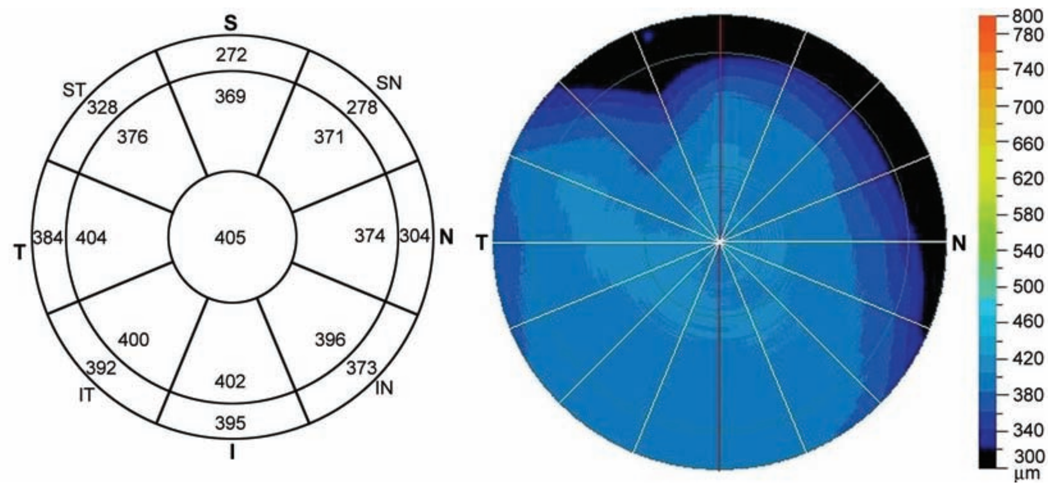

Fig. 3.27 Keratoglobus. OCT pachymetry map; notice the generalized thinning.

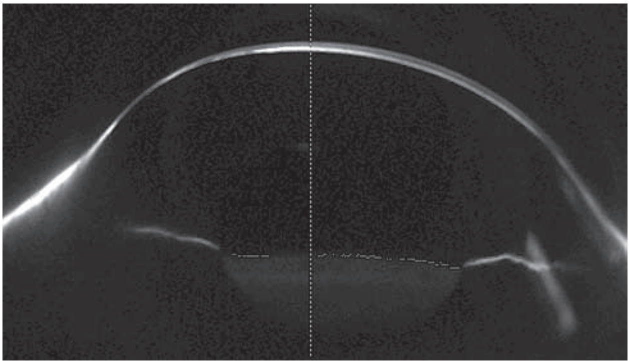

Fig. 3.28 Keratoglobus. Scheimpflug image; notice the generalized thinning.

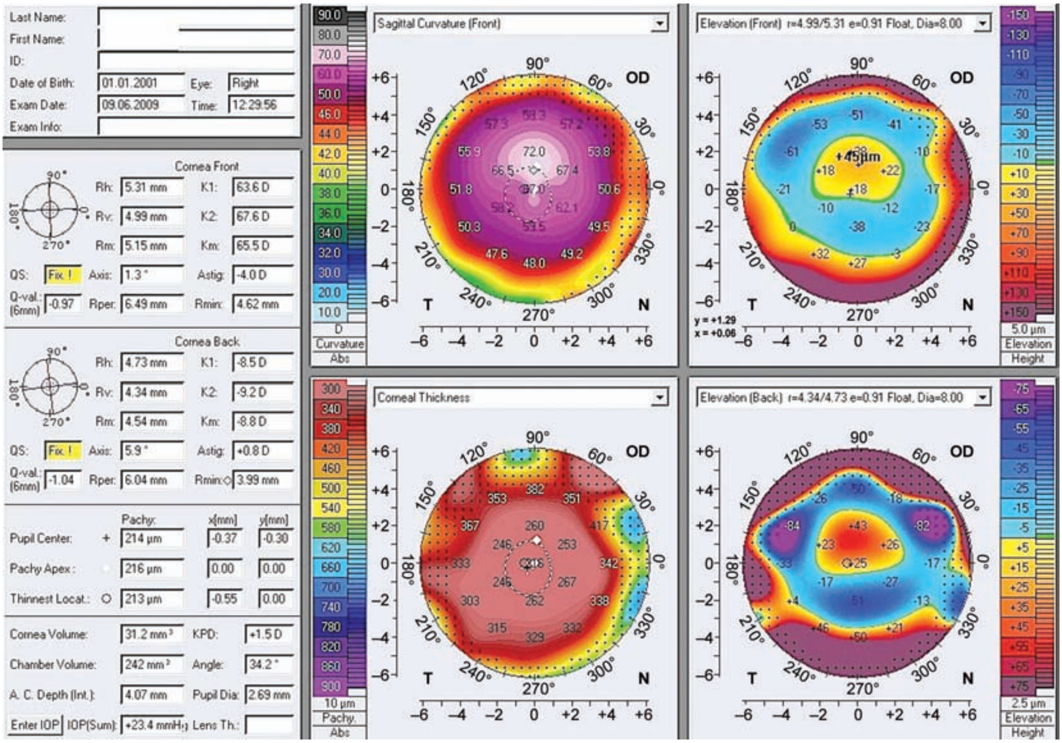

Fig. 3.29 Keratoglobus. Corneal tomography; notice the generalized thinning.

surgical peeling is the solution. When the opacity is superficial as in SBC and superficial corneal haze, PTK is the solution.

2. What is the depth of PTK:

   Figures 3.30 and 3.31 represent corneal haze after surface ablation. On OCT, depth of haze from the surface is measured. As a guideline, it is recommended not to ablate more than 80 µm without the epithelium. Therefore, if the distal depth of the opacity from the surface is 150 µm and the measured epithelium is 50 µm, the opacity is 150 – 50 = 100 µm deep in the

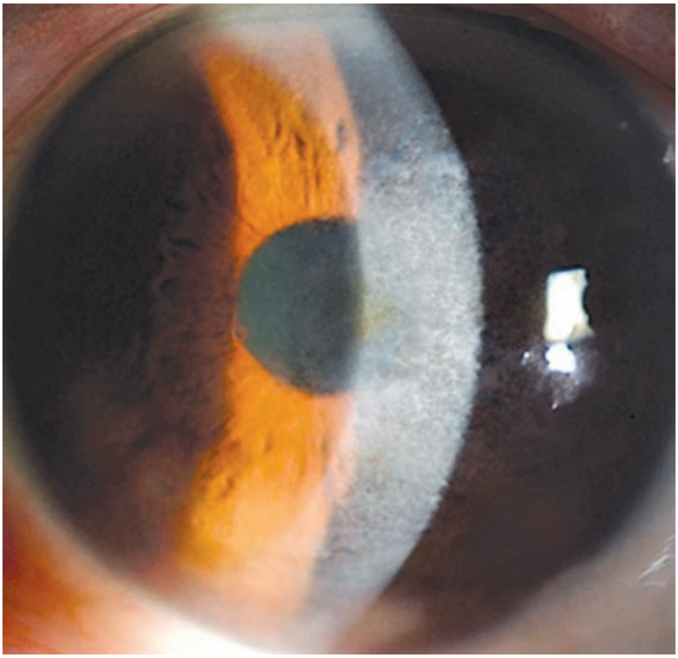

Fig. 3.30 Corneal haze after surface ablation.

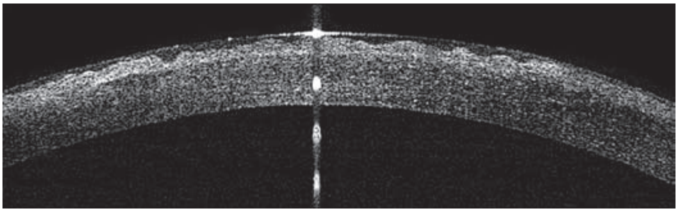

Fig. 3.31 OCT view of corneal haze after surface ablation.

stroma. According to the mentioned guideline, about 100 – 80 = 20 µm of the opacity will remain; in spite of this, visual acuity will significantly improve since the bulk of the opacity has been removed.

3. What is the induced refractive error:
   PTK induces a small amount of refractive error, which can be treated either during or after the surgery. The amount of induced refractive error can be calculated using the formula:
   [–0.29 + 0.141 x (PTK depth – CET) – 0.159 x (CET – PET) – refractive ablation setting]
   Where: CET is central epithelial thickness; PET is peripheral epithelial thickness; refractive ablation setting = the amount of attempted correction if any; i.e. if no correction is attempted, this will be 0.

Photoablation Enhancement

Post photorefractive enhancement is not rare, but in case of faint corneal haze, OCT pachymetry is much more accurate than tomography pachymetry.

Post Corneal Cross Linking Follow-up

Corneal cross linking (CXL) is indicated to stop progression of KC and ectatic corneal disorders (see chapter 5). In CXL, the anterior part of the cornea is crosslinked; therefore, a demarcation line separating the anterior crosslinked part from the posterior uncross linked part appears on OCT (Fig. 3.32). This demarcation line occurs due to the difference in light reflectivity between the two parts (virtual dotted lines). This phenomenon appears by the third postoperative month. In case of absence of this phenomenon, CXL should be repeated since it has failed.

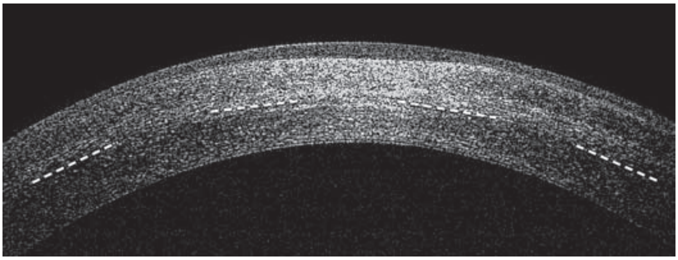

Fig. 3.32 OCT view of the demarcation line encountered after corneal cross linking. The virtual dotted white line indicates the level of the demarcation line.

Implantation of Phakic IOLs (PIOLs)

OCT gives measurements to ACD and ACA and can help in decision-making for glaucoma and for PIOL implantation (see chapter 5).

Before implanting a PIOL, OCT measures WTW, ACD and ACA. After implanting a posterior PIOL, OCT measures the vault (space between PIOL and the crystalline lens). The ideal vault is 350–700 µm. When the vault is <350 µm, there is a risk of touch and cataract formation, a risk of PIOL rotation which is visually important in case of toric PIOL and a risk of continuous sulcus and iris irritation. When the vault is >700 µm, there is a risk of pupillary block unless a peripheral iridotomy is patent or the new design with a central hole is used.

In glaucoma, OCT gives measurements that are more accurate than Scheimpflug-based tomography. ACA measurements are given by means of three terms: angle (Fig. 3.33), angle opening distance at 500 µm (AOD_{500}) and trabecular-iris space at 500 µm ($TISA_{500}$) (Fig. 3.34). In spite of the importance of AOD and TISA, they still need to be normalized.

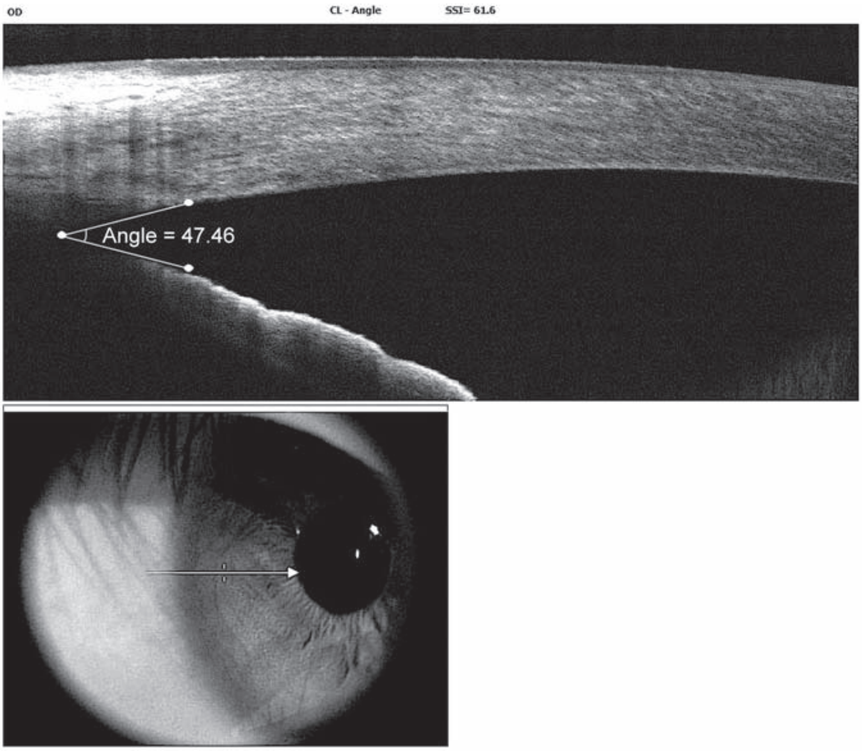

Fig. 3.33 Anterior chamber angle measured with OCT.

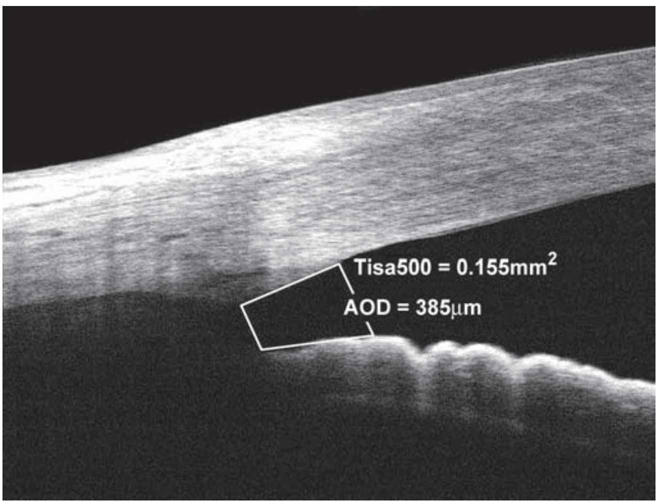

Fig. 3.34 Parameters of Anterior chamber angle measured with OCT.

TAKE-HOME MESSAGE

- OCT is an essential investigational tool in refractive surgery for diagnosis and treatment
- It is important to diagnose corneal lesions, LASIK flap complications, double AC after DALK, keratoconus detection, keratoglobus and glaucoma
- It is important in guiding PTK, LASIK enhancement, CXL follow up and planning for PIOL implantation

BIBLIOGRAPHY

1. Baïkoff G, Lutun E, Ferraz C, et al. Static and dynamic analysis of the anterior segment with optical coherence tomography. J. Cataract Refract Surg. 2004;30(9):1843-50.
2. Baïkoff G, Lutun E, Wei J, et al. Contact between 3 phakic intraocular lens models and the crystalline lens: an anterior chamber optical coherence tomography study. J Cataract Refract Surg. 2004;30(9):2007-12.
3. Ceylan OM, Turk A, Erdurman C et al. Comparison of Oculus Pentacam and Stratus optical coherence tomography for measurement of central corneal thickness. Cornea. 2011;30(6):670-4.
4. Dada T, Sihota R, Gadia R, et al. Comparison of anterior segment optical coherence tomography and ultrasound biomicroscopy for assessment of the anterior segment. J Cataract Refract Surg. 2007;33(5):837-40.
5. Das S, Link B, Seitz B. Salzmann's nodular degeneration of the cornea: a review and case series. Cornea. 2005;24(7):772-7.
6. Dawczynski J, Koenigsdoerffer E, Augsten R, et al. Anterior optical coherence tomography: a non-contact technique for anterior chamber evaluation. Graefe's Arch Clin. Exp. Ophthalmol. 2007;245(3):423-5.
7. Dinc U, Gorgun E, Oncel B, et al. Assessment of anterior chamber depth using Visante optical coherence tomography, slitlamp optical coherence tomography, IOL master, Pentacam and Orbscan II. Ophthalmologica. 2010;224(6):341-6.
8. Fujimoto JG. Optical coherence tomography: introduction. In: Bourna BE, Tearney GJ. Handbook of Optical Coherence Tomography. New York: Marcel Dekker. 2002;1-40.
9. Gabriele ML, Wollstein G, Ishikawa H, et al. Optical coherence tomography: history, current status, and laboratory work. Invest. Ophthalmol Vis. Sci. 2011;52(5):2425-36.
10. Garcia JPS, Rosen RB. Anterior segment imaging: optical coherence tomography versus ultrasound biomicroscopy. Ophthalmic Surg. Lasers Imaging. 2008;39(6):476-84.
11. Goins KM, Wagoner MD. Focal points: Imaging the anterior segment. American academy of ophthalmology. 2009;27(11):1-17.
12. Goldsmith JA, Li Y, Chalita MR, et al. Anterior chamber width measurement by high-speed optical coherence tomography Ophthalmology. 2005;112(2):238-44.
13. Huang D, Swanson EA, Lin CP, et al. Optical coherence tomography. Science. 1991;254(5035):1178-81.
14. Hurmeric, V, Yoo SH, Karp CL, et al. In vivo morphologic characteristics of Salzmann nodular degeneration with ultra-high-resolution optical coherence tomography. Am. J. Ophthalmol. 2011;151(2):248-56.
15. Hurmeric V, Wang J and Yoo SH. Ultra-high-resolution optical coherence tomography imaging in LASIK. ASCRS (Abstract 983431); 2011.
16. Ide T, Wang J, Tao A, et al. Intraoperative use of three-dimensional spectral-domain optical coherence tomography. Ophthalmic Surg. Lasers Imaging. 2010;41(2):250-4.
17. Ide T, Yoo SH, Kymionis G, et al. Double Descemet's membranes after penetrating keratoplasty with anterior segment optical coherence tomography. Ophthalmic Surg. Lasers Imaging. 2008;39(5):422-5.
18. Jagow von B, Kohnen T. Corneal architecture of femtosecond laser and microkeratome flaps imaged by anterior segment optical coherence tomography. J. Cataract Refract. Surg. 2009;35(1):35-41.
19. Kalev-Landoy M, Day AC, Cordeiro MF, et al. Optical coherence tomography in anterior segment imaging. Acta Ophthalmol. 2007;85(4):427-30.

20. Karnowski K, Kaluzny BJ, Szkulmowski M, et al. Corneal topography with high-speed swept source OCT in clinical examination. Biomed Opt Express. 2011;2(9):2709-20.
21. Kymionis GD, Suh LH, Dubovy SR, et al. Diagnosis of residual Descemet's membrane after Descemet's stripping endothelial keratoplasty with anterior segment optical coherence tomography. J. Cataract Refract Surg. 2007;33(7):1322-4.
22. Li Y, Meisler DM, Tang M, et al. Keratoconus diagnosis with optical coherence tomography pachymetry mapping Ophthalmology. 2008;115(12):2159-66.
23. Li Y, Netto M, Shekhar R, et al. A longitudinal study of LASIK flap and stromal thickness with high-speed optical coherence tomography. Ophthalmology. 2007;114(6):1124-32.
24. Lim LS, Aung HT, Aung T, et al. Corneal imaging with anterior segment optical coherence tomography for lamellar keratoplasty procedures. Am. J. Ophthalmol. 2008;145(1):81-90.
25. Milla M, Piñero DP, Amparo F, et al. Pachymetric measurements with a new Scheimpflug photography-based system: intra observer repeatability and agreement with optical coherence tomography pachymetry. J. Cataract Refract Surg. 2011;37(2):310-6.
26. Nakagawa T, Maeda N, Higashiura R, et al. Corneal topographic analysis in patients with keratoconus using 3-dimensional anterior segment optical coherence tomography. J Cataract Refract Surg. 2011;37(10):1871-8.
27. Nolan W. Anterior segment imaging: ultrasound biomicroscopy and anterior segment optical coherence tomography. Curr. Opin. Ophthalmol. 2008;19(2):115-21.
28. Rosas SCH, Li Y, Zhang X, et al. Repeatability of laser in situ keratomileusis flap thickness measurement by Fourier-domain optical coherence tomography. J Cataract Refract Surg. 2011;37(4):649-54.
29. Schuman JS. Ophthalmic imaging and diagnostics. Ophthalmology Clinics of North America. 1998;11:1-490.
30. Shen M, Wang MR, Yuan Y, et al. SD-OCT with prolonged scan depth for imaging the anterior segment of the eye. Ophthal. Surg. Lasers Imaging. 2010;41(6):S65-9.
31. Shousha MA, Perez VL, Wang J, et al. Use of ultra-high-resolution optical coherence tomography to detect in vivo characteristics of Descemet's membrane in Fuchs' dystrophy. Ophthalmology. 2010;117(6):1220-7.
32. Stahl JE, Durrie DS, Schwendeman FJ, et al. Anterior segment OCT analysis of thin Intralase femtosecond flaps. J Refract Surg. 2007;23(6):555-8.
33. Suh LH, Shousha MA, Ventura RU, et al. Epithelial ingrowth after Descemet stripping automated endothelial keratoplasty: description of cases and assessment with anterior segment optical coherence tomography. Cornea. 2011;30(5):528-34.
34. Tan AN, Sauren LDC, de Brabander J, et al. Reproducibility of anterior chamber angle measurements with anterior segment optical coherence tomography. Invest. Ophthalmol. Vis. Sci. 2011;52(5):2095-9.
35. Tang M, Chen A, Li Y, et al. Corneal power measurement with Fourier-domain optical coherence tomography. J Cataract Refract Surg. 2010;36(12):2115-22.
36. Vajzovic LM, Karp CL, Haft P, et al. Ultra high-resolution anterior segment optical coherence tomography in the evaluation of anterior corneal dystrophies and degenerations. Ophthalmology. 2011;118(7):1291-6.
37. Wollstein G, Paunescu LA, Ko TH, et al. Ultrahigh-resolution optical coherence tomography in glaucoma. Ophthalmology. 2005;112(2):229-37.
38. Wylegała E, Nowińska A. Usefulness of anterior segment optical coherence tomography in Descemet membrane detachment. Eur. J. Ophthalmol. 2009;19(5):723-8.
39. Yazici AT, Bozkurt E, Alagoz C, et al. Central corneal thickness, anterior chamber depth, and pupil diameter measurements using Visante OCT, Orbscan, and Pentacam. J Refract Surg. 2010;26(2):127-33.
40. Yoo SH, Hurmeric V. Femtosecond laser-assisted keratoplasty. Am J Ophthalmol. 2011;151(2):190-1.
41. Yoo SH, Kymionis GD, Deobhakta AA, et al. One-year results and anterior segment optical coherence tomography findings of Descemet stripping automated endothelial keratoplasty combined with phacoemulsification. Arch Ophthalmol. 2008;26(8):1052-5.

CHAPTER 4

Corneal Biomechanics

INTRODUCTION

CORE MESSAGE

- Corneal biomechanics explain some post-refractive surgery phenomena
- Corneal biomechanics are related to the visco-elastic structure of the cornea
- Corneal biomechanics are expressed by many parameters, of which the most important is corneal hysteresis and corneal resistance factor
- Ocular response analyzer measures corneal biomechanics

Definitions

Before going into corneal biomechanics in details, some definitions should be known.

1. *Elasticity:* The property of a substance that enables it to change its length, volume, or shape in *direct* response to a force and to recover its original form upon the removal of the force.
2. *Strain:* It is the deformation that is directly proportional to stress (applied force), independent of the length of time or the rate at which the force is applied.
3. *Viscosity:* Resistance of a fluid (liquid or gas) to a change in shape, or movement of neighboring portions relative to one another. The more viscous a fluid is, the more it resists flow. Honey, for example, has a greater viscosity than water. Resistance to an applied force depends primarily on the speed at which the force is applied.
4. *Damping:* Restraining of vibratory motion, such as mechanical oscillations, by dissipation of energy. Viscous fluids or gasses are employed to accomplish this.
5. *Hysteresis:* The phenomenon was physically identified and the term coined, by Sir James Alfred Ewing in 1890. Hysteresis is a property of physical systems that do not instantly follow the forces applied to them, but react slowly, or do not return completely to their original state.

   The term is medically identified by David Luce, PhD: Corneal Hysteresis (CH) is the difference in the inward and outward pressure values obtained during the dynamic bidirectional applanation process employed in the Ocular Response Analyzer, as a result of viscous damping in the cornea.

Corneal Tissue

Corneal tissue is composed of collagen fibers and a matrix. Collagen fibers are bonded and both fibers and the bonds give the cornea its elastic property, whereas the matrix gives it its viscosity.

Corneal tissue is unique since it is viscoelastic; the more the bonds and fibers are, the more elastic the cornea is, and the more the matrix is, the more viscous the cornea is. In normal cornea, there is a balance between elasticity and viscosity with a slight preponderance towards viscosity. In KC and ectatic corneal disorders the cornea is more viscous. Beside the two main properties of the cornea (viscosity and elasticity), the cornea has rigidity, which is the force resisting flaccidity and keeps the cornea stable. In KC and ectatic corneal disorders, there is a reduction in rigidity. What CXL does is increasing rigidity to stabilize the cornea although it is still viscous.

On the other hand, the anterior two thirds (most important is Bowman layer) of the cornea are more elastic than the posterior third and they are responsible for biomechanical stability. This means that any disturbance in the integrity of the anterior two-thirds will weaken the cornea and will increase the risk of ectasia. This effect is more prominent with deep ablations (such as LASIK) rather than surface ablations (such as PRK) and it is more prominent with larger ablation depth and less residual stromal bed.

CLINICAL IMPACT OF CORNEAL BIOMECHANICS

Biomechanical properties explain many of post refractive surgery phenomena such as regression, iatrogenic irregularities, ectasia and incorrect IOP measurements.

Biomechanics and Myopic Treatment

In old myopic ablation profiles (see chapter 5), ablation leaves a rim at the borders of the treated zone (Fig. 4.1). The elevated rim shrinks (Fig. 4.2), the formed mass bulges inward the anterior chamber (Fig. 4.3), and finally the central part of the cornea bulges outwards (Fig. 4.4) causing myopic regression. This explains myopic regression after myopic ablation especially in high myopic corrections.

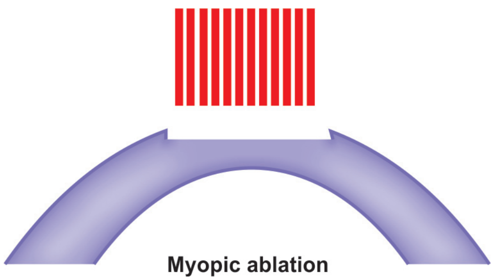

Fig. 4.1 Corneal biomechanics in myopic treatment. Old ablation profiles (no transitional zone) leave a rim of collagen fibers at the borders of the ablated zone.

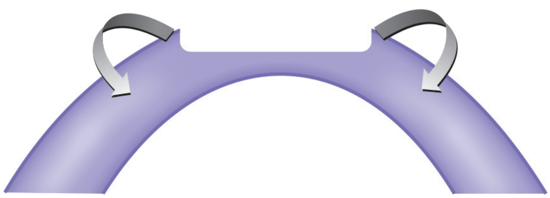

Fig. 4.2 Corneal biomechanics in myopic treatment. Collagen tissue at the rim shrinks inwards.

Biomechanics and Hyperopic Treatment

In hyperopic correction, corneal periphery is ablated (Fig. 4.5) in order to steepen the central part of the cornea and change the slope of the cornea (Fig. 4.6). Since the peripheral part of the cornea is weakened by this ablation, IOP will influence the peripheral part more than the central part (Fig. 4.7), leading to re-flattening of the central part (Fig. 4.8) and hyperopic regression. This effect increases with higher hyperopic corrections.

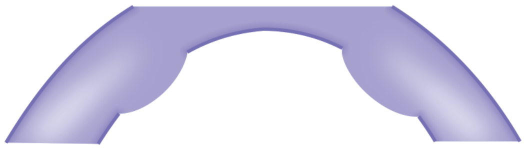

Fig. 4.3 Corneal biomechanics in myopic treatment. Shrunk rim bulges into anterior chamber.

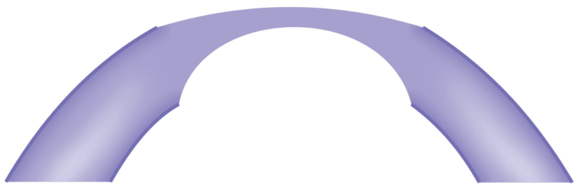

Fig. 4.4 Corneal biomechanics in myopic treatment. Central out bulging is the end stage and myopia regresses.

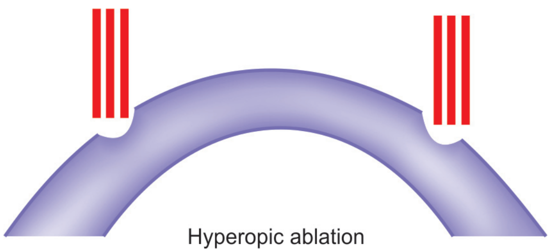

Fig. 4.5 Corneal biomechanics in hyperopic treatment. Corneal periphery is ablated.

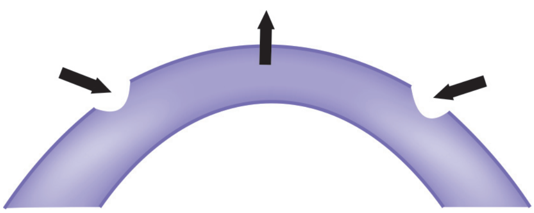

Fig. 4.6 Corneal biomechanics in hyperopic treatment. Central part of the cornea bulges out to compensate for hyperopia.

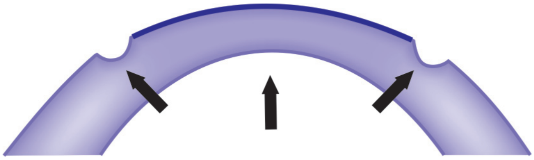

Fig. 4.7 Corneal biomechanics in hyperopic treatment. Ablated area constitutes a weak area that falls under the influence of IOP.

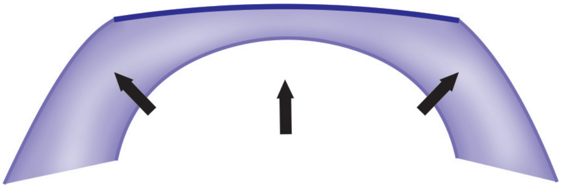

Fig. 4.8 Corneal biomechanics in hyperopic treatment. Under the influence of IOP, the weak zone bulges out causing flattening of corneal center, this in turn causes hyperopic regression.

Biomechanics and Postoperative Induced Irregularities

Whenever there is a difference of ≥ 1D between K-max and steep K, there is an irregularity in the cornea. Figure 4.9 shows a hot spot (high K-max) due to a posterior surface irregularity. Treating hyperopia in such a cornea (Fig. 4.10), will put the cornea under irregular forces (Figs 4.11 and 4.12) and will lead to postoperative irregularity (Figs 4.13 and 4.14).

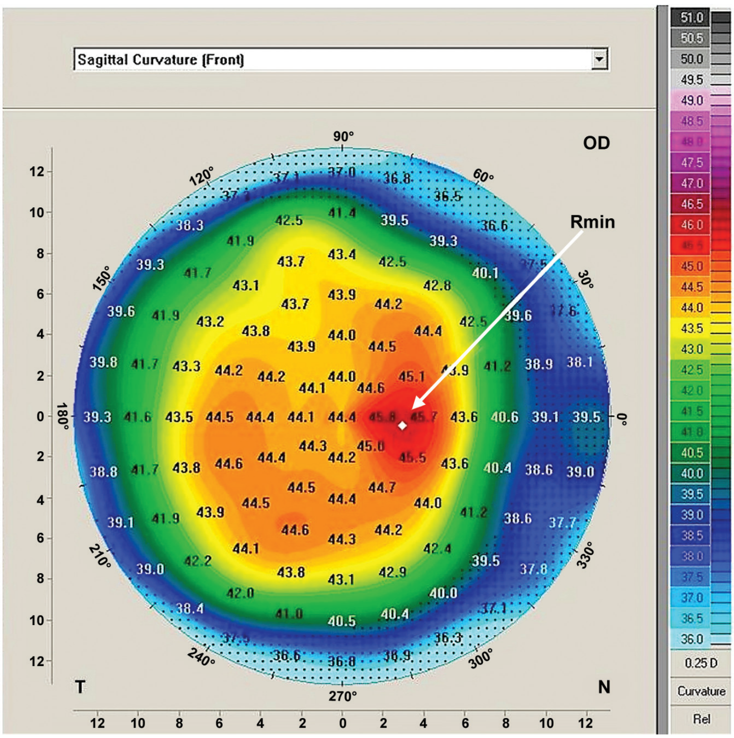

Fig. 4.9 Irregular cornea as it appears on anterior curvature sagittal map. There is > 1D difference between K-max and steep K.

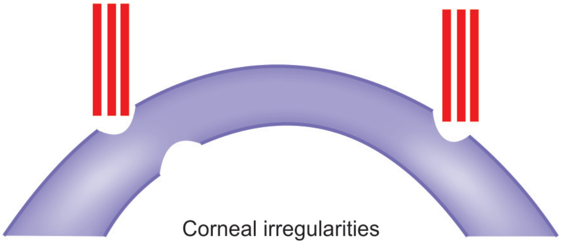

Fig. 4.10 Corneal biomechanics in hyperopic treatment on an irregular cornea.

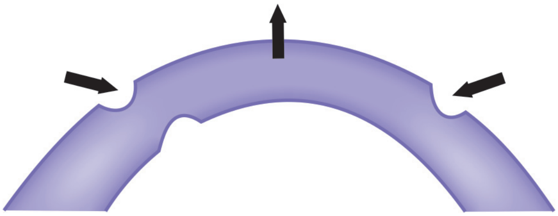

Fig. 4.11 Corneal biomechanics in hyperopic treatment on an irregular cornea. Central part of the cornea bulges out to compensate for hyperopia.

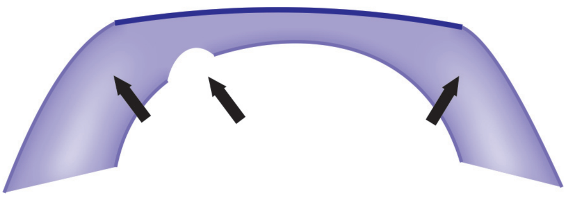

Fig. 4.12 Corneal biomechanics in hyperopic treatment on an irregular cornea. Posterior irregularity falls under the influence of unequal pressure forces.

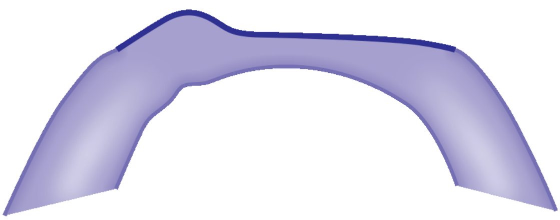

Fig. 4.13 Corneal biomechanics in hyperopic treatment on an irregular cornea. Posterior irregularity causes anterior irregularity.

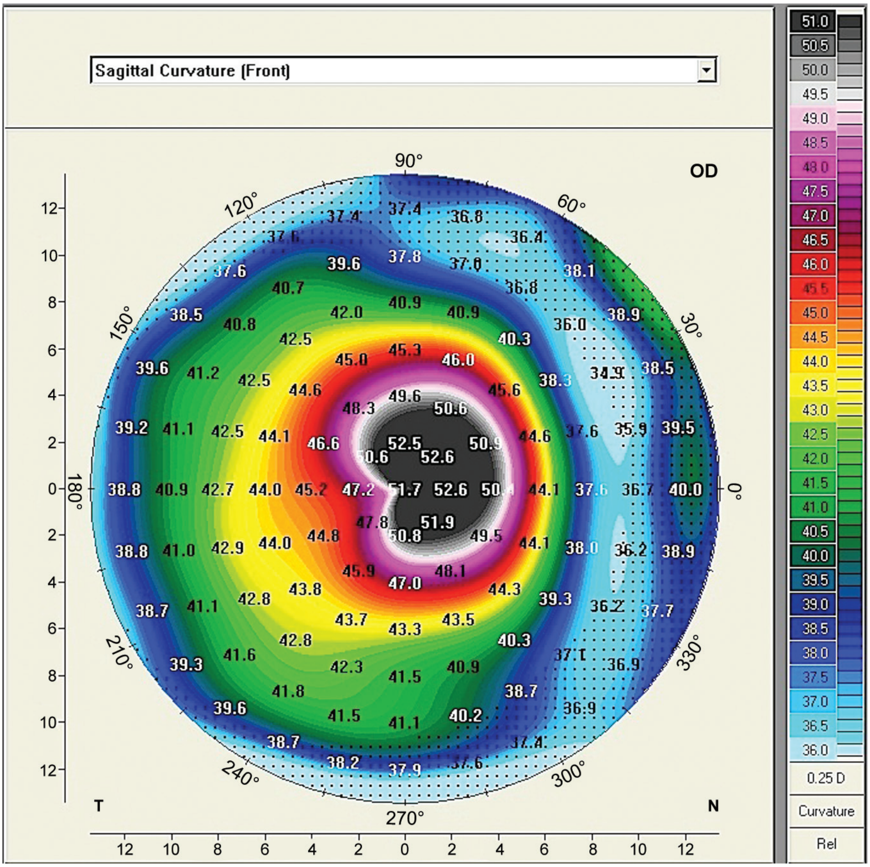

Fig. 4.14 Corneal biomechanics in hyperopic treatment on an irregular cornea. Postoperative irregularity due to preoperative irregularity.

Biomechanics and Induced Ectasia

Corneal biomechanics is the major factor in post surgical iatrogenic ectasia. One of the main risk factors for ectasia is abnormal preoperative tomographic patterns (see chapter 8). Many studies have proven a strong relationship between these abnormal patterns and abnormal corneal biomechanics. On the other hand, it has been shown that there are abnormal biomechanics in corneas with FFKC. Therefore, apparently normal corneas may have the potential of post surgical ectasia and can be discovered by measuring corneal biomechanics.

Biomechanics and Postoperative IOP Measurements

IOP measurements are incorrect after keratorefractive surgeries especially when simply measured by Goldman applanation tonometer since corneal thickness and curvature have changed. The best method to measure IOP in such cases is the Pascal since it is not affected by thickness changes. If unavailable, several methods were suggested. IOP can be measured by Goldman and the readings should be modified according to Pentacam suggestions. Tonopen is

used on the mid periphery of the cornea. Air puff roughly gives approximate readings. Finally, ocular response analyzer (ORA) gives accurate measurements.

MEASURING CORNEAL BIOMECHANICS

Corneal Biomechanics are measured using ORA.

Principle of ORA

A light source directs a parallel light beam towards the cornea and since the cornea is convex the light beam will be reflected as a diverging beam (Fig. 4.15). A light receptor receives the reflected beam and measures its intensity. When the reflected beam is divergent, its intensity is smaller than that of the incident parallel beam. A central perpendicular air puff is sent from a source to indent the cornea; the cornea moves in five phases:

a. *First convex phase:* The air puff has not been sent yet (Fig. 4.15).
b. *First applanation phase (Fig. 4.16):* The air puff pushes the cornea inwards.
c. *Excavation phase (Fig. 4.17):* The cornea is excavated under the influence of the air puff.
d. *Second applanation phase (Fig. 4.18):* The cornea comes outwards after the influence of the air puff has finished.
e. *Second convex phase:* The cornea takes its primary shape (Fig. 4.19).

The light beam changes in these phases in the following five manners:

a. Divergent reflected beam, which intensity is less than the incident parallel beam (Fig. 4.15).
b. Parallel reflected beam, which intensity is equal to the incident beam (Fig. 4.16).
c. Convergent reflected beam, which intensity is less than the incident beam (Fig. 4.17).
d. Parallel reflected beam, which intensity is equal to the incident beam (Fig. 4.18).

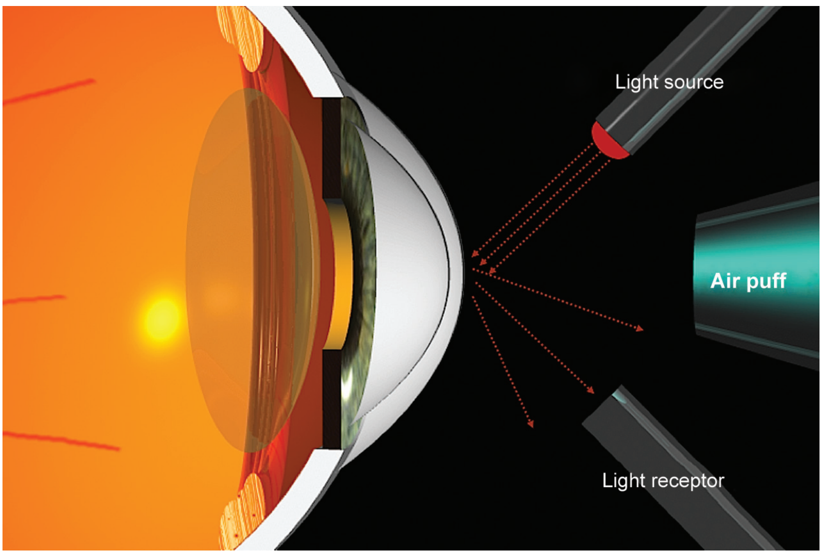

Fig. 4.15 Principle of measuring corneal biomechanics with ORA. First convex phase.

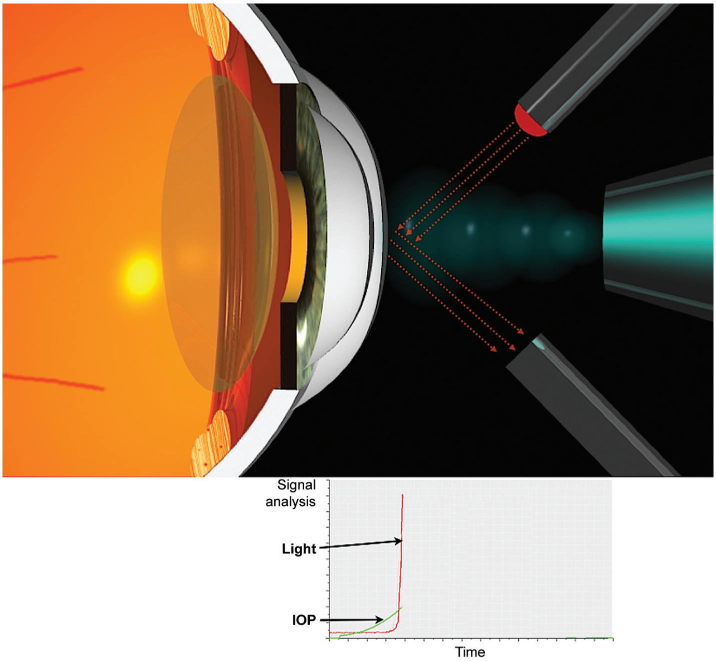

Fig. 4.16 Principle of measuring corneal biomechanics with ORA. First applanation phase.

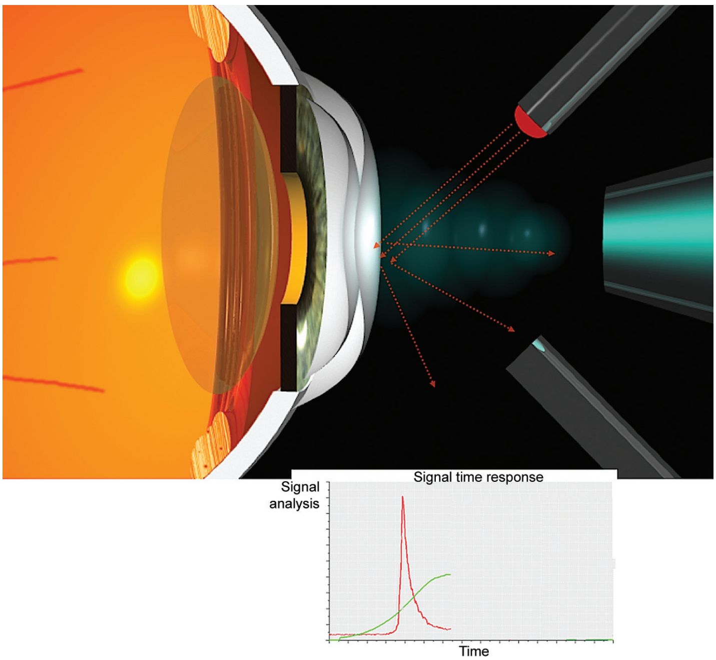

Fig. 4.17 Principle of measuring corneal biomechanics with ORA. Excavation phase.

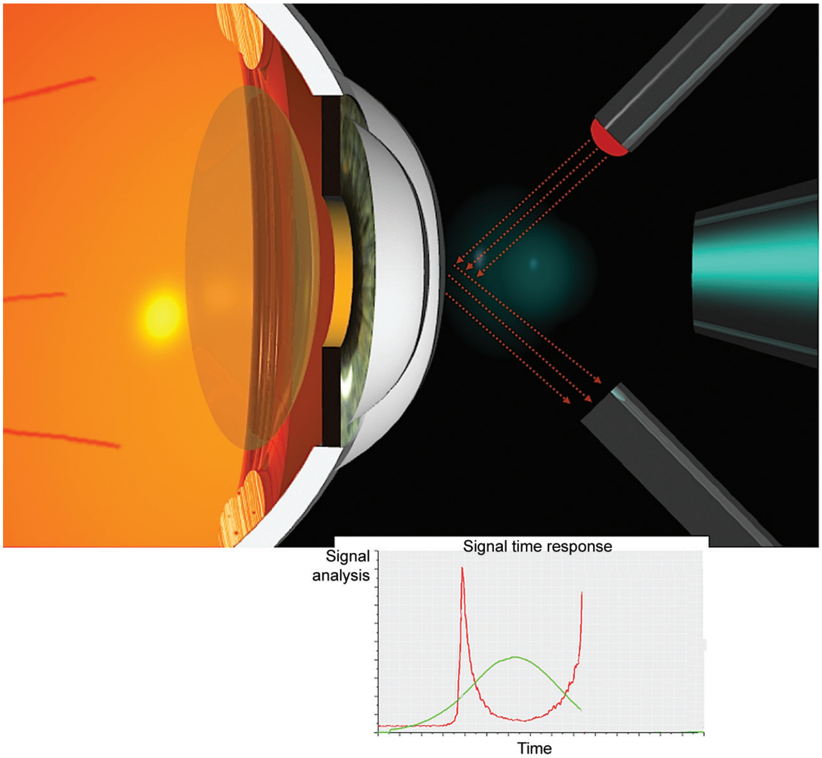

Fig. 4.18 Principle of measuring corneal biomechanics with ORA. Second applanation phase.

e. Divergent reflected beam, which intensity is less than the incident parallel beam (Fig. 4.19). During this process, IOP changes in a bell-shape curve (see the green curve in Fig. 4.20).

The Waveform

The computer of the machine measures the intensity of the reflected beam and the changes in IOP during the whole process and displays that in a diagram shown in Figure 4.20. The diagram consists of a curve and a waveform:

1. The green curve for IOP.
2. The red Waveform for light intensity, which has two peaks:
   a. In-peak: It corresponds to the inward movement of the cornea.
   b. Out-peak: It corresponds to the outward movement of the cornea.

The green curve and the red waveform intersect in two points of different levels. The difference between these two levels represents the delay of the outward movement of the cornea and expresses what is named corneal hysteresis (CH).

Normal distribution of CH was studied in normal corneas, corneas with KC and corneas with Fuch's dystrophy (diseased thick cornea) as shown in Figure 4.21. According to this distribution:

- CH < 8 is always abnormal.
- CH >13 is always normal.
- CH in between may be normal or abnormal.

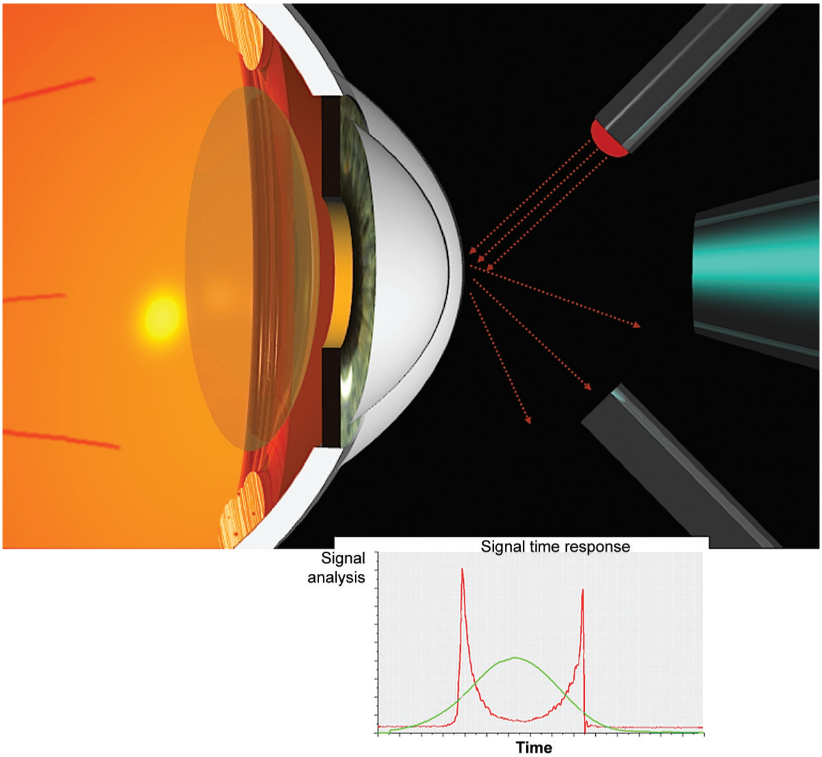

Fig. 4.19 Principle of measuring corneal biomechanics with ORA. Second convex phase.

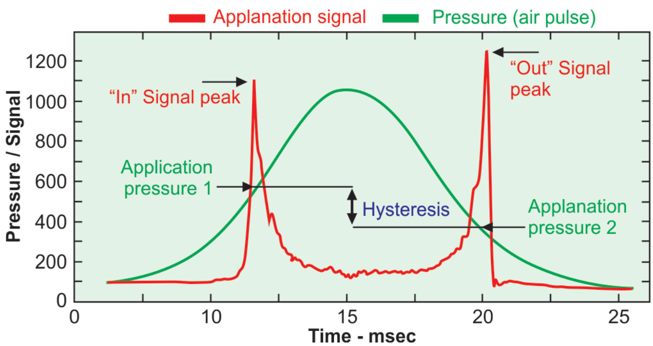

Fig. 4.20 The waveform displayed by ORA.

It is also clear that Fuchs cornea is as bad as KC in spite of its high thickness; this means that thick corneas may have a risk as much as thin corneas in keratorefractive surgeries.

Figure 4.22 shows the waveform of a normal cornea and Figure 4.23 shows the waveform of a KC. In the latter, the magnitude of the peaks is smaller than that in the former, in addition to the fluctuation seen after the second peak (blue arrow), which is the hallmark of KC and ectatic disorders even with normal CH value.

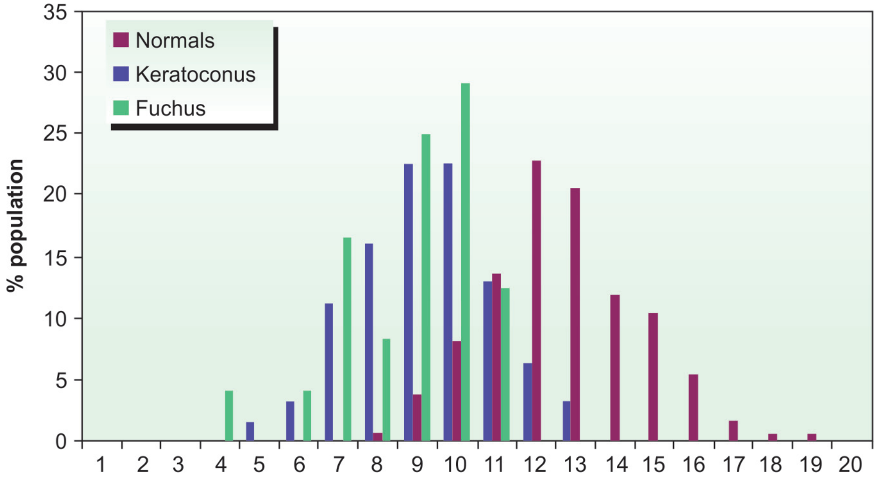

Fig. 4.21 Normal distribution of corneal hysteresis in normal, KC and Fuch's.

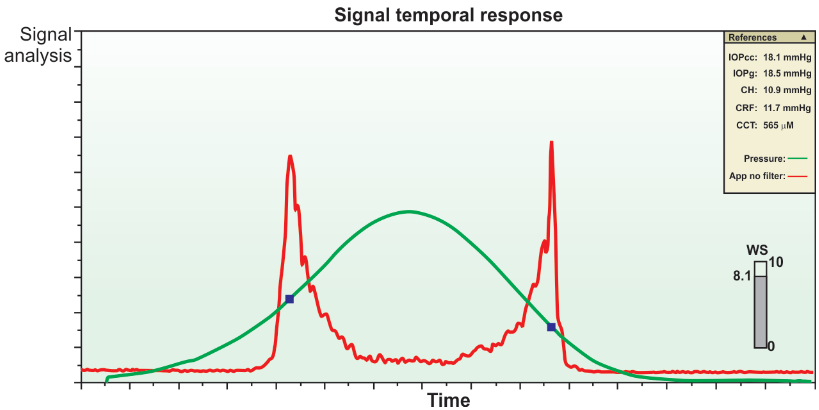

Fig. 4.22 Waveform in normal cornea.

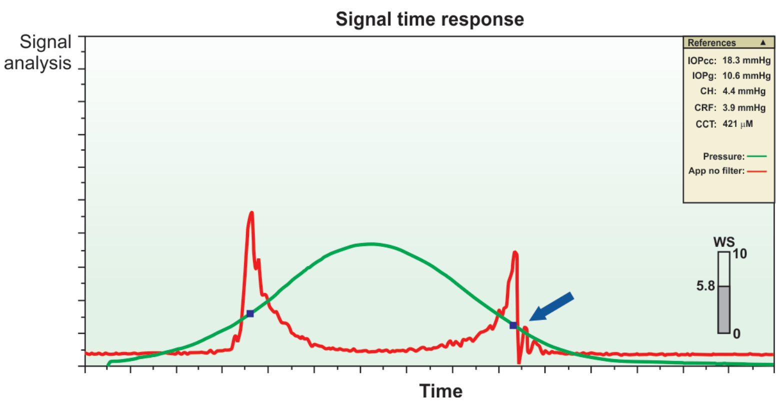

Fig. 4.23 Waveform in a cornea with keratoconus. The blue arrow points at the fluctuation after the second peek which is the hallmark of KC and other ectatic corneal disorders.

Remarks

1. Corneal viscoelasticity is affected neither by CXL nor by intracorneal ring segment (ICRs) implantation.
2. Beside CH, there is an important indicator of corneal biomechanics known as corneal resistance factor (CRF), which reflects corneal resistance towards changes.
3. With comparable flap thickness and attempted ablation volumes, myopic photoablation profiles were associated with greater decreases in CRF and CH than hyperopic profiles. Results indicate that preoperative corneal biomechanical status, ablation volume and the spatial distribution of ablation are important factors that affect corneal resistance and viscous dissipative properties differently. Preferential tissue removal in the natively thicker paracentral cornea in hyperopia may partially account for the rarity of ectasia after hyperopic LASIK.
4. Corneal rigidity (stiffness) increases with age.
5. The recent software of ORA studies 38 indices to increase the sensitivity and specificity for diagnosis. It also suggests KC match probabilities (Fig. 4.24), where percentage of probability of having abnormality is displayed.
6. Goldman tonometer does 'static' measurements of IOP. IOP is derived from the force measured during a steady state applanation of the cornea.
7. The ORA does a 'dynamic' measurement, monitoring the movement of the cornea in response to a rapid air impulse.
8. Recent studies have shown a role of CH in predicting progression of glaucoma in glaucoma patients, eyes with lower CH have faster rates of visual field loss than those with higher CH.

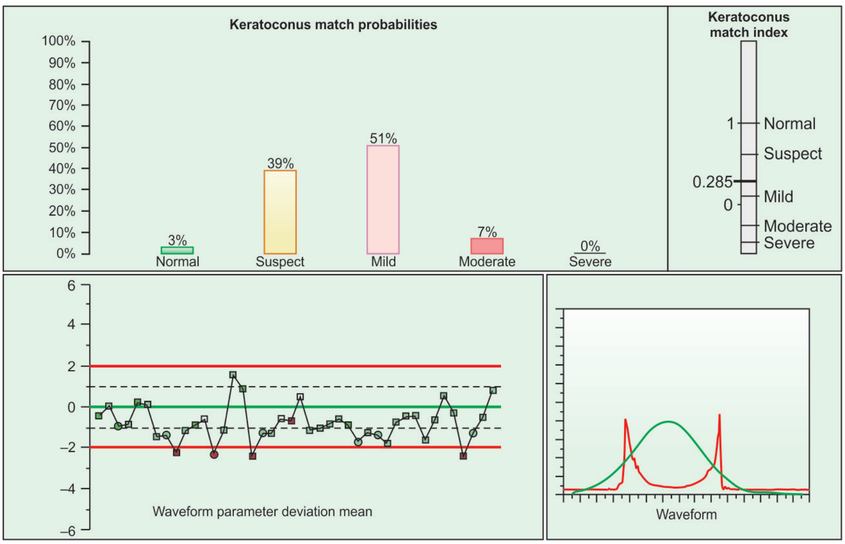

Fig. 4.24 Diagram of KC match probabilities. In this example, the probability of this case to be normal is only 3%.

TAKE-HOME MESSAGE

- Corneal biomechanics have a great negative impact on keratorefractive surgery results
- Post myopic and post hyperopic correction regression is related to corneal biomechanics
- Some of iatrogenic corneal irregularities are related to corneal biomechanics
- Post keratorefractive ectasia is directly related to corneal biomechanics
- Corneal biomechanics is the cause behind incorrect post keratorefractive IOP measurements
- Corneal biomechanics is taking more important role in glaucoma prediction and treatment

BIBLIOGRAPHY

1. Abitbol O, Bouden J, Doan S, et al. Corneal hysteresis measured with the Ocular Response Analyzer® in normal and glaucomatous eyes. Acta Ophthalmol (Oxf). 2010;88:116-9.
2. Agarwal DR, Ehrlich JR, Shimmyo M, et al. The Relationship between Corneal Hysteresis and the Magnitude of Intraocular Pressure Reduction with Topical Prostaglandin Therapy. The British Journal of Ophthalmology. 2012;96(2):254-7.
3. Ahearne M, Yang Y, Then KY, et al. An indentation technique to characterize the mechanical and viscoelastic properties of human and porcine corneas. Ann Biomed Eng 35:1608-1616. Available at:http://link.springer.com/article/10.1007%2Fs10439-007-9323-9. Accessed December. 2007;4:2012.
4. Ambekar R, Toussaint KC, Wagoner Johnson A. The effect of keratoconus on the structural, mechanical, and optical properties of the cornea. J Mech Behav Biomed Mater. 2011;4:223-36.
5. Anand A, De Moraes CG, Teng CC, et al. Corneal Hysteresis and Visual Field Asymmetry in Open Angle Glaucoma. Investigative Ophthalmology Visual Science. 2012;51(12):6514-8.
6. Andreassen TT, Simonsen AH, Oxlund H. Biomechanical properties of keratoconus and normal corneas. Exp Eye Res. 1980;31:435-441.
7. Asaoka R, Kotecha A, White E, et al. The effects of maximum air pulse pressure and intraocular pressure on corneal hysteresis measurements with the Reichert Ocular Response Analyser. Program and abstracts of the Association for Research in Vision and Ophthalmology Annual Meeting; Fort Lauderdale, Florida. Abstract 703; 2008.
8. Bayoumi NHL, Bessa AS, El Massry AAK. Ocular Response Analyzer and Goldman applanation tonometry: a comparative study of findings. J Glaucoma. 2010;19:627-31.
9. Bochmann F, Ang GS, Azuara-Blanco A. Lower Corneal Hysteresis in Glaucoma Patients with Acquired Pit of the Optic Nerve (APON). Graefe's Archive for Clinical and Experimental Ophthalmology. 2008;246(5):735-8.
10. Congdon NG, Broman AT, Bandeen-Roche K, et al. Central Corneal Thickness and Corneal Hysteresis Associated with Glaucoma Damage. American Journal of Ophthalmology. 2006;141(5):868-75.
11. Dauwe C, Touboul D, Roberts CJ, et al. Biomechanical and morphological corneal response to placement of intrastromal corneal ring segments for keratoconus. J Cataract Refract Surg. 2009;35(10):1761-7.
12. De Mederios FW, Sinha-Roy A, Alves MR, et al. Differences in the early biomechanical effects of hyperopic and myopic laser in situe keratomileusis. J Cataract Refract Surg. 2010;36(6):947-53.
13. Del Buey MA, Cristóbal JA, Ascaso FJ, et al. Biomechanical Properties of the Cornea in Fuchs' Corneal Dystrophy. Investigative Ophthalmology Visual. 2009;50(7):3199-202.
14. Del Buey MA, Cristóbal JA, Ascaso FJ, et al (2009). Biomechanical properties of the cornea in Fuchs' corneal dystrophy. Invest Ophthalmol Vis Sci 50:3199–3202Available at: http://www.iovs.org/content/50/7/3199.full.pdf. Accessed July 8, 2011.
15. Detry-Morel M, Jamart J and Pourjavan S. Evaluation of corneal biomechanical properties with the Reichert Ocular Response Analyzer. Eur J Ophthalmol. 2011;21:138-48.
16. Dupps WJ Jr, Netto MV, Herekar S, et al. Surface wave elastometry of the cornea in porcine and human donor eyes. J of Refract Surg. 2007;23(1):66-75.
17. Edmund C. Corneal elasticity and ocular rigidity in normal and keratoconic eyes. Acta Ophthalmol (Copenh). 1988;66:134-40.
18. Ehrlich JR, Haseltine S, Shimmyo M, et al. Evaluation of Agreement between Intraocular Pressure Measurements Using Goldman Applanation Tonometry and Goldman Correlated Intraocular Pressure by Reichert's Ocular Response Analyser. Eye (London). 2010;24(10):1555-60.
19. Elsheikh A, Alhasso D, Rama P. Biomechanical properties of human and porcine corneas. Experimental eye research. 2008;86(5):783-90.
20. Elsheikh A, Wang D, Brown M, et al. Assessment of corneal biomechanical properties and their variation with age. Current eye research. 2007;32(1):11-9.
21. Elsheikh A, Wang D, Rama P, et al (2008). Experimental assessment of human corneal hysteresis. Curr Eye Res 33(3):205-13. doi: 10.1080/02713680701882519.

22. Fontes BM, Ambrósio R, Salomão M, et al. Biomechanical and tomographic analysis of unilateral keratoconus. J Refract Surg. 2010;26:677-81.
23. Fontes BM, Ambrósio R, Velarde GC, et al. Ocular response analyzer measurements in keratoconus with normal central corneal thickness compared with matched normal control eyes. J Refract Surg. 2011;27:209-15.
24. Fontes BM, Ambrosio R Jr, Jardim D, et al. Corneal biomechanical metrics and anterior segment parameters in mild keratoconus. Ophthalmology. 2010;117(4):673-9.
25. Gatinel D, Chaabouni S, Adam PA, et al. Corneal Hysteresis, Resistance Factor, Topography, and Pachymetry after Corneal Lamellar Flap. J of Refract Surg. 2007;23(1):76-84.
26. Glass DH, Roberts CJ, Litsky AS, et al. A viscoelastic biomechanical model of the cornea describing the effect of viscosity and elasticity on hysteresis. Investigative ophthalmology and visual science. 2008;49(9):3919-26.
27. Glass DH, Roberts CJ, Litsky AS, et al. Evaluation of the deformation response to an air puff in healthy and diseased in vivo human corneas. Program and abstracts of the Association for Research in Vision and Ophthalmology. Annual Meeting Fort Lauderdale, Florida. Abstract 646; 2008.
28. Glass DH, Roberts CJ, Litsky AS, et al (2008). A viscoelastic biomechanical model of the cornea describing the effect of viscosity and elasticity on hysteresis. Invest Ophthalmol Vis Sci. 2008;49:3919–3926Available at:http://www.iovs.org/cgi/reprint/49/9/3919. Accessed July 8, 2011.
29. Gore C, Weinreb RN, Sample PA, et al. Differences in corneal biomechanical properties between African-Americans and Caucasians. Program and abstracts of the Association for Research in Vision and Ophthalmology 2008 Annual Meeting Fort Lauderdale, Florida. Abstract 692; 2008.
30. Hamilton DR, Johnson RD, Lee N, et al. Differences in the Corneal Biomechanical Effects of Surface Ablation Compared with Laser in Situ Keratomileusis Using a Microkeratome or Femtosecond Laser. J Cataract Refract Surg. 2008;34(12):2049-56.
31. Kamiya K, Shimizu K, Ohmoto F. Effect of aging on corneal biomechanical parameters using the Ocular Response Analyzer. J Refract Surg. 2009;25:888-93.
32. Kerautret J, Colin J, Touboul D, et al. Biomechanical Characteristics of the Ectatic Cornea. J Cataract Refract Surg. 2008;34(3):510-3.
33. Kirwan C, O'Keefe M, Lanigan B. Corneal Hysteresis and Intraocular Pressure Measurement in Children Using the Reichert Ocular Response Analyzer. American Journal of Ophthalmology. 2006;142(6):990-2.
34. Kirwan C, O'Malley D, O'Keefe M. Corneal hysteresis and corneal resistance factor in keratoectasia: findings using the Reichert Ocular Response Analyzer. Ophthalmologica. 2008;222:334-7.
35. Kotecha A, Elsheikh A, Roberts CR, et al (2006). Corneal thickness- and age-related biomechanical properties of the cornea measured with the Ocular Response Analyzer. Invest Ophthalmol Vis Sci. 47:5337–5347. Available at:http://www.iovs.org/cgi/reprint/47/12/5337. Accessed July 8, 2011.
36. Lam A, Chen D, Chiu R, et al. Comparison of IOP Measurements Between ORA and GAT in Normal Chinese. Optometry and Vision Science. 2007;84(9):909-14.
37. Lam AK, Chen D, Tse J. The Usefulness of Waveform Score from the Ocular Response Analyzer. Optometry and vision science : official publication of the American Academy of Optometry; 2010.
38. Lanchares E, Del Buey MA, Cristóbal JA, et al. Biomechanical property analysis after corneal collagen cross-linking in relation to ultraviolet A irradiation time. Graefes Arch Clin Exp Ophthalmol. 2011;249:1223-7.
39. Liu J, He X, Pan X, et al. Ultrasonic model and system for measurement of corneal biomechanical properties and validation on phantoms. Journal of Biomechanics. 2007;40(5):1177-82.
40. Luce DA. Determining in Vivo Biomechanical Properties of the Cornea with an Ocular Response Analyzer. J Cataract Refract Surg. 2005;31(1):156-62.
41. McMonnies CW (2012). Assessing corneal hysteresis using the Ocular Response Analyzer. Optom Vis Sci 89(3):E343-9. doi: 10.1097/OPX.0b013e3182417223.
42. Medeiros FA, Meira-Freitas D, Lisboa R, et al (2013). Corneal Hysteresis as a Risk Factor for Glaucoma Progression: A Prospective Longitudinal Study. Ophthalmology. 2013 May 1. pii: S0161-6420(13)00047-X. doi: 10.1016/j.ophtha.2013.01.032. [Epub ahead of print]

43. Mirza SN, Schonlau D, Mahmoud AM, et al (2008). The measurement of biomechanical parameters as a function of peak applied pressure in the Reichert Ocular Response Analyzer, in a glaucomatous population. Program and abstracts of the Association for Research in Vision and Ophthalmology 2008 Annual Meeting Fort Lauderdale, Florida. Abstract 704.
44. Ogbuehi KC, Almubrad TM. Evaluation of the intraocular pressure measured with the Ocular Response Analyzer. Curr Eye Res. 2010;35:587-96.
45. Ortiz D, Pinero D, Shabayek MH, et al. Corneal biomechanical properties in normal, post-laser in situ keratomileusis, and keratoconic eyes. J Cataract Refract Surg. 2007;33(8):1371-5.
46. Pepose JS, Feigenbaum SK, Qazi MA, et al. Changes in corneal biomechanics and intraocular pressure following LASIK using static, dynamic, and noncontact tonometry. Am J Ophthalmol. 2007;143:39-47.
47. Roberts CJ, Peterson JD, Mahmoud AM, et al (2008). The influence of age on anatomic and biomechanical ocular parameters in “stiffer” and “softer” normal healthy eyes. Program and abstracts of the Association for Research in Vision and Ophthalmology 2008 Annual Meeting Fort Lauderdale, Florida. Abstract 2045.
48. Saad A, Lteif Y, Azan E, et al. Biomechanical properties of keratoconus suspect eyes. Invest Ophthalmol Vis Sci. 2020;51:2912-6.
49. Schweitzer C, Roberts CJ, Mahmoud AM, et al. Screening of forme fruste keratoconus with the ocular response analyzer. Invest Ophthalmol Vis Sci. 2010;51:2403-10.
50. Schweitzer C, Roberts CJ, Mahmoud AM, Colin J, et al (2010). Screening of forme fruste keratoconus with the Ocular Response Analyzer. Invest Ophthalmol Vis Sci 51:2403–2410. Available at:http://www.iovs.org/content/51/5/2403.full.pdf. Accessed July 8, 2011.
51. Shah S, Laiquzzaman M, Bhojwani R, et al. Assessment of the biomechanical properties of the cornea with the ocular response analyzer in normal and keratoconic eyes. Investigative ophthalmology & visual science. 2007;48(7):3026-31.
52. Touboul D, Bénard A, Mahmoud AM, et al. Early biomechanical keratoconus pattern measured with an ocular response analyzer: Curve analysis. J Cataract Refract Surg. 2011;37(12):2144-50.
53. Touboul D, Roberts C, Kérautret J, et al. Correlations between corneal hysteresis, intraocular pressure, and corneal central pachymetry. J Cataract Refract Surg. 2008;34:616-22.
54. Vu DM, Silva FQ, Haseltine SJ, et al (2013). Relationship between corneal hysteresis and optic nerve parameters measured with spectral domain optical coherence tomography. Graefes Arch Clin Exp Ophthalmol. 2013 Mar 22. [Epub ahead of print]
55. Wang J, Chagnon M, Bayoumi A, et al (2008). Correlation between glaucoma damage, ocular biomechanical properties and vasospasm. Program and abstracts of the Association for Research in Vision and Ophthalmology 2008 Annual Meeting; Fort Lauderdale, Florida. Abstract 4599.
56. Wasielica-Poslednik J, Berisha F, Aliyeva S, et al. Reproducibility of ocular response analyzer measurements and their correlation with central corneal thickness. Graefes Arch Clin Exp Ophthalmol. 2010;248:1617-22.
57. Wells AP, Garway-Heath DF, Poostchi A, et al (2008). Corneal hysteresis but not corneal thickness correlates with optic nerve surface compliance in glaucoma patients. Invest Ophthalmol Vis Sci 49:3262–3268. Available at: http://www.iovs.org/content/49/8/3262.full.pdf. Accessed July 8, 2011.
58. Wollensak G, Spoerl E, Seiler T. Stress-strain measurements of human and porcine corneas after riboflavin-ultraviolet-A-induced cross-linking. J Cataract Refract Surg. 2003;29(9):1780-5.

Step Two

Main Refractive Options

CHAPTER 5

Main Refractive Options

PHOTO REFRACTIVE TREATMENT (PRT)

CORE MESSAGE

- Photo refractive treatment (PRT) uses excimer laser to ablate and reshape the cornea to compensate for refractive errors and treat LOAs and HOAs
- There are three main types of PRT, surface, lamellar and surface-lamellar
- Surface ablation (SA) includes photorefractive keratectomy (PRK), laser subepithelial keratomileusis (LASEK), Epipolis LASIK (Epi-LASIK) and trans epithelial photorefractive keratectomy (TE-PRK). Phototherapeutic keratectomy (PTK) is a type of SA used to treat some corneal pathologies
- Lamellar ablation (LA) is known as laser in situ keratomileusis (LASIK)
- Surface-Lamellar ablation (SLA) is known as sub Bowman keratomileusis (SBK)
- There are indications, contraindications, pros and cons for each type
- Regardless of PRT type, ablation profiles include plain, optimized, aspheric, aspheric aberration-free and wavefront-guided
- The choice of treatment profile depends on visual acuity, patient's complaint and RMS related to HOAs

The 193-nm argon-fluoride (ArF) excimer laser treats refractive error by ablating the anterior corneal stroma to create a new radius of curvature in order to compensate for the refractive error.

Types of PRT

Three major refractive surgical techniques use excimer laser ablation: surface ablation (SA), lamellar ablation (LA) and surface-lamellar ablation (SLA).

Surface Ablation (SA)

In SA, Bowman layer is exposed and the ablation profile is applied on this layer and on anterior stroma.
SA includes four types:

a. **Photorefractive Keratectomy (PRK):** The epithelium is debrided and removed either mechanically or by 20% alcohol (Fig. 5.1).
b. **Laser Subepithelial Keratomileusis (LASEK):** The epithelium is *loosened* by 20% alcohol and *moved aside*, but ultimately preserved, then re-positioned after ablation (Fig. 5.2).
c. **Epipolis LASIK (Epi-LASIK):** The epithelium is *moved* mechanically by a mechanical microkeratome (MMK), but ultimately preserved, then re-positioned after ablation (see Fig. 5.2).

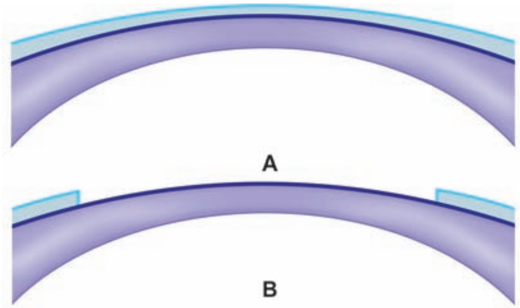

Fig. 5.1 PRK. The epithelium is removed either mechanically or after alcohol application.

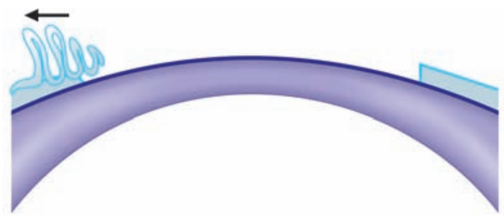

Fig. 5.2 LASEK and Epi-LASIK. In LASEK, the epithelium is loosened by alcohol and moved aside; in Epi-LASIK, the epithelium is mechanically moved aside using a MMK.

d. **Transepithelial Photorefractive Keratectomy (TE-PRK):** The epithelium is not removed but ablated with a specific profile designed to remove the epithelium and simultaneously correct the refractive error.
   In irregular corneas, Bowman layer is irregular and the epithelium is as well. If an eye presents with irregular topography, by definition the epithelium has reached its maximum compensatory function which is known as "filling characteristic." In the filling characteristic the epithelium thickens to fill in troughs in the stromal surface, and thins to compensate for peaks in the stromal surface (Fig. 5.3); therefore, topography and wavefront measurements are inaccurate means of describing the irregularity on the stromal surface. Therefore, if PRK, LASEK or Epi-LASIK is planned, the ablation will be performed on irregular Bowman surface, leading to irregular correction (Fig. 5.4). In such cases, the TE-PRK has the advantage of

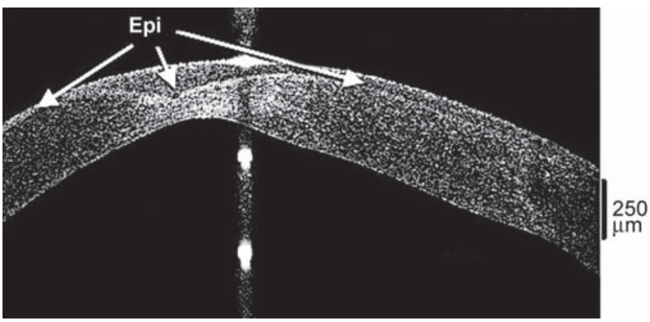

Fig. 5.3 Filling characteristic of the epithelium. Notice the smooth anterior surface in spite of irregular Bowman layer.

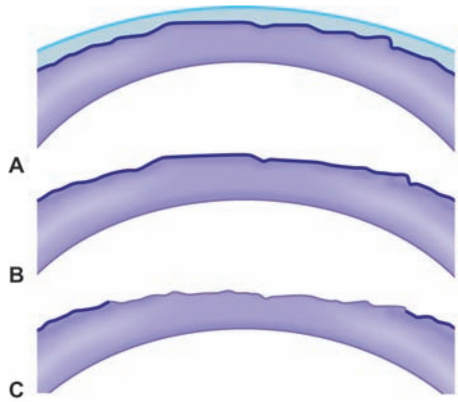

Fig. 5.4 Irregular treatment over irregular surface. In case of irregular Bowman layer, if SA is performed, the result will be an irregular treatment. A) Epithelium on irregular Bowman; B) Epithelium removed; C) Ablation applied on an irregular surface leading to more irregularity which may or may not be remodeled by the epithelium.

ablating a definite amount of epithelium (and parts of Bowman) all over the ablation zone creating a smooth and regular surface for refractive correction (Fig. 5.5). The disadvantage of this technique is that it assumes that the thickness of the epithelial layer is uniform in all eyes, which is not true; therefore, there will be some under- or over-corrections, particularly in small amounts of correction. However, this technique is best indicated in irregular corneas or when treating mild to moderate keratoconus cases with simultaneous SA and CXL.

e. **Photo Therapeutic Keratectomy (PTK):** It is one of the SA types used to treat superficial corneal opacities and some of postoperative flap complications such as micro and macro striae (see chapter 8).
As mentioned in chapter 3, OCT imaging of the cornea is mandatory for this type of treatment to measure corneal thickness and the depth and thickness of the opacity.

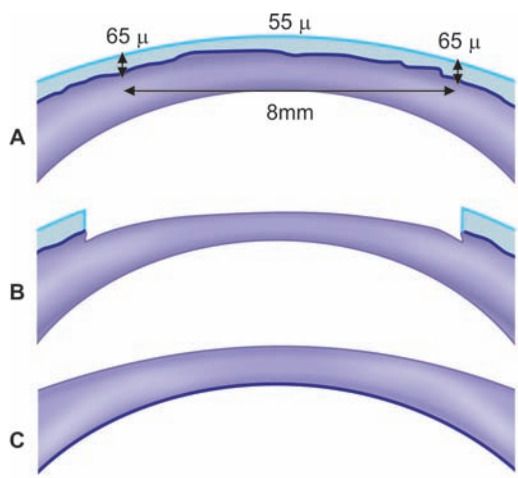

Fig. 5.5 TE-PRK. (A) The epithelium and Bowman layer are removed by the laser profile; (B) This creates a smooth regular stromal bed; (C) Postoperative smooth and regular surface.

Surgical Techniques in SA

1. **Pre-op:** Patients are often administered 5 mg of diazepam on the day of or the night before the procedure to reduce anxiety. Females are recommended to avoid eye makeup for at least one weak preoperatively since the particles of the makeup substances may contaminate and may act as toxic agents.
2. **Anesthesia, Sterilization and Draping:** After the eye has been anesthetized with either topical proparacaine or tetracaine, the periocular skin is prepped with 10% povidone-iodine (Betadine) and 4% povidone-iodine drops are applied to the ocular surface for two minutes and then irrigated. Patients then receive additional topical anesthetic and antibiotic drops, the eyelids are draped and a lid speculum is placed to optimize corneal exposure. The other eye is occluded. Topical anesthesia is obtained with proparacaine 0.5% or tetracaine 0.5% drops.
3. **Alignment and Registration:** Registration is a technique in which a fixed landmark is used at the time of aberrometry or tomography and treatment to apply the ablation to the correct area of the cornea; it does not rely on the pupil for laser centration. The step of registration should be done before removing epithelium. This step will be discussed in details in chapter 6.
4. **Epi-Off:** In the evolution of PRK, several methods were developed to debride the epithelium. Some techniques involve complete removal and disposal of the epithelium; other methods offer the option of preserving and repositioning the epithelium following stromal excimer laser ablation. None involve creation of a corneal stromal flap.
    a. The original PRK techniques utilize mechanical epithelial removal with a sharp blade, blunt spatula, or a rotating corneal brush. Some surgeons prefer using alcohol 20% to loosen the intact epithelium. Central cornea is marked with an 8.0 mm OZ marker delineating the area for epithelial removal and the epithelial removal method of choice is begun. In case of alcohol method, a solution of 20% alcohol is applied for 20 to 30 seconds in a "well" created by pressing an 8 or 9 mm diameter OZ marker onto the corneal surface, to restrict the alcohol to the area to be de-epithelialized (Fig. 5.6). After the desired exposure time, the alcohol is removed from the "well" by absorption into a microsurgical spear sponge (Fig. 5.7) and the ocular surface is copiously irrigated with balanced salt solution (BSS).

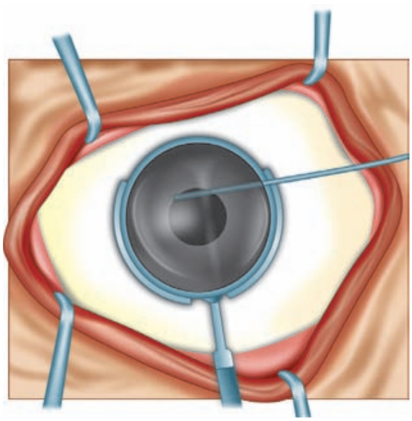

Fig. 5.6 Surgical technique in PRK. De-epithelialization by alcohol. Application of 20% alcohol in a "well."

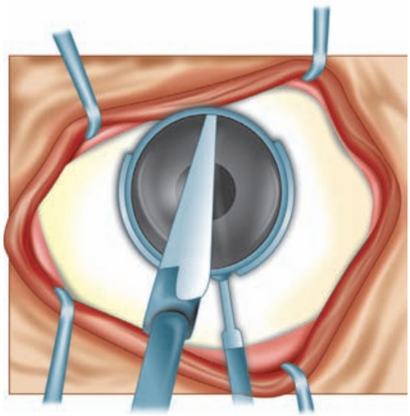

Fig. 5.7 Surgical technique in PRK. De-epithelialization by alcohol. Drying alcohol before removing the "well."

A special brush is used to debride the loosened epithelium (Fig. 5.8) and bare the stromal bed (Fig. 5.9).

b. TE-PRK was developed to allow for a no-touch removal technique that is helpful when trying not to disturb the underlying stroma (as in previous radial keratotomy patients) or dislodge a previous LASIK flap.

c. LASEK was developed in an attempt to preserve the epithelium. Alcohol is applied in the same manner described with PRK. Epithelial trephine and spatula are used sequentially to score and roll up the epithelium, which remains attached at the hinge (Figs 5.10 and 5.11). After photoablation is performed, the epithelium is replaced.

d. The Epi-LASIK procedure does not use alcohol, which is toxic to the epithelium. Instead, a MMK with a modified dull blade and a thin applanation plate is used to cleave the epithelium. In the absence of alcohol, Epi-LASIK may preserve more-viable epithelial cells. This could improve epithelial flap adherence, reduce postoperative discomfort, and improve visual outcomes compared to LASEK. In both LASEK and Epi-LASIK, around

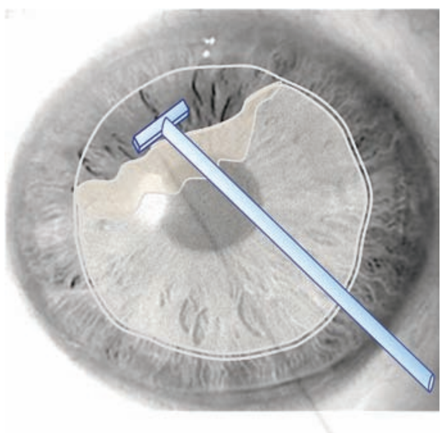

Fig. 5.8 Surgical technique in PRK. Debridement of the loosened epithelium using a special brush.

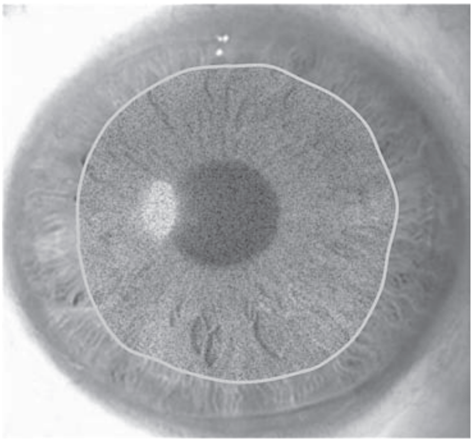

Fig. 5.9 Surgical technique in PRK. Bare stromal bed after removing the epithelium.

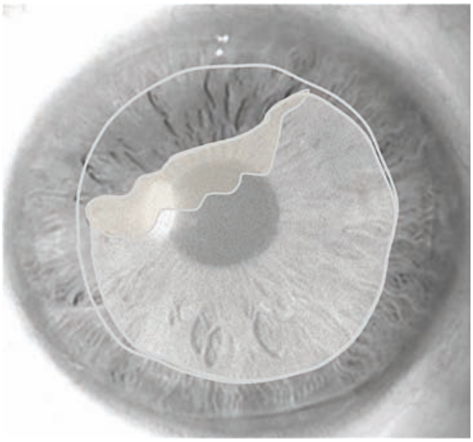

Fig. 5.10 Surgical technique in LASEK. De-epithelialization by 20% alcohol.

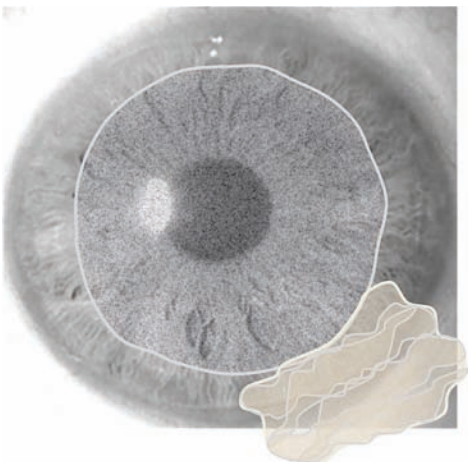

Fig. 5.11 Surgical technique in LASEK. A flap of epithelium is moved aside.

20% of the epithelial flaps are sloughed off or become necrotic postoperatively and the purported benefit of the epithelium is lost. Both LASEK and Epi-LASIK are similar to PRK in that the epithelium is removed and the photoablation is performed directly on Bowman's membrane and the anterior stroma. The visual results are comparable in all three procedures and Epi-LASIK and LASEK have not been proven to be beneficial over PRK in decreasing corneal haze or significantly reducing postoperative discomfort.

e. After the epithelium has been removed with any of the three techniques, a surgical cellulose sponge lightly moistened with an artificial tear lubricant (such as carboxymethylcellulose) is lightly brushed over the surface of the cornea to remove residual epithelium and to smooth the surface. The OZ must be free of epithelial cells, debris and excess fluid before ablation. The epithelium should be removed quickly and consistently in order to prevent dehydration of the stroma, which increases the rate of excimer laser ablation resulting in an overcorrection.

5. **Centring and Applying the Ablation Beam:** Each excimer laser machine has its own pattern of lights for centring the ablation beam (cross, meniscuses, spot lights, etc.). The ablation beam should be coaxial with the fixating blinking target, at which the patient should be asked to fixate (Figs 5.12 and 5.13). It is mandatory to be sure that the eye tracker has recognised the pupil and it is active; otherwise, decentred ablation will result leading to postoperative decentred zone, which is the main cause of postoperative induced coma. Tracking systems, although effective, do not reduce the importance of keeping the reticule centred on the patient's entrance pupil. If the patient is unable to maintain fixation, the illumination of the operating microscope should be reduced. If decentration occurs and the ablation does not stop automatically, the surgeon should immediately stop the treatment until adequate re-fixation is achieved. It is still important for the surgeon to monitor for excessive eye movement, which can result in decentration despite the tracking device. Once the patient confirms that the fixation light of the excimer laser is still visible and that he or she is looking directly at it, ablation begins. During ablation, the surgeon must monitor the patient to ensure that fixation is maintained throughout the treatment. Neither tracking nor registration is a substitute for accurate patient fixation. It is important to initiate stromal ablation promptly, before excessive stromal dehydration takes place.

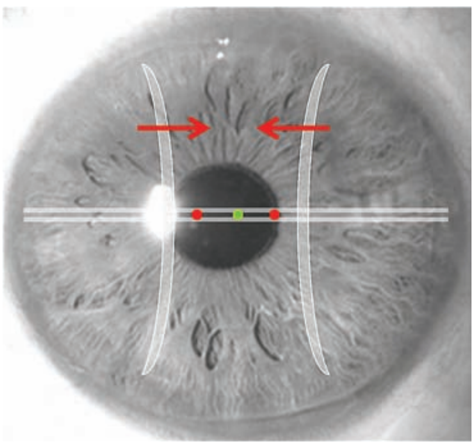

Fig. 5.12 Centering the ablation beam. The eye fixates on the blinking green light. Light crescents and the two red spots are moved to superimpose the green light.

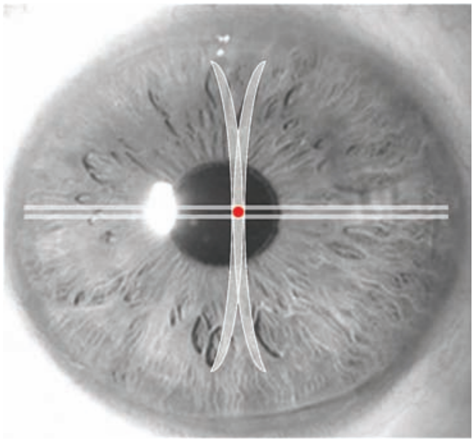

Fig. 5.13 Centering the ablation beam. The light crescents and the two red spots are superimposed with the green fixating target.

The change in illumination and in patient position (i.e., lying down) can cause pupil centroid shift. In most patients, the pupil moves nasally and superiorly when it is constricted. It is therefore important to use the registration technique in cases sensitive to pupil position as will be discussed later in chapter 6.

6. **Addressing the Eye:** After photoablation, many surgeons irrigate the ablated stromal surface with chilled BSS and/or apply iced BSS on surgical spears to control postoperative pain and possibly reduce the incidence of corneal haze. Drops of antibiotic and corticosteroid are instilled, followed by placement of a bandage contact lens (BCL). If Epi-LASIK or LASEK are performed, the surgeon first places the epithelial sheet back into position with an irrigating canula filled with BSS before applying drops and the BCL.

Post SA Management

1. **Sedation:** During the first 24 to 48 hours, patients experience a variable amount of pain, which may need to be treated with an oral narcotic, non steroidal anti inflammatory drugs (NSAID), analgesics (e.g. gabapentin and pregabalin) and topical 0.5% morphine.
2. **Medication:** As long as the BCL is in place, patients are prescribed antibiotics and corticosteroids, 4 times daily and preservative-free artificial tears. Corticosteroids can be postponed till complete epithelialisation and BCL removal. Patients should be followed closely until the epithelium is completely healed, which usually occurs within 3 to 4 days. At this point BCL and antibiotics are discontinued. Topical corticosteroids modulate postoperative wound healing, reduce anterior stromal haze and reduce regression of the refractive effect. The strength of steroid and the duration of use remain controversial. Many surgeons still advocate a tapering dose of topical corticosteroid drops (4 times a day for 1 month, 2 times a day for 1 month, once a day for 1 month) and then stop them. Other surgeons feel that patients with low refractive errors (<–4 D), shallow ablation depth (AD) (<70 μm), or those receiving Mitomycin C (MMC) are at lesser risk to develop postoperative corneal haze and may require a shorter course of corticosteroid postoperatively. Duration of occupational sun exposure has an impact on haze formation; it is therefore advised to use sun glasses after SA for a long period of time in addition to intraoperative application of MMC (see below).

Adjunctive Intraoperative Mitomycin C (MMC) in SA

Because corneal haze is a major complication associated with SA, a soaked pledged of MMC, usually 0.02% or 0.2 mg/ml, can be placed on the ablated surface for 12 seconds to 2 minutes at the end of the laser treatment (Fig. 5.14). MMC is an alkylating agent that inhibits DNA synthesis. It is used to reduce the chance of corneal subepithelial haze in eyes at high risk for this complication, including higher corrections corresponding to ablations of more than 80 µm, or in eyes that have undergone prior corneal surgery such as penetrating keratoplasty, radial keratotomy, or LASIK. Some surgeons use MMC in patients with a history of keloid formation or in those subjected to prolonged sunlight exposure because ultraviolet radiation causes postoperative corneal haze. The length of time that the pledged is in place depends on surgeon preference. Recent studies indicate that shorter application times are equally effective in primary SA, hence, the trend to 12-second applications, while 1- to 2-minute MMC applications are reserved for high-risk cases. Irrigation of the corneal surface with copious amounts of BSS (30 ml) to remove the excess MMC and minimize the toxicity is crucial. To prevent damage to limbal stem cells, the surgeon should avoid exposing the limbus or conjunctiva to MMC. The use of adjunctive topical MMC to prevent postoperative corneal haze in refractive surgery is an off-label use of the medication. Human confocal microscopy studies have demonstrated less haze in eyes treated with MMC and an associated reduction in keratocytes. Vision threatening complications associated with the drug have been reported many years after glaucoma and pterygium surgeries, but these cases involved different techniques, higher concentration and more-prolonged exposure.

N.B. using MMC may cause overcorrection of myopia. Some surgeons recommended reducing the spherical myopic component by 10–15% depending on patients age; the older the patient the higher the percentage to reduce. On the other hand, in case of myopic astigmatism, the plus cylinder equation is used; e.g. a 25 y/o patient has –4D sph –2D cyl @ 120°, it should be converted into –6 D sph +2 D cyl @ 30°, then the –6 D sph may be reduced by 10%; therefore, the patient will be corrected for –5.4 D sph +2 D cyl @ 30°. Another example, a 55 y/o patient with –2

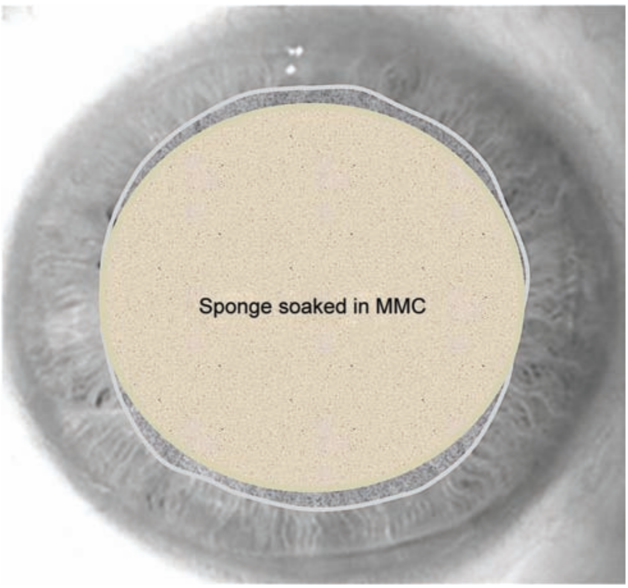

Fig. 5.14 Mitomycin C (MMC) application. A sponge soaked with MMC 0.02% is applied on the treated stromal bed.

D sph –1 D cyl @ 180°, it should be converted into –3 D sph +1 D cyl @ 90°, then the –3 D sph will be reduced by 15%; therefore, the patient will be corrected for –2.55 D sph +1 D cyl @ 90°.

Surgical Technique in PTK

PTK is mainly used to treat superficial corneal opacities and in case of post operative micro- and macrostriae in LASIK flap.

1. For superficial opacities, AD of PTK is calculated by OCT. The same surgical technique of TE-PRK is used, except that centration is not always mandatory; in case of decentered opacity, the tracker can be switched off and the laser beam is directed towards the area of opacity. Application of MMC 0.02% for 60–120 seconds is strongly recommended after ablation.
2. For micro and macrostriae, AD of PTK should be about 20–30 µm. A viscous substance of very low viscosity (commercially available such as LASERVIS®) is used as a masking agent to fill the valleys and leave the peaks apparent and prominent to laser ablation. After draping, corneal surface is irrigated then dried using a spear sponge. One drop of the masking agent is installed over the cornea; the surgeon should wait for about 1–3 seconds then immediately apply PTK. In this technique, only the peaks of the striae will be ablated and the surface will be smoothened. If this masking agent is not available, a drop of BSS can be used. There is no need to use MMC at the end of this treatment.

TAKE-HOME MESSAGE

- Several methods are available for removal of epithelium in SA, some are mechanical, others are by alcohol or laser ablation
- It has not been proven that Epi-LASIK and LASEK are beneficial over PRK in decreasing corneal haze or significantly reducing postoperative discomfort
- Centration and alignment are very important concepts in every PRT procedure
- Eye tracker does not exclude the role of surgeon's observation during laser application
- PTK is a therapeutic procedure mainly performed for treating superficial corneal opacities and micro- and macrostriae

Lamellar Ablation (LA)

Photoablation is performed on anterior stroma under a lamellar flap created with either a MMK or femtosecond laser (Fig. 5.15). The lamellar type is called laser in situ keratomileusis (LASIK). Since surgical technique and postoperative follow up resembles that for the surface-lamellar ablation (SLA), these will be discussed in the next paragraph.

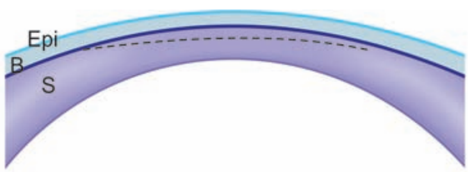

Fig. 5.15 Level of flap cut in LASIK.

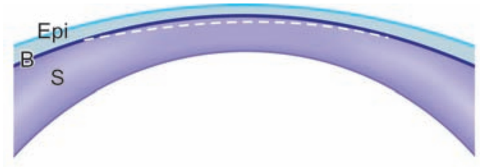

Fig. 5.16 Level of flap cut in SBK.

Surface-Lamellar Ablation (SLA)

Photoablation is performed just sub Bowman layer under a very thin lamellar flap created with either a MMK or femtosecond laser (Fig. 5.16); therefore, it is called sub Bowman keratomileusis (SBK). This type has the advantages of both SA and LA types.

Surgical Techniques in LA and SLA

1. Steps one (pre-op) and two (anesthesia, sterilization and draping) are same as in SA.
2. **Alignment and Registration:** As mentioned in SA, registration is a technique in which a fixed landmark is used at the time of aberrometry or tomography and treatment to apply the ablation to the correct area of the cornea; it does not rely on the pupil for laser centration. The step of registration should be done before flap creation. This step will be discussed in details in chapter 6.
3. **Decentration (Off-set Pupil):** In case of high angle kappa, > 1D astigmatism or in hyperopia, it is recommended to decenter the ablation beam in order to shift the center of ablation to be coaxial with the visual axis.
   In Placido-based topographers, angle kappa is measured and offset pupil (or decentration) can be performed either manually by input of x and y values of angle kappa or automatically by wavefront-guided profiles.
   In Scheimpflug-based topographers, angle kappa is not measured and offset pupil (or decentration) can be performed either manually by input of half x and y values of pupil center coordinates or automatically by the wavefront-guided profiles.
   In both methods, great care of the location of the flap should be taken; decentration holds the risk of applying part of the photoablation beam out of treatment bed leading to irregular treatment and hence, introducing high order aberrations (mainly coma). Therefore, the flap should also be decentered to compensate for the decentered photoablation beam.
   Decentring the flap is done in the following manner (Figs 5.17 to 5.20):
   a. Perform beam decentration by input of decentered values in the software of the excimer machine (offset pupil).
   b. Press the pedal test to see the new location of the center of the ablation beam.
   c. While keep pressing the pedal test, put a mark on the cornea at the place of the beam.
   d. Use this mark as the center of the suction ring either with MMK or femtosecond.
   e. Create the "decentered" flap.

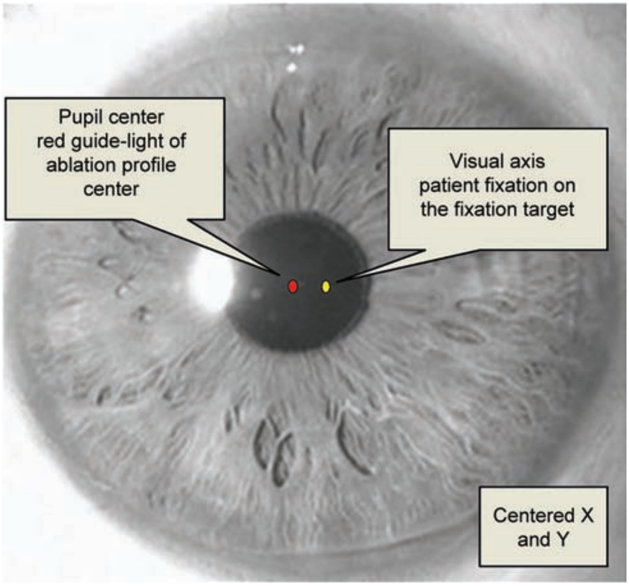

Fig. 5.17 Step one in Decentration technique "off-set pupil." The eye is fixating on the fixation target.

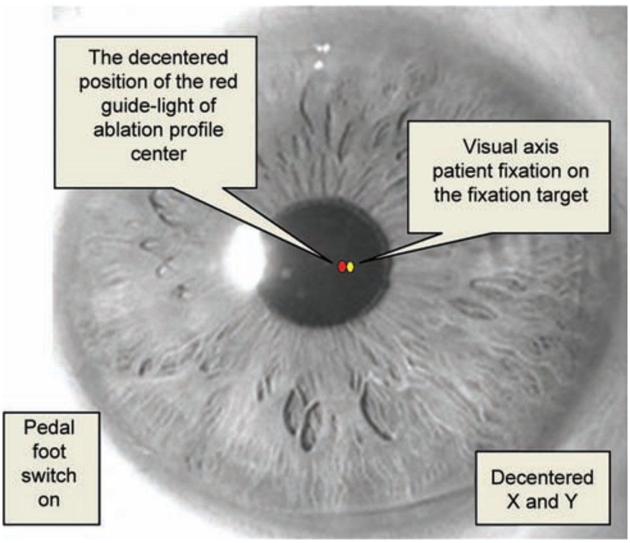

Fig. 5.18 Step two in Decentration technique "off-set pupil." Laser beam is decentered in machine computer to compensate for angle kappa. Pedal foot switch is pressed on. The red-guide-light moves the amount that the laser beam has been decentered for.

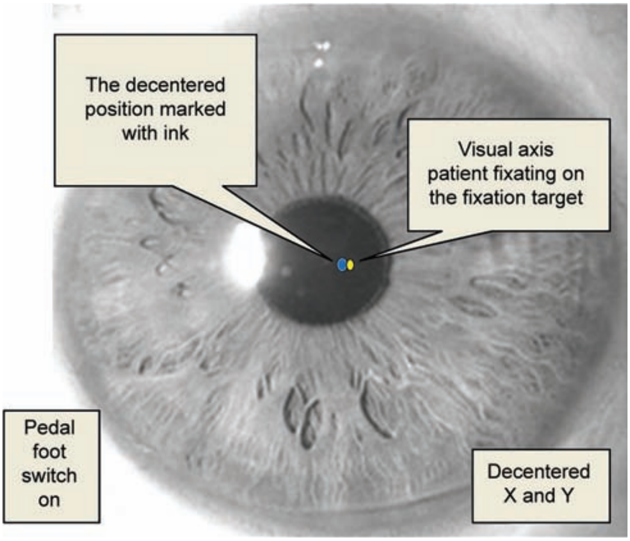

Fig. 5.19 Step three in Decentration technique "off-set pupil." The decentered position is marked with ink.

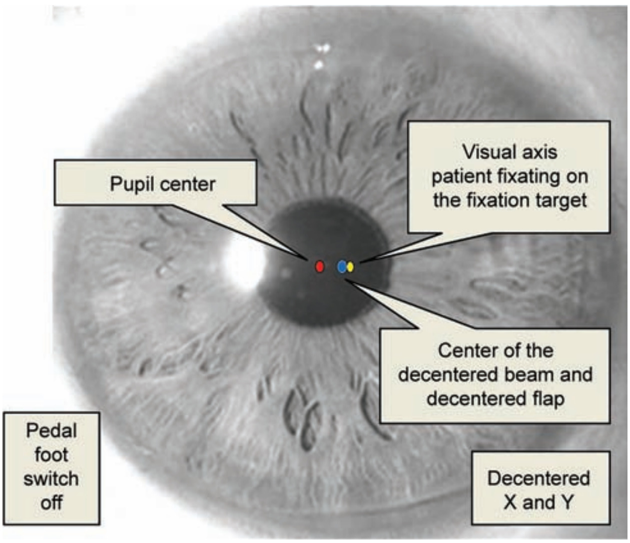

Fig. 5.20 Step four in Decentration technique "off-set pupil." Pedal foot switch is off. The cornea is marked for the center of the ablation beam. The flap will be created centered with this mark.

4. **Flap Creation:** Creating the flap can be performed using either a MMK or a femtosecond laser.
   It is recommended to create a flap with a diameter of 0.5 to 1.0 mm larger than the total ablation zone. Usually, the total ablation zone diameter is 6 to 9.5 mm in myopic treatment and 8.5 to 10 mm in hyperopic treatment.
   a. Marking the Cornea (Fig. 5.21). Make asymmetric sterile ink marks in the corneal periphery, away from the intended flap hinge, just before placement of the suction ring. These marks can aid in alignment of the flap at the end of surgery and in proper orientation in the rare event of a free cap.
   b. Creating the flap.
      – The MMK suction ring has two functions: adhering to the globe, providing a stable platform for the MMK cutting head; and raising the IOP to a high level, which stabilizes the cornea.
      – The dimensions of the suction ring determine the diameter of the flap and the size of the stabilizing hinge. The thicker the vertical dimension of the suction ring and the smaller the diameter of the ring opening, the less the cornea will protrude and hence a smaller-diameter flap will be produced (see also chapter 6, average K rule).
      – The suction ring is connected to a vacuum pump, which is typically controlled by an on-off-foot pedal.
      – The MMK cutting head has several key components. The highly sharpened disposable cutting blade is discarded after each patient, either after a single eye or after bilateral treatment.
      – The applanation head, or plate, flattens the cornea in advance of the cutting blade. The length of the blade that extends beyond the applanation plate and the clearance between the blade and the applanation surface are the principal determinants of flap thickness.
      – The motor, either electrical or gas-driven turbine, oscillates the blade rapidly, typically between 6000 and 15,000 cycles per minute. The same motor or a second motor is used to mechanically advance the cutting head, which is attached to the suction ring, across the cornea; although in some models the surgeon manually controls the advance of the cutting head (this carries potential personal errors).

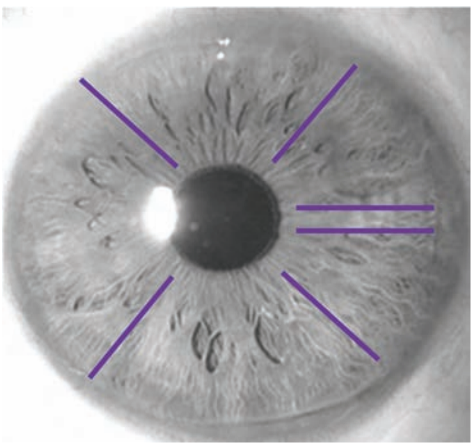

Fig. 5.21 Marking the cornea using asymmetric marking lines to facilitate repositioning the flap.

- Smaller and thinner flap size and longer hinge cord length are more important than hinge location in sparing the nerves and reducing the incidence and severity of dry eye. Regardless of hinge type, patients generally recover corneal sensation to preoperative levels within 6–12 months after surgery.
- The ring should be positioned either symmetrical to the limbus, or centered with the ink mark that has been put in case of decentration.
- Once the ring is properly positioned, suction is activated (Fig. 5.22). The IOP should be assessed at this point because low IOP can result in a poor-quality, thin, or incomplete flap. It is essential to have both excellent exposure of the eye, allowing free movement of the MMK and proper suction ring fixation. Inadequate suction may result from blockage of the suction ports from eyelashes under the suction ring or from redundant or scarred conjunctiva. To avoid the possibility of pseudo suction (occlusion of the suction port with conjunctiva but not sclera), the surgeon can confirm the presence of true suction by observing that the eye moves when the suction ring is gently moved, the pupil is mildly dilated and the patient can no longer see the fixation light or can see it blurred.
- Prior to the flap cut, the surface of the cornea is moistened with proparacaine with glycerin or with preservative-free artificial tears. BSS should be avoided at this point because mineral deposits may develop within the MMK and interfere with its proper function. The surgeon places the MMK on the suction ring (Fig. 5.23) and checks that its path is free of obstacles such as the eyelid speculum, drape, or overhanging eyelid.
- The MMK is then activated, passed over the cornea until halted by the hinge-creating stopper and then reversed off the cornea. It is important to maintain a steady translation speed to avoid creating irregularities in the stromal bed.
- Before surgery, the MMK and vacuum unit are assembled, carefully inspected and tested to ensure proper function. The importance of meticulously maintaining the MMK and carefully following the manufacturer's recommendations cannot be overemphasized.
- In addition, the surgeon should be aware that, regardless of the label describing the flap thickness of a specific device, the actual flap thickness varies with the type of

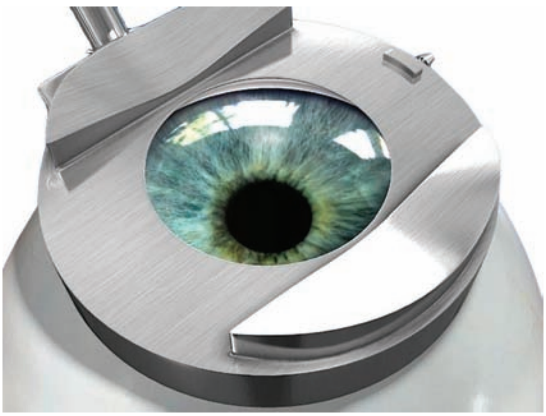

Fig. 5.22 Application of the suction ring.

Fig. 5.23 Application of the MMK head on the suction ring and creating the flap.

MMK, quality of the blade, patient age, preoperative corneal thickness, preoperative keratometry, preoperative astigmatism, corneal diameter, IOP, first eye vs. second eye and translation speed of the MMK pass.

b. Femtosecond laser.
   - A femtosecond laser also creates flaps by performing a lamellar dissection within the stroma. Each laser pulse creates a discrete area of photo disruption of the collagen. The greater the number of laser spots and the more the spots overlap, the more easily the tissue will separate when lifted.
   - The femtosecond laser allows adjustments for several variables involved in making the flap, including flap thickness, flap diameter, hinge location, hinge angle, bed energy and spot separation.
   - Although the goal is to try to minimize the total energy used in flap creation, a certain level of power is necessary to ensure complete photo disruption and greater overlap of spots allows for easier flap lifting.
   - With the computer programmed for flap diameter, depth and hinge location and size, thousands of adjacent pulses are scanned across the cornea in a controlled pattern that results in a flap.
   - With a femtosecond laser, the side cut of the corneal flap can be modified in a manner that may reduce the incidence of epithelial ingrowth.
   - The use of a femtosecond laser generally takes more time than a MMK because it requires several extra steps. First, the suction ring is centred over the pupil (symmetrical with the limbus) or centered with the mark of decentration in case of it. Suction is applied. Proper centration of the suction ring is critical and is performed under a separate microscope, either the microscope from the adjacent excimer laser or an auxiliary microscope in the laser suite. The docking procedure is initiated under the femtosecond laser's microscope, while the patient's chin and forehead are kept level and the suction ring is kept parallel to the eye. The applanation lens is then centred over the suction ring and lowered into place using the joystick and the suction ring is unclipped to complete the attachment to the docking device. Complete applanation of the cornea must be achieved, or an incomplete flap or incomplete side cut may occur. Adjustment of centration can be performed by the laser's computer and once it

has confirmed centration, the surgeon administers the femtosecond laser treatment (Fig. 5.24). The vacuum is then released, the suction ring is removed and the patient is positioned under the excimer laser.

– A spatula with a semi sharp edge identifies and scores the flap edge near the hinge (Fig. 5.25).
– A blunt instrument is then passed across the flap along the base of the hinge (Fig. 5.26), and the flap is lifted by sweeping inferiorly and separating the flap interface, dissecting one-third of the flap at a time and thus reducing the risk of tearing (Fig. 5.27).

5. **Centring and Applying the Ablation Beam:** This step is similar to that for SA added that the flap must be lifted and reflected and the stromal bed should be uniformly dry prior to treatment (Fig. 5.28).

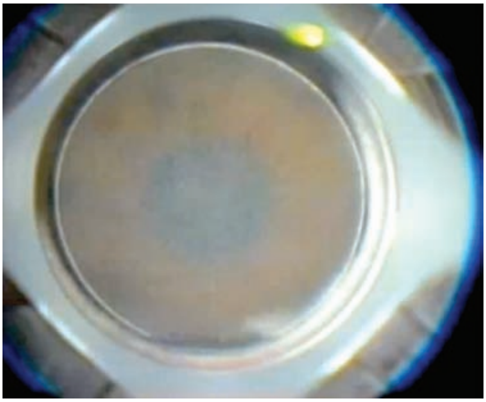

Fig. 5.24 View after flap cut with femtosecond laser.

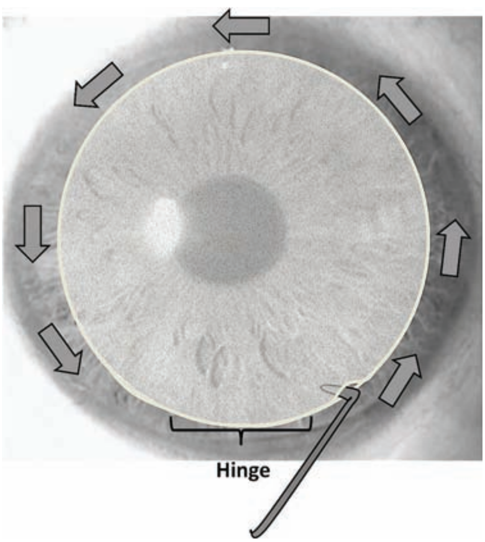

Fig. 5.25 Flap dissection. The flap is separated at its periphery from the cornea using a semi sharp spatula.

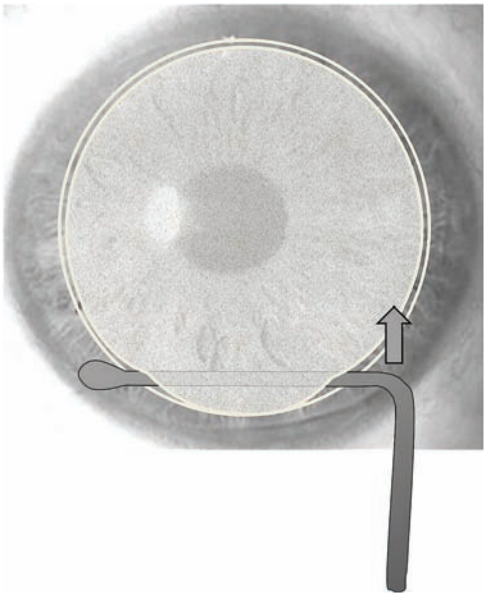

Fig. 5.26 Flap dissection. A blunt instrument is inserted across the flap along the base of the hinge to dissect the flap.

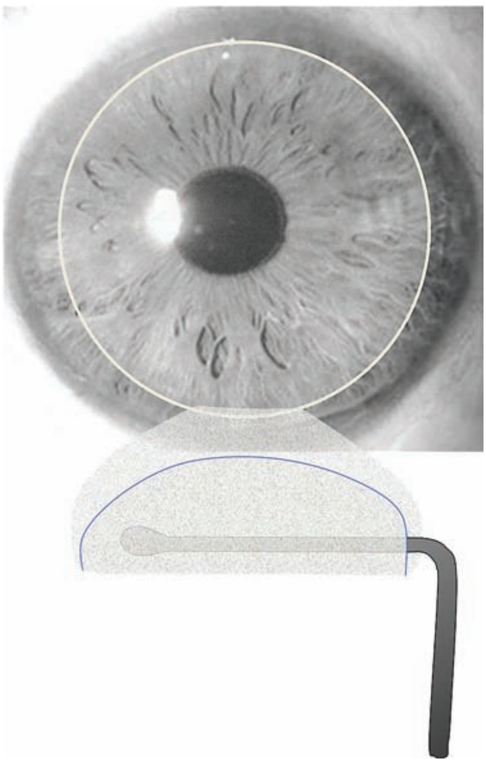

Fig. 5.27 Lifting the flap.

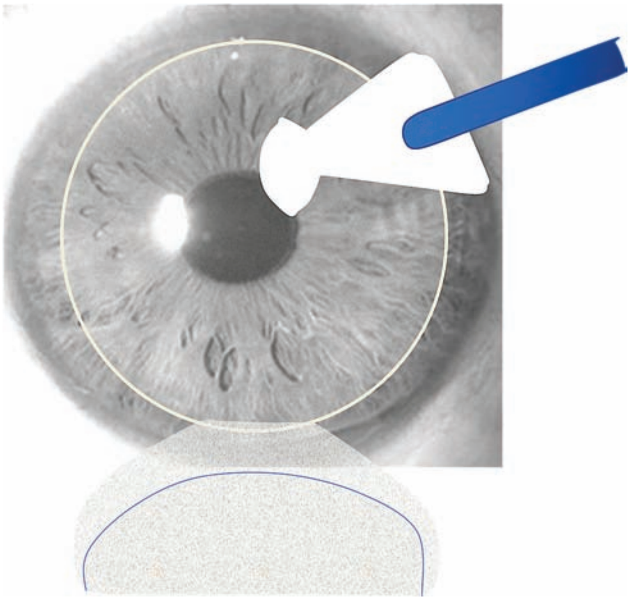

Fig. 5.28 Drying the stromal bed.

6. **Addressing the Eye:** After the ablation is completed, the flap is replaced onto the stromal bed. The interface is irrigated until all interface debris are eliminated (which is better seen with oblique rather than coaxial illumination) (Fig. 5.29). The surface of the flap is gently stroked with a smooth instrument, such as an irrigation canula or a moistened microsurgical spear sponge, from the hinge, or centre, to the periphery to ensure that wrinkles are eliminated and that the flap settles back into its original position, as indicated by realignment of the corneal

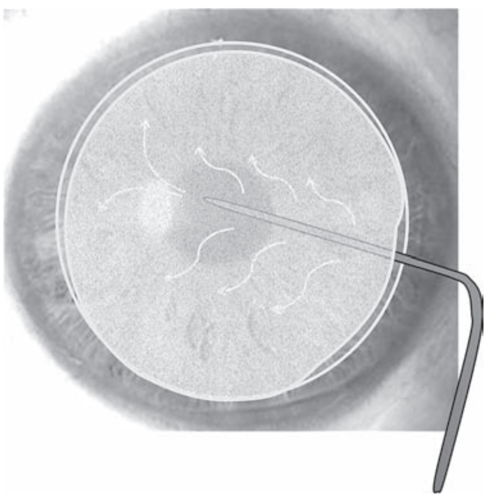

Fig. 5.29 Irrigating the interface after flap repositioning to remove debris.

marks made earlier (Fig. 5.30). The peripheral gutters should be symmetric and even. The physiologic dehydration of the stroma by the endothelial pump will begin to secure the flap in position within several minutes. If a significant epithelial defect or a large loose sheet of epithelium is present, a BCL should be placed. Once the flap is adherent, the eyelid speculum is removed carefully so as not to disturb the flap. Most surgeons place varying combinations of antibiotic and corticosteroid drops on the eye at the conclusion of the procedure. The flap is usually rechecked at the slit lamp before the patient leaves to make sure it has remained in proper alignment. A clear shield or protective goggles are often placed to guard against accidental trauma that could displace the flap. Patients are instructed not to rub or squeeze their eyes.

Post LA Management

Many surgeons instruct their patients to use topical antibiotics and corticosteroids postoperatively for 3–7 days. With femtosecond laser procedures, some surgeons prescribe more frequent applications of corticosteroid eye drops or a longer period of use. In addition, it is very important for the surface of the flap to be kept well lubricated in the early postoperative period. Patients are advised to keep their eyes closed for at least 2 hours immediately after the procedure. Patients may be told to use the protective shield for 1 week when they shower or sleep and to avoid swimming and hot tubs for 2 weeks. Patients are examined 1 day after surgery to ensure that the flap has remained in proper alignment and that there is no evidence of infection or excessive inflammation. In the absence of complications, the next examinations are typically scheduled at approximately 1 week, 1 month, 3 months, 6 months and 12 months, postoperatively.

Pros and Cons

Table 5.1 summarizes types of PRT and the cons and pros of each type.
Table 5.2 compares SA with LASIK.

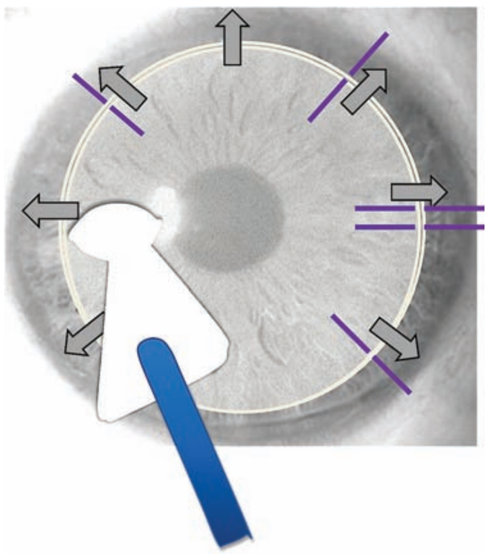

Fig. 5.30 Removing liquid from interface by massaging the flap. Corneal marks should be aligned.

Table 5.3 presents advantages of SBK.
Table 5.4 presents advantages of TE-PRK
Table 5.5 presents results of SA.
Table 5.6 summarizes advantages and disadvantages of femtosecond laser over MMK.
Table 5.7 is a comparison between a femtosecond created flap and an MMK created flap.

TABLE 5.1 Types of Photorefractive Surgery

<table>
<tr><th rowspan="2">Factor PRK</th><th colspan="4">Surface Ablation</th><th rowspan="2">SBK*</th><th rowspan="2">LASIK</th></tr>
<tr><th>TE-PRK^</th><th>LASEK</th><th>Epi-LASEK</th><th></th></tr>
<tr><td>Range of correction</td><td colspan="6">Up to –8 D Sph
Up to +4 D Sph
Up to 6 D Cyl</td></tr>
<tr><td>Postoperative pain</td><td colspan="4">Mild to moderate, may extend for 24–72 hours</td><td colspan="2">Minimum, may extend for 12 hours</td></tr>
<tr><td>Postoperative medications</td><td colspan="4">1–3 months</td><td colspan="2">1 week</td></tr>
<tr><td>Functional vision recovery</td><td colspan="4">3–7 days</td><td colspan="2"><24 hours</td></tr>
<tr><td>Refractive stability</td><td colspan="4">3 weeks to 3 months</td><td colspan="2">1 week to 3 months</td></tr>
<tr><td>Specific complications</td><td colspan="2">Haze formation, scarring</td><td colspan="2">Haze formation, scarring, incomplete epithelial flap, stromal incursions</td><td>Flap complications†, Bowman cracks, diffuse lamellar keratitis (DLK)</td><td>Flap complications†, ectasia, diffuse lamellar keratitis (DLK)</td></tr>
<tr><td>Better for</td><td colspan="4">EBMD (epithelial basement membrane corneal dystrophy), thin corneas, flap trauma risk, flat corneas, steep corneas, ectasia susceptible, nerve injury, moderate to severe dry eye syndrome, wide scotopic pupil, LASIK complications in the fellow eye, irregular astigmatism (TE-PRK is superior), early keratoconus (TE-PRK + corneal cross linking), glaucoma suspect, recurrent erosion syndrome, deep-set orbits, narrow palpebral fissures, corneal vascularization, corneal nodules, prior history of ocular surgery with significant conjunctival scarring and/or irregular tissue near the limbus</td><td>Thinner corneas, ectasia susceptible, surface healing issues</td><td>Infection risk, surface healing issues, concern of postoperative pain, requirement of rapid visual recovery</td></tr>
<tr><td>Worse for</td><td colspan="2">Concern about postoperative pain, requirement of rapid visual recovery</td><td colspan="2">Concern about postoperative pain, requirement of rapid visual recovery, glaucoma, scleral buckle, deep set eyes, small palpebral fissure</td><td colspan="2">Thin corneas, wide pupils, recurrent corneal erosion syndrome, glaucoma, scleral buckle, deep set eyes, small palpebral fissure</td></tr>
</table>

† Refer to Table 5.2
* Refer to Table 5.3
^ Refer to Table 5.4

TABLE 5.2 Comparison of Surface Ablation and LASIK

Advantages of SA over LASIK	Weakens the cornea by approximately 5–10% vs. 15–30% for LASIK* Quick and safe procedure No LASIK corneal flap complications: • No free flap • No buttonhole formation in the corneal flap • No incomplete flaps • No flap melt • No risk for postoperative traumatic flap dislocation • No flap striae • No epithelial ingrowth • No interface debris • No interface fluid accumulation • No diffuse lamellar keratitis (DLK) • Better biomechanical stability • No compromise of the deep collagen layers and the peripheral circular fibers • Decreased risk for postoperative corneal ectasia* • No epithelial erosions from the MMK • Decreased development or exacerbation of dry eye syndrome • Less postoperative reduction in corneal sensation • Decreased risk for postoperative corneal edema associated with preoperative cornea guttata • No HOAs associated with LASIK flap creation • Treatment of irregular corneas has better results with TE-PRK • Wavefront-guided treatment (WFGT) has better results with SA • Easier enhancement (2–3 times) in case of good thickness
Advantages of LASIK over SA	More rapid visual rehabilitation More rapid stabilization of refraction Decreased postoperative discomfort Minimal corneal haze (third generations of excimer lasers has less haze with SA) Less risk of infection Reduced frequency and intensity of topical steroids postoperatively Fewer postoperative visits

*creation of a flap reduces corneal strength:
80 µm flap = 14% loss of corneal strength
140 µm flap = 25% loss of corneal strength
160 µm flap= 29% loss of corneal strength
180 µm flap = 33% loss of corneal strength

TABLE 5.3 Advantages of SBK

- Less impact on corneal biomechanics
- Better corneal stability - reduced ectasia risk
- Less corneal nerve injury - less dryness
- Faster visual recovery
- Allows for higher corrections in thinner corneas

TABLE 5.4 Advantages of TE-PRK

- Best for irregular corneas
- Less traumatic
- De-epithelialization is restricted to the treatment zone
- Less re-epithelialization time
- Less inflammation and pain (intensity and duration)
- Less recovery time

TABLE 5.5 Results with Surface Ablation

Myopic Correction	The lower the corrections the better the prognosis, best in low myopic corrections (–1 to –6 D) with up to 96% success. A transient hyperopia followed by regression may occur, this is related to the amount of correction. Predictability up to 98.8% (low myopia) Efficacy: high Safety: high
Hyperopic Correction	The lower the corrections the better the prognosis, best in low hyperopic corrections (+1.5 to +3.5 D) with a success rate lower that in myopic correction Regression is possible and common Efficacy: almost 76% Safety: best in low corrections

TABLE 5.6 Advantages and Disadvantages of Femtosecond Laser over MMK

Advantages	*Disadvantages*
1. Less increase in IOP 2. More control over flap diameter 3. Size and thickness of flap less dependent on corneal contour 4. Centration easier to control 5. Epithelial defects on flap are rare 6. Less risk of free flap, buttonhole and displaced flap 7. More reliable flap thickness 8. Hemorrhage from limbal vessels less likely 9. Ability to re-treat immediately if incomplete femtosecond laser ablation	1. Longer suction time 2. More flap manipulation 3. Opaque bubble layer may interfere with excimer ablation 4. Bubbles in the anterior chamber may interfere with tracking and registration 5. Increased overall treatment time 6. Difficulty lifting flap > 6 months 7. Increased risk of diffuse lamellar keratitis 8. Increased coast 9. Need to acquire new skills 10. Delayed photosensitivity or good acuity plus photosensitivity (GAPP), which may require prolonged topical corticosteroid therapy

TABLE 5.7 A Comparison between Femto-created and Microkeratome-created Flaps

	Femtosecond	*MMK*
Safety in small steep cornea	safer	Less safe
Epithelial defect in old females	Less likely	More likely
Thickness	Consistent	Inconsistent
Parallel Faces	Yes	No (except pendular MMK)
Biological Interaction	Potentially High (energy-dependent)	Low
Side Cut	Angled	Meniscus
Reproducibility	High	Low

TAKE-HOME MESSAGE

- There are two main techniques in LA, LASIK and SBK which can be considered as a combination between SA and LA
- In general, SA is safer than LA
- The most specific complications in SA are haze and scarring, whereas the most specific complications in LA are flap complications and ectasia
- Decentration of the flap is mandatory when the laser beam is decentered
- Flap diameter should be 0.5 to 1.0 mm larger than the treatment zone
- Marking the cornea is important
- Check good suction fixation of the eye before flap cut
- The most advantages of femtosecond over mechanical MMK are less increase in IOP and more control of flap diameter, thickness and centration
- Both LA and SA have pros and cons, but the new tradition today is "back to surface"

Potential Contraindications to PRT

Table 5.8 summarizes potential contraindications to PRT.

PRT Profiles

During the last couple of years, a great development occurred in photorefractive treatment profiles in order to achieve optimal refractive results regarding quality and quantity of visual acuity.

TABLE 5.8 Potential Contraindications to PRT

1. Connective tissue disease
   a. Rheumatoid arthritis
   b. Systemic lupus erythematosus
   c. Sjogren syndrome
   d. Wegener granulomatosis
2. Dry eye syndrome
3. Neurotrophic corneas
4. Previous herpes simplex
5. Previous herpes zoster ophthalmicus
6. Fuchs corneal dystrophy
7. Corneal stromal dystrophies
8. Corneal ectatic disorders (unless surface ablation is combined with corneal cross-linking)
9. Glaucoma (especially if a large bleb is present)
10. Blepharophimosis
11. Monocular patients
12. Large pupil size
13. Medications
    a. Isotrentinoin (Accutane) (contraindicaiton for surface ablation)
    b. Amiodarone hydrochloride such as Cordarone and Pacerone (contra for surface types)
    c. Antihistamines (contraindication for surface ablation)
    d. Anticoagulants (contraindication for lamellar, SBK and Epi-lasik)
14. Uncontrolled systemic diabetes
15. Diabetic retinopathy
16. Systemic or retinal vascular diseases
17. Thyroid eye disease
18. Monocular patients
19. Patients who are pregnant or nursing or planning to be pregnant in the next 6–12 months
20. Patients with unreasonable expectations or unwilling to take the risk of possible complications
21. Patients who are unable to commit to postoperative instructions and care plan
22. Patients younger than 18 years, preferably 21 years and more.

Plain Ablation Profile

Primary photoablation profiles were designed to correct spherocylindrical refractive errors; little knowledge about corneal slope and ocular aberrations was available at that time.

In this type, laser beam is applied on a small OZ (5–5.5 mm) with all ablation pulses equal in power along the ablated area as shown in Figure 5.31. Since corneal surface is convex, the peripheral laser pulses in this profile fall obliquely rather than perpendicularly losing some of their energy (Fig. 5.32) and creating a plain or even a slightly concave zone. This creates an abrupt transition between the plain treated zone and the convex corneal midperiphery inducing spherical aberration presenting as night glare and halos. Three factors contribute in the resulting spherical aberration, the small OZ vs. pupil, the plain shape of the OZ due to equal power of all laser pulses and the corruption of corneal slope. In addition, this profile has the worst biomechanical disturbance as mentioned in chapter 4. This profile is no longer used.

Fig. 5.31 Plain ablation profile.

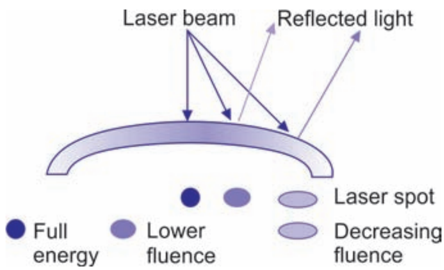

Fig. 5.32 Loss of laser energy at corneal periphery in plain ablation profile.

Optimized Ablation Profile

To improve the plain profile and avoid inducing spherical aberrations, a true aspheric OZ is created by: first, enlarging the OZ; second, increasing the power of peripheral pulses to compensate for the oblique incidence of laser beam and to create a convex ablation zone (Fig. 5.33); third, adding the concept of the transitional zone (Fig. 5.34).

Aspheric (Q-Guided) Profile

Although the optimized profile produces a true aspheric OZ, its effect is limited to low refractive errors (myopia < 3 D, astigmatism < 2 D or hyperopia < 3 D). Whenever the desired correction should go beyond these limits, asphericity of the cornea will be affected and hence the need for the aspheric profile.

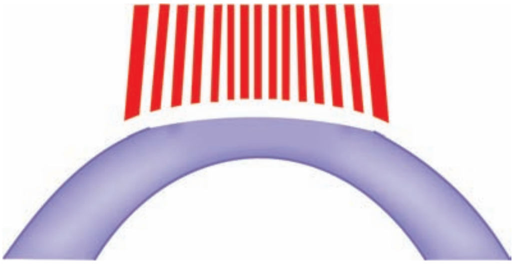

Fig. 5.33 Optimized ablation profile.

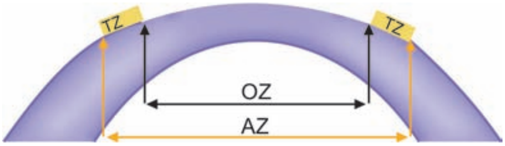

Fig. 5.34 Transitional zone concept. TZ: transitional zone; OZ: optical zone; AZ: ablation zone. The machine software adjusts an optimal TZ depending on amount of correction, K-readings and corneal slope.

On the other hand, this profile can be used to re-adjust Q-value either in case of abnormal value or in the management of presbyopia. This will be discussed in details in chapter 6.

The principle of the aspheric profile is the same as the optimized one added that it reshapes the treated surface by adding more prolate peripheral ablation and optimizing the transitional zone (the larger the transitional zone the higher the spherical aberration), thereby reducing spherical aberration and maintaining or achieving normal Q-value even in relatively high refractive errors (see Fig. 5.35 and compare it with 5.33).

Aspheric Aberration-Free Profile

It is not uncommon that photoablation may induce iatrogenic HOA(s) or at least may change the native (preexisting) HOA(s).

All human eyes have different amounts of native HOAs, but not all eyes suffer from them. Several mechanisms contribute in the compensation for asymptomatic HOAs such as neural adaptation to native aberrations, depth of focus and wide field of vision. When these aberrations are increased or changed (e.g. switching from coma to trefoil), decompensation occurs.

Patients who have subjective complaints and irregular corneas following PRT can have 2.3 to 3.5 times more HOAs than those who are asymptomatic and have normal corneas.

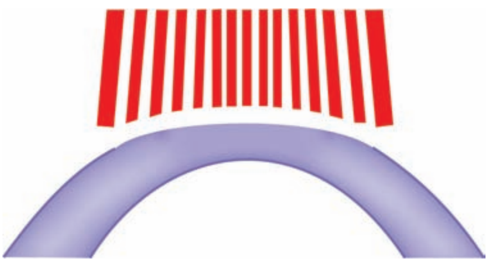

Fig. 5.35 Aspheric ablation profile.

Aspheric aberration-free profile was designed to maintain the pre-existing normal asphericity in addition to maintain the compensated asymptomatic native aberrations.

Wavefront-Guided Treatment (WFGT)

It is also named *custom treatment*. It is a variation of the surgery, where rather than applying a sphero-cylindrical correction to the cornea, laser is instructed to ablate a sophisticated spatially variant pattern based on measurements from an Aberrometer. The goal of achieving a more optically perfect ablation depends on appropriate patient selection, high-quality wavefront data, successful surgery and accurately predicting and managing the change that occur during healing. WFGT has two types according to the source of data, corneal WFGT and ocular WFGT.

Corneal WFGT

It is also known as "topography-guided treatment" since it depends on corneal topography (in fact corneal tomography) to treat corneal irregularity without treating associated refractive errors. If refractive errors need to be treated, they should be added to the profile.

This profile is calculated from corneal elevation data derived from corneal tomography measurements. The profile is then transformed to the excimer laser machine software, which analyses and instructs the profile in a shape that neutralizes corneal irregularities. To understand this, look at Figure 5.36, the right side is corneal tomography of a keratoconic cornea and the left side is the instructed treatment profile. The white arrows point at the steep area in tomography and to the corresponding ablation in the profile. The blue arrows point at the flat area in tomography and to the corresponding minimal ablation in the profile, whereas the yellow arrow in the profile points at the peripheral ablation to steepen the area at which the blue arrow in tomography points.

To have a good idea about the ablation profiles, the followings are ablation profiles of several situations:

Figure 5.37 is the ablation profile to correct positive spherical aberration in an eye with no refractive error.

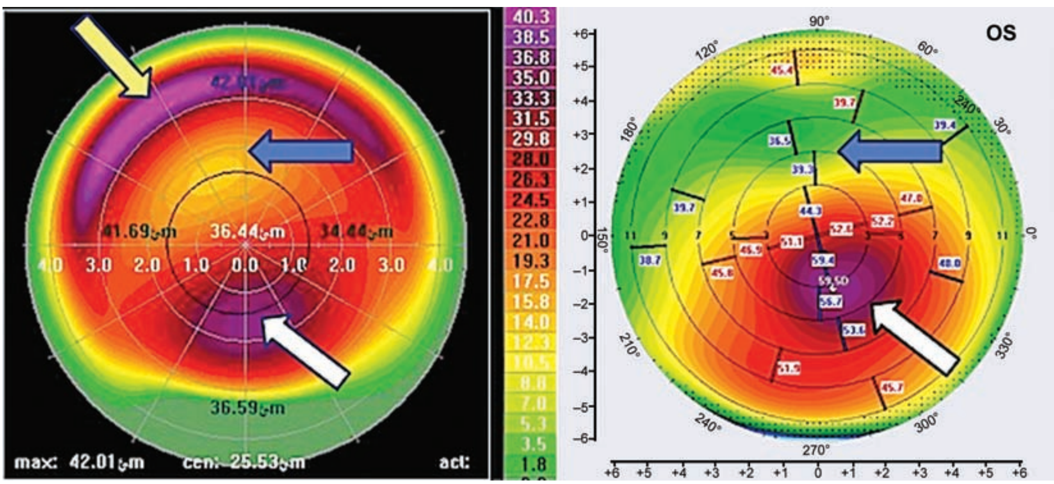

Fig. 5.36 Wavefront guided treatment.

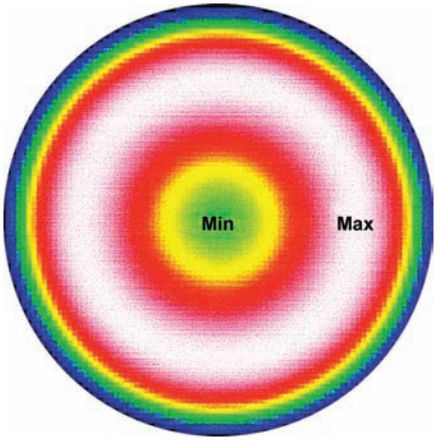

Fig. 5.37 Ablation profile to correct positive spherical aberration. Maximum ablation is peripheral, while minimum ablation is central.

Figure 5.38 is the ablation profile to correct spherical aberration in a hyperopic eye.

Figure 5.39 is the ablation profile to correct spherical aberration in a myopic eye.

Notice the difference among the last three figures; the maximal AD is peripheral in the first two figures contrary to the third one.

Figure 5.40 is the ablation profile to correct coma.

Figure 5.41 is the ablation profile to correct trefoil.

Corneal wavefront-guided profile is usually used to treat early to moderate cases of keratoconus and keratoectasia in conjunction with CXL. It is also indicated in the treatment of irregular astigmatism (Fig. 5.42), decentered OZ (Fig. 5.43), central island (Fig. 5.44) and to enlarge small OZs (Fig. 5.45). But it has to be kept in mind that this profile may introduce or change the refractive status of the eye; therefore, it requires a good experience from the surgeon and a good understanding from the patient. This treatment aims at reducing corneal irregularities and the related HOAs to improve the quality (and may be the quantity) of the uncorrected and best corrected visual acuity.

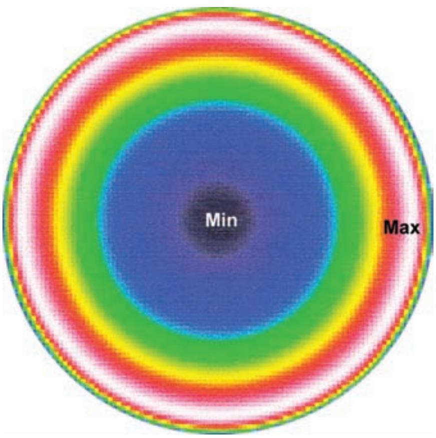

Fig. 5.38 Ablation profile to correct spherical aberration in a hyperopic eye.

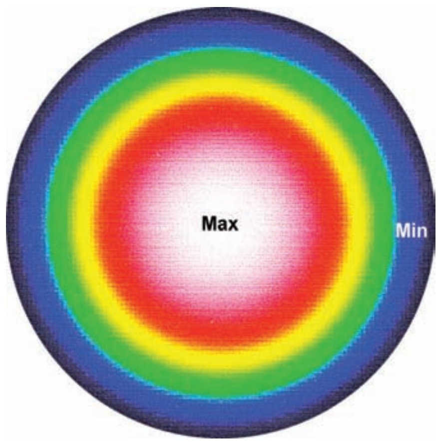

Fig. 5.39 Ablation profile to correct spherical aberration in a myopic eye.

Corneal wavefront-guided ablation may not be appropriate for use after cataract surgery, particularly with multifocal IOLs.

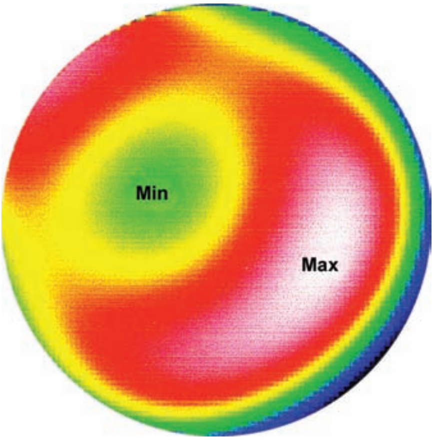

Fig. 5.40 Ablation profile to correct coma.

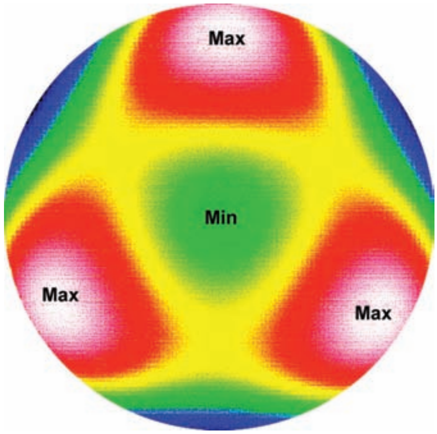

Fig. 5.41 Ablation profile to correct trefoil.

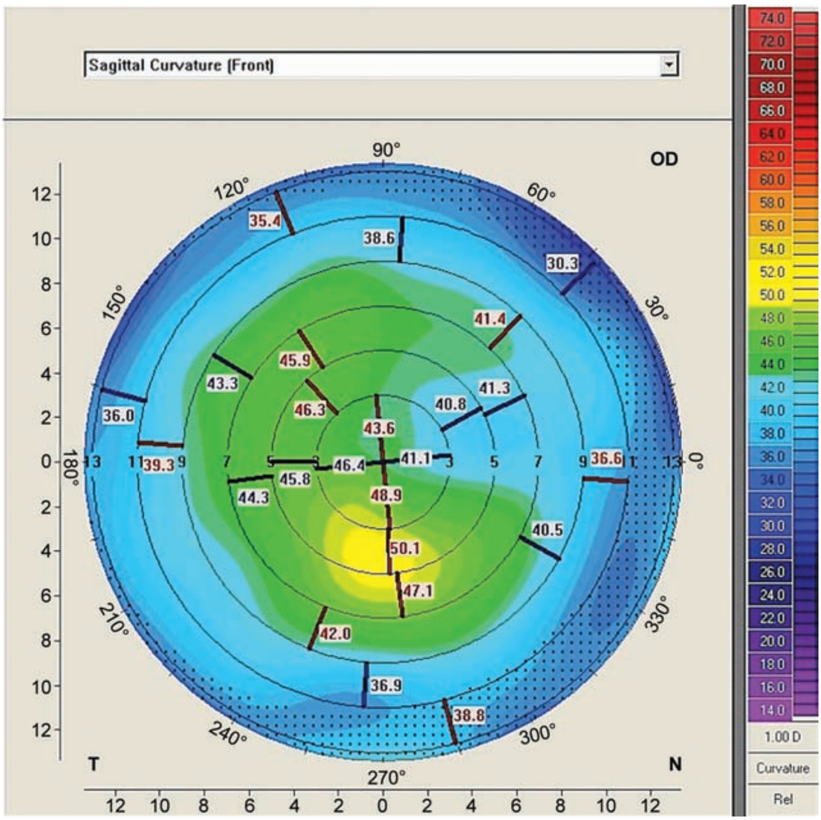

Fig. 5.42 Irregular astigmatism.

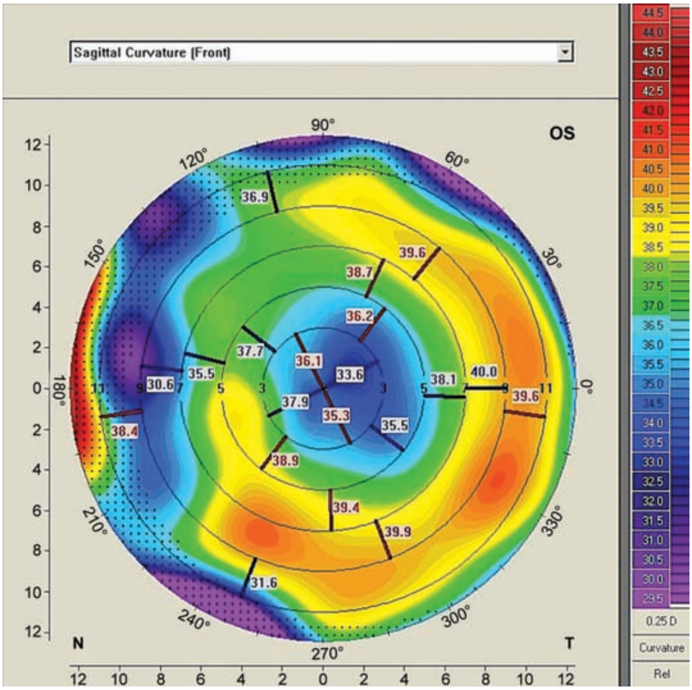

Fig. 5.43 Decentered ablation zone.

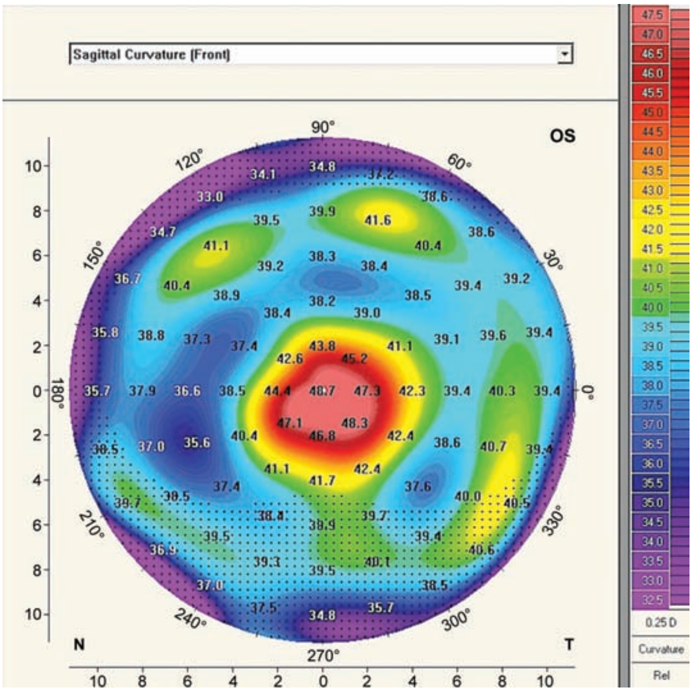

Fig. 5.44 Central island.

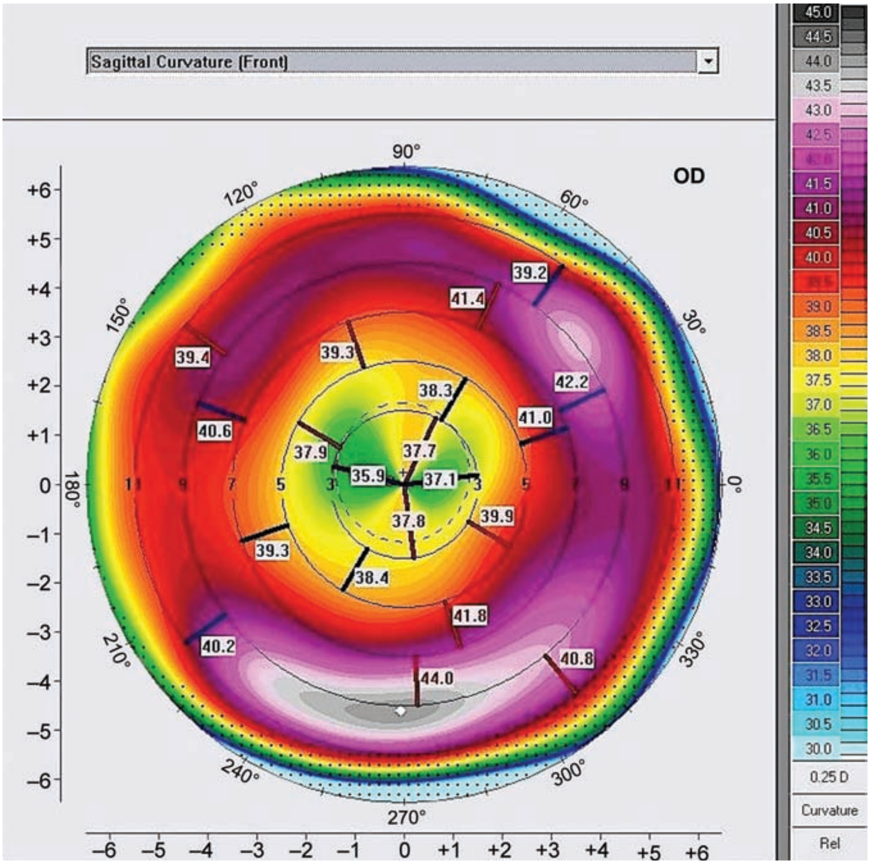

Fig. 5.45 Small optical zone.

Ocular WFGT

It is also known as "total WFGT". Total HOAs are measured by the aberrometer, which at the same time measures the objective refractive error, giving a profile that contains both total HOAs and objective refractive error of the examined eye.

The principle of ocular WFGT is the same as corneal WFGT, but there are three major differences:

First, ocular WFGT measures and corrects total HOAs produced by all refractive media of the eye, contrary to corneal WFGT that measures and treats corneal HOAs.

Second, ocular WFGT measures and treats objective refractive error, contrary to corneal WFGT where subjective refractive error should be added. For more details, see "Manifest Refraction" and "Data Analysis" below.

Third, in very irregular corneas or in eyes with small pupils, wavefront data may be hard to obtain by ocular WFGT, in such cases, corneal WFGT is superior and an alternative.

Finally, similar to corneal WFGT, ocular WFGT may induce some refractive error, but not to that extent encountered with corneal WFGT.

N.B. 1: In the last three profiles, high speed eye tracker, auto centration and compensation for cyclotorsion are mandatory.

N.B. 2: In the last two profiles, the higher the resolution of the aberrometer is, the more accurate the results and the less adverse the side effects are.

N.B. 3: In the last two profiles, correcting HOAs may generate new HOAs up to twice as many. Furthermore, since HOAs change with increased age, the optimum results may persist for a limited time. Therefore, treatment with the last two profiles should be done with caution and be limited to specific cases as will follow in the decision tree.

Key Elements in WFGT

There are key elements of a preoperative wavefront-guided PRT examination to perform a custom procedure and to achieve successful results. These key elements are wavefront capture, manifest refraction, data analysis, profile creation, topography, tomography, pachymetry, pupillometry and patients counseling. In addition, there are intraoperative key elements, which include alignment and registration, centration, eye tracking, nomogram adjustment and flap creation.

1. **Preoperative Key Elements:**
   a. *Wavefront Capture:* The quality of laser ablation and hence visual outcomes are precisely related to the quality of wavefront capture. The saying "garbage-in, garbage-out" exactly applies to the wavefront capture.
      – *Monitoring scan capture.* Unless the surgeon performs all the wavefront measurements, an attentive and well-trained technician is a must. Centration during taking the capture influences exam results; any slight decentration causes dramatic differences in maps.
      – *Multiple exams* are mandatory, they allow for evaluation of scatter. Use only reliable multiple captures and discard the outliers.
      – *Validation.* In case of corneal wavefront-guided (topography-guided), captures should be validated by comparing their K readings with those of ocular wavefront and keratometry.
      – *Tear film effect.* The quality of each capture needs to be monitored by assessing the lenslet pattern and dropout points. Let the patient blink and close eyes repeatedly and open wide just before taking the capture. Transient dropout that varies between captures usually indicates a dry spot on the cornea, whereas an area of consistent dropout can indicate opacity in the optical system (Fig. 5.46). The captures should

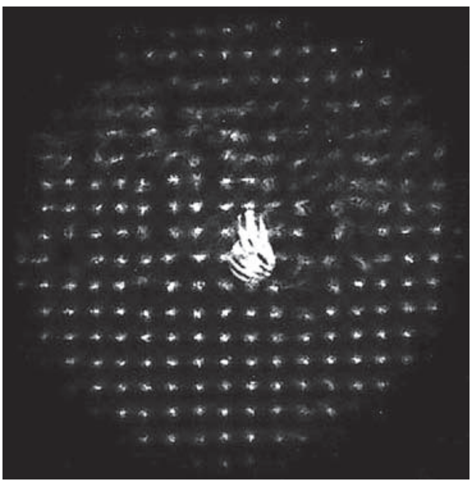

Fig. 5.46 Dropout in wavefront capture.

be repeated as needed to obtain high-quality images. The variability in the derived defocus (sphere) between captures is a useful tool to ensure accurate measurements.

- *Memory effect.* Corneal tissue has a memory to deformation such as measuring IOP by applanation which causes indentation of corneal surface and should be avoided at least six hours before taking the capture.
- *Considering pupil size and accommodation.* In ocular WFGT, the size of the entrance pupil should be at least as large as intended treatment zone to get raw data over entire treatment area. Therefore, the wavefront unit should be located in a dim room to allow a large pupil capture. A pupil size of 5 mm is generally accepted as the minimum (better 6 mm) and is a requirement for the laser system. Some physicians use low-strength tropicamide to increase the pupil size for the aberrometer capture, although there is some concern about the potential shift in the pupil centroid. Manufacturers have designed their wavefront units to minimize the tendency for a patient to accommodate (instrument myopia). Despite this, accommodation during a capture is always a concern and needs to be monitored and minimized in laser systems that base their capture on a natural pupil. Checking the difference between the manifest (subjective) sphere and the wavefront-derived (objective) sphere is required. Careful instruction to patients can help, such as not allowing them to read just beforehand and telling them to "look beyond the instrument" during the capture. Some laser systems rely on a cycloplegic capture, which allows for a large pupil capture without accommodation concern, but again there is some concern about the potential shift in the pupil centroid.
- *Raw data.* Do not use captures with extrapolated data within the diameter of treatment zone. In corneal WFGT, sagittal and tangential maps provide just different views (optical and power), but they do not influence corneal height (elevations) profile and the resulting treatment ablation profile.

b. *Manifest Refraction:* Even though ocular wavefront provides the treatment profile, including sphere and cylinder, a manifest refraction is still necessary. It is primarily used to assess the accuracy of the wavefront capture and to help determine refractive stability. This refraction should be "push plus" to eliminate accommodation as well as a careful determination of the astigmatism, typically using a Jackson Cross Cylinder. It is important to know the exact refractive status of each patient to assess the wavefront data properly. It is also important to assess and record visual acuity and determine the pre- and postoperative visual capability. In this regard, it is useful to assess the full visual potential beyond 1.0 (Snell) where this can be achieved.
   Finally, in case of significant disparity between subjective and objective refractive errors by ocular wavefront, the former should be used.
c. *Data Analysis:* Depending on the laser system, a series of images is selected to calculate the ablation profile. Only the highest-quality images should be used.
   In ocular WFGT, there is often a difference between the wavefront-derived sphere/cylinder (objective refraction) and the manifest sphere/cylinder (subjective refraction). This difference can be due to several factors: the accuracy of the wavefront and manifest refraction; accommodation during either the wavefront capture or manifest refraction; or the influence of HOAs on the manifest refraction. Manufacturers generally provide guidance. Before proceeding with surgery, it is important to determine the acceptable differences between components of the manifest, cycloplegic and wavefront refractions

to assess acceptability of wavefront data. If the difference between the wavefront and manifest refraction exceeds the manufacturer's guidelines, there are several options to consider:

   i. Repeat both refractions. The wavefront capture, or the manifest refraction, may be more minus if the patient is accommodating.
   ii. Repeat the manifest refraction using the wavefront-derived sphere and cylinder as a starting point. The wavefront-derived cylinder and axis may more accurately define the patient's astigmatism as demonstrated by an improvement in best-corrected vision.
   iii. Check the cycloplegic refraction. If after these steps the difference still exceeds the manufacturer's guidelines for the laser system, an ocular wavefront-guide treatment may not be suited to this candidate and corneal WFGT may be better.

d. *Profile Creation:* After the selection of the most suitable wavefront image, an ablation profile is created within the corneal wavefront device or the aberrometer (according to which type). In aberrometer, both LOAs (sphere and cylinder) and HOAs are incorporated. The optical path deviation from the wavefront is converted into a spatial pattern that can correct the aberrations on the corneal surface. The profile is then transferred to the laser via an SD card or USB memory stick.
e. *Pupillometry and Patient Counseling:* The importance of pupillometry in the preoperative work-up has been controversial. Most studies of conventional PRT have not shown a relationship between the diameter of the scotopic pupil and disturbing visual symptoms postoperatively. On the other hand, patients with larger pupils who undergo WFGT appear to have no increase in symptoms and may perhaps have fewer symptoms. One of the most important benefits of WFGT compared to a conventional treatment may be in low-light conditions when the pupil dilates. That is where a reduction, or less induction, of HOAs may be most apparent. Despite the fact that WFGT results in fewer post-op complaints, irrespective of pupil size, it is important for potential patients to understand that still there might be a risk for night vision problems after surgery. (See Pupil size rule in chapter 6).

2. **Intraoperative Key Elements:**
   a. *Alignment and Registration:* Registration and alignment of the ablation profile is mandatory in WFGT. This step will be discussed in details in chapter 6.
   b. *Centration:* Proper centration of ablation is critical to ensuring good outcomes. Decentration of 0.5 mm or less can result in debilitating visual symptoms. Accurate centration is even more important when treating HOAs. Centration is based on matching the aberrometer-derived ablation profile either to the limbus, the pupil margin or iris details. The center of the pupil (pupil centroid) can change positions up to 0.7 mm as the pupil dilates or constricts. For laser systems based on pupil margins, it is important to compensate for this centroid shift to avoid an ablation decentration. Iris recognition systems do this by using the limbus and iris details as reference points.
   c. *Eye Tracking:* Even with proper initial centration and alignment, eye movement during surgery can have a deleterious effect on the outcome. All custom-capable excimer laser systems employ sophisticated eye trackers. Most systems utilize an infrared camera to track the edge of the iris because of the contrast between the iris and pupil. A passive eye tracker monitors eye motion and interrupts the laser treatment if the eye movement exceeds a certain threshold. An active eye tracker drives a complex mirror system that

directs the excimer laser beam onto the proper location on the cornea. Laser systems can employ both methods, steering the laser if eye movements are slight but pausing the laser if movements are too large. This is important because active eye trackers do not account for the change in effective laser energy as the curvature of the cornea changes during movement. Hence, even with a properly working eye tracker, the surgeon needs to monitor centration continually during the procedure.

d. *Nomogram Adjustment:* Potential sources of variability in custom LASIK outcomes include surgical technique, local conditions such as the temperature and humidity and patient characteristics such as gender and age. Just as nomogram adjustments are often needed to fine-tune the efficacy of conventional LASIK, adjustments may be needed to improve the efficacy of a custom treatment.
e. *Flap Creation:* The quality of the flap is even more important when performing custom LASIK. Besides, the flap needs to be large enough for the custom ablation and be well centered. In comparison with MMK flap, the femtosecond laser flap results in an improved outcome and better quality of vision. Reasons postulated for this observation are that the femtosecond laser flaps are more reliable and consistent, produce fewer HOAs and are less prone to epithelial injury (see Tables 5.6 and 5.7).

Postoperative Management

Postoperative management after custom treatment is identical to conventional treatment.

Decision Tree

Corrected distance visual acuity (CDVA), contrast sensitivity, CWF, OWF, internal wavefront (IWF), media transparency and patient's complaints of HOAs are the trunk of the decision tree.
See Figure 5.47 before going in details:

1. If the RMS of OWF (measured in diopters) is ≤ 0.25 D, use:
   a. The optimized profile for low refractive errors, or
   b. The aspheric or aspheric aberration-free profiles for low, moderate and high refractive errors.

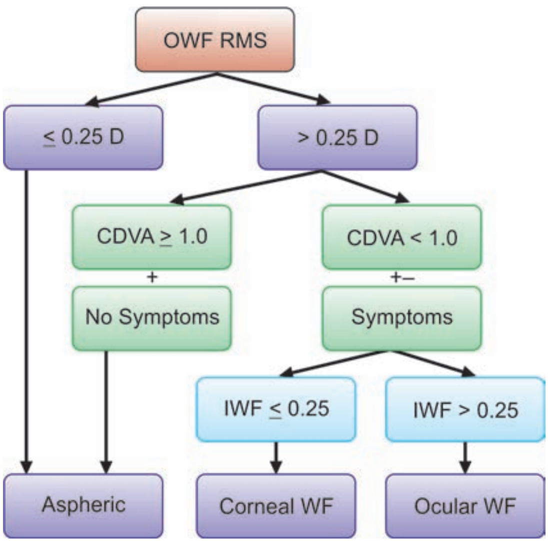

Fig. 5.47 Decision tree in wavefront guided treatment. OWF: ocular wavefront; RMS: root mean square, related to HOAs; CDVA: corrected distance visual acuity; IWF: internal wavefront.

2. If the RMS of OWF (measured in diopters) is >0.25 D and:
   a. CDVA is ≥1.0 (Snellen) and there are no complaints indicating HOAs such as night glare, halos, starbursts or ghost images, use:
      i. The optimized profile for low refractive errors, or
      ii. The aspheric or aspheric aberration-free profiles for low, moderate and high refractive errors.
   b. CDVA is <1.0 (Snellen) and/or there are complaints indicating HOAs such as night glare, halos, starbursts or ghost images, you have to know the source of HOAs (corneal or internal):
      i. If the RMS of the IWF is ≤0.25 D, the cornea is the source of HOAs; perform corneal WFGT.
      ii. If the RMS of the IWF is >0.25 D, the internal media are the source of HOAs; perform OWF treatment.

TAKE-HOME MESSAGE

- Plain profile has the worst effect on corneal biomechanics and it is no longer used
- Optimized ablation profile is suitable for low refractive errors
- Aspheric ablation profile is suitable for low to moderately high refractive error
- Aspheric aberration free profile may help in reducing the iatrogenic HOAs
- WFGT profiles are used to treat irregular cornea and HOAs
- Corneal WFGT profile does not include refractive error correction unless it has been added to the profile
- Ocular WFGT profile includes objective refractive error correction unless it has been excluded from the profile
- Both types of WFGT profiles may induce refractive errors
- Pay attention to key elements in WFGT including wavefront capture, manifest refraction, data analysis, profile creation, pupillometry and patient counseling in addition to intraoperative key elements including alignment and registration, centration, eye tracking, nomogram adjustment and flap creation

SURFACE ABLATION COMBINED WITH CORNEAL COLLAGEN CROSS LINKING

CORE MESSAGE

- SA in conjunction with CXL is indicated in treating refractive errors in corneas with early to moderate ectatic diseases including post LASIK ectasia or corneas having the potential risk of post PRT ectasia
- The aim of this treatment is to improve the quality of vision by reducing the amount of irregular astigmatism

In the last few years, the combination of SA and CXL has mounted and indicated in the treatment of:
1. Refractive errors in early to moderate ectatic corneal disorders such as KC, PMD, FFKC and post-PRT ectasia.
2. Refractive errors in corneas with potential risk of post-PRT ectasia.
3. Irregular corneas such as post-corneal grafts.

During the surgery, customized PRT (most often using corneal wavefront-guided surface ablation profile) is done first; thereafter CXL is applied in the same session.

The aim of this treatment is to regularize the cornea by reducing the amount of irregular astigmatism, correcting part of the refractive error, improving the quality and quantity of visual acuity by reducing the amount of HOAs and to stabilize the ectatic corneal disorders or

prevent the induction of ectasia in corneas with a potential risk. CXL strengthens the cornea by approximately 300–500%.

Conditions

1. In ectatic corneal diseases, there are two limits:
    a. The AD should not exceed 50 µm.
    b. The RSB should be >400 µm at the end of photoablation before CXL application.
2. In irregular corneas and in corneas with potential risk of ectasia:
    a. It is recommended that the AD does not exceed 80–90 µm according to the OZ.
    b. The RSB should be >400 µm at the end of photoablation before CXL application.

To measure the central thickness before CXL application, there are two methods, online pachymetry integrated in some excimer machines and ultrasound pachymetry. In case of 370–400 µm of RSB, still one can use hypotonic riboflavin for 10 min to swell the stroma, then continue with the normal riboflavin and then apply CXL whenever the RSB has reached 400 µm, otherwise the endothelium will be damaged.

Recommendation

CXL has a flattening effect on the cornea causing hyperopic shift. Therefore; it is recommended to undercorrect the eye for –0.75 D to –1 D in case of myopic ablation to compensate for the flattening effect and avoid the hyperopic shift.

Contraindications

1. A RSB of <400 µm after photoablation and before CXL application, unless hypotonic CXL is to be used.
2. K-max >58 D since there is a high incidence of CXL failure.
3. High visual expectations because this treatment aims at reducing the amount of HOAs induced by irregular astigmatism.
4. Corneal epithelial healing disorders.
5. Previous herpes keratitis.
6. Corneal melting disorders (such as rheumatoid arthritis).
7. Pregnancy.
8. Continuous eye rubbing habits especially when associated with the following systemic conditions: Down syndrome, atopic disease, CL wear, floppy eyelid syndrome and nervous habitual eye rubbing.
9. Corneal scaring.

Considerations

Corneal wavefront-guided surface ablation profile is usually used in this kind of treatment. In this profile, most ablation is spent for regularizing the cornea and reducing irregular astigmatism; therefore, the amount of AD per diopter is larger than that in other profiles. Since only a maximum of 50 µm of AD is recommended, may be 2–3 D of refractive error can be corrected.

On the other hand, in irregular corneas, HOAs are due to irregular astigmatism; therefore, it is wise to give the priority for correcting the astigmatism rather than the spherical component of the refractive error in such cases.

TAKE-HOME MESSAGE

- In ectatic corneal diseases or post LASIK ectasia, the recommended AD is 50 µm at most
- In corneas carrying the potential risk of ectasia, the recommended AD is 80 µm to 90 µm at most
- In all cases, the RSB should be at least 400 µm before CXL application
- Should the RSB be 370 µm, hypotonic CXL is to be used
- The main concern should be for correcting irregular astigmatism

PHAKIC IOL (PIOL)

CORE MESSAGE

- Phakic IOLs (PIOLs) are additive lenses implanted to compensate for the refractive error and preserve the normal crystalline lens
- There are three types of PIOLs according to the location of implantation
- PIOL implantation is one of the refractive options for treating refractive errors. It is indicated in moderate to high refractive errors, in which it can be considered as an alternative to PRT. It is also indicated where PRT is contraindicated
- There are special considerations and careful work up to be done before the decision of PIOL implantation has been taken

Phakic IOLs (PIOLs) are additive lenses implanted into the anterior or posterior chambers of the eye to compensate for refractive errors and at the same time preserving the crystalline lens and accommodation.

Types

Three types of PIOLs are currently available:
1. Angle-Supported (anterior chamber)
2. Iris-Fixated (anterior chamber)
3. Sulcus-Supported (posterior chamber)

The power of a phakic lens is independent of the axial length of the eye. Rather, it depends on central corneal power (K-readings), ACD and patient refraction (preoperative refraction). The most common formula for calculating the power of PIOL is the following:

$$P = \frac{n}{\frac{n}{K+R} - d} - \frac{n}{\frac{n}{K} - d}$$

Where:
- P : power of PIOL
- n : refractive index of aqueous (1.336)
- K : central corneal power in diopters
- R : refraction at the corneal vertex
- d : effective lens position in mm

Indications

PIOLs are usually indicated where photoablation is relatively or absolutely contraindicated. PIOLs are implanted in case of:
1. High refractive errors (myopia ≥ −5 D, Hyperopia ≥ +4 D).
2. Thin corneas.

3. Abnormal (suspicious) corneal tomography.
4. Dry eye.

Conditions

1. Age: Age of the candidate should be <45 years, otherwise the patient would be presbyopic and there might be changes in the crystalline lens and ACD has decreased.
2. Endothelial cell count: It should be >2500 cells/mm^2 at age of 20 years and >2000 cells/mm^2 at age of 40 years.
3. ACD: It should be >3.0 mm.
4. ACA: It should be >30°.
5. IOP: It should be <20 mmHg (after modification according to corneal thickness).
6. Any intraocular pathology is a contraindication for PIOL implantation.

Work up

Work up for PIOLs consists of full estimation of the eye and general health. A thorough approach of the refractive surgery candidate will be discussed in chapter 7 in details. In general, eye examination includes determination of the magnitude and type of the refractive error; uncorrected distance visual acuity (UDVA) and CDVA; slitlamp biomicroscopy; tonometry; ocular motility; pupil size, shape and location; specular biomicroscopy; corneal tomography and pachymetry; biometry; white-to-white measurement and fundus examination.

UDVA and CDVA for both near and distance should be reasonable to deserve such an operation.

Refractive error magnitude affects the plan of treatment; in severe cases, bioptics including the combination of PIOLs implantation with other refractive surgeries (e.g. PRT) would be on the table.

ACD and ACA are key elements in decision-making. Corneal tomography, OCT and ultrasound biomicroscopy (UBM) can measure ACD and ACA; whereas, IOL Master and immersion A scan can measure ACD including corneal thickness, hence the need to deduct central corneal thickness to find out the real ACD. Another concern is the progressive decrease in ACD with age. Multiple studies have shown a 12–17 µm/year decrease in the anterior chamber depth with aging. If a PIOL patient is assumed to have a 50-year lifespan, the overall decline in ACD may add up to 0.6–0.85 mm, long-term data about the this effect are not available.

Pachymetry is important to detect thinning disorders and for future laser enhancement capability.

Tonometry is of much importance as a routine test especially that high myopic patients are at increased risk for glaucoma. Risks for glaucoma with PIOLs includes temporary postoperative retained viscoelastic, pigmentery dispersion, inflammation, crowded angle, too large implant, angle damage, angle supported PIOLs and synechiae (see chapter 8).

Ocular motility should be checked for possible phoria and tropia with and without glasses. It is to be kept in mind that the intraocular lenses unlike glasses, have no prismatic effect that counteracts phorias or tropias.

Scotopic pupil should be measured since the implants have fixed OZ and there is some risk of glare and halos in case of large pupil diameter. Decentered pupil is an important issue. Full dilatation of the pupil should be evaluated in clinic to avoid the surprise of partial dilatation in the operation room.

Endothelial cell count is important since there will be a certain amount of loss (nearly 2%/year) especially in anterior chamber lenses. Endothelial cell count should be followed yearly after the operation.

Sulcus-supported IOLs need to be implanted in the ciliary sulcus which may have various diameters among individuals; therefore, anterior chamber diameter needs to be measured with a calliper or with the use of eye imaging systems such as Scheimpflug-based tomographers, IOL Master, OCT or UBM. A calliper and imaging systems measure the external limbus-to-limbus diameter of anterior chamber (white-to-white diameter) which provides an approximate estimation of AC diameter, but the UBM offer a more adequate measurement of the sulcus diameter (sulcus-to-sulcus diameter) and should be used when available.

Patient Education

Appropriate expectations of surgery and postoperative results should be explained. Risks of the surgery should be discussed and included in the consent form. These risks include glare, halo, residual refractive error, loss of best corrected visual acuity, corneal edema, hyphema, infection, uveitis, cystoid macular edema, lens dislocation, cataract, secondary glaucoma, retinal detachment and additional surgery to readjust a rotated toric PIOL, or to remove or to replace the lens.

Aspheric PIOL

PIOLs can be customised; in other words an aspheric IOL can be implanted to correct refractive error and counteract abnormal asphericity of the eye. As mentioned in chapters 1 and 2, spherical aberrations can be positive or negative; therefore, a PIOL of positive asphericity can be implanted to compensate for negative ocular spherical aberrations and vice versa. The ocular spherical aberration is the one to be measured and compensated for rather than the corneal spherical aberration.

TAKE-HOME MESSAGE

- PIOL implantation is indicated to correct refractive error in case of (≥ –5 D or ≥ +4 D), thin corneas, abnormal tomography, or dry eye
- PIOL implantation is contraindicated when patient's age is > 45 years; endothelial cell count < 2500 cells/mm^2 at 20-year-old or <2000 cells/mm^2 at 40-year-old; ACD < 3.0 mm; ACA <30°; IOP > 20 mmHg and any intraocular pathology
- Work up for PIOL implantation consists of corrected and uncorrected visual acuity, manifest and cycloplegic refraction, slitlamp biomicroscopy, tonometry, ocular motility, pupil size, shape and location, specular biomicroscopy, corneal tomography, biometry, white-to-white measurement and fundus examination

REFRACTIVE LENS EXCHANGE (RLE)

CORE MESSAGE

- Refractive lens exchange (RLE) is extracting the clear crystalline lens and implantation of an IOL to compensate for refractive errors
- It can be considered as one of the refractive options to treat refractive errors, but has very limited indications and carries almost the same risks of cataract extraction

Refractive lens exchange (RLE) is usually considered only if alternative refractive procedures are not feasible and there is a strong reason why spectacles or CLs are unacceptable alternatives. If

the cornea is too thin, too flat, or too steep, or if the refractive error exceeds the limit for corneal refractive surgery, RLE with IOL implantation is an option. RLE may be preferable to a PIOL in the presence of a lens opacity that is presently visually insignificant but that may soon progress and cause visual loss, or in case of patients older than 45 years.

Patient Selection and Criteria

Age

Age represents the primary criterion for patient selection for RLE. Young individuals with intact accommodation cannot understand what loss of accommodation may be like; even at the age of 39, individuals presenting for LASIK do not always imagine the requirement for reading glasses after the surgery. Despite thorough counseling and informed consent, those who do not yet feel the sufferings form presbyopia are rarely candidates for RLE.

Myopia

The axial length and risk for retinal detachment or other retinal complications should be considered despite prophylactic treatment. With this in mind, other phakic refractive modalities should be considered in extremely high myopic patients. If RLE is performed in these patients, complete informed consent regarding the long-term risks for retinal complications should be emphasized preoperatively.

Life Style and Personality

Optical aberrations, dysphotopsias and poorly defined states of asthenopia, the likelihood of foreign body sensation, odd light reflections and unanticipated color perception are some of the postoperative complaints. Obsessive-compulsive, depressed, highly motivated personality types fare poorly with refractive surgery of all types. Utilization of accommodative or multifocal IOLs in patients who complain excessively, are highly introspective, or obsess over body image and symptoms should be avoided. In addition, conservative use of these lenses is recommended when evaluating patients with occupations that include frequent night driving and occupations that put high demands on vision and near work (e.g. artists, architects and engineers).

Preoperative Evaluation

Beside the thorough work up for refractive surgery that will be discussed in details in chapter 7, the followings are important for RLE.

Biometry

Axial length measurement remains an indispensable technique for IOL power calculation. There are several techniques for biometry, some are optically-based and others are ultrasound-based. A commonly used optical biometry method called partial coherence interferometry (PCI). It provides a measurement of axial length, lens thickness, ACD and corneal curvature. It also includes software for the calculation of an intraocular lens power using a selection of formulae. It is not appropriate for eyes with dense cataracts or severe corneal edema, in which case ultrasonography is preferable. On the other hand, optical biometry may be superior in eyes with posterior staphyloma because of more precise localization of the fovea. There are two types of

ultrasound-based methods, immersion technique and applanation technique. The former is more accurate. A near-perfect correlation of immersion ultrasound and optical coherence biometry measurement techniques indicates the high level of accuracy of both of these methodologies.

Corneal Tomography

Corneal tomography is necessary for the following reasons:

1. Diagnosing and planning for treating coexisting ectatic corneal disorders or corneal irregularities.
2. Measuring corneal spherical aberration to choose the aspheric IOL that compensates for it.
3. IOL power calculations especially in case of irregular cornea, where keratometry readings do not meet topography K-readings.

Keratometry and IOL Power Calculation

IOL power calculations for cataract and RLE surgery have become much more precise with the current generation of theoretical formulas and newer biometry devices. However, IOL power calculation remains a challenge in eyes with prior keratorefractive surgery. The difficulty in these cases lies in accurately determining corneal refractive power.

- Calculating Corneal Refractive Power: In a normal cornea, standard keratometry and computed corneal topography are accurate in measuring four sample points to determine the steepest and flattest meridians of the cornea, thus yielding accurate values for the central corneal power. In irregular corneas having undergone keratorefractive surgery or keratoplasty, the four sample points are not sufficient to provide an accurate estimate of the central corneal refractive power. Traditionally, there have been three methods to calculate the corneal refractive power in these eyes. These include the historical method, the hard CL method and values derived from standard keratometry or corneal topography. The historical method remains limited by its reliance on the availability of refractive data prior to the keratorefractive surgery. The CL method is not applicable in patients with significantly reduced visual acuity. The use of simulated or actual keratometry values almost invariably leads to a hyperopic refractive surprise. It has been suggested that using the average central corneal power rather than topography-derived keratometry may offer improved accuracy in IOL power calculation following corneal refractive surgery.
- Holladay II Formula: The IOL calculation formula plays a critical role in obtaining improved outcomes. The Holladay II formula is designed to improve determination of the final effective lens position by taking into account disparities in the relative size of the anterior and posterior segments of the eye. To accomplish this goal, the formula incorporates the corneal white-to-white measurement and the phakic lens thickness and uses the keratometry (effective refractive power or *EffRP*) values not only to determine corneal power but also to predict effective lens position. The use of the Holladay II formula has increased the accuracy of our IOL power calculations. Many new formulas with improving accuracy in IOL power determination have been published in recent years and it would be wise to compare the results from multiple sources before choosing the lens implant.
- Informed Consent: It is wise to tell patients as part of the informed consent process that IOL calculations following keratorefractive surgery remain a challenge and that refractive surprises do occur. Explain that further surgery may be necessary in the future to enhance uncorrected visual acuity. Defer any secondary procedures until a full three months postoperatively and document refractive stability before proceeding.

Surgical Technique

RLE succeeds in creating spectacle independence only if the final postoperative refraction includes less than 1 D of astigmatism. It is, thus, very important that incision construction be appropriate with respect to size and location. A clear corneal incision at the temporal periphery that is 3.5 mm or less in width and 2 mm long is highly recommended. The surgeon must also be able to utilize one of the many modalities for addressing preoperative astigmatism. Although arcuate keratotomies at the 7 mm OZ can be utilized, there is an increasing trend favouring 600 µm deep limbal relaxing incisions for the reduction or elimination of pre-existing astigmatism. In preparation for phacoemulsification, hydro delineation and cortical cleaving hydro dissection are important because they facilitate lens disassembly and complete cortical clean-up. Complete and fastidious cortical clean-up will reduce the incidence of posterior capsule opacification (PCO) whose presence, even in very small amounts, will inordinately degrade the visual acuity with multifocal IOLs and impede the function of accommodative IOLs. It is because of this phenomenon that patients implanted with multi focal lenses may require Nd:YAG laser posterior capsulotomies earlier than patients implanted with monofocal IOLs. Key elements of the surgical technique when implanting accommodative IOLs include temporal clear corneal phacoemulsification, with construction of a 3.5 mm incision for implantation. A round, centred 4.0 mm capsulorrhexis ensures in-the-bag fixation of the IOL optic.

Intraocular Lens Selection

Monofocal IOLs

Designs of Monofocal IOLs

1. **Flexible IOLs** are now in general use and allow introduction into the eye through a very small incision. For insertion they may be folded in half with special forceps or loaded into an injector delivery system, then unfolded or unrolled inside the eye. Injector-based delivery has become increasingly popular, as it allows introduction without lens contact with the ocular surface, so reducing the risk of bacterial contamination. Injection also allows insertion through a slightly smaller incision than folding. Flexible materials available are discussed below; there seems to be no distinct superiority of one over another and a combination IOL can also be used.
   a. ***Silicone*** IOLs are available in both loop haptics (1- or 3-piece) and plate haptics (1-piece) conformations. Silicone IOLs may exhibit greater biocompatibility, exciting less inflammatory reaction, than hydrophobic acrylic IOLs. They may be particularly prone to significant silicone deposition in silicone oil-filled eyes.
   b. ***Acrylic*** IOLs, 3-piece or 1-piece, may be hydrophobic (water content <1%) or hydrophilic, with much higher water content.
      – Hydrophobic acrylic materials have a greater refractive index than hydrophilic lenses and are consequently thinner. They tend to produce a greater reaction in uveitic eyes, and some surgeons prefer not to use them in this scenario.
      – Hydrophilic acrylic (hydrogel), in theory, offers superior biocompatibility and so should be better tolerated by uveitic eyes. PCO rates are probably higher than with other materials.
   c. ***Collamer*** is composed of collagen, a poly-HEMA based copolymer and a UV-absorbing chromophore.

2. **Rigid IOLs** are made entirely from polymethylmethacrylate (PMMA). They cannot be folded or injected so require an incision larger than the diameter of the optic, typically 5 mm, for insertion. For economic reasons, they continue to be widely used in developing countries. PCO rates are higher with PMMA lenses than silicone and acrylic. Some surgeons favor heparin-coated (see below) IOLs in uveitic eyes, particularly in children.
3. **Sharp/square-edged optics** are significantly associated with a lower rate of PCO compared with round-edged optics and the former is now the predominant design. Lens material seems to have a less important effect than shape on PCO.
4. **Blue light filters.** Although essentially all IOLs contain ultraviolet light filters, a number also include filters for blue wavelengths, in order to reduce the possibility of damage to the retina.
5. **Aspheric optics** counteract spherical aberration and improve contrast, particularly in mesopic conditions and are available in some newer IOLs. Monofocal lenses can be spheric or customized; they can be positive or negative aspheric to compensate for corneal abnormal asphericity. Here, corneal asphericity is the concern rather than the ocular asphericity, which is the concern in case of PIOL. That is because in RLE, the internal component of the ocular asphericity has been removed and the major impact comes from the cornea. In other words, in PIOL, ocular asphericity should be compensated for, while in RLE and IOL implantation, corneal asphericity should be compensated for.
6. **Heparin coating** reduces the attraction and adhesion of inflammatory cells, and this may have particular application in eyes with uveitis. However, there is no clear evidence about whether heparin-surface modification is clinically beneficial and indeed about which IOL material is superior for use in cataract surgery on eyes with uveitis.
7. **Toric IOLs** have an integral cylindrical refractive component to compensate for pre-existing corneal astigmatism. The main potential problem is rotation within the capsular bag, which occurs in 10–20%, following which surgical repositioning may be carried out.
8. **Adjustable IOLs** allow the alteration of refractive power following implantation. One version uses low-level ultraviolet irradiation at the slit-lamp about a week after surgery to induce polymerization of its constituent molecules in specific patterns with precise spherical and cylindrical (astigmatism) correction.

Selection of Monofocal IOLs

1. Occasionally, implantation of bilateral distance focused monovision IOLs may represent an appropriate choice for RLE. In particular, extremely hyperopic patients who require bilateral piggyback IOL implantation may be satisfied with correction of their refractive error alone.
2. Patients with a history of successful monovision CL wear may find RLE with pseudophakic monovision an appealing option.
3. Patients with a high degree of TA may require implantation of toric IOLs in addition to limbal relaxing incisions to achieve adequate reduction of their refractive cylinder.

Multifocal Lenses (MFIOLs)

MFIOLs are designed to increase depth of focus and enhance near vision in eyes with cataract and have been reported as effective. Different types of MFIOLs have been developed using different optical design approaches. At present, there are two main types, refractive and a hybrid mix of refractive–diffractive and each general type comprises different designs. The optics of both types have concentric bifocal circular or annular regions and contain powers suitable for distance or near correction. The pure diffractive MFIOL is rarely used due to its irregular surface

which enhances cell growth. At present, most so-called diffractive IOLs are in essence a hybrid combination of refractive and diffractive lenses.

Types of MFIOLs

- Refractive MFIOL. In this type, refractive power changes from centre to periphery of the lens and produces many foci; therefore, 100% of the light reaches the retina, in contrast to the diffractive MFIOL. Refractive MFIOL has at least one aspherical surface; thus, there is a smooth change in the zonal power of the lens from its center to its edge. The ReZoom lens (Advanced Medical Optics [AMO]) is a refractive lens that has five anterior surface zones for distance and near and the grading between the zones provides intermediate vision.
- Diffractive MFIOL. This type uses Fresnel diffractive optics; it uses light diffraction at an interference grid to separate the incoming light into two focal points, one for near objects and one for distance objects, which means they are effectively bifocal lenses. The overall spherical shape of the surfaces produces an image for distance vision. The posterior surface has a stepped structure and the diffraction from these multiple rings produces a second image, with an effective add power. About 20% of the light entering the pupil is absorbed in this process and optical aberrations with diffractive IOLs can be particularly troublesome. The second generation of this type included two lenses, the AcrySof ReSTOR IOL (Alcon, Ft Worth, TX) and the TECNIS ZM900 lens (AMO). The first one has the diffractive grating on its anterior surface and it is apodized, which means there is a gradual tapering of the diffractive steps from the centre to the outside edge of the lens to create a smooth transition of light between the distance, intermediate and near focal points. The second one has the diffractive grating on the entire back surface and adds an aspheric anterior surface, whereas the first lens does not have aspheric surface.

Pupil Size Effect

The performance of MFIOLs depends on pupil size. A typical MFIOL comprises concentric annular OZs; thus, pupil size influences the image quality at distance and near. To enhance near vision with a MFIOL, the desirable effective pupil diameter is 3.4 mm or larger. Pupil size affects the optical characteristics of refractive MFIOL. It can also affect the optical performance of the refractive–diffractive IOLs. On the other hand, in principle, the basic optical characteristics of pure diffractive MFIOLs are unaffected by changes in pupil diameter because according to their design, distance and near correction are simultaneously present across the full area of the pupil.

Limitations

Preoperative astigmatism is one of the most important issues. It is the most common reason for wearing glasses after MFIOL implantation; therefore, it is wise to avoid patients with more than 1 D of preoperative astigmatism.

MFIOL Selection

Selection of a multifocal IOL for a particular patient rests on several details of IOL design. One of the key optical differences between the ReZoom lens and the ReSTOR lens, apart from the fact that the former is a refractive lens while the later is a refractive-diffractive lens, is the strength of the add power. The ReZoom lens provides 3.5 D of additional power for near while the ReSTOR lens provides 4.0 D. At the spectacle plane these powers translate to approximately 2.5 D for the ReZoom lens and 3.2 D for the ReSTOR lens. Therefore, the optimal near point for reading will be about 16 inches for ReZoom lens and 14 inches for the ReSTOR lens. A patient who frequently

uses a computer monitor may find greater benefit with the slightly more distant near focal point, while a patient who reads paperback books may have greater satisfaction with the closer focus. Another key difference between these MFIOLs is their dependence on pupil size. With a pupil of less than 3 mm the ReZoom lens becomes distinctly distant dominant (because the central zone is distance-focused), while with a small pupil the ReSTOR lens splits light evenly between distance and near (40% distance, 40% near, and 20% loss to destructive interference). On the other hand, a larger pupil enhances the near function of the ReZoom lens and the distance function of the ReSTOR lens. For a frequent night driver, there may be an advantage in the design of the ReSTOR lens, while someone who needs to read in dim light may find an advantage in the ReZoom lens. Because postoperative pupil size after lens extraction and IOL implantation is somewhat unpredictable based on preoperative pupil size, it is important to know the technique of photomydriasis. The argon or diode laser can be used to enlarge the pupil and provide near function. It is often useful to demonstrate improved near function with a drop of phenylephrine before undertaking this procedure. Additional points of distinction between the ReZoom lens and the ReSTOR lens concern structural design differences of the optics and haptics. The acrylic ReZoom lens optic is based on the AR40e platform, while the ReSTOR lens is currently available on the SA60, SN60, or MN60 platform. The 3600 sharp posterior design of the AR40e inhibits the development of PCO by creating a capsular bend. The SA60AT also features a sharp posterior edge, but PCO may develop through lens epithelial cell migration at the haptic-optic junction. The three-piece construction of the AR40e enables placement of the IOL in the ciliary sulcus, if there is intraoperative compromise of capsular support. If the anterior capsule remains intact in this situation, it is recommended to capture the optic posterior to the capsulorrhexis. While the SA60AT or ReSTOR lens should not be placed in the sulcus, it is noted for its stability within the capsular bag. These points of difference may influence IOL selection. Table 5.9 summarises clinical difference between refractive and refractive-diffractive MFIOLs.

Accommodative Lenses

Accommodative IOLs offer to patients satisfactory near vision by restoring to some degree a dynamic component of the ocular ability for near vision. By implementing several designs of the haptic and the optic part of the IOL, the target is to take advantage of the axial movement of the ciliary muscle and of the vitreous in order to change position and shape. The position of the

TABLE 5.9 Clinical difference between Refractive and Refractive-Diffractive Multifocal IOLs

		Refractive	*Refractive-Diffractive*
Pupil Size	Effect	+++	+
	<3 mm	Distance	Distance + Near
	>3 mm	Distance + Near	Distance > Near
	Driving at night	+	+++
	Reading in dim light	+++	+
The Add Power		+3.5 D	+4.0 D
The Clinical Add Power		+2.5 D	+3.2 D
The optimal Near Point for Reading		16 inch	14 inch
PCO		Most probably not	May be
Placement in the Ciliary Sulcus		Can be done	Should not be done

TABLE 5.10 Phakic IOLs vs. Refractive Lens Exchange		
Procedure	*Better for*	*Worse for*
Phakic IOLs	High myopia	Endothelial dysfunction
	Ectasia susceptible	Large pupils
	Sever dry eye/surface issues	Early lens changes
Refractive lens exchange	Higher hyperopia	Retinal detachment risk
	Early lens changes	Lower refractive errors
	Presbyopic correction	

accommodative IOL changes axially by 0.5–0.7 mm to achieve a change of the overall dioptric power of the eye and the facilitation of near vision.

Precise biometry and IOL power calculation are mandatory for this type. Applanation biometry is not sufficiently accurate and must be abandoned. Immersion A-scan is used as a confirmatory test, if there are variable test results with the IOL Master (0.1 mm in one eye or 0.2 mm between eyes). Autokeratometry from the optical biometers (IOL Master), supplemented by simulated keratometry values from topography measurements, yields good results. In patients who have had previous incisional keratorefractive surgery use the *EffRP* from the Holladay Diagnostic Summary of the EyeSys Corneal Topographer, or consider using Scheimpflug tomographers to determine corneal power. Once accurate keratometry and axial length are obtained, the Holladay II formula can be used to determine the IOL power. It takes into account seven variables to determine the effective lens position. Haigis-L or other modern regression formula can also be used.

Before going to the operating room, make sure the patient has reasonable expectations and thoroughly understands the informed consent for this procedure. Hyperopic patients with presbyopia may be extremely happy even with this worst-case scenario. High myopic patients with presbyopia may be among the very happiest RLE patients and demonstrate remarkably good uncorrected distance and near vision. Low myopic patients with presbyopia may not be happy and should be approached a bit more cautiously. It is wise to ask these people about their activities to determine if they live in a distant-dominant or near-dominant world before choosing the appropriate refractive procedure for them.

Table 5.10 summarizes the indications of PIOLs vs. RLE.

TAKE-HOME MESSAGE

- RLE is indicated just where no other refractive options are indicated
- When RLE is an option, there are special considerations including age, myopia, lifestyle and personality
- RLE work up is similar to that for cataract extraction in addition to corneal tomography for diagnosing and planning for treating coexisting ectatic corneal disorders or corneal irregularities, or if simultaneous astigmatic keratotomy is indicated
- Selection of IOL is an important issue in RLE success
- Each type of IOLs has pros and cons and its selection depends on many considerations

BIBLIOGRAPHY

1. Alio JL and Azar DT (Eds.). Management of Complications in Refractive Surgery. Springer; 2008.
2. Alio JL, de La Hoz F, Perez-Santoja JJ, et al. Phakic anterior chamber lenses for the correction o myopia: a 7-year cumulative analysis of complications in 26 cases. Ophthalmology. 1999;106(3):458-66.

3. Alió JL, El Aswad A, Vega-Estrada, et al. Laser in situ keratomileusis for high hyperopia (>5.0 diopters) using optimized aspheric profiles: Efficacy and safety. J Cataract Refract Surg. 2013;39(4):519-27.
4. Alio JL and Javaloy J. Corneal inflammation following corneal photoablative refractive surgery with excimer laser. Surv Ophthalmol. 2013;58:11-25.
5. Alpins N and Stamatelatos G. Customized photo astigmatic refractive keratectomy using combined topographic and refractive data for myopia and astigmatism in eyes with forme fruste and mild keratoconus. J Cataract Refract Surg. 2007;33:591-602.
6. Ambrosio R Jr, Wilson S. LASIK vs. LASEK vs. PRK: advantages and indications. Semin Ophthalmol. 2003;18:2-10.
7. American Academy of Ophthalmology (2012-2013 edition). Basic and Clinical Science Course. Section 13: Refractive Surgery.
8. American Academy of Ophthalmology (2012-2013 edition). Basic and Clinical Science Course. Section 3: Clinical Optics.
9. Arne JL, Lesueur LC and Hulin HH. Photorefractive keratectomy or laser in situ keratomileusis for residual refractive error after phakic intraocular lens implantation. J Cataract Refract Surg. 2003;29:1167-73.
10. Asano-Kato N, Toda I, Hori-Komai Y, et al. Experience with the Artisan phakic intraocular lens in Asian eyes. J Cataract Refract Surg. 2005;31(5):910-5.
11. Azar DT, Gatinel D, Hoang-Xuan T. Refractive surgery. Philadelphia: Mosby Elsevier; 2007.
12. Barisic A, Dekaris I, Gabric N, et al. Comparison of Diffractive and Refractive Multifocal Intraocular Lenses in Presbyopic Treatment. Coll. Antropol. 32 Suppl. 2008;2:27-31.
13. Bartels M, Santana N, Budo C, et al. Toric phakic intraocular lens for the correction of hyperopia and astigmatism. J Cataract Refract Surg. 2006;32:243-9.
14. Battle J. Toric phakic IOL may be alternative for treating keratoconus. Ophthalmology Times Meeting E-News. Available via http://www.ophthalmologytimes.com/ophthalmologytimes; 2004.
15. Bedei A, Marabotti A, Giannecchini I, et al. Photorefractive keratectomy in high myopic defects with or without intraoperative Mitomycin C: 1-year results. Eur J Ophthalmol. 2006;16(2):229-34.
16. Benedetti S, Casamenti V, Marcaccio L, et al. Correction of myopia of 7 to 24 diopters with the Artisan phakic intraocular lens: two-year follow-up. J Refract Surg. 2005;21(2):116-26.
17. Boxer Wachler BS, Scruggs RT, Yuen LH, et al. Comparison of the Visian ICL and Verisyse phakic intraocular lenses for myopia from 6.00 to 20.00 diopters. J Refract Surg. 2009;25(9):765-70.
18. Brightbill FS, McDonnell PJ, McGhee CNJ, et al. Corneal Surgery: Theory, Technique and Tissue. Mosby Elsevier; 2009.
19. Candal EM, Majmudar PA. Surface ablation with prophylactic MMC for high myopia and high-risk patients. In: Probst L, ed. LASIK: advances, controversies and custom. Thorofare, NJ, Slack. 2004;325-32.
20. Carones F, Vigo L, Scandola E, et al. Evaluation of the prophylactic use of Mitomycin C to inhibit haze formation after photorefractive keratectomy. J Cataract Refract Surg. 2002;28:2088-95.
21. Corbett MC, Verma S, O'Brart DP, et al. Effect of ablation profile on wound healing and visual performance 1 year after excimer laser photorefractive keratectomy. Br J Ophthalmol. 1996;80(3):224-34.
22. Davidorf JM, Eghbali F, Ondinx T, et al. Effect of varying the optical zone diameter on the results of hyperopic laser in situ keratomileusis. Ophthalmology. 2001;108(7):1261-5.
23. Davison JA, Johnson Sc. Intraoperative complications of LASIK flaps using the Intralase femtosecond laser in 3009 cases. J Refract Surg. 2010;26(11):851-7.
24. Dejaco-Ruhswurm I, Scholz U, Pieh S, et al. Long-term endothelial changes in phakic eyes with posterior chamber intraocular lenses. J Cataract Refract Surg. 2002;28(9):1589-93.
25. Dementiev DD, Hoffer KJ, Sonecka A. PRL-Medennium posterior chamber phakic intraocular lens. In: Alio JL, Perez-Santonja JJ (Eds) Refractive surgery with phakic IOLs. Fundamentals and practice. Highlights of Ophthalmology International, El Dorado, Republic of Panama; 2004.
26. Dick H, Ali. J, Bianchetti M, et al. Toric phakic intraocular lens: European multicenter study. Ophthalmology. 2003;110:150-62.

27. Donnenfeld ED, Ehrenhaus M, Solomon R, et al. Effect of hinge width on corneal sensation and dry eye after laser in situ keratomileusis. J Cataract Refract Surg. 2004;30(4):790-7.
28. Durrie DS (2011). Rapid vision recovery after PRK: The next frontier. Paper presented at: The American Academy of Ophthalmology Subspecialty Day; October 22, 2011; Orlando, Fla. Reported at: http://eyewiretoday.com/view.asp?20111022-corneal_shield_may_improve_visual_results_and_increase_epithelial_healing_after_PRK.
29. Durrie DS, Kezirian GM. Femtosecond laser versus mechanical keratome flaps in wavefront guided laser in situ keratomileusis: prospective contralateral eye study. J Cataract Refract Surg. 2005;31(1):120-6.
30. El Danasoury MA, el Maghraby A, Klyce SO, et al. Comparison of photorefractive keratectomy with excimer laser in situ keratomileusis in correcting low myopia (from - 2.00 to -5.50 diopters): a randomized study. Ophthalmology. 1999;106(2):411-20.
31. Endl MJ, Martinez CE, Klyce SD, et al. Effect of larger ablation zone and transition zone on corneal optical aberrations after photorefractive keratectomy. Archives of ophthalmology. 2001;119(8):1159-64.
32. Faktorovich EG and Basbaum AI. Effect of topical 0.5% morphine on postoperative pain after photorefractive keratectomy. J Refract Surg. 2010;26:934-41.
33. Feder RS, Rapuano. The lasik handbook: a case-based approach. Lippincott Williams & Wilkins; 2007.
34. Felipe A, Dı´az-Llopis M. Image quality with multifocal intraocular lenses and the effect of pupil size Comparison of refractive and hybrid refractive–diffractive designs J Cataract Refract Surg. 2007;33:2111-7.
35. Fernandez AP, Jaramillo J, Jaramillo M. Comparison of photorefractive keratectomy and laser in situ keratomileusis for myopia of -6 0 or less using the Nidek EC•5000 laser. J Refract Surg. 2000;16(6):711-5.
36. Fernandez-Vega L, Alfonso JF and Villacampa T. Clear lens extraction for the correction of high myopia. Ophthalmology. 2003;110:2349-54.
37. Fink AM, Gore C, Rosen ES. Refractive lensectomy for hyperopia. Ophthalmology. 2000;107(8):1540- 8.
38. Gambato C, Ghirlando A, Moretto E, et al. Mitomycin C modulation of corneal wound healing after photorefractive keratectomy in highly myopic eyes. Ophthalmology. 2005;112:208-18.
39. Guell J (2013). The use of a novel device for removal of the epithelium in surface ablation procedures. Abstract presented at: Winter Meeting of the European Society of Cataract and Refractive Surgeons; February 15-17, 2013; Warsaw, Poland. Available at: http://escrs.org/warsaw2013/programme/posters-details.asp?id=15682. Accessed on May 3, 2013.
40. Guo H, Goncharov AV, Dainty C. Comparison of retinal image quality with spherical and customized aspheric intraocular lenses. Biomed Opt Express. 2012;3(4):681-91.
41. Holz.er MP, Rabsilber TM, Auffarth Gu. Femtosecond laser- assisted corneal flap cuts: morphology accuracy, and histopathology. Invest Ophthalmol Vis Sci. 2006;47(7):2828-3l.
42. Horgan N, Condon PI, Beatty S. Refractive lens exchange in high myopia: long term follow-up. Br J Ophthalmol. 2005;89:670-2.
43. Huang D, Schallhorn SC, Sugar A, et al. Phakic intraocular lens implantation for the correction of myopia: a report by the American Academy of Ophthalmology. Ophthalmology. 2009;116(11):2244- 58.
44. Kamiya K, Shimizu K, Igarashi A, et al. Komatsu M. Four-year follow-up of posterior chamber phakic intraocular lens implantation for moderate to high myopia. Arch Ophthalmol. 2009;127(7):845-50.
45. Kanellopoulos AJ. Comparison of sequential vs. same-day simultaneous collagen cross-linking and topography-guided PRK for treatment of keratoconus. J Refract Surg. 2009;25(9).
46. Kanellopoulos AJ, Binder PS. Collagen cross-linking (CCL) with sequential topography-guided PRK: a temporizing alternative for keratoconus to penetrating keratoplasty. Cornea. 2007;26(7):891-5.
47. Kanellopoulos AJ, Binder PS. Management of Corneal Ectasia after LASIK with Combined, Same-Day, Topography-Guided Partial Transepithelial PRK and Collagen Cross-Linking: The Athens Protocol. J Refract Surg. 2010;5:1-9.
48. Keir NJ, Simpson T, Jones UV, et al. Wavefront-guided LASIK for myopia: effect on visual acuity, contrast sensitivity, and higher order aberrations. J Refract Surg. 2009;25(6):524-33.

49. Kezirian GM, Stonecipher KG. Comparison of the Intralase femtosecond laser and mechanical keratomes for laser in situ keratomileusis. J Cataract Refract Surg. 2004;30:804-11.
50. Kohnen T, Bühren J, Kühne C, et al. Wavefront-guided LASIK with the Zyoptix 3.1 system for the correction of myopia and compound myopic astigmatism with 1-year follow-up: clinical outcome and change in higher order aberrations. Ophthalmology. 2004;111(12):2175-85.
51. Kohnen T, Knorz MC, Cochener B, et al. AcrySof phakic angle-supported intraocular lens for the correction of moderate- to-high myopia: one-year results of a multicenter European study. Ophthalmology. 2009;116(7):1314-21.
52. Koller T, Iseli HP, Hafezi F, et al. Q-factor customized ablation profile for the correction of myopic astigmatism. J Cataract Refract Surg. 2006;32(4):584-9.
53. Krueger RR, Applegate RA, MacRae SM. Wavefront customized visual correction. Slack Inc; 2004.
54. Kumano y, Matsui H, Zushi I, et al. Recovery of corneal sensation after myopic correction by laser in situ keratomileusis with a nasal or superior hinge. J Cataract Refract Surg. 2003;29(4):757-6l.
55. Kuo IC, Jabbur NS, O'Brien TP. Photorefractive keratectomy for refractory laser in situ keratomileusis flap striae. J Cataract Refract Surg. 2008;34:330-3.
56. Kymionis GD, Portaliou DM, Diakonis VF, et al. Management of post laser in situ keratomileusis ectasia with simultaneous topography guided photorefractive keratectomy and collagen cross-linking. Open Ophthalmol J. 2011;11(5):11-3.
57. Kymionis GD, Portaliou DM, Kounis GA, et al. Simultaneous topography-guided photorefractive keratectomy followed by collagen corneal cross-linking for keratoconus. Am J Ophthalmol. 2011;152(5):748-55.
58. Kymionis GD, Karavitaki AE, Kounis GA, et al. Management of pellucid marginal corneal degeneration with simultaneous customized photorefractive keratectomy and collagen crosslinking. J Cataract Refract Surg. 2009;35:1298-301.
59. Kymionis GD, Kontadakis GA, Kounis GA, et al. Simultaneous topography-guided PRK followed by corneal collagen cross-linking for keratoconus. J Refract Surg. 2009;25:S807-11.
60. Lacayo GO 3rd and Randleman JB. Surface ablation. Int Ophthalmol Clin. 2008;48:17-28.
61. Law RW, Li RT, Ng IS, et al. Refractive lensectomy in extreme myopia. Cataract Refract Surg. 2001;27(12):1899-900.
62. Lee DH, Chung HS, Jeon YC, et al. Photorefractive keratectomy with intraoperative Mitomycin C application. J Cataract Refract Surg 31. 2005;(12):2293-8.
63. Lichtinger AA, Schanzlin DJ, Purcell T, et al. The use of gabapentin for postoperative pain after photorefractive keratectomy. Poster 482. Presented at: Annual Meeting of the American Academy of Ophthalmology; October 16-19; Chicago, Ill; 2010.
64. Lim T, Yang S, Kim M, et al. Comparison of the Intralase femtosecond laser and mechanical microkeratome for laser in situ keratomileusis. Am J Ophthalmol. 2006;141(5):833-9.
65. Lovisolo CF, Giacomotti E. Implantation of phakic intraocular lenses for hyperopia correction. In: Ali. JL, Perez-Santonja JJ (Eds) Refractive surgery with phakic IOLs. Fundamentals and practice. Highlights of Ophthalmology International, El Dorado, Republic of Panama; 2004.
66. Lovisolo CF, Pesando PM. Posterior chamber phakic intraocular lenses. In: Ali. JL, Perez-Santonja JJ (Eds) Refractive surgery with phakic IOLs. Fundamentals and practice. Highlights of Ophthalmology International, El Dorado, Republic of Panama; 2004.
67. Lovisolo CF, Reinstein DZ. Phakic intraocular lenses. Surv Ophthalmol. 2005;50(6):549-87.
68. Majmudar PA, Forstot SL, Nirankari VS, et al. Topical Mitomycin C for subepithelial fibrosis after corneal surgery. Ophthalmology. 2000;107:89-94.
69. Marinho A ARTIFLEX: a new phakic IOL. In: Garg A, Pandey S, Chang D et al (Eds) Advances in ophthalmology 2. Jaypee Brothers, New Delhi; 2005.
70. Menezo JL, Peris-Mart.nez C, Cisneros AL, et al. Phakic intraocular lenses to correct high myopia: Adatomed, STAAR, and Artisan. J Cataract Refract Surg. 2004;30(1):33-44.

71. Moshirfar M, Gardiner JP, Schliesser JA, et al. Laser in situ keratomileusis complications using mechanical microkeratome versus femtosecond laser: retrospective comparison. J Cataract Refract Surg. 2010;36:1925-33.
72. Mrochen M, Donitzky C, Wüllner C, et al. Wavefront-optimized ablation profiles: theoretical background. J Cataract Refract Surg. 2004;30(4):775-85.
73. Muller LT, Candal EM, Epstein RJ, et al. Transepithelial phototherapeutic keratectomy/photorefractive keratectomy with adjunctive Mitomycin C for complicated LASIK flaps. J Cataract Refract Surg. 2005;31:291-6.
74. Muñoz G, Cardoner A, Albarrán-Diego C, et al. Iris-fixated toric phakic intraocular lens for myopic astigmatism. J Cataract Refract Surg. 2012;38(7):1166-75.
75. Nachiketa N and Munshi V. Refractive lensectomy in extreme myopia. J Cataract Refract Surg. 2001;27(12):1900-1.
76. Nanavaty MA, Spalton DJ, Boyce J, et al. Wavefront aberrations, depth of focus, and contrast sensitivity with aspheric and spherical intraocular lenses: fellow-eye study. J Cataract Refract Surg. 2009;35(4):663-71.
77. Neuhann T, Neuhann IM, Hassel JM. Aspheric profiles for refractive laser ablation of the cornea. Ophthalmologe. 2008;105(3):241-7.
78. Nissman SA, Tractenberg RE, Babbar-Goel A, et al. Oral gabapentin for the treatment of postoperative pain after photorefractive keratectomy. Am J Ophthalmol. 2008;145:623-9.
79. O'Keefe M, Kirwan C. Laser epithelial keratomileusis in 2010 - a review. Clinical and experimental ophthalmology. 2010;38(2):183-91.
80. Packer M, Fine IH, Hoffman RS. Refractive lens exchange. Focal points: American academy of ophthalmology; 2007.
81. Patel SV, Maguire LJ, McLaren JW, et al. Femtosecond laser versus mechanical microkeratome for LASIK: a randomized controlled study. Ophthalmology. 2007;114(8):1482-90.
82. Price FW. LASIK. Clinical Modules for Ophthalmologists. Focal Points: American Academy of Ophthalmology; 2000.
83. Rajan MS, Jaycock P, O'Brart D, et al. A long-term study of photorefractive keratectomy: 12-year follow-up. Ophthalmology. 2004;111(10):1813-24.
84. Randleman JB, Perez-Straziota CE, Hu MH, et al. Higher-order aberrations after wavefront-optimized photorefractive keratectomy and laser in situ keratomileusis. J Cataract Refract Surg. 2009;35(2):260- 4.
85. Rekas M, Krix-Jachym K, Zelichowska B. Comparison of high order aberrations with spherical and aspheric IOLs compared to normal phakic eyes. Eur J Ophthalmol. 2008;18(5):728-32.
86. Richoz O, Mavrakanas N, Pajic B, et al. Corneal collagen cross-linking for ectasia after LASIK and photorefractive keratectomy: long term results. Ophthalmology. 2013;120(7):1354-9.
87. Sanders D, Vukich JA. Comparison of implantable collamer lens (ICL) and laser-assisted in situ keratomileusis (LASIK) for low myopia. Cornea. 2006;25:1139-46.
88. Sanders DR. Matched population comparison of the Visian Implantable Collamer Lens and standard LASIK for myopia of –3.00 to –7.88 Diopters. J Refract Surg. 2007;23:537-53.
89. Sanders DR, Doney K, Poco M. ICL in Treatment of Myopia Study Group. US FDA clinical trial of the Implantable Collamer Lens (ICL) for moderate to high myopia: three-year follow-up. Ophthalmology. 2004;111:1683-92.
90. Sanders DR, Schneider D, Martin R, et al. Toric Implantable Collamer Lens for moderate to high myopic astigmatism. Ophthalmology. 2007;114:54-61.
91. Sanders DR, Vukich JA, Doney K, et al; Implantable Contact Lens in Treatment of Myopia Study Group. U.S. Food and Drug Administration clinical trial of the Implantable Contact Lens for moderate to high myopia. Ophthalmology. 2003;110(2):255-66.
92. Sarver EJ, Sanders DR, Vukich JA. Image quality in myopic eyes corrected with laser in situ keratomileusis and phakic intraocular lens. J Refract Surg. 2003;19:397-404.

93. Schallhorn SC, Amesbury EC, Tanzer DJ. Avoidance, recognition, and management of LASIK complications. Am J Ophthalmol. 2006;141(4):733-9.
94. Schallhorn SC, Farjo AA, Huang D, et al. Wavefront-guided LASTK for the correction of primary myopia and astigmatism: a report by the American Academy of Ophthalmology. Ophthalmology. 2008;115(7):1249-61.
95. Schwartz GS, Park DH, Lane SS. Custom Cornea wavefront retreatment after conventional laser in situ keratomileusis. J Cataract Refract Surg. 2005;31:1502-5.
96. Shortt AJ, Allan BD, Evans JR. Laser-assisted in-situ keratomileusis (LASIK) versus photorefractive keratectomy (PRK) for myopia. Cochrane Database Syst Rev. 1:CD005135; 2013.
97. Sinjab MM. Quick Guide to the management of keratoconus. Springer; 2012.
98. Slade SG, Durrie OS, Binder PS. A prospective, contralateral eye study comparing thin-flap LASIK (sub-Bowman keratomileusis) with photorefractive keratectomy. Ophthalmology. 2009;116(6):1075-82.
99. Smadja D, Reggiani-Mello G, Touboul D, et al (2012). [Ablation profiles in refractive surgery. Part 1: in search of excellence]. J Fr Ophthalmol. 35(2):126-35. doi: 10.1016/j.jfo.2011.09.004. Epub 2012 Jan 4. [Article in French]
100. Solomon R, Eric D, Donnenfeld ED. Innovations in Advanced Surface Laser Refractive Surgery. Focal Points: American Academy of Ophthalmology. 2010;28(2):1-14.
101. Stein HA, Salim AG, Stein RM, et al. Corneal cooling and rehydration during photorefractive keratectomy to reduce postoperative corneal haze. J Refract Surg. 1999;15:S232-33.
102. Steinert RF, Ashrafzadeh A, Hersh PS. Results of phototherapeutic keratectomy in the management of flap striae after LASIK. Ophthalmology. 2004;111:740-6.
103. Stonecipher K, Ignacio TS, Stonecipher M Advances in refractive surgery: microkeratome and femtosecond flap creation in relation to safety, efficacy, predictability, and biomechanical stability. Curr Opin Ophthalmol. 2006;17:368-72.
104. Stonecipher KG, Kezirian GM. Wavefront-optimized versus wavefront-guided LASIK for myopic astigmatism with the ALLEGRETTO WAVE: three-month results of a prospective FDA trial. J Refract Surg. 2008;24(4):S424-30.
105. Stulting RD, John ME, Maloney RK, et al U.S. Verisyse Study Group. Three-year results of Artisan/Verisyse phakic intraocular lens implantation. Results of the United States Food and Drug Administration clinical trial. Ophthalmology. 2008;115(3):464-72.
106. Sugar A, Rapuano CJ, Culbertson WW, et al. Laser in situ keratomileusis for myopia and astigmatism: safety and efficacy: a report by the American Academy of Ophthalmology. Ophthalmology. 2002;109(1):175-87.
107. Taieb M, Bar-On Y, Fink A, et al. Epi-Bowman keratectomy: an alternative method for corneal epithelial removal. Cataract and Refractive Surgery Today, Europe 30-31; 2013.
108. Titiyal JS, Sharma N, Mannan R, et al. Iris-fixated intraocular lens implantation to correct moderate to high myopia in Asian-Indian eyes: Five-year results. J Cataract Refract Surg. 2012;38(8):1446-52.
109. Tole OM, McCarty OJ, Couper T, et al. Comparison of laser in situ keratomileusis and photorefractive keratectomy for the correction of myopia of -6.00 diopters or less. Melbourne Excimer Laser Group. J Refract Surg. 2001;17(1):46-54.
110. Torun N, Bertelmann E, Klamann M, et al. Posterior chamber phakic intraocular lens to correct myopia: Long-term follow-up, J Cataract Refract Surg (article in press); 2013.
111. Tuwairqi WS and Sinjab MM. Safety and efficacy of simultaneous corneal collagen cross-linking with topography-guided PRK in managing low-grade keratoconus: 1-year follow-up. J Refract Surg. 2012;28(5):341-5.
112. United States Food and Drug Administration. Summary of Safety and Effectiveness Data. Artisan Phakic Lens. PMA: P030028. Date of approval: 9/10/04.
113. United States Food and Drug Administration. Summary of Safety and Effectiveness Data. STAAR Visian ICL (Implantable Collamer Lens). PMA: P030016. Date of approval: 2/22/05.

114. Varley GA, Huang 0, Rapuano CJ, et al. LASIK for hyperopia, hyperopic astigmatism, and mixed astigmatism: a report by the American Academy of Ophthalmology. Ophthalmology. 2004;111(8):1604-17.
115. Verma A. Phakic IOL Myopia. At http://emedicine.medscape.com/article/1221908-overview; 2008.
116. Virasch VV, Majmudar PA, Epstein RJ, et al. Reduced application time for prophylactic Mitomycin C in photorefractive keratectomy. Ophthalmology. 2010;117(5):885-9.
117. Watson SL, Bunce C, Alan BDS. Improved safety in contemporary LASIK. Ophthalmology. 2005;112(8):1375-80.
118. Zolotaryov AV. Prophylactic intraoperative MMC: on the way to haze-free PRK? Am Acad Ophthalmology, annual meeting; 2002.

Step Three

Rules and Guidelines in Refractive Surgery

CHAPTER 6

Rules and Guidelines in Refractive Surgery

CORE MESSAGE

- There are no strict rules in refractive surgery as much as they are recommendations and guidelines
- There are 9 rules related to corneal thickness
- There are 4 rules related to K readings and astigmatism
- There is a rule for sub optimal correction, a rule for Q-value and a rule for pupil centre coordinates and angle kappa
- There are considerations related to pupil size
- There are recommendations for cyclotorsion and recommendations for amblyopia
- Enhancement if required, special concepts should be well known

Although, there are no definite rules in refractive surgery as much as there are general guidelines that should be followed and certain limits that should not be exceeded, in order to avoid complications. In this chapter, I tried to simplify and clarify the rules, although some are still controversial.

THICKNESS RULES

To understand thickness rules and imagine what the excimer laser does, Munnerlyn formula and thickness ablation profiles should be understood first.

Munnerlyn formula for myopic and myopic astigmatism states that AD (µm) = 1/3 x (OZ diameter [mm])^2 x (intended correction [D]).

For instance, correcting –4 D for an OZ = 6.5 mm indicates an AD = 1/3 x (6.5)^2 x 4 = 56 µm.

This formula is very helpful in calculating the amount of AD for different OZs; i.e. when the scotopic pupil is small, a small OZ can be chosen to save tissue. For example, if the scotopic pupil size is 5 mm, an OZ of 5.5 mm can be chosen and the corresponding AD is almost 10 µm per 1 D of correction. However, a 6.5 mm OZ will be used in the calculations and decision-making in this book.

Figure 6.1 is the ablation profile for myopia. The maximum AD is at the centre of the cornea. It resembles removing a positive meniscus from corneal tissue.

Figure 6.2 is the ablation profile for hyperopia. The maximum AD is at corneal periphery. It resembles removing a negative meniscus where no tissue is removed at the centre.

Figure 6.3 is the ablation profile for myopic astigmatism. The AD is maximum on the steeper meridian (including the centre) and minimum on the perpendicular flatter meridian. It resembles removing a positive meniscus from corneal tissue with different amount according to the meridian, but in all situations it is maximum at the centre.

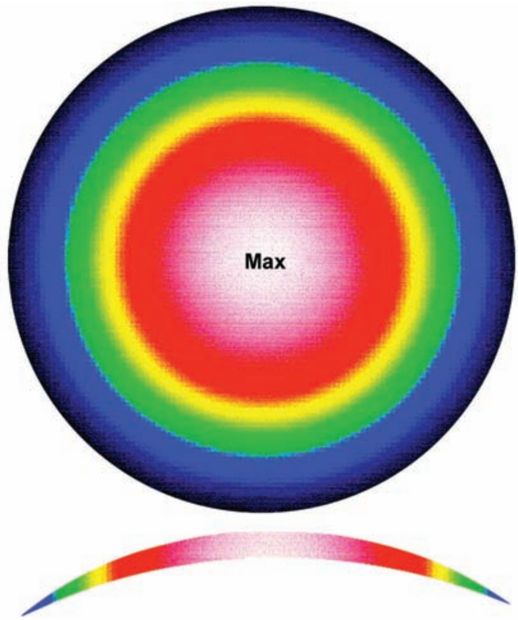

Fig. 6.1 Ablation profile to correct myopia.

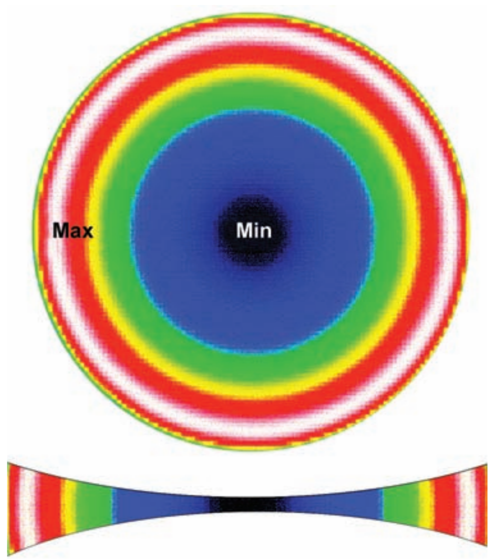

Fig. 6.2 Ablation profile to correct hyperopia.

Figure 6.4 is the ablation profile for hyperopic astigmatism. The AD is maximum at the periphery on the flatter meridian and no tissue is ablated at the perpendicular steeper meridian or centre. It resembles removing a negative meniscus at one meridian.

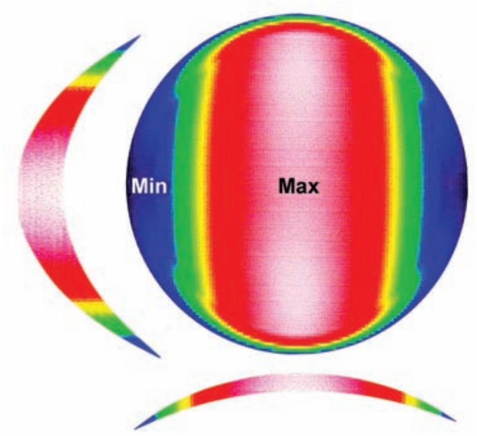

Fig. 6.3 Ablation profile to correct myopic astigmatism.

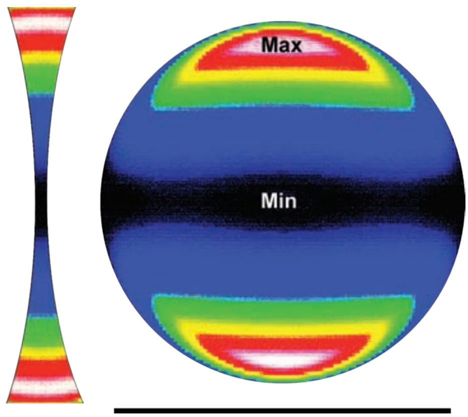

Fig. 6.4 Ablation profile to correct hyperopic astigmatism.

Figure 6.5 is the ablation profile for mixed astigmatism. It resembles removing a positive meniscus at the steeper meridian and a negative meniscus at the flatter meridian. The amount of ablation at the centre is related to the amount of spherical component of the refractive error using the plus cylinder equation.

In the following: rules 1 to 6 are for myopic and myopic astigmatism, rule 7 is for hyperopia and hyperopic astigmatism, rule 8 is for mixed astigmatism and rule 9 is for correcting refractive errors and HOAs.

Finally, it is advised to measure pachymetry intraoperatively and not to rely on pachymetry measurement made on a different day.

RSB Rule 1

In LA, thickness of the RSB should be at least 55% of the original corneal thickness *at the thinnest location* AND to be at least 250 μm (preferably 270 μm).

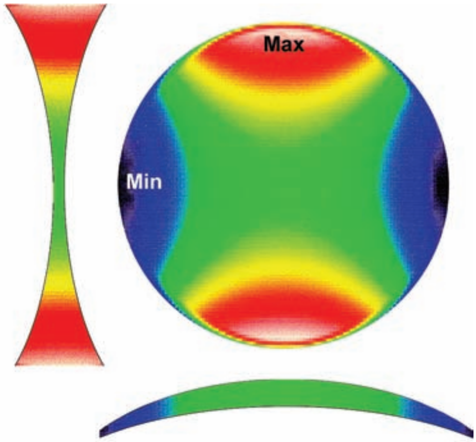

Fig. 6.5 Ablation profile to correct mixed astigmatism.

Example 1: an original corneal thickness of 500 µm means a RSB of 500 x 55 = 275 µm, which is >270 µm.

Example 2: an original corneal thickness of 480 µm means a RSB of 480 x 55 = 264 µm, which is not favourable.

RSB Rule 2

In LA, at most 20% of the original corneal thickness *at the thinnest location* can be ablated.
Example 3: an original corneal thickness of 500 µm means a recommended AD of at most 500 x 20 = 100 µm. In case of 100 µm flap, the RSB will be: 500 (thickness) – 100 (flap) – 100 (AD) = 300 µm.

Example: 4: an original corneal thickness of 600 µm means an AD of at most 600 x 20 = 120 µm. In case of 100 µm flap, the RSB will be: 600 (thickness) – 100 (flap) – 120 (AD) = 380 µm.

RSB Rule 3

In LA, the AD differs according to OZ diameter and profile. In general, correcting –1 D sph ablates an average of 14 µm and 16–17 µm for 6 mm and 6.5 mm OZ, respectively. For easy calculations, 15 µm will be used.

Example 5: an original corneal thickness of 500 µm with –5 D sph and 100 µm flap means a RSB of: 500 – (5 x 15) – 100 = 325 µm.

Example 6: an original corneal thickness of 600 µm with –8 D sph and 100 µm flap means a RSB of: 600 – (8 x 15) – 100 = 380 µm.

RSB Rule 4

Use the most conservative rule from rules 1, 2 and 3.
Example 7: an eye with an original corneal thickness of 500 µm and –6 D sph refractive error:

1. RSB rule 1: RSB = 500 x 55% = 275 µm; therefore, the recommended AD for a 100 µm flap is 500 – 100 – 275 = 125 µm
2. RSB rule 2: AD = 500 x 20% = 100 µm; therefore, the RSB for a 100 µm flap = 500 – 100 – 100 = 300 µm

3. RSB rule 3: AD = 6 x 15µm = 90 µm; therefore, the RSB for a 100 µm flap = 500 – 100 – 90 = 310 µm
4. To be conservative, ablate 90µm and leave 310 µm RSB (rule 3).

Example 8: an eye with an original corneal thickness of 520 µm and –8 D sph refractive error:

1. RSB rule 1: RSB = 520 x 55% = 286 µm; therefore, the recommended AD for a 100 µm is 520 – 100 – 286 = 134 µm
2. RSB rule 2: AD = 520 x 20% = 104 µm; therefore, the RSB for a 100 µm flap = 520 – 100 – 104 = 316 µm
3. RSB rule 3: AD = -8 x 15 µm = 120 µm; therefore, the RSB for a 100 µm flap = 520 – 100 – 120 = 300 µm
4. To be conservative, ablate 104 µm and leave 296 µm RSB (rule 2); therefore, only 104/15 ≈ –7.0 D sph can be corrected and a residual refractive error of –1.0 D sph will remain.

RSB Rule 5

In SA, it is recommended not to exceed 80–90 µm of AD in order to avoid haze; therefore, in case of 6.5 mm OZ, about 6 D can be corrected. On the other hand, a minimum of 400 µm of final RSB including the epithelium should be left. For example, an eye with an original corneal thickness of 490 µm can be ablated for 80–90 µm, while an eye with an original corneal thickness of 470 µm can be ablated for 70 µm. The AD is thereafter divided by 15 µm to calculate the recommended refractive correction.

Example 9: an eye with an original corneal thickness of 490 µm and –5 D sph; the AD = 5 x 15 = 75 µm, this is within the recommended range either for the RSB (490 – 75 = 415 µm) or for the maximum recommended AD (≤ 90 µm).

Example 10: an eye with an original corneal thickness of 480 µm and –6.5 D sph; the AD (6.5 mm OZ) = 6.5 D x 15 µm = 97.5 µm, which is not recommended.

RSB Rule 6

In PRT, use the absolute sum of the refractive error in calculating the RSB.

Example 11: the amount of AD for a refractive error of –4 D sph/–3 D cyl @120 is (4 + 3) x 15 = 105 µm.

RSB Rule 7

In hyperopic treatment (either pure hyperopia or hyperopic astigmatism), the central ablation is zero, whereas the maximum AD is peripheral where the cornea is thick. Therefore, the previous rules cannot be applied. However, the trend nowadays is to correct no more than + 4 D by PRT in order to minimize biomechanical responses which may impact the results.

In general, the preoperative thinnest location should be > 470 µm.

RSB Rule 8

For calculations in mixed astigmatism, the equation should be converted into plus cylinder formula.

Example 12: in a refractive error of +2 D sph/–4 D cyl, the plus cylinder equation should be used: –2 D sph/+4 D cyl. Thereafter, the RSB rules are applied for –2 D sph.

RSB Rule 9

In WFGT profiles, the AD differs according to the type and severity of HOA(s). Therefore, it is difficult to establish a rule for HOA correction; for instance look at table 6.1 to see how AD differs.

In this example, the patient has –2 D sphere with HOAs. As shown in this table, the AD increases by almost 20% when only spherical aberration is add to treatment profile, whereas the AD increases by almost 60% when all HOAs are added (mainly spherical, coma and trefoil).

Therefore, it is recommended to chose the proper profile and let the excimer machine software calculate the central AD and the rules can be followed accordingly.

Example 13: Figure 6.6 represents the wavefront-guided ablation profile for an eye with +2 D sphere, coma = 4 µm, trefoil = 1.97 µm, spherical aberration = –0.29 µm, and RMS related to HOAs = 4.85 µm. The central AD is 22.13 µm and the maximum AD is 103 µm.

In the previous example, if the eye is myopic, more central ablation will be needed.

TABLE 6.1 AD (µm) for –2 D myopic treatment

Profile	*OZ*	
	6 mm	*6.5 mm*
Aspheric	27	34
Aspheric with correction of spherical aberration	32	40
Aspheric with correction of all HOAs	43	55

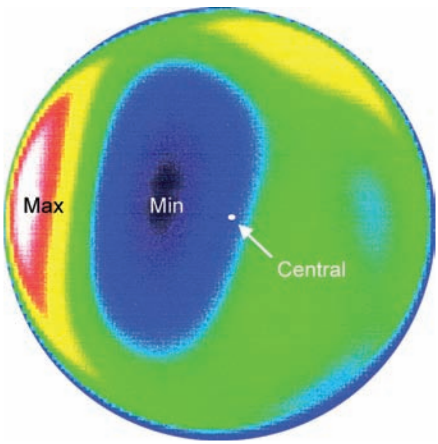

Fig. 6.6 Wavefront-guided ablation profile to correct an eye with +2 D sphere, coma = 4 µm, trefoil = 1.97 µm, spherical aberration = –0.29 µm, and RMS related to HOAs = 4.85 µm.

TAKE-HOME MESSAGE

In LA and LSA:
- RSB 1: Keep at least 270 µm of RSB
- RSB 2: Ablate at most 20% of original corneal thickness at thinnest location
- RSB 3: Actual AD differs according to the diameter of the OZ. In average, 15 µm per -1 D for an OZ = 6.5 mm
- RSB 4: Follow the most conservative rule among rules 1, 2 and 3

Contd...

Contd...

In SA:
- RSB 5: Ablate at most 80–90 µm and keep at least 400 µm of RSB including epithelium

In PRT:
- RSB 6: Use the absolute sum of the refractive error in calculating RSB

In hyperopic treatment:
- RSB 7: The preoperative thinnest location should be ≥ 470 µm and it is recommended not to go beyond +4 D of correction

In mixed astigmatism:
- RSB 8: convert the equation to use the plus cylinder formula

In WFGT:
- RSB 9: the AD differs according to the type and severity of HOA(s); the rules should be followed on site

K-READING RULES

The recommended amount of correction should be calculated according to RSB rules first and according to K-readings rules thereafter.

Flat K Rule

In myopic ablation, look at flat K. Correction of –1 D reduces flat K by 0.75 D. Calculate the final flat K according to the amount of myopic ablation. The final flat K should be > 34 D.

Example 14: an eye with flat K = 43 D and –6 D sph; final flat K = 43 – (6 x 0.75) = 39 D (recommended).

Example 15: an eye with flat K = 40 D and –8 D sph; final flat K = 40 – (8 x 0.75) = 34 D (not recommended).

Steep K Rule

In hyperopic ablation, look at steep K. Correction of +1 D increases steep K by 1.2 D. Calculate the final steep K according to the amount of hyperopic ablation. The final steep K should be <49 D.

Example 16: an eye with steep K = 43 D and +4 D sph; final steep K = 43 + (4 x 1.2) = 47.8 D (recommended).

Example 17: an eye with steep K = 44 D and +5 D sph; final steep K = 44 + (5 x 1.2) = 50 D (not recommended).

N.B: when there is > 1 D difference between K-max and steep K, the former should be used in the calculations.

Average K (mean K or Km)

There are two main flap complications related to K-readings: the free flap and the button hole or pseudo button hole. When Km is <40 D, a free flap may happen regardless of the type of MMK or femtosecond used. When Km is >46 D, a button hole or pseudo button hole may happen regardless of the type of MMK or femtosecond used. Figures 6.7 and 6.8 show the mechanism of formation of a button hole or pseudo button hole, respectively. During application of the MMK or the femtosecond cone or handpiece, the central cornea will be applanated. When the cornea is steep (Km > 46 D), the apex of the cornea will indent inwards resulting in irregular cut and a button hole or pseudo button hole formation. The difference between the button hole and pseudo button hole is that the latter still has a thin layer of epithelium occluding the hole.

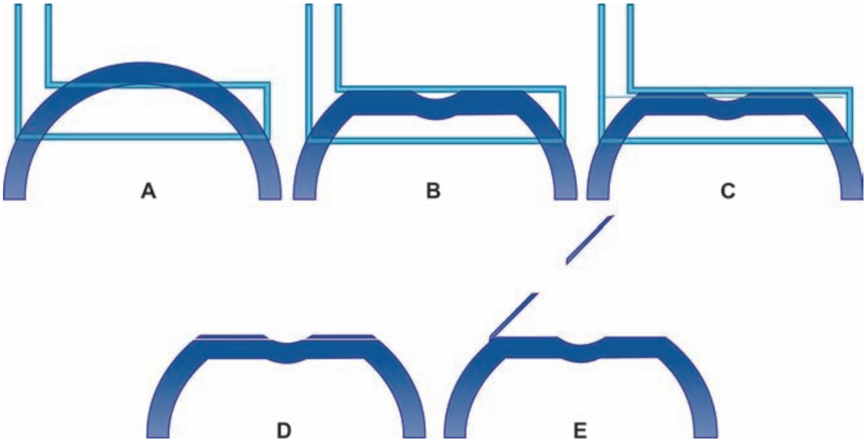

Fig. 6.7 Mechanism of button hole formation.

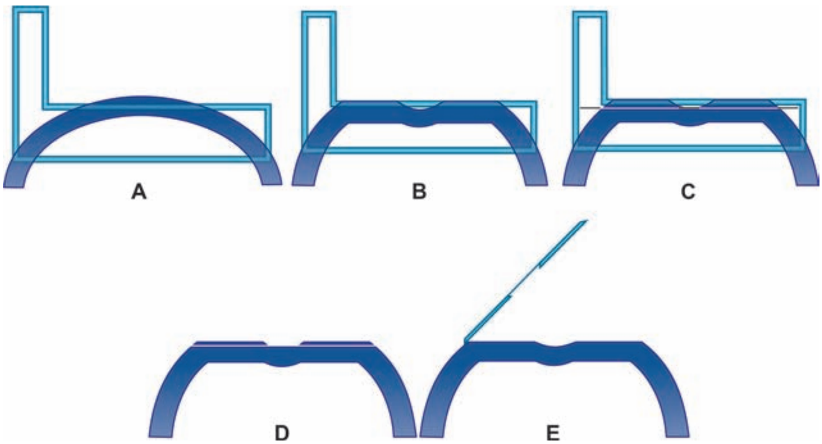

Fig. 6.8 Mechanism of pseudo button hole formation.

To avoid such complications, three parameters should be adjusted: flap diameter, hinge width and hinge length. However, hinge width and hinge length are correlated in a proportional relationship. Figure 6.9 illustrates the relationship among K-readings, flap diameter and hinge width. The flatter the cornea, the smaller the diameter of the flap should be and vice versa. The flatter the cornea, the wider the hinge of the flap should be and vice versa. For example, if Km is 42 D, 8.5 mm flap diameter and 0.6 mm hinge width should be adjusted to avoid free flap complication. However, manufacturers usually provide nomogram for such a purpose.

Use a larger flap when treating a patient with mixed astigmatism, hyperopic astigmatism or hyperopia.

Corneal diameter must be considered when a large flap is required. It should be noticed that edges of large flaps may be near the limbus; therefore, the flap may be more difficult to lift and small vessels bleeding may be bothersome.

Astigmatism Rules

Figure 6.10 describes the principle of corneal astigmatism; "a" is the steep meridian, "b" is the flat meridian, and "ab" represents corneal or topographic astigmatism (TA).

There are three principles in treating corneal astigmatism with photorefractive surgery.

1. Flattening the steep meridian by ablating this meridian for the same amount of corneal astigmatism (Fig. 6.11). The computer applies this profile when treating myopic astigmatism.
2. Steepening the flat meridian by ablating the periphery of this meridian for the same amount of corneal astigmatism (Fig. 6.12). The computer applies this profile when treating hyperopic astigmatism.
3. Performing both 1 and 2 in half steps. The computer applies this profile when treating mixed astigmatism (Fig. 6.13).

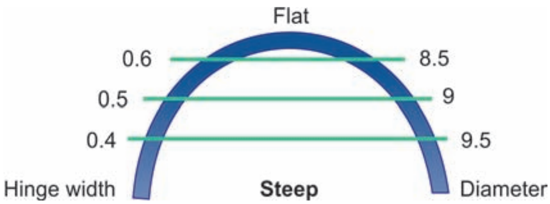

Fig. 6.9 Relationship among K-readings, flap diameter and hinge width.

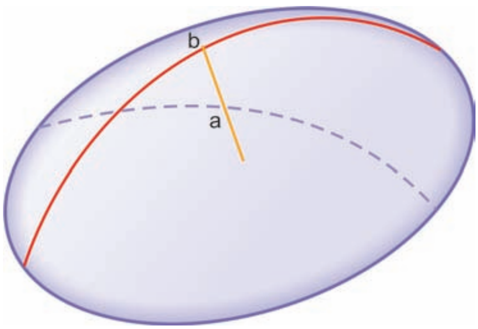

Fig. 6.10 Corneal (topographical) astigmatism. It is the difference "ab" between the steep "a" and flat "b" meridians.

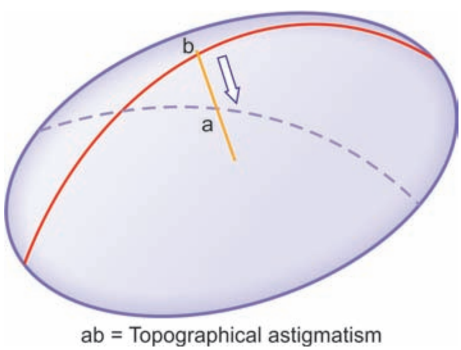

Fig. 6.11 Principle of correcting myopic astigmatism.

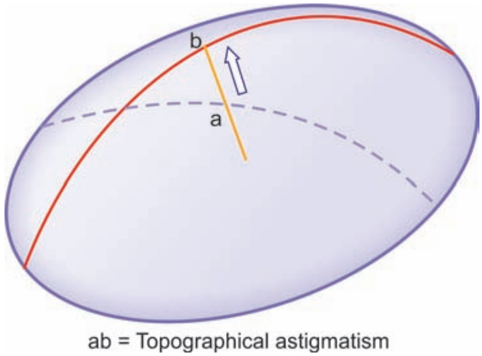

Fig. 6.12 Principle of correcting hyperopic astigmatism.

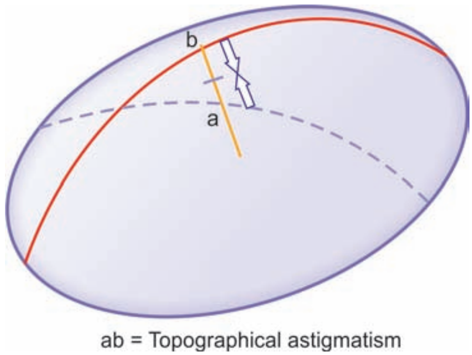

Fig. 6.13 Principle of correcting mixed astigmatism.

Myopic Astigmatism Rule

If an eye has myopic astigmatism, look at the steep K for the astigmatic correction and at the flat K for the myopic spherical correction.

Example 18: an eye with a refractive error of –4 D sph/–2 D cyl and K readings of 44 D and 45.5 D. To have accurate calculations fill in a table and see Table 6.2 as an example.

Explanation: in this example, the astigmatic correction flattens the steep K and brings it to flat K, which is not affected by the astigmatic correction. Thereafter, the spherical correction flattens all.

Hyperopic Astigmatism Rule

If an eye has hyperopic astigmatism, look at the flat K for the astigmatic correction and at the steep K for the hyperopic spherical correction.

Example 19: an eye with a refractive error of +4 D sph/+2 D cyl and K readings of 40 D and 42.4 D. To have accurate calculations fill in a table and see table 6.3 as an example.

Explanation: in this example, the astigmatic correction steepens the flat K and brings it to steep K, which is not affected by the astigmatic correction. Thereafter, the spherical correction steepens all.

TABLE 6.2 Final K in Myopic Correction

Original K	*Astigmatic correction (–2 D)*	*Myopic correction (–4 D)*	*Final K*
K_f 44 D	(0) K_f = 44 D	(4 x 0.75 = 3 D) K_f = 44 – 3 = 41 D	41 D
K_s 45.5 D	(2 x 0.75 = 1.5 D) K_s = 45.5 – 1.5 = 44 D	(4 x 0.75 = 3 D) K_s = 44 – 3 = 41 D	

K_f : flat K
K_s : steep K

TABLE 6.3 Final K in Hyperopic Correction

Original K	*Astigmatic correction (+2 D)*	*Hyperopic correction (+4 D)*	*Final K*
K_f 40 D	(2 x 1.2 = 2.4) K_f = 40 + 2.4 = 42.4 D	(4 x 1.2 = 4.8 D) K_f = 42.4 + 4.8 = 47.2 D	47.2 D
K_s 42.4 D	(0) K_s = 42.4 D	(4 x 1.2 = 4.8 D) K_s = 42.4 + 4.8 = 47.2 D	

K_f : flat K
K_s : steep K

Mixed Astigmatism Rule

In mixed astigmatism, use the plus cylinder equation, look at flat K for the astigmatic correction and look at steep K for the myopic spherical correction.

Example 20: an eye with a refractive error of +2 D sph/–4 D cyl @180 and K readings of 40 D and 44.8 D. To have accurate calculations, use the plus cylinder equation: –2 D sph/+4 D cyl @ 90, fill in a table and see table 6.4 as an example.

Explanation: in this example, the astigmatic correction steepens the flat K and brings it to steep K, which is not affected by the astigmatic correction. Thereafter, the spherical correction flattens all.

N.B: As you noticed in the previous three examples, the spherical correction affected both K readings after the astigmatic correction had affected one of them.

TABLE 6.4 Final K in Hyperopic Correction

Original K	*Astigmatic correction (+4 D)*	*Myopic correction (–2 D)*	*Final K*
K_f 40 D	(4 X 1.2 = 4.8 D) K_f = 40 + 4.8 = 44.8 D	(2 x 0.75 = 1.5 D) K_f = 44.8 – 1.5 = 43.3 D	43.3 D
K_s 44.8 D	(0) K_s = 44.8 D	(2 x 0.75 = 1.5 D) K_s = 44.8 – 1.5 = 43.3 D	

K_f : flat K
K_s : steep K

TAKE-HOME MESSAGE

- Flat K: look at flat K in myopic correction. Correcting –1 D flattens the K by 0.75 D. Final K should be >34 D
- Steep K: look at steep K in hyperopic correction. Correcting +1 D steepens the K by 1.2 D. Final K should be <49 D
- Average K (Km): flap complications are found in Km <40 D and Km >46 D. In general, the flatter the cornea the smaller the diameter of the flap and the wider the hinge of the flap should be
- Myopic astigmatism: look at the steep K for astigmatic correction, and at the flat K for myopic spherical correction
- Hyperopic astigmatism: look at the flat K for astigmatic correction and at the steep K for hyperopic spherical correction
- Mixed astigmatism: use the plus cylinder equation, look at flat K for astigmatic correction and look at steep K for myopic spherical correction

DISPARITY BETWEEN TOPOGRAPHIC ASTIGMATISM (TA) AND MANIFEST ASTIGMATISM (MA)

Clinical MA occasionally differs from the TA. This disparity may be either in values, axes or both.

Etiology

1. Misalignment during the capture.
2. Corneal irregularity. It is more obvious on the tangential curvature map.
3. Hot spot.
4. Tear film disturbance.
5. Corneal opacities, particularly central.
6. Lenticular astigmatism. Corneal astigmatism may be accompanied with lenticular astigmatism and in some cases, the whole clinical astigmatism may be lenticular. One of the important causes of the lenticular astigmatism is lens subluxation or dialysis; but the most important thing is when there is a subtle cataract, particularly, posterior subcapsular cataract, it may present itself with astigmatism before it becomes clear on the slit lamp, hence the importance of studying Scheimpflug image, lens densitometry and re-examining the patient more carefully with the pupil dilated. Figure 6.14 is Scheimpflug image showing lens opacity causing MA and TA disparity.

Management

There are 9 probabilities in this regard. They are as follows:

1. TA and MA are WTR and the amount of the former is more than the latter.
2. TA and MA are WTR and the amount of the former is less than the latter.
3. TA and MA are ATR and the amount of the former is more than the latter.
4. TA and MA are ATR and the amount of the former is less than the latter.
5. TA is WTR and MA is ATR with the amount of the former is more than the latter.
6. TA is WTR and MA is ATR with the amount of the former is less than the latter.
7. TA is ATR and MA is WTR with the amount of the former is more than the latter.
8. TA is ATR and MA is WTR with the amount of the former is less than the latter.
9. TA and/or MA are oblique with more than 15° difference between their axes.

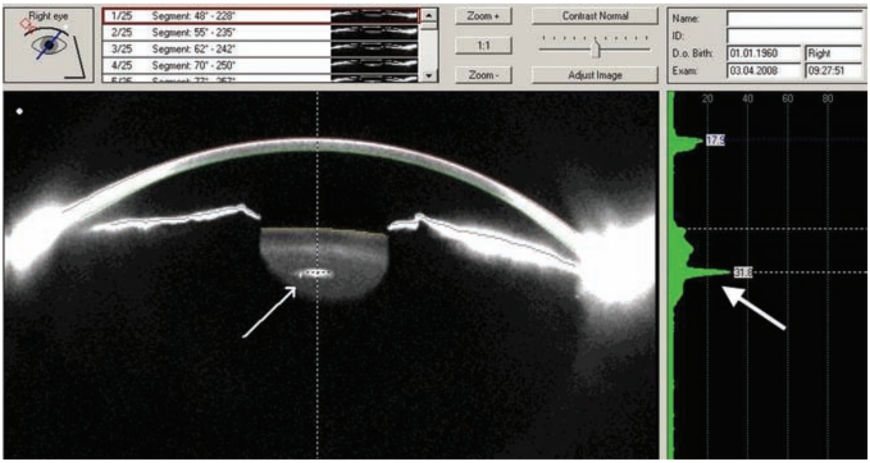

Fig. 6.14 Scheimpflug image showing lens opacity. On the right side, densitometry shows a corresponding peak (white arrow) with a 31.8 reading. Readings > 30 are significant.

Table 6.5 summarizes the 9 probabilities.

N.B 1: When axes of TA and MA are perpendicular, usually there is no much difference in their amounts.

Let us explain the nine probabilities by examples. To simplify the cases, MA will be myopic.

Example 21: TA is –3 D @ 180 and MA is –2 D @ 180 (Fig. 6.15)

Correcting the MA completely leaves a residual TA of about –1 @ 180. This will be acceptable by the patient since it is WTR and it is consistent with the pre-op WTR astigmatism.

Example 22: TA is –2 D @ 180 and MA is –3 D @ 180 (Fig. 6.16)

Correcting the MA completely induces an ATR TA of about –1 @ 90. This will not be acceptable by the patient since it is ATR and not consistent with his/her pre-op WTR astigmatism even with post-op UDVA 1.0 (Snellen). In such a case, it is better to be limited to the amount of the TA and depend on the spherical equivalent (S.E). For example: a patient with –2 D sph –3 D cyl @ 180, and the TA is –2 D @ 180, it is recommended to treat –2.5 D sph –2 D cyl @ 180.

TABLE 6.5 Probabilities of the Disparity Between Topographic Astigmatism (TA) and Manifest Astigmatism

Amount	*MA*	*TA*	*Probability*
TA > MA	WTR	WTR	1
TA < MA	WTR	WTR	2
TA > MA	ATR	ATR	3
TA < MA	ATR	ATR	4
TA > MA	ATR	WTR	5
TA < MA	ATR	WTR	6
TA > MA	WTR	ATR	7
TA < MA	WTR	ATR	8
?	Oblique	Oblique	9

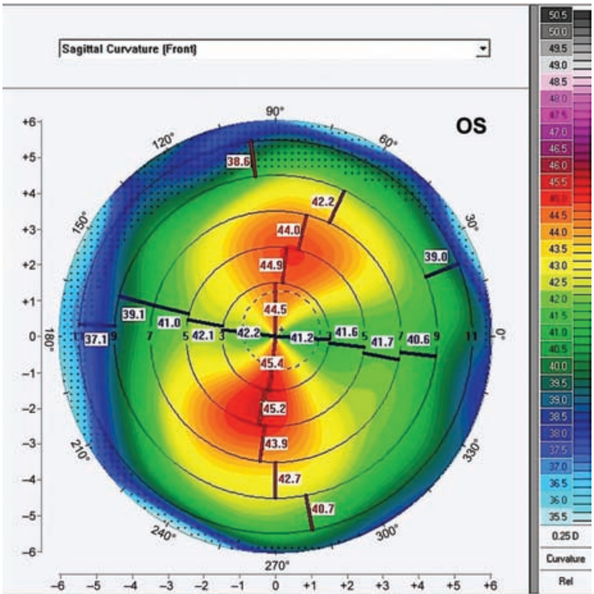

	Cyl	Axis
TA	–3	180
MA	–2	180

Fig. 6.15 MA and TA disparity. First probability.

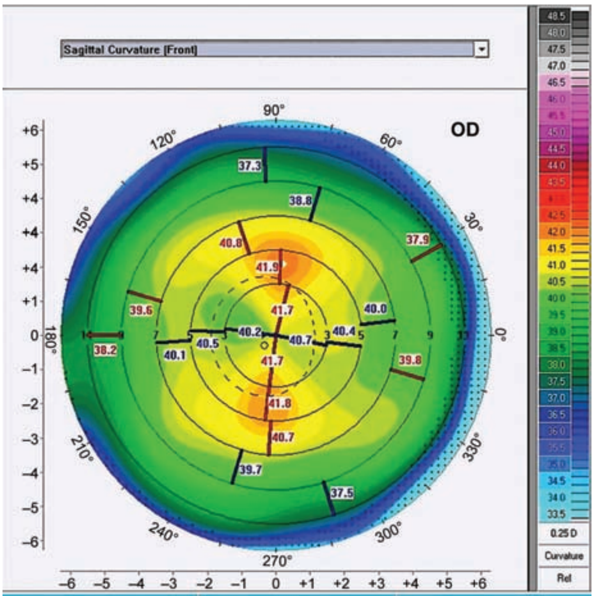

	Cyl	Axis
TA	–2	180
MA	–3	180

Fig. 6.16 MA and TA disparity. Second probability.

Example 23: TA is –3 D @ 90 and MA is –2 D @ 90 (Fig. 6.17).

Correcting the MA completely leaves a residual TA of about –1 @ 90. This will be acceptable by the patient since it is consistent with the pre-op ATR astigmatism.

Example 24: TA is –2 D @ 80 and MA is –3 D @ 80 (Fig. 6.18).

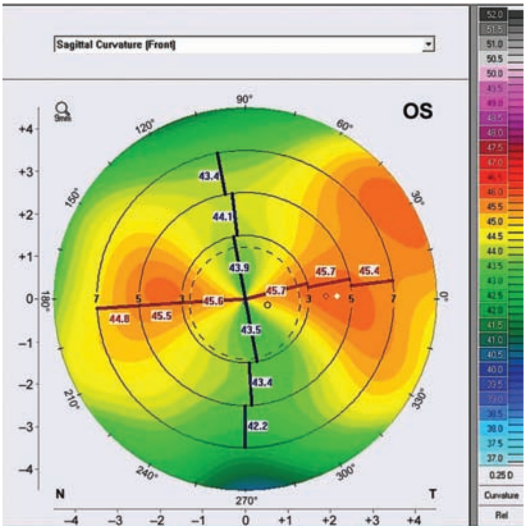

	Cyl	Axis
TA	–3	90
MA	–2	90

Fig. 6.17 MA and TA disparity. Third probability.

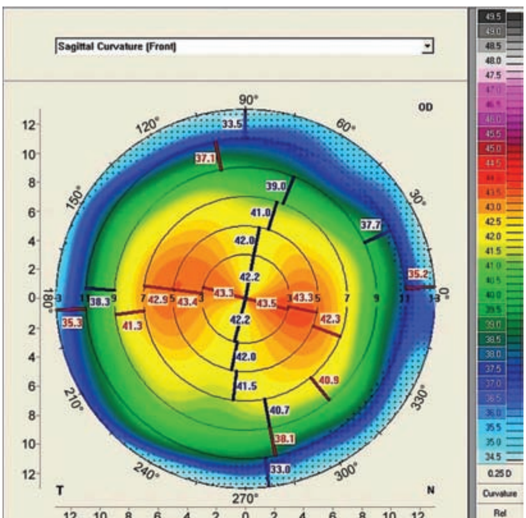

	Cyl	Axis
TA	–2	80
MA	–3	80

Fig. 6.18 MA and TA disparity. Fourth probability.

Correcting MA completely induces WTR TA of about −1 @ 170. This will be acceptable by the patient since it is WTR although it is not consistent with the pre-op ATR astigmatism. If the induced WTR TA is within 1 D, it will be tolerable, otherwise it will not be; in such a case the proposed induced WTR TA should be limited to 0.5 D to 1 D and the S.E should be modified accordingly. For example: a patient with −2 D sph −4 D cyl @ 80, and the TA is −2 D cyl @ 80, it is recommended to treat −2.5 D sph −3 D cyl @ 80. In this case, the induced TA is not more than −1 D cyl @ 170.

Example 25: TA is −1.5 D @ 180 and MA is −1 D @ 90 (Fig. 6.19)

First, we have to look for any cause behind this disparity especially in the crystalline lens. Correcting MA completely induces WTR TA of about −2.5 D cyl @ 180! This will be completely very odd. In such a case, it is recommended to re-check the manifest refraction and try to modify it to be with at least astigmatism as possible. For example: a patient with −2 D sph −0.75 D cyl @ 90, the CDVA is 0.9 (Snellen), and the TA is −1.5 D @ 180, it is recommended to adjust the refraction to be, for example, −2.25 D sph without cylindrical correction although the CDVA may be 0.8 (Snellen). As mentioned before, it is unusual to see much difference between MA and TA amounts when their axes are completely perpendicular.

Example 26: TA is −1 D @ 180 and MA is −1.5 D @ 90 (Fig. 6.20)

What applies on example 25 applies here also.

Example 27: TA is −1.5 D @ 80 and MA is −1 D @ 170 (Fig. 6.21)

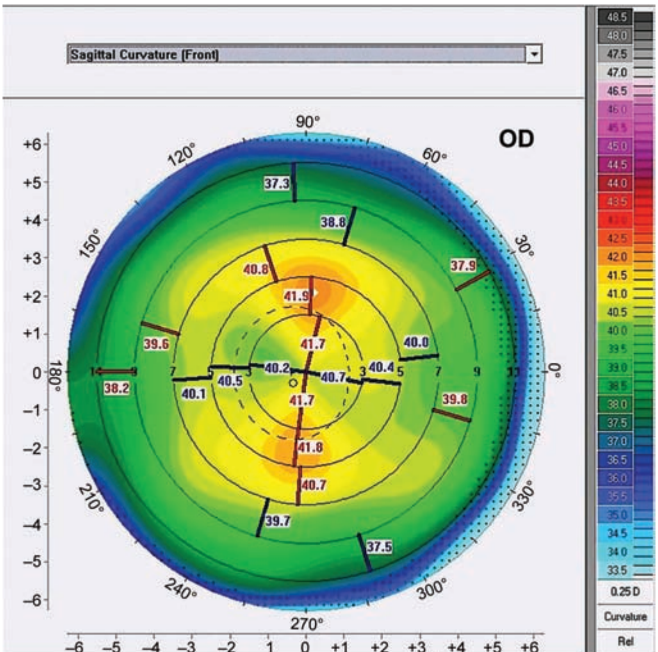

	Cyl	Axis
TA	−1.5	180
MA	−1	90

Fig. 6.19 MA and TA disparity. Fifth probability.

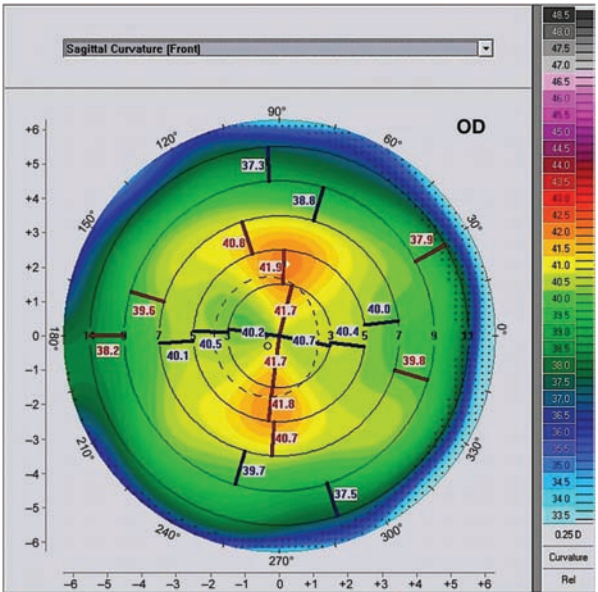

	Cyl	Axis
TA	–1	180
MA	–1.5	90

Fig. 6.20 MA and TA disparity. Sixth probability.

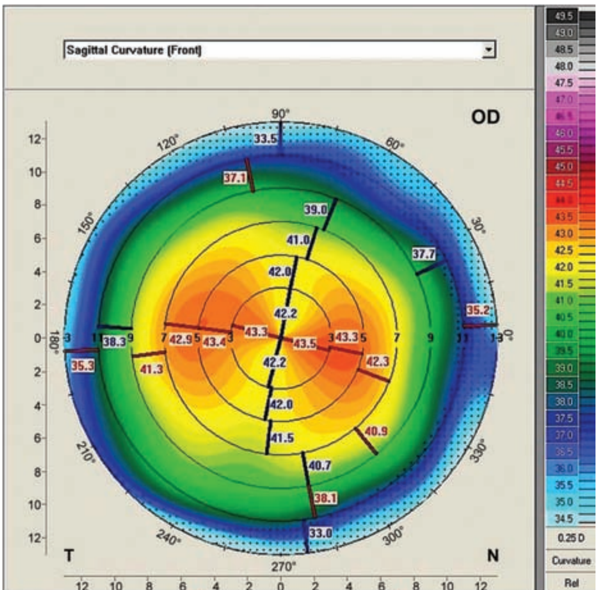

	Cyl	Axis
TA	–1.5	80
MA	–1	170

Fig. 6.21 MA and TA disparity. Seventh probability.

The problem encountered in examples 25 and 26 will be exaggerated in this example; the TA is ATR and will be increased by the operation if the MA has been completely corrected. Thus, we have two factors in this example that make the patient disturbed with the correction; the ATR factor and the amount of this astigmatism. In such a case, it is recommended to re-check the manifest refraction and try to modify it to be with at least astigmatism as possible. For example: a patient with –2 D sph –0.75 D cyl @ 80, the CDVA is 0.9 (Snellen), and the TA is –1.5 D @ 170, it is recommended to adjust the refraction to be, for example, –2.25 D sph without cylindrical correction although the CDVA may be 0.8 (Snellen).

Example 28: TA is –1 D @ 80 and MA is –1.5 D @ 170 (Fig. 6.22)

What applies on example 27 applies here also.

Example 29: TA is –2 D @ 135 and MA is –2.5 D @ 100 (Fig. 6.23)

It is not uncommon to encounter such an example in our clinical practice. Suspicion in cataract or corneal irregularities especially faint scaring should be very high. If such causes and other possible causes were excluded, it is wise to take time in thinking about the final correction. Re-examining the patient with fine tuning of the MA axis and amount is very necessary. If the difference persists, the MA should be chosen. It is also wise to tell the patient that there might be a need for future enhancement.

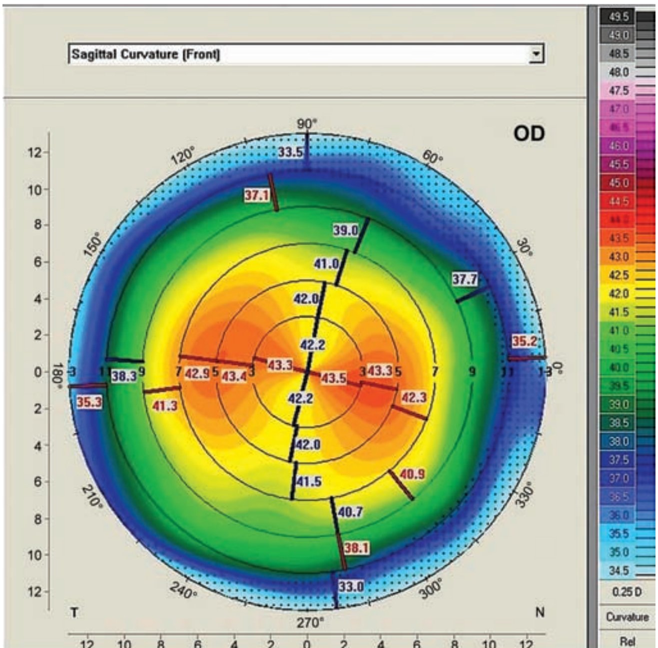

	Cyl	Axis
TA	–1	80
MA	–1.5	170

Fig. 6.22 MA and TA disparity. Eighth probability.

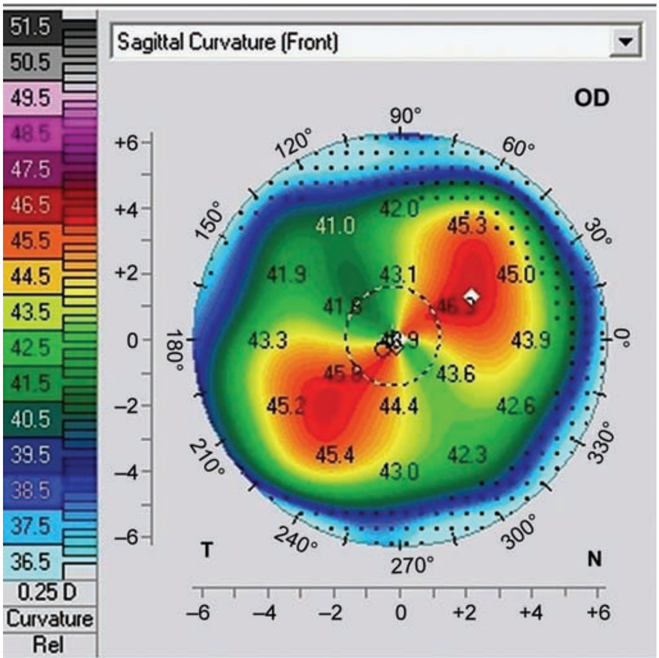

	Cyl	Axis
TA	– 2	135
MA	– 2.5	100

Fig. 6.23 MA and TA disparity. Ninth probability.

SUBOPTIMAL CORRECTION RULE

In case of suboptimal correction due to limitations in thickness, the expected residual refractive error should be planned to be on the account of the spherical component rather than the astigmatic component of the refractive error.

Example 30: an eye has –5 D sph/–2 D cyl. According to thickness rule, this is considered (–5 + –2) = –7 D. Assuming that only –6 D can be corrected due to thickness limitations, it is wise to correct –4 D sph/–2 D cyl rather than correcting –5 D sph/–1 D cyl. The residual refractive error will be –1 D sph.

Example 31: an eye has +1 D sph/–4 D cyl. According to mixed astigmatism rule and thickness rule, this is considered –3 D sph/+4 D cyl. Therefore, the –3 D is taken into consideration for thickness rules. Assuming that only –2 D sph can be corrected, the correction will be –2 D sph/ +4 D cyl. The residual refractive error will be –1 D sph.

Example 32: an eye has –4 D sph/–3 D cyl and significant HOAs. Assuming that the wavefront-guided treatment requires an AD that exceeds thickness limits by 1.5 D, one of two options can be applied: reducing the amount of spherical correction to be –2.5 D sph, or reducing the amount of astigmatic correction to be –1.5 D cyl. It is wise to correct –2.5 D sph/–3 D cyl especially that most HOAs are induced by irregular astigmatism.

TAKE-HOME MESSAGE

- In case of suboptimal correction, it is recommended for the residual refractive error to be sphere rather than to be astigmatism

Q-VALUE RULE AND ASSIS NOMOGRAM

As mentioned in chapter 1, Q-value represents the asphericity of the cornea; it has a positive value (>0) when the cornea is oblate, zero value when the cornea is spheric and negative value (<0) when the cornea is prolate (see figures 1.54 to 1.57). Myopic correction shifts the cornea towards being oblate, where Q becomes less negative or more positive (Fig. 6.24) which usually leads to positive spherical aberrations. On the other hand, hyperopic correction shifts the cornea towards being hyperprolate, where Q becomes more negative (Fig. 6.25) which leads to negative spherical aberrations. This problem may be insignificant in small refractive errors (myopia < 3 D, astigmatism < 2 D or hyperopia < 3 D). In case of higher corrections, Q value will go beyond the accepted range [–1 , 0] leading to spherical aberrations.

Studies have shown that even with the use of aspheric or wavefront-guided profiles, there was a +0.18 change in the Q value (more positive) for each diopter of myopic treatment, whereas there was an induction of – 0.17 of asphericity (more negative) for each diopter of hyperopic treatment. Table 6.6 shows the effect of myopic correction on Q-value assuming that the original Q = –0.4, and Table 6.7 shows the effect of hyperopic correction on Q-value assuming that the original Q = –0.4.

This table shows that at almost –3 D and more of myopic treatment, Q-value is shifted to be positive.

This table shows that at almost +3 D and more of hyperopic treatment, Q-value is shifted to be very negative.

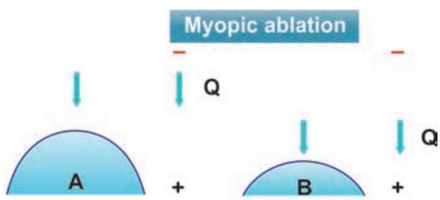

Fig. 6.24 Corneal asphericity. After myopic ablation, the cornea becomes oblate and Q becomes more positive (less negative). (A) before treatment; (B) after treatment.

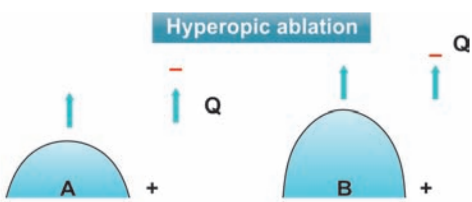

Fig. 6.25 Corneal asphericity. After hyperopic ablation, the cornea becomes hyperprolate and Q becomes more negative. (A) before treatment; (B) after treatment.

TABLE 6.6: Effect of Myopic Correction on Q-value (Aspheric or Wavefront-guided Profiles) for an Original Q = –0.4

Myopic Correction (D)	*Resultant Q*
–1	–0.22
–2	–0.04
–3	+0.14
–4	+0.32
–5	+0.50
–6	+0.68
–7	+0.86
–8	+1.04

TABLE 6.7 Effect of Hyperopic Correction on Q-value for an Original Q = –0.4

Hyperopic Correction (D)	*Resultant Q*
+1	–0.57
+2	–0.74
+3	–0.91
+4	–1.08
+5	–1.25
+6	–1.42

Although the aspheric or wavefront-guided profiles are used, these two tables show that Q value is still affected by high corrections. However, if Q adjustment is indicated for monovision or treating abnormal Q-value ± refractive errors, the following steps should be followed assuming that the aspheric or wavefront profiles will be used:

1. Calculate the Q-value that will result from the treatment (assumed resultant Q).
2. Suggest a target Q, preferably –0.4.
3. Calculate ΔQ = assumed resultant Q – target Q.
4. Use ASSIS Nomogram (see below) to calculate the amount of sphere adjustment.
5. Adjust the refractive error to be treated.

ASSIS found that each 0.1 change in Q-value is associated with an amount of change in refractive error as shown in Table 6.7.

We will study some examples.

Example 33: an eye with –6 D of myopia. Preoperative Q at 6 mm is –0.2.

1. Correcting each –1 D reduces Q by 0.18: –6 x 0.18 = –1.08. The assumed resultant Q = –0.2 – (–1.08) = +0.88.
2. Target Q = –0.4.
3. ΔQ = +0.88 – (–0.4) = 1.28, which is 12.8 folds of 0.1 ΔQ.
4. In ASSIS Nomogram, when treating -6 D: –0.2 x 12.8 = –2.56 D should be adjusted.
5. The refractive error that should be treated –6 – (–2.56) = –3.44 D. This will achieve emmetropia in addition to –0.4 Q-value.

TABLE 6.8 ASSIS sphere adjustment nomogram for customized Q (for 6.5 mm OZ)

Hyperopia			
Add +0.16 D per 0.1 ΔQ for any sphere			
Myopia (D)			
Subtract	−0.20	Per 0.1 ΔQ When correcting:	−1.00
	−0.30		−2.00
	−0.27		−3.00
	−0.25		−4.00
	−0.22		−5.00
	−0.20		−6.00

Example 34: an eye with −4 D of myopia. Preoperative Q at 6 mm is −0.1.

1. Correcting each −1 D reduces Q by 0.18: −4 x 0.18 = −0.72. The assumed resultant Q = −0.1 − (−0.72) = +0.62.
2. Target Q = −0.4.
3. ΔQ = +0.62 − (−0.4) = 1.02, which is 10.2 folds of 0.1 ΔQ.
4. In ASSIS Nomogram, when treating −4 D: −0.25 x 10.2 = −2.55 D should adjusted.
5. The refractive error that should be treated −4 − (−2.55) = −1.45 D. This will achieve emmetropia in addition to −0.4 Q-value.

Example 35: an eye with +4 D of hyperopia. Preoperative Q at 6 mm is −0.3.

1. Correcting each +1 D increases Q by 0.17: +4 x 0.17 = +0.68. The assumed resultant Q = −0.3 − (+0.68) = −0.98.
2. Target Q = −0.4.
3. ΔQ = −0.98 − (−0.4) = −0.58, which is 5.8 folds of 0.1 ΔQ.
4. In ASSIS Nomogram, when treating +4 D: = 0.16 x 5.8 = +0.93 D should adjusted.
5. The refractive error that should be treated +4 + (+0.93) = +4.93 D. This will achieve emmetropia in addition to −0.4 Q-value.

Example 36: an eye with +5 D of hyperopia. Preoperative Q at 6 mm is −0.2.

1. Correcting each +1 D increases Q by 0.17: 5 x 0.17 = 0.85. The assumed resultant Q = −0.2 − 0.85 = −1.05.
2. Target Q = −0.2 (maintain same Q).
3. ΔQ = −1.05 − (−0.2) = −0.85, which is 8.5 folds of 0.1 ΔQ.
4. In ASSIS Nomogram, when treating +5 D: 0.16 x 8.5 = +1.36 D should adjusted.
5. The refractive error that should be treated +5 + (+1.36) = +6.36 D. This will achieve emmetropia in addition to maintaining the native −0.2 Q-value.

Nevertheless, as mentioned in chapter 5, Q-adjustment is indicated to maintain the preoperative normal Q and to improve a preoperative abnormal Q. Maintaining normal Q is achieved by targeting Q to be equal to the preoperative value of the flattest meridian of the cornea (example 37). Improving an abnormal Q is achieved by targeting Q to be as the closest value which lies in the normal range [−1 , 0]; this is indicated when preoperative Q > 0.0 (oblate cornea) (examples 38 and 39), or when there is a difference of >0.1 between the flattest and steepest meridians values (examples 40 and 41). However, it should be noted that in such cases, the refractive status will be altered and should therefore be adjusted accordingly.

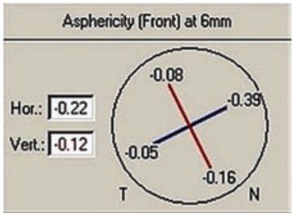

Fig. 6.26 Q-value demonstrated in two meridians with average vertical and average horizontal.

Finally, target Q value should not be so far from the preoperative Q value for two reasons: to avoid so much ablation of tissue (the farer the target Q, the larger the amount of AD) and to avoid much alteration of the refractive status of the eye, which may need a big adjustment in case of far target Q.

Example 37: Figure 6.26 shows Q value of the flattest and the steepest meridians. As shown in this figure, the flat Q = –0.12 and the steep Q = –0.22; both are normal and target Q can be adjusted to be –0.12.

Example 38: A cornea has flat Q = +0.3, steep Q = +0.2 and average Q = +0.25; all are abnormal indicating an oblate cornea. The closest normal Q = 0.0 or –0.1; therefore, target Q = 0.0 or –0.1 (preferably –0.1).

Example 39: A cornea has flat Q = +0.5, steep Q = +0.4 and average Q = +0.45; all are abnormal indicating very oblate cornea. The closest normal Q = 0.0 or –0.1; therefore, target Q = 0.0 or –0.1 (preferably 0.0).

Example 40: A cornea has flat Q = –0.2, steep Q = –0.4 and average Q = –0.3; all are normal but the difference between flat and steep is 0.2 (>0.1). Q can be targeted to be as the flat = –0.2.

Example 41: A cornea has flat Q = +0.3, steep Q = +0.1 and average Q = +0.2; all are abnormal and the difference between flat and steep is 0.2 (>0.1). Q cannot be targeted to be as the flat, but to be the closest normal = 0.0 or –0.1 (preferably –0.1).

TAKE-HOME MESSAGE

- Q-value is affected by PRT even when aspheric or wavefront-guided profiles are used; however, such affection is minor with the use of these profiles
- Myopic treatment shifts Q towards more positive and vice versa for the hyperopic treatment. The higher the magnitude of corrected refractive error, the higher the shift will be
- Q is shifted towards positive by +0.18 increments per diopter of myopic treatment and is shifted towards negative by –0.17 decrements per diopter of hyperopic treatment
- It is recommended to use the aspheric profile even for small refractive errors in virgin eyes
- It is recommended to adjust a target Q to maintain the original native Q
- When adjusting abnormal Q, target Q should be the closest to normal range
- Q-adjustment showed follow 5 steps: calculate the assumed resultant Q, suggest a target Q, calculate ΔQ, use ASSIS Nomogram for sphere adjustment and adjust the sphere

PUPIL CENTRE AND ANGLE KAPPA RULE

Angle Kappa is the angle between the visual axis and the axis that passes through pupil centre (Fig. 6.27). Unlike Scheimpflug-based topographers, Placido-based topographers measure angle kappa. This raises the need to find a way to estimate this angle in Scheimpflug-based topographers. However, clinical trials have shown that visual axis passes somewhere in between

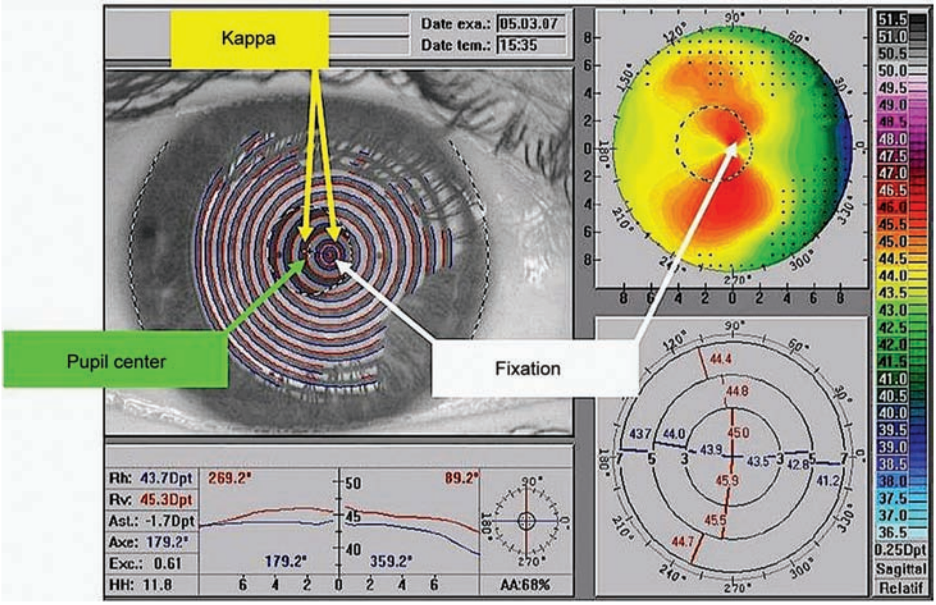

Fig. 6.27 Angle kappa.

pupil centre and apex of the cornea and might be half the distance. Therefore, it is reasonable to consider half values of x and y pupil centre coordinates in Scheimpflug based as if they were angle kappa in Placido based topographers.

Angle kappa is considered significant when it exceeds 0.1 mm (100 µm) or > 5°. This is important for the following reasons:

- When angle kappa is >0.1 mm (>100 µm), the capture should be repeated to exclude misalignment.
- When a patient has a wide angle kappa, his/her topography may display false positives or false negatives such as the skewed pattern of elevation maps.
- When treating refractive errors with PRT (particularly hyperopia and astigmatism), optimal results can be achieved when the centre of ablation coincides with the optical axis of the patient. This can be achieved by decentring the ablation profile for the amount of angle kappa; this is called "offset pupil" or "decentration" as mentioned in chapter 5.

Finally, decentred pupil (corectopia) is a case of concern especially when PIOL implantation is indicated.

TAKE-HOME MESSAGE

- Angle kappa is measured by Placido-based topographers and estimated by pupil coordinates in Scheimpflug-based tomographers
- When angle kappa is significant (>100 µm), the capture should be repeated to exclude misalignment
- It is recommended to compensate for significant angle kappa in PRT by decentration (offset pupil) in case of hyperopic or astigmatic treatment
- Decentration (offset pupil) can be achieved by manual input of angle kappa coordinates (in Placido-based) or half values of pupil coordinates (in Scheimpflug-based)
- Decentration (offset pupil) is automatically performed when using wavefront-guided profile

PUPIL DIAMETER CONSIDERATIONS

In PRT, there are special considerations in adjusting OZ treatment:

1. The diameter of the OZ should be at least 0.5 mm larger than the scotopic pupil in order to avoid night glare.
2. Light-colored iris usually has a pupil diameter larger than that of dark-colored one.
3. The higher the amount of corrected refractive error the smaller the actual resultant OZ (efficient OZ). For example, when treating –8 D sph with an OZ of 6.5 mm, the efficient OZ will be about 5.5 mm. Therefore, choosing a small OZ to gain more correction in high refractive errors carries the risk of night glare.
4. In SA, OZ < 6 mm increases the risk of postoperative haze.

TAKE-HOME MESSAGE

- OZ in PRT should be 0.5 mm larger than scotopic pupil
- Correction of high refractive error results in an efficient OZ smaller than the assumed one
- Colored iris usually has a pupil size larger than that of dark-colored one

CYCLOTORSION

Cyclotorsion in corneal meridians usually happens with change of head position or when transferring from the setting position (status of capturing tomography) to the supine position (status of operation). It has been shown that eyes can undergo up to 9.5° of cyclotorsion (usually ex-cyclotorsion) when a patient goes from the setting position measured on the aberrometer to the supine position under the excimer laser.

Cyclotorsion impacts correction of astigmatism and HOAs; in such cases, treatment profile derived from imaging machines should exactly match where it should be applied on the cornea, otherwise a tortional effect will result leading to what is known as surgically induced astigmatism in case of astigmatism, or surgically induced aberrations in case of aberrations.

To understand this concept, Figure 6.28 illustrates the relationship between resultant astigmatism magnitude as a percentage of preoperative magnitude and angle of error (misalignment or cyclotorsion). As shown in this figure, an almost 3°, 8° and 15° of misalignment results in 10%, 25% and 50% of reduction of effect respectively; whereas, 30° of misalignment results in no effect (same amount) but on different axis and a 90° of misalignment results in doubling of initial cylinder.

Compensation for cyclotorsion is indicated in case of >1 D astigmatism and in case of WFGT.

Several systems have been developed to ensure alignment. The most basic technique is to mark the limbus, typically at the 3 o'clock and 9 o'clock positions, while the patient is seated immediately prior to surgery. These marks are then used to align the head when the patient is lying under the laser. A more sophisticated system ensures that the eye alignment during aberrometry matches the alignment under the laser. Limbal marks are captured and recorded by the aberrometer immediately prior to surgery. An ablation profile is then computed. Under the laser, the same limbal marks are used to manually match the alignment to the wavefront image.

The most recent technology advancement, iris registration, has further improved and automated the alignment process. Unique iris details are recorded by the aberrometer and relayed to the laser. A sophisticated camera and computer system in the excimer machine records and matches iris details to the aberrometer. Scleral registration is another technique to ensure

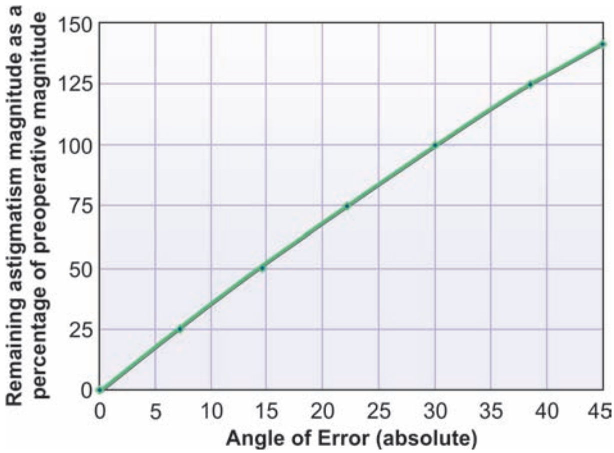

Fig. 6.28 Error in astigmatic correction due to cyclotorsion.

proper cyclo-alignment. This system recognizes unique limbal vessels at both the aberrometer and laser and automatically compensates for misalignment.

There are two types of cyclotorsion compensation, static cyclotorsion compensation (SCC) and dynamic cyclotorsion compensation (DCC). SCC is performed at the beginning of the surgery, where the profile is adjusted according to the preoperative registered landmarks. SCC should be done before epithelium removal or flap creation. DCC is automatically performed during the surgery by continuous adjustment of the profile according to the registered landmarks.

TAKE-HOME MESSAGE

- Compensation for cyclotorsion is necessary in treating > 1 D of astigmatism and HOAs
- A cyclotorsion of 8° results in a residual astigmatism which magnitude equals 25% of the original astigmatism but on a new meridian

AMBLYOPIA

Do not assume the patient has refractive amblyopia unless a careful refraction has been done. Wavefront technology can help with refraction even if custom surgery is not being done.

In case of amblyopia, the patient should know that the expected post operative UDVA may not be better than the preoperative CDVA.

Treatment decision depends on the severity of amblyopia and the refractive status of both eyes. As shown in Figure 6.29, the decision depends on CDVA in the amblyopic eye. When the CDVA in the amblyopic eye is <0.2 (Snellen), refractive surgery is contraindicated in both eyes. When the CDVA is 0.2 to 0.5, decision depends on the refractive status; in case of intolerable anisoconia due to anisometropia, refractive surgery is indicated, otherwise the case is questionable and should be discussed carefully with the patient. When the CDVA is ≥0.5, refractive surgery can be performed. Some surgeons may prefer to operate on the amblyopic eye first, but this may induce tropia.

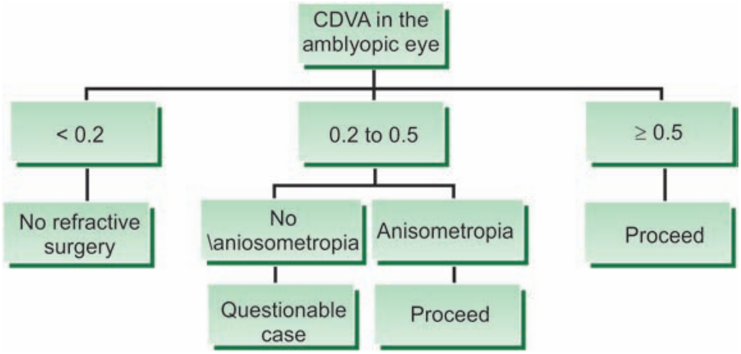

Fig. 6.29 Flow chart of decision making for refractive surgery in amblyopia.

TAKE-HOME MESSAGE

- In case of amblyopia, decision of treatment depends on the severity of amblyopia and the refractive status of both eyes
- In case of mild amblyopia, refractive surgery is not contraindicated
- In case of moderate amblyopia with anisometropia, refractive surgery is not contraindicated
- In case of moderate amblyopia without anisometropia, refractive surgery is questionable
- In case of severe amblyopia, refractive surgery is contraindicated

ENHANCEMENT CONCEPTS

Thickness Concept

After calculation, make certain that the patient will have enough RSB for enhancement.

K-readings Concept

Try not to come to the end of borderline K from the first surgery; i.e. make certain that the patient will be able for enhancement without compromising the K. For example, do not go below 36 D or over 46 D of flat K and steep K, respectively, by the first surgery.

Time Concept

Allow adequate time for the cornea to stabilize, particularly when the patient cannot be refracted to 1.0 (Snellen) and there is no other cause. Three to six months are usually sufficient for the refractive status to stabilize.

Refraction Concept

The CR and MR may be significantly different despite 1.0 (Snellen) vision with each. The retreatment should be based on the CR.

WGT Concept

Custom enhancement may be considered in patients who have subjective complaints out of proportion to the measured refractive error. This is true regardless of whether the patient had custom LASIK, initially.

Multiple Enhancements

A patient can be retreated more than once if the refractive error, corneal tomography, slit lamp examination of the cornea and wavefront maps are stable. Pachymetry must be adequate.

Enhancement by LA vs. SA

If further laser enhancement is required due to regression, surface ablation of the flap may be a better alternative. MMC prophylaxis may be required in order to prevent significant haze but with adjustment of sphere to compensate for the flattening effect of MMC.

Surface enhancement is usually a better alternative than re-cutting when working with poor-quality flaps and no information about the original LASIK surgery.

BIBLIOGRAPHY

1. Alio JL, Azar DT (Eds.). Management of Complications in Refractive Surgery. Springer; 2008.
2. Al-Mezaine HS, Al-Amro SA, Al-Obeidan S. Incidence, management, and visual outcomes of buttonholed laser in situ keratomileusis flaps. J Cataract Refract Surg. 2009;35(5):839-45.
3. American Academy of Ophthalmology (2012-2013 edition). Basic and Clinical Science Course, Section 13: Refractive Surgery.
4. Amoils SP, Deist MB, Gous P, et al. Iatrogenic keratoectasia after laser in situ keratomileusis for less than -4.0 to -7.0 diopters of myopia. J Cataract Refract Surg. 2000;26:967-77.
5. Arbelaez MC, Vidal C, Arba-Mosquera S (2008). Clinical outcomes of corneal vertex versus central pupil references with aberration-free ablation strategies and LASIK. Invest Ophthalmol Vis Sci. 49(12):5287-94. doi: 10.1167/iovs.08-2176. Epub 2008 Jul 24.
6. ASSISS Nomogram. Available on line http://ebookbrowse.com/nomogram-assis-sphere-adjustment-for-custom-q-pdf-d233602880.
7. Belin MW, Ambrosio R, Jr. Corneal ectasia risk score: statistical validity and clinical relevance. J Refract Surg. 2010;26(4):238-40.
8. Binder PS. Analysis of ectasia after laser in situ keratomileusis: risk factors. J Cataract Refract Surg. 2007;33:1530-8.
9. Binder PS. Risk factors for ectasia after LASIK. J Cataract Refract Surg. 2008;34:2010-1.
10. Binder PS, Lindstrom RL, Stulting RD, et al. Keratoconus and corneal ectasia after LASIK [letter]. J Cataract Refract Surg. 2005;31:2035-8.
11. Bottos KM, Leite MT, Aventura-Isidro M, et al. Corneal asphericity and spherical aberration after refractive surgery. J Cataract Refract Surg. 2011;37:1109-15.
12. Brightbill FS, McDonnell PJ, McGhee CNJ, et al. Corneal Surgery: Theory, Technique and Tissue. Mosby Elsevier; 2009.
13. Bühren J, Kühne C, Kohnen T. Influence of pupil and optical zone diameter on higher-order aberrations after wavefront-guided myopic LASIK. J Cataract Refract Surg. 2005;31(12):2272-80.
14. Caster Ai, Friess DW, Potvin RJ. Absence of keratoectasia after LASIK in eyes with preoperative central corneal thickness of 450 to 500 microns. J Refract Surg. 2007;23(8):782-8.

15. Chan CC, Hodge C, Sutton G. External analysis of the Randleman Ectasia Risk Factor Score System: a review of 36 cases of post LASIK ectasia. Clinical and Experimental Ophthalmology. 2010;38(4):335-40.
16. Dawson DG, Randleman JB, Grossniklaus HE, et al. Corneal ectasia after excimer laser keratorefractive surgery: histopathology, ultra structure, and pathophysiology. Ophthalmology. 2008;115:2181-91.e1
17. Feder RS, Rapuano. The lasik handbook: a case-based approach. Lippincott Williams & Wilkins; 2007.
18. Geggel HS, Talley AR. Delayed onset keratoectasia following in situ keratomileusis. J Cataract Refract Surg. 1999;25:582-6.
19. Jain V, Mhatre K, Shome D. Flap buttonhole in thin-flap laser in situ keratomileusis: case series and review. Cornea. 2010;29(6):655-8.
20. Krueger RR, Applegate RA, MacRae SM. Wavefront customized visual correction. Slack Inc; 2004.
21. Kymiosis GD, Bouzoukis D Diakonis V, et al. Long-term results of thin corneas after refractive laser surgery. Am J Ophthalmol. 2007;144(2):181-5.
22. Kremer I, Bahar I, Hirsh A, et al. Clinical outcome of wavefront-guided laser in situ keratomileusis in eyes with moderate to high myopia with thin corneas. J Cataract Refract Surg. 2005;31(7):1366-71.
23. Lifshitz T, Levy J, Klemperer I, et al. Late bilateral keratoectasia after LASIK in a low myopic patient. J Refract Surg. 2005;2:494-6.
24. Majmudar PA. LASIK complications. Focal Points: American Academy of Ophthalmology. 2004;12(13):1-14.
25. Okamoto S, Kimura K, Funakura M, et al. Comparison of wavefront-guided aspheric laser in situ keratomileusis for myopia: Coaxially sighted corneal-light-reflex versus line-of-sight centration. J Cataract Refract Surg. 2011;37(11):1951-60.
26. Pallikaris IG, Kymionis GD, Astyrakakis NI. Corneal ectasia induced by laser in situ keratomileusis. J Cataract Refract Surg. 2001;27(11):1796-802.
27. Rad AS, Jabbarvand M, Saifi N. Progressive keratoectasia after laser in situ keratomileusis. J Refract Surg. 2004;20(5 Suppl):S718-22.
28. Randleman JB. Post-laser in-situ keratomileusis ectasia: current understanding and future directions. Current opinion in ophthalmology. 2006;17(4):406-12.
29. Randleman JB. Evaluating risk factors for ectasia: what is the goal of assessing risk? J Refract Surg. 2010;26(4):236-7.
30. Randleman JB, Banning CS, Stulting RD. Corneal ectasia after hyperopic LASIK. J Refract Surg. 2007;2:98-102.
31. Randleman JB, Russell B, Ward MA, et al. Risk factors and prognosis for corneal ectasia after LASIK. Ophthalmology. 2003;110:267-75.
32. Randleman JB, Trattler WB, Stulting RD. Validation of the Ectasia Risk Score System for preoperative laser in situ keratomileusis screening. Am J Ophthalmol. 2008;145:813-8.
33. Randleman JB, Woodward M, Lynn MJ, et al. Risk assessment for ectasia after corneal refractive surgery. Ophthalmology. 2008;115:37-50.
34. Rao SN, Epstein RJ. Early onset keratoectasia following laser in situ keratomileusis: case report and literature review. J Refract Surg. 2002;18:177-84.
35. Saad A, Gatinel D. Bilateral corneal ectasia after laser in situ keratomileusis in patient with isolated difference in central corneal thickness between eyes. J Cataract Refract Surg. 2010;36:1033-5.
36. Seiler T, Quurke AW. Iatrogenic keratoectasia after LASIK in a case of forme fruste keratoconus. J Cataract Refract Surg. 1998;24:1007-9.
37. Sinjab MM. Step by Step Reading Pentacam Topography (Basics and Case Study Series). Jaypee - Highlights Medical Publishers, New Delhi; 2010.
38. Sinjab MM. A guide to interpreting corneal tomography. J Cataract Refract Surg Today 20-24; 2012.
39. Sinjab MM. A Quick Guide to the Management of Keratoconus: A Systematic Step-by-Step Approach. Springer, Heidelberg; 2012.
40. Sinjab MM. Corneal Topography in Clinical Practice (Pentacam System): Basics and Clinical Interpretation. Jaypee-Highlights Medical Publishers, Inc; 2012.

41. Solomon R, Eric D. Donnenfeld ED. Innovations in Advanced Surface Laser Refractive Surgery. Focal Points: American Academy of Ophthalmology. 2010;28(2):1-14.
42. Tabbara KF, Kotb AA. Risk factors for corneal ectasia after LASIK. Ophthalmology. 2006;113(9):1618-22.
43. Khachikian SS, Belin MW and Ciolino JB. Intrasubject corneal thickness asymmetry. J Refract Surg. 2008;24(6):606-9.
44. Tobias Koller T, Iseli HP, Hafezi F, et al. Q-factor customized ablation profile for the correction of myopic astigmatism. J Cataract Refract Surg. 2006;32:584-9.
45. Winkler von Mohrenfels C, Salgado JP, et al. [Keratoectasia after refractive surgery]. Klinische Monatsblatter fur Augenheilkunde. 2011;228(8):704-11.

Step Four

Start Off

CHAPTER 7

Clinical Approach

CORE MESSAGE

- Candidate for refractive surgery should be evaluated psychologically and medically
- Patient history taking should include social history, ocular history, general history and family history
- Ocular history should include refractive history, use of CLs, tear film disturbance including dry eye syndrome (DES) and tearing, chronic allergy and infections, ocular trauma, previous surgeries, KC and ectatic corneal disorders, glaucoma and previous glaucoma surgery and other pathologies
- General history should include diabetes, hypertension, allergy and atopic disease, collagen vascular diseases and inflammatory disorders, keloid formation diseases, pregnancy and nursing, immunodeficiency, medications, and other conditions
- Examination of the candidate should include visual acuity, clinical refraction, pupillometry, tear film tests, IOP measurements, determination of the non-dominant eye, ocular motility, orbital and eye anatomy, external examination and slitlamp biomicroscopy and fundoscopy

A thorough preoperative evaluation of the refractive surgery candidate is critically important for successful refractive outcomes. Clinical evaluation should include psychosocial and medical evaluation. The latter consists of ocular, general and family history taking in addition to clinical examination.

PSYCHOSOCIAL APPROACH

Two of the most important criteria in determining candidates for refractive surgery are the patients' personalities and expectations for the procedure. Patients need to have reasonable expectations and understand that there is no guarantee that vision correction surgery will improve vision. There is no guarantee that patients will not need eyeglasses or CLs after surgery to perform daily activities. Even when an excellent outcome is achieved, eyeglasses for night driving and reading may be needed. In addition, eyes may change over time whether patients have vision correction surgery or not and if patients have surgery, they may require additional surgery to continue to have their best vision, just as they might need to change their eyeglasses or CL prescription over time. Patients who are difficult or demanding in scheduling their appointment, stopping their CL wear, or discussing finances may be demonstrating warning signs that they are not ideal candidates for an elective procedure like refractive surgery. In addition, very exacting, "type-A," compulsive personalities may also be less than ideal candidates because of their unrealistic expectations and potential problems dealing with the surgeon and the surgeon's staff, especially if the results are less than perfect, or the patients are slow in healing. Patient's psychosocial candidacy should also be assessed during history taking as well as during examination.

A good candidate for refractive surgery should:
1. Be capable of understanding the risks of the procedure and that risk-free surgery does not exist.
2. Be able to follow instructions before, during and after surgery.
3. Be able to be available for postoperative follow-up.
4. Have personal characteristics of the best PRT patients including an easygoing nature, a positive outlook, a well-adjusted personality, currently using less than a full refractive error correction and a willingness to wear glasses for reading or night driving.

A good surgeon should:
1. Avoid making grandiose statements regarding the surgical outcome or even promises about the quality of vision that will be achieved after surgery.
2. Tell the patient what level of visual acuity is reasonable to expect after surgery, with a subsequent enhancement procedure if needed.
3. Mention the surgeon's rate of enhancement for patients with similar refractive error.
4. Not confuse visual acuity with visual function. A patient with 1.0 (Snellen) may be unhappy due to loss of near vision, ghosting, decreased contrast sensitivity, glare, or other problems that affect the quality of vision.
5. Know that refractive surgeries are elective and a patient properly advised against surgery can be a potential referral source, while a patient made unhappy with refractive surgery will usually speak negatively about the surgeon and the office.

TAKE-HOME MESSAGE

- Patients with unreasonable high expectations and those with very exacting, type-A, compulsive personalities are not good candidates for refractive surgery
- A good candidate is that who understands that the refractive surgery is not risk-free, follows instructions, is willing to wear glasses after the surgery
- A good surgeon is that who does not give unreal promises, tells that patient the reasonable expected visual acuity and visual function and discusses the issue of enhancement

MEDICAL APPROACH

In general, the most reproducible results are obtained when refractive surgery is performed on a healthy patient with healthy eyes.

Patient History

Social History

Visual requirements of the patient's profession should be determined since certain jobs require that best vision be at a specific distance. For example, a highly myopic jeweller, who is used to examining objects without glasses a few inches from the eyes, may not be happy with postoperative emmetropia, while soldiers, fire fighters, or police may have restrictions on the type of refractive surgery they can have. On the other hand, the type of sports and recreational activities a patient prefers may help select the best refractive procedure or determine whether that patient is even a good candidate for refractive surgery. For example, a SA may be preferable to a LA for a patient who wrestles, boxes, or rides horses and is at high risk of ocular trauma.

Ocular History

A patient's ocular history helps to identify any potential postoperative problems that may arise and allows for adjustment, postponement, or cancellation of the procedure in question if necessary.

The ocular history should include refractive history, dry eye, tearing, chronic infections, chronic allergies, use of CLs, ocular trauma, previous surgeries, ectatic corneal disorders and other pathologies.

1. **Refractive History:**
   a. *Onset of refractive error:*
      1. If started around puberty, think of KC.
      2. If started after 30, think of PMD.

   b. *Stability of refractive error:* While PRT is approved for patients at least 18 to 21 years of age, many patients will not have attained refractive stability by this age. The refractive history should contain questions about refractive stability. Ideally, the refraction should be stable for at least one year before refractive surgery is considered. If glasses or CLs change by more than 0.50 D within one year, the patient should be re-evaluated at 6-month intervals until the measurement is stable. More rapid changes should be questioned.

   c. *Anisometropia:* An anisometropia of > 1 D is significant and ectatic corneal diseases should be excluded. On the other hand, if a large degree of anisometropia is fully corrected, diplopia is a risk. Motility function should be evaluated with full CL correction to be sure the patient is asymptomatic.

   d. *Age and Presbyopia:*
      1. Age of the candidate is important for predicting postoperative satisfaction. Loss of near vision with aging should be discussed with the candidate. Generally, patients younger than 40 years do not need reading adds for near targets. Patients older than 40 years should understand that if they are made emmetropic with refractive surgery, they will require reading glasses. On the other hand, myopic patients approaching age 40 may require reading glasses postoperatively even that they were able to see near targets with their myopic glasses or CLs, preoperatively. Such patients should understand this phenomenon and be willing to use reading glasses after surgery. A trial with CLs will approximate the patient's reading ability after surgery.
      2. Monovision should be discussed with patients who are presbyopic or in the presbyopic age group (including myopic patients approaching the age of 40). Monovision is achieved by targeting the non-dominant eye for near and the dominant eye for distance. The non-dominant eye can be targeted to be –0.75 D (mini monovision), –1.5 D (monovision), or –2.5 D (high monovision); this depends on surgeon's preferences and patient's demands. While improving the near vision, loss of perception and anisometropia may be unwanted side effects from the high monovision in some patients. However, simulating post operative monovision should be done with CLs for a period of time at home, at work and during leisure activities. This will be also helpful for determining the preferred eye for near, which may rarely be the dominant eye rather than the non-dominant eye.

         In the last few years, models of monovision were developed such as adjusting Q value, multifocal cornea and small aperture inlays. All these options should be discussed with the patient.
      3. Determination of the non-dominant eye will be discussed later in clinical examination.

2. **Use of Contact Lens:** Contact lens history should be obtained. Important information includes the type of lens (e.g., PMMA, rigid gas permeable or soft); the wearing schedule (e.g., daily wear disposable, daily wear frequent replacement, overnight wear indicating number of nights worn); the type of cleaning, disinfection and enzyming; and how old the lenses are. Occasionally, a patient may have been happy with CL wear and only needs a change in lens material or wearing schedule to eliminate the recent onset of discomfort symptoms.
   Using CLs should be stopped 2–4 weeks prior to examination since it:
   - alters the topographic features of corneal surface (corneal warpage) and may be the cause of apparent irregular astigmatism
   - changes the amount, type and axis of astigmatism
   - is one of the causes of the hot spot formation on the anterior surface of the cornea
   - can alter corneal thickness; it is more accurate to measure corneal thickness after the patient has stopped using CLs for at least 1–2 weeks
3. **Dry Eye Syndrome (DES):**
   a. *Definition:* Dry eye syndrome (DES) is defined as a multifactorial disease of tears and ocular surface that results in symptoms of discomfort, visual disturbance and tear film instability, with potential damage to ocular surface. It is accompanied by increased osmolarity of the tear film and inflammation of the ocular surface.
   Due to the very important impact of DES on refractive surgery results, it will be discussed in details.
   b. *Pathophysiology:* In DES, tear water evaporation and tear osmolarity increase. Tear water evaporation composes 33% of the total tear flow in normal eyes; whereas, it composes 75% in DES. Tear film osmolarity is an expression of the balance between normal tear production and normal tear evaporation. In case of normal tear production and normal tear evaporation, osmolarity is 296–308 mOsm/L. In case of normal tear production and increased evaporation, osmolarity increases to cause hyperosmolarity; but the most increase is in case of reduced tear production and increased evaporation. Hyperosmolarity is able to produce an inflammatory response in ocular surface evidenced by inflammatory cell infiltrate and CD54 expression on conjunctival epithelium. Epithelium is thereafter damaged by apoptosis which also involves loss of goblet cells leading to disturbance of mucin expression leading to tear film instability. This instability exacerbates ocular surface hyperosmolarity and completes a vicious cycle. Tear film instability can also be initiated by several etiologies, including xerosing medication, xerophthalmia, ocular allergy, topical preservative use and CL wear. The major causes of tear hyperosmolarity are reduced aqueous tear flow, resulting from lacrimal failure and/or increased evaporation from tear film.
   c. *Classification:* DES may result from one or more factors.
   Figure 7.1 is a flow chart representing the etiologic classification of DES.
   d. *Investigations:* The aim of investigation is to confirm and quantify the diagnosis of dry eye. Unfortunately, although the repeatability of symptoms is good, that of clinical tests is poor, as is the correlation between symptoms and tests. The reliability of tests improves as the severity of dry eye increases. The tests measure the following parameters:
      - Stability of the tear film. Tear film break-up time (BUT).
      - Tear production. Schirmer, flourescein clearance and tear osmolarity.
      - Ocular surface disease. Corneal stains and impression cytology.

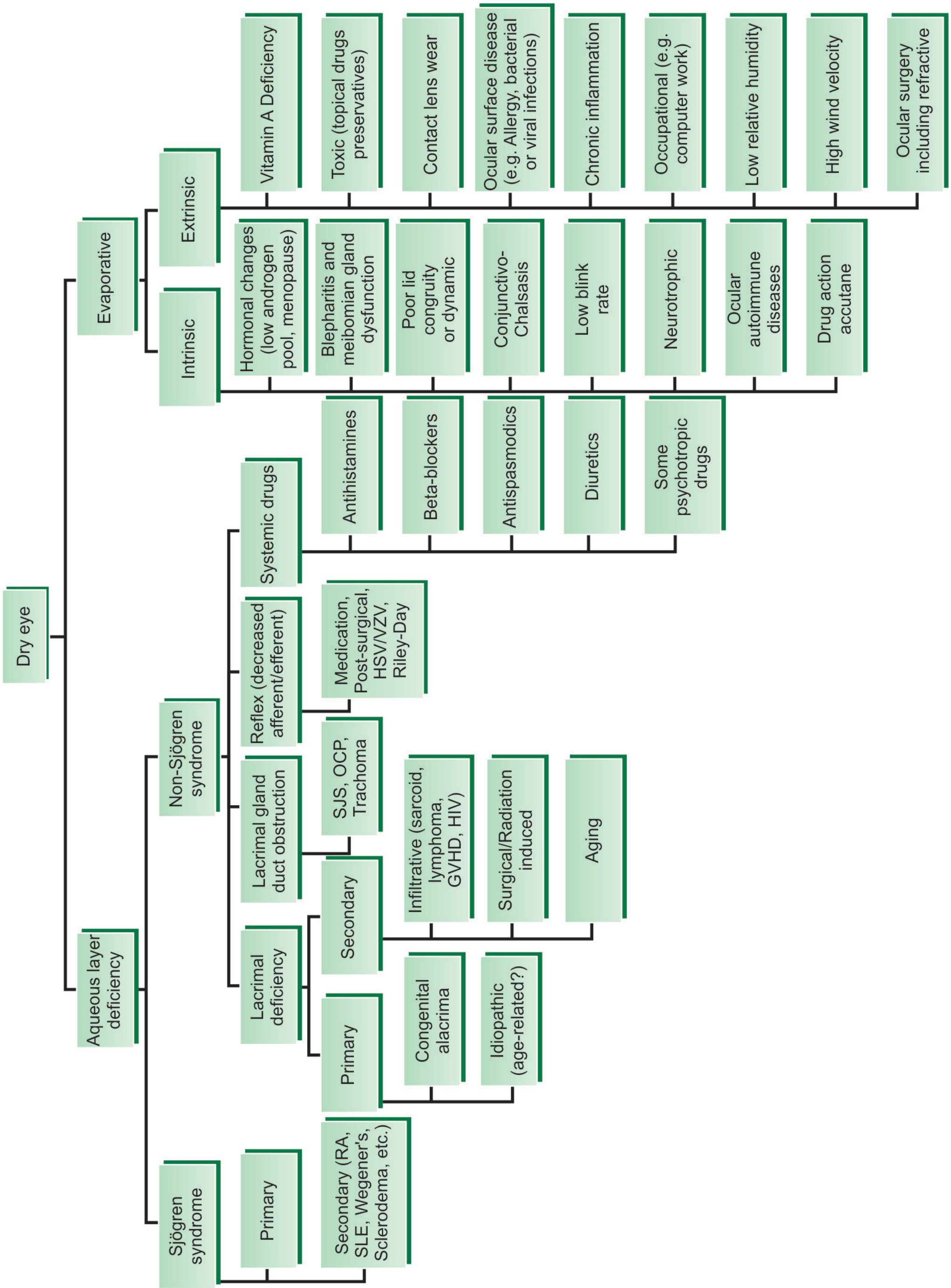

Fig. 7.1 Diagnostic classification scheme for DES.

There is no clinical test to confirm the diagnosis of evaporative dry eye. It is therefore a presumptive diagnosis based on the presence of meibomian gland disease. Tarsal transillumination to visualize the meibomian glands, can give an indication of gland drop-out. It is suggested that BUT should be performed first, Schirmer second and staining third, because the Schirmer strip paper can damage ocular surface and cause staining.

e. *DES and PRT:* DES is one of the major challenges in refractive surgery since several factors contribute in DES and in many cases treatment is not straight forward. In addition, it:
   - affects refractive error determination
   - affects visual outcome
   - may be the cause of intra- or postoperative complications especially with LA
   - exaggerates the normal transient dryness that happens after keratorefractive surgery
   - may be severe enough to make keratorefractive surgery contraindicated and to go for alternatives such as PIOLs.

   On the other hand, it is important to differentiate between DES and dry eye symptoms. The latter is just mild symptoms without significant signs and does not interfere with PRT decision. However, dry eye symptoms after LA are common, generally respond to treatment, and usually return to the preoperative state after three to six months postoperatively.

f. *Predisposing factors for DES after PRT:*
   1. High refractive error correction.
   2. High ablation depth.
   3. Low preoperative Schirmer's test.
   4. Pre-op DES.
   5. Sex. Females are more prone than males. The incidence of DES in females and males > 55 y/o is 5.7–9.8% and 3.5%, respectively.
   6. Hypermetropia treatment.
   7. Wearing CLs for many hours a day.

g. *Prevention and Treatment:*
   1. *Preoperative evaluation:*
      i. Ask about dry eye symptoms (e.g. CL intolerance).
      ii. Investigate.
   2. *Preoperative treatment:* In case of DES, it is recommended to avoid PRT. However, in mild cases, get the best ocular surface as long as possible before surgery by:
      i. Avoiding CL.
      ii. Using one or more of the following measures: artificial tears, steroids, lid hygiene, punctual plugs, oral tetracyclines, 0.05% cyclosporine, omega 3 and autologous serum (see below).
      iii. Treatment of blepharitis or meibomian gland dysfunction. Blepharitis should be diagnosed and treated aggressively because the adnexa, especially the lids are nearly always the source of the offending organisms in endophthalmitis and post-LASIK infections. In case of recalcitrant DES and/or blepharitis, look for Demodex Mites.
      iv. Encouraging good oral hydration. This is important in patients who exercise heavily. Low ambient humidity in the patient's work or home environment will be unfavorable for the borderline dry eye patient.
      v. Waiting six months before excluding patients as LA candidates.

vi. Thereafter, if there are no symptoms and examination is normal, offer surgery and continue treatment for at least six months after the surgery.
vii. If significant tear deficiency remains despite these measures, LA should be avoided. However, in severe cases, even SA may be contraindicated. PIOL implantation is a good alternative.

3. *Intraoperative preventive measures:*
   There are three recommendations to reduce DES following LA:
   i. Perform small flaps with large hinges to save as much of the entering nerves as possible.
   ii. Perform thin planner flaps since deep cuts cause transection of deeper corneal nerves during flap creation.
   iii. Perform bevelled-in side cut to improve corneal nerve apposition.
4. *Postoperative treatment:*
   i. Keep the eyes closed as long as possible during the early hours.
   ii. Continue preoperative medication for at least six months after the surgery.

h. *General Treatment of DES:*
   1. *Tear Substitutes:*
      i. Drops and Gels:
         – Cellulose derivatives are appropriate for mild cases.
         – Carbomers adhere to the ocular surface and so are longer lasting.
         – Polyvinyl alcohol increases the persistence of the tear film and is useful in mucin deficiency.
         – Sodium hyaluronate may be useful in promoting conjunctival and corneal epithelial healing.
         – Autologous serum may be used in very severe cases.
         – Povidone and sodium chloride.
      ii. *Ointments* containing petrolatum mineral oil can be used at bedtime, as daytime use is precluded by marked blurring.
      iii. *Minims* are preservative free. Preservatives are a potential source of toxicity, especially after punctal occlusion. Non-preserved drops should therefore be used whenever possible.
   2. *Mucolytic Agents:* Acetylcysteine 5% drops q.i.d. may be useful in patients with corneal filaments and mucous plaques. It may cause irritation following instillation. Debridement of filaments may also be useful.
   3. *Punctal Occlusion:* Punctal occlusion reduces drainage and thereby preserves natural tears and prolongs the effect of artificial tears. It is of greatest value in patients with moderate to severe DES who have not responded to frequent use of topical treatment. On the other hand, punctal occlusion may provoke bacterial conjunctivitis especially with lack of immune natural tear film and accumulation of fluids rich in debris.
      i. *Temporary* occlusion can be achieved by inserting collagen plugs into the canaliculi; these dissolve in 1–2 weeks. The main aim is to ensure that epiphora does not occur following permanent occlusion.
         – Initially, the inferior puncta are occluded and the patient is reviewed after 1 or 2 weeks.
         – If the patient is now asymptomatic and without epiphora, the plugs can be removed or kept until resolved and the inferior canaliculi permanently occluded.
         – In severe DES, both the inferior and superior canaliculi can be plugged.

ii. *Reversible* prolonged occlusion can be achieved with silicone or long-acting (2–6 months) collagen plugs.
- Problems include extrusion, granuloma formation and distal migration.
- Plugs that pass into the horizontal portion of the canaliculus cannot be visualized, but when it causes epiphora, it might not be possible to flush it out with saline.

iii. *Permanent* occlusion should be undertaken only in patients with severe DES with repeated Schirmer test values of 5 mm or less and who have had a positive response to temporary plugs without epiphora. It should not be performed if possible in young patients who may have reversible pathology. All four puncta should not be occluded at the same time.
- Permanent occlusion is performed following punctal dilatation by coagulating the proximal canaliculus with cautery; following successful occlusion, it is important to watch for signs of recanalization.
- Diode laser cautery is less effective than thermal coagulation, with higher rates of recanalization.

4. *Anti-inflammatory Agents:*
   i. *Low dose topical steroids* are effective supplementary treatment for acute exacerbations. The risks of long-term treatment must be balanced against the potential benefits of increased comfort.
   ii. *Topical ciclosporin* (0.05%, 0.1%) reduces T-cell mediated inflammation of lacrimal tissue, resulting in an increase in the number of goblet cells and reversal of squamous metaplasia of the conjunctiva.
   iii. *Systemic tetracyclines* may control associated blepharitis and reduce inflammatory mediators in the tears.
5. *Contact Lenses:* Special designs of CLs may play a role in treatment by the reservoir effect of fluid trapped behind the lens.
   i. *Low water* content HEMA lenses may be successfully fitted to moderately dry eyes.
   ii. *Occlusive* gas permeable scleral CLs provide a reservoir of saline over the cornea. They can be worn on an extremely dry eye with exposure.
6. Conservation of Existing Tears:
   i. *Reduction of room temperature* to minimize evaporation of tears.
   ii. *Room humidifiers, moist chamber goggles and side shields to glasses*.

4. **Tearing:** Tearing can be a result of hyperlacrimation or hypersecretion. It is important since:
   a. It affects visual outcome and may cause complications.
   b. Tear pooling during the operation is a cause of infection and DLK.
5. **Chronic Allergy and Infection:** There are three things related to other three things in this regard:
   a. Constant rubbing and development of keratoconus.
   b. Constant rubbing and post LASIK complications such as flap dislocation, macrostriae and microstriae.
   c. Chronic infections and post surgery complications.
6. **Ocular Trauma:** Asking the patient about previous ocular trauma (even minor) is necessary because it may explain:
   a. Pathological findings such as retinal tears or atrophy, or optic nerve head atrophy.
   b. Corneal opacities and scars.

c. Iridodenesis.
d. Lens subluxation.

7. **Previous Surgeries:** Identification and evaluation of a patient's previous ocular surgery status are critical to the success of subsequent refractive surgery.
   The patient may forget to mention previous ocular surgeries such as squint surgery especially if this surgery was performed in early childhood. On the other hand, some patients may think that what they underwent (such as phacoemulsification) was not a surgery and therefore do not mention that to the doctor!
   It is necessary to ask about previous ocular surgeries for the following reasons:
   a. A previous PRT will change the decision and the plan of treatment and may explain the complaints; e.g. post operative aberrations (not the residual refractive error) may be the cause behind reduced visual acuity.
   b. In case of a previous cataract surgery:
      i. The type of incision should be noted since it affects corneal tomography.
      ii. The approximate date of the surgery should be known, since at least six months post phacoemulsification and twelve months post extra capsule cataract extraction should pass until the refractive status of the eye (in general) and the cornea (in particular) stabilizes.
      iii. The type of the implanted IOL should be known if possible; e.g. spheric, aspheric, toric, etc., since it guides us to the proper next intervention and to the type of the additive IOL, if this is the decision.
   c. Previous retinal surgery: The refractive status of the eye differs according to the type of surgery; e.g. buckle, vitrectomy. etc. The refractive index is altered by the silicone oil, if it is inside. The kind of the silicon oil should be known and whether there is a future plan to extract it. On the other hand, the buckle may interfere with suction ring application.
   d. Previous squint surgery: A history of a previous squint surgery indicates a presence of muscular imbalance and carries the risk for phoria to become tropia, hence the need for a squint consultation. On the other hand, limbal conjunctival scars may be the cause of irregular corneal astigmatism and may interfere with suction ring application.
   e. Previous pterygium surgery: The patient who underwent a pterygium surgery should be informed that the pterygium may recur, which will affect the refractive surgery results. On the other hand, the scar left after pterygium removal may be the cause of irregular astigmatism and may interfere with suction ring application.
8. **KC and Ectatic Corneal Disorders:** It is logic to ask the patient: do you have keratoconus? The patient may know that he has KC and may think that LASIK is helpful! On the other hand, some of the modern modalities of KC management are refractive such as wavefront-guided PRT.
   The patient should also be asked about a family history of ectatic corneal disorders.
9. **Glaucoma and Previous Glaucoma Surgery:** Glaucoma patients or those with a pre-existing optic neurotrophy might be better served with SA.
   Using steroids after refractive surgery may impact the IOP, especially when used for a long period (after PRK for example).
   The bleb may be the cause of irregular astigmatism and may interfere with suction ring application.

During application of the suction ring, IOP is raised to unfavourable levels for relatively significant period of time; this has an impact on optic nerve fibres and causes additional damage in case of glaucoma.

10. **Other Pathologies:** A history of recurrent corneal erosion, corneal ulceration or ocular infections may have an impact on patient's candidacy for PRT and put other options of refractive surgeries on the horizon.
    Patients who have neurotrophic corneas are not candidates for PRT because of problems with healing.
    Patients with a history of herpes simplex or herpes zoster keratitis are not good candidates for SA because of a significant risk of recurrence of keratouveitis and they also often have underlying neurotrophic corneas.

TAKE-HOME MESSAGE

- Visual requirements determine the amount and type of refractive correction
- New onset of refractive error around puberty alerts for KC
- New onset of refractive error after thirty alerts for PMD
- An anisometropia should alert for ectatic corneal disorders
- Refraction should be stable at least 1 year before refractive surgery is considered
- Presbyopia is a major concern in refractive surgery
- CLs should be stopped 2–4 weeks before evaluation and investigation
- Dry eye syndrome (DES) is a major concern in refractive surgery and should b diagnosed, classified and treated for at least six months before considering PRT
- Look and ask for previous surgeries including refractive surgeries
- KC and ectatic corneal disorders should be diagnosed and classified since they have their own managements
- Glaucoma may contraindicate refractive surgery

General History

Any underlying systemic disease associated with corneal healing abnormalities should be considered. In addition, some systemic diseases have an impact on refractive surgery. They include diabetes, hypertension, medications, allergy and atopic diseases, keloid formation diseases, collagen vascular diseases and rheumatologic diseases, pregnancy and nursing, and immunodeficiency.

1. **Diabetes:** Regardless of its type, uncontrolled diabetes is a contraindication to refractive surgery. Diabetics, in addition to retinal ischemia and edema, may have poor healing process, poor epithelial adhesion, increasing the risk of erosion. They may also be more likely to have cataract and infections. Diabetes has also an impact on the stability of refractive error and the refractive status after surgery. In general, the percentage of post refractive surgery complications increases from 7% in non diabetics to 47% in diabetics.
2. **Hypertension:** Refractive surgery is contraindicated when hypertension is uncontrolled or malignant.
3. **Allergy and Atopic Disease:** Systemic atopy is a relative contraindication to PRT in general and to refractive management of KC (intracorneal ring segments [ICRs] implantation, CXL, topography-guided PRK, etc.). This is because it may increase the risk of corneal haze following SA and it is usually accompanied with constant eye rubbing, which is one of the main causes for:
    a. Postoperative flap complications
    b. Post surgical ectasia
    c. Complications of ICRs implantation
    d. CXL failure

4. **Collagen Vascular Diseases and Inflammatory Disorders:** A relative contraindication to SA is a history of autoimmune or connective tissue disease such as systemic lupus erythematosus, rheumatoid arthritis, multiple sclerosis, hyperthyroidism and Crohn's disease. Most patients with collagen vascular diseases have very mild symptoms and use very little medication. Such diseases are associated with less predictable wound healing and greater potential for corneal melting. In case of positive rheumatoid factor and the patient has uncontrolled collagen vascular disease, refractive surgeries are contraindicated. However, patients with well-controlled autoimmune diseases have been reported to achieve excellent outcomes without complications after refractive surgery, especially LASIK.
5. **Keloid Formation Diseases:** Keloid formation diseases such as sclerosis, Marfan syndrome, dysosteosis and Ehler-Danlos were initially considered a contraindication to ICR implantation and to PRT (particularly PRK); however, recent investigations have determined that this is no longer the case.
6. **Pregnancy and Nursing:** Pregnant or nursing candidates may have unstable refractions and transitory topographical variations. It is best to delay surgery until six to twelve weeks after nursing has ended. Females who become pregnant after PRT should understand that a refractive error change may result from the pregnancy and may not be a postoperative regression. This should be discussed preoperatively. The change may resolve after delivery without retreatment.

   On the other hand, it is recommended that a plan of pregnancy should be delayed for six to twelve months, post PRT.
7. **Immunodeficiency:** Patients who are immunecompromised may be at greater risk of infection.
8. **Medications:**
   a. Anticoagulants: They predispose to conjunctival hemorrhage or expulsive choroidal hemorrhage during intraocular refractive surgery.
   b. Isotrentoin (Roccutaine), Amiodaron (Cordarone), hormone replacement therapy and antihistamines. These medications have an impact on corneal epithelial healing and may cause poor results with PRT. In addition, isotrentoin causes a significantly decreased tear production. This drug should be stopped for at least six months before surgery.
   c. Immunosuppressants and high dose systemic steroids. They predispose to infections.
   d. 5-Hydroxy-tryptamine (Sumatriptin). There is an increased risk of vascular occlusion when IOP is raised during application of suction ring. This drug should be stopped for at least one month before treatment.
9. **Other Conditions:**
   a. Caution should be taken in performing any excimer laser surgery in patients with cardiac pacemakers and implanted defibrillators, due to the unknown effects of the laser's electromagnetic emissions.
   b. Epilepsy: The patient must be able to remain relatively still during the PRT procedure. Therefore, only patients that have not had an epileptic episode for twelve months or more may be considered for treatment.
   c. History of frequent fainting: These patients may have a low threshold for vasovagal attack. Patients that have a low oculocardiac reflex would also be unsuitable.
   d. Hepatitis B and C: Patients with these conditions will not be considered for surgery in many clinics due to the potential risk to surgical staff.

Family History

A thorough family history may elucidate potential contraindications or concerns with refractive surgery and long-term visual prognosis. A positive history of any of the followings warrants further careful ocular evaluation prior to surgical intervention:

a. KC and ectatic corneal disorders.
b. Glaucoma.
c. Past history of high intraocular pressure after topical steroid application.
d. Corneal dystrophy or degeneration.
e. Retinal pathology (e.g. retinal holes, tears, or detachment).

TAKE-HOME MESSAGE

- Uncontrolled diabetes contraindicates refractive surgery
- Complications of refractive surgery have higher incidence with uncontrolled diabetes
- Allergy and atopic diseases should be controlled before PRT
- Uncontrolled collagen vascular diseases contraindicate refractive surgeries
- Keloid formation diseases are not contraindications for refractive surgeries
- Refractive surgeries are contraindicated during pregnancy until 2 to 12 weeks after end of nursing
- Immunodeficient people are at great risk of post surgical infections
- Medications of concern are anti coagulants, Isotrentoin, Amiodaron, hormone replacements, antihistamines, immunosuppressants and 5-hydroxy-tryptamine
- Great caution should be taken with candidates using pacemakers and implanted defibrillators and those with epilepsy, a history of frequent fainting and hepatitis B and C
- Family history is important

EXAMINATION

A thorough ocular evaluation should be performed for both eyes. This includes uncorrected and best corrected visual acuity for distance, intermediate and near, refraction, pupillometry, tear film tests, IOP measurement, determination of dominant and non-dominant eyes, studying ocular motility, orbital anatomy, slitlamp biomicroscopy and fundoscopy.

A standardized refractive surgery form, designed for recording the history and examination, can assist the surgeon in documenting pertinent information in an orderly manner. The chance of inadvertent oversight in the evaluation can be reduced by using such a form. There is an advantage to using a form in which the results of multiple postoperative visits can be recorded on a single page. This format facilitates the ability to track postoperative findings.

Visual Acuity

Visual acuity at distance, intermediate (75cm) and near should be measured with and without correction. The preoperative CDVA should be at least 1.0 (Snellen). If it is less than 1.0 (Snellen), the surgeon must seek an explanation. If the acuity is reduced because of refractive amblyopia the patient may still be a candidate for surgery, provided the patient has realistic expectations for postoperative vision (see chapter 6 for amblyopia). Reduced preoperative visual acuity related to irregular corneal astigmatism is a contraindication for conventional refractive surgeries and an indication for WFGT.

Potential visual acuity should be measured with CLs in case of high refractive errors to avoid the effect of magnification of glasses on visual acuity. On the other hand, measuring potential visual acuity in patients with irregular corneas using hard CLs is necessary to estimate visual function and put a good plan and prognosis for any treatment.

Clinical Refraction

At the beginning, if the patient uses CLs, lens wear needs to be discontinued. The surgery cannot safely be done until the refraction becomes stable. In general, refractive stability for hard CL (HCL) users takes a longer period than that for soft CL (SCL) users. The duration of lens wear and the intensity of lens wear are also important factors affecting the time to achieve refractive stability after lens removal. A rule of thumb for patients wearing SCL or HCL for ten years would be to discontinue lens wear for two or four weeks, respectively. Longer duration of lens wear will likely require longer periods of abstinence.

Clinical refraction includes two types: the manifest refraction (MR) and the cycloplegic refraction (CR).

1. MR: it is also known as dry refraction or subjective refraction. In determination of MR, the following rules are to be followed:
   a. Determine the least myopic correction that gives the best corrected visual acuity, but do not over minus.
   b. Do not use the Duochrome test since it usually leads to over minus the examined eye.
   c. Determine the most hyperopic correction that gives the best corrected visual acuity.
2. Cycloplegic refraction (CR): it is also known as objective refraction.

In myopia, the MR should not differ from the CR by more than 0.50 D, and the axis of cylinder should not differ by more than 15 degrees.

In hyperopia, the difference should not be more than 0.75 D, otherwise the MR should be repeated after the cycloplegia has resolved and this is known as post medriatic test (PMT). Hyperopic patients need to be educated about the possible need for distance glasses after surgery and that it may take up to six months for the refraction to stabilize.

Anisometropia is one of the preoperative risk factors for ectasia, especially, if it is on the account of astigmatism.

Pupillometry

Accurate pupil measurement is an absolute necessity prior to corneal laser surgery as 1 mm can make a huge difference to the amount of tissue that needs to be ablated. For example, using the Munnerlyn formula, a – 5.00 D error requires a 60 μm AD for 6 mm OZ, whereas a 7 mm zone requires an AD of 81.7 μm. The evaluation of pupil size should be carried out under mesopic and scotopic light conditions. The size of the treatment zone is usually set so that the *efficient* OZ diameter is 0.5 mm greater than the scotopic pupil diameter. This is necessary to minimise the risk of glare, ghost images and halos after treatment. The bigger the pupil size, the larger the OZ and the larger the amount of corneal tissue removed. This may render some eyes unsuitable for treatment as a stromal bed thickness of at least 270 μm must remain after treatment to minimise the risk of ectasia.

Candidate should also be examined for a relative afferent pupillary defect.

Pupil measurement can be done either by topography, direct comparison (Morton's pupillometer), projected method (Magnani's pupillometer), light amplification pupillometry (Clovard pupillometer) or infrared dynamic pupillometer (Procyon dynamic pupillometer).

Tear Film Tests

Have been described in DES.

IOP Measurements

PRT thins the cornea and typically causes a falsely low measurement of IOP postoperatively. The most accurate method to measure the IOP pre- and postoperatively is Pascal since it is not affected by the change in central corneal thickness (CCT). On the other hand, if Pascal is not available, Goldman readings should be modified according to CCT as given by the Pentacam. The Tonopen is also useful should the measurement be taken at corneal mid periphery to avoid the central part of the cornea which has been altered by PRT.

Measuring the IOP before PRT is essential for the following reasons:

1. In case of glaucoma, doing LA is questioned since suction ring application raises IOP to unfavorable levels leading to more injury to optic nerve fibres.
2. The use of steroids postoperatively most often has an impact on IOP, especially when used for a long period of time to avoid haze after SA, hence the need for a regular monitoring of IOP.
3. When there is a myopic shift, some surgeons may prefer to extend the use of topical steroids, which may have an impact on IOP.

The Non-dominant Eye

Ocular dominance can be determined by asking the patient to wink. Generally, patients have difficulty winking the dominant eye. Hand the patient a disposable camera and ask the patient to pretend to take a picture. The camera will be held in front of the dominant eye. Finally, the patient can be asked to make the okay sign with the fingers of either hand. He or she is then asked to sight on a distant object through the circle formed with the thumb and forefinger. The hand is then brought toward the eyes and usually the hand will move toward the dominant eye.

Determination of the non-dominant eye is necessary in case of presbyopic treatment, such as monovision or corneal inlay techniques; in such cases the non-dominant eye is targeted for near vision. But it has to be noticed that true monovision may not be comfortable for some patients and a CL trial will help determine the eye and the appropriate lens power. Do not just assume that the non-dominant eye is the best eye for reading correction.

Ocular Motility

Patients with an asymptomatic tropia or phoria may develop symptoms after refractive surgery, if the change in refraction causes the motility status to break down. If a patient, for example, has myopia and esophoria, and he/she underwent PRT and he/she had been overcorrected, his/her accommodation will be triggered and he/she will have decompensation and may have intermittent esotropia. If there is a history of strabismus or there is a concern regarding ocular alignment postoperatively, a trial with CLs before surgery should be considered. An orthoptic evaluation can be obtained preoperatively, if strabismus is an issue. Confrontation test should be performed in all patients.

On the other hand, patients who have accommodative esotropia and are prepared to PRT should know that they may still have esotropia after the surgery. One of the methods to avoid such situation is to perform the correction based on CR since even one diopter of residual refractive error may trigger esotropia, but this option will induce myopia especially in young patients. At the same time, if correction is done based on MR in order to avoid overcorrection,

there will be a possibility of postoperative esotropia or even recurrence of esotropia after it has been surgically corrected.

Nevertheless, motility function should be assessed to rule out a latent condition that might become symptomatic in the event of significant postoperative anisometropia. This is especially true in the patient considering monovision treatment or a patient with a past history of strabismus surgery. A patient able to control a significant phoria may develop diplopia, if fusion has been disturbed. A patient with a moderate to large-angle alternating tropia may tolerate monovision, because this individual currently fails to use the eyes together and is capable of using either eye independently. Monovision may not be suitable for a patient with a constant tropia and a strong fixation preference for one eye. Monovision would force this patient to use the deviated, non-dominant eye for near vision, which might seem unnatural.

Orbital and Eye Anatomy

There is less risk when the orbital and lid anatomy allow adequate exposure for the MMK.
The surgeon should determine if the degree of lid laxity, orbital aperture, prominence of the brow, position of the globe and palpebral fissure height are adequate to accommodate the MMK.

Deep set eyes, narrow palpebral fissure or protruded superior orbital rim will interfere with the application of the suction ring; in such cases, SA (except Epi-LASIK) may be preferable.

External Examination and Slitlamp Biomicroscopy

A careful external examination is required to rule out external eye diseases such as acne rosacea, which can be associated with inflammatory eye disease and may require treatment before surgery.

Slitlamp examination should begin with an assessment of the lids and lashes. Inflammation in this area such as blepharitis and meibomitis should be controlled prior to surgery. It is critically important to rule out the presence of corneal pathology. CL wearing patients may have peripheral corneal neovascularization, punctate keratopathy, sterile keratitis, or peripheral subepithelial fibrosis. Keratitis and punctate keratopathy may be reversible and clear after a period of time with no lens wear. Active keratitis is a contraindication to refractive surgery. If it does not clear spontaneously, a treatment regimen should be initiated and the patient re-evaluated. Subepithelial fibrosis and neovascularization are permanent changes that may impact the decision to do surgery or the planning related to proposed surgery.

1. **Lids:** Significant lagophthalmos and associated exposure may be problematic post LA given the temporary neurotrophic status of the flap. On the other hand, lid abnormalities such as ectropion, entropion, trichiasis, dystichiasis and ptosis impact refractive surgery in general and PRT in particular and should be evaluated and treated before any assessment.
   As mentioned before, blepharitis and meibomitis should be addressed prior to any refractive surgery, since they cause complications and impact visual outcomes, especially, when they are associated with DES.
2. **Cornea:**
   a. Superficial corneal blood vessels can bleed during surgery and interfere with the laser ablation. LA has the added risk of blood accumulating beneath the flap, causing DLK or affecting healing. Although deep corneal vessels are less likely to be transected or bleed

with SA, compared to LA, this finding should prompt the surgeon to investigate for any underlying cause of chronic inflammation that might preclude one's candidacy for any form of refractive surgery. When pannus or neovascularization is present, consider flap diameter and its implications since the risk of bleeding increases with small corneas and large flaps. Balance the need to protect the peripheral cornea with the need to accommodate a large treatment zone. Femtosecond, if available, can be helpful.

b. Corneal scarring within the treatment zone is a contraindication to refractive surgery unless it was superficial and can be treated by PTK. Scarring in the periphery with minimal thinning may be acceptable, provided the cause is not a prior herpes simplex keratitis. Herpes viral infections can be reactivated by the ultraviolet radiation of the excimer laser or even by the surgical trauma of any refractive surgery.
c. The presence of epithelial basement membrane dystrophy or recurrent corneal erosion syndrome may indicate a possible defect in epithelial adhesion. Such patients are more likely to experience epithelial sloughing due to MMK and possibly having DLK or epithelial ingrowth after lamellar ablation. These patients are better served with PRK, because the abnormal epithelium is removed as part of the procedure and the new epithelium has better adherence to the cornea.
d. Females older than 40 years are at increased risk of epithelial defects during creation of LASIK flap. Femtosecond is safer than MMK in this regard.
e. The endothelium should be examined carefully, looking for signs of Fuchs dystrophy, cornea guttata and other dystrophies. Patients with confluent guttata or Fuchs dystrophy may be at risk for poor flap adhesion postoperatively, if the endothelial pump functions poorly. An abnormally thick cornea, especially in the early morning, may be a sign of abnormal endothelial pump function. In general, confluent guttata and Fuchs dystrophy are contraindications to refractive surgery.

3. **Conjunctiva:** Conjunctival scars may indicate previous ocular surgeries that the patient may have not mentioned. On the other hand, such scars may interfere with the application of the suction ring and make SA a better choice. The same can be said for a pre-existing glaucoma filtering blebs or scleral buckles.
4. **Anterior Segment:** All abnormalities of the anterior segment should be noted.
   a. *The lens:* Careful undilated and dilated evaluation of the crystalline lens for clarity is essential especially in patients over age 50. The presence of a cataract is a contraindication to any refractive surgery except RLE. It is best to avoid PRT in patients with a visually significant or progressive cataract.

   Lens-induced myopia from a nuclear cataract can be misinterpreted as a regression. A patient could mistakenly believe that progressive vision loss or glare due to cataract is due to PRT failure.

   If a small peripheral cataract is found in the preoperative examination, it is wise to follow up the patient until it can be determined whether or not the cataract is progressive. The patient who decides to proceed with PRT should be informed that, although the cataract may appear to be stable and not visually significant, it could unexpectedly progress and undermine the photorefractive result.

   Postoperatively, if a cataract surgery is needed, determination of the IOL power will be more challenging than it otherwise would be. If standard keratometry is used in biometry for a cataract patient after PRT has been done, the selected lens implant may

be underpowered. Therefore, it is wise to provide the patient with his/her preoperative and intraoperative refractive and keratometric data to be used when cataract surgery is needed in the future.

b. *ACD:* It is necessary for PIOL implantation. However, the ACD cannot be determined by slitlamp; it should be measured accurately using several methods such as ultrasound, OCT, IOL Master or tomography.

Fundoscopy

The dilated fundus examination is an essential part of the preoperative evaluation. While it need not be done during an initial screening examination, it must be done prior to surgery. If significant abnormalities are found, the patient should be informed.

Fundus examination is particularly important for a myopic patient who is at greater risk for retinal detachment. In the presence of peripheral retinal pathology, a consultation from a retinal specialist is advisable. The result of this consultation should be included in the record. Preoperative prophylactic treatment can be delivered, if required. The retina surgeon should determine the timing of refractive surgery, following any treatment. If a retinal problem were to develop postoperatively, the patient will already have a relationship with a specialist.

Diabetic retinopathy if present may impact the decision to do refractive surgery. Patients with evidence of significant retinal ischemia may be at risk for an ischemic event related to extreme IOP elevation. Macular edema, epiretinal membranes and degenerative changes in the macula may limit the postsurgical visual outcome. These issues should be discussed with the patient. It is not uncommon for a previously undiagnosed retinal disease to be uncovered during the refractive evaluation.

If the optic disc does not appear normal, an evaluation of optic nerve function should be conducted. This evaluation will include measurement of central acuity, pupil reactivity, color vision, brightness comparison and visual field. Obviously, some of this evaluation may already have been done before fundus examination. Highly myopic patients often have tilted discs with peripapillary atrophy.

TAKE-HOME MESSAGE

- Potential visual acuity is as much important as visual acuity
- Determine manifest refraction (MR), cycloplegic refraction (CR) and post medriatic test (PMT)
- Anisometropia is one of the preoperative risk factors for ectasia
- Scotopic pupillometry is important to determine OZ and AD
- OZ should be 0. 5mm larger than scotopic pupil size
- BUT and Schirmer's test should be routinely done, other investigations for DES can by performed accordingly
- The best to measure IOP is Pascal since it is not affected by CCT
- IOP taken by Applanation tonometer should be modified according to CCT
- Tonopen gives an idea should the IOP be taken at corneal midperiphery
- IOP should be monitored postoperatively in case of prolonged use of steroids
- The non-dominant eye should be determined for monovision treatment and for other treatments of presbyopia
- A complete evaluation of ocular motility is mandatory especially in case of significant phoria, intermittent tropia, or prominent tropia and a trial of CL should be done before the decision of surgery is taken
- Orbital and eye anatomy has an impact of surgical choice
- Detailed external and internal eye examination is mandatory since any pathology may lead to significant complications

BIBLIOGRAPHY

1. Artola A, Gala A, Belda JI, et al. LASIK in myopic patients with dermatological Keloids. J Refract Surg. 2006;22(5):505-8.
2. Alio JL, Azar DT (Eds.). Management of Complications in Refractive Surgery. Springer; 2008.
3. Alio JL, Perez-Santonja JJ Rodriguez-Prats J. LASIK in patients with rheumatic diseases: a pilot study. Ophthalmology. 2005;12:1948-54.
4. American Academy of Ophthalmology. Is LASIK for me? A Patient's Guide to Refractive Surgery; 2008.
5. American Academy of Ophthalmology. Preferred Practice Patterns Committee, Cornea/External Disease Panel. Dry Eye Syndrome; 2008.
6. American Academy of Ophthalmology. Preferred Practice Patterns Committee, Cornea/External Disease Panel. Blepharitis; 2008.
7. American Academy of Ophthalmology (2012-2013 edition). Basic and Clinical Science Course. Section 13: Refractive Surgery.
8. American Academy of Ophthalmology (2012-2013 edition). Basic and Clinical Science Course. Section 3: Clinical Optics.
9. Barbazzetto IA, Pizzarello LD. Ocular changes during pregnancy. Compr Ophthalmol Update. 2007;8(3):155-67.
10. Bilgihan K, Hondur A, Sul S, Ozturk S. Pregnancy-induced progression of keratoconus. Cornea. 2011;30(9):991-4.
11. Binder PS, Lindstrom RL, Stulting RD, et al. Keratoconus and corneal ectasia after LASIK. J Cataract Refract Surg. 2005;31(11):2035-8.
12. Brightbill FS, McDonnell PJ, McGhee CNJ, et al (2009, 4th edition). Corneal Surgery: Theory, Technique and Tissue. Mosby Elsevier.
13. Bron AJ, Tiffany JM. The contribution of meibomian disease to dry eye. Owl Surf. 2004;2(2):149- 65.
14. Cobo-Soriano R, Beltran J, Baviera J. LASIK outcomes in patients with underlying systemic contraindications: a preliminary study. Ophthalmology. 2006;113:e1-8.
15. Cua IY, Pepose JS. Late corneal scarring after photorefractive keratectomy concurrent with development of systemic lupus erythematosus. J Refract Surg. 2002;18:750-2.
16. Diaz-Valle D. Late-onset severe diffuse lamellar keratitis associated with uveitis after LASIK in a patient with ankylosing spondylitis. J Refract Surg. 1995;25:623.
17. Driver PL, Lemp MA. Meibomian gland dysfunction. Surv Ophthalmol. 1996;40(5):343-67.
18. Edwards JD. Burka JM, Bower KS, et al. Effect of brimonidine tartrate 0.15% on night-vision difficulty and contrast testing after refractive surgery. J Cataract Refract Surg. 2008;34(9):1538-41.
19. Ersanli D, Akin T, Karadayi K. Aggravation of proliferative diabetic retinopathy after LASIK (letter). J Cataract Refract Surg. 2005;31:1086-7.
20. Feder RS, Rapuano. The lasik handbook: a case-based approach. Lippincott Williams & Wilkins; 2007.
21. Fraunfelder FW, Rich LF. Laser-assisted in situ keratomileusis complications in diabetes mellitus. Cornea. 2002;21:246-8.
22. Ghanbari H, Ahmadieh H. Aggravation of proliferative diabetic retinopathy after laser in situ keratomileusis. J Cataract Refract Surg. 2003;29:2232-3.
23. Golas L, Manche EE. Dry eye after laser in situ keratomileusis with femtosecond laser and mechanical keratome. J Cataract Refract Surg. 2011;37(8):1476-80.
24. Halkiadakis I, Belfair N, Gimbel HV. Laser in situ keratomileusis in patients with diabetes. J Cataract Refract Surg. 2005;31:1895-8.
25. Herse PR. A Review of manifestations of diabetes mellitus in the anterior eye and cornea. Am J Optom Physiol Opt. 1988;224-30.
26. Hoogewoud F, Gatzioufas Z, Hafezi F. Transitory topographical variations in keratoconus during pregnancy. J Refract Surg. 2013;29(2):144-6.

27. International Dry Eye WorkShop. The definition and classification of dry eye disease: report of the Definition and Classification Subcommittee of the International Dry Eye WorkShop. Ocul Surf. 2007;5(2):75-92.
28. Kadyan A, Edmunds MR (2010). Intraocular surgery with warfarin anticoagulation. J Cataract Refract Surg 36(4):701; author reply 701-2. DOI:10.1016/j.jcrs.2010.01.008.
29. Kanski JJ, Bowling B (2011, 7th edition). Clinical Ophthalmology: A Systematic Approach. Ch. 4: Dry Eye Disorders. Elsevier.
30. Kenyon K, Wafai Z, Michels R, et al. Corneal basement membrane abnormality in diabetes mellitus [ARVO abstract]. Invest Ophthalmol Vis Sci (suppl). 1978;17:245.
31. Kohnen T. Excimer laser refractive surgery in autoimmune disease (Letter to the Editor). J Cataract Refract Surg. 2006;32:1241.
32. Lee JH, You YS, Choe EM, Lee ES. Efficacy of brimonidine tartrate 0.2% ophthalmic solution in reducing halos after laser in situ keratomileusis. J Cataract Refract Surg. 2008;34(6):963-7.
33. Lemp MA. Advances in understanding and managing dry eye disease. Am J Ophthalmol. 2008;146(3):350-6.
34. Levinson EA, Rapuano CJ, Cohen EJ, et al. Referrals to the Wills Eye Institute Cornea Service after laser in situ keratomileusis: reasons for patient dissatisfaction. J Cataract Refract Surg. 2008;34(1):32-9.
35. Li Y, Li HY. [Analysis of clinical characteristics and risk factors of corneal melting after laser in situ keratomileusis]. [Chinese]. Zhonghua Yan Ke Za Zhi. 2005;41:330-4.
36. Lopez-Prats MJ, Hidalgo-Mora JJ, Sanz-Marco E, et al. [Influence of pregnancy on refractive parameters after LASIK surgery]. Arch Soc ESsp Oftalmol. 2012;87(6):173-8.
37. Majmudar PA. LASIK complications. Focal Points: American Academy of Ophthalmology. 2004;12(13):1-14.
38. Moshirfar M, Feiz V, Feilmeier MR, et al. Laser in situ keratomileusis in patients with corneal guttata and family history of Fuchs endothelial dystrophy. J Cataract Refract Surg. 2005;31(12):2281-6.
39. Pflugfelder SC, Beuerman RW, Stern ME (Eds). Dry Eye and Ocular Surface Disorders. New York: Informa Healthcare; 2004.
40. Pop M, Payette Y. Risk factors for night vision complaints after LASIK for myopia. Ophthalmology. 2004;111(1):3-10.
41. Preferred Practice Pattern® Guidelines. www.aao.org/ppp.
42. Rezende RA, Uchoa UC, Cohen EJ, et al. Complications associated with anterior basement membrane dystrophy after laser in situ keratomileusis. J Cataract Refract Surg. 2004;30:2328-31.
43. Rosario Cobo-Soriano R, Jaime Beltrán J, Baviera J. LASIK Outcomes in Patients with Underlying Systemic Contraindications: A Preliminary Study Ophthalmology. 2006;113(7):1118.e1–1118.e8.
44. Saini JS, Khandalavia B. Corneal epithelial fragility in diabetes mellitus. Can J Ophthalmol. 1995;30:142-6.
45. Salib GM, McDonald MB, Smolek M. Safety and efficacy of cyclosporine 0.05% drops versus unpreserved artificial tears in dry-eye patients having laser in situ keratomileusis. J Cataract Refract Surg. 2006;32(5):772-8.
46. Salomão MQ, Ambrósio R Jr, Wilson SE (2009). Dry eye associated with laser in situ keratomileusis: Mechanical microkeratome versus femtosecond laser. J Cataract Refract Surg 35(10):1756-60. doi: 10.1016/j.jcrs.2009.05.032.
47. Samuelson TW. Refractive surgery in glaucoma. Curr Opill Ophthalmol. 2004;15(2):112-8.
48. Sanchez-Thorin JC. The Cornea in Diabetes Mellitus. Int Ophthalmol Clin. 1998;38:19-36.
49. Schallhorn SC, Kaupp SE, Tanzer DJ, et al. Pupil size and quality of vision after LASIK. Ophthalmology. 2003;110(8):1606-14.
50. Schmidt GW, Yoon M, McGwin G, et al. Evaluation of the relationship between ablation diameter, pupil size, and visual function with vision-specific quality-of-life measures after laser in situ keratomileusis. Arch Ophthalmol. 2007;125(8):1037-42.
51. Schultz RO, Peters MA, Sobocinski K, et al. Diabetic corneal neuropathy. Trans Am Ophthalmol Soc. 1983;81:107-24.

52. Seiler T, Wollensak J. Complications of laser keratomileusis with the excimer laser. Klin Monatsbl Augenheilkd. 1992;200:642-53.
53. Smith RJ, Maloney RK. Laser in situ keratomileusis in patients with autoimmune diseases. J Cataract Refract Surg. 2006;32(8):1292-5.
54. Solomon R, Eric D, Donnenfeld ED. Innovations in Advanced Surface Laser Refractive Surgery. Focal Points: American Academy of Ophthalmology. 2010;28(2):1-14.
55. Stern ME, Pflugfelder Sc. Inflammation in dry eye. Ocul Surf. 2004;2(2):124-30.
56. Toda I, Asano-Kato N, Hori-Komai, et al. Laser-assisted in situ keratomileusis for patients with dry eye. Arch Ophthalmol. 2002;120(8):1024-8.
57. Toda T, Vagi Y, Hata S, et al. Excimer laser photorefractive keratectomy for patients with contact lens intolerance caused by dry eye. Br J Opl1thafmol. 1996;80(7):604-9.
58. Weintrob AC, Sexton DJ. Susceptibility to infections in persons with diabetes mellitus. UpToDate. Updated 2012; (2012).
59. Wilson SE, Klyce SD. Screening for corneal topographic abnormalities before refractive surgery. Ophthalmology. 1994;101(1):147-52.
60. Wilson SE. Laser in situ keratomileusis-induced (presumed) neutrophilic epitheliopathy. Ophthalmology. 2001;108:1082-7.

CHAPTER 8

Avoidable Refractive Surgery Complications

CORE MESSAGE

- Refractive surgery complications are not rare but many of them can be avoided
- There are complications related to PRT, some are related to flap, interface or stroma
- There are complications related to PIOL
- There are complications related to CLE, most important are retinal detachment and choroidal neovascularization

Refractive surgery is not risk-free. There are many complications may happen during and after refractive surgery; but many of them can be avoided.
This chapter will discuss main refractive complications, their causes and how to avoid them.

COMPLICATIONS RELATED TO PRT

Intraoperative and Early Postoperative Complications

Before discussing intraoperative complications, it is wise to know that when an untoward event happens in the first eye, it is often best not to proceed with surgery on the fellow eye at the same day, because there may be delayed visual rehabilitation with suboptimal final results and there is a higher risk of a similar problem in the fellow eye.

Flap Complications

1. **Thin, Irregular, Buttonhole Flap (Fig. 8.1):**
   a. *Predisposing Factors:*
      – Preoperative Km >46 D (see Fig. 6.9).
      – History of collagen vascular disease.
      – Conjunctival scarring after previous ocular surgery.
      – Previous incisional keratotomy.
      – Previous ocular, specifically cornea injury.
      – Previous scleral buckling surgery.
      – Patient with unusually thick epithelial layer (>90 μm).
   b. *Etiology:*
      – Attempted creation of very thin corneal flap (<100 μm).
      – Poor applanation with MMK or femtosecond contact glass.
      – Loss of suction during flap cut.
      – Patient movement during the procedure.

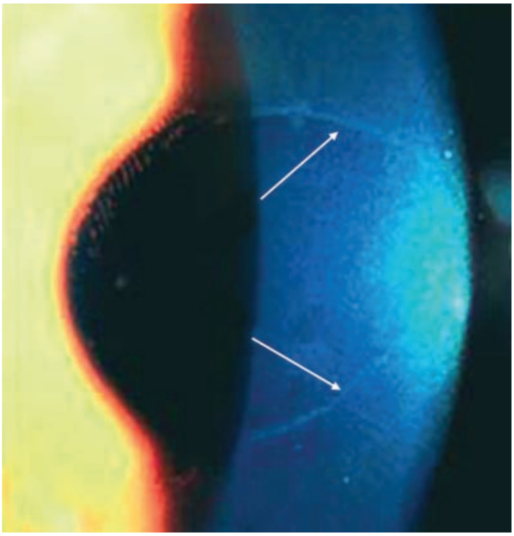

Fig. 8.1 Button hole flap. White arrows point at borders of the button hole.

- Low or reduction in patient IOP.
- Poor lubrication of corneal surface or MMK malfunction.
- Excess tissue being compressed beyond applanation by the MMK foot plate, causing indentation of the cornea (see Figs 6.7 and 6.8). Indentation may happen also in case of multiple applications of the suction ring which lead to IOP reduction, or in case of fast MMK movement.

c. *Prevention and Treatment:*
   - Identify patients at risk for flap complications.
   - Carefully set up and review your microkeratome, laser and surgical protocol.
   - Secure a wide and safe path for the MMK head until it reaches the intended hinge position by careful draping, using adjustable speculum in patients with tight eyelids, and gently lifting the globe after suction activation.
   - Be aware of these complications and suspect them in any uncertain situation.
   - Do not ablate a poor quality bed.
   - Replace the flap, put a BCL, use topical antibiotics and steroids for few days and then remove BCL.
   - Wait for a stable refraction before the second intervention (at least 3 months, some surgeons wait for 6 months). Thereafter:
     - If a second flap cut is planned, it should be at a deeper level and with a larger flap diameter than the first attempt.
     - If SA is planned, MMC 0.02% (0.2 mg/ml) should be applied after the ablation for up to 2 min to reduce haze and scarring. A reduction in the amount of minus sphere treatment also must be considered to compensate for the diminished healing response due to MMC.

2. **Incomplete Flap (Fig. 8.2):**

   a. *Predisposing factors:* It happens due to premature stopping of the MMK head before reaching the intended hinge position. This is commonly due to:

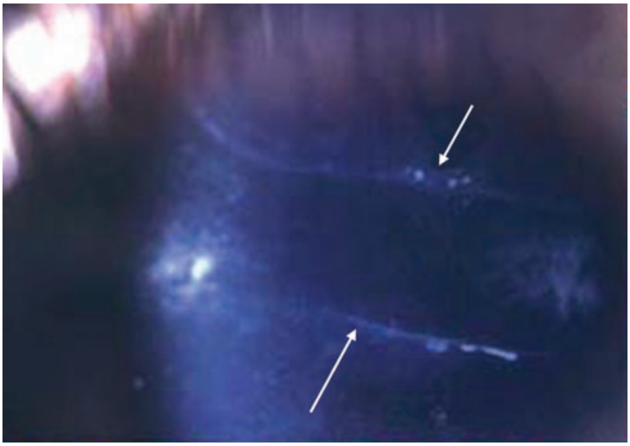

Fig. 8.2 Incomplete flap. White arrows point at borders of the defect.

- Mechanical obstacles such as lashes, drapes, loose epithelium and precipitated salt from the irrigating solution.
- MMK malfunction.
- Facial features such as deep-seated eyes, tight lids or blepharospasm.

b. *Prevention and treatment:*
Same as the previous complication added that:
- Do not lock the MMK until you are sure that the surgical area is wide enough and free of any thing that may obstacle the microkeratome.
- The MMK should be locked easily, otherwise there is something inside.
- Press gently on the eye during fixing the suction ring, slightly raise the suction ring with the eye after being sure of good suction, lock the MMK smoothly, press the eye gently again during MMK pass.

3. **Free Flap:**
a. *Predisposing factors:* The main predisposing factor is flat cornea (Km <40 D). Small interpalpebral fissure and poor patient cooperation are also important contributing factors.
b. *Etiology:* Inconsistent flap diameter, hinge width and Km (see Fig. 6.9).
c. *Prevention and treatment:*
- In case of flat cornea, make sure that MMK or femtosecond parameters are adjusted to create a flap of a small diameter and a wide hinge.
- Make sufficiently long-lasting ink marks.
- Make marks sufficiently long, to allow the edge of the flap to be crossed by the marks.
- Make asymmetric marks that are distinguishable in the event that the flap is repositioned inversely (epithelium vs. stroma).
- When removing the microkeratome from the eye, make sure the flap is on the cornea.
- In the case of a free flap, reinforce the marks or even make stromal incisions.
- If the marks are lost completely, then try to reposition the free flap using the epithelial details from the edge of the flap.
- Inadequate repositioning (rotation) leads to mixed astigmatism, generally accompanied by reduced CDVA.

– In case of induced mixed astigmatism discovered after the operation due to intraoperative free flap rotation, solve the problem by repositioning the flap. Calculate the angle for which the flap should be rotated by the following steps:
  - Measure the induced (postoperative) refractive error (manifest mixed astigmatism).
  - Use the plus astigmatism equation.
  - Use the axis of the plus astigmatism in one of the following two equations to calculate the angle of error of the recent position of the flap:
    1. *Equation one.* Flap error angle of rotation = 2 x postoperative axis –90. It is used when the flap has been cut horizontally (horizontal MMK).
    2. *Equation two.* Flap error angle of rotation = 2 x postoperative axis –270. It is used when the flap has been cut vertically (rotational MMK).
  - If the resulting angle of error is positive, turn the flap clockwise, otherwise turn it counterclockwise.
  - Example 1: post surgical induced refractive error is –1 D sph/+2 D cyl @ 30° and the flap has been cut vertically. Angle of error = 2 x 30 – 270 = –210°. Since it is a negative value, rotate the flap counterclockwise for 210°.
  - Example 2: post surgical induced refractive error is –1.5 D sph/+3 D cyl @ 100° and the flap has been cut horizontally. Angle of error = 2 x 100 – 90 = +110°. Since the angle is positive, rotate the flap clockwise for 110°.

4. **Distorted (Displaced) Flap (Fig. 8.3):**
   a. *Presentation:* Intraoperatively, it appears as wrinkled flap with a gap at an edge.
   Postoperatively, the epithelium fills the gap and the case presents either like macrostriae or microstriae. The former can be seen clearly by slitlamp biomicroscopy without staining, while the latter can be missed unless seen with staining, where it takes a negative staining as shown in Figure 8.4.
   Traumatic flap displacement can occur long after surgery. LASIK patients need to be examined at a slit lamp after ocular trauma to make sure the flap was not disturbed.

Fig. 8.3 Distorted flap. Notice the vertical striate.

b. *Etiology:*
   - Intraoperatively:
     - Copious irrigation under the flap leads to viscous interface and predisposing to flap slippage.
     - Improper replacement of the flap, especially if no adequate time was given to the flap to dry and adhere.
     - A superior hinge, 70-degree side cut angle may reduce the incidence.
   - Postoperatively:
     - Rubbing the eye.
     - Dryness during the first 3–4 hours due to anesthesia and reduced blinking reflex.
     - Closing the eyes for 2–3 hours postoperatively, frequent lubrication, especially in the first few hours after surgery and avoidance of brimonidine perioperatively, will reduce the incidence.

c. *Management:*
   - Early postoperatively (first 24 hours):
     - If the case is mild (microstriae) with no visual impact, nothing should be done since the epithelium has the filling property (remodeling).
     - If the case is moderate to severe (macrostriae) with visual impact, refloating the flap accompanied with debridement of the epithelium and hydration, is usually successful. It is important to brush back epithelium that has grown onto the stromal bed and under surface of the flap to reduce the risk of epithelial ingrowth.
   - Late postoperatively:
     - If the case is mild (microstriae) with visual impact, mild PTK is sufficient (see chapter 5).
     - If the case is moderate to severe (macrostriae), refloating the flap accompanied with debridement of the epithelium and *suturing*, is usually successful.

Fig. 8.4 Microstriae. They can be visible by flourescein negative staining.

Flap-Interface Complications

After flap repositioning at the end of the surgery, endothelial pump starts its function within few minutes to adhere the flap. On OCT view, normal interface appears as a silver line differentiating the stromal bed from the flap. Ideal interface should be regular with no gap or debris as shown in Figure 8.5. The following are the most common (although rare) complications related to the interface.

1. **Infectious Keratitis (Fig. 8.6):**
   a. *Etiology:*
      – Infections presenting early after LASIK (within 1 week) are commonly caused by gram-positive organisms.
      – Delayed onset (2–3 weeks) is commonly due to atypical mycobacterium.
      – Fungal infections are suspected in those cases lacking improvement after early broad-spectrum therapy and associated with severe visual loss.
   b. *Differential Diagnosis:* Persistence of interface inflammation or appearance of corneal infiltrate after LASIK should be presumed infectious unless proven otherwise. Differential diagnosis consists of the followings:
      – DLK.
      – Pressure induced interface stromal keratitis (PISK).
      – Central toxic keratitis (CTK).
      – Interface debris.
      – Edema:
         - Due to bandage contact lens.
         - Due to trauma.
         - Due to epithelial effect.
      – Sterile peripheral infiltrate (staphylococcus marginal).
      – Epithelial ingrowth.
      – Post-viral reactivation.
   c. *Preventive measures:*
      – Preoperatively:
         - Avoid makeup for at least 1 week.
         - Sterilization and good scrubbing.
      – Intraoperatively:
         - Sterilization.
         - Avoid entrance of meibomian gland secretions under the flap.
         - Avoid pooling of liquids during the surgery (speculum with suction is preferable).

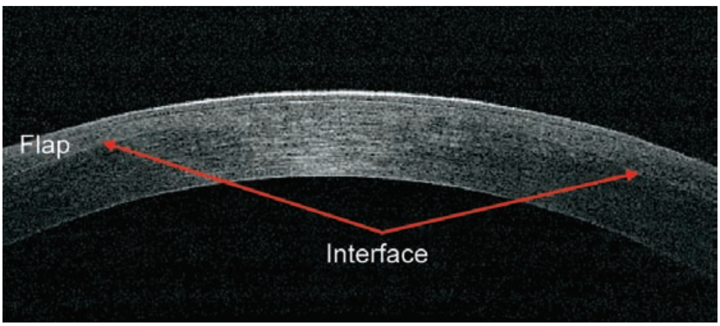

Fig. 8.5 Normal flap-bed interface after LASIK.

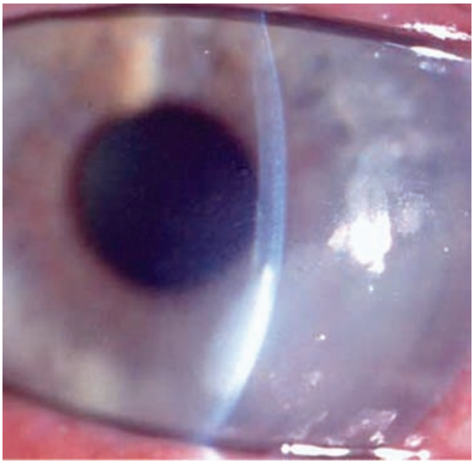

Fig. 8.6 Post-LASIK infectious keratitis.

- Postoperatively:
  - Plastic cover over night for five days.
  - Avoid rubbing.
  - Avoid makeup, swimming, sleeping with cats and puppies, or working with plants for at least one week.
  - Proper use of topical antibiotics.
  - Proper treatment of dry eye.

d. *Management:*
- Early lifting of corneal flap for microbiological tests (smear and culture) for bacteria, fungus and atypical mycobacterium followed by aggressive topical broad spectrum antibiotic therapy.
- Initial therapy may be modified based on culture results and clinical response.

2. **Diffuse Lamellar Keratitis (DLK):**

a. *Definition:* It is a rare early postoperative complication appearing as an inflammatory response of the corneal lamellae.

b. *Predisposing factors and prevention:* Entrance of toxic and oxidative materials during the surgery under the flap is the main cause. Materials may be oil, wax, talc powder (in gloves), mascara (eye makeup), metallic material and bacterial cell proteins that have accumulated on the autoclaved instruments. Epithelial defects during the surgery may trigger the inflammation.

Treatment of blepharitis and avoiding makeup preoperatively, is critical for prevention. Wiping the MMK with alcohol, then rinsing with BSS before mounting may also prevent DLK.

In some cases, DLK may be non toxic; it may occur as an inflammatory reaction to intra- or postoperative trauma. Intraoperative trauma happens due to aggressive manipulation of the flap or due to epithelial defects on the flap. It is, therefore, recommended to replace loose epithelium to its original location at the end of the LA.

Late-onset DLK can occur from ocular surface problems such as corneal abrasions, recurrent erosions and HSV dendritic keratitis, but it can also be a sign of indolent flap interface infection, such as with atypical mycobacterium or fungus.

c. *Grading and Treatment:*
   i. Grade I (Fig. 8.7): Seen within 24 hours postoperatively. Fine, white cells in the stroma, usually in the inferior periphery. No clumping of cells in the interface or in the central portion of the cornea. Visual axis is free. Treatment is by extensive topical steroids.
   ii. Grade II (Fig. 8.8): Usually seen within 48–72 hours postoperatively but may be seen within 24 hours. Fine, white cells in the stroma extending to the center of the cornea. Yet, no clumping of cells in the interface is present. Treatment is by extensive topical steroids.
   iii. Grade III (Fig. 8.9): Usually seen with 48–72 hours postoperatively. Fine, white cells in the stroma and clumped slightly in the interface slightly central or just inferior to the center of the cornea. Requires flap lifting, scrubbing of the bed and the inner face of the flap and flap repositioning to prevent permanent scarring.
   iv. Grade IV (Fig. 8.10): Seen after one week postoperatively. Results from stromal melting and scarring. It appears as mud cracks and central scar leading to loss of central

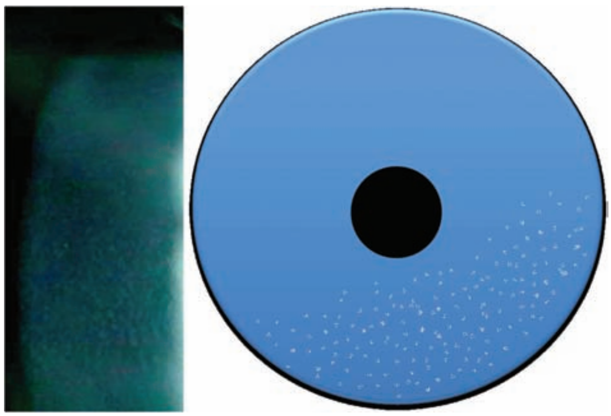

Fig. 8.7 Grade I DLK.

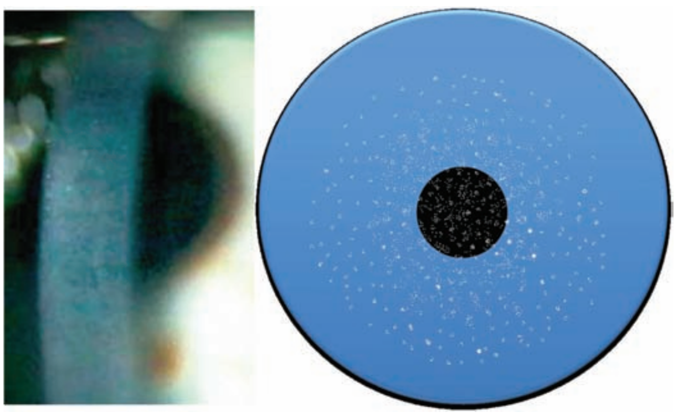

Fig. 8.8 Grade II DLK.

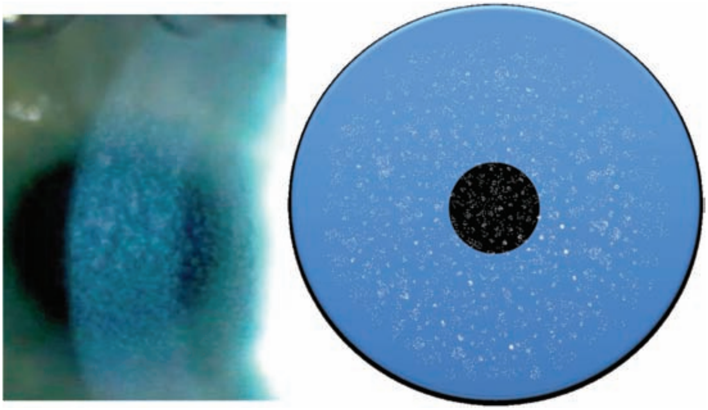

Fig. 8.9 Grade III DLK.

Fig. 8.10 Grade IV DLK.

volume, hyperopic shift and flattening of central cornea; this can be seen clearly on the OCT pachymetry map (Fig. 8.11, red circle). Treatment is of little help. Three to six months should pass to decide for lamellar keratoplasty. In some cases, melting may be very severe and appears on OCT as a thickened cornea, infiltrated stroma and flap and a gap filled with dead tissue in the interface as shown in Figure 8.12.

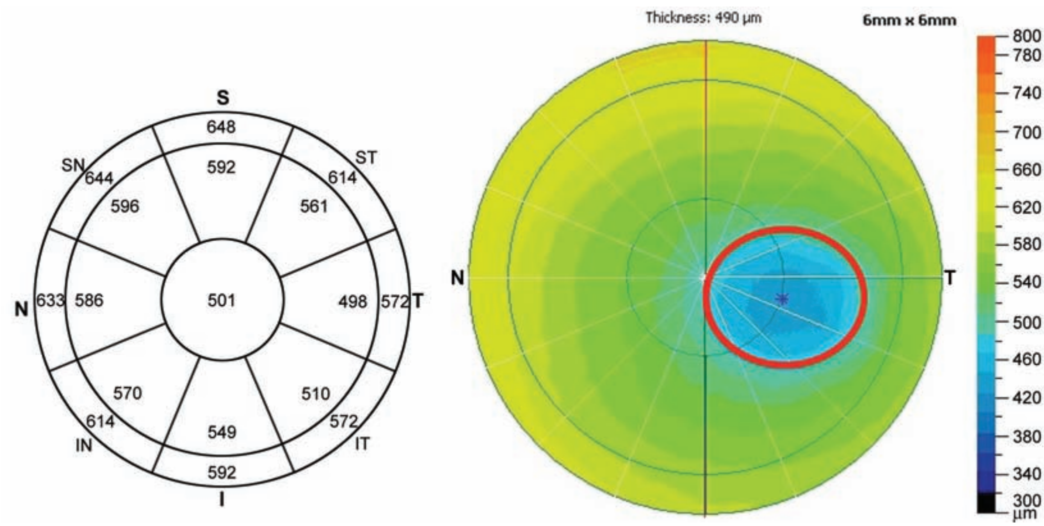

Fig. 8.11 OCT pachymetry map of a cornea with grade IV DLK. The red circle indicates a flat thin area.

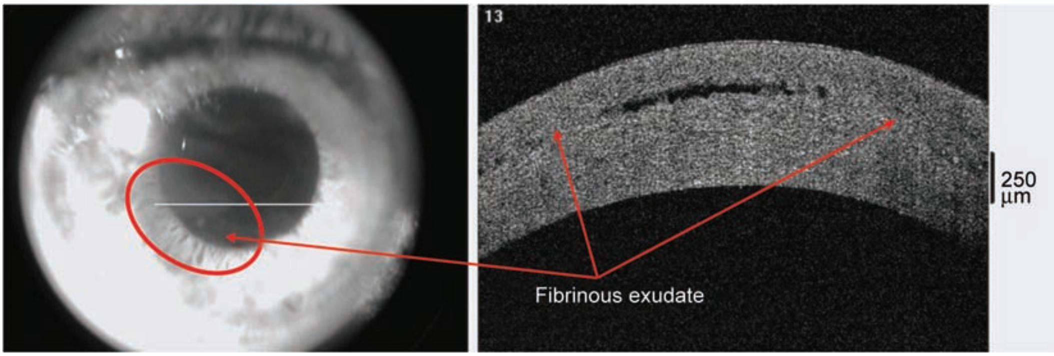

Fig. 8.12 OCT view of corneal melting in severe DLK. The red circle indicates the melted area, and on the right appears a thickened cornea with a fibrinous exudate within the interface.

3. **Pressure Induced Interface Stromal Keratitis (PISK) (Fig. 8.13):**
   a. *Etiology:* Steroid induced accumulation of fluid in the interface due to increased IOP. Fluid accumulation may be space occupying and results in falsely low IOP measurements on applanation tonometry (4 or 5 mmHg), or may be non-space occupying leading to accurate IOP measurements. In case of space occupying type, a fluid cleft behind the flap can be seen by slit lamp and OCT.
   b. *Differential diagnosis and treatment:*
   PISK should be differentiated from DLK. The main differences between both are:
      – DLK usually starts within 24 hours postoperatively, but late onset after weeks or months may happen in the setting of trauma, corneal abrasions or erosions, while PISK starts after a week.
      – DLK responds to topical steroids, while PISK worsens.
      – PISK responds to discontinuation of steroids and using IOP lowering agents.
      – OCT view. In DLK grade I to III, the stroma and interface are infiltrated without a gap in the interface (Fig. 8.14, white arrow). In the space occupying type of PISK, there is a gap filled with fluids in the interface (Fig. 8.15, white arrows).

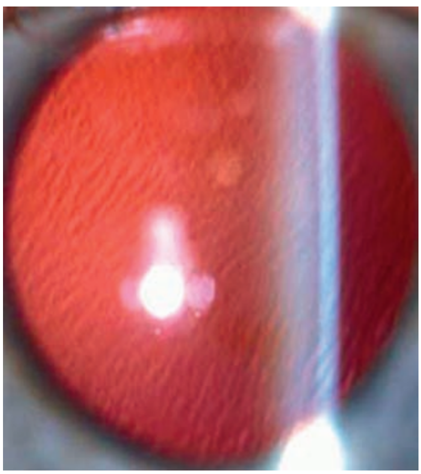

Fig. 8.13 PISK.

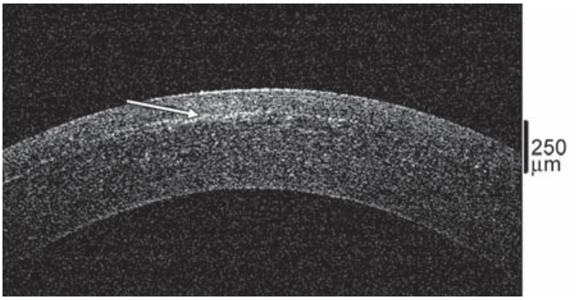

Fig. 8.14 OCT view of infiltrated interface in DLK. The white arrow points at the interface.

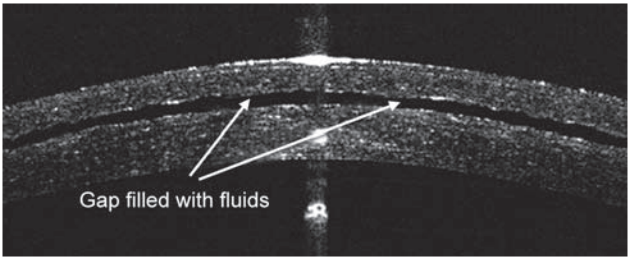

Fig. 8.15 OCT view of space occupying PISK.

4. **Central Toxic Keratitis (CTX) (Fig. 8.16):** It is a toxic inflammatory reaction which has the same etiology and predisposing factors of DLK. It is a DLK-grade-IV-like entity which (unlike grade IV DLK) presents within 1-5 days postoperatively. On the other hand, CTX does not respond to steroids and needs only observation. OCT view is same in both complications, where a central area of very high reflectivity extends through all corneal thickness as shown in Figure 8.17. The process may take several months to resolve or may leave a scar just like DLK grade IV. The decision of treatment can be made thereafter.

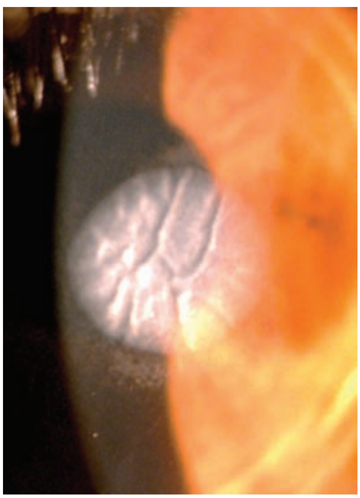

Fig. 8.16 CTX.

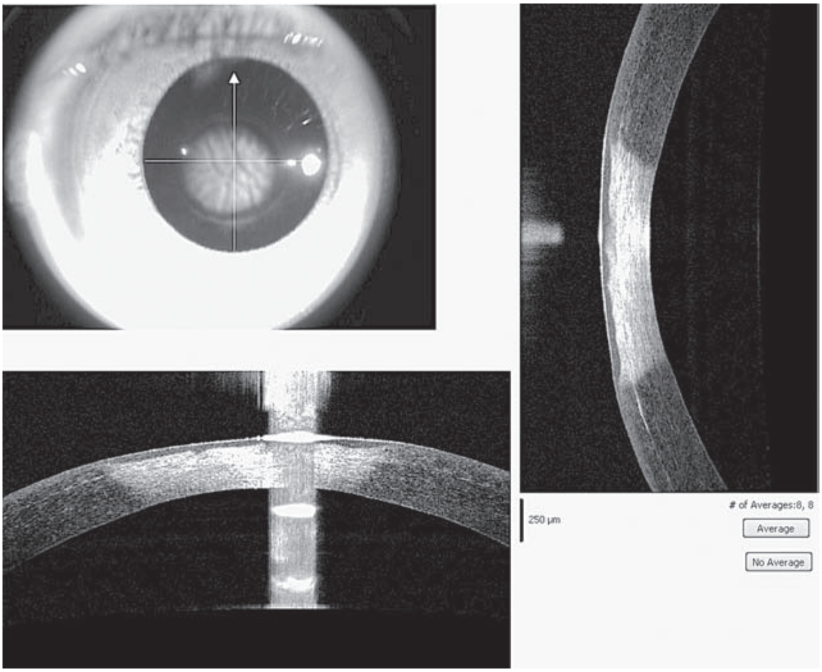

Fig. 8.17 OCT view of CTK.

5. **Marginal Sterile Corneal Infiltrates (Fig. 8.18):**
   a. *Definition:* A bilateral noninfectious inflammatory process that is characterized by multiple marginal subepithelial white infiltrates with intact epithelium localized peripheral to flap edge. Similar to catarrhal infiltrate, there is an intervening clear zone between the involved area and the limbus.
   b. *Clinical presentation:* The case presents within the first few days postoperatively with a sluggish onset of clinical signs with mild to lack of symptoms. Visual acuity is not affected.

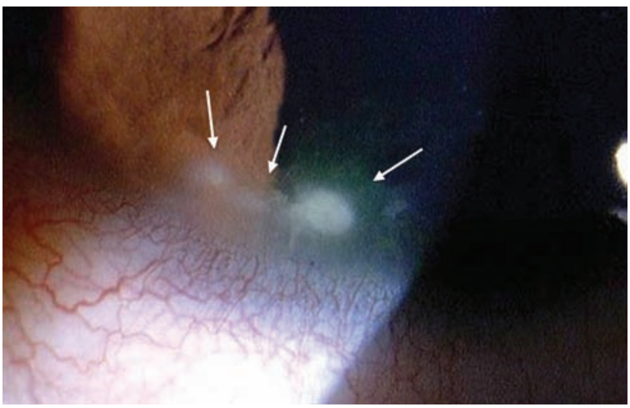

Fig. 8.18 Marginal sterile corneal infiltrates. The white arrows point at the infiltrates.

There is a mild to moderate redness with no anterior chamber reaction. The patient may complain of mild pain, foreign body sensation and tearing.

c. *Predisposing factors:*
   - In LA: blepharitis.
   - In SA: use of tight contact lenses, use of NSAIDs without topical steroids and blepharitis.
d. Treatment and Differential Diagnosis:
   - Intensive high penetration topical steroids every 1–2 hour while the patient is awake.
   - Re-evaluation of the case every day until the condition is under control.
   - Short doses of systemic steroids are to be considered, if the inflammation is not responsive to topical intense treatment and as long as there are no severe signs or epithelial defect.
   - In situations, where the clinical presentation is more severe (as with dense infiltrates, edema, epithelial defect, purulent discharge, considerable pain and decreased vision), it is advised to get material for microbiological cultures and laboratory workup, as well as to treat these cases empirically as bacterial infections until the cultures come back negative, to increase the use of topical and systemic steroids.
   - Myopic regression is often seen after proper treatment.
   - If enhancement is needed, recurrence rate of infiltrates is high in those who had them after the first treatment. Therefore, a prophylactic treatment with high penetration steroids should be initiated days before enhancement.
   - Differential diagnosis also includes herpes simplex keratitis.

Corneal Melting

a. Corneal melting is the final common response of the stroma to a variety of insults.
b. Predisposing factors include:
   - DES.
   - Autoimmune diseases.
   - Epithelial defects during the operation.
   - Use of NSAIDs.
   - Epithelial ingrowth.
   - Interface infections
   - Epithelial and stromal herpes.
   - Adenoviral infection.
   - The classic course of the disease is a self-limited phenomenon, but treatment is indicated in severe cases to avoid scarring.

Late Postoperative Complications

DES

It has been discussed in chapter 7.

Epithelial Ingrowth (Fig. 8.19)

It is one of the interface complications. It occurs when epithelium finds a port to go through under the flap. The ingrowth consists of two portions, the tunnel, which is the pathway of the

feeding epithelium, extending from corneal periphery into under the flap and the nests and islands of epithelium which are fed by corneal epithelium through the tunnel as shown in Figure 8.20. OCT view shows a gap in the interface being occupied by the ingrowing epithelial cells (Fig. 8.21); it also detects the gap at the flap edge through which the ingrowing cells find their way in (Fig. 8.22). Figure 8.23 shows well-opposed edges after flap repositioning.

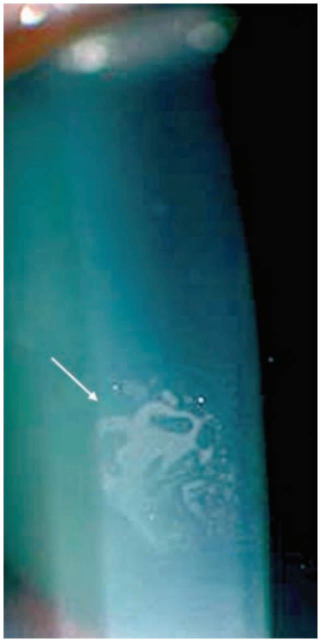

Fig. 8.19 Epithelial ingrowth. The white arrow points at nests of epithelium.

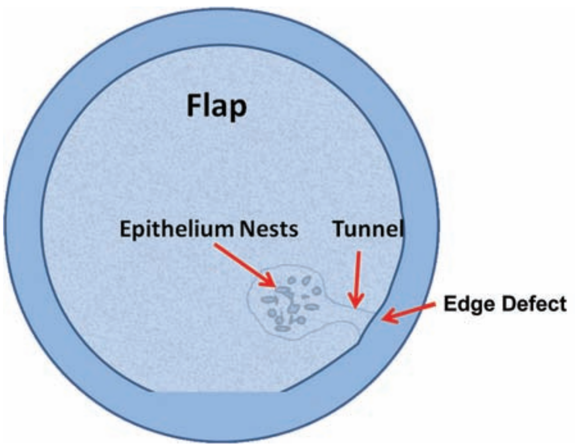

Fig. 8.20 Epithelial ingrowth. This diagram shows etiology of the complication; a defect in the flap edge forms an entrance for cell migration into the interface via a tunnel.

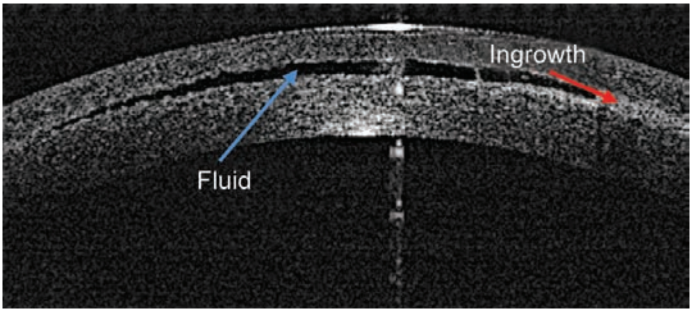

Fig. 8.21 Epithelial ingrowth. OCT view along the tunnel showing a space occupying defect with nests of epithelial cells at its end.

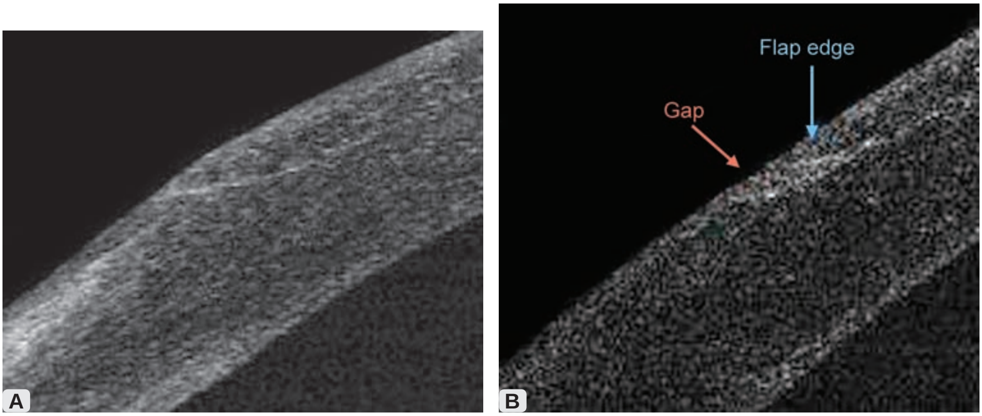

Figs 8.22A and B Epithelial ingrowth. OCT shows the defect at flap edge. (A) is the intact flap edge; (B) is the defected flap edge with the gap filled by epithelium.

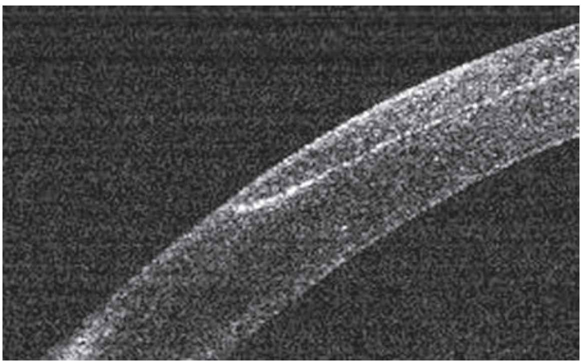

Fig. 8.23 OCT section taken after flap repositioning shows well-opposed edge.

a. **Predisposing factors and prevention:**
   - Flap striae or folds, as when the flap dislocates after surgery due to trauma or poor adhesion.
   - Excessive manipulation of the flap with forceps or with sponges.

- Excessive irrigation or careless surgery without enough time dedicated to the flap desiccation, resulting in poor adhesion of the flap. This leaves a virtual space between the flap and the residual stroma that is infiltrated by epithelial cells.
- Any complication that occurs during flap creation may lead to epithelial ingrowth, such as buttonhole, irregular flaps, decentered flaps, or flaps with an irregular gutter.
- Use of defective MMK with uneven and or irregular advancement, with poor or intermittent suction, blades with non-smooth or sharp borders. All of these can cause irregular stromal bed or a defect in Bowman layer at the edge of the flaps, a known cause of epithelial ingrowth.
- Aggressive relifting of the flap carries a higher incidence of epithelial ingrowth.
- Epithelial defects created by the surgery, such as "fluffy epithelium" caused by a defected MMK, or bad manipulation of the flap, especially in patients older than 40 years of age.
- When the flap is smaller than the ablation zone, a part of the laser beam will fall out of stromal bed which may create a gap that could be an open window for the epithelium to enter and grow.
- Surgery over previous surgeries such as LASIK over radial keratotomy cuts.

b. **Classification:**
Grade I: Epithelium under the flap as localized island at the periphery. It does not block the red reflex.
Grade II: Epithelium grows diffusely at the periphery of the flap, with a faint line in front of it. It distorts red reflex.
Grade III: Diffuse epithelium under the flap with total blockage of the red reflex.

c. **Management:** The main stay of the treatment is observation since management of this complication is difficult and has a high incidence of recurrence (10%). On the other hand, lifting the flap introduces the danger of spreading the cells under the flap or even activating epithelial cell growth.
Surgical treatment is indicated in the following situations:
1. When epithelial ingrowth progresses toward the visual axis and CDVA is in danger.
2. When epithelial ingrowth is not progressing, but the cyst forms an elevation that causes irregular and un-correctable astigmatism.
3. When the flap starts to melt.

The principle of the treatment is to close the tunnel and remove the nests. The suggested surgical technique is as follows:
- Debride the epithelium from bed and the inner face of the flap.
- Irrigate with sterile distilled water to turn the epithelial ingrowth cells white for better visualization.
- Close and seal the tunnel by one of the followings:
  - Ethyl Alcohol 100% to 18%.
  - Tissue glue (super glue).
  - Suture with 10-0 or 11-0 Nylon.
  - Cryopexy of tunnel opening.
  - PTK to the bed and flap at the tunnel.
  - Cocaine 4%.
  - ND: YAG Laser.
  - Use SCL until tunnel closed.

Ectasia

Definition

Corneal ectasia is an iatrogenic keratoconus triggered by keratorefractive surgery, especially by LASIK. It is characterized by a progressive thinning, unstable refraction and a topographic evidence of asymmetric inferior corneal steepening on the anterior sagittal curvature map, or a tomographic evidence of abnormal elevations on either of corneal surfaces. It is a progressive disorder. The progression is monitored by one or more of the followings:

1. Increase in Kmax > 1 D per 6 months.
2. Increase in TA > 1 D per 6 months.
3. Increase in MA > 1 D per 6 months.
4. Thinning of the cornea at the thinnest location >30 μm per 6 months.
5. Increase of HOAs per 6 months (as mentioned in chapter 2).

Risk Factors

Since the first reports in 1998, a variety of risk factors have been identified; however, patients have also developed ectasia without any of these predisposing risk factors.

Risk factors for ectasia include preoperative abnormal corneal tomography, FFKC, frank KC and PMD; high ablation depth; low preoperative corneal thickness; low RSB thickness; young age; and high myopia. Abnormal preoperative tomography is associated with the greatest relative risk for ectasia.

High Myopia

High myopia (> –12 D) has been reported to be a risk factor for ectasia; however, ectasia can also occur in eyes with low preoperative myopia and myopia is a poor predictor of ectasia in multivariate analysis. However, it is widely recommended to avoid correction of > –8 D by PRT.

Thin Corneas

In comparative studies, ectasia cases had significantly thinner corneas preoperatively than did controls. A thin cornea may be a marker for subclinical ectatic corneal disorders and it increases the risk of low RSB and thicker than expected flaps. The cornea is considered thin when it is < 450 μm if no other risk factors exist; otherwise <500 μm is considered thin.

Low RSB

Ectasia cases have had a significantly lower RSB than controls in comparative studies. Low RSB has always been thought to be one of the most significant risk factors for postoperative ectasia and a generally accepted minimum RSB of 250 μm has been established. In spite of this, many surgeons prefer not to go below 270 μm, or even 300 μm.

Factors contributing to low RSB include treatment of high refractive errors, thin preoperative corneas, excessively thick flaps and deeper than expected stromal ablations. There can be significant variability in the thickness of corneal flaps depending on microkeratome technology. While most of the microkeratome plate markings overestimate average actual flap thickness, flap thickness can vary widely with MMK and to less extent with femtosecond lasers. Previous studies have also demonstrated that actual AD is usually greater than estimated AD.

While a 250 μm RSB is commonly accepted as a safe cut-off for LASIK, ectasia has occurred after LASIK in numerous eyes with calculated RSB greater than 250 μm, including eyes with RSB greater than 300 μm confirmed by intraoperative pachymetry and after PRK in eyes with RSB

greater than 350 µm. Conversely, many eyes have undergone successful LASIK with RSB less than 225 µm. Thus, decreasing RSB likely represents a continuum of postoperative ectasia risk rather than a definitive safety cut-off.

Only 31% of respondents to the ISRS/AAO survey, routinely measure flap or RSB thickness intraoperatively. Using a probability model that accounts for imprecision in corneal thickness, flap thickness and laser ablation depth measurements, Reinstein and colleagues determined that, depending on the microkeratome used, up to 33% of eyes with calculated RSB thickness of 250 µm could have actual RSB less than 200 µm. Therefore, It is recommended that surgeons initially perform intraoperative pachymetry to become familiar with the performance of their microkeratomes and at least for those patients at risk for low RSB, if not for all LASIK cases. It is not necessary to perform intraoperative pachymetry on a routine basis once initial microkeratome evaluation has been performed.

Multiple enhancements further reduce RSB. Corneal thickness measurements taken months after initial LASIK usually overestimate RSB thickness especially with corneal tomography devices, hence, the importance of anterior OCT. If preoperative information is not available, accurate assessment of actual RSB prior to retreatment is critical to avoid excessive ablation of the posterior stroma. This can be accomplished by utilizing intraoperative pachymetry measurements prior to laser ablation at the time of retreatment, or by utilizing confocal microscopy or OCT prior to retreatment, as these instruments can accurately measure RSB thickness without ever lifting the flap.

Young Age

Patients who develop ectasia, especially those without classical, recognized risk factors, tend to be younger than average patients undergoing LASIK. This observation may be explained by the fact that younger corneas are more susceptible to structural deformation due to decreased collagen crosslinking that naturally increases with age, or the fact that some younger patients are destined to develop clinical KC in their 4th to 6th decades of life, but have not yet manifested any of the clinical or topographic findings of the disease process.

Ectatic Corneal Disorders and Forme Fruste Keratoconus

Ectatic disorders, including KC, PMD and defined abnormal topographic patterns, such as FFKC, are the most significant risk factors for postoperative ectasia. Corneal tomography should be carefully studied in both eyes before proceeding with surgery. Many surgeons rely heavily on objective classification given by software indices adopted in devices programs. However, sensitivity and specificity of such indices are not 100% and there might be false positives as well as false negatives which means that there might be subtle changes that cannot be estimated by the software. Therefore, subjective skillful reading of the maps is very important.

Other factors, such as contact lens warpage and keratoconjunctivitis sicca, can create tomographic changes that resemble those of FFKC. These factors may make it more challenging to differentiate normal from abnormal tomographies. It is therefore recommended to repeat tomographic examinations at a later time in questionable cases, and if available, utilizing multiple technologies, since a variety of imaging systems can provide unique information and decrease the odds of artifactual readings.

Other Potential Risk Factors

In addition to the aforementioned risk factors, other factors should be considered, including HOA especially coma, multiple enhancements, chronic trauma (eye rubbing), family history of

KC and refractive instability (increasing refractive cylinder) with preoperative CDVA worse than 1.0 (Snellen).

General risk factors are also as important as ocular ones. Collagen disorders that have high incidence of accompanying KC or keratoglobus are contraindications for keratorefractive surgeries even with apparently normal corneal tomography. Such disorders include Ehler-Danlos, osteogenesis imperfecta, mitral valve prolapse, joint hypermobility, Marfan disease and others. In such cases, corneal hysteresis is usually abnormal.

Ectasia Risk Score System

Randleman et al. established "Ectasia Risk Score System" to score the candidate of refractive surgery and help the surgeon in taking the decision. This system consists of two steps.
Step number 1 (Table 8.1) gives an accumulative score of the case depending on five factors: preoperative topography pattern, assumed postoperative RSB, age, preoperative CCT and preoperative manifest refractive spherical equivalent (MRSE).
Step 2 (Table 8.2) grades the risk of the case for PRT.

Example 1: a case with normal topography, a calculated RSB = 290 µm, age of the candidate = 20 y/o, CCT = 500 µm, and MRSE = –6 D. The score of this case is 0+1+3+2+0 = 6. According to Table 6.2, PRT should be avoided.

Example 2: a case with asymmetrical bowtie, RSB = 310 µm, age = 31 y/o, CCT = 520 µm and MRSE = –6 D. The score of this case is 1+0+0+0+0 = 1. According to Table 6.2, both LA and SA can be performed.

However, Randleman scoring system does not consider corneal tomography, which in many cases shows abnormal elevation or pachymetry maps in spite of normal topography; it does consider central thickness rather than thickness at the thinnest location, which is more accurate in abnormal corneas. Due to these two major reasons, many surgeons do not follow this score system. But still, the mentioned five factors are of importance.

TABLE 8.1 The Ectasia Risk Score System for Identifying Eyes at High Risk of Developing Ectasia After Lasik

Pattern	*Points*				
	4	*3*	*2*	*1*	*0*
Topography	Abnormal topography	Inferior steepening/ skewed radial axis		Asymmetrical bowtie	Normal/ symmetrical bowtie
RSB (µm)	< 240	240 – 259	260 – 279	280 – 299	≥300
Age (years)		18 – 21	22 – 25	26 – 29	≥30
CCT (µm)	< 450	451 – 480	481 – 510		≥510
MRSE (D)	> –14.00	> –12.00 to –14.00	> –10.00 to –12.00	> –8.00 to –10.00	–8.00 or less

TABLE 8.2 Grading the Risk of Ectasia According to the Scoring System Shown in Table 8.1

Total Risk Score	*Relative Risk*	*Recommendations*
0 – 2	Low	Proceed with LA or SA
3	Moderate	Proceed with caution, special informed consent, safety of SA unknown
4	High	Do not perform any

For more detail about ectasia and the predisposing risk factors, please refer to the second edition of my book (Corneal Topography in Clinical Practice) and (Keratoconus: When, Why and Why Not) by Jaypee Highlight 2012.

Haze

a. **Definition:** It is a marginal loss of corneal clarity due to a subepithelial stromal opacity (Figs 8.24 and 8.25). Its mechanism consists of abnormal collagen deposition.
   Although it is usually seen after SA, it can be encountered after LA.
b. **Predisposing Factors:**
   – Ablation depth >80 µm.
   – OZ diameter < 6 mm.
   – Magnitude of correction > –6 D.
   – Slope of wound surface; e.g. in aspheric profile is less common than that in plain profile.
   – Postoperative surface irregularity.

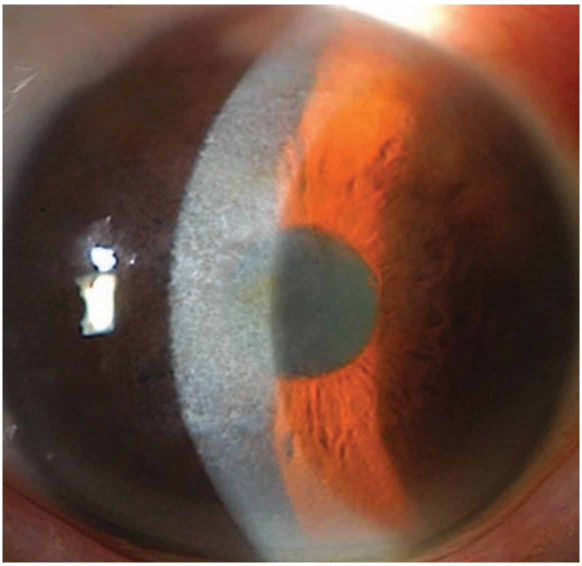

Fig. 8.24 Corneal haze after surface ablation.

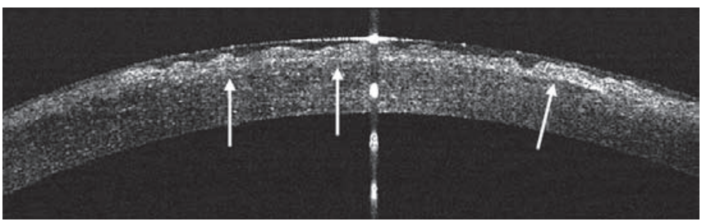

Fig. 8.25 OCT view of corneal haze. The white arrows point at irregular collagen deposition which forms an irregular hazy layer under the epithelium.

- High tear TGF-Beta levels.
- In broadband lasers is more common than flying-spot lasers.

c. **Grading:** Haze is graded from 0 to 4 as shown in Table 8.3.

d. **Prevention:**
- Intraoperative application of MMC 0.02%.
- Postoperative oral vitamin C to:
  - Prevent UV damage produced by excimer.
  - Reduce keratocyte activation.
- Postoperative sunglasses for UV protection.
- Postoperative weak steroids for a period that may last for 3 months. Monitor the IOP.

e. **Treatment:** There are several choices to treat established haze. Some are medical and some are surgical. Some surgeons use topical steroids for a long period of time. Others do PTK or even lamellar keratoplasty. However, MMC application was also described.

Some surgeons do the following steps:
1. Anterior OCT to measure epithelium thickness and the depth of haze.
2. Removal of epithelium by PTK according to OCT measurements (almost 50–60 μm) followed by PTK for haze (no more than 80 μm).
3. Application of MMC 0.02% for 2–3 min according to severity of haze (longer time for more severe haze).
4. Copious irrigation of cornea and conjunctiva with BSS.
5. BCL.
6. Topical antibiotics till complete epithelialization and removal of BCL.
7. After complete epithelialization, start weak topical steroids for at least three months with IOP monitoring.

TABLE 8.3 Grading of Haze

Grade	*Description of the image by the slit lamp*
0	No Haze
0.5	Trace
1	Haze not interfering with visibility of fine iris details
2	Mild obscuration of iris details
3	Moderate obscuration of the iris and lens
4	Complete opacification

Complications Related to PIOL

As mentioned in chapter 5, there are three types of PIOLs, anterior chamber iris-supported, anterior chamber angle-supported and posterior chamber PIOLs. Each of these types has its own complications, but there are general complications that will be discussed.

Intraoperative Complications

Intraoperative complications include ocular hypotony, iris prolapse, choroidal hemorrhage, damage to the natural crystalline lens, endothelium or iris. These are usually due to inappropriate surgical technique or IOL size and design.

Postoperative Complications

Ocular Hypertension

Ocular hypertension can be seen as an early onset during the first few days postoperatively, or as a late onset seen between the second and the fourth week after the surgery.

Early onset happens due to three mechanisms:

1. Incomplete removal of the viscoelastic substance, which results in blockage of drainage at the trabecular meshwork. The best viscoelastic to use is methylcellulose since it is easy to remove and any small remnants will be rapidly absorbed postoperatively.
2. Blockage in circulation due to entrapment behind the lens (especially in posterior chamber PIOL).
3. Rarely, malignant glaucoma.

Early onset can be avoided by good removal of the viscoelastic at the end of the surgery. It can be treated by using antihypertensive and hyperosmotic agents. In nonresponding cases, surgical intervention to remove the viscoelastic or to manage malignant glaucoma is needed.

Late onset is likely related to steroids. It is, therefore, important to have regular IOP check-ups during the treatment period.

Pupillary Block Glaucoma

It may happen with all types of PIOL even with patent peripheral iridectomy.

Acute Uveitis

Surgical trauma causes mild transient uveitis that can be controlled by postoperative medications. In case of severe reaction, full work up for uveitis should be done and endophthalmitis should be kept in mind.

Chronic Inflammation

A kind of chronic inflammation (described as an increase in aqueous flare) is found in all types of PIOLs, being more with the anterior chamber types. This inflammation is one of the major causes of progressive loss of endothelium and it may contribute to the development of cataract.

Decentration, Displacement, or Rotation of IOL

Decentration, displacement, or rotation of the PIOL is usually due to inappropriate surgical technique or IOL sizing. This requires repositioning or replacement with another lens of appropriate size.

Dislocation of PIOL

Traumatic and spontaneous PIOL dislocations have been reported in anterior chamber iris-supported PIOLs.

Corneal Edema

It is usually due to excessive manipulation during surgery, inflammation, or ocular hypertension.

Progressive Endothelial Cell Loss

This complication happens with all types of PIOL, even with posterior chamber type. Very roughly, there is about 2–2.5% loss per year. When endothelial cell loss exceeds 30%, corneal decompensation happens. This complication is one of the indications for PIOL explantation.

Residual Refractive Error

This can be managed by replacing the PIOL with another one or can be corrected with PRT.

Pigment Dispersion

It has been observed in approximately 3% of eyes that underwent posterior chamber PIOLs, but there are no reports of related glaucoma.

Cataract

Anterior subcapsular cataracts are related to posterior chamber PIOLs and mostly related to the beginning of the surgeon's learning curve. Nuclear cataract has been reported in anterior chamber angle-supported PIOLs with no reasonable correlation.

Iris Atrophy and Pupil Ovalization

It may happen with the anterior chamber angle-supported PIOLs. When the pupil margin extends beyond the edge of the PIOL, diplopia may occur and explantation of the PIOL may be indicated.

COMPLICATIONS IN REFRACTIVE LENS EXCHANGE

Refractive lens exchange (RLE) is usually performed in extreme cases, where no other refractive options are suitable. One of these extreme cases is high myopia. In high myopia, there is an increased risk of retinal detachment (RD) in general and after RLE or cataract surgery in particular. Incidence of RD after RLE differs among studies and the main reason is the period of follow up, the longer the period the higher the incidence, but in general it ranges between 1.3% and 8.1% of cases. One of the predisposing factors for RD after RLE is posterior capsule rupture during the surgery.

Of the important complications are choroidal neovascularization (CNV) and macular degeneration (MD). Unlike hyperopic patients, myopic patients are subject to the effects of the retinal stretching that can lead to premature macular CNV and MD. The incidence of these two complications can be reduced by using IOLs provided with blue-light-blocking pigments and looking for premature onset of age-related macular degeneration (AMD) and family history of AMD.

In addition to the above complications, RLE has same complications of cataract surgery.

BIBLIOGRAPHY

1. Alfonso JF, Lisa C, Cueto LF, et al. Clinical outcomes after implantation of a posterior chamber collagen copolymer phakic intraocular lens with a central hole for myopic correction. J Cataract Refract Surg. 2013;39(6):915-21.
2. Ali. JL, Ruiz-Moreno JM, Shabayek MH, et al. The risk of retinal detachment in high myopia after small incision coaxial phacoemulsification. Am J Ophthalmol. 2007;144:93-8.
3. Alio JL, Azar DT (Eds.). Management of Complications in Refractive Surgery. Springer; 2008.
4. Al-Mezaine HS, Al-Amro SA, Al-Obeidan S. Incidence, management, and visual outcomes of buttonholed laser in situ keratomileusis flaps. J Cataract Refract Surg. 2009;35(5):839-45.
5. Ambrsio R Jr, Periman LM, Netto MV, et al. Bilateral marginal sterile infiltrates and diff use lamellar keratitis after laser in situ keratomileusis. J Refract Surg. 2003;19:154-8.
6. American Academy of Ophthalmology (2012-2013 edition). Basic and Clinical Science Course. Section 13: Refractive Surgery.

7. Amoils SP, Deist MB, Gous P, et al. Iatrogenic keratoectasia after laser in situ keratomileusis for less than -4.0 to -7.0 diopters of myopia. J Cataract Refract Surg. 2000;26:967-77.
8. Asai T, Nakagami T, Mochizuki M, et al. Three cases of corneal melting after instillation of a new non steroidal anti inflammatory drug. Cornea. 2006;25:224-7.
9. Asano-Kato N, Toda I, Hori-Komai Y, et al. Epithelial ingrowth after laser in situ keratomileusis: clinical features and possible mechanisms. Am J Ophthalmol. 2002;134(6):801-7.
10. Ashrafzadeh A, Steinert RF. Results of phototherapeutic keratectomy in the management of flap striae after LASIK before and after developing a standardized protocol: long term follow-up in an expanded patient population. Ophthalmology. 2007;114:1118-23.
11. Belin MW, Ambrosio R, Jr. Corneal ectasia risk score: statistical validity and clinical relevance. Journal of refractive surgery. 2010;26(4):238-40.
12. Belin MW, Hannush SB, Yau CW, et al. Elevated intraocular pressure-induced interlamellar stromal keratitis. Ophthalmology. 2002;109:1929-33.
13. Bielory BP, O'Brien TP. Allergic complications with laser-assisted in-situ keratomileusis. Curr Opin Allergy Clin Immunol. 2011;11(5):483-91.
14. Bigham M, Enns CL, Holland SP, et al. Diffuse lamellar keratitis complicating laser in situ keratomileusis: post-marketing surveillance of an emerging disease in British Columbia, Canada, 2000–2002. J Cataract Refract Surg. 2005;31:2340-4.
15. Binder PS. One thousand consecutive Intralase laser in situ keratomileusis flaps. J Cataract Refract Surg. 2006;32:962-9.
16. Binder PS. Analysis of ectasia after laser in situ keratomileusis: risk factors. J Cataract Refract Surg. 2007;33:1530-8.
17. Binder PS. Risk factors for ectasia after LASIK. J Cataract Refract Surg. 2008;34:2010-1.
18. Binder PS, Lindstrom RL, Stulting RD, et al. Keratoconus and corneal ectasia after LASIK [letter]. J Cataract Refract Surg. 2005;31:2035-8.
19. Biser SA, Bloom AH, Donnenfeld ED, et al. Flap folds after femtosecond LASIK. Eye Contact Lens. 2003;29:252-4.
20. Brightbill FS, McDonnell PJ, McGhee CNJ, et al (2009, 4th edition). Corneal Surgery: Theory, Technique and Tissue. Mosby Elsevier.
21. Bron AJ, Tiffany JM. The contribution of meibomian disease to dry eye. Owl Surf. 2004;2(2):149- 65.
22. Buxey K. Delayed onset diffuse lamellar keratitis following enhancement LASIK surgery. Clin Exp Optom. 2004;87:102-6.
23. Caster Ai, Friess DW, Potvin RJ. Absence of keratoectasia after LASIK in eyes with preoperative central corneal thickness of 450 to 500 microns. J Refract Surg. 2007;23(8):782-8.
24. Chan CC, Hodge C, Sutton G. External analysis of the Randleman Ectasia Risk Factor Score System: a review of 36 cases of post LASIK ectasia Clinical and Experimental Ophthalmology. 2010;38(4):335-40.
25. Chang MA, Jain S, Azar DT. Infections following laser in situ keratomileusis: an integration of the published literature. Surv Ophthalmol. 2004;49:269-80.
26. Choi CJ, Melki SA. Loose anchoring suture to secure a free flap after laser in situ keratomileusis. J Cataract Refract Surg. 2012;38(7):1127-9.
27. Choi MS, Melki SA. Maddox rod effect to confirm the visual significance of laser in situ keratomileusis flap striae. J Cataract Refract Surg. 2011;37:1748-50.
28. Cimberle Michael. Retinal detachment rates for lens exchange, phakic IOLs comparable. Ocular Surgery News, 15 June 2006, pp 3–6 (Report on Alicante International Refractive Meeting); 2006.
29. Cobo-Soriano R, Beltran J, Baviera J. LASIK outcomes in patients with underlying systemic contraindications: a preliminary study. Ophthalmology. 2006;113:e1-8.
30. Cua IY, Pepose JS. Late corneal scarring after photorefractive keratectomy concurrent with development of systemic lupus erythematosus. J Refract Surg. 2002;18:750-2.
31. Davidson RS, Brandt ID, Mannis MJ. Intraocular pressure- induced interlamellar keratitis after LASIK surgery. Glaucoma. 2003;12:23-6.

32. Dawson DG, Randleman JB, Grossniklaus HE, et al. Corneal ectasia after excimer laser keratorefractive surgery: histopathology, ultra structure, and pathophysiology. Ophthalmology. 2008;115:2181-91.e1
33. De Rojas Silva MV, Diez Feijo E, Rodrguez Ares MT, et al. Confocal microscopy of stage 4 diffuse lamellar keratitis with spontaneous resolution. J Refract Surg. 2004;20:391-6.
34. Dejaco-Ruhswurm I, Scholz U, Pieh S, et al. Long-term endothelial changes in phakic eyes with posterior chamber intraocular lenses. J Cataract Refract Surg. 2002;28(9):1589-93.
35. Diaz-Valle D. Late-onset severe diffuse lamellar keratitis associated with uveitis after LASIK in a patient with ankylosing spondylitis. Journal of Refract Surg. 1995;25:623.
36. Dogru M, Stern ME, Smith JA, et al. Changing trends in the definition and diagnosis of dry eyes. Am J Ophthalmol. 2005;140:507-8.
37. Donnenfeld ED, O'Brien TP, Solomon R, et al. Infectious keratitis after photorefractive keratectomy. Ophthalmology. 2003;110(4):743-7.
38. Durrie DS, Kezirian GM. Femtosecond laser versus mechanical keratome flaps in wavefront-guided laser in situ keratomileusis: prospective contralateral eye study. J Cataract Refract Surg. 2005;31:120-6.
39. Edelhauser HF, Sanders DR, Azar R, et al. Corneal endothelial assessment after ICL implantation. J Cataract Refract Surg. 2004;30:576-83.
40. El-Sheikh HF, Tabbara KF. Cataract following posterior chamber phakic intraocular lens. J Refract Surg. 2003;19:72-3.
41. Feder RS, Rapuano. The lasik handbook: a case-based approach. Lippincott Williams and Wilkins; 2007.
42. Fernandez-Vega L, Alfonso JF, Villacampa T. Clear lens extraction for the correction of high myopia. Ophthalmology. 2003;110:2349-54.
43. Fogla R, Padmanabhan P. Interrupted sutures at the hinge site to manage a free flap during laser in situ keratomileusis. J Cataract Refract Surg. 2004;30:2235-8.
44. Frucht-Pery J, Landau D, Raiskup F, et al. Early transient visual acuity loss after LASIK due to steroid-induced elevation of intraocular pressure. J Refractive Surgery. 2007;23:244-51.
45. Gabison EE, Chastang P, Menashi S, et al. Late corneal perforation after photorefractive keratectomy associated with topical diclofenac: involvement of matrix metalloproteinase. Ophthalmology. 2003;110:1626-31.
46. Galal A, Artola A, Belda I, et al. Interface corneal edema secondary to steroid-induced elevation of intraocular pressure simulating diffuse lamellar keratitis. J Refract Surg. 2006;22:441-7.
47. Gambato C, et al. Mitomycin C modulation of corneal wound healing after photorefractive keratectomy in highly myopic eyes. Ophthalmology. 2005;112:208-18.
48. Geggel HS, Talley AR. Delayed onset keratoectasia following in situ keratomileusis. J Cataract Refract Surg. 1999;25:582-6.
49. Golas L, Manche EE. Dry eye after laser in situ keratomileusis with femtosecond laser and mechanical keratome. J Cataract Refract Surg. 2011;37(8):1476-80.
50. Gonnermann J, Klamann MKJ, Maier A, et al. Visual outcome and complications after posterior iris-claw aphakic intraocular lens implantation J Cataract Refract Surg. 2012;38(12):2139-43.
51. Gris O, Guell JL, Wolley-Dod C, et al. Diffuse lamellar keratitis and corneal edema associate with viral keratoconjunctivitis 2 years after laser in situ keratomileusis. J Cataract Refract Surg. 2004;30:1366-70.
52. Guo N, Zhou YH, Qu J, et al. [Evaluation of diffuse lamellar keratitis after LASIK with confocal microscopy]. [Chinese]. Zhonghua Yan Ke Za Zhi. 2006;42:330-3.
53. Hadden OB, McGhee CNJ, Morris AT, et al. Outbreak of diffuse lamellar keratitis caused by marking-pen toxicity. J Cataract Refract Surg. 2008;34:1121-4.
54. Hamilton DR, Manche EE, Rich LF, et al. Steroid-induced glaucoma after laser in situ keratomileusis associated with interface fluid. Ophthalmology. 2002;109(4):659-65.
55. Haw WW, Manche EE. Treatment of progressive or recurrent epithelial ingrowth with ethanol following laser in situ keratomileusis. J Refract Surg. 2001;17(1):63-8.
56. Hayashi K, Ohno-Matsui K, Futagami S, et al. Choroidal neovascularization in highly myopic eyes after cataract surgery. Jpn J Ophthalmol. 2006;50:345-8.

57. Hoff man RS, Fine IH, Packer M. Incidence and outcomes of LASIK with diffuse lamellar keratitis treated with topical and oral corticosteroids. J Cataract Refract Surg. 2003;29:451-6.
58. Hoffman RS, Fine IH, Packer M. Incidence and outcomes of LASIK with diffuse lamellar keratitis treated with topical and oral corticosteroids. J Cataract Refract Surg. 2003;29(3):451-6.
59. Horgan N, Condon PI, Beatty S. Refractive lens exchange in high myopia: long term follow-up. Br J Ophthalmol. 2005;89:670-2.
60. Hovanesian JA, Maloney RK. Treating astigmatism after a free laser in situ keratomileusis cap by rotating the cap. J Cataract Refract Surg. 2005;31:1870-6.
61. Hsu JK, Johnston WT, Read RW, et al. Histopathology of corneal melting associated with diclofenac use after refractive surgery. J Cataract Refract Surg. 2003;29:250-6.
62. Huang 0, Schallhorn se, Sugar A, et al. Phakic intraocular lens implantation for the correction of myopia: a report by the American Academy of Ophthalmology. Ophthalmology. 2009;116(11):2244-58.
63. International Dry Eye WorkShop. The definition and classification of dry eye disease: report of the Definition and Classification Subcommittee of the International Dry Eye WorkShop. Ocul Surf. 2007;5(2):75-92.
64. Ito M, Hori-Komai Y, Toda I, et al. Risk factors and retreatment results of intraoperative flap complications in LASIK. J Cataract Refract Surg. 2004;30:1240-7.
65. Jackson DW, Hamill MB, Koch DD. Laser in situ keratomileusis flap suturing to treat recalcitrant flap striae. J Cataract Refract Surg. 2003;29:264-9.
66. Jacobs JM, Taravella MJ. Incidence of intraoperative flap complications in laser in situ keratomileusis is. J Cataract Refract Surg. 2002;28(1):23-8.
67. Jain V, Mhatre K, Shome D. Flap buttonhole in thin-flap laser in situ keratomileusis: case series and review. Cornea. 2010;29(6):655-8.
68. Jin GJ, Lyle WA, Merkley KH. Late-onset idiopathic diffuse lamellar keratitis after laser in situ keratomileusis. J Cataract Refract Surg. 2005;31:435-7.
69. Kamburoglu G, Ertan A. Epithelial ingrowth after femtosecond laser-assisted in situ keratomileusis. Cornea. 2008;27(10):1122-5.
70. Kamiya K, Shimizu K, Igarashi A, et al. Komatsu M. Four-year follow-up of posterior chamber phakic intraocular lens implantation for moderate to high myopia. Arch Ophthalmol. 2009;127(7):845-50.
71. Kanski JJ, Bowling B (2011, 7th edition). Clinical Ophthalmology: A Systematic Approach. Ch. 4: Dry Eye Disorders. Elsevier.
72. Karp CL, Tuli SS, Yoo SH. Infectious keratitis after LASIK. Ophthalmology. 2003;110:503-10.
73. Katsanevaki VJ, Tsiklis NS, Astyrakakis NI, et al. Intraoperative management of partial flap during LASIK. Ophthalmology. 2005;112:1710-3.
74. Kezirian GM, Stonecipher KG. Comparison of the Intralase femtosecond laser and mechanical keratomes for laser in situ keratomileusis. J Cataract Refract Surg. 2004;30:804-11.
75. Khoueir Z, Haddad NM, Saad A, et al. Traumatic flap dislocation 10 years after LASIK. Case report and literature review. J Fr Ophtalmol. 2013;36(1):82-6.
76. Kim JY, Kim MJ, Kim TI, et al. A femtosecond laser creates a stronger flap than a mechanical microkeratome. Invest Ophthalmol Vis Sci. 2006;47:599-604.
77. Knorz MC. Flap and interface complications in LASIK. Curr Opin Ophthalmol. 2002;13:242-5.
78. Kohnen T. Excimer laser refractive surgery in autoimmune disease (Letter to the Editor). J Cataract Refract Surg. 2006;32:1241.
79. Kohnen T, Knorz MC, Cochener B, et al. AcrySof phakic angle-supported intraocular lens for the correction of moderate- to-high myopia: one-year results of a multicenter European study. Ophthalmology. 2009;116(7):1314-21.
80. Kuo IC, Jabbur NS, O'Brien TP. Photorefractive keratectomy for refractory laser in situ keratomileusis flap striae. J Cataract Refract Surg. 2008;34:330-3.
81. Kuo IC, Lee SM, Hwang DG. Late-onset corneal haze and myopic regression after photorefractive keratectomy (PRK). Cornea. 2004;23:350-5.

82. KurianM, Shetty R, Shetty BK, et al. In vivo confocal microscopic findings of interlamellar stromal keratopathy induced by elevated intraocular pressure. J Cataract Refract Surg. 2006;32:1563-6.
83. Lahners WJ, Hardten DR, Lindstrom RL. Peripheral keratitis following laser in situ keratomileusis. J Refract Surg. 2003;19:671-5.
84. Lemp MA. Advances in understanding and managing dry eye disease. Am J Ophthalmol. 2008;146(3):350-6.
85. Leopoldo Spadea, Valerio Verrecchia. Effectiveness of Scraping and Mitomycin C to Treat Haze After Myopic Photorefractive Keratectomy. Open Ophthalmol J. 2011;5:63-5.
86. Letko E, Price MO, Price FW Jr. Influence of original flap creation method on incidence of epithelial ingrowth after LASIK retreatment. J Refract Surg. 2009;25(11):1039-41.
87. Levinger S, Landau D, Kremer I, et al. Wiping microkeratome blades with sterile 100% alcohol to prevent diffuse lamellar keratitis after laser in situ keratomileusis. J Cataract Refract Surg. 2003;29:1947-9.
88. Levy J, Lapid-Gortzak R, Klemperer I, et al. Herpes simplex virus keratitis after laser in situ keratomileusis. J Refract Surg. 2005;21:400-2.
89. Li Y, Li HY. [Analysis of clinical characteristics and risk factors of corneal melting after laser in situ keratomileusis]. [Chinese]. Zhonghua Yan Ke Za Zhi. 2005;41:330-4.
90. Lichter H, Russell GE, Waring GO III. Repositioning the laser in situ keratomileusis flap at the slit lamp. J Refract Surg. 2004;20:166-9.
91. Lifshitz T, Levy J, Klemperer I, et al. Late bilateral keratoectasia after LASIK in a low myopic patient. J Refract Surg. 2005;2:494-6.
92. Lifshitz T, Levy J, Mahler O, et al. Peripheral sterile corneal infiltrates after refractive surgery. J Cataract Refract Surg. 2005;31:1392-5.
93. Lim T, Yang S, Kim M et al. Comparison of the Intralase femtosecond laser and mechanical microkeratome for laser in situ keratomileusis. Am J Ophthalmol. 2006;141:833-9.
94. Lin JM, Tsai Y, Tseng SH. Spontaneous regression of dense epithelial ingrowth after laser in situ keratomileusis. J Refract Surg. 2005;21:300-2.
95. Linebarger EJ, Hardten DR, Lindstrom RL. Diffuse lamellar keratitis: recognition and management. In: Buratto L, Brint SF (Eds) Custom LASIK surgical techniques and complications. Slack, Thorofare, N.J. 2003;pp745-50.
96. Lois N, Wong D. Pseudophakic retinal detachment. Surv Ophthalmol. 2003;48:467-87.
97. Long Q, Chu R, Zhou X, et al. Correlation between TGF-beta1 in tears and corneal haze following LASEK and Epi-LASIK. J Refract Surg. 2006;22(7):708-12.
98. Luchs JI. Evaluating Flap Complications. Cataract and Refractive Surgery Today 2007. Available Online at http://www.crstoday.com/PDF%20Articles/0907/CRST0907_16.php. 2007.
99. Ly Y, Li HY. Analysis of clinical characteristics and risk factors of corneal melting after laser in situ keratomileusis. Zhonghua Yan Ke Za Zhi. 2005;41:330-4.
100. Mackool RJ, Monsanto VR. Sequential lift and suture technique for post-LASIK corneal striae. J Cataract Refract Surg. 2003;29:785-7.
101. Majmudar PA. LASIK complications. Focal Points: American Academy of Ophthalmology. 2004;12(13):1-14.
102. Marinho A Phakic IOLs: what could go wrong? Ophthalmol Times. 2006;2:29-33.
103. Martinez-Castillo V, Boixadera A, Verdugo A, et al. Rhegmatogenous retinal detachment in phakic eyes after posterior chamber phakic intraocular lens implantation for severe myopia. Ophthalmology 11. 2005;2(4):580-5.
104. Menezo JL, Cisneros A, Cervera M, et al. Iris claw phakic lens immediate and long-term corneal endothelial changes. Eur J Implant Refract Surg. 1994;6:195-9.
105. Menezo JL, Peris-Mart.nez C, Cisneros AL, et al. Phakic intraocular lenses to correct high myopia: Adatomed, STAAR, and Artisan. J Cataract Refract Surg. 2004;30:40-51.
106. Menezo JL, Peris-Martinez C, Cisneros A, et al. Rate of cataract formation in 343 highly myopic eyes after implantation of three types of phakic intraocular lenses. J Refract Surg. 2004;20:317-24.

107. Meyers SM, Ostrovsky MA. Bonner RFA model of spectral filtering to reduce photochemical damage in age-related macular degeneration. Trans Am Ophthalmol Soc. 2004;102:83.
108. Miljanovic B, Trivedi KA, Dana MR, et al. Relation between dietary n-3 and n-6 fatty acids and clinically diagnosed dry eye syndrome in women. Am J Clin Nutr. 2005;82:887-93.
109. Miller DG, Singerman LJ. Vision loss in younger patients: a review of choroidal neovascularization. Optom Vis Sci. 2006;83:316-25.
110. Mohamed TA, Hoffman RS, Fine IH , et al. Post-laser assisted in situ keratomileusis epithelial ingrowth and its relation to pre-treatment refractive error. Cornea. 2011;30(5):550-2.
111. Mohan RR, Hutcheon AE, Choi R, et al. Apoptosis, necrosis, proliferation, and myofibroblast generation in the stroma following LASIK and PRK. Exp Eye Res. 2003;76:71-87.
112. Moilanen JA, Holopainen JM, Helinto M, et al. Keratocyte activation and inflammation in diffuse lamellar keratitis after formation of an epithelial defect. J Cataract Refract Surg. 2004;30:341-9.
113. Moon SJ, Mann PM, Matoba AY. Microsporidial keratoconjunctivitis in a healthy patient with a history of LASIK surgery. Cornea. 2003;22:271-2.
114. Mori T, Yokoyama S, Kojima T, et al. Factors affecting rotation of a posterior chamber collagen copolymer toric phakic intraocular lens. J Cataract Refract Surg. 2012;38(4):568-73.
115. Moshirfar M, Gardiner JP, Schliesser JA, et al. Laser in situ keratomileusis flap complications using mechanical microkeratome versus femtosecond laser: Retrospective comparison. J Cataract Refract Surg. 2010;36(11):1925-33.
116. Moya Calleja T, Iribarne Ferrer Y, Sanz Jorge A, et al. Steroid-induced interface fluid syndrome after LASIK. J Refract Surg. 2009;25(2):235-9.
117. Muller LT, Candal EM, Epstein RJ, et al. Transepithelial phototherapeutic keratectomy/ photorefractive keratectomy with adjunctive Mitomycin-C for complicated LASIK flaps. J Cataract Refract Surg. 2005;31:291-6.
118. Muñoz G, Cardoner A, Albarrán-Diego C, et al. Iris-fixated toric phakic intraocular lens for myopic astigmatism J Cataract Refract Surg. 2012;38(7):1166-75.
119. Narváez J, Chakrabarty A, Chang K. Treatment of epithelial ingrowth after LASIK enhancement with a combined technique of mechanical debridement, flap suturing, and fibrin glue application. Cornea. 2006;25(9):1115-7.
120. Nassaralla BA, McLeod SD, Boteon JE, et al. The effect of hinge position and depth plate on the rate of recovery of corneal sensation following LASIK. Am J Ophthalmol. 2005;139:118-24.
121. Nassaralla BA, McLeod SD, Nassaralla JJ Jr. Effect of myopic LASIK on human corneal sensitivity. Ophthalmology. 2003;110:497-502.
122. Neal RE, Bettelheim FA, Lim C, et al. Alterations in human vitreous humour following cataract extraction. Exp Eye Res. 2005;80:337-47.
123. Netto MV, Chalita MR, Krueger RR. Corneal haze following PRK with Mitomycin C as a retreatment versus prophylactic use in the contralateral eye. J Refract Surg. 2007;23:96-8.
124. Netto MV, Mohan RR, Sinha S, et al. Stromal haze, myofibroblasts, and surface irregularity after PRK. Exp Eye Res. 2006;82:788-97.
125. Netto MV, Mohan RR, Ambrosio R Jr, et al. Wound healing in the cornea: a review of refractive surgery complications and new prospects for therapy. Cornea. 2005;24:509-22.
126. Nordlund MI, Grimm S, Lane S, et al. Pressure induced interface keratitis: a late complication following LASIK. Cornea. 2004;23:225-34.
127. Pallikaris IG, Kymionis GD, Astyrakakis NI. Corneal ectasia induced by laser in situ keratomileusis. J Cataract Refract Surg. 2001;27(11):1796-802.
128. Pechméja J, Guinguet J, Colin J, et al. Severe endothelial cell loss with anterior chamber phakic intraocular lenses J Cataract Refract Surg. 2012;38(7):1288-92.
129. Perez-Santonja JJ, Galal A, Cardona C, et al. Severe corneal epithelial sloughing during laser in situ keratomileusis as a presenting sign for silent epithelial basement membrane dystrophy. J Cataract Refract Surg. 2005;31:1932-7.

130. Petternel V, Koppl CM, Dejaco-Ruhswurm, et al. Effect of accommodation and pupil size on the movement of a posterior chamber lens in the phakic eye. Ophthalmology. 2004;111:325-31.
131. Pflugfelder SC, Beuerman RW, Stern ME, (Eds). Dry Eye and Ocular Surface Disorders. New York: Informa Healthcare; 2004.
132. Pop M, Payette Y. Initial results of endothelial cell counts after Artisan Lens for Phakic Eyes. Ophthalmology. 2004;111:309-17.
133. Pop M, Payette Y. Risk factors for night vision complaints after LASIK for myopia. Ophthalmology. 2004;111:3-10.
134. Rad AS, Jabbarvand M, Saifi N. Progressive keratoectasia after laser in situ keratomileusis. Journal of refractive surgery. 2004;20(5 Suppl):S718-22.
135. Rajan MS, et al. Effect of exogenous keratinocyte growth factor on corneal epithelial migration after photorefractive keratectomy. J Cataract Refract Surg. 2004;30:2200-6.
136. Rajan MS, et al. Effects of ablation diameter on long-term refractive stability and corneal transparency after photorefractive keratectomy. Ophthalmology. 2006;113:1798-806.
137. Randleman JB. Post-laser in-situ keratomileusis ectasia: current understanding and future directions. Current opinion in ophthalmology. 2006;17(4):406-12.
138. Randleman JB. Evaluating risk factors for ectasia: what is the goal of assessing risk? Journal of refractive surgery. 2010;26(4):236-7.
139. Randleman JB, Banning CS, Stulting RD. Corneal ectasia after hyperopic LASIK. J Refract Surg. 2007;2:98-102.
140. Randleman JB, Russell B, Ward MA, et al. Risk factors and prognosis for corneal ectasia after LASIK. Ophthalmology. 2003;110:267-75.
141. Randleman JB, Trattler WB, Stulting RD. Validation of the Ectasia Risk Score System for preoperative laser in situ keratomileusis screening. Am J Ophthalmol. 2008;145:813-8.
142. Randleman JB, Woodward M, Lynn MJ, et al. Risk assessment for ectasia after corneal refractive surgery. Ophthalmology. 2008;115:37-50.
143. Rao SN, Epstein RJ. Early onset keratoectasia following laser in situ keratomileusis: case report and literature review. J Refract Surg. 2002;18:177-84.
144. Rapuano CJ. Management of Epithelial Ingrowth After Laser In Situ Keratomileusis on a Tertiary Care Cornea Service. Cornea. 2010;29(3):307-13.
145. Ravalico G, Michieli C, Vattovani O, et al. Retinal detachment after cataract extraction and refractive lens exchange in highly myopic patients. J Cataract Refract Surg. 2003;29:39-44.
146. Rezende RA, Uchoa UC, Cohen EJ, et al. Complications associated with anterior basement membrane dystrophy after laser in situ keratomileusis. J Cataract Refract Surg. 2004;30:2328-31.
147. Ripandelli G, Scassa C, Parisi V, et al. Cataract surgery as a risk factor for retinal detachment in very highly myopic eyes. Ophthalmology. 2003;110:2355-61.
148. Ruiz-Moreno JM, Alio JL. Incidence of retinal diseases following refractive surgery in 9,239 eyes. J Refract Surg. 2003;19:534-47.
149. Ruiz-Moreno JM, de la Vega C, Ruiz-Moreno O, et al. Choroidal neovascularization in phakic eyes with anterior chamber intraocular lenses to correct high myopia. J Cataract Refract Surg. 2003;29:270-4.
150. Ruiz-Moreno JM, Montero J, de la Vega C, et al. Retinal detachment in myopic eyes after phakic intraocular lens implantation. J Refract Surg. 2006;22:247-52.
151. Ruiz-Moreno JM, Montero JA, de la Vega C, et al. Macular choroidal neovascularization in myopic eyes after phakic intraocular lens implantation. J Refract Surg. 2006;22:689-94.
152. Saad A, Gatinel D. Bilateral corneal ectasia after laser in situ keratomileusis in patient with isolated difference in central corneal thickness between eyes. J Cataract Refract Surg. 2010;36:1033-5.
153. Salaroli CHR, Li Y, Huang D. High-resolution optical coherence tomography visualization of LASIK flap displacement. J Cat Refract Surg. 35(9):1640-2.
154. Salib GM, McDonald MB, Smolek M. Safety and efficacy of cyclosporine 0.05% drops versus unpreserved artificial tears in dry-eye patients having laser in situ keratomileusis. J Cataract Refract Surg. 2006;32(5):772-8.

155. Salomão MQ, Ambrósio R Jr, Wilson SE (2009). Dry eye associated with laser in situ keratomileusis: Mechanical microkeratome versus femtosecond laser. J Cataract Refract Surg 35(10):1756-60. doi: 10.1016/j.jcrs.2009.05.032.
156. Sanchez-Galeana CA, Smith RJ, Sanders DR, et al. Lens opacities after posterior chamber phakic intraocular lens implantation. Ophthalmology. 2003;110:781-5.
157. Sanders D, Vukich JA. Comparison of implantable collamer lens (ICL) and laser-assisted in situ keratomileusis (LASIK) for low myopia. Cornea. 2006;25:1139-46.
158. Sanders DR. ICL in Treatment of Myopia Study Group. Postoperative inflammation after implantation of the implantable contact lens. Ophthalmology. 2003;110:2335-41.
159. Sanders DR. Matched population comparison of the Visian Implantable Collamer Lens and standard LASIK for myopia of –3.00 to –7.88 Diopters. J Refract Surg. 2007;23:537-53.
160. Sanders DR. Anterior subcapsular opacities and cataracts 5 years after surgery in the Visian Implantable Collamer Lens FDA trial. J Refract Surg. 2008;24(6):566-70.
161. Sanders DR, Doney K, Poco M. ICL in Treatment of Myopia Study Group. US FDA clinical trial of the Implantable Collamer Lens (ICL) for moderate to high myopia: three-year follow-up. Ophthalmology. 2004;111:1683-92.
162. Sanders DR, Schneider D, Martin R, et al. Toric Implantable Collamer Lens for moderate to high myopic astigmatism. Ophthalmology. 2007;114:54-61.
163. Sanders DR, Vukich JA, Doney K, et al. Implantable Contact Lens in Treatment of Myopia Study Group. U.S. Food and Drug Administration clinical trial of the Implantable Contact Lens for moderate to high myopia. Ophthalmology. 2003;110:255-66.
164. Sarver EJ, Sanders DR, Vukich JA. Image quality in myopic eyes corrected with laser in situ keratomileusis and phakic intraocular lens. J Refract Surg. 2003;19:397-404.
165. Schallhorn SC, Kaupp SE, Tanzer DJ, et al. Pupil size and quality of vision after LASIK. Ophthalmology. 2003;110:1606-14.
166. Seiler T, Quurke AW. Iatrogenic keratoectasia after LASIK in a case of forme fruste keratoconus. J Cataract Refract Surg. 1998;24:1007-9.
167. Seiler T, Wollensak J. Complications of laser keratomileusis with the excimer laser. Klin Monatsbl Augenheilkd. 1992;200:642-53.
168. Singhal S, Sridhar MS, Garg P. Bilateral peripheral infiltrative keratitis after LASIK. J Refract Surg. 2005;21:402-4.
169. Smith RJ, Maloney RK. Diffuse lamellar keratitis. A new syndrome in lamellar refractive surgery. Ophthalmology. 1998;105:1721-6.
170. Smith RJ, Maloney RK. Laser in situ keratomileusis in patients with autoimmune disease. J Cataract Refract Surg. 2006;32:1292-5.
171. Solomon R, Donnenfeld ED, Azar DT, et al. Infectious keratitis after laser in situ keratomileusis: results of an ASCRS survey. J Cataract Refract Surg. 2003;29:2001-6.
172. Solomon R, Donnenfeld ED, Perry HD, et al. Slitlamp stretching of the corneal flap after laser in situ keratomileusis to reduce corneal striae. J Cataract Refract Surg. 2003;29:1292-6.
173. Solomon R, Donnenfeld ED, Perry HD, et al. Methicillin-resistant Staphylococcus aureus infectious keratitis following refractive surgery. Am J Ophthalmol. 2007;143(4):629-34.
174. Steinert RF, Ashrafzadeh A, Hersh PS. Results of phototherapeutic keratectomy in the management of flap striae after LASIK. Ophthalmology. 2004;111:740-6.
175. Stern ME, Pflugfelder Sc. Inflammation in dry eye. Ocul Surf. 2004;2(2):124-30.
176. Stojanovic A, Ringvold A, Nitter T. Ascorbate prophylaxis for corneal haze after photorefractive keratectomy. J Refract Surg. 2003;19:338-43.
177. Stonecipher K, Ignacio TS, Stonecipher M. Advances in refractive surgery: microkeratome and femtosecond flap creation in relation to safety, efficacy, predictability, and biomechanical stability. Curr Opin Ophthalmol. 2006;17:368-72.

178. Stulting RD, Jolm ME, Maloney RK, et al. U.S. Verisyse Study Group. Three-year results of Artisan/Verisyse phakic intraocular lens implantation. Results of the United States Food and Drug Administration clinical trial. Ophthalmology. 2008;115(3):464-72.
179. Stulting RD, Randleman JB, Couser JM, et al. The epidemiology of diffuse lamellar keratitis. Cornea. 2004;23:680-8.
180. Tabbara KF, Kotb AA. Risk factors for corneal ectasia after LASIK. Ophthalmology. 2006;113(9):1618-22.
181. Tahzib NG, Bootsma SJ, Eggink FA, et al. Functional outcomes and patient satisfaction after laser in situ keratomileusis for correction of myopia. J Cataract Refract Surg. 2005;31:1943-51.
182. Tehrani M, Dick H. Short-term follow-up after implantation of a foldable iris-fixated intraocular lens in phakic eyes. Ophthalmology. 2005;112:2189-95.
183. Tekwani NH, Huang D. Risk factors for intraoperative epithelial defect in laser in-situ keratomileusis. Am J Ophthalmol. 2002;134(3):311-6.
184. Titiyal JS, Sharma N, Mannan R, et al. Iris-fixated intraocular lens implantation to correct moderate to high myopia in Asian-Indian eyes: Five-year results. J Cataract Refract Surg. 2012;38(8):1446-52.
185. Toda I, Asano-Kato N, Hori-Komai, Tsubota K. Laser-assisted in situ keratomileusis for patients with dry eye. Arch Ophthalmol. 2002;120(8):1024-8.
186. Torun N, Bertelmann E, Klamann MKJ, et al. Posterior chamber phakic intraocular lens to correct myopia: Long-term follow-up. J Cataract Refract Surg (article in press); 2013.
187. Tosi GM, Casprini F, Malandrini A, et al. Phacoemulsification without intraocular lens implantation in patients with high myopia: long-term results. J Cataract Refract Surg. 2003;29:1127-31.
188. Toso A, Morselli S. Visual and aberrometric outcomes in eyes with an angle-supported phakic intraocular lens. J Cataract Refract Surg. 2012;38(9):1590-4.
189. Ţuru L, Alexandrescu C, Stana D, et al. Dry eye disease after LASIK. J Med Life. 2012;5(1):82-4.
190. Varley GA, Huang D, Rapuano CJ, et al. LASIK for hyperopia, hyperopic astigmatism, and mixed astigmatism: a report by the American Academy of Ophthalmology. Ophthalmology. 2004;111:1604-17.
191. Waring GO III. Epithelial ingrowth after laser in situ keratomileusis. Am J Ophthalmol. 2001;131(3):402-3.
192. Weisenthal RW, Salz J, Sugar A, et al. Photorefractive keratectomy for treatment of flap complications in laser in situ keratomileusis. Cornea. 2003;22(5):399-404.
193. Winkler von Mohrenfels C, Salgado JP, et al. [Keratoectasia after refractive surgery]. Klinische Monatsblatter fur Augenheilkunde. 2011;228(8):704-11.
194. Wroblewski KJ, Pasternak JF, Bower KS, et al. Infectious keratitis after photorefractive keratectomy in the United States Army and Navy. Ophthalmology. 2006;113(4):520-5.

Step Five

Case Study

CHAPTER 9

Case Study

INTRODUCTION

Refractive surgery candidate should be evaluated thoroughly in order to:

1. Check his/her candidacy for the refractive surgery.
2. Exclude predisposing risk factors for post PRT ectasia.
3. Chose the best option of refractive surgery.
4. Avoid intra- and postoperative complications as much as possible.

This can be done by full clinical approach as described in chapter 7 in addition to conducting proper investigations and skilful interpretation of results.

In our case study, only positive clinical findings will be presented.

READING AND INTERPRETING CORNEAL TOMOGRAPHY

Key Points

1. Do not "normalize" a topographic and/or tomographic pattern by considering other patient's information.
2. Review topography and tomography as stand-alone entity and then include other data in your overall evaluation.
3. Compare findings in both eyes.
4. Compare TA with MA.

Steps of the Study

1. The Qualification Step: it aims at looking for abnormal findings and risk factors by:
   a. Displaying the four composite maps.
   b. Studying each map separately.
   c. Studying thickness profiles.
   d. Qualification of corneal parameters. This includes: quality specification (QS); Q-value; K-readings; astigmatism; parameters of thickness and coordinates at pupil centre, apex and thinnest location; anterior chamber depth, angle and volume; and scotopic pupil diameter.
2. The Quantitative Step: it aims at choosing the best treatment decision by following the rules mentioned in chapter 6.

3. Discussion Step: it aims at discussing all findings and the proper treatment options.

READING AND INTERPRETING WAVEFRONT

Key Points

1. Do not "normalize" a wavefront pattern by considering other patient's information.
2. Review wavefront as stand-alone entity and then include other data in your overall evaluation.
3. Compare findings in both eyes.
4. Compare findings with topography and tomography.
5. Compare objective refraction measured by wavefront with subjective refraction.

Select your Goal

Before performing wavefront mapping for the candidate, a question should be asked: what is it for?

1. When the cornea is irregular and a customized ablation is required; *this is for treatment.*
2. When the best spectacle corrected visual acuity is not optimal; *this is for diagnosis and treatment.*
3. When the patient suffers from symptoms of HOAs (halos, ghost images, etc.), despite good visual acuity; *this is for diagnosis and treatment.*

Steps of the Study

1. The Qualification Step: it aims at estimating types and severity of aberrations by studying the:
   a. PFS.
   b. RMS related to HOAs.
   c. Zernike Coefficients.
   d. Coma, spherical and trefoil aberrations.
2. The Quantitative Step: it aims at taking the decision of the type of treatment by evaluating:
   a. RMS related to HOAs.
   b. Zernike Coefficients.
3. Discussion Step: In our case study, whenever wavefront analysis is needed, this step will be merged with the third step of interpreting tomography.

CASE 1

A 20-year-old male has a stable refractive error with no other complaints. Eye examination is normal. His MR and VA are shown in Table 9.1.1. His CR is shown in Table 9.1.2.

TABLE 9.1.1 Manifest Refraction and Visual Acuity

	UDVA	*Sph*	*Cyl*	*Axis*	*CDVA (G)*	*CDVA (G+PH)*
OD	0.1	−3.0	−1.5	180	1.0	1.2
OS	0.1	−3.0	−1.0	180	1.0	1.2

UDVA= uncorrected distance visual acuity; CDVA (G)= corrected distance visual acuity (by glasses); CDVA (G+PH)= corrected distance visual acuity (by glasses and pin hole)

TABLE 9.1.2 Cycloplegic Refraction

	Sph	*Cyl*	*Axis*
OD	−2.75	−2	170
OS	−2.75	−1.5	10

Figure 9.1.1 represents corneal tomography of the right eye, which will be studied as an example.

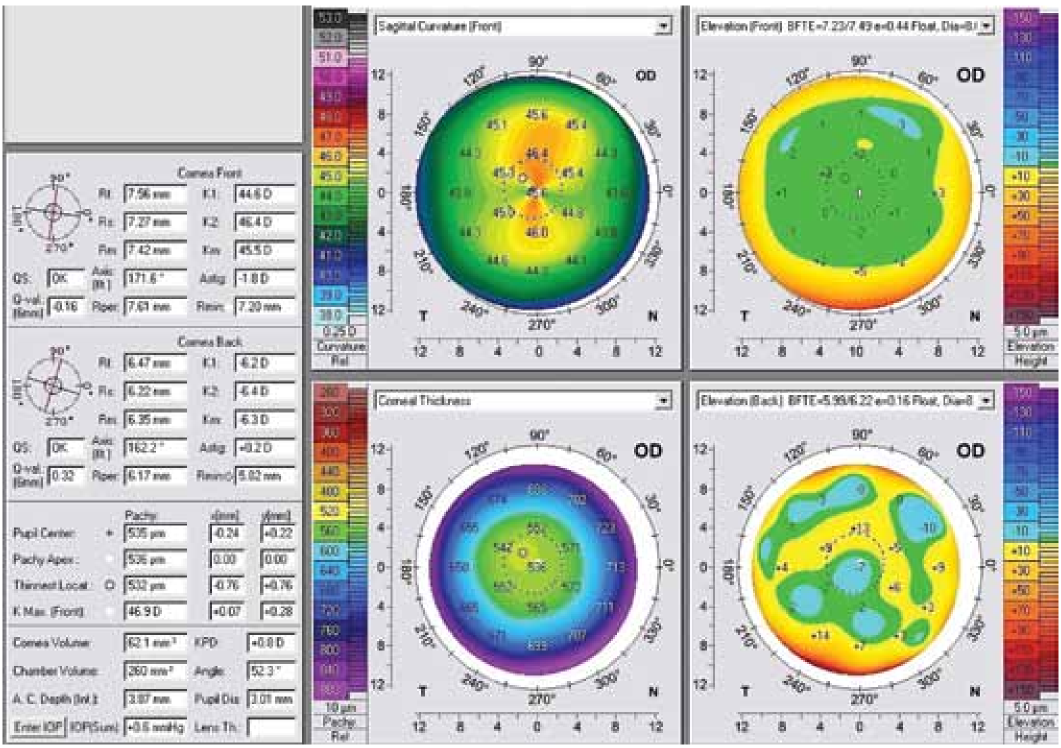

Fig. 9.1.1 The four composite maps.

1. **The Qualification Step:**
   a. In a general look, the sagittal curvature map has a SB pattern oriented vertically indicating WTR astigmatism. Nothing seems abnormal in the elevation and pachymetry maps.
   b. Studying single maps:
      i. The anterior sagittal curvature map (Fig. 9.1.2) shows an almost SB with neither SRAX nor significant inferior-superior difference.
      ii. The anterior elevation map:
         1. In BFS mode (Fig. 9.1.3): almost symmetric sandy watch pattern.
         2. In BFTE mode (Fig. 9.1.4): normal values within the central 5 mm circle.
      iii. The posterior elevation map:
         1. In BFS mode (Fig. 9.1.5): asymmetric sandy watch pattern.
         2. In BFTE mode (Fig. 9.1.6): normal values within the central 5 mm circle.
      iv. The pachymetry map (Fig. 9.1.7) shows a normal shape in spite of the superior displacement of the thinnest location (white arrow). There is no significant inferior superior difference.
      v. Thickness profiles (Fig. 9.1.8) show normal slopes with normal average (0.9).

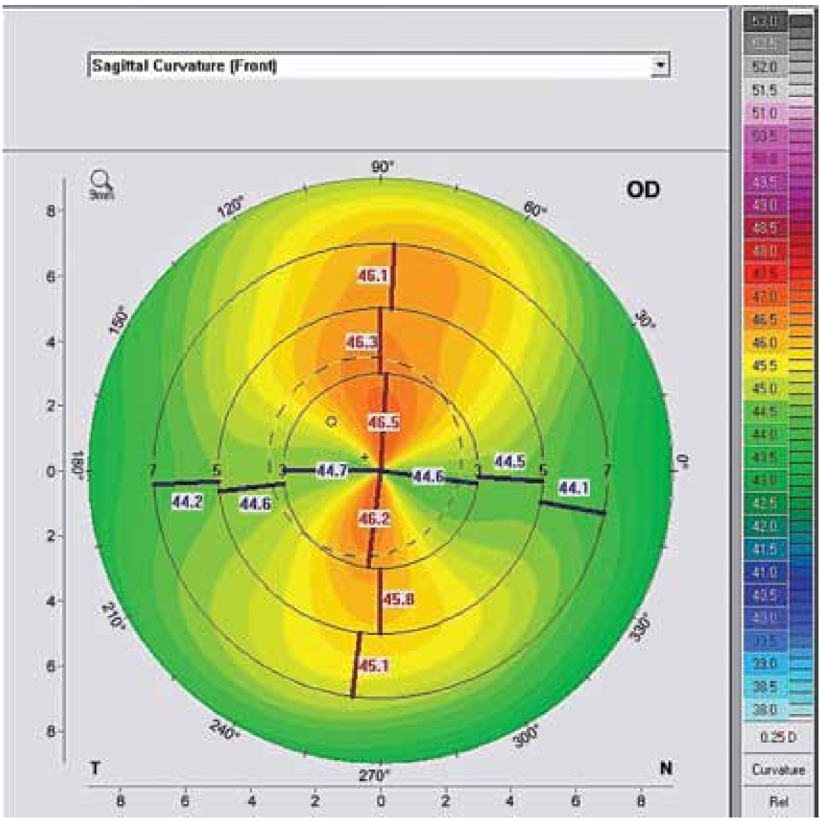

Fig. 9.1.2 The anterior curvature sagittal map. SB pattern.

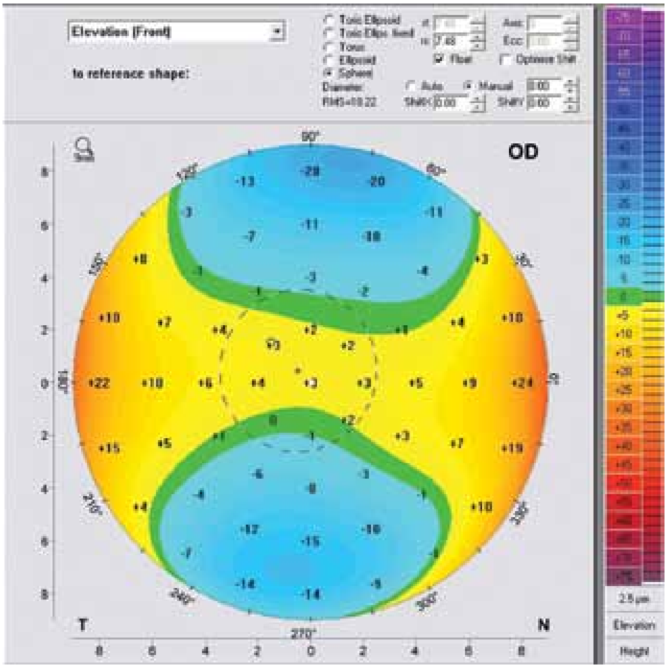

Fig. 9.1.3 The anterior elevation map with BFS reference body. Sandy watch pattern.

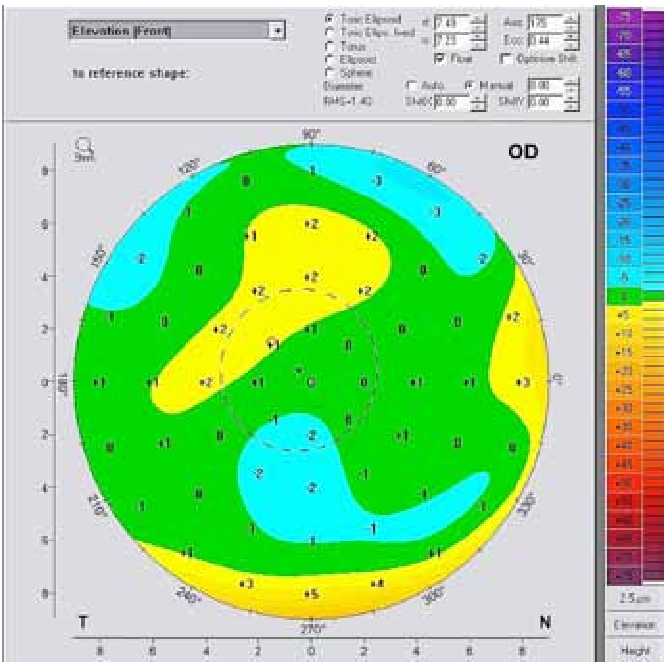

Fig. 9.1.4 The anterior elevation map with BFTE reference body.

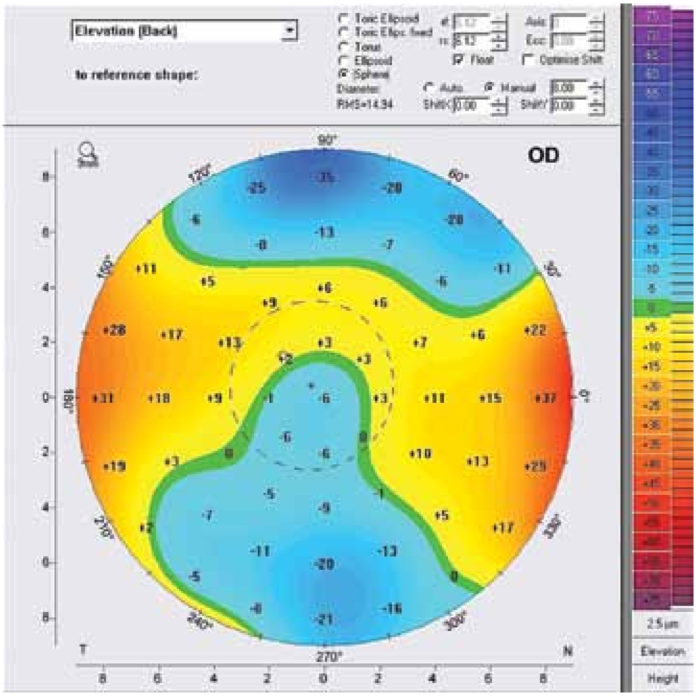

Fig. 9.1.5 The posterior elevation map with BFS reference body.

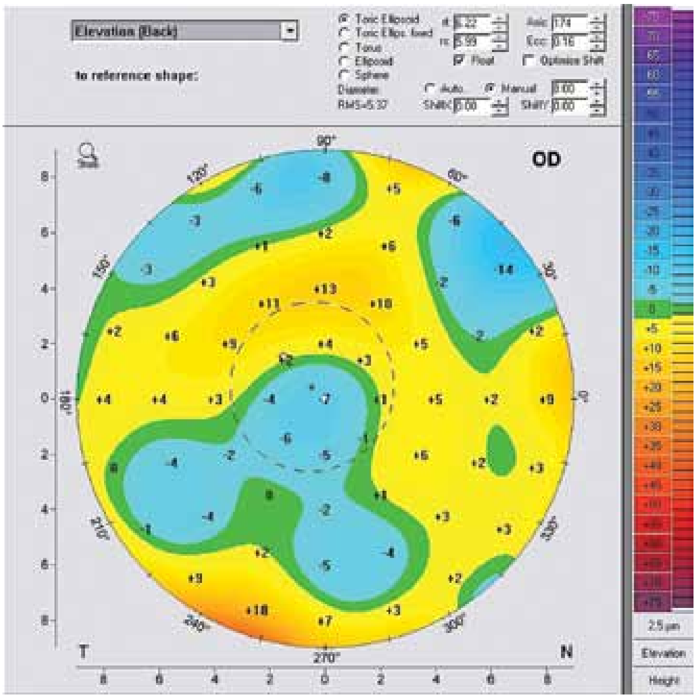

Fig. 9.1.6 The posterior elevation map with BFTE reference body.

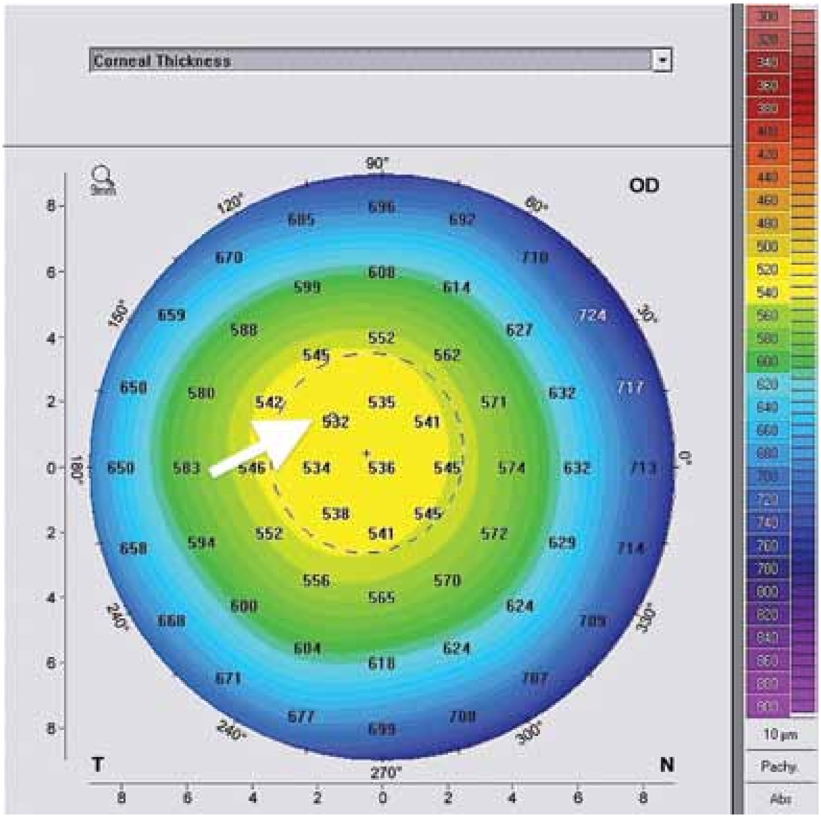

Fig. 9.1.7 The pachymetry map. The white arrow points at the superiorly displaced thinnest location.

c. Qualification of values (Fig. 9.1.9):
   i. QS is OK.
   ii. K readings including K-max are <48 D.
   iii. K-max-steep K is < 1 D.
   iv. Astigmatism is < 6 D.
   v. Thickness at the thinnest location is >500 µm.
   vi. Pachy-Thinnest difference in thickness is <10 µm.
   vii. *Y*-coordinate of the thinnest location is positive, which means that it is displaced upwards (rare but normal).
   viii. ACD, ACA and ACV are normal.
   ix. Mesopic pupil diameter is 3 mm.
   x. Pupil coordinates indicate almost central pupil and significant angle Kappa.

2. **The Quantitative Step:** Since, there is no significant difference between MR and CR, the former will be quantified.
   a. Thickness concepts:
      i. RSB Law 1: According to this law, RSB should be at least 532 x 55% = 292.6 µm (>270 µm); therefore, the allowed AD = 532 – 100 (flap) – 292.6 = 139.4 µm.

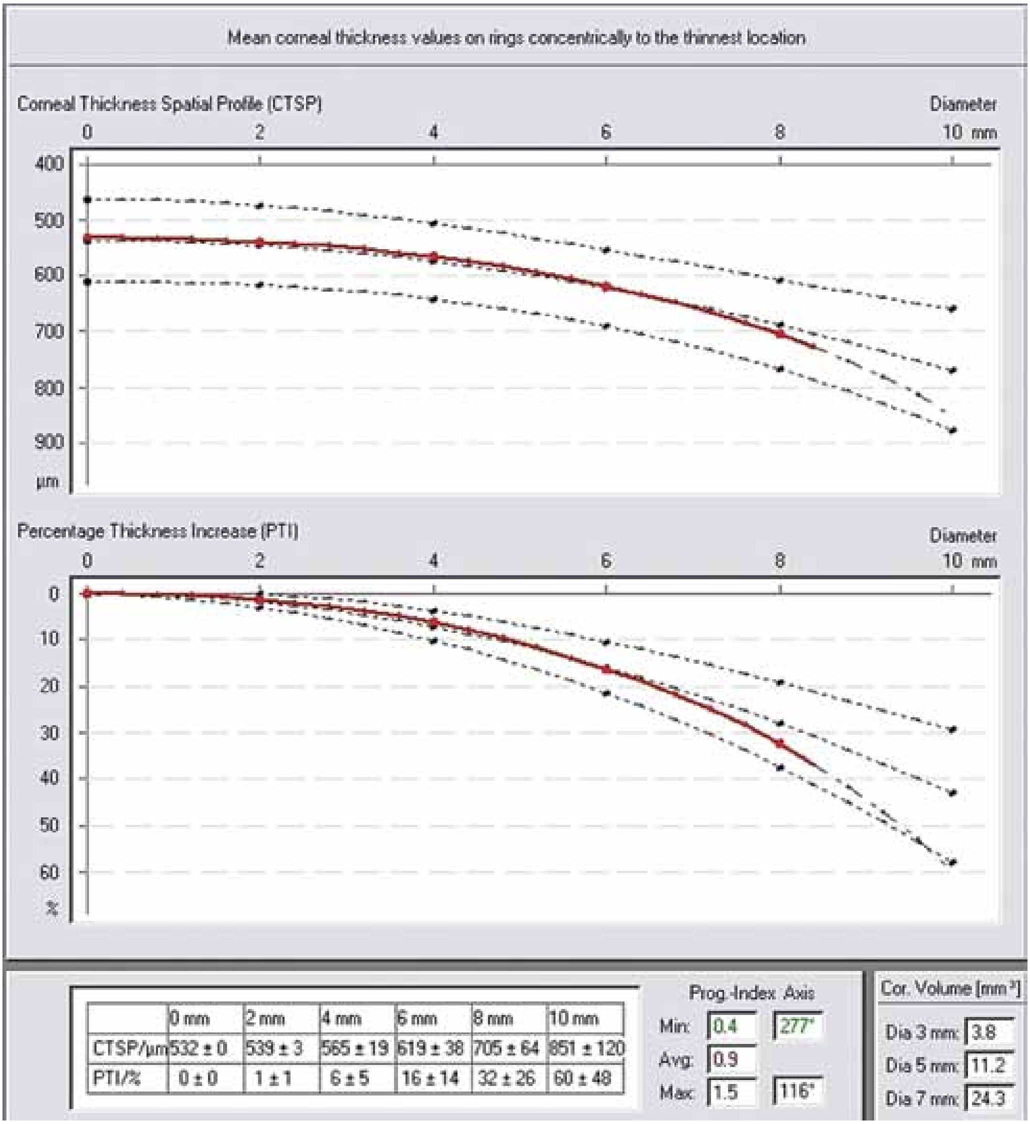

Fig. 9.1.8 Thickness profiles.

ii. RSB Law 2: According to this law, the AD should be at most 532 x 20% = 106.4 µm; therefore, the RSB = 532 – 100(flap) – 106.4 µm = 325.6 µm
iii. RSB Law 3: According to this law, the actual AD (6.5 mm OZ) is: AD = (3 + 1.5) x 15 = 67.5 µm; therefore the actual RSB = 532 – 100 – 67.5 = 364.5 µm.
iv. RSB Law 4: The most conservative in this case is RSB law 3.
v. RSB Law 5: If SA is planned, the AD = (3 + 1.5) x 15 = 67.5 µm (<80 µm) and the RSB = 532 - 67.5 = 464.5 µm (>400 µm).
vi. Table 9.1.3 summarizes the thickness concepts.

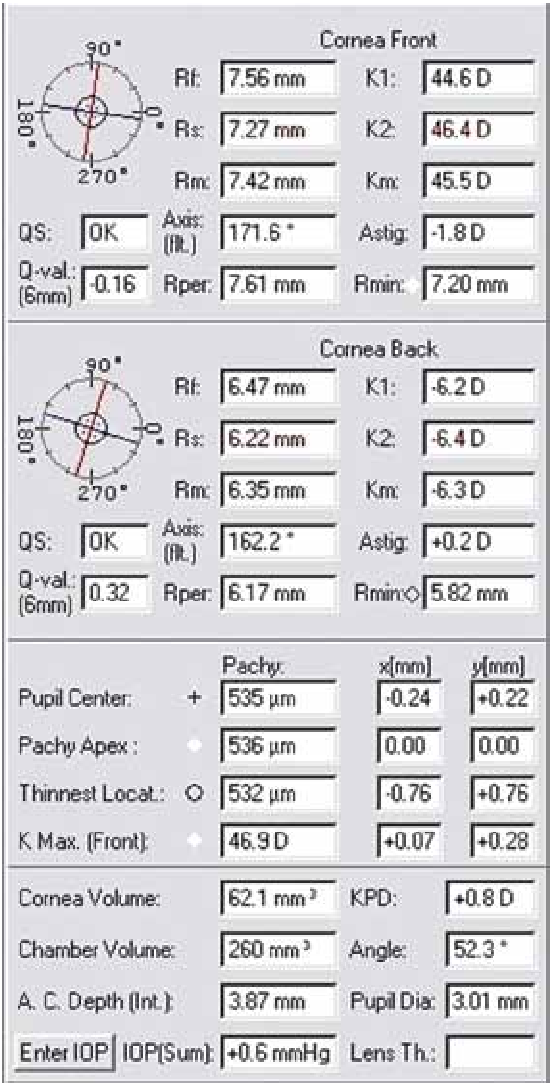

Fig. 9.1.9 Corneal parameters.

TABLE 9.1.3 Thickness Concepts

RSB Law		*RSB (µm)*	*AD (µm)*
LA	1	At least 292.6	139.4
	2	325.6	At most 106.4
	3	364.5	67.5
	4	364.5	67.5
SA	5	414.5	67.5

RSB = residual stromal bed for a 100 µm flap; AD= ablation depth

b. K-readings and Astigmatism Concept:
   i. According to RSB laws, the refractive error can be completely corrected.
   ii. It is a myopic astigmatism case; therefore, the myopic astigmatism law should be used (Table 9.1.4).

TABLE 9.1.4 Final K

Refractive error	*Original K*	*Astigmatic correction*	*Myopic correction*	*Final K*
−3 sph	K_f = 44.6 D	(0) K_f = 44.6 D	(3 x 0.75 = 2.25 D) K_f = 44.6 – 2.25 = 42.35 D	42.7 D in average
−1.5 cyl	K_s = 46.4 D	(1.5 x 0.75 = 1.13 D) K_s = 46.4 – 1.13 = 45.27 D	(3 x 0.75 = 2.25 D) K_s = 45.27 – 2.25 = 43.02 D	

K_f : flat K
K_s : steep K

DISCUSSION

The patient is still young and eye examination is normal; therefore, RLE option is excluded. The refractive error is moderate; the spherical equivalent is < 8 D of myopia; therefore, both PRT and PIOL options are on table.

According to tomography, thickness and K-readings concepts, the case is straight forward for PRT. At the same time, ACD, ACA and pupil centre coordinates are suitable for a PIOL. In my opinion, PRT is better than PIOL implantation in this case, since the refractive error is small and does not worth an intraocular surgery.

If PRT is indicated, the MR will be used since the manifest astigmatism (MA) is more accurate than the cycloplegic astigmatism (CA) and there is little difference between manifest sphere (MS) and cycloplegic sphere (CS). In general, up to 0.5 D difference between MS and CS is reasonable due to the cycloplegic effect and even if the patient was overcorrected for 0.5 D, his young age enables him to compensate for this hyperopic shift by accommodation.

If PRT is indicated, both LA and SA are suitable since the refractive error is small and thickness is suitable. In either case, aspheric profile should be used. Decentration is not necessary despite significant angle kappa since the case is myopia with < 2 D myopic astigmatism. Compensation for cyclotorsion is also recommended since the astigmatism is > 1 D.

N.B: Scotopic pupillometry was performed and found 5.5 mm; therefore, a 6 mm OZ can be used to save tissue.

CASE 2

A 20-year-old female has a stable refractive error with no complaints. Eye examination is normal. Her MR and VA are shown in Table 9.2.1. Her CR is shown in Table 9.2.2.

TABLE 9.2.1 Manifest Refraction and Visual Acuity

	UDVA	*Sph*	*Cyl*	*Axis*	*CDVA (G)*	*CDVA (G+PH)*
OD	0.04	−6.0	−2	180	0.9	1.0
OS	0.04	−7.0	−1.0	180	0.8	1.0

UDVA= uncorrected distance visual acuity; CDVA (G)= corrected distance visual acuity (by glasses); CDVA (G+PH)= corrected distance visual acuity (by glasses and pin hole)

TABLE 9.2.2 Cycloplegic Refraction

	Sph	*Cyl*	*Axis*
OD	−5.5	−2.25	175
OS	−6.5	−1.5	13

Figure 9.2.1 represents corneal tomography of the left eye which will be studied as an example.

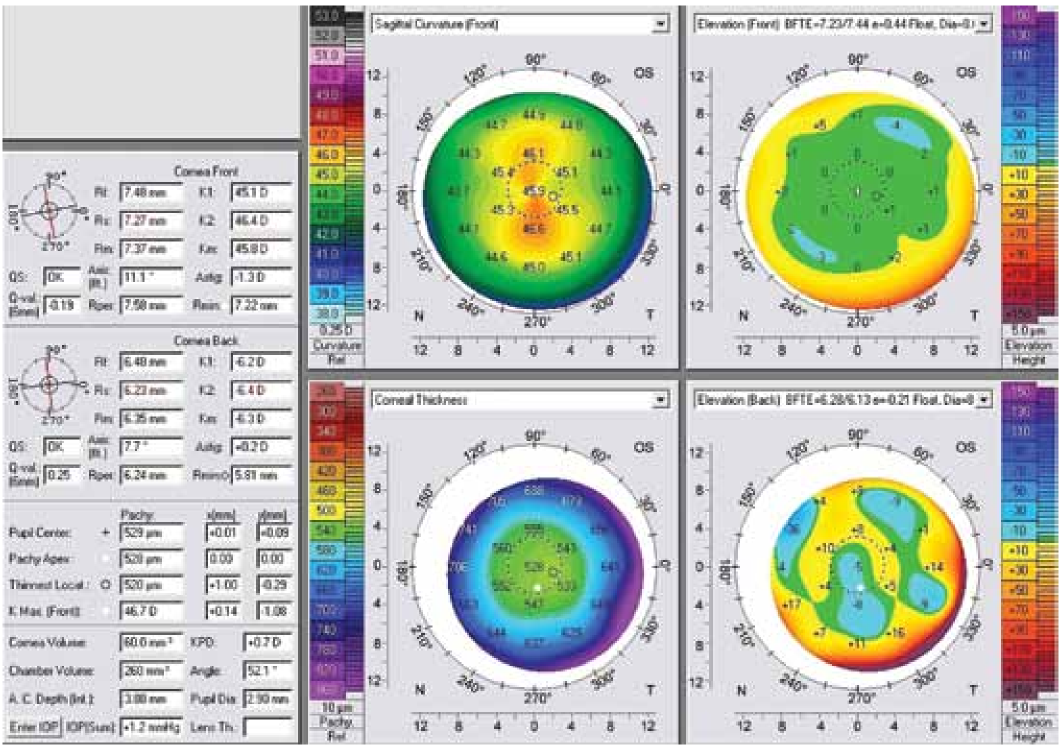

Fig. 9.2.1 The four composite maps.

1. **The Qualification Step:**
   a. In a general look, the sagittal curvature map has a vertical SB indicating WTR astigmatism. Nothing seems abnormal in the elevation and the pachymetry maps.
   b. Studying single maps:
      i. The anterior curvature sagittal map (Fig. 9.2.2) shows an almost SB with neither SRAX nor significant inferior-superior difference.
      ii. The anterior elevation map:
         1. In BFS mode (Fig. 9.2.3): Almost symmetric sandy watch pattern.
         2. In BFTE mode (Fig. 9.2.4): Normal values within the central 5 mm circle.
      iii. The posterior elevation map:
         1. In BFS mode (Fig. 9.2.5): irregular pattern.
         2. In BFTE mode (Fig. 9.2.6): normal values within the central 5 mm circle.
      iv. The pachymetry map (Fig. 9.2.7) shows a normal shape in spite of the temporal displacement of the thinnest location (white arrow). There is no significant inferior superior difference.
      v. Thickness profiles (Fig. 9.2.8): The red curves take a normal slope although they deviate after the 6 mm circle. The average is normal (1.0).

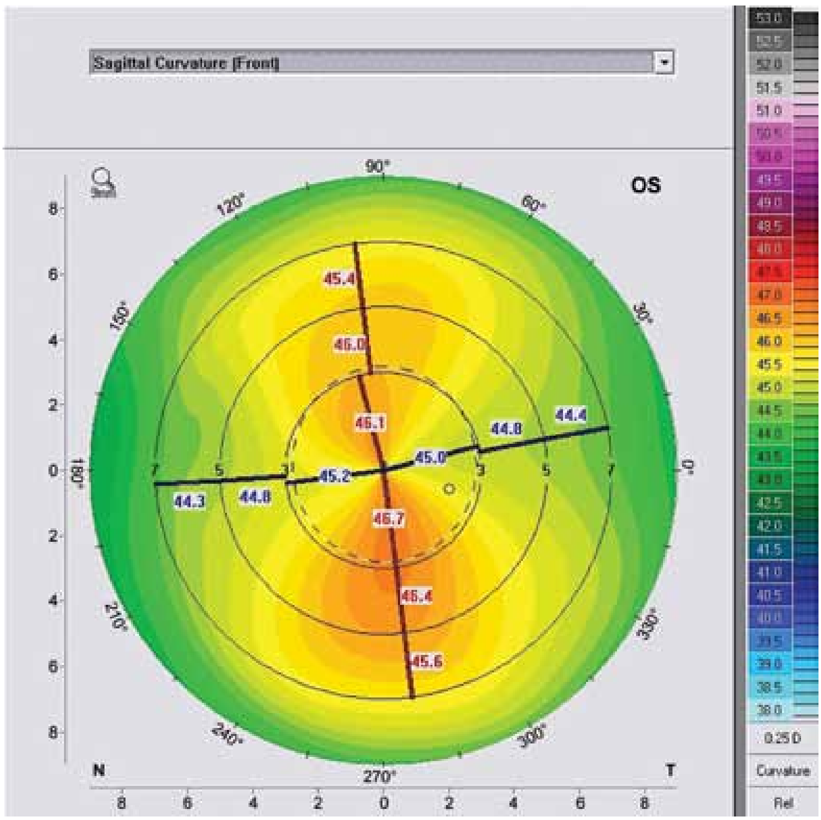

Fig. 9.2.2 The anterior curvature sagittal map. SB pattern.

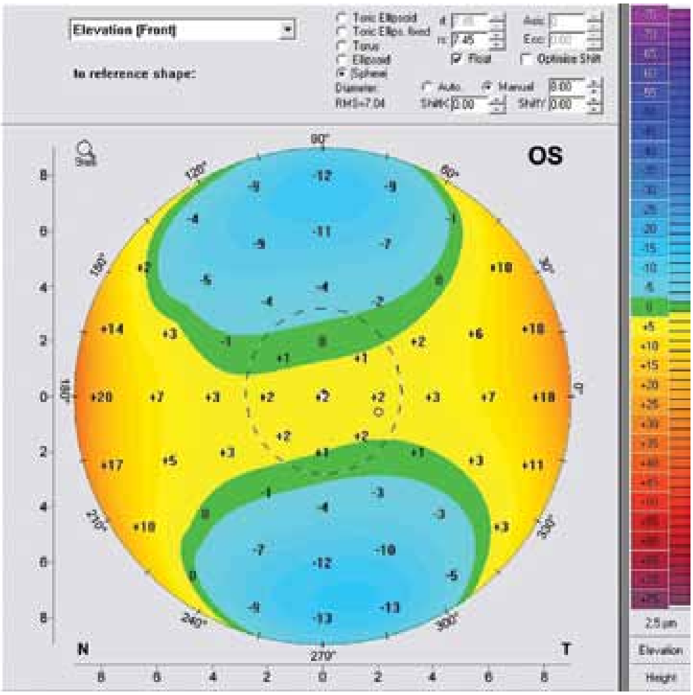

Fig. 9.2.3 The anterior elevation map with BFS reference body. Sandy watch pattern.

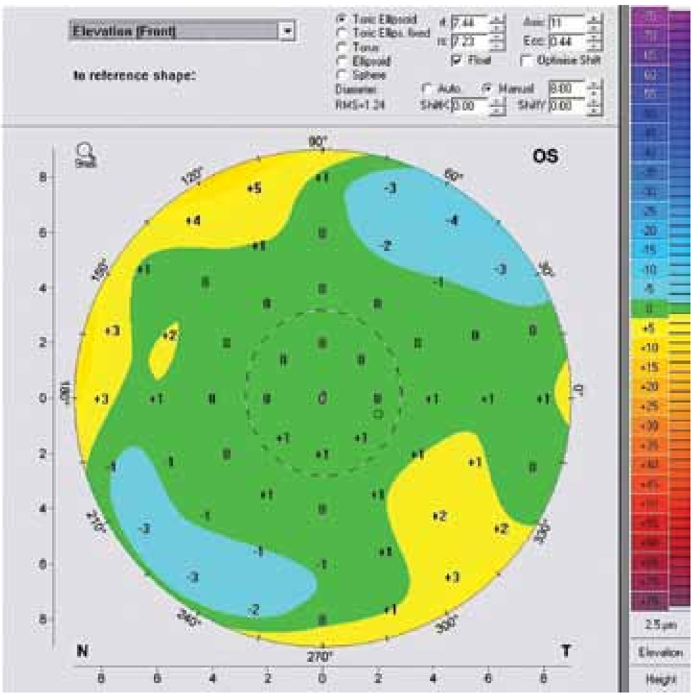

Fig. 9.2.4 The anterior elevation map with BFTE reference body.

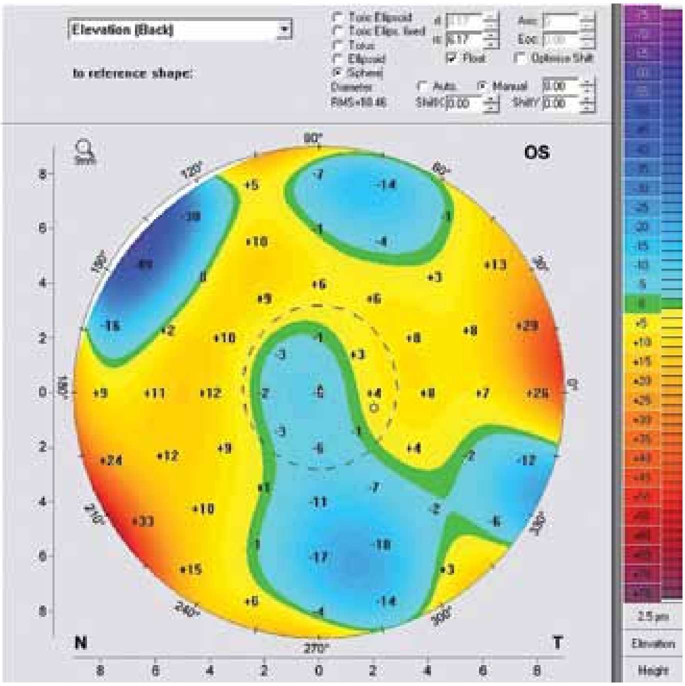

Fig. 9.2.5 The posterior elevation map with BFS reference body. Tongue-like extension.

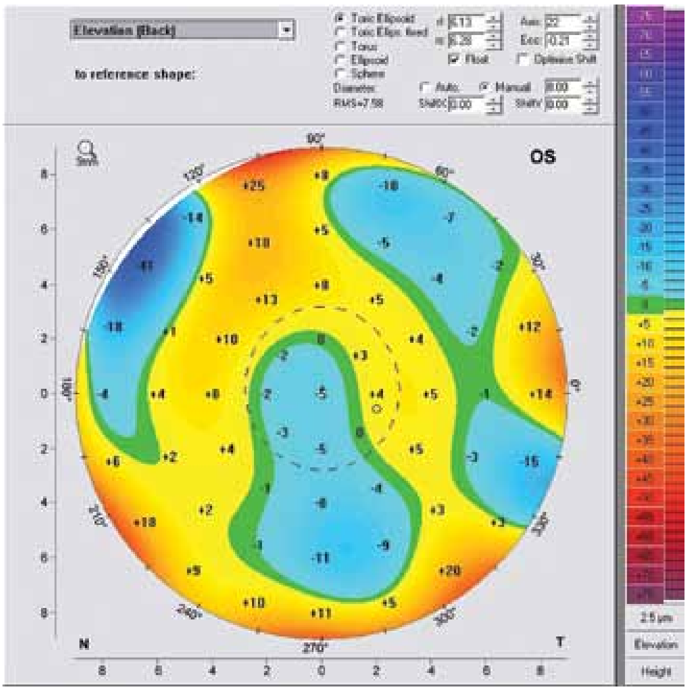

Fig. 9.2.6 The posterior elevation map with BFTE reference body.

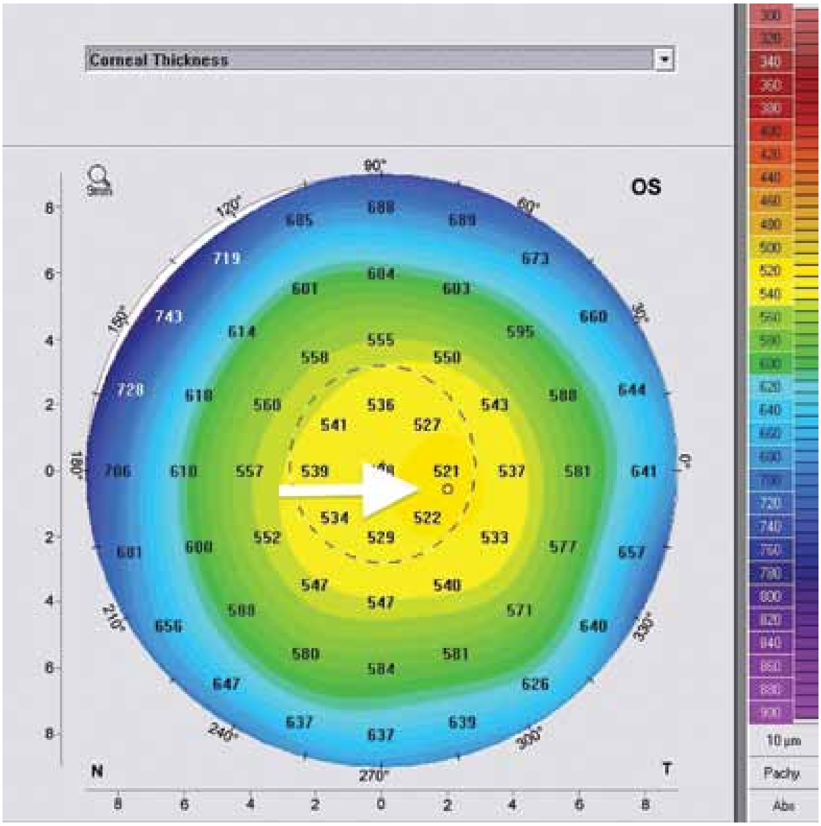

Fig. 9.2.7 The pachymetry map. The white arrow points at the horizontally displaced thinnest location.

c. Qualification of values (Fig. 9.2.9):
   i. QS is OK.
   ii. K readings including K-max are <48 D.
   iii. K-max-steep K is < 1 D.
   iv. Astigmatism is < 6 D.
   v. Thickness at the thinnest location is >500 µm.
   vi. Pachy-Thinnest difference in thickness is <10 µm.
   vii. *Y*-coordinate of the thinnest location is less than –500 µm (–290 µm).
   viii. ACD, ACA and ACV are normal.
   ix. Mesopic pupil diameter is 2.90 mm.
   x. Pupil coordinates indicate central pupil and insignificant angle Kappa.

2. **The Quantitative Step:**
   a. Thickness concepts:
      i. RSB Law 1: According to this law, RSB should be at least 520 x 55% = 286 µm (>270 µm); therefore, the allowed AD = 520 – 100 (flap) – 286 = 134 µm.
      ii. RSB Law 2: According to this law, the AD should be at most 520 x 20% = 104 µm; therefore, the RSB = 520 – 100(flap) – 104 µm = 316 µm.

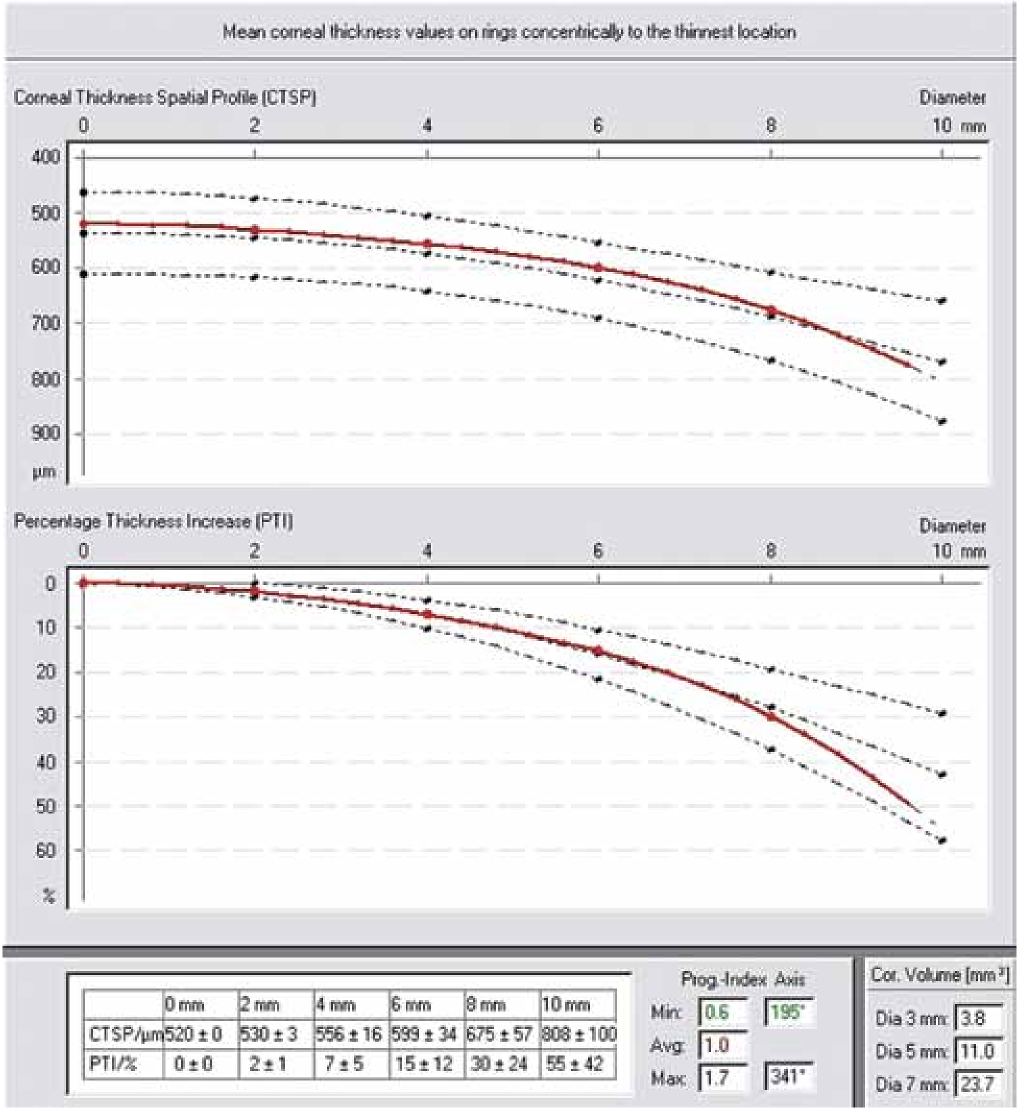

Fig. 9.2.8 Thickness profiles.

iii. RSB Law 3: According to this law, the actual AD (6.5 mm OZ) = (7 + 1) x 15 = 120 µm; therefore the actual RSB = 520 – 100 – 120 = 300 µm.
iv. RSB Law 4: The most conservative in this case is RSB law 2. According to this, the allowed correction of refractive error is 104 / 15 = 7 D, which results in almost 1 D of residual refractive error for this OZ.
v. RSB Law 5: If SA is planned, the AD (6.5 mm OZ) = (7 + 1) x 15 = 120 µm (which is >80 µm) and the RSB = 520 -120 = 400 µm. The allowed refractive correction is 80 / 15 ≈ 5.5 D, and the RSB = 520 - 80 = 440 µm (>400 µm).
vi. Table 9.2.3 summarizes the thickness concept.

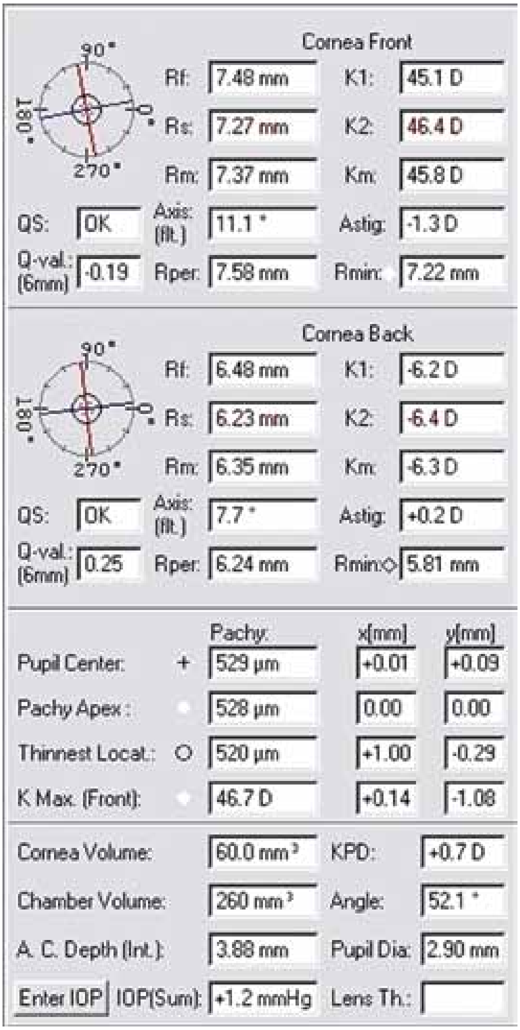

Fig. 9.2.9 Corneal parameters.

TABLE 9.2.3 Thickness Concepts

RSB Law		*RSB (μm)*	*AD (μm)*
LA	1	At least 286	134
	2	316	At most 104
	3	300	120
	4	316	104
SA	5	440	80

RSB = residual stromal bed for 100 μm flap; AD = ablation depth

b. K-readings and Astigmatism Concept:
   i. According to RSB law, the refractive error cannot be completely corrected; 7 D can be corrected.
   ii. According to sub optimal correction rule (chapter 6), it is wise to correct -6 D sph and -1 D cyl.
   iii. It is a myopic astigmatism case; therefore, the myopic astigmatism rule should be used (Table 9.2.4)

TABLE 9.2.4 Final K

Refractive error	*Original K*	*Astigmatic correction*	*Myopic correction*	*Final K*
–6 sph	K_f = 45.1 D	(0) K_f = 45.1 D	(6 x 0.75 = 4.5 D) K_f = 45.1 – 4.5 = 40.6 D	40.9 D in average
–1 cyl	K_s = 46.4 D	(1 x 0.75 = 0.75 D) K_s = 46.4 – 0.75 = 45.65 D	(6 x 0.75 = 4.5 D) K_s = 45.65 – 4.5 = 41.15 D	
K_f : flat K K_s : steep K				

As shown in this table, the final K is > 34 D.

DISCUSSION

The minification effect of glasses explains the suboptimal corrected visual acuity, this is proven by the improvement found with pin hole test.

The patient is still young and eye examination is normal; therefore, RLE option is excluded.

The refractive error is moderately high; the spherical equivalent is –7.5 D; therefore, both PRT and PIOL options are on table.

According to tomography, thickness and K-readings concepts, the refractive error cannot be completely corrected by PRT if a 6.5 mm OZ was chosen. Scotopic pupil was measured by pupillometry and found 5 mm. Using an OZ = 5.5 mm is reasonable and saves tissue but we have to remember that in case of high refractive errors, postoperative efficient OZ will be smaller than the desired; in addition, OZ < 6 mm increases the risk of post SA haze.

If PRT is the option, sub optimal correction will be on the account of myopia; a residual refractive error of -1 D sph will be the result. The case should be discussed with the patient after doing the same calculations for the right eye. On the other hand, using an OZ = 6 mm will allow for full correction.

ACD, ACA and pupil centre coordinates are suitable for a PIOL. The PIOL can be chosen to be either aspheric or toric since the amount of astigmatism is small.

If PRT is indicated, aspheric or aspheric aberration-free profiles should be used. Both decentration and compensation for cyclotorsion are not necessary since the amount of astigmatism is 1 D.

In my opinion, implantation of a toric PIOL is superior to PRT in this case.

CASE 3

A 43-year-old female is complaining of high refractive error. She is using SCL, but unsatisfied due to recurrent conjunctivitis and the feeling of dryness. CLs have been stopped since two weeks.

Eye examination reveals mild dry eye; tear film BUT is 8 seconds and primary Schirmer's test is 7mm/5min.

Her MR and VA are shown in Table 9.3.1. Her CR is shown in Table 9.3.2.

TABLE 9.3.1 Manifest Refraction and Visual Acuity

	UDVA	*Sph*	*Cyl*	*Axis*	*CDVA (G)*	*CDVA (G+PH)*
OD	0.04	–6.0	–4.0	5	0.8	1.0
OS	0.04	–5.5	–3.0	175	0.8	1.0

UDVA= uncorrected distance visual acuity; CDVA (G)= corrected distance visual acuity (by glasses); CDVA (G+PH)= corrected distance visual acuity (by glasses and pin hole)

TABLE 9.3.2 Cycloplegic Refraction

	Sph	*Cyl*	*Axis*
OD	–6	–3.5	175
OS	–5.5	–2.75	180

Figure 9.3.1 shows corneal tomography of the right eye which will be studied as an example.

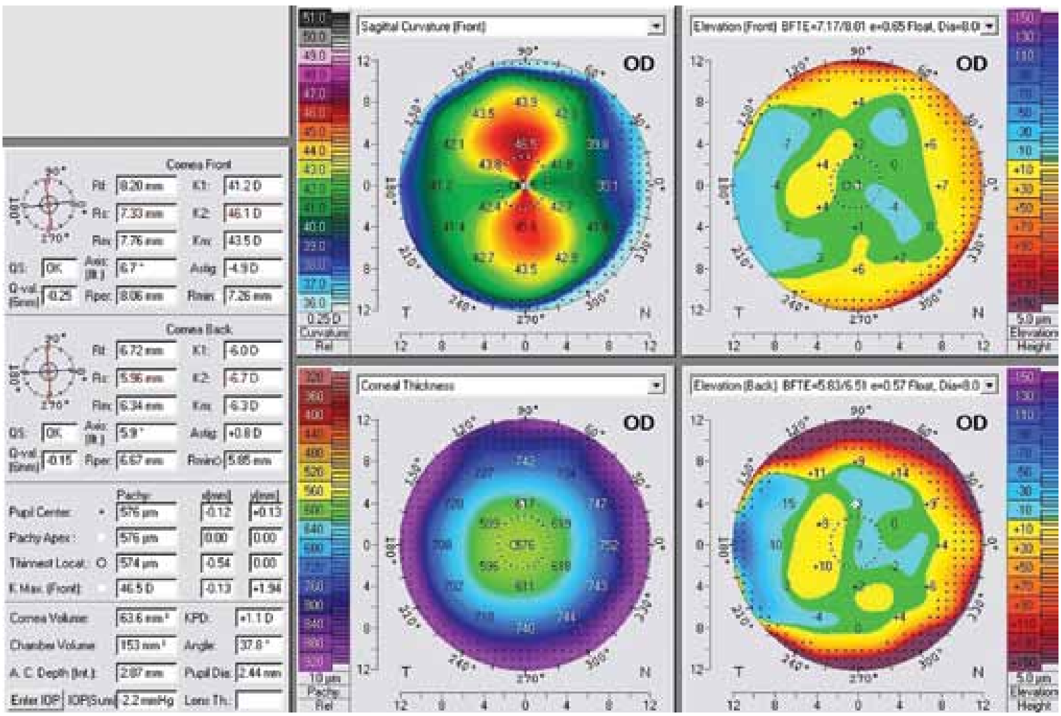

Fig. 9.3.1 The four composite maps.

1. **The Qualification Step:**
   a. In a general look, the sagittal curvature map has a vertical SB pattern indicating WTR astigmatism. Nothing seems abnormal in the elevation maps and the pachymetry map.
   b. Studying single maps:
      i. The anterior sagittal curvature map (Fig. 9.3.2) shows SB with neither SRAX nor significant inferior-superior difference.
      ii. The anterior elevation map:
         1. In BFS mode (Fig. 9.3.3): almost symmetric sandy watch pattern.
         2. In BFTE mode (Fig. 9.3.4): normal values within the central 5 mm circle.
      iii. The posterior elevation map:
         1. In BFS mode (Fig. 9.3.5): almost symmetric sandy watch pattern.
         2. In BFTE mode (Fig. 9.3.6): normal values within the central 5 mm circle.
      iv. The pachymetry map (Fig. 9.3.7) shows normal shape in spite of the temporal displacement of the thinnest location (white arrow). There is no significant inferior-superior difference.
      v. Thickness profiles (Fig. 9.3.8): The red curves take a normal slope. The average is normal (0.9).

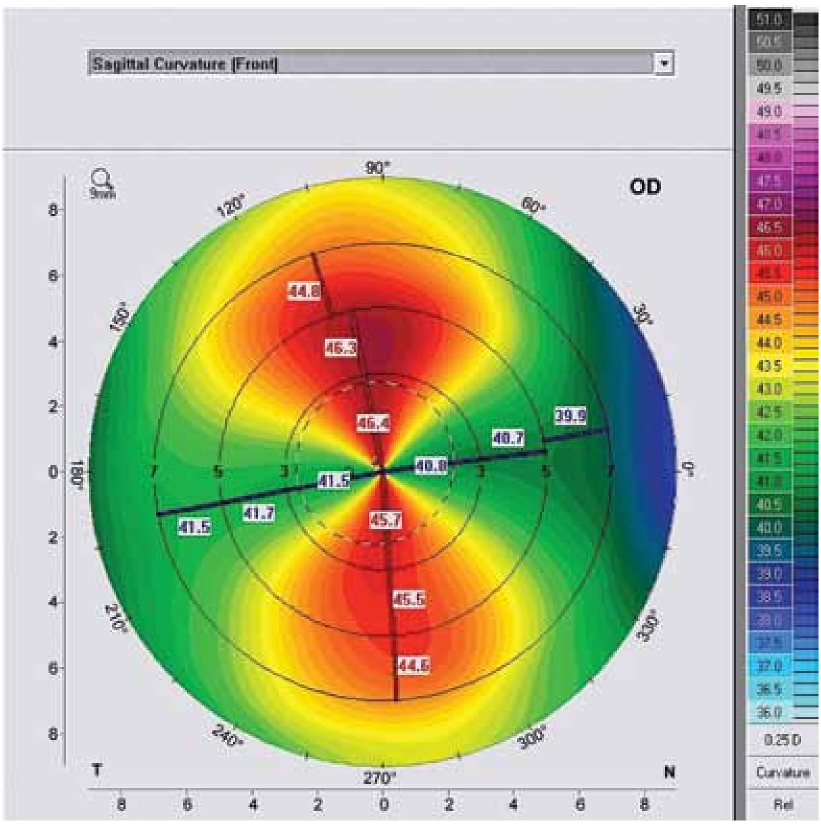

Fig. 9.3.2 The anterior curvature sagittal map. SB pattern.

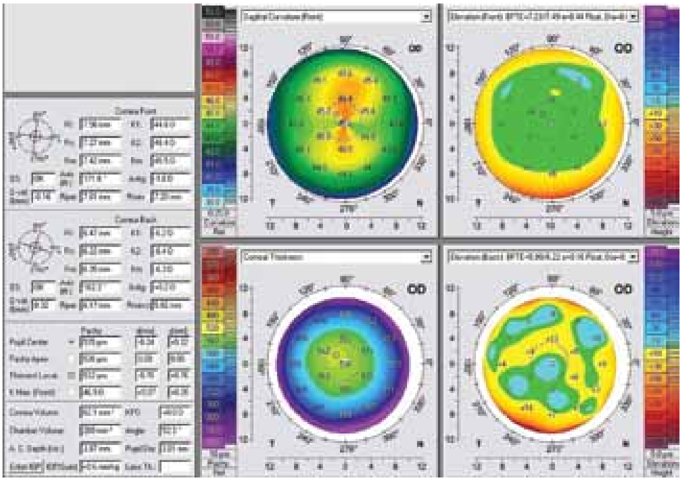

Fig. 9.3.3 The anterior elevation map with BFS reference body. Sandy watch pattern.

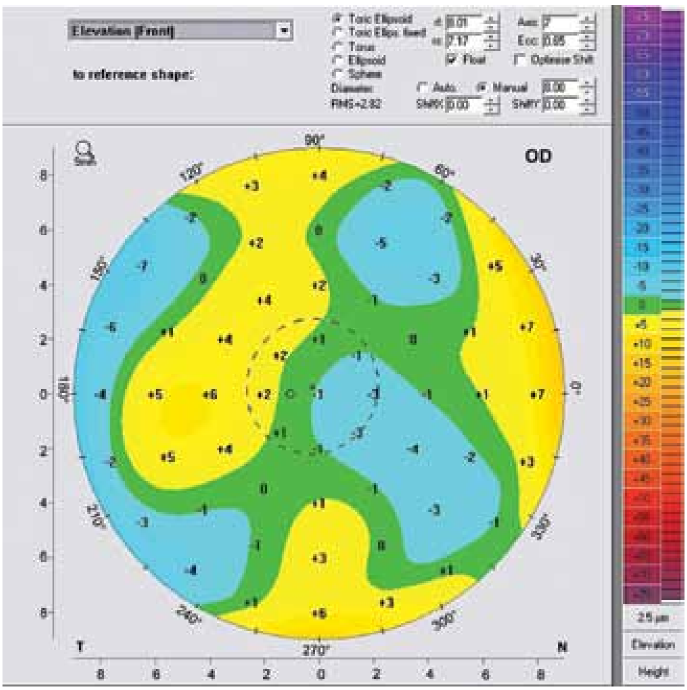

Fig. 9.3.4 The anterior elevation map with BFTE reference body.

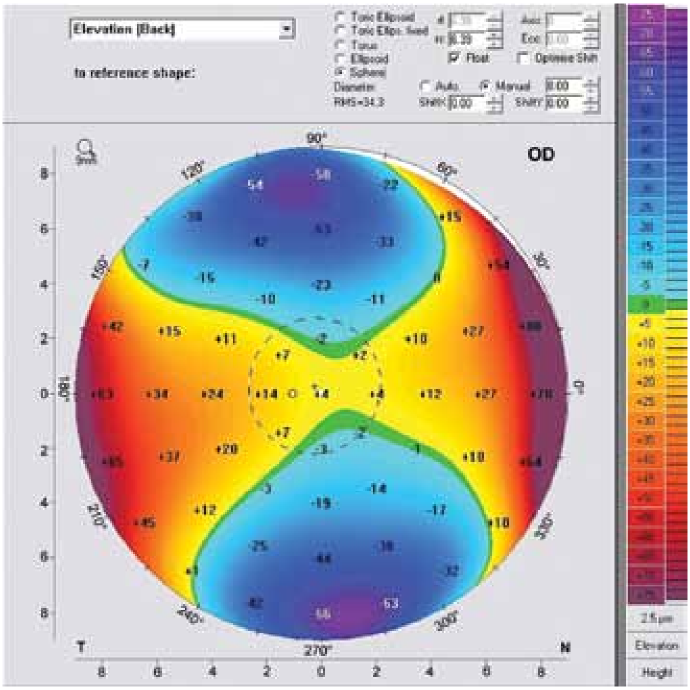

Fig. 9.3.5 The posterior elevation map with BFS reference body. Almost symmetric sandy watch pattern.

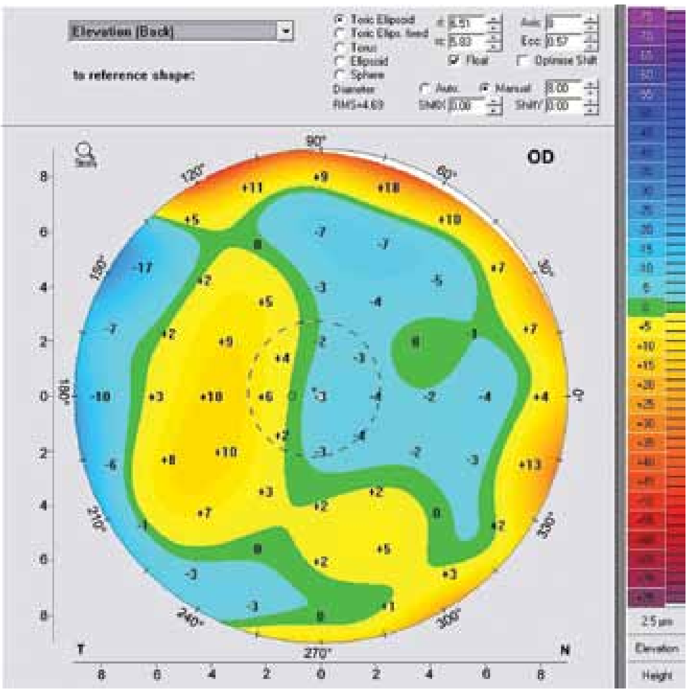

Fig. 9.3.6 The posterior elevation map with BFTE reference body.

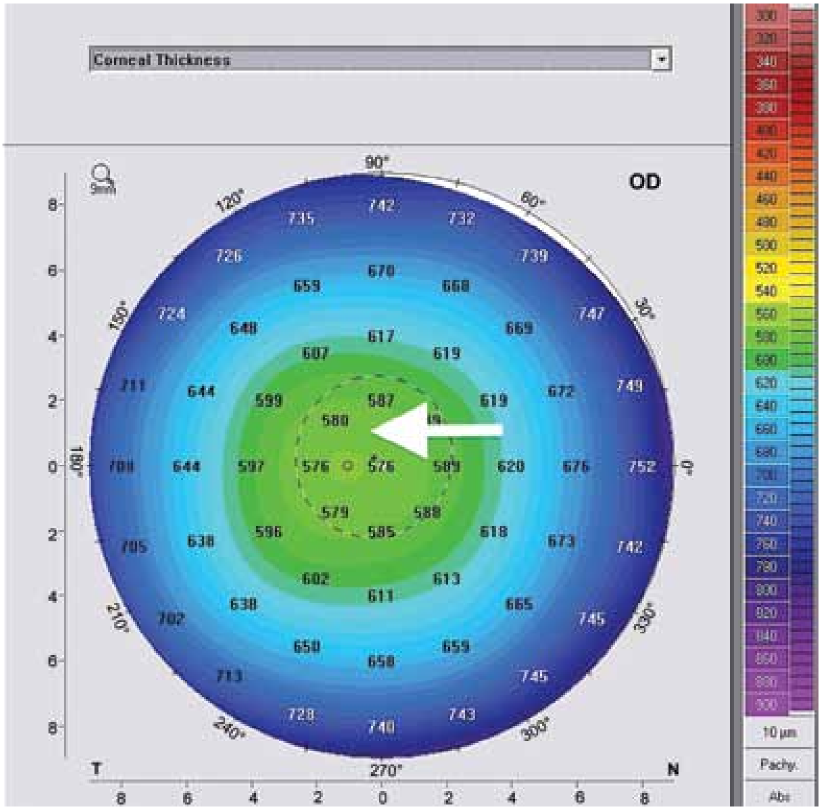

Fig. 9.3.7 The pachymetry map. The white arrow points at the horizontally-displaced thinnest location.

c. Qualification of values (Fig. 9.3.9):
   i. QS is OK.
   ii. K readings including Kmax are <48 D.
   iii. K-max-steep K is < 1 D.
   iv. Astigmatism is < 6 D.
   v. Thickness at the thinnest location is > 500 µm.
   vi. Pachy-Thinnest difference in thickness is < 10 µm.
   vii. *Y*-coordinate of the thinnest location is less than –500 µm (0 µm).
   viii. ACD, ACA and ACV are normal.
   ix. Mesopic pupil diameter is 2.44 mm.
   x. Pupil coordinates indicate central pupil and insignificant angle Kappa.

2. **The Quantitative Step:**
   a. Thickness concepts:
      i. RSB Law 1: According to this law, RSB should be at least 574 x 55% = 315.7 µm (>270 µm); therefore, the allowed AD = 574 – 100 (flap) – 315.7 = 158.3 µm.
      ii. RSB Law 2: According to this law, the AD should be at most 574 x 20% = 114.8 µm; therefore, the RSB = 574 – 100(flap) – 114.8 µm = 359.2 µm.
      iii. RSB Law 3: According to this law, the actual AD (6.5mm OZ) = (6 + 4) x 15 = 150 µm; therefore, the actual RSB = 574 – 100 – 150 = 324 µm. MR has been used in calculations.

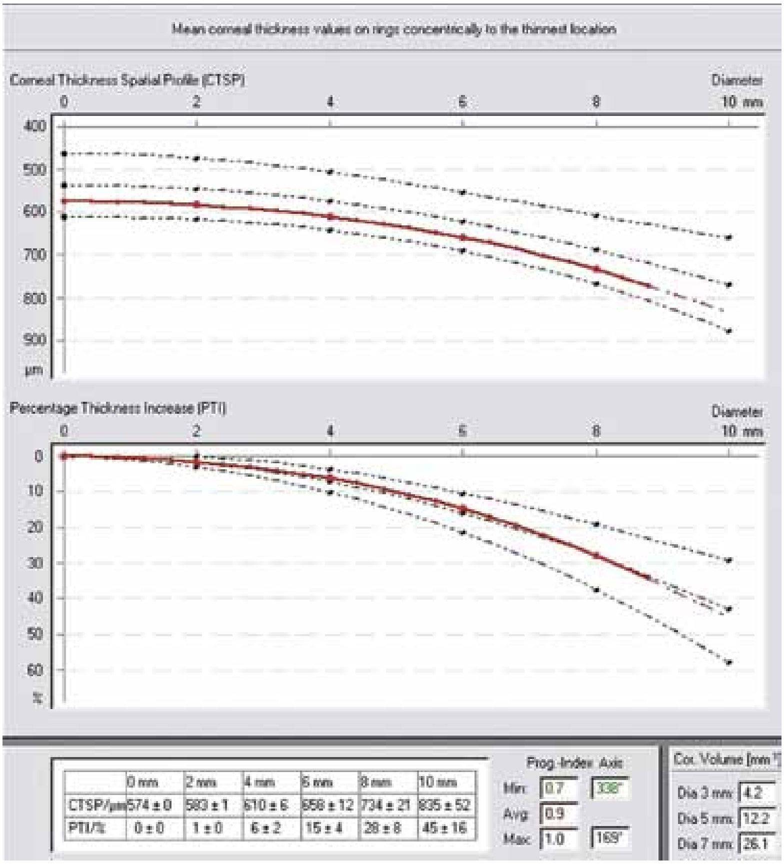

Fig. 9.3.8 Thickness profiles.

iv. RSB Law 4: The most conservative in this case is RSB law 2. According to this, the allowed correction of refractive error is 114.8 / 15 = 7.65 D, which results in almost 2.5 D residual refractive error for a 6.5 mm OZ.

b. K-readings and Astigmatism Concept:

i. According to RSB laws, nearly –8 D can be corrected. K-reading laws will be applied assuming that –4 D sph and –4 D cyl will be corrected leaving almost –2 D sph.

ii. It is a myopic astigmatism case; therefore, the myopic astigmatism law should be used (Table 9.3.3).

TABLE 9.3.3 Final K

Refractive error	*Original K*	*Astigmatic correction*	*Myopic correction*	*Final K*
–4 sph	K_f = 41.2 D	(0) K_f = 41.2 D	(4 x 0.75 = 3D) K_f = 41.2 – 3 = 38.2 D	39.15 D in average
–4 cyl	K_s = 46.1 D	(4 x 0.75 = 3 D) K_s = 46.1 – 3 = 43.1 D	(4 x 0.75 = 3 D) K_s = 43.1 – 3 = 40.1 D	

K_f : flat K
K_s : steep K

As shown in this table, the final K is >34 D.

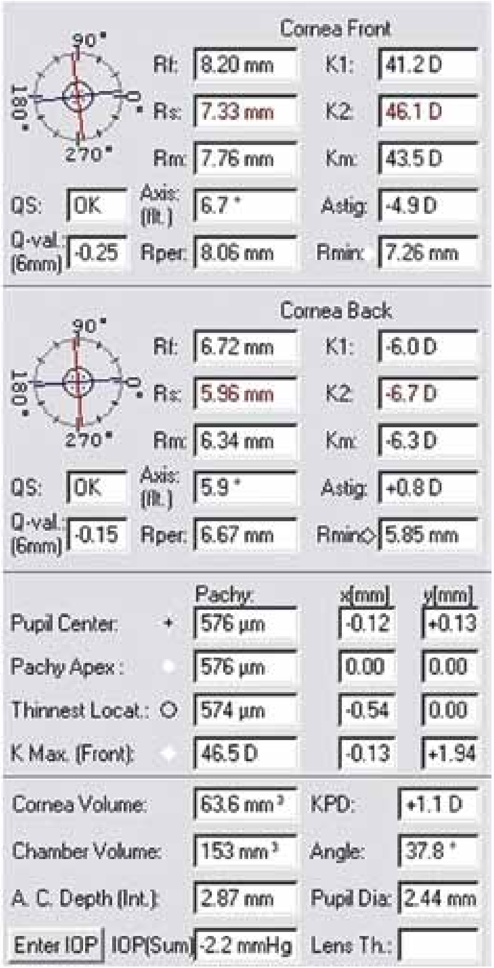

Fig. 9.3.9 Corneal parameters.

DISCUSSION

The minification effect of glasses explains the suboptimal corrected visual acuity, this is proven by the improvement found with pin hole test.

Since the patient is 43 years old, all refractive options, including RLE, are on table.

Although the refractive error is high (SE= –8D), PIOL option is not on table since the ACD is < 3 mm.

On the other hand, according to tomography, thickness and K-readings concepts, the refractive error cannot be completely corrected by PRT unless smaller OZ is used. Scotopic pupil was measured by pupillometry and found 5.2 mm. Using an OZ = 5.7 mm is reasonable and saves tissue, but we have to remember that in case of high refractive errors, the efficient OZ will be smaller than the desired; in addition, OZ < 6 mm increases the risk of post SA haze. However,

using an OZ = 6 mm in our case increases the amount of correction. I advise the reader to do the calculations himself to find out the amount of correction for the 6 mm OZ.

Therefore, the patient has two options, RLE and implantation of a toric IOL and partial correction with PRT (unless smaller OZ is used).

If PRT is to be performed, dry eye should be treated first, aspheric or aspheric aberration-free profiles should be used and decentration and cyclotorsion compensation are mandatory since the astigmatism is >2 D. If dryness persists in spite of treatment, RLE and implanting a toric IOL will be the choice.

CASE 4

A 25-year-old male has a refractive error in both eyes. He is complaining of unfavorable appearance of his glasses and imperfect vision with them.
His MR and VA are shown in Table 9.4.1. His CR is shown in Table 9.4.2.

TABLE 9.4.1 Manifest Refraction and Visual Acuity

	UDVA	*Sph*	*Cyl*	*Axis*	*CDVA (G)*	*CDVA (G+PH)*
OD	0.08	–4.5	–0.75	10	0.9	1.0
OS	0.08	–4.5	–1	170	0.9	1.0

UDVA= uncorrected distance visual acuity; CDVA (G)= corrected distance visual acuity (by glasses); CDVA (G+PH)= corrected distance visual acuity (by glasses and pin hole)

TABLE 9.4.2 Cycloplegic Refraction

	Sph	*Cyl*	*Axis*
OD	–4	–1	180
OS	–4	–1.5	180

Figures 9.4.1 to 9.4.11 are tomography and wavefront for the right eye and Figures 9.4.12 to 9.4.22 are tomography and wavefront for the left eye.

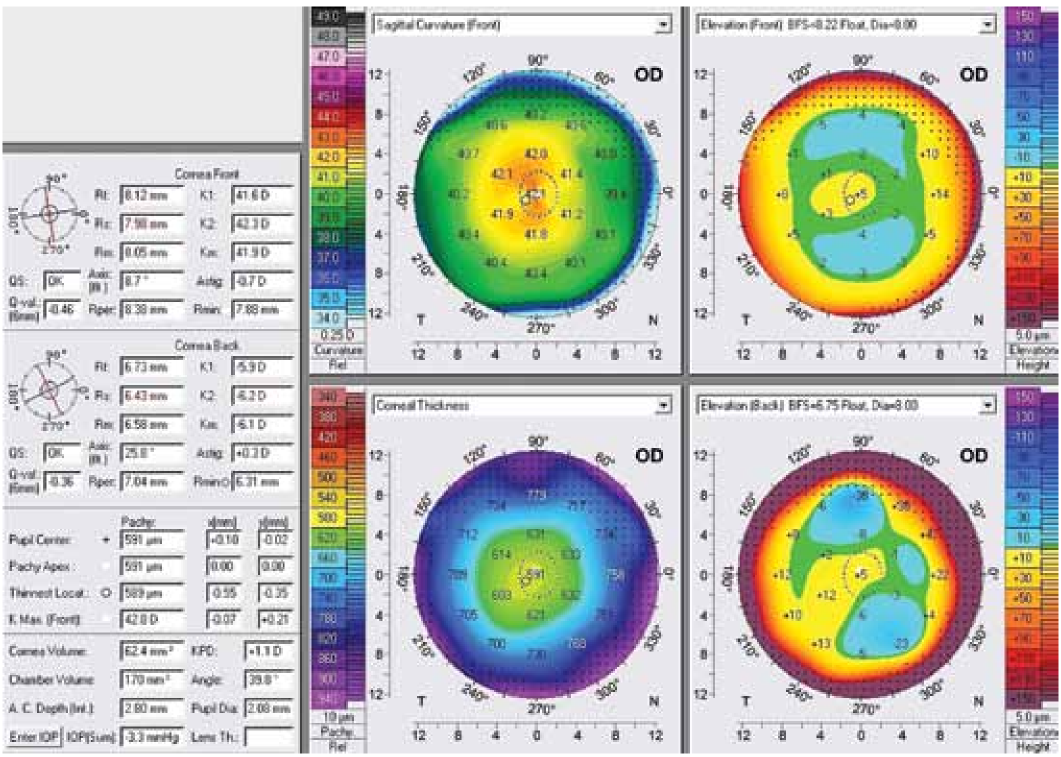

Fig. 9.4.1 OD. The four composite maps.

1. **The Qualification Step:**
   Right Eye:
   a. In a general look, there are some irregularities in all maps (Fig. 9.4.1).
   b. Studying single maps:
      i. The anterior sagittal curvature map (Fig. 9.4.2): It is SB/SRAX; there is >22° between the segments' axes. There is no significant inferior-superior difference (not shown on this map).
      ii. The anterior elevation map:
         1. In BFS mode (Fig. 9.4.3): tongue-like extension or almost an isolated island.
         2. In the BFTE mode (Fig. 9.4.4): normal values within the central 5 mm circle.
      iii. The posterior elevation map:
         1. In BFS mode (Fig. 9.4.5): tongue-like extension.
         2. In BFTE mode (Fig. 9.4.6): normal values within the central 5 mm circle.
      iv. The pachymetry map (Fig. 9.4.7): Mild dome-like shape with displacement of thinnest location (white arrow); (see coordinates in Figs 9.4.1 and 9.4.9).
      v. Thickness profiles (Fig. 9.4.8): Although the red curves seem to be normal, at the end of the curves there is a small S-shape (blue arrows). The average is normal (0.8).

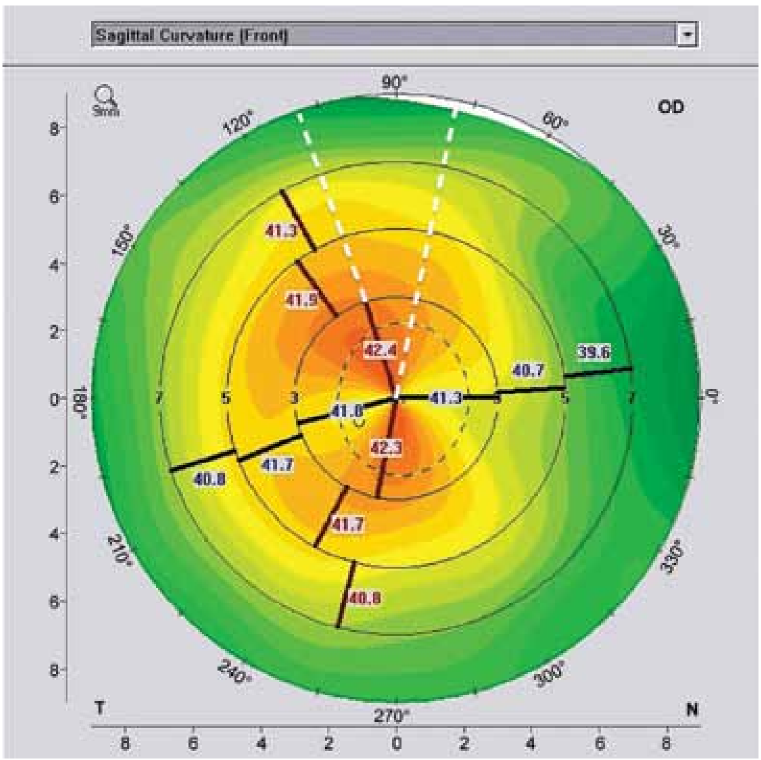

Fig. 9.4.2 OD. The anterior curvature sagittal map. SB/SRAX pattern.

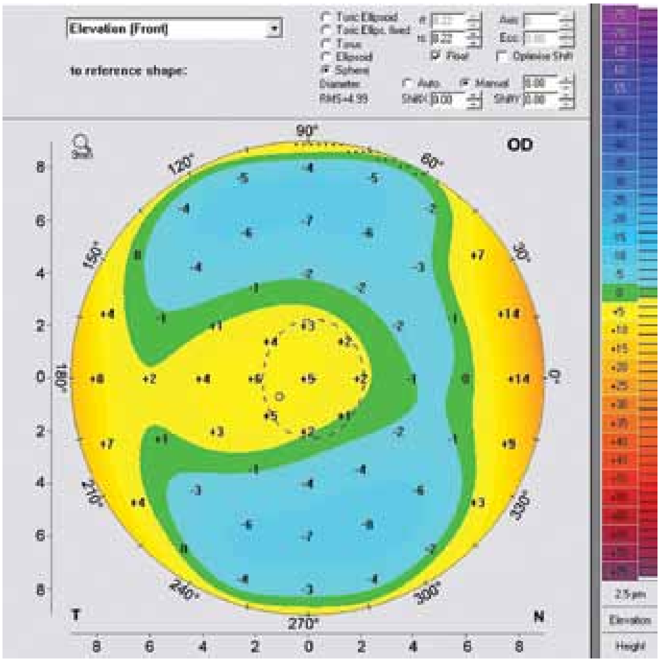

Fig. 9.4.3 OD. The anterior elevation map with BFS reference body. Tongue-like extension.

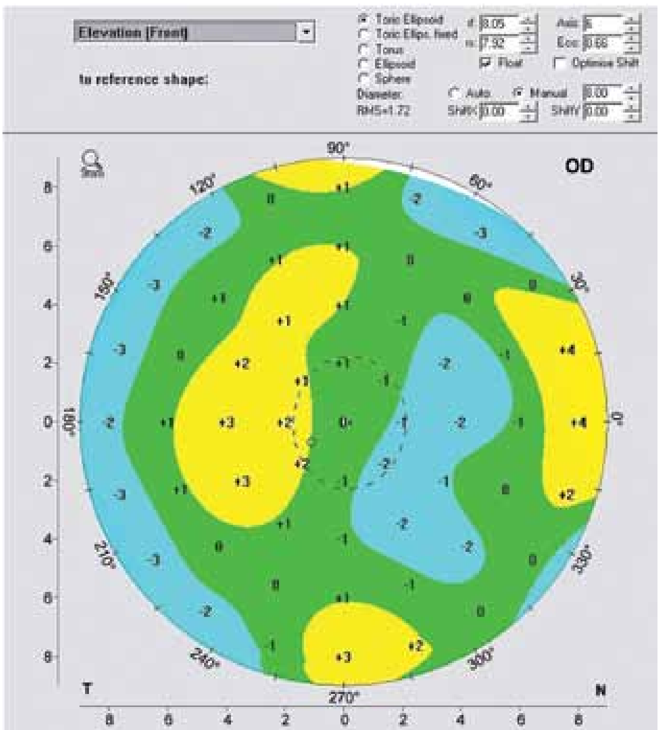

Fig. 9.4.4 OD. The anterior elevation map with BFTE reference body.

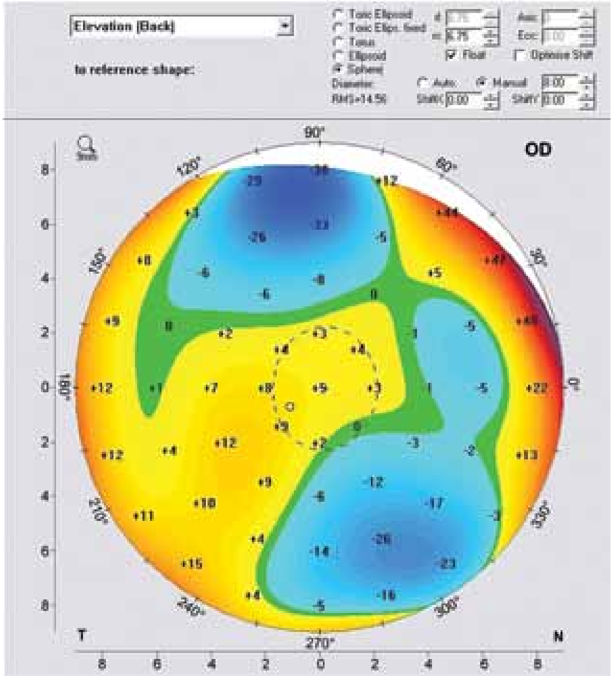

Fig. 9.4.5 OD. The posterior elevation map with BFS reference body. Tongue-like extension.

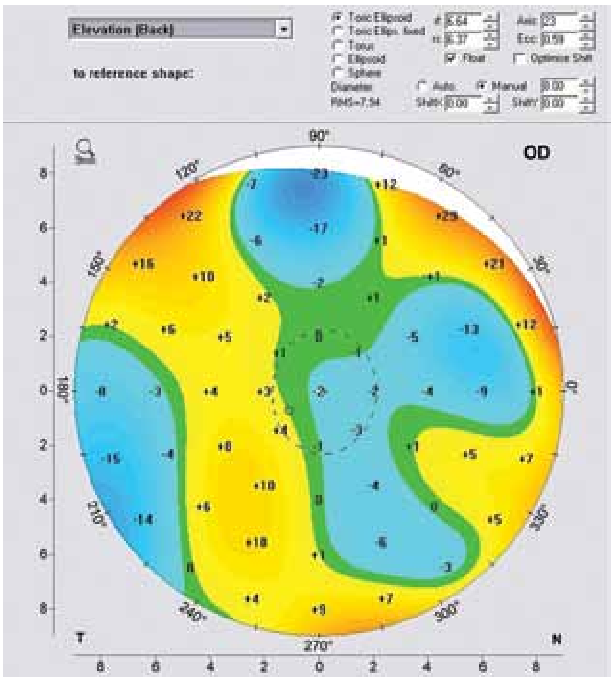

Fig. 9.4.6 OD. The posterior elevation map with BFTE reference body.

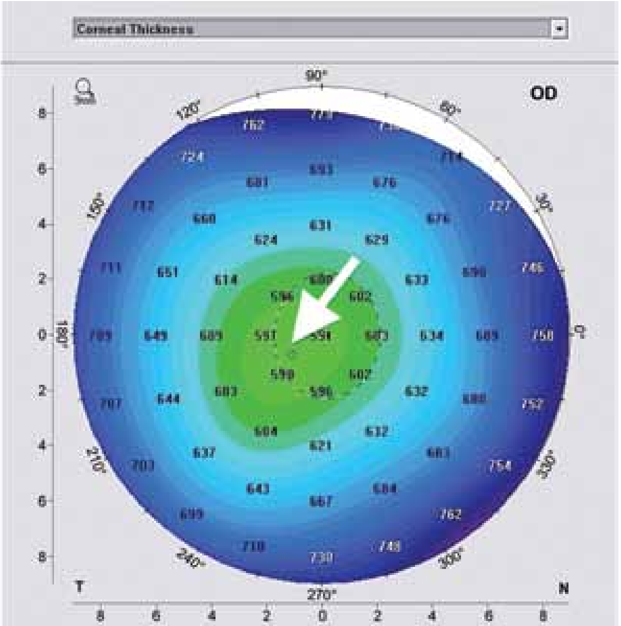

Fig. 9.4.7 OD. The pachymetry map. The white arrow points at the dome-like pattern and displaced thinnest location.

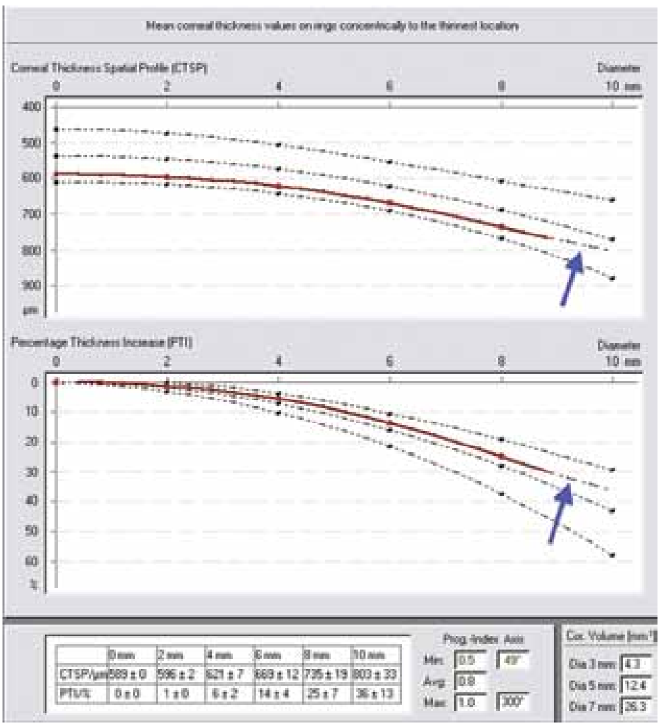

Fig. 9.4.8 OD. Thickness profiles. The blue arrows point at the S-shape pattern.

c. Qualification of values (Fig. 9.4.9):
   i. QS is OK.
   ii. K readings including K-max are <48 D.
   iii. K-max-steep K is <1 D.
   iv. Astigmatism is < 6 D.
   v. Thickness at the thinnest location is >500 µm.
   vi. Pachy-Thinnest difference in thickness is <10 µm.
   vii. *Y*-coordinate of the thinnest location is less than –500 µm (–350 µm).
   viii. ACD, ACA and ACV are normal.
   ix. Mesopic pupil diameter is 2.08 mm.
   x. Pupil coordinates indicate central pupil and borderline angle Kappa.

d. Qualification of Wavefront:
   i. The objective refractive error measured by wavefront (Fig. 9.4.10 red arrow) is consistent with the MR (Table 9.4.1).

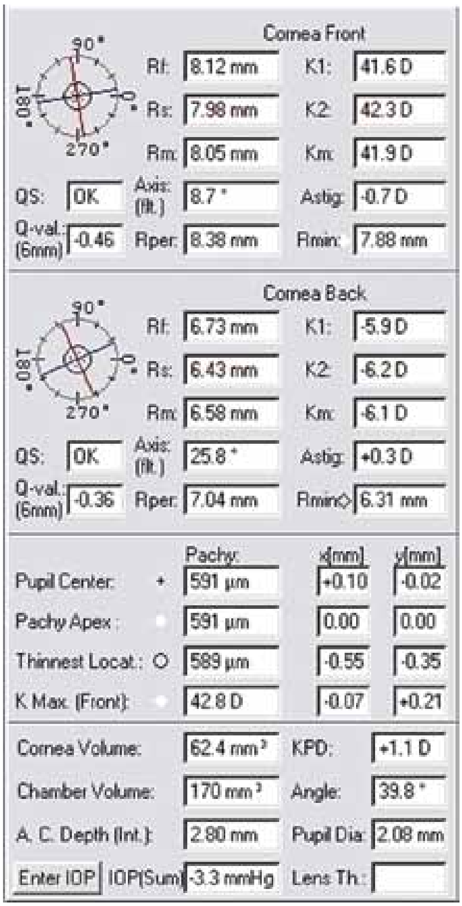

Fig. 9.4.9 Case 4, OD. Corneal parameters.

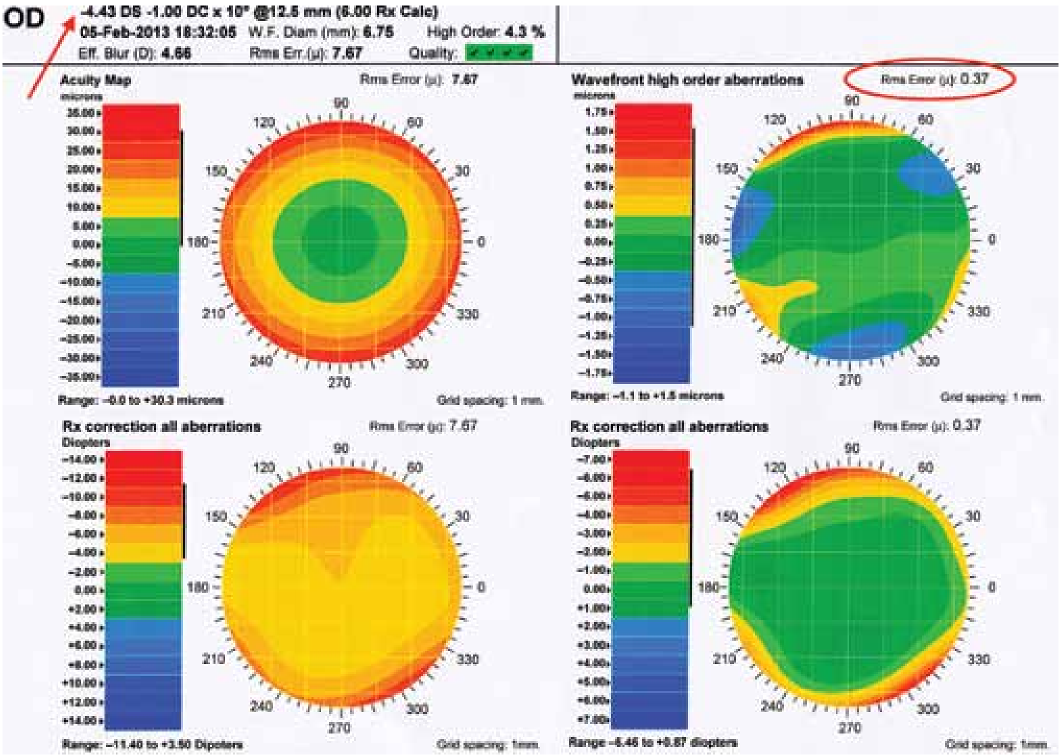

Fig. 9.4.10 OD. Ocular wavefront. The red arrow points at the objective refractive error. The red ellipse indicates RMS related to HOAs.

  ii. RMS related to HOAs is 0.37 (> 0.3) (Fig. 9.4.10 red ellipse).
  iii. PSF related to HOAs is spread over 5 minutes of arc, which is considered very small (Fig. 9.4.11 blue ellipse).
  iv. Zernike coefficient is almost 0.29, which is in the range of [0.25–0.50] and mainly produced by trefoil aberrations (Fig. 9.4.11 green arrows).

Left Eye

a. In a general look, there are some irregularities in all maps (Fig. 9.4.12).
b. Studying single maps:
  i. The anterior sagittal curvature map (Fig. 9.4.13): Although it seems to be AB, there is no significant inferior-superior difference.
  ii. The anterior elevation map:
    1. In BFS mode (Fig. 9.4.14): Tongue-like extension.
    2. In the BFTE mode (Fig. 9.4.15): Normal values within the central 5 mm circle.
  iii. The posterior elevation map:
    1. In BFS mode (Fig. 9.4.16): Tongue-like extension.
    2. In BFTE mode (Fig. 9.4.17): Normal values within the central 5 mm circle.
  iv. The pachymetry map (Fig. 9.4.18) shows dome shape with displacement of the thinnest location (white arrow). (See coordinates in Figs 9.4.12 and 9.4.20).
  v. Thickness profiles (Fig. 9.4.19) show normal slope of the red curves. The average is normal (0.9).

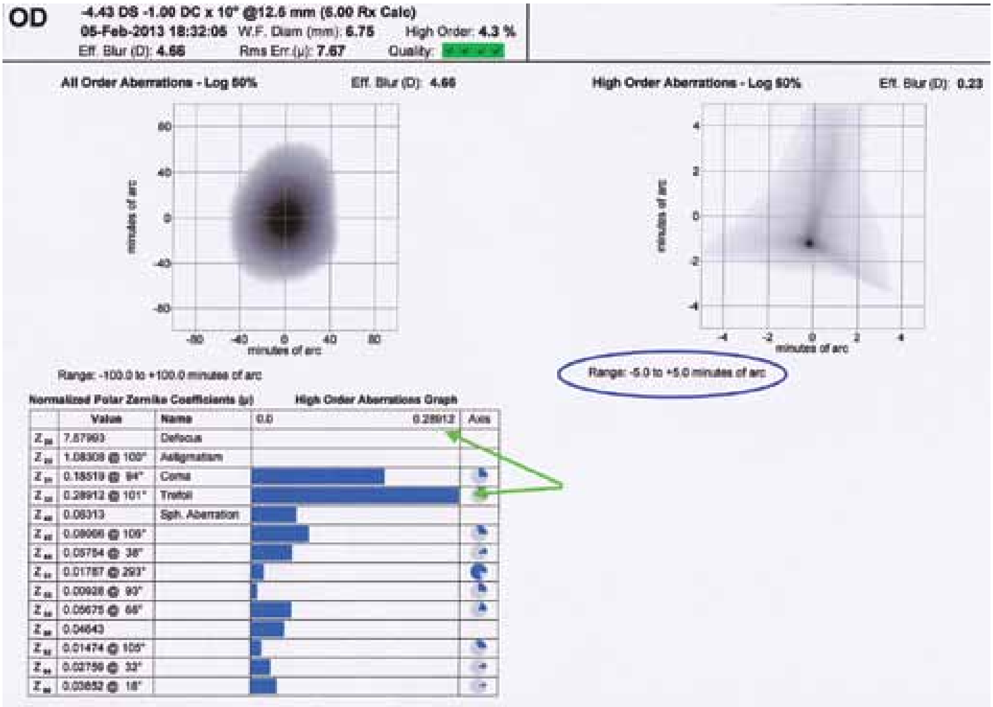

Fig. 9.4.11 OD. Ocular wavefront. The green arrows point at ZC of HOAs which mainly consists of trefoil. The blue ellipse indicates the range of PSF.

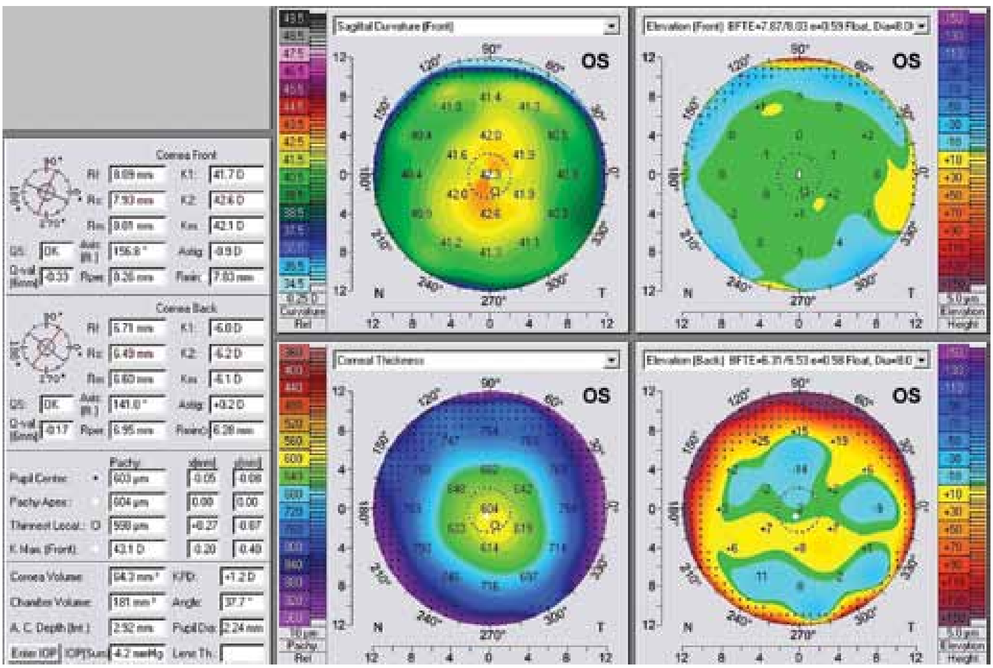

Fig. 9.4.12 OS. The four composite maps.

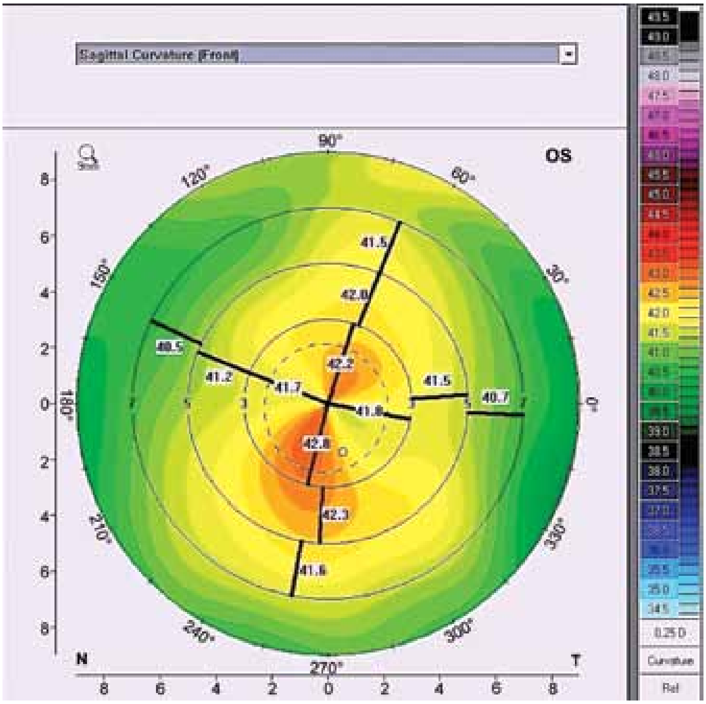

Fig. 9.4.13 OS. The anterior curvature sagittal map. AB pattern.

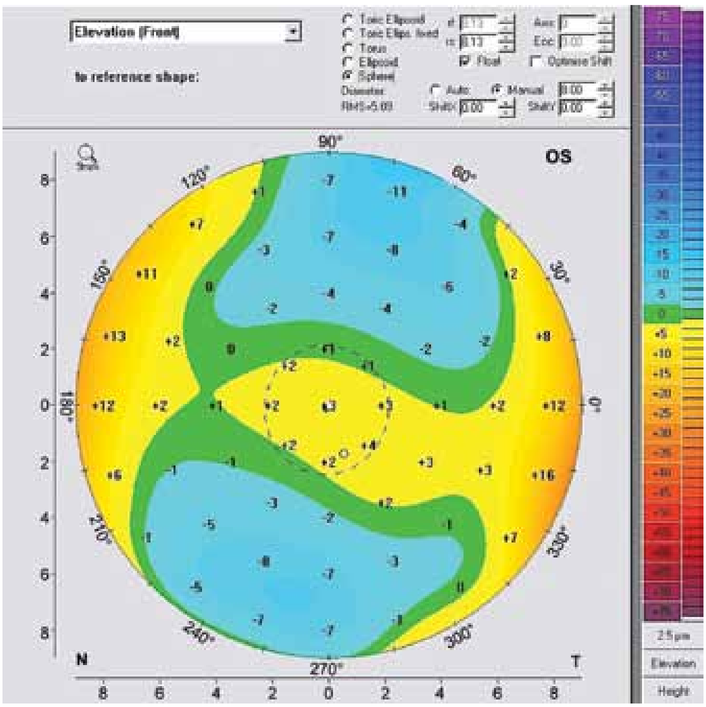

Fig. 9.4.14 OS. The anterior elevation map with BFS reference body. Tongue-like extension.

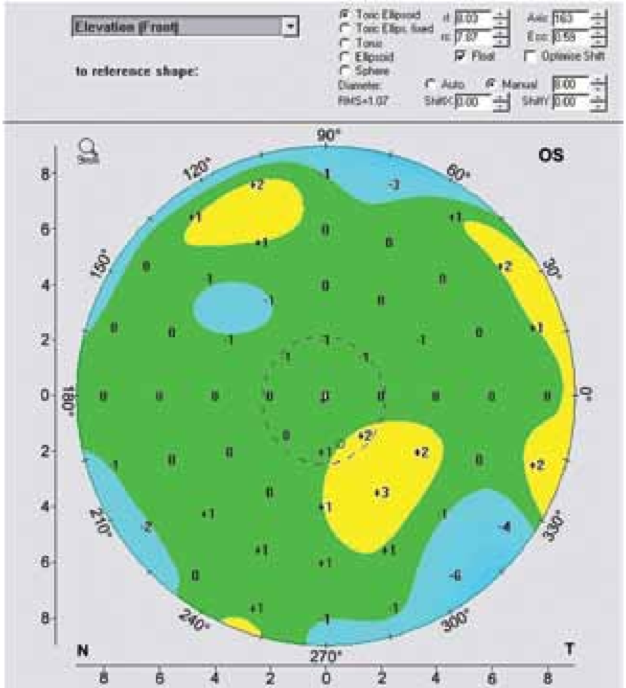

Fig. 9.4.15 OS. The anterior elevation map with BFTE reference body.

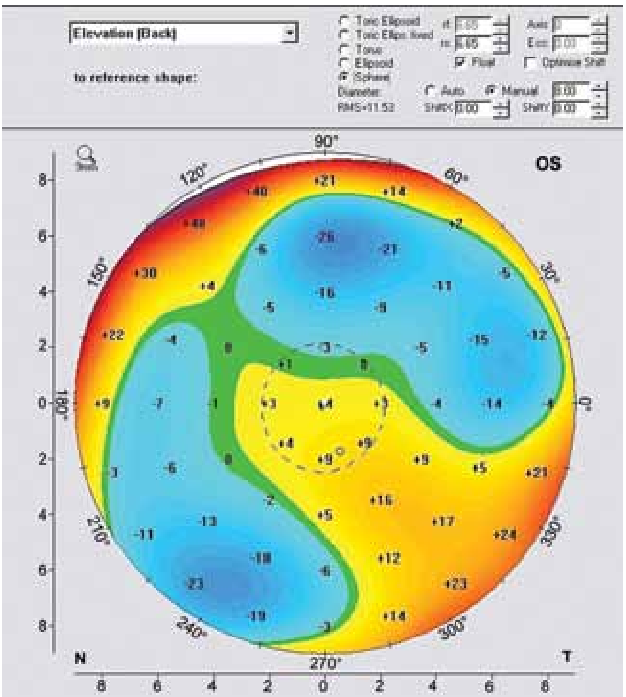

Fig. 9.4.16 OS. The posterior elevation map with BFS reference body. Tongue-like extension.

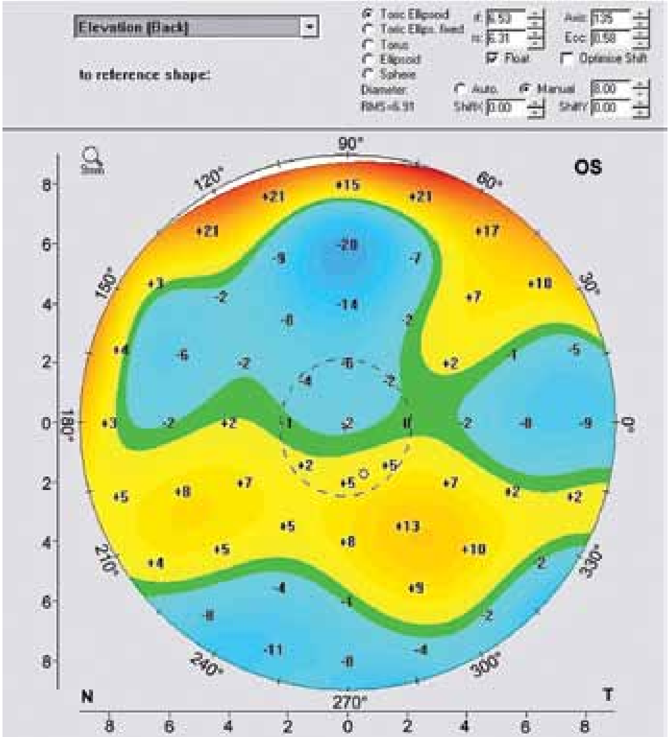

Fig. 9.4.17 OS. The posterior elevation map with BFTE reference body.

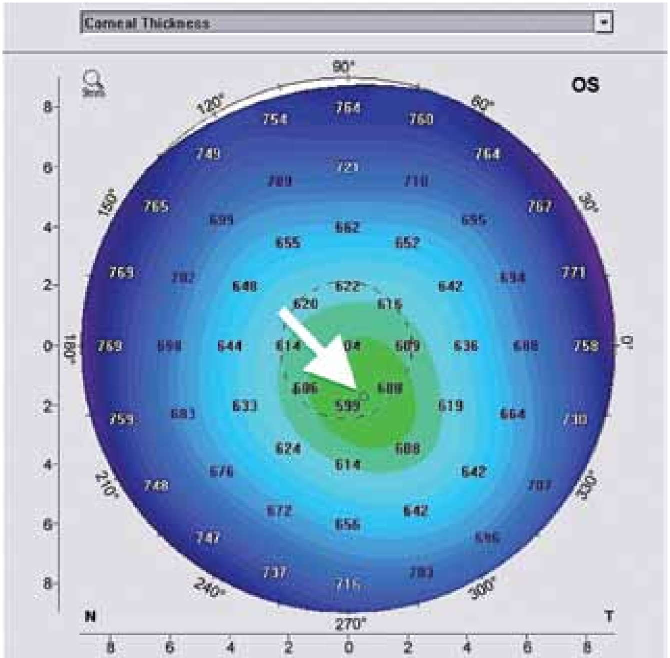

Fig. 9.4.18 OS. The pachymetry map. The white arrow points at the dome-like pattern and displaced thinnest location.

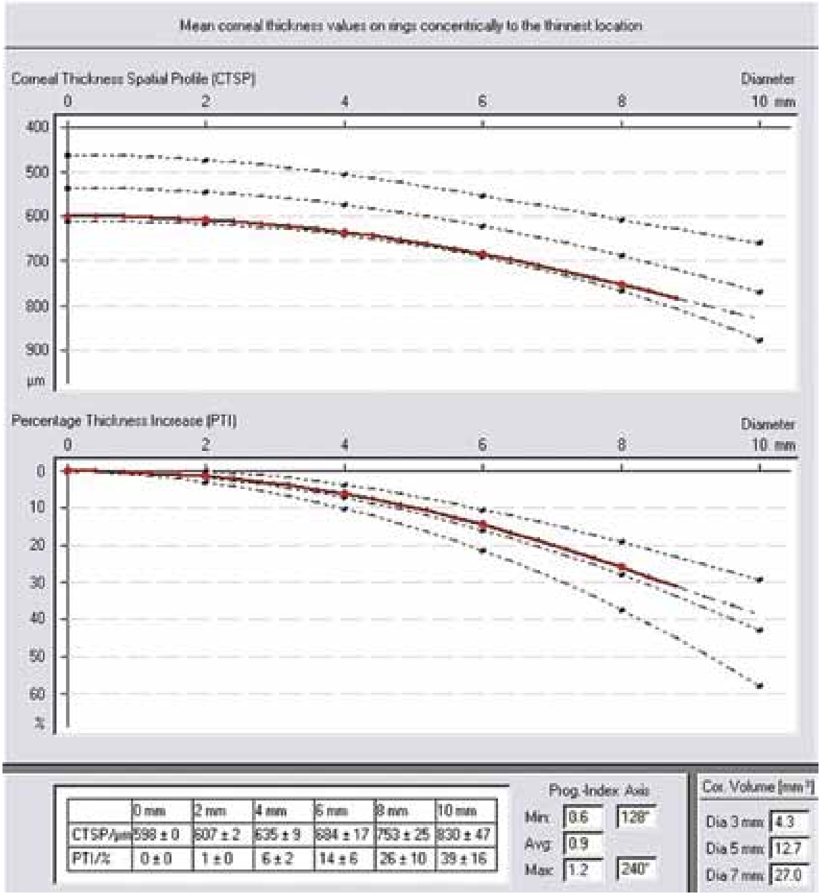

Fig. 9.4.19 OS. Thickness profiles.

c. Qualification of values (Fig. 9.4.20):
   i. QS is OK.
   ii. K readings including K-max are <48 D.
   iii. K-max-steep K is < 1 D.
   iv. Astigmatism is < 6 D.
   v. Thickness at the thinnest location is >500 µm.
   vi. Pachy-Thinnest difference in thickness is <10 µm.
   vii. *Y*-coordinate of the thinnest location is >–500 µm (–870 µm).
   viii. ACD, ACA and ACV are normal.
   ix. Mesopic pupil diameter is 2.24 mm.
   x. Pupil coordinates indicate central pupil and insignificant angle Kappa.
d. Qualification of Wavefront:
   i. The objective refractive error measured by wavefront (Fig. 9.4.21 red arrow) is consistent with the MR (Table 9.4.1).
   ii. RMS related to HOAs is 0.19 (<0.3) (Fig. 9.4.21 red ellipse).

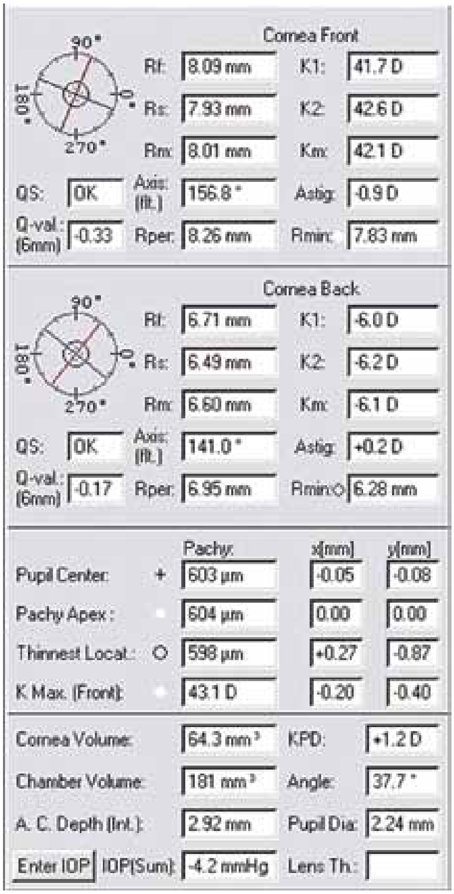

Fig. 9.4.20 OS. Corneal parameters.

iii. PSF related to HOAs is spread over 5 minutes of arc, which is considered very small (Fig. 9.4.22 blue ellipse).

iv. Zernike coefficient is almost 0.14 (<0.25) and mainly produced by coma aberration (Fig. 9.4.22 green arrows).

2. **Discussion Step:**
   It is better to discuss the case before proceeding with the quantitative step.
   Although, the minification effect of glasses may explain the suboptimal corrected visual acuity (proven by the improvement found with pin hole test), HOAs may have a role.
   Tomographic and wavefront figures show some irregularity with some risk factors including the followings:
   a. SRAX >22° in the right anterior curvature map.
   b. Tongue-like extensions on the elevation maps (BFS mode) in both eyes.
   c. Inferior displacement in the thinnest location in the left eye.
   d. S-shape of thickness profile in the right eye.

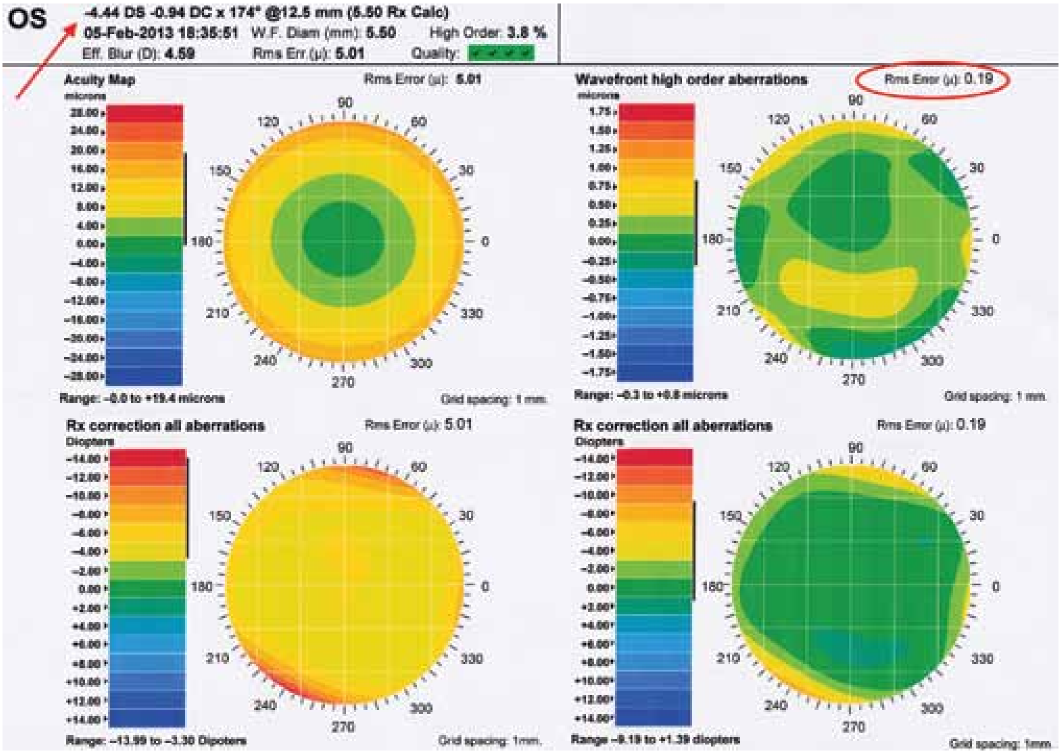

Fig. 9.4.21 OS. Ocular wavefront. The red arrow points at the objective refractive error. The red ellipse indicates RMS related to HOAs.

e. Abnormal RMS and Zernike coefficient in the right eye. Although, the main HOA in the right eye is trefoil, the patient is not complaining of night symptoms, since the left eye HOAs are within normal limits and may compensate for the right eye trefoil.

These risk factors should emphasise asking about a family history of KC (this question should of course be a routine in the work up). On the other hand, these risk factors put a limitation for PRT option especially that the patient is still young. In case of PRT option, SA is a better choice than LA. In the right eye, treatment profile should be corneal wavefront or ocular wavefront guided depending on the internal wavefront (see Fig. 5.47). In the left eye, aspheric or aspheric aberration free profile should be used. Cyclotorsion compensation is mandatory in the right eye since HOAs are to be treated. Decentration is not necessary in both eyes since pupil coordinates and hence, angle kappa are not significant and the astigmatism is < 2 D.

The other option is PIOLs implantation, bearing in mind that coma and trefoil cannot be correct by this option; the only HOA that can be compensated for in PIOL option is the spherical aberration by using special designs of aspheric PIOLs. Unfortunately, PIOLs are contraindicated in this case, since the ACD is < 3.0 mm in both eyes.

RLE is not on table since the patient is young and the refractive error is not high.

The right decision in this case is either to stay on glasses, use contact lenses or do SA. In our case, either SA or SA with CXL can be performed; the latter is preferable since there are risk factors and the patient is still young. In case CXL is added, a reduction of myopic correction

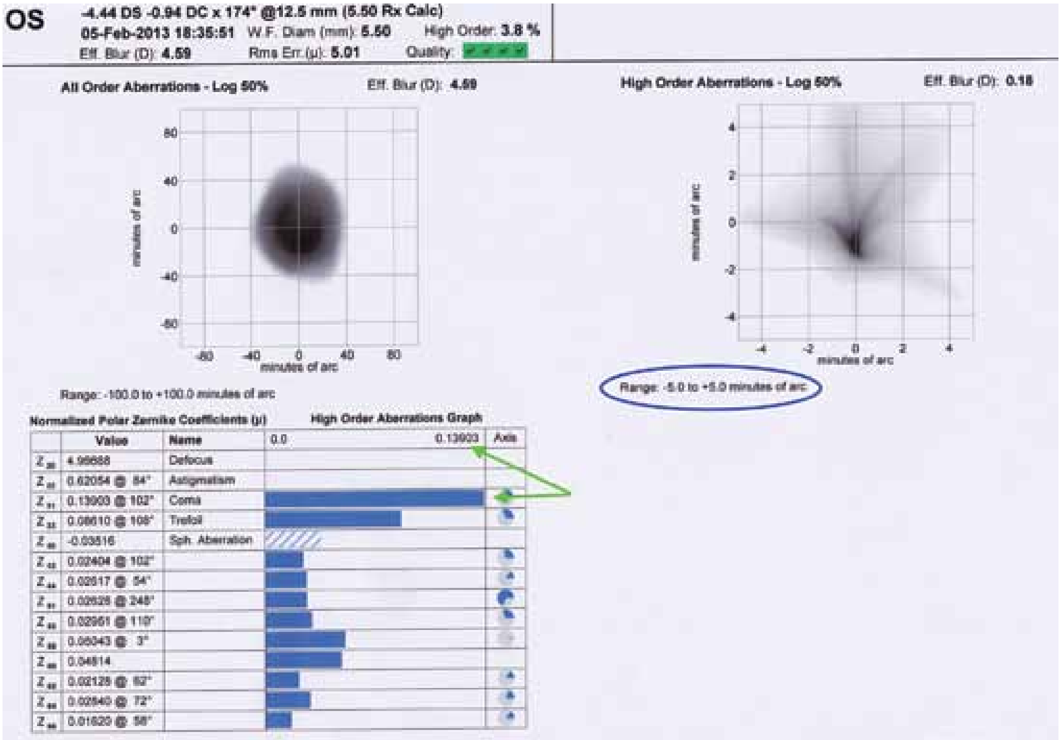

Fig. 9.4.22 OS. Ocular wavefront. The green arrows point at ZC of HOAs which mainly consists of coma. The blue ellipse indicates the range of PSF.

by −0.5 to −0.75 D may be done to compensate for the flattening effect and hyperopic effect that the CXL does. Therefore, the recommended refraction for correction will be as shown in Table 9.4.3.

TABLE 9.4.3 Recommended Refraction for SA and CXL

	Sph	*Cyl*	*Axis*
OD	−4	−0.75	10
OS	−4	−1	170

3. **The Quantitative Step:**
   The case will be studied as a candidate for SA.
   Right Eye:
   Since wavefront-guided treatment is indicated in the right eye, more tissue per diopter will be ablated depending on the severity and type of HOAs. In our case, an average of 19 *μm per diopter* is ablated for 6.5 mm OZ and will be used in our quantification.
   a. **Thickness concepts:** MR will be used in calculations.
      RSB Law 5: the AD = (4.5 + 0.75) x 19 ≈ 100 μm, which is >80 μm; the recommended ablation is 80 μm, which can correct 80/19 ≈ 4.25 D, leading to suboptimal correction. The RSB = 591−80 = 511 μm, unless a smaller OZ is used. Scotopic pupil was measured by pupillometry and found 4.5 mm. Using an OZ = 5 mm is reasonable and saves tissue but

we have to remember that OZ < 6 mm increases the risk of post SA haze. Using an OZ = 6 mm in this case will allow for full correction.

b. **K-readings and Astigmatism Concept:** It is a myopic astigmatism case; therefore, the myopic astigmatism law should be used (Table 9.4.4). The MR will be used assuming that the refractive error can be completely corrected.

TABLE 9.4.4 Final K

Refractive error	*Original K*	*Astigmatic correction*	*Myopic correction*	*Final K*
–4.5 sph	K_f = 41.6 D	(0) K_f = 41.6 D	(4.5 x 0.75 ≈ 3.4D) K_f = 41.6 – 3.4 = 38.2 D	38.27 D in average
–0.75 cyl	K_s = 42.3 D	(0.75 x 0.75 = 0.56 D) K_s = 42.3 – 0.56 = 41.74 D	(4.5 x 0.75 = 3.4D) K_s = 41.74 – 3.4 = 38.34 D	

K_f : flat K
K_s : steep K

As shown in this Table, the final K is >34 D.

Left Eye

a. **Thickness concepts:** MR will be used in calculations.
RSB Law 5: The AD = (4.5 + 1) x 15 = 82.5 μm, which is ≈ 80 μ and therefore, the refractive error can be completely corrected since the RSB ≈ 509 μm.

b. **K-readings and Astigmatism Concept:** It is a myopic astigmatism case; therefore, the myopic astigmatism law should be used (Table 9.4.5).

TABLE 9.4.5 Final K

Refractive error	*Original K*	*Astigmatic correction*	*Myopic correction*	*Final K*
–4.5 sph	K_f = 41.7 D	(0) K_f = 41.7 D	(4.5 x 0.75 ≈ 3.4 D) K_f = 41.7 – 3.4 = 38.3 D	38.38 D in average
–1.0 cyl	K_s = 42.6 D	(1 x 0.75 = 0.75 D) K_s = 42.6 – 0.75 = 41.85 D	(4.5 x 0.75 = 3.4 D) K_s = 41.85 – 3.4 = 38.45 D	

K_f : flat K
K_s : steep K

As shown in this table, the final K is >34 D.

CONCLUSION

Full correction with SA is possible in the right eye, but with an OZ = 6 mm, wavefront-guided profile and compensation for cyclotorsion. Whereas, full correction with aspheric or aspheric aberration-free profiles is possible in the left eye.

CASE 5

A 32-year-old female has a refractive error. She is complaining of headache and ghost images. She has seen different doctors and optometrists, but their prescriptions were neither identical to each others nor satisfactory as she stated.
Her previous glasses and corresponding VA are shown in Table 9.5.1.

TABLE 9.5.1 Old Glasses and Visual Acuity

	UDVA	*Sph*	*Cyl*	*Axis*	*CDVA (G)*
OD	0.1	−3.0	−1	180	0.8
OS	0.1	−3.0	−1	175	0.8

UDVA= uncorrected distance visual acuity; CDVA (G)= corrected distance visual acuity (by glasses)

Her MR and corresponding VA are shown in Table 9.5.2. Her CR is shown in Table 9.5.3.

TABLE 9.5.2 Manifest Refraction and Visual Acuity

	UDVA	*Sph*	*Cyl*	*Axis*	*CDVA (G)*	*CDVA (G+PH)*
OD	0.1	−3.25	−0.5	135	0.9	1.0
OS	0.1	−3.25	−0.5	45	0.9	1.0

UDVA= uncorrected distance visual acuity; CDVA (G)= corrected distance visual acuity (by glasses); CDVA (G+PH)= corrected distance visual acuity (by glasses and pin hole)

TABLE 9.5.3 Cycloplegic Refraction

	Sph	*Cyl*	*Axis*
OD	−3	−1	130
OS	−3	−1	50

Figures 9.5.1 to 9.5.9 are corneal tomography for the right eye which will be studied as an example.

1. **The Qualification Step:**
   a. In a general look, the four composite maps seem normal (Fig. 9.5.1).
   b. Studying single maps:
      i. The anterior sagittal curvature map (Fig. 9.5.2) shows SB with neither SRAX nor significant inferior superior difference.
      ii. The anterior elevation map:
         1. In BFS mode (Fig. 9.5.3): although it is not an ideal sandy watch, it can be considered normal because of symmetry.
         2. In the BFTE mode (Fig. 9.5.4): normal values within the central 5 mm circle.
      iii. The posterior elevation map:
         1. In BFS mode (Fig. 9.5.5): although it is not an ideal sandy watch, it can be considered normal because of symmetry.
         2. In BFTE mode (Fig. 9.5.6): normal values within the central 5 mm circle.
      iv. The pachymetry map (Fig. 9.5.7) shows normal shape but with horizontally-displaced thinnest location (white arrow).
      v. Thickness profiles (Fig. 9.5.8): The red curves are normal in spite of the deviation since the latter is after the 6 mm zone (green arrows). The average is abnormal (1.2).

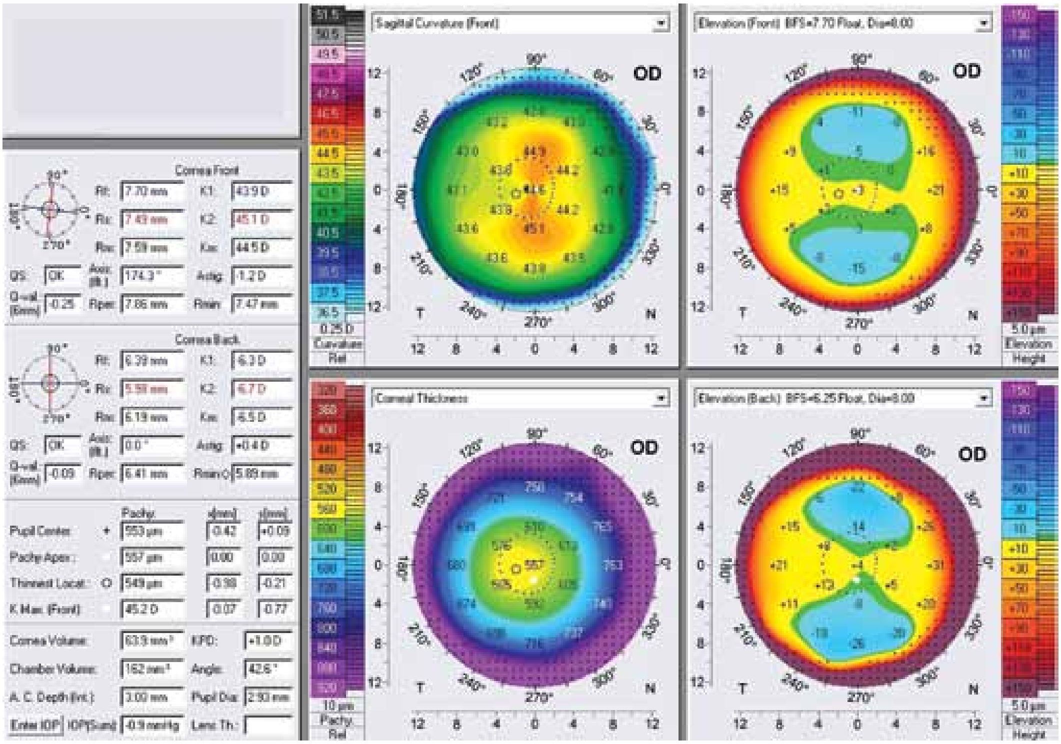

Fig. 9.5.1 OD. The four composite maps.

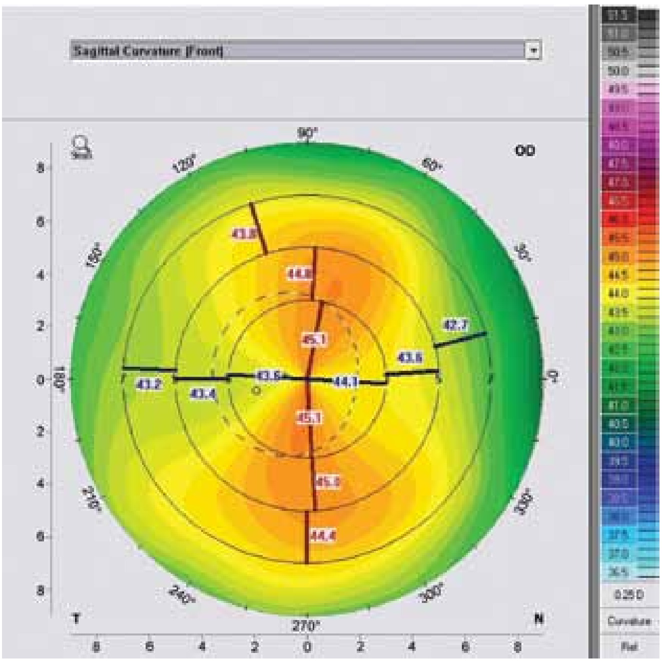

Fig. 9.5.2 OD. The anterior curvature sagittal map. SB pattern.

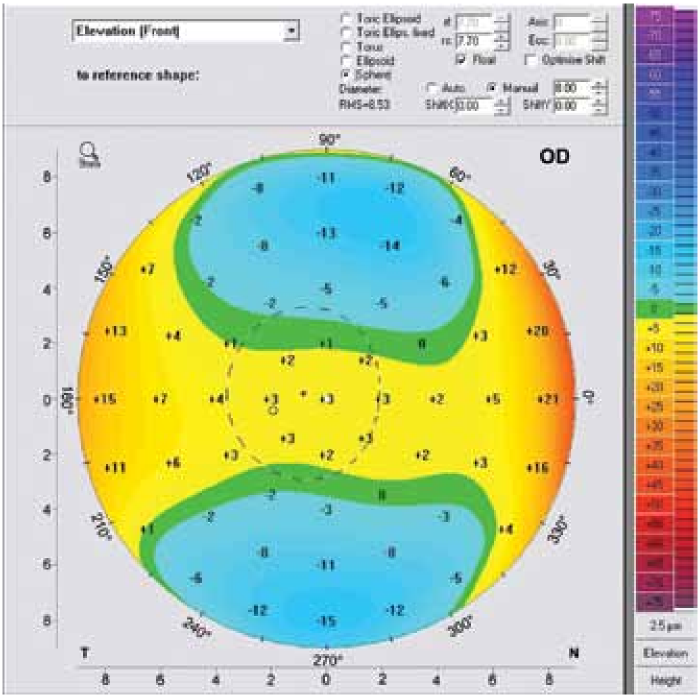

Fig. 9.5.3 OD. The anterior elevation map with BFS reference body. Sandy watch pattern although not ideal.

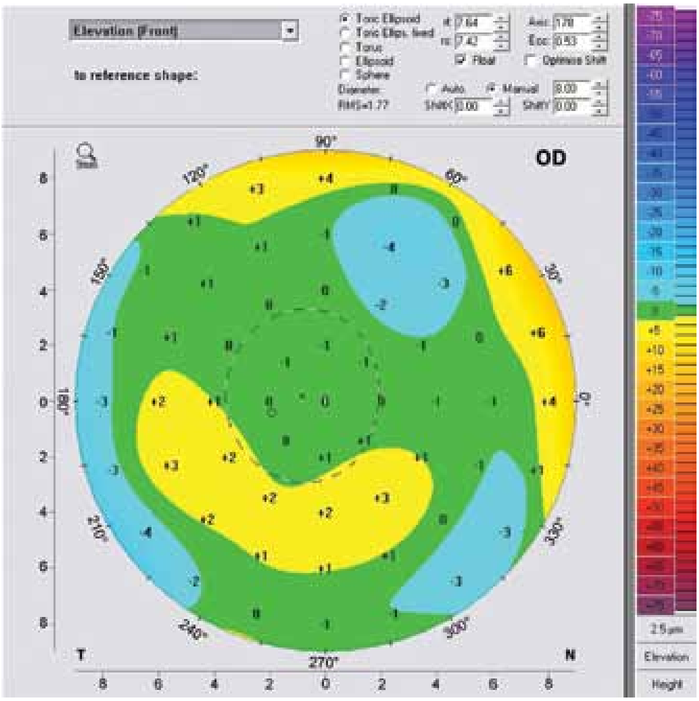

Fig. 9.5.4 OD. The anterior elevation map with BFTE reference body.

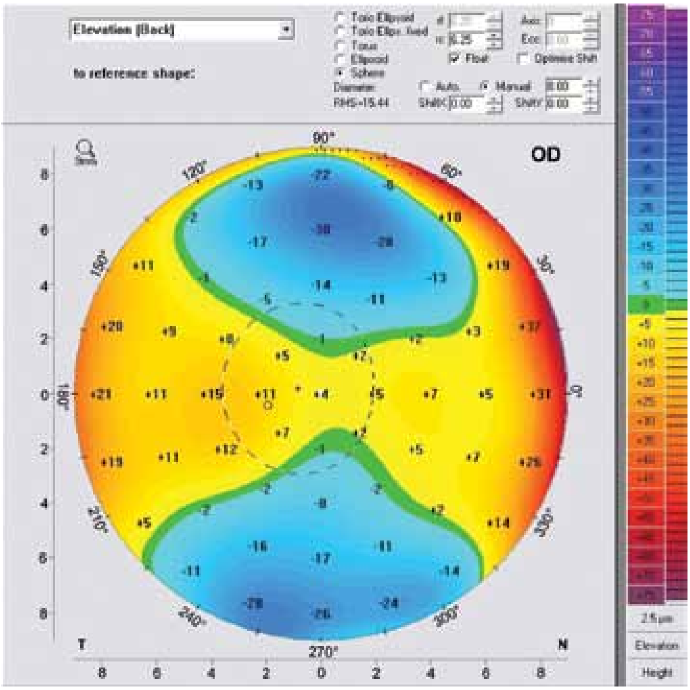

Fig. 9.5.5 OD. The posterior elevation map with BFS reference body. Sandy watch pattern.

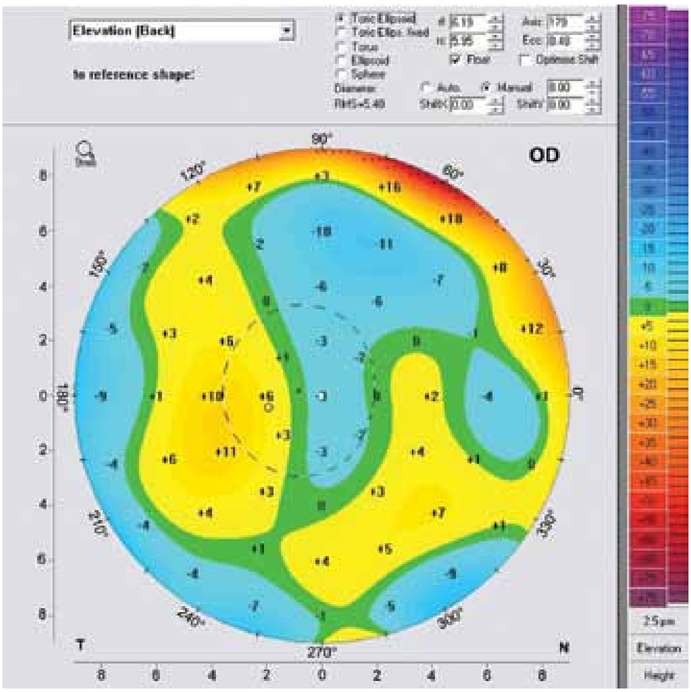

Fig. 9.5.6 OD. The posterior elevation map with BFTE reference body.

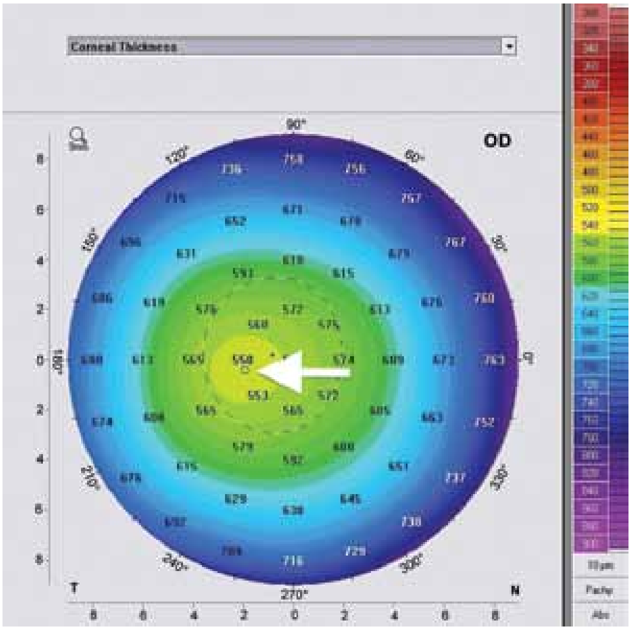

Fig. 9.5.7 OD. The pachymetry map. The white arrow points at the horizontally-displaced thinnest location.

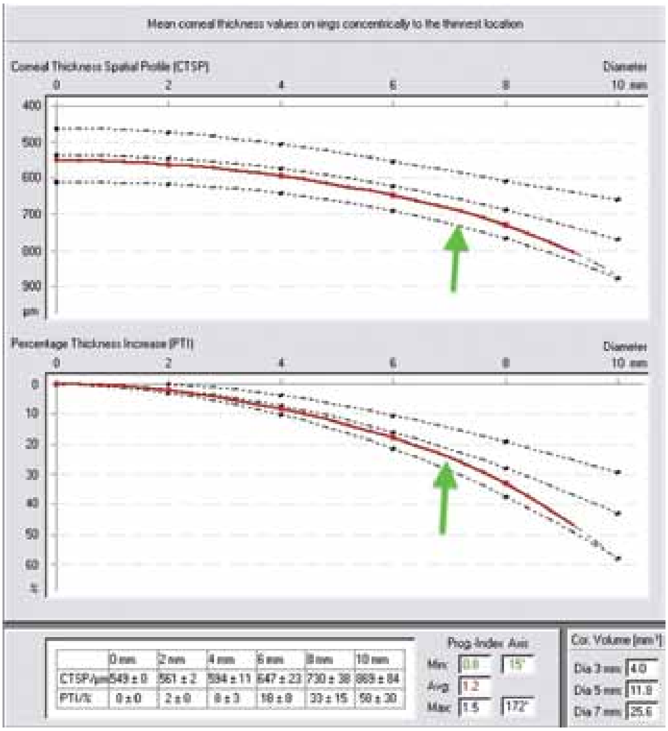

Fig. 9.5.8 OD. Thickness profiles. The curves leave the slope after 6 mm (green arrows).

c. Qualification of values (Fig. 9.5.9):
   i. QS is OK.
   ii. K readings including K-max are <48 D.
   iii. K-max-steep K is < 1 D.
   iv. Astigmatism is < 6 D.
   v. Thickness at the thinnest location is >500 µm.
   vi. Pachy-Thinnest difference in thickness is < 10 µm.
   vii. *Y*-coordinate of the thinnest location is less than –500 µm (–210 µm).
   viii. ACD, ACA and ACV are normal.
   ix. Mesopic pupil diameter is 2.93 mm.
   x. Pupil X-coordinate indicates significant angle kappa.

d. Qualification of Wavefront: Wavefront analysis should be done because of:
   – Disparity among glasses, TA and MA.
   – Symptoms that the patient is suffering from.

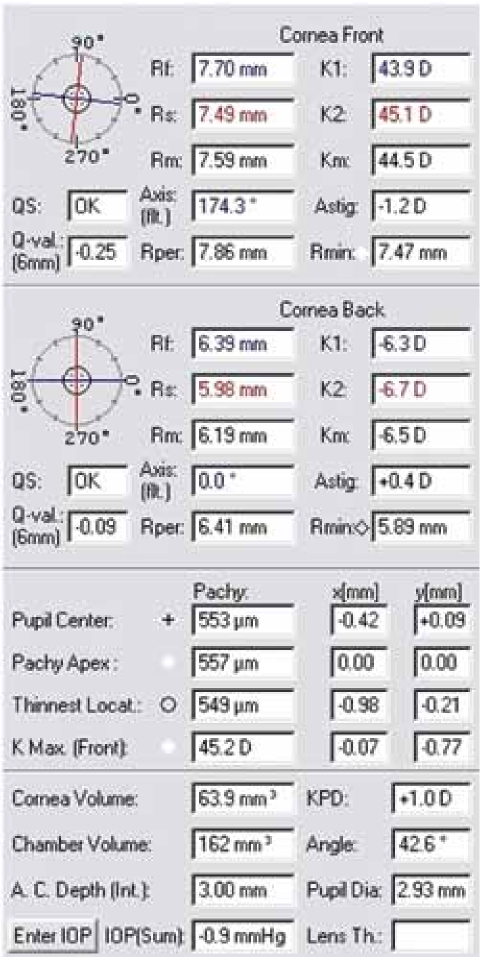

Fig. 9.5.9 OD. Corneal parameters.

Figures 9.5.10 and 9.5.11 represent wavefront of the right eye:

i. The objective refractive error measured by wavefront (Fig. 9.5.10 red arrow) is consistent with the MR (see Table 9.5.1).
ii. RMS related HOAs is 0.55 (>0.3) (Fig. 9.5.10 red ellipse).
iii. PSF related HOAs is spread over 10 minutes of arc, which is considered moderate (Fig. 9.4.11 blue ellipse).
iv. Zernike coefficient is almost 0.43, which is in the range of [0.25–0.50], and mainly produced by coma (Fig. 9.5.11 green arrows).

2. **Discussion:**

Patient's complaints can be explained by coma and the disparity between MA and TA. All causes of disparity should be excluded (refer to chapter 6).

PRT is an option in spite of one abnormal finding in tomography: the abnormal average in thickness profiles. However, SA can be done safely in this case but with the following considerations:

a. The disparity between MA and TA is of oblique type (probability number 9, see example 29 in chapter 6). In this case, there are two methods to follow. The first one is to correct the MR, since it is consistent with the wavefront objective refractive error. In this method, a new astigmatism with a new axis and amount will be created on the anterior corneal surface. This may impact the quality of vision postoperatively in spite of the achieved

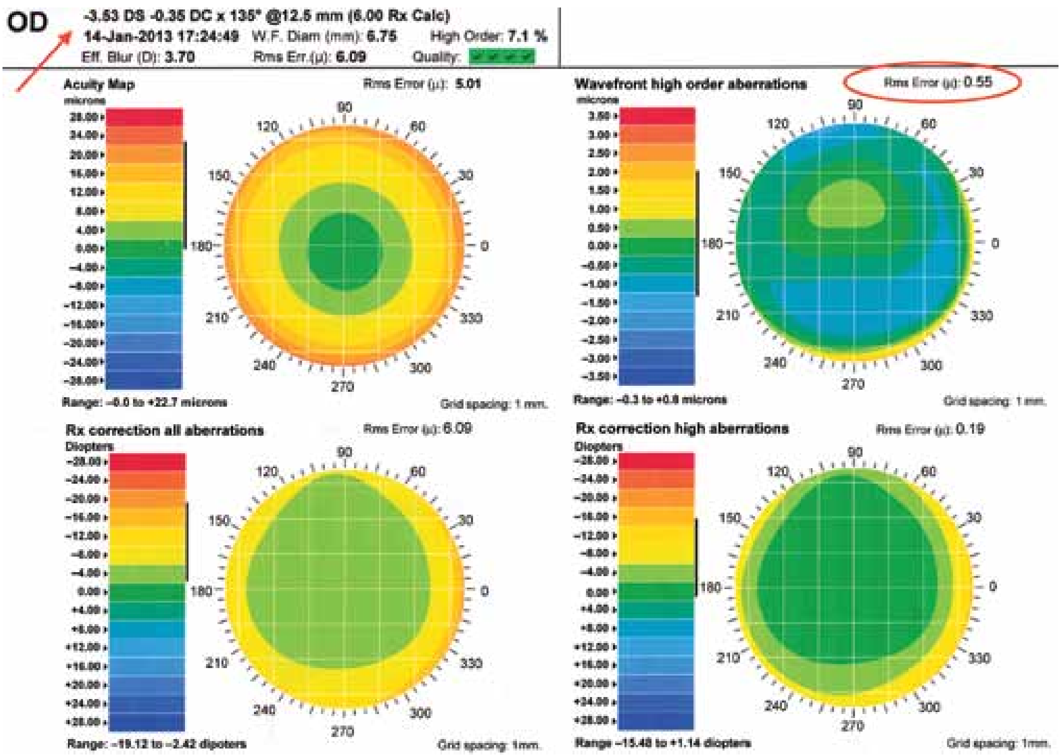

Fig. 9.5.10 OD. Ocular wavefront. The red arrow points at the objective refractive error. The red ellipse indicates RMS related to HOAs.

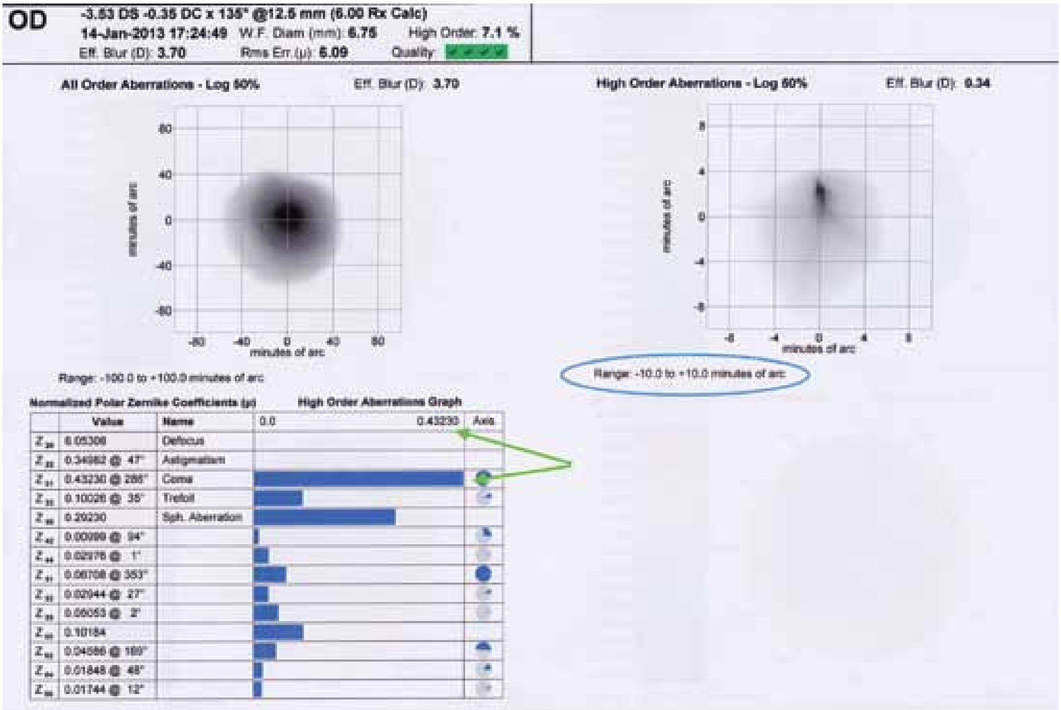

Fig. 9.5.11 OD. Ocular wavefront. The green arrows point at ZC of HOAs which mainly consists of coma. The blue ellipse indicates the range of PSF.

emmetropia and there might be a need for enhancement. The second one is to correct either the spherical equivalent or only the spherical component since the MA is <1 D. In this method, enhancement may also be required. The second option is preferred in order to maintain the original astigmatism and avoid anterior surface distortion.

b. Wavefront analysis indicates wavefront-guided ablation profile with cyclotorsion compensation.

c. The relatively large angle kappa indicates decentration.
CLE is excluded since the patient is 32-years-old and his refractive error is mild.
ACD is suitable for PIOL implantation, but this option is questionable because of mild refractive error, presence of coma (which cannot be corrected by PIOLs) and the astigmatic disparity.

3. **Quantitative Step:**
If SA is indicated, it is wise to know that wavefront-guided treatment ablates more tissue per diopter depending on the severity and type of HOAs. In general, an average of *19 μm per diopter* is ablated for 6.5 mm OZ and will be used in our quantification.
Since, the preferred method in this case is to correct the sphere only, it will be dealt with as a myopic case.

a. Thickness concepts: MR will be used in calculations.
RSB Law 5: the AD = (3.25) x 19 = 61.75 μm, which is < 80 μm and therefore, the refractive errors can be completely corrected since the RSB = 549 – 61.75 ≈ 487 μm.

b. K-readings Concept (Table 9.5.4):

TABLE 9.5.4 Final K

Refractive error	*Original K*	*Astigmatic correction*	*Myopic correction*	*Final K*
–3.25 sph	K_f = 43.9 D	(0) K_f = 43.9 D	(3.25 x 0.75 = 2.44 D) K_f = 43.9 – 2.44 = 41.46 D	38.7 D in average
0 cyl	K_s = 45.1 D	(0) K_s = 45.1 D	(3.25 x 0.75 = 2.44 D) K_s = 45.1 – 2.44 = 35.9 D	

K_f : flat K
K_s : steep K

As shown in this Table, the final K is >34 D.

4. **Conclusion:** Full correction of sphere with SA is possible, but with wavefront-guided profile, compensation for cyclotorsion and decentration.

CASE 6

A 54-years-old male has a refractive error. He is complaining of anisometropia.
His MR and VA are shown in Table 9.6.1. His CR is shown in Table 9.6.2.

TABLE 9.6.1 Manifest refraction and visual acuity

	UDVA	*Sph*	*Cyl*	*Axis*	*CDVA (G)*	*CDVA (G+PH)*
OD	0.1	−3			1.0	1.0
OS	0.3	+2			0.7	0.7

UDVA= uncorrected distance visual acuity; CDVA (G)= corrected distance visual acuity (by glasses); CDVA (G+PH)= corrected distance visual acuity (by glasses and pin hole)

TABLE 9.6.2 Cycloplegic refraction

	Sph	*Cyl*	*Axis*
OD	−3	−0.5	175
OS	+3	−0.25	180

Figures 9.6.1 to 9.6.9 represent corneal tomography of the right eye and Figures 9.6.10 to 9.6.18 represent corneal tomography of the left eye.

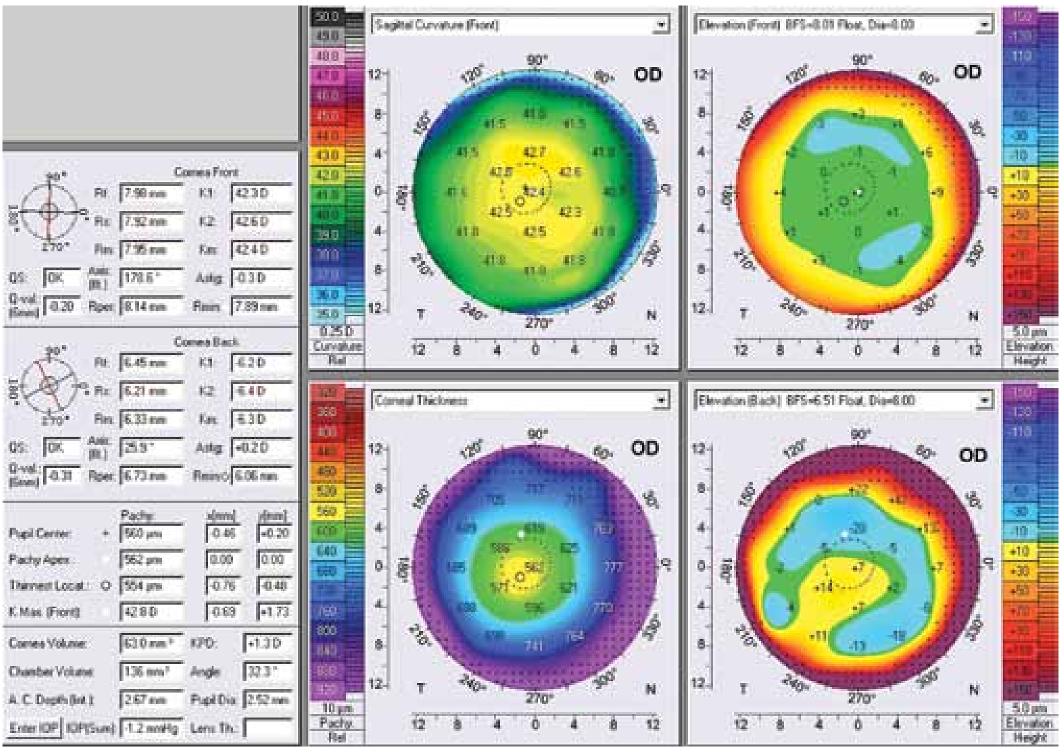

Fig. 9.6.1 OD. The four composite maps.

1. **The Qualification Step:**
   Right Eye:
   a. In a general look, there are some irregularities in all maps (Fig. 9.6.1).
   b. Studying single maps:
      i. The anterior sagittal curvature map (Fig. 9.6.2) shows mild irregularity with border line SRAX (almost 22°). There is no significant inferior-superior difference.
      ii. The anterior elevation map:
         1. In BFS mode (Fig. 9.6.3): isolated island.
         2. In the BFTE mode (Fig. 9.6.4): normal values within the central 5 mm circle.
      iii. The posterior elevation map:
         1. In BFS mode (Fig. 9.6.5): Tongue-like extension.
         2. In BFTE mode (Fig. 9.6.6): Abnormal values (>15) within the central 5 mm circle (black arrow).
      iv. The pachymetry map (Fig. 9.6.7) shows mild dome shape with horizontally-displaced thinnest location (white arrow). (See *X*-coordinate in Figs 9.6.1 and 9.6.9).
      v. Thickness profiles (Fig. 9.6.8) show normal slopes but with high average (1.2).

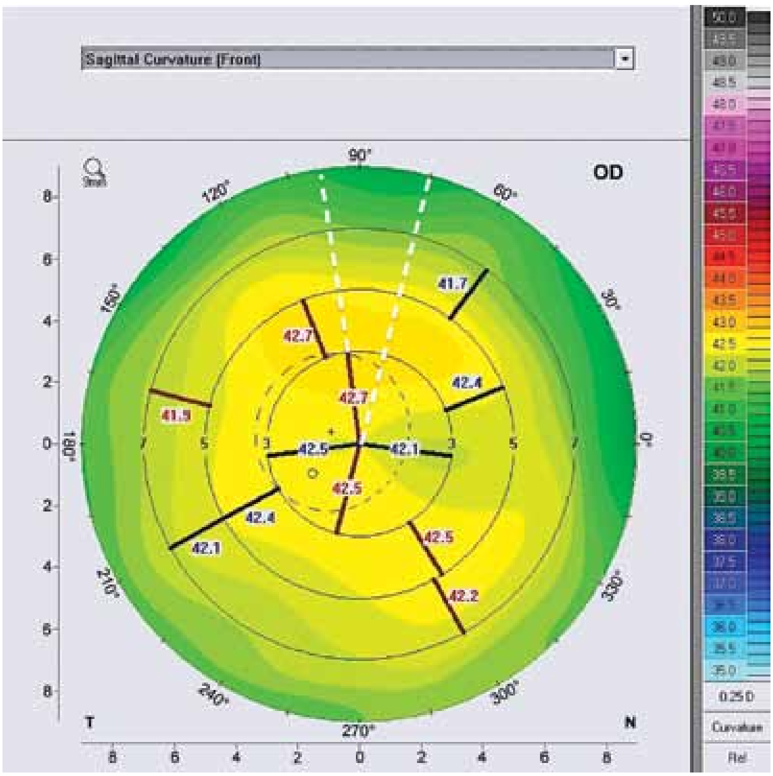

Fig. 9.6.2 OD. The anterior curvature sagittal map. Mild irregularity with borderline SRAX.

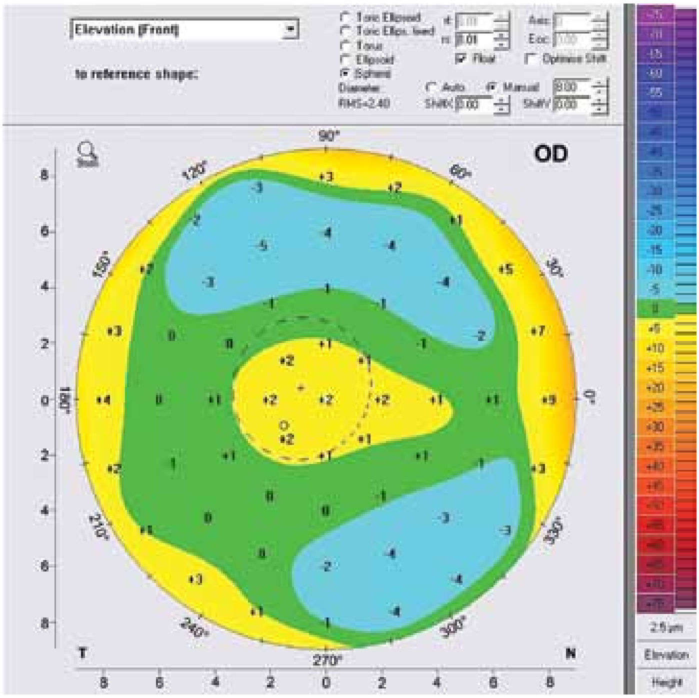

Fig. 9.6.3 OD. The anterior elevation map with BFS reference body. Isolated island.

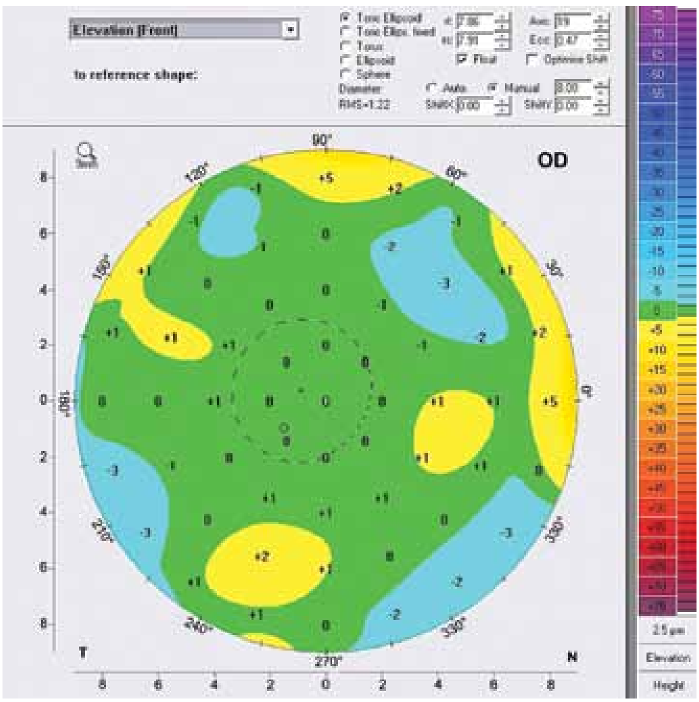

Fig. 9.6.4 OD. The anterior elevation map with BFTE reference body.

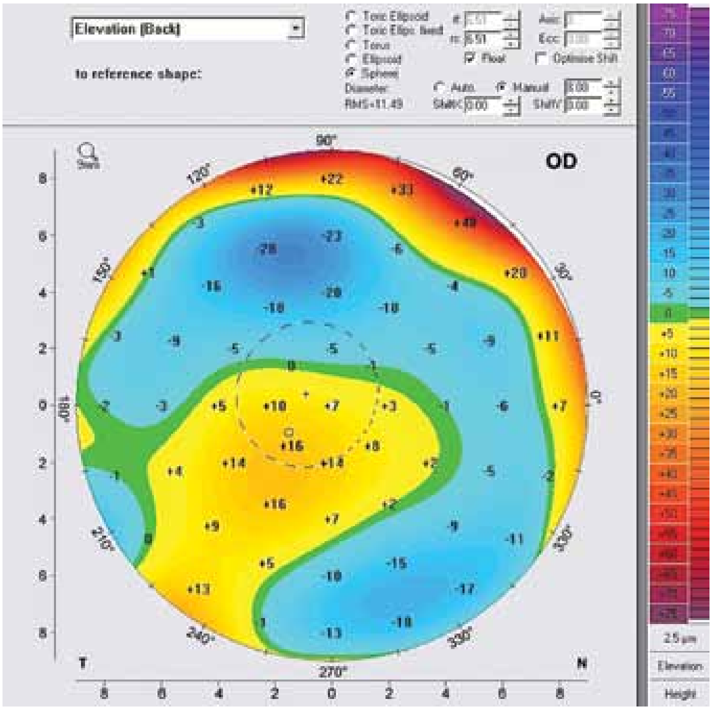

Fig. 9.6.5 OD. The posterior elevation map with BFS reference body. Tongue-like extension.

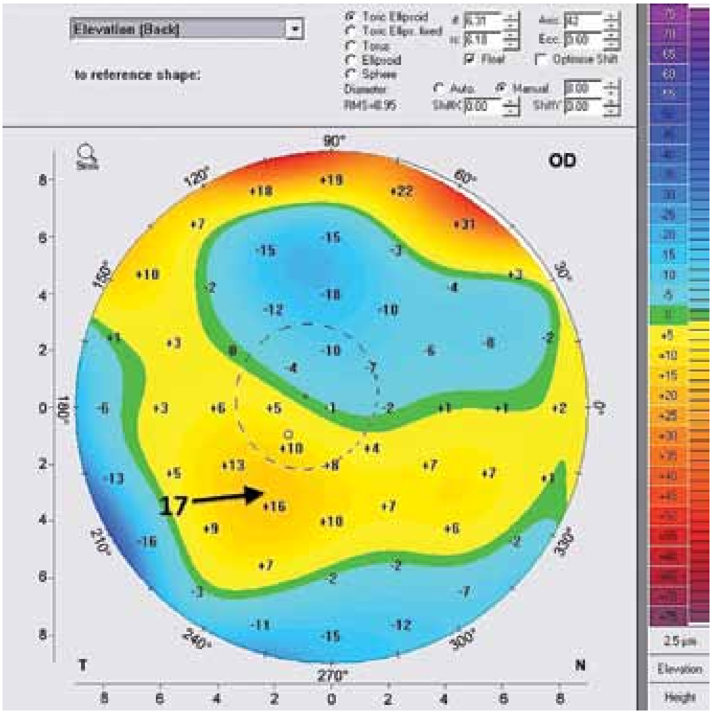

Fig. 9.6.6 OD. The posterior elevation map with BFTE reference body. Abnormal values (black arrow).

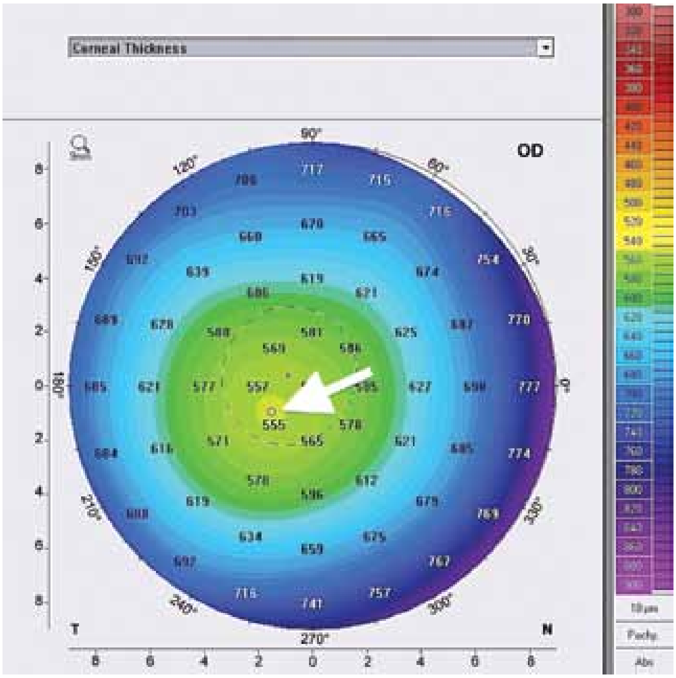

Fig. 9.6.7 OD. The pachymetry map. The white arrow points at the horizontally-displaced thinnest location and mild dome-like pattern.

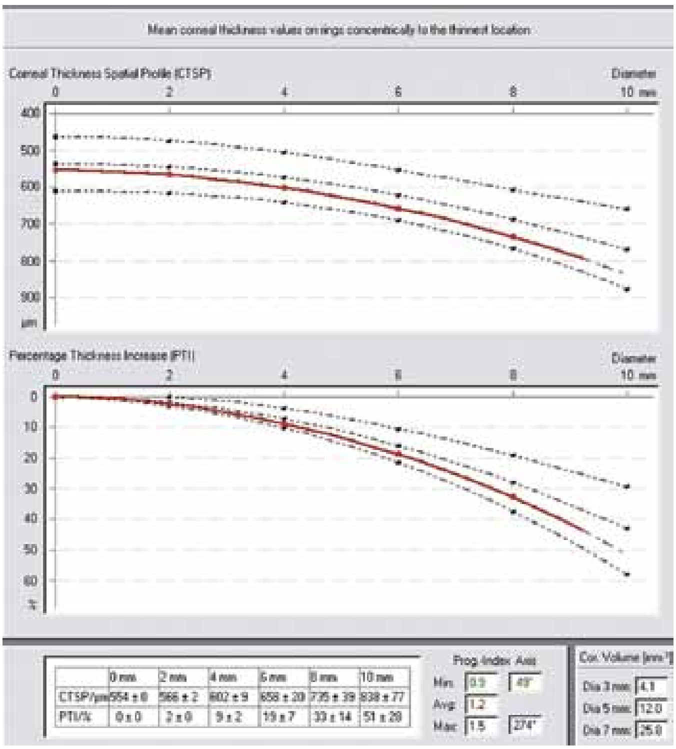

Fig. 9.6.8 OD. Thickness profiles.

c. Qualification of values (Fig. 9.6.9):
   i. QS is OK.
   ii. K readings including K-max are <48 D.
   iii. K-max-steep K is < 1 D
   iv. Astigmatism is < 6 D.
   v. Thickness at the thinnest location is >500 µm.
   vi. Pachy-Thinnest difference in thickness is <10 µm.
   vii. *Y*-coordinate of the thinnest location is border line (–480 µm).
   viii. Although ACD is normal (>2.4 mm), it is <3.0 mm. ACA and ACV are normal (>24° and >100 mm^3, respectively).
   ix. Mesopic pupil diameter is 2.52 mm.
   x. Pupil coordinates indicate decentred pupil and significant angle Kappa.

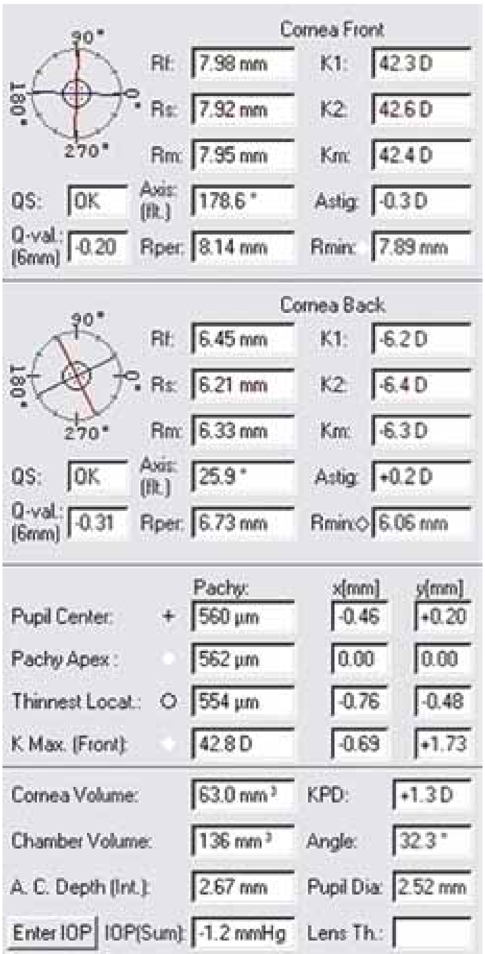

Fig. 9.6.9 OD. Corneal parameters.

Left Eye:

a. In a general look, there are some irregularities in all four maps (Fig. 9.6.10).

b. Studying single maps:

   i. The anterior sagittal curvature map (Fig. 9.6.11):
      Although it seems to be AB, there is neither SRAX nor significant inferior superior difference.

   ii. The anterior elevation map:
      1. In BFS mode (Fig. 9.6.12): Tongue-like extension.
      2. In the BFTE mode (Fig. 9.6.13): normal values within the central 5 mm circle.

   iii. The posterior elevation map:
      1. In BFS mode (Fig. 9.6.14): tongue-like extension.
      2. In BFTE mode (Fig. 9.6.15): abnormal values (>15) within the central 5 mm circle (black arrow).

   iv. The pachymetry map (Fig. 9.6.16) shows mild dome shape with a horizontal displacement (white arrow). (See *X*-coordinate in Figs 9.6.10 and 9.6.18).

   v. Thickness profiles (Fig. 9.6.17) show normal slope of the red curves. The average is abnormal (1.2).

c. Qualification of values (Fig. 9.6.18):

   i. QS is OK.
   ii. K readings including K-max are <48 D.
   iii. K-max-steep K is <1 D.
   iv. Astigmatism is < 6 D.

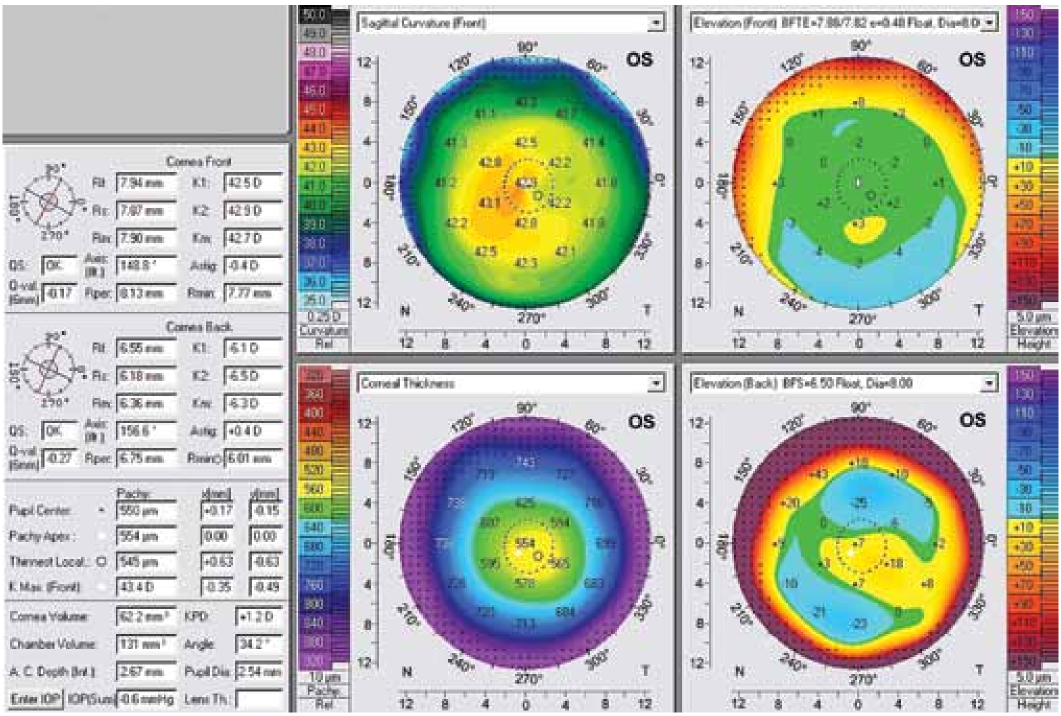

Fig. 9.6.10 OS. The four composite maps.

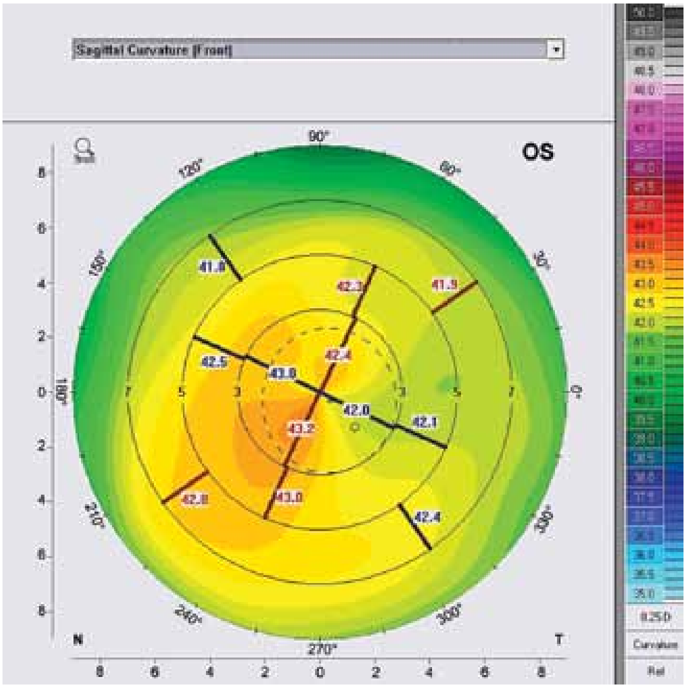

Fig. 9.6.11 OS. The anterior curvature sagittal map. AB/IS.

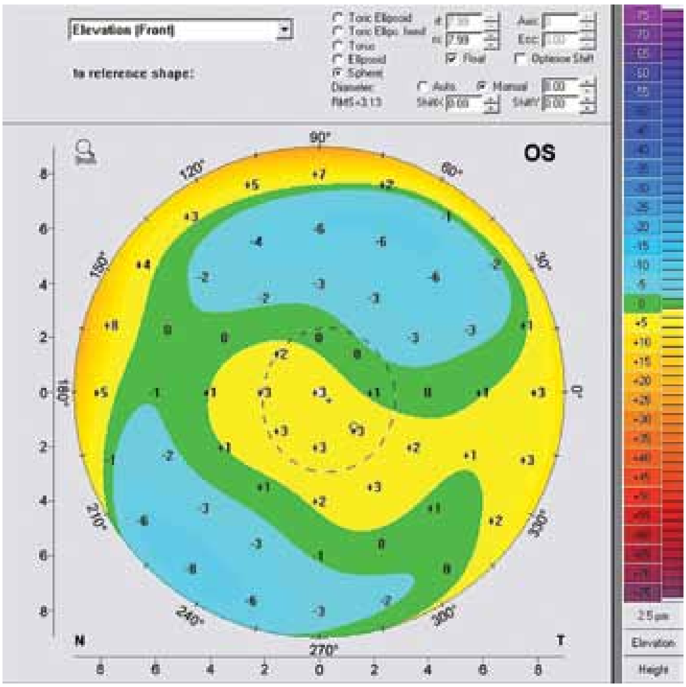

Fig. 9.6.12 OS. The anterior elevation map with BFS reference body. Tongue-like extension.

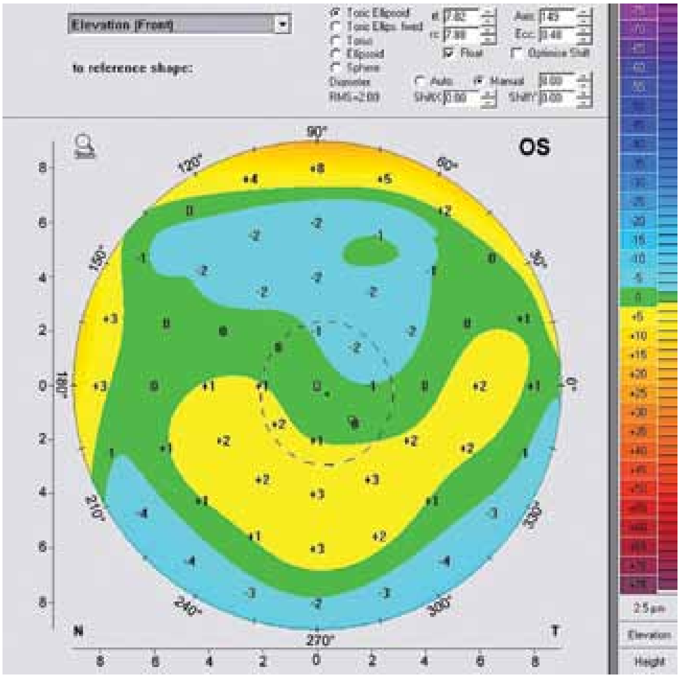

Fig. 9.6.13 OS. The anterior elevation map with BFTE reference body.

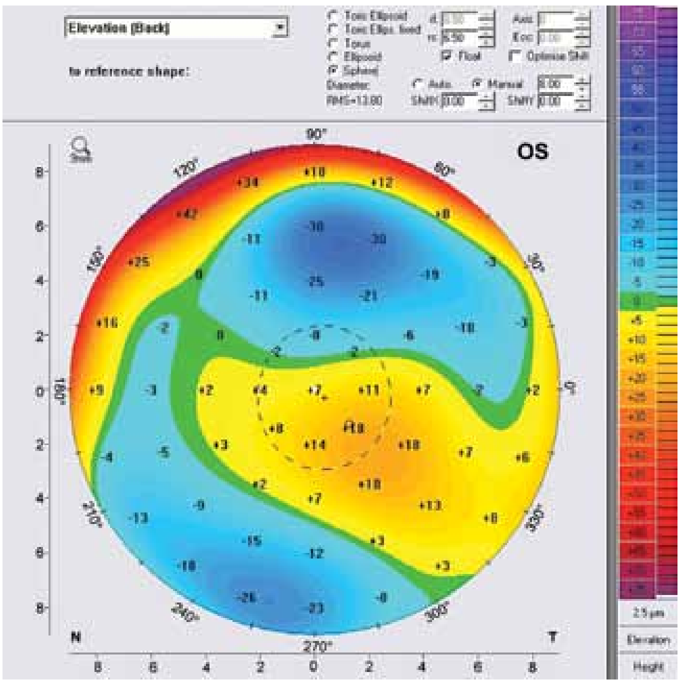

Fig. 9.6.14 OS. The posterior elevation map with BFS reference body. Tongue-like extension.

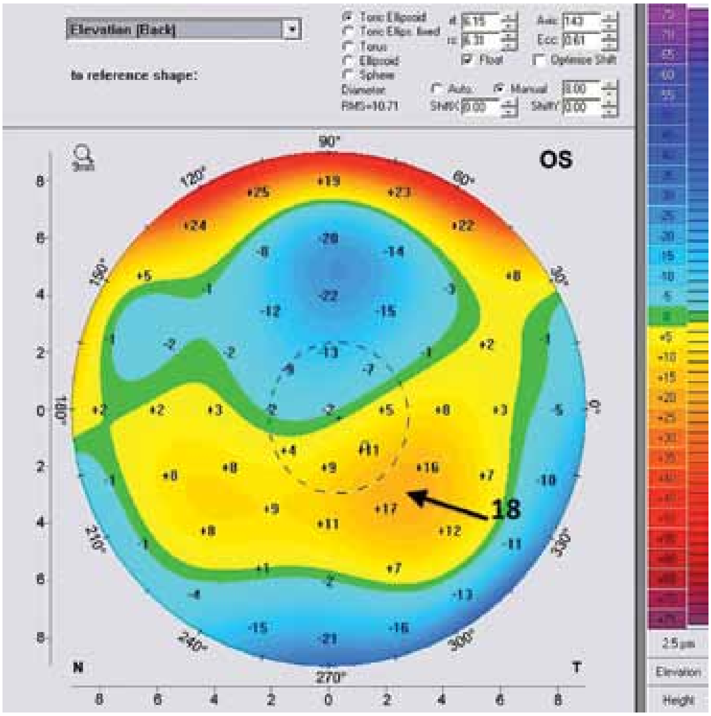

Fig. 9.6.15 OS. The posterior elevation map with BFTE reference body. Abnormal values (black arrow).

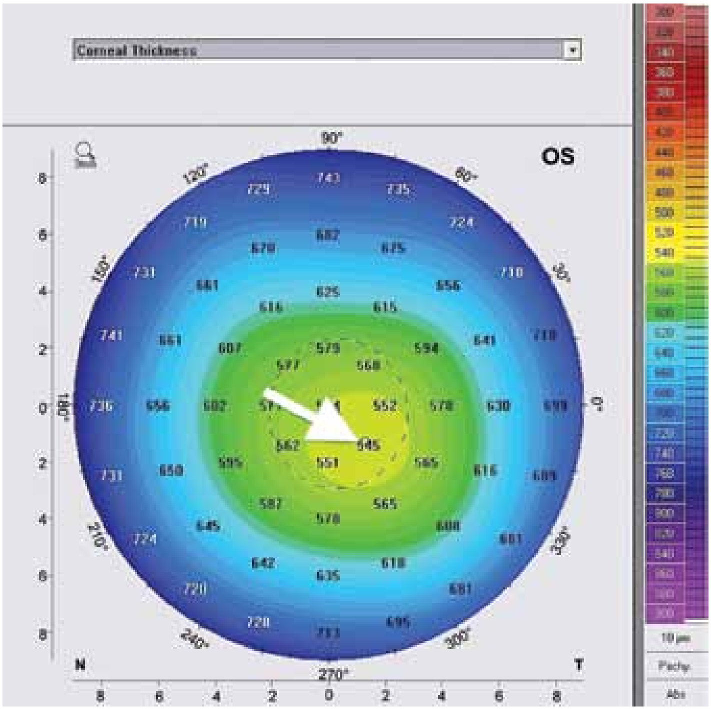

Fig. 9.6.16 OS. The pachymetry map. The white arrow points at the horizontally-displaced thinnest location and mild dome-like pattern.

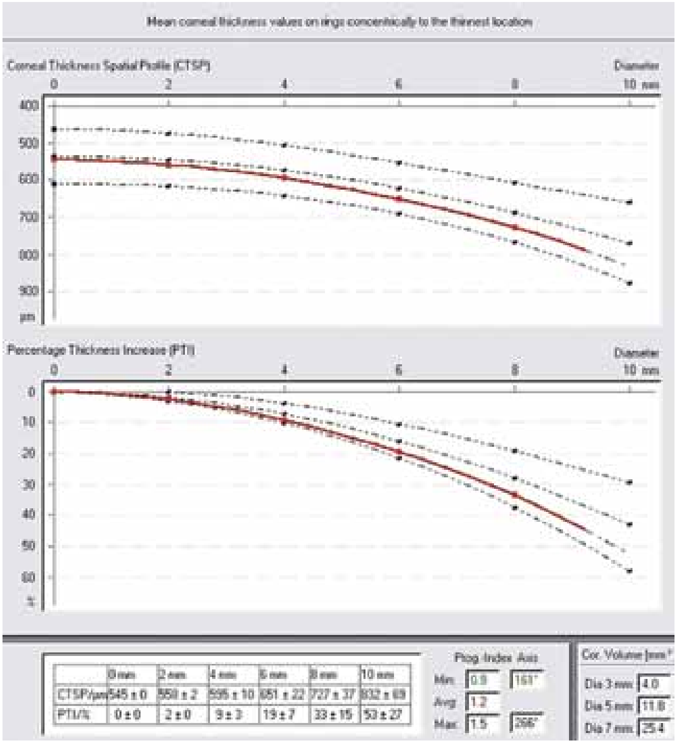

Fig. 9.6.17 OS. Thickness profiles.

v. Thickness at the thinnest location is >500 µm.
vi. Pachy-Thinnest difference in thickness is <10 µm.
vii. *Y*-coordinate of the thinnest location is >–500 µm (–630 µm).
viii. Although ACD is normal (>2.4 mm), it is <3.0 mm, ACA and ACV are normal (>24° and >100 mm^3, respectively).
ix. Mesopic pupil diameter is 2.54 mm.
x. Pupil coordinates indicate central pupil and insignificant angle Kappa.

2. **Discussion:**

The patient has anisometropia with amblyopia in the hyperopic eye proven by amblyopia tests.

The question is: is this anisometropia related to difference in ocular axial length? Biometry was done. The axial length of the right eye was 0.75 mm longer than that of the left eye, which explains some of the refractive difference meaning that there might be additional causes related to the lens or to the cornea. Causes related to the lens are either index-based such as sclerosis or nuclear cataract, or curvature-based such as lentiglobus. Causes related to cornea are curvature-based meaning that the myopic eye should have K readings higher than the other eye, but this is not the situation in our case. Careful slitlamp re-examination of the patient revealed grade I nuclear sclerosis in the right eye.

Qualification of corneal tomography of both eyes shows the following risk factors:

a. Irregular shape of the anterior sagittal map.
b. Abnormal shapes in anterior and posterior elevation maps (BFS mode).

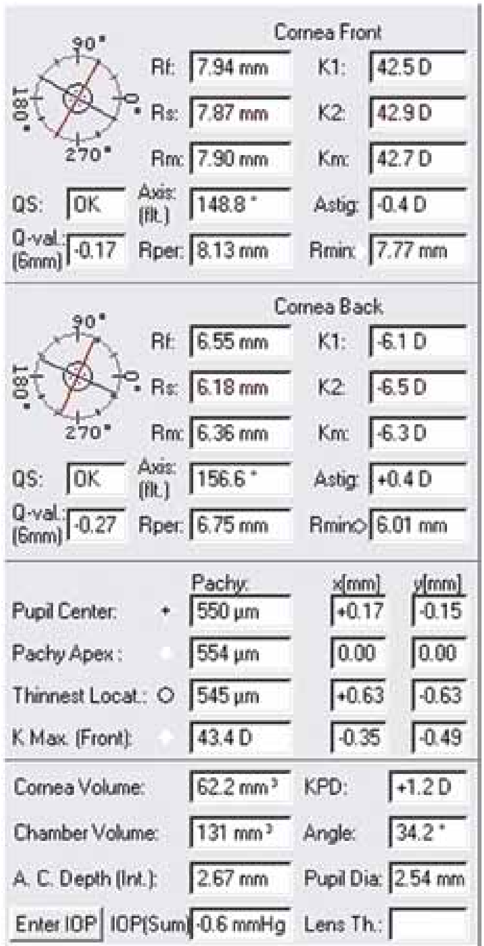

Fig. 9.6.18 OS. Corneal parameters.

c. Abnormal values in posterior elevation maps (BFTE mode).
d. Abnormal shape of the pachymetry map, especially in the left eye.
e. Abnormal average in thickness profiles.
f. Abnormal Y-coordinate of the thinnest location, especially in the left eye.

In spite of these abnormalities, SA is still an option, especially that the patient is 54-years-old indicating a relatively stiff cornea.

PIOL is not an option because of patient's age, small refractive error and the ACD is <3.0 mm.

RLE may be indicated in both eyes since there is grade I nuclear sclerosis in the right eye and the patient is 54-year-old.

Following the rule of amblyopia (see Fig. 6.29), refractive treatment can be performed for both eyes.

In summary, two options are available, SA and RLE. In my opinion, RLE outweighs SA.

In case of SA, decentration is not that important since it is pure myopia in the right eye and the angle is insignificant in the left eye. Postoperatively, the patient should be provided with all

pre-, intra- and postoperative data since he is in the potential age for cataract development. IOL calculations after keratorefractive surgery are not as accurate as prior to corneal surgery. The more preoperative information you provide the patient, the better his chance of having more accurate IOL calculations for post SA cataract surgery. In such cases, patients need to know that they may need corrective lenses or additional surgery in order to achieve better visual acuity after cataract surgery.

3. **Quantitative Step four SA Option:**
   Right Eye
   a. Thickness concepts:
      MR will be used in calculations.
      RSB Law 5: the AD (6.5 mm OZ) = 3 x 15 = 45 μm, which is <80 μm and therefore, the refractive errors can be completely corrected since the RSB = 554 - 45 = 509 μm.
   b. K-readings Concept (Table 9.6.3):

TABLE 9.6.3 Final K

Refractive error	*Original K*	*Astigmatic correction*	*Myopic correction*	*Final K*
–3.0 sph	K_f = 42.3 D	(0) K_f = 42.3 D	(3.0 x 0.75 = 2.25D) K_f = 42.3 – 2.25 = 40.05 D	40.2 D in average
0	K_s = 42.6 D	(0) K_s = 42.6 D	(3 x 0.75 = 2.25D) K_s = 42.6 – 2.25 = 40.35 D	

K_f : flat K
K_s : steep K

As shown in this table, the final K is >34 D.

Left Eye
   a. Thickness concepts:
      Full correction of CR will be used since the case is hyperopia and the patient is 54-year-old.
      RSB Law 7: the preoperative thinnest location is >470 μm.
   b. K-readings Concept (Table 9.6.4):

TABLE 9.6.4 Final K

Refractive error	*Original K*	*Astigmatic correction*	*Hyperopic correction*	*Final K*
+3.0 sph	K_f = 42.5 D	(0) K_f = 42.5 D	(3.0 x 1.2 = 3.6 D) K_f = 42.5 + 3.6 = 46.1 D	46.3 D in average
	K_s = 42.9 D	(0) K_s = 42.9 D	(3.0 x 1.2 = 3.6 D) K_s = 42.9 + 3.6 = 46.5 D	

K_f : flat K
K_s : steep K

As shown in this table, the final K is < 49 D.

CASE 7

A 24-year-old female has a refractive error. She is complaining of blurring vision, strain and headache after near vision work even with glasses.
Her recent glasses and corresponding VA are shown in Table 9.7.1.

TABLE 9.7.1 Recent Glasses and Visual Acuity

	UDVA	*Sph*	*Cyl*	*Axis*	*CDVA (G)*
OD	0.4	+3	−0.5	10	0.8
OS	0.4	+2.5			0.9

UDVA= uncorrected distance visual acuity; CDVA (G)= corrected distance visual acuity (by glasses)

Her MR and corresponding VA are shown in Table 9.7.2.

TABLE 9.7.2 Manifest Refraction and Visual Acuity

	UDVA	*Sph*	*Cyl*	*Axis*	*CDVA (G)*
OD	0.4	+3	−1	60	1.0
OS	0.4	+2.5	−0.5	95	1.0

UDVA= uncorrected distance visual acuity; CDVA (G)= corrected distance visual acuity (by glasses)

Her CR is shown in Table 9.7.3.

TABLE 9.7.3 Cycloplegic Refraction

	Sph	*Cyl*	*Axis*
OD	+6	−1	65
OS	+6	−0.5	100

Since there is >0.75 D difference between MR and CR, PMT should be performed.
PMT and corresponding VA are shown in Table 9.7.4.

TABLE 9.7.4 Post-medriatic Refraction and Visual Acuity

	UDVA	*Sph*	*Cyl*	*Axis*	*CDVA (G)*
OD	0.4	+4	−1	60	1.0
OS	0.4	+4	−0.5	95	1.0

UDVA= uncorrected distance visual acuity; CDVA (G)= corrected distance visual acuity (by glasses)

Figures 9.7.1 to 9.7.9 represent right eye tomography. Figures 9.7.10 to 9.7.18 represent left eye tomography.

1. **Qualification Step:**

   Right Eye:

   a. In a general look, there are some irregularities in the anterior curvature map and posterior elevation map (Fig. 9.7.1).
   b. Studying single maps:
      i. The anterior sagittal curvature map (Fig. 9.7.2) shows a horizontal AB pattern indicating ATR astigmatism.

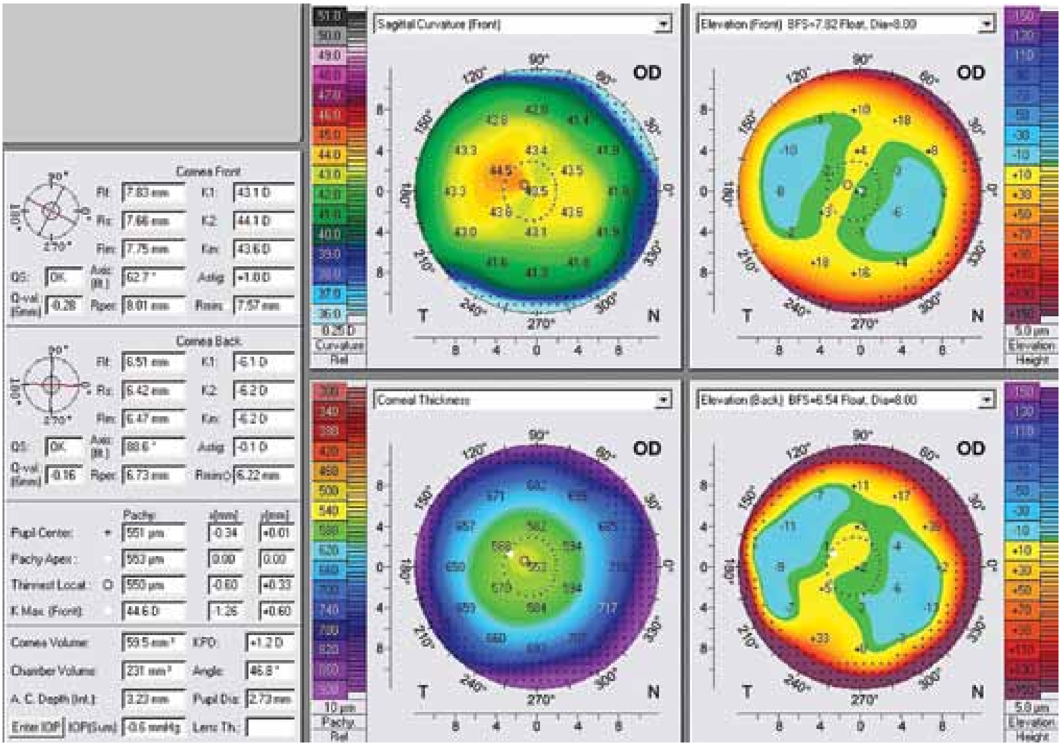

Fig. 9.7.1 OD. The four composite maps.

ii. The anterior elevation map:
   1. In BFS mode (Fig. 9.7.3): although it is not an ideal sandy watch, it can be considered normal because of symmetry.
   2. In the BFTE mode (Fig. 9.7.4): normal values within the central 5 mm circle.

iii. The posterior elevation map:
   1. In BFS mode (Fig. 9.7.5): Tongue-like extension.
   2. In BFTE mode (Fig. 9.7.6): Normal values within the central 5 mm circle.

iv. The pachymetry map (Fig. 9.7.7) shows normal shape although the thinnest location is superio-temporally-displaced (white arrow).

v. Thickness profiles (Fig. 9.7.8) show normal slopes and normal average (0.8).

c. Qualification of values (Fig. 9.7.9):
   i QS is OK.
   ii. K readings including K-max are <48 D.
   iii. K-max-steep K is < 1 D.
   iv. Astigmatism is < 6 D.
   v. Thickness at the thinnest location is >500 µm.
   vi. Pachy-Thinnest difference in thickness is <10 µm.
   vii. *Y*-coordinate of the thinnest location is positive due to superior displacement which is rare but normal.
   viii. ACD is >3.0 mm, ACA and ACV are normal (>24° and >100 mm^3, respectively).
   ix. Mesopic pupil diameter is 2.73 mm.
   x. Pupil coordinates indicate decentred pupil and significant angle Kappa.

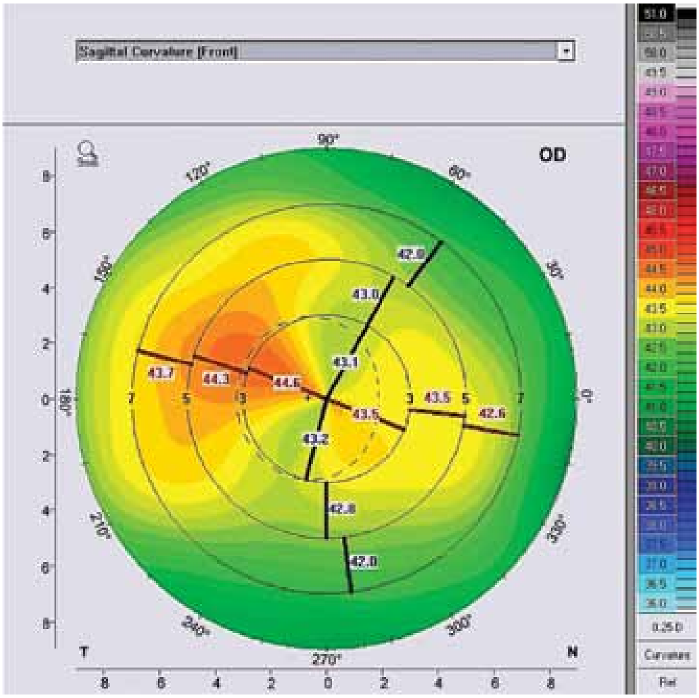

Fig. 9.7.2 OD. The anterior curvature sagittal map. ATR astigmatism.

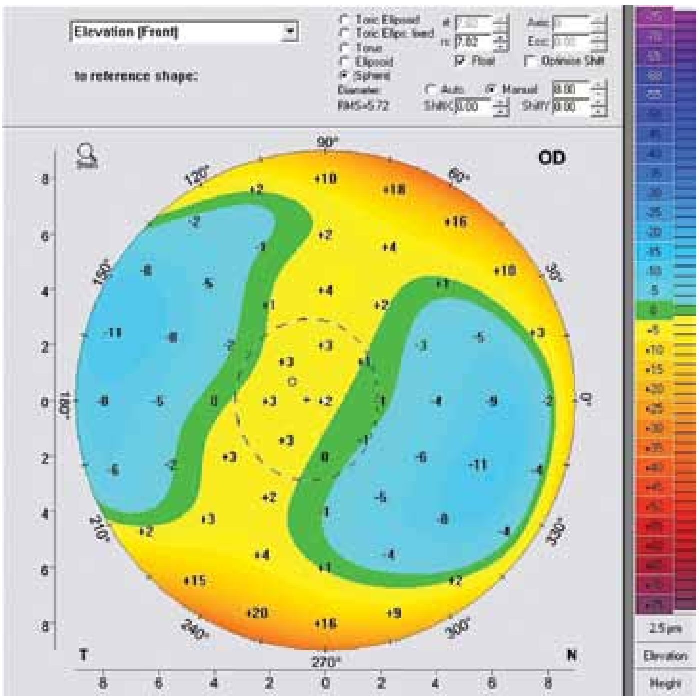

Fig. 9.7.3 OD. The anterior elevation map with BFS reference body. Horizontal sandy watch pattern.

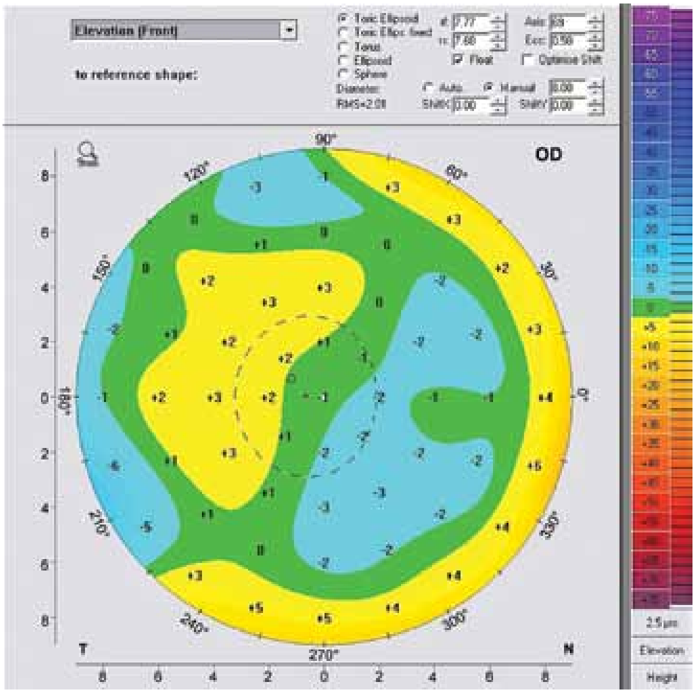

Fig. 9.7.4 OD. The anterior elevation map with BFTE reference body.

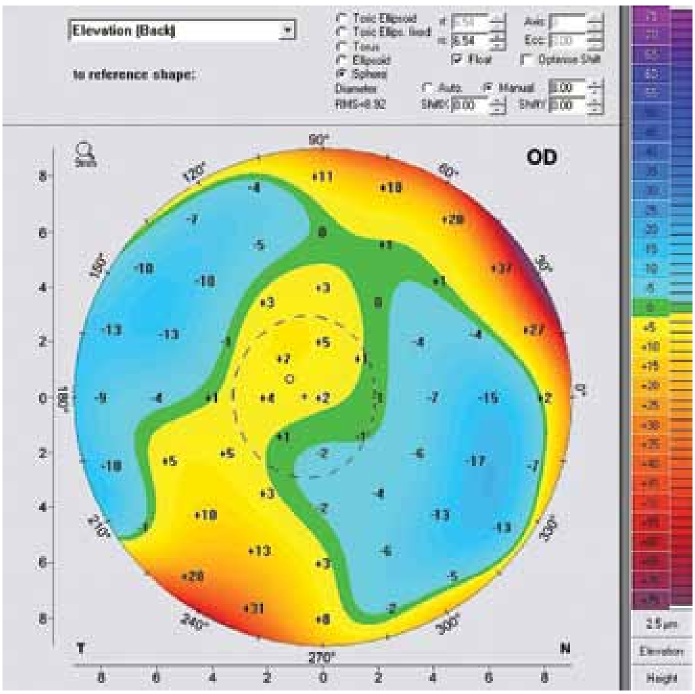

Fig. 9.7.5 OD. The posterior elevation map with BFS reference body. Tongue-like extension.

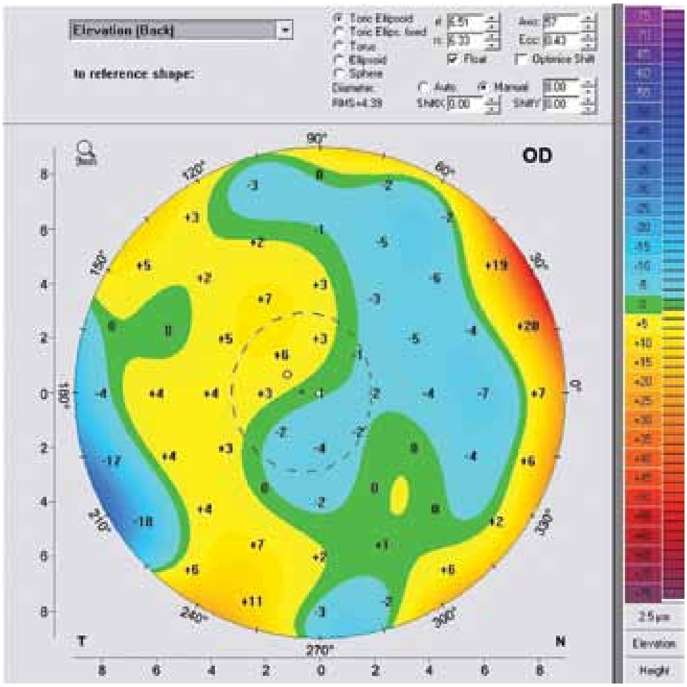

Fig. 9.7.6 OD. The posterior elevation map with BFTE reference body.

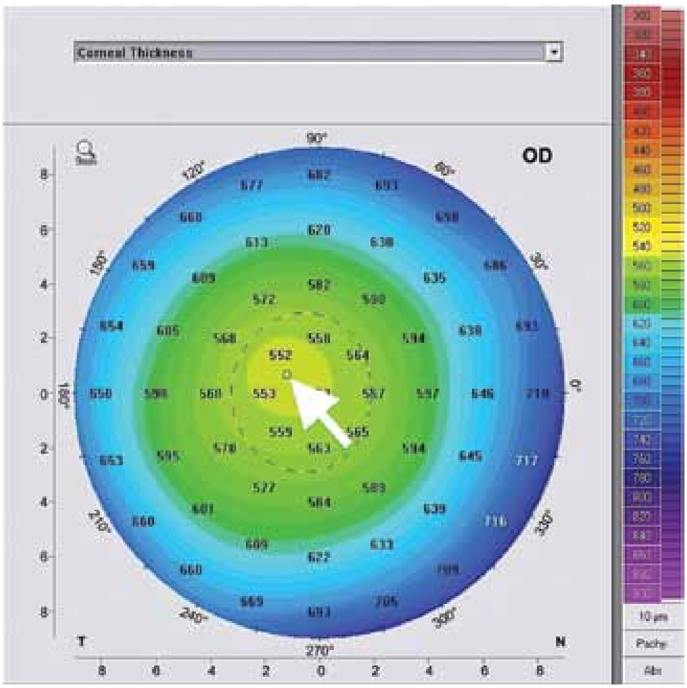

Fig. 9.7.7 OD. The pachymetry map. The white arrow points at the horizontally and superiorly-displaced thinnest location.

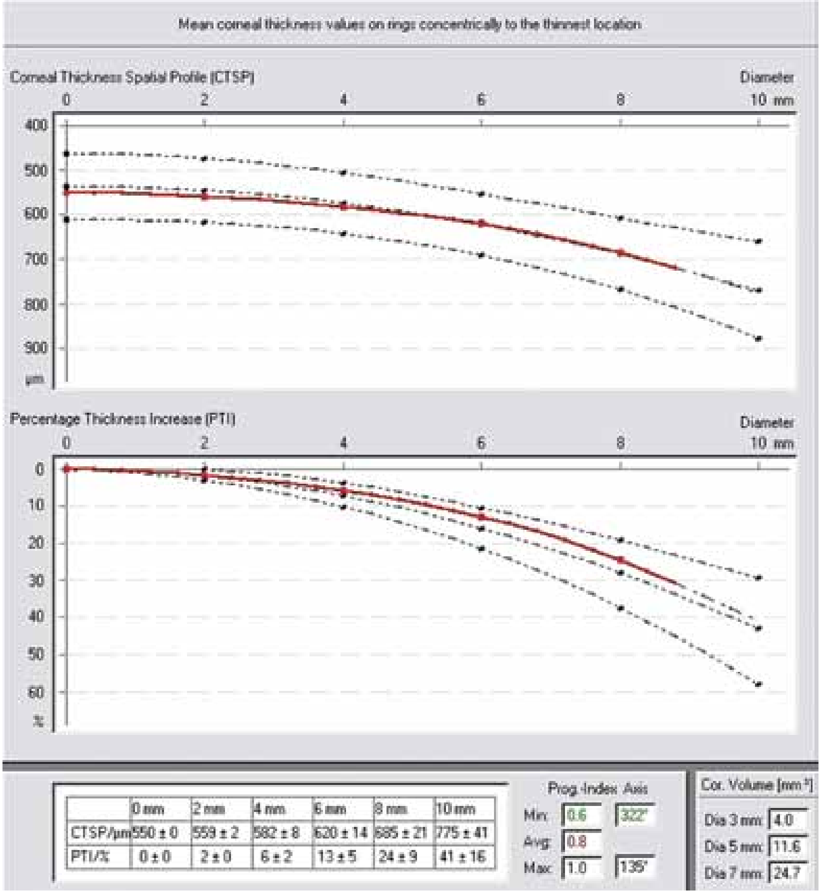

Fig. 9.7.8 OD. Thickness profiles.

Left Eye:

a. In a general look, there is some irregularity in the anterior curvature map (Fig. 9.7.10).
b. Studying single maps:
   i. The anterior sagittal curvature map (Fig. 9.7.11):
      Although it seems irregular, it can be considered horizontal SB indicating an ATR astigmatism.
   ii. The anterior elevation map:
      1. In BFS mode (Fig. 9.7.12): Tongue-like extension.
      2. In the BFTE mode (Fig. 9.7.13): Normal values within the central 5 mm circle.
   iii. The posterior elevation map:
      1. In BFS mode (Fig. 9.6.14): Irregular.
      2. In BFTE mode (Fig. 9.7.15): Normal values within the central 5 mm circle.
   iv. The pachymetry map (Fig. 9.7.16) shows normal shape.
   v. Thickness profiles (Fig. 9.7.17) show normal slope with normal average (0.8).

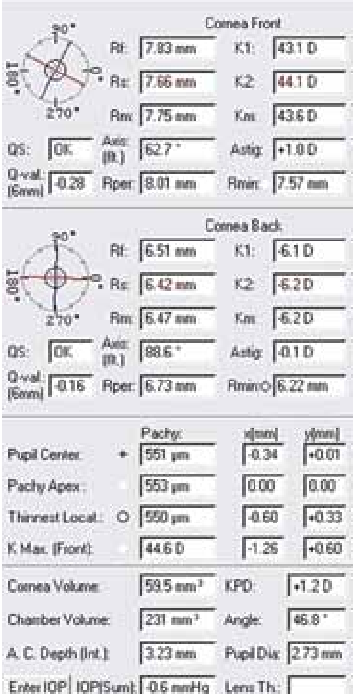

Fig. 9.7.9 OD. Corneal parameters.

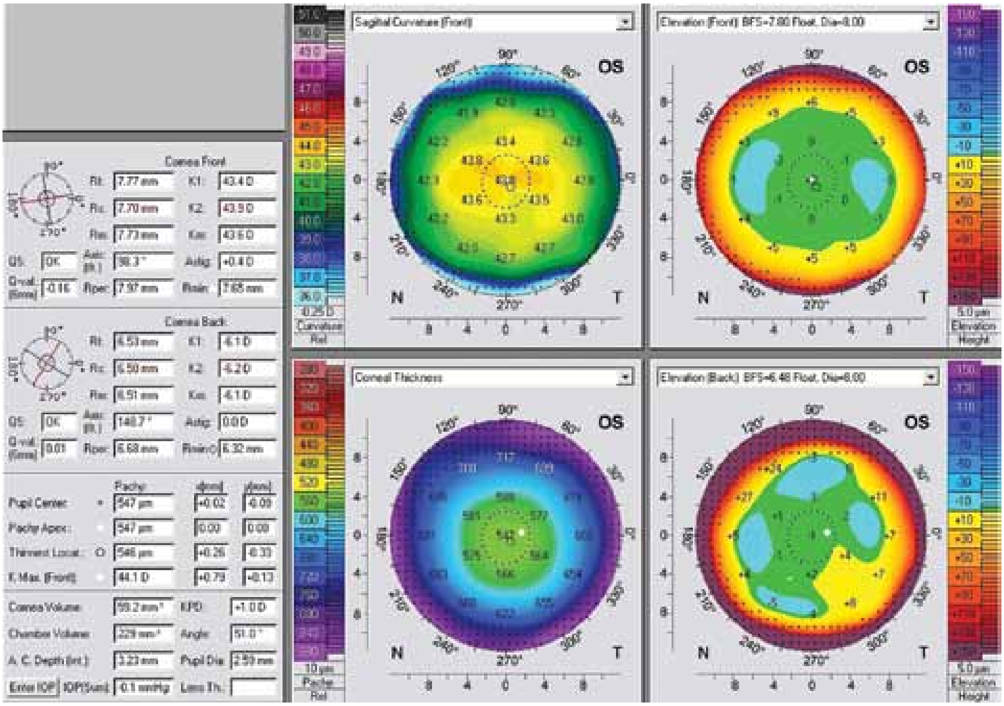

Fig. 9.7.10 OS. The four composite maps.

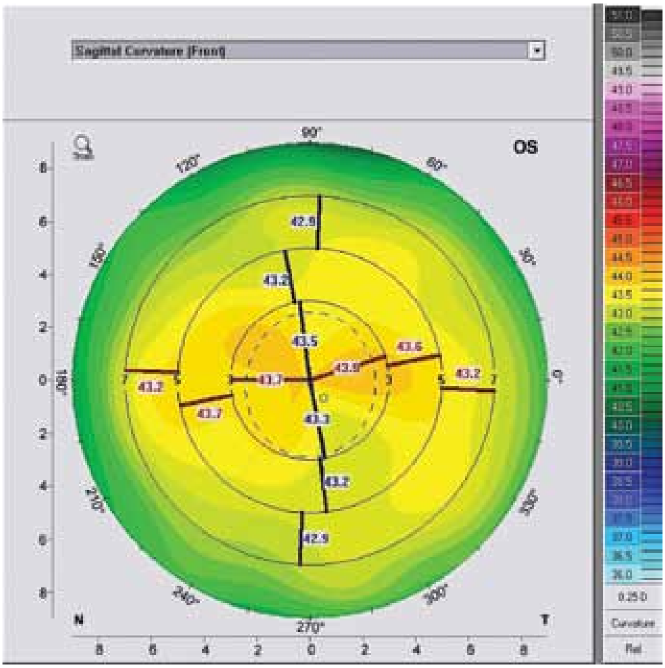

Fig. 9.7.11 OS. The anterior curvature sagittal map. ATR astigmatism.

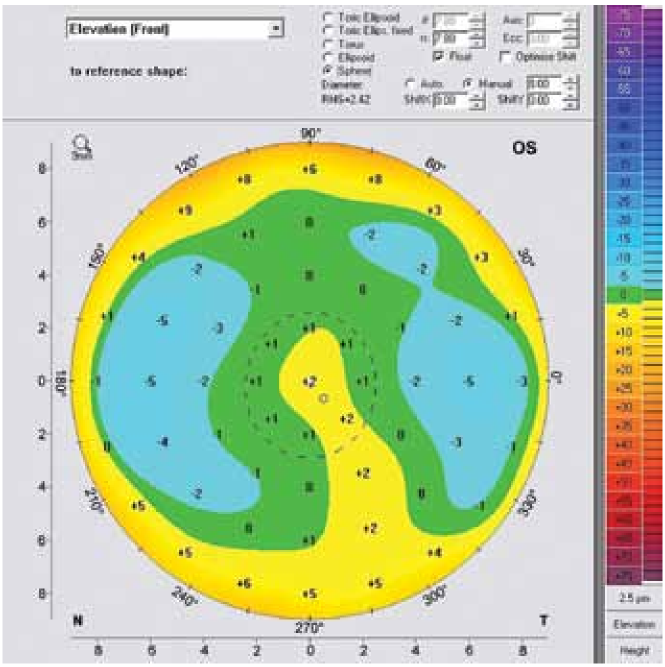

Fig. 9.7.12 OS. The anterior elevation map with BFS reference body. Tongue-like extension.

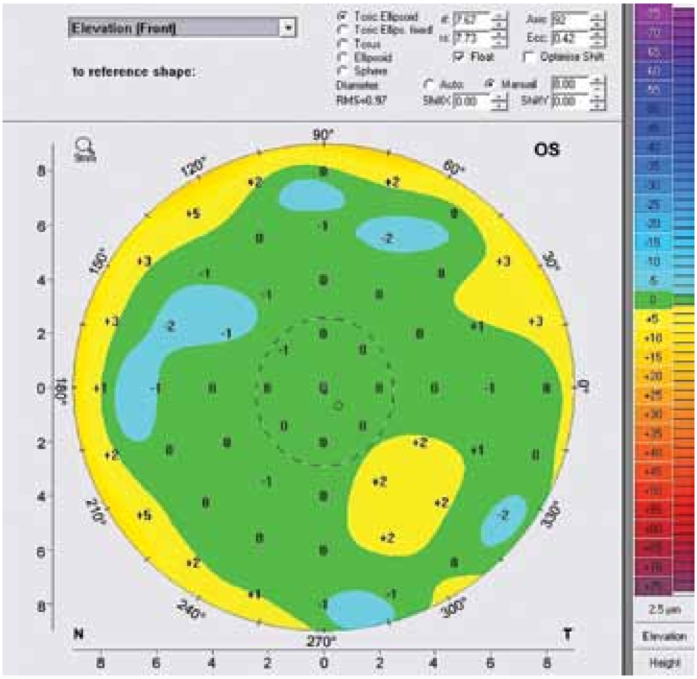

Fig. 9.7.13 OS. The anterior elevation map with BFTE reference body.

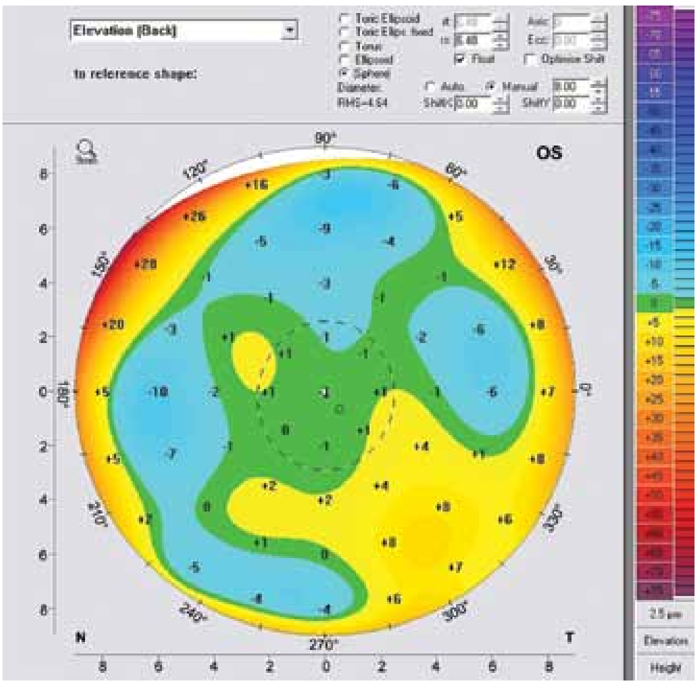

Fig. 9.7.14 OS. The posterior elevation map with BFS reference body. Sandy watch pattern.

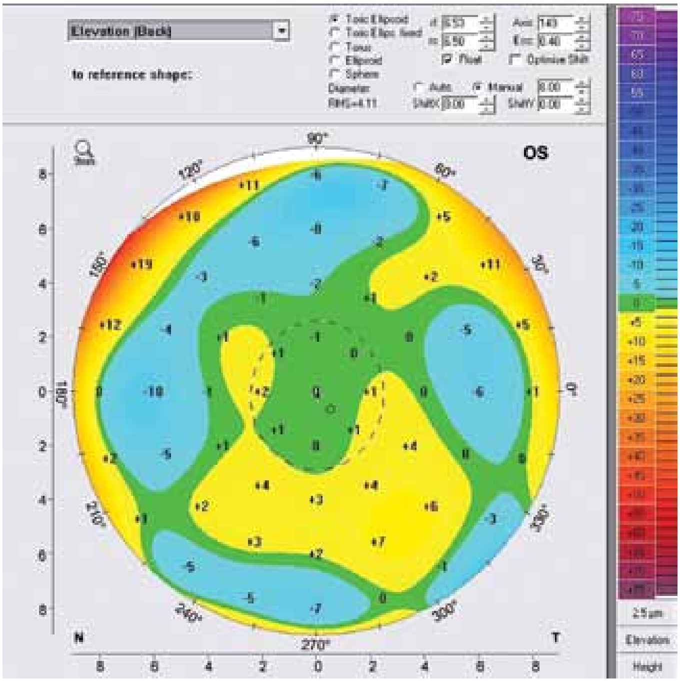

Fig. 9.7.15 OS. The posterior elevation map with BFTE reference body.

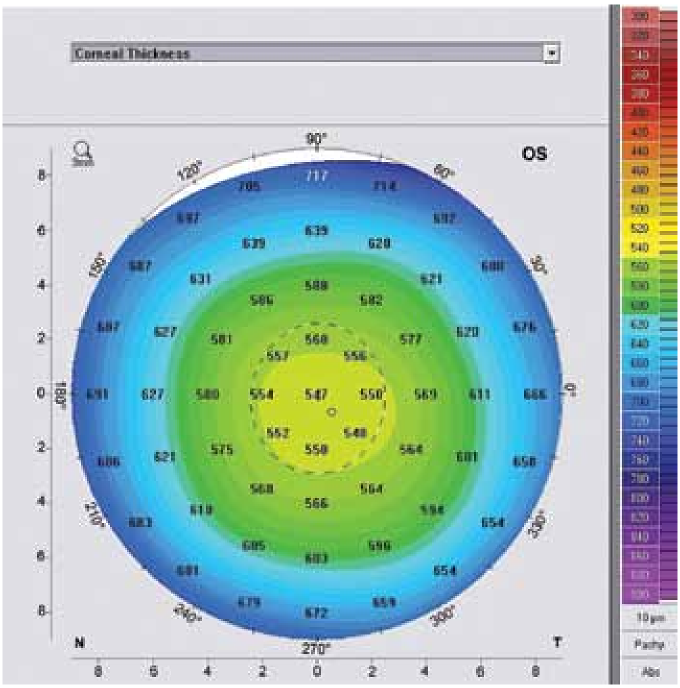

Fig. 9.7.16 OS. The pachymetry map.

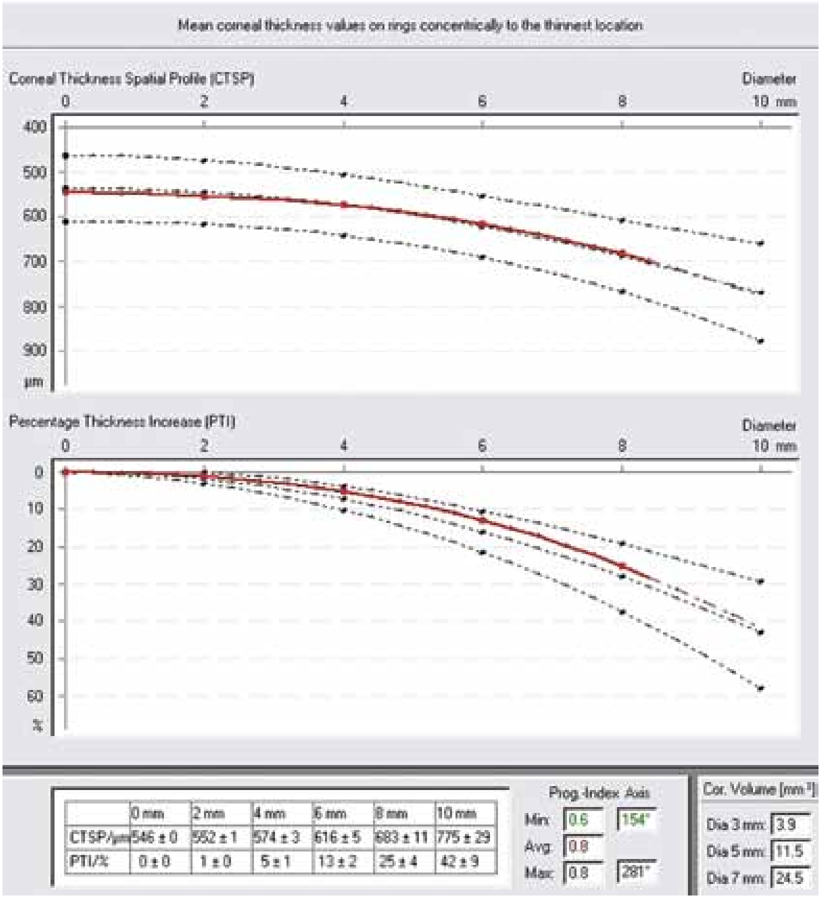

Fig. 9.7.17 OS. Thickness profiles.

c. Qualification of values (Fig. 9.7.18):
   i. QS is OK.
   ii. K readings including K-max are <48 D.
   iii. K-max-steep K is < 1 D.
   iv. Astigmatism is < 6 D.
   v. Thickness at the thinnest location is >500 µm.
   vi. Pachy-Thinnest difference in thickness is <10 µm.
   vii. *Y*-coordinate of the thinnest location is <–500 µm.
   viii. ACD is >3.0mm, ACA and ACV are normal (>24° and >100 mm^3, respectively).
   ix. Mesopic pupil diameter is 2.59 mm
   x. Pupil coordinates indicate central pupil and insignificant angle Kappa.

2. **Quantitative Step:**
   Since, the case is hyperopia and there is a big difference among MR, CR and PMT, it is wise to try contact lenses or glasses depending on PMT correction for a couple of weeks, then recheck the patient for higher correction till the highest tolerable correction is reached, the decision can be taken thereafter. In our case, the expected optimal correction is shown in Table 9.7.5.

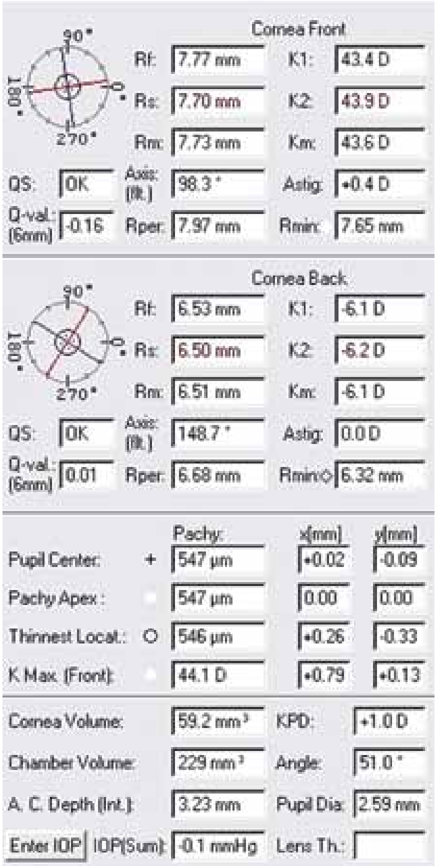

Fig. 9.7.18 OS. Corneal parameters.

TABLE 9.7.5 Potential Refractive Error

	UDVA	*Sph*	*Cyl*	*Axis*	*CDVA (G)*
OD	0.4	+5	–1	60	1.0
OS	0.4	+5	–0.5	95	1.0

UDVA= uncorrected distance visual acuity; CDVA (G)= corrected distance visual acuity (by glasses)

For correct calculations, positive cylinder equation will be used in the quantitative step.

Right Eye:

a. Thickness concept:
   RSB Law 7: the preoperative thinnest location is >470 µm.
b. K-readings Concept (Table 9.7.6):

TABLE 9.7.6 Final K for +5D sph/-1D cyl = +4D sph/+1D cyl				
Refractive error	*Original K*	*Astigmatic correction*	*Hyperopic correction*	*Final K*
+4.0 sph	K_s = 44.1 D	(0) K_s = 44.1 D	(4.0 x 1.2 = 4.8D) K_s = 44.1 + 4.8 = 48.9 D	49 D in average
+1 cyl	K_f = 43.1 D	(1.0 x 1.2 = 1.2) K_f = 43.1 + 1.2 = 44.3 D	(4.0 x 1.2 = 4.8D) K_f = 44.3 + 4.8 = 49.1 D	
K_f : flat K K_s : steep K				

As shown in this table, full correction of the refractive error slightly exceeds the borderline of K readings.

Left Eye:

a. Thickness concepts:
   RSB Law 7: the preoperative thinnest location is >470 μm.
b. K-readings Concept (Table 9.7.7):

TABLE 9.7.7 Final K for +5D sph/-0.5D cyl = +4.5D sph/+0.5D cyl				
Refractive error	*Original K*	*Astigmatic correction*	*Hyperopic correction*	*Final K*
+4.5 sph	K_s = 43.9 D	(0) K_s = 43.9 D	(4.5 x 1.2 = 5.4 D) K_s = 43.9 + 5.4 = 49.3 D	49.35 D in average
+0.5 cyl	K_f = 43.4 D	(0.5 x 1.2 = 0.6) K_f = 43.4 + 0.6 = 44 D	(4.5 x 1.2 = 5.4 D) K_f = 44 + 5.4 = 49.4 D	
K_f : flat K K_s : steep K				

As shown in this table, full correction of the refractive error exceeds the borderline of K readings.

3. **Discussion:**
   There are no significant risk factors in corneal tomography.
   The patient is hyperopic and her symptoms come from improper spectacle correction. Her MR, CR and PMT show a high latent hyperopia and accommodation spasm, which results from both improper correction and the presence of astigmatism. Fortunately, there is neither amblyopia nor significant phoria.
   In our case, PRT is not a good option unless the patient agrees with suboptimal correction; i.e. +3.5 D sph/+1 D cyl for OD and +4 D sph/+0.5 D cyl for OS. The residual refractive error will not be significant, especially that the case is hyperopia and the patient is still young with good accommodation, but an early presbyopia is expected.
   PIOL implantation is a good and reasonable option since the ACD is suitable and the potential refractive error is relatively high.
   RLE is not an option since the patient is young and there is no reasonable indication for that.
4. **Conclusion:**
   The best solution in my opinion is PIOL implantation. PRT comes as a second choice.

CASE 8

A 20-year-old male has a refractive error. He is thinking of refractive correction. He never tried contact lenses. His refractive error was stable during the last year. There are no other complaints. His MR and VA are shown in Table 9.8.1. His CR is shown in Table 9.8.2.

TABLE 9.8.1 Manifest Refraction and Visual Acuity

	UDVA	*Sph*	*Cyl*	*Axis*	*CDVA (G)*	*CDVA (G+PH)*
OD	0.2	−1.5	−1	135	0.9	1.0
OS	0.3	−1.75	−0.75	40	0.9	1.0

UDVA= uncorrected distance visual acuity; CDVA (G)= corrected distance visual acuity (by glasses); CDVA (G+PH)= corrected distance visual acuity (by glasses and pin hole test)

TABLE 9.8.2 Cycloplegic Refraction

	Sph	*Cyl*	*Axis*
OD	−1.5	−1.25	140
OS	−1.75	−1	25

Figures 9.8.1 to 9.8.9 represent right eye tomography. Figures 9.8.10 to 9.8.18 represent left eye tomography.

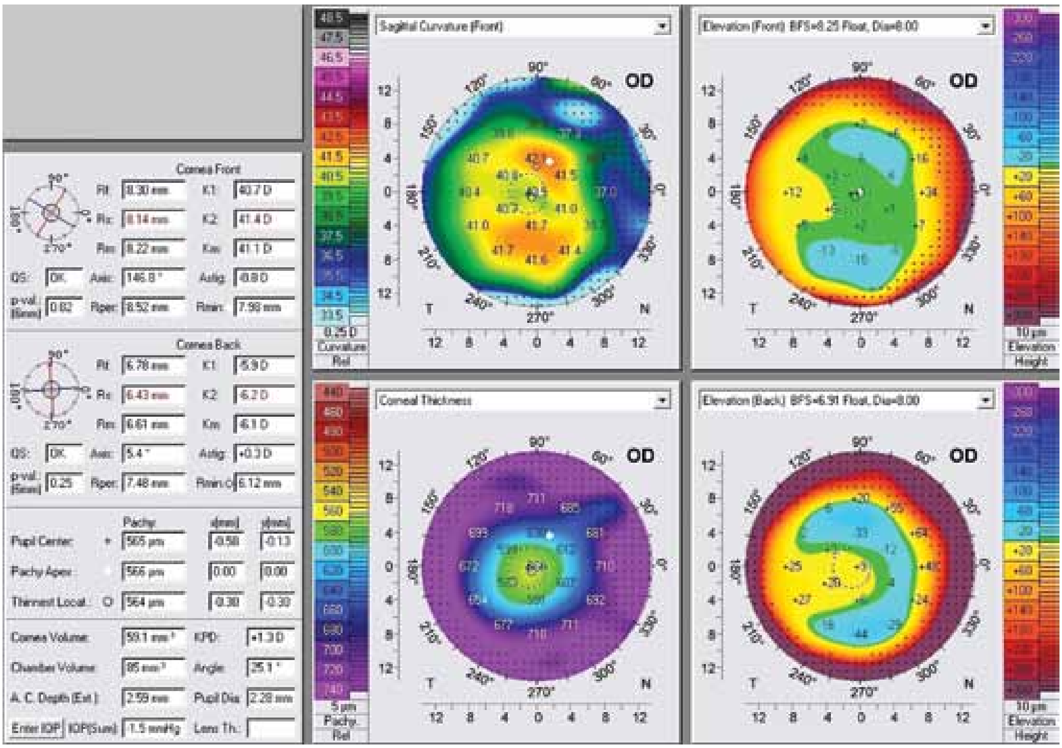

Fig. 9.8.1 OD. The four composite maps.

1. **Qualification Step:**
   Right Eye:
   a. In a general look, there are some irregularities in the anterior curvature map and posterior elevation map (Fig. 9.8.1).
   b. Studying single maps:
      i. The anterior sagittal curvature map (Fig. 9.8.2):
         It is irregular pattern, but there is no significant inferior-superior difference.
      ii. The anterior elevation map:
         1. In BFS mode (Fig. 9.8.3): Tongue-like extension.
         2. In the BFTE mode (Fig. 9.8.4): Normal values within the central 5 mm circle.
      iii. The posterior elevation map:
         1. In BFS mode (Fig. 9.8.5): Tongue-like extension.
         2. In BFTE mode (Fig. 9.8.6): Abnormal values within the central 5 mm circle (black arrow).
      iv. The pachymetry map (Fig. 9.8.7) shows apparently normal shape.
      v. Thickness profiles (Fig. 9.8.8) show S-shape slopes (black arrows) with normal average (0.9).

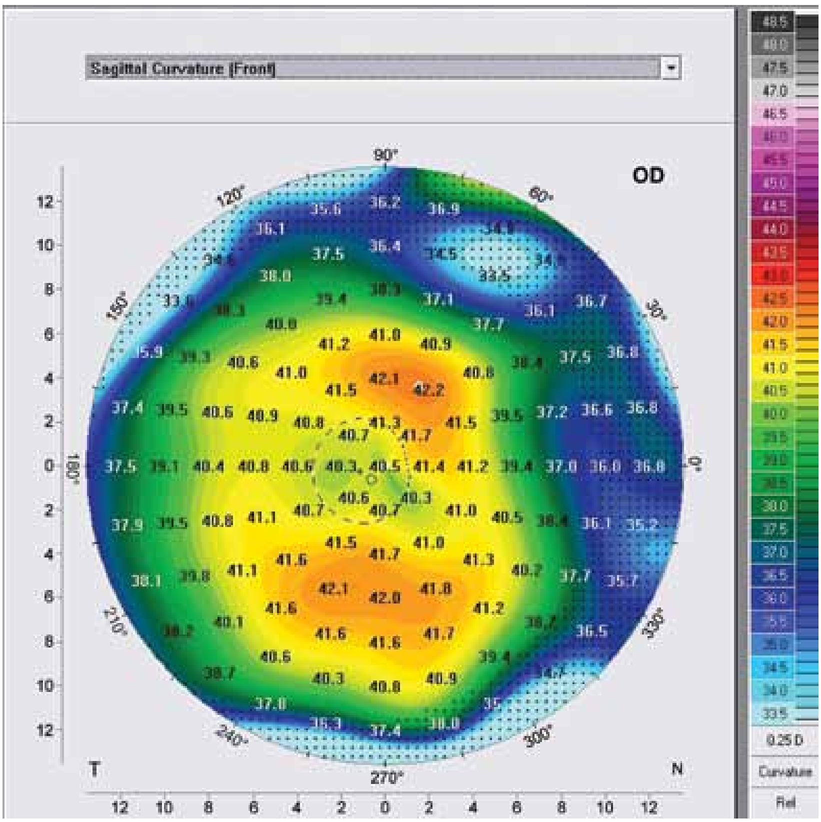

Fig. 9.8.2 OD. The anterior curvature sagittal map. Mild irregular pattern.

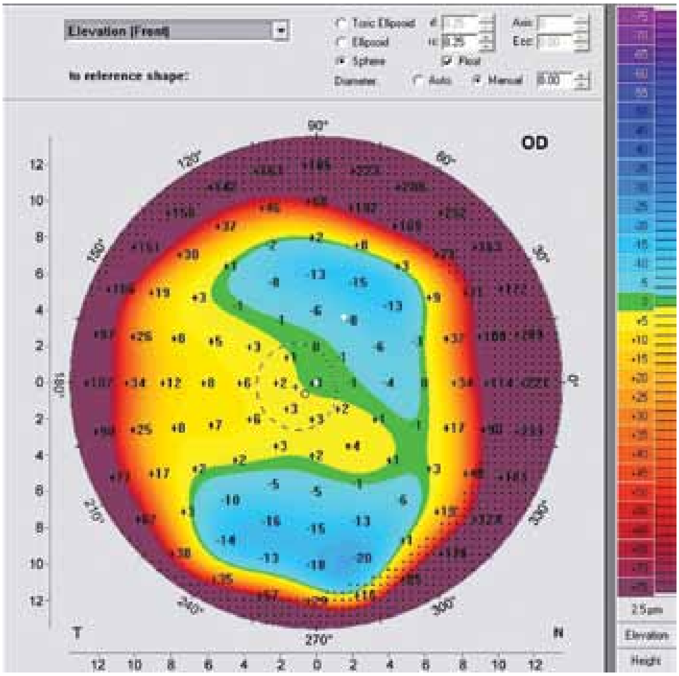

Fig. 9.8.3 OD. The anterior elevation map with BFS reference body. Tongue-like extension.

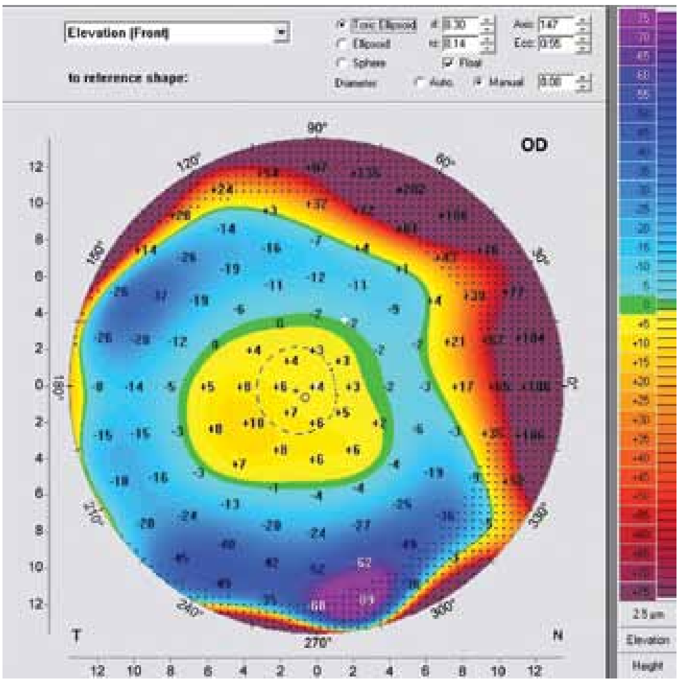

Fig. 9.8.4 OD. The anterior elevation map with BFTE reference body.

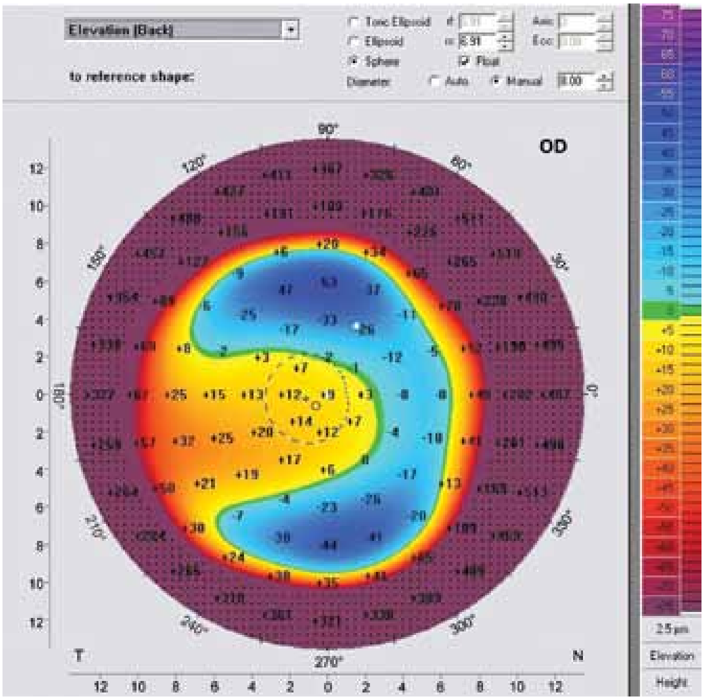

Fig. 9.8.5 OD. The posterior elevation map with BFS reference body. Tongue-like extension.

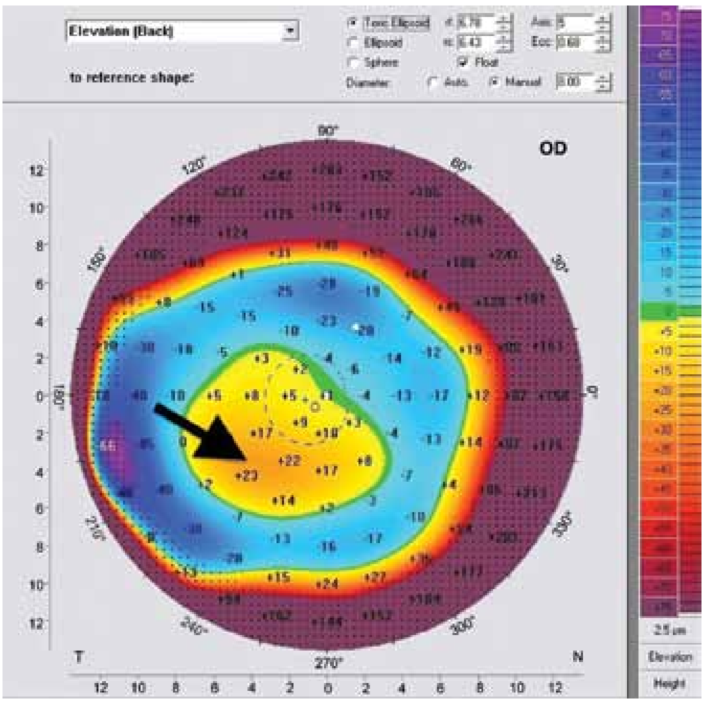

Fig. 9.8.6 OD. The posterior elevation map with BFTE reference body. Abnormal values (black arrow).

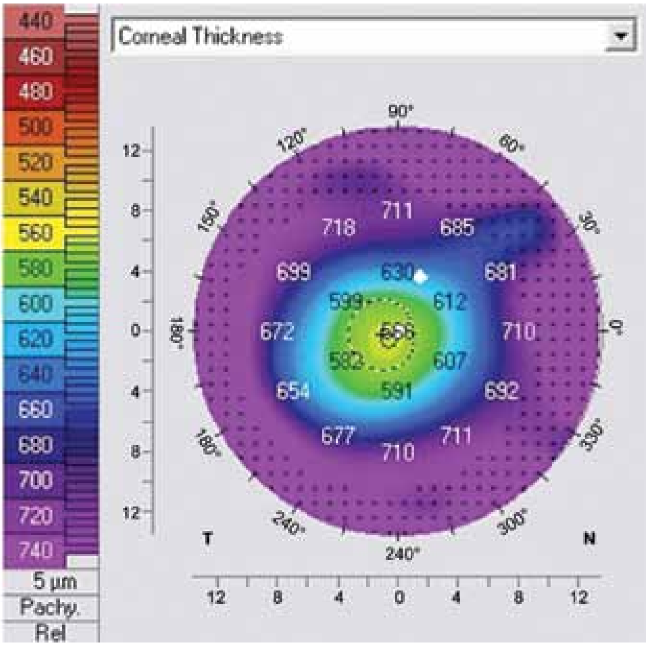

Fig. 9.8.7 OD. The pachymetry map.

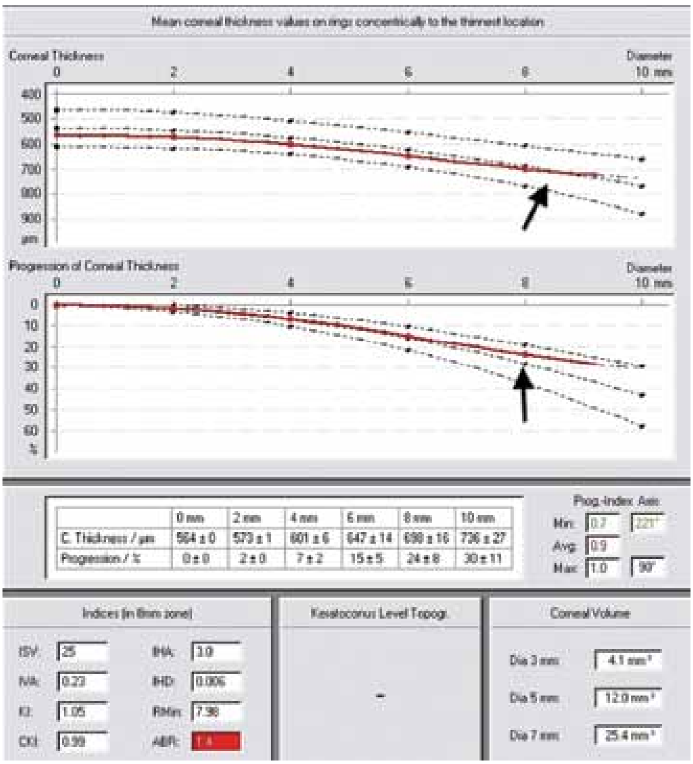

Fig. 9.8.8 OD. Thickness profiles. The black arrows point at the S-shape.

c. Qualification of values (Fig. 9.8.9):
   i. QS is OK.
   ii. K readings including K-max are <48 D.
   iii. K-max-steep K is < 1 D (not shown).
   iv. Astigmatism is < 6 D.
   v. Thickness at the thinnest location is >500 µm.
   vi. Pachy-Thinnest difference in thickness is <10 µm.
   vii. *Y*-coordinate of the thinnest location is <–500 µm.
   viii. ACD and ACV are abnormal (2.59 mm and 85 mm^3), ACA is normal (>24°).
   ix. Mesopic pupil diameter is 2.28 mm.
   x. Pupil coordinates indicate decentred pupil and significant angle Kappa.

Left Eye:

a. In a general look, there is some irregularity in the anterior curvature and posterior elevation maps (Fig. 9.8.10).
b. Studying single maps:
   i. The anterior sagittal curvature map (Fig. 9.8.11) shows SS pattern in spite of normal I-S difference.

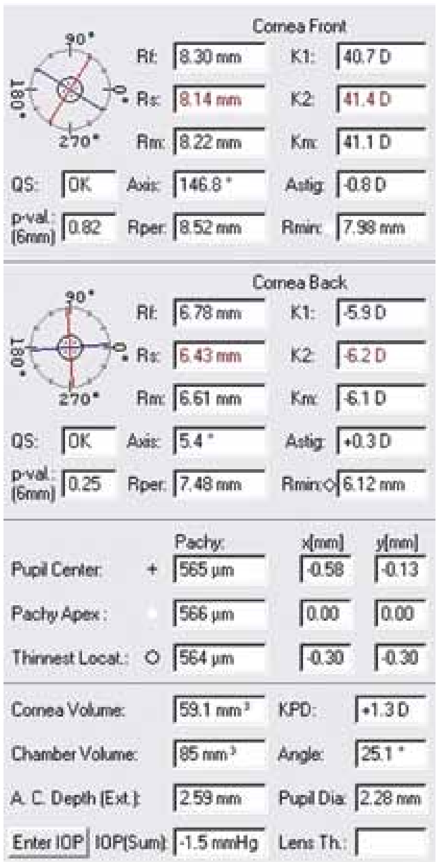

Fig. 9.8.9 OD. Corneal parameters.

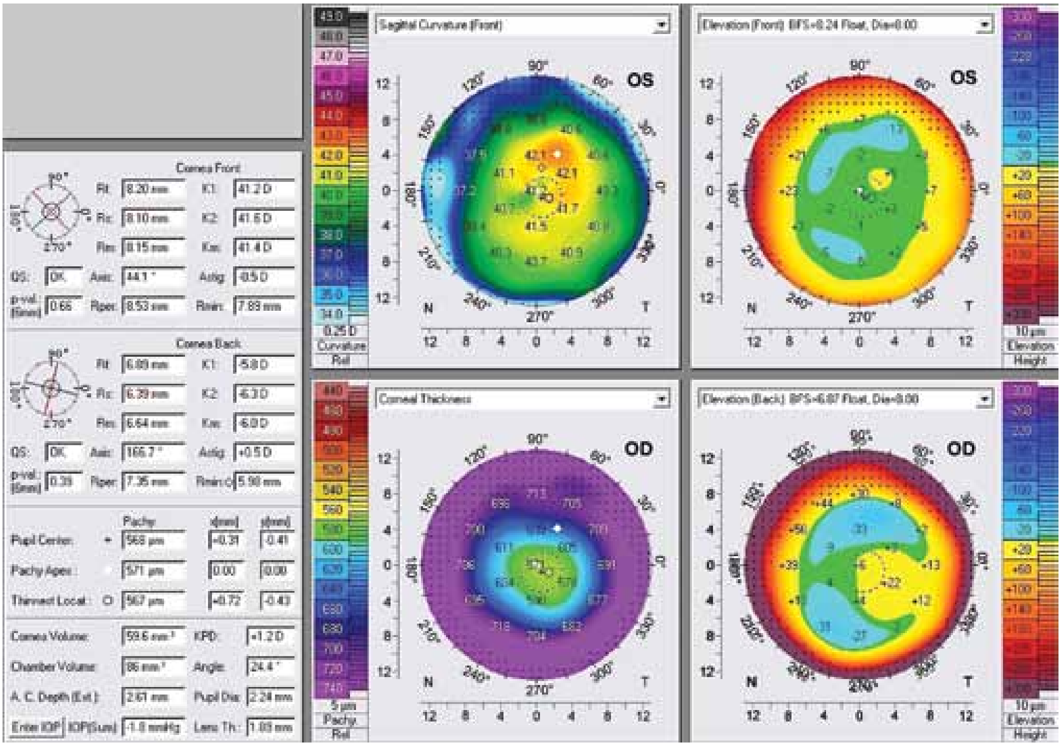

Fig. 9.8.10 OS. The four composite maps.

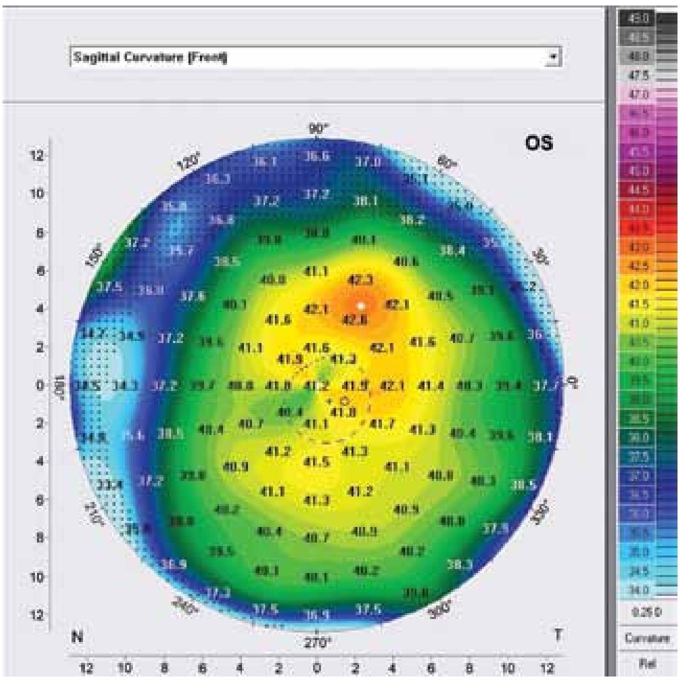

Fig. 9.8.11 OS. The anterior curvature sagittal map. SS pattern.

ii. The anterior elevation map:
   1. In BFS mode (Fig. 9.8.12): tongue-like extension.
   2. In the BFTE mode (Fig. 9.8.13): normal values within the central 5 mm circle.
iii. The posterior elevation map:
   1. In BFS mode (Fig. 9.8.14): tongue-like extension.
   2. In BFTE mode (Fig. 9.8.15): abnormal values within the central 5 mm circle (black arrow).
iv. The pachymetry map (Fig. 9.8.16) shows normal shape with horizontal displacement of thinnest location (white arrow). (See *X*-coordinates on Fig. 9.8.18).
v. Thickness profiles (Fig. 9.8.17) show slight S-shape at the extreme end (black arrows). The average is normal (0.8).

c. Qualification of values (Fig. 9.8.18):
   i. QS is OK.
   ii. K readings including K-max are <48 D.
   iii. K-max-steep K is < 1 D (not shown).
   iv. Astigmatism is < 6 D.
   v. Thickness at the thinnest location is >500 μm.
   vi. Pachy-Thinnest difference in thickness is <10 μm.

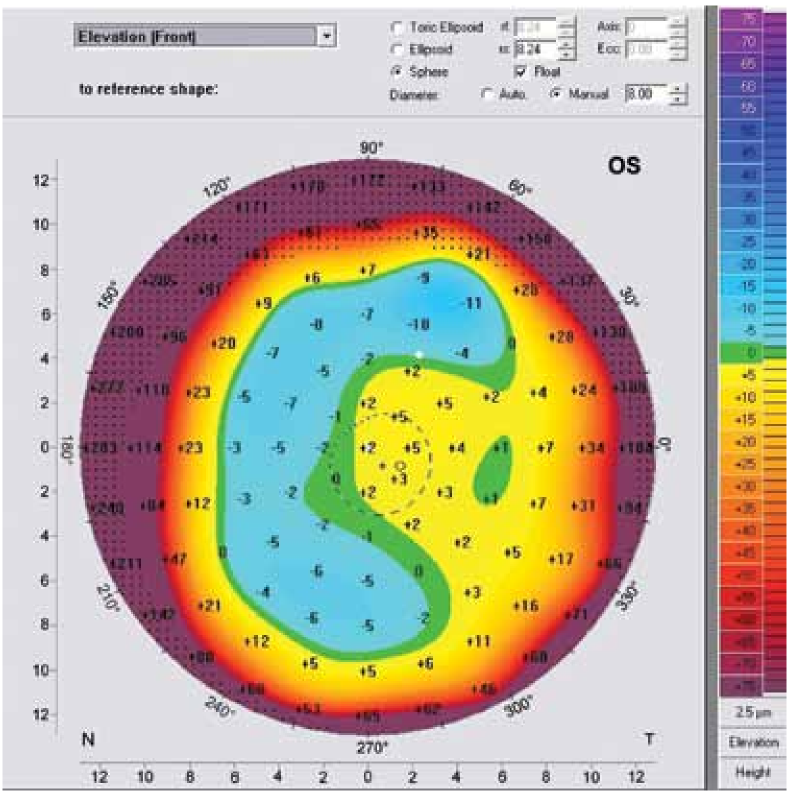

Fig. 9.8.12 OS. The anterior elevation map with BFS reference body. Tongue-like extension.

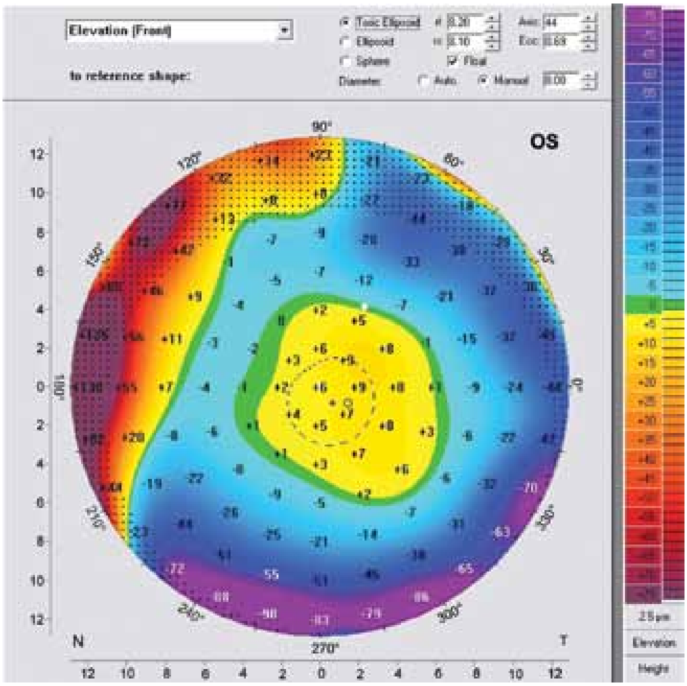

Fig. 9.8.13 OS. The anterior elevation map with BFTE reference body.

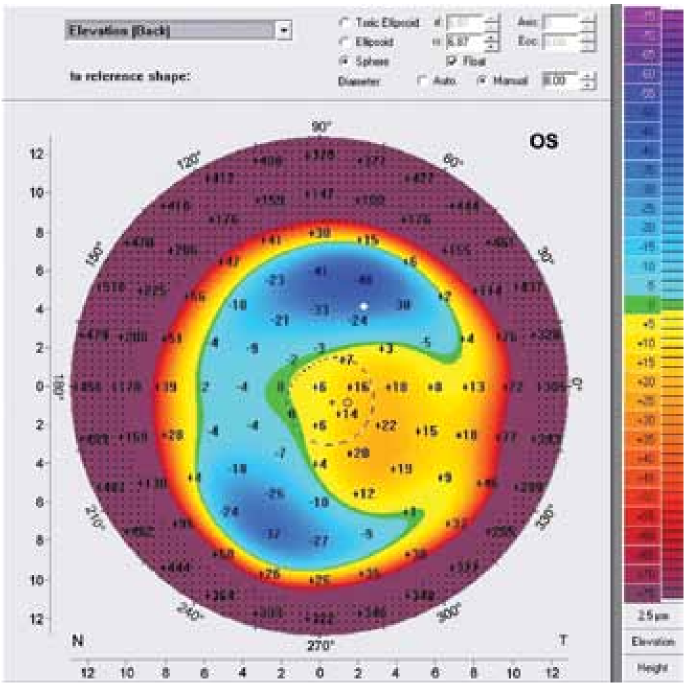

Fig. 9.8.14 OS. The posterior elevation map with BFS reference body. Tongue-like extension.

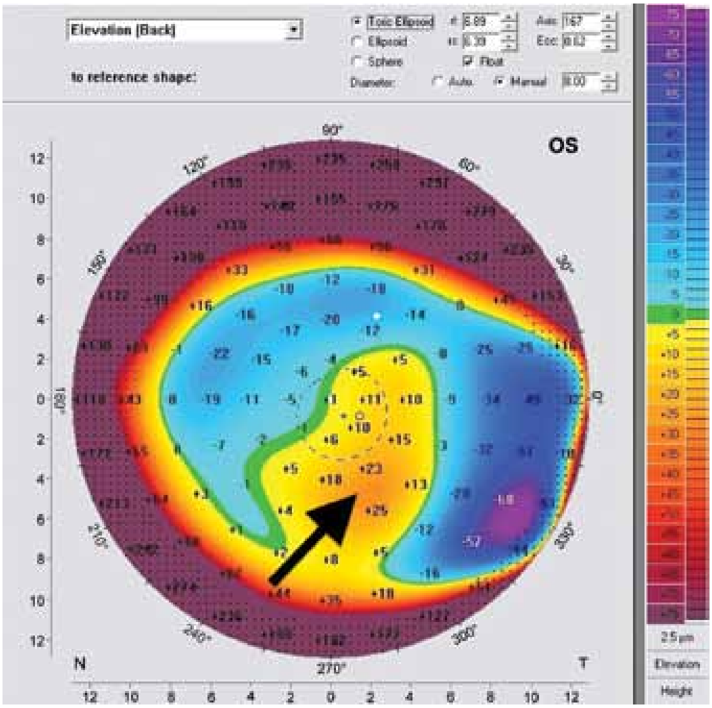

Fig. 9.8.15 OS. The posterior elevation map with BFTE reference body. Abnormal values (black arrow).

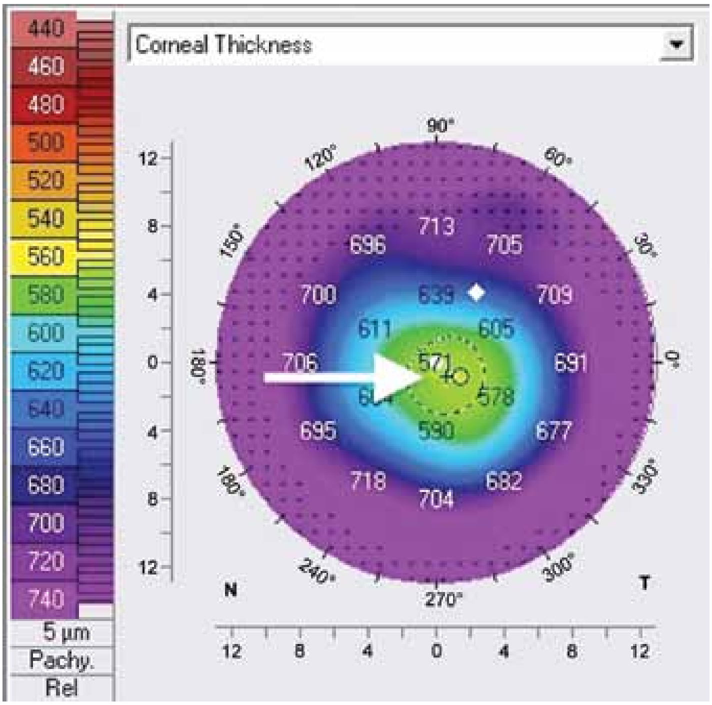

Fig. 9.8.16 OS. The pachymetry map. The white arrow points at the horizontally-displaced thinnest location.

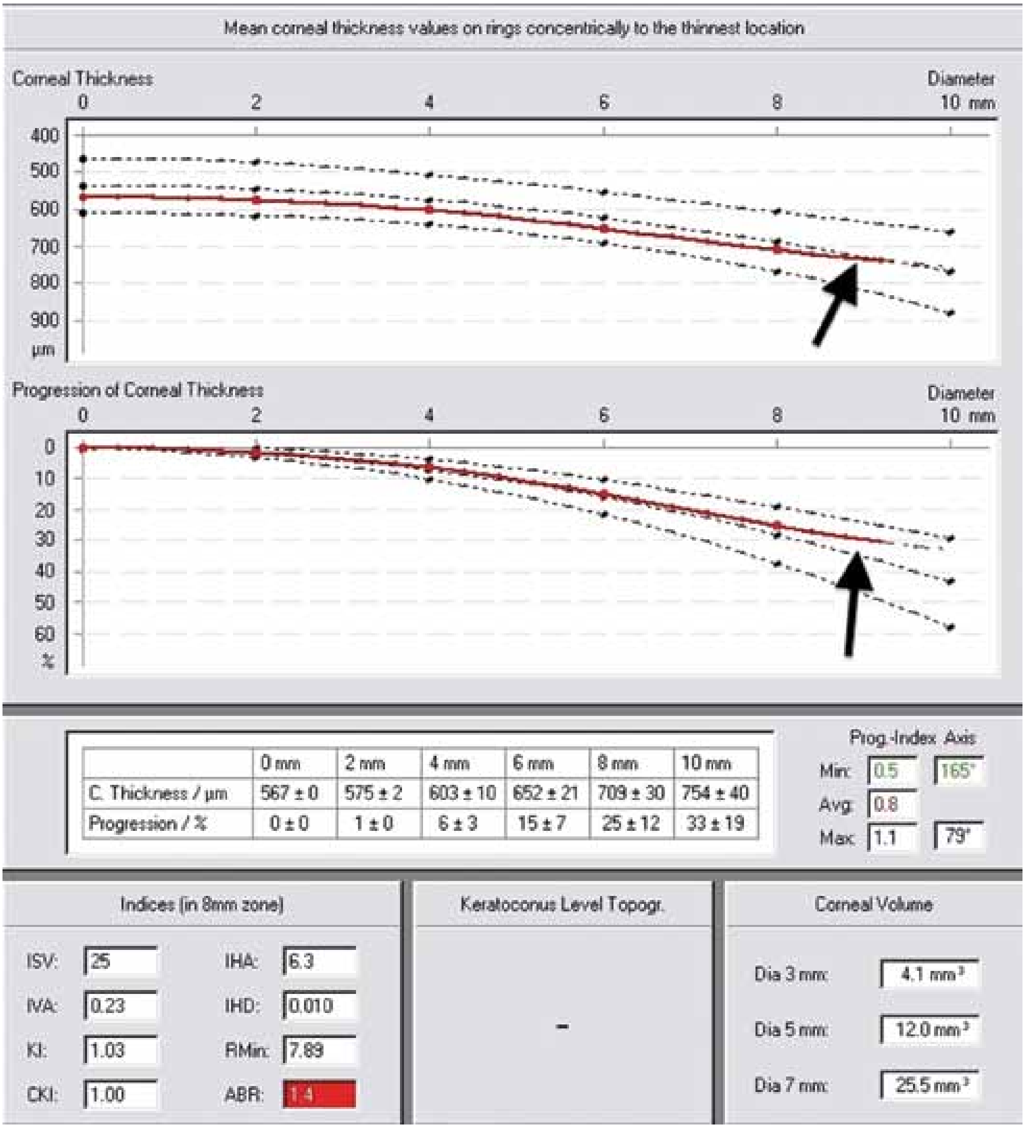

Fig. 9.8.17 OS. Thickness profiles. The black arrows point at S-shape pattern.

vii. *Y*-coordinate of the thinnest location is <–500 µm.
viii. ACD and ACV are abnormal (2.61 mm and 86 mm^3), ACA is normal (>24°).
ix. Mesopic pupil diameter is 2.24 mm.
x. Pupil coordinates indicate decentered pupil and significant angle kappa.

2. **Discussion Step:**
It is wise to discuss the case before proceeding with the quantitative step.
Although K readings are normal, the anterior sagittal map is visibly irregular in both eyes. The anterior and posterior elevation maps show tongue-like extension and only the

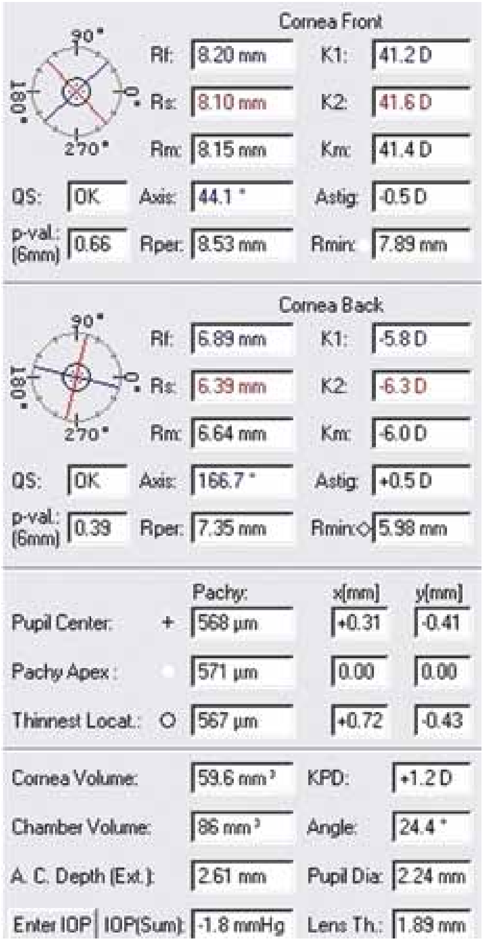

Fig. 9.8.18 OS. Corneal parameters.

posterior show abnormal values in both eyes. Pachymetry profile takes an S-shape in both eyes. All these findings classify the case as FFKC. This diagnosis directs us towards family KC suspect. This patient was asked to bring his 18-year-old brother for corneal tomography and surprisingly he was found to have apparently normal cornea in the right eye and KC in the left eye (Figs 9.8.19 and 9.8.20).

This patient in this case has FFKC in respect to its definition. This explains the sub optimal CDVA and puts the patient at risk of ectasia if PRT was done unless SA and CXL were performed.

Other refractive options are not on the table; the ACD is not suitable for PIOL and the patient is still young for RLE. This is apart from the small refractive error, which does not warrant PIOL implantation or performing RLE.

Regardless of refractive surgery, the patient should be monitored for KC development unless successful CXL is performed.

In case of SA and CXL option, it is recommended to perform WFGT and undercorrect myopia to compensate for the flattening effect of CXL.

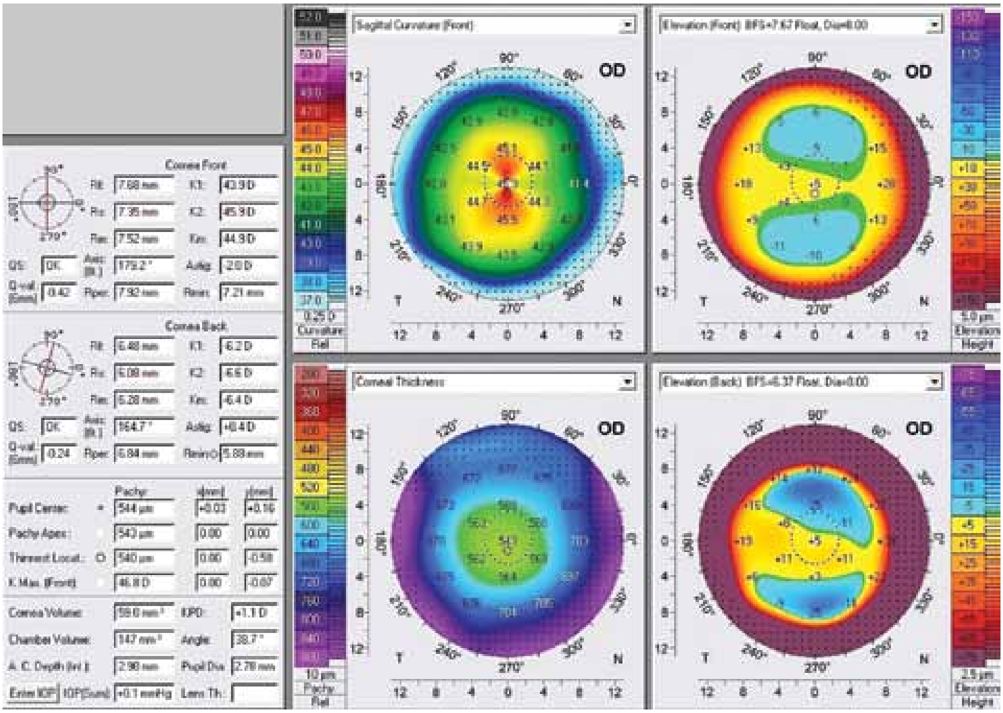

Fig. 9.8.19 The four composite maps of the right eye of patient's brother.

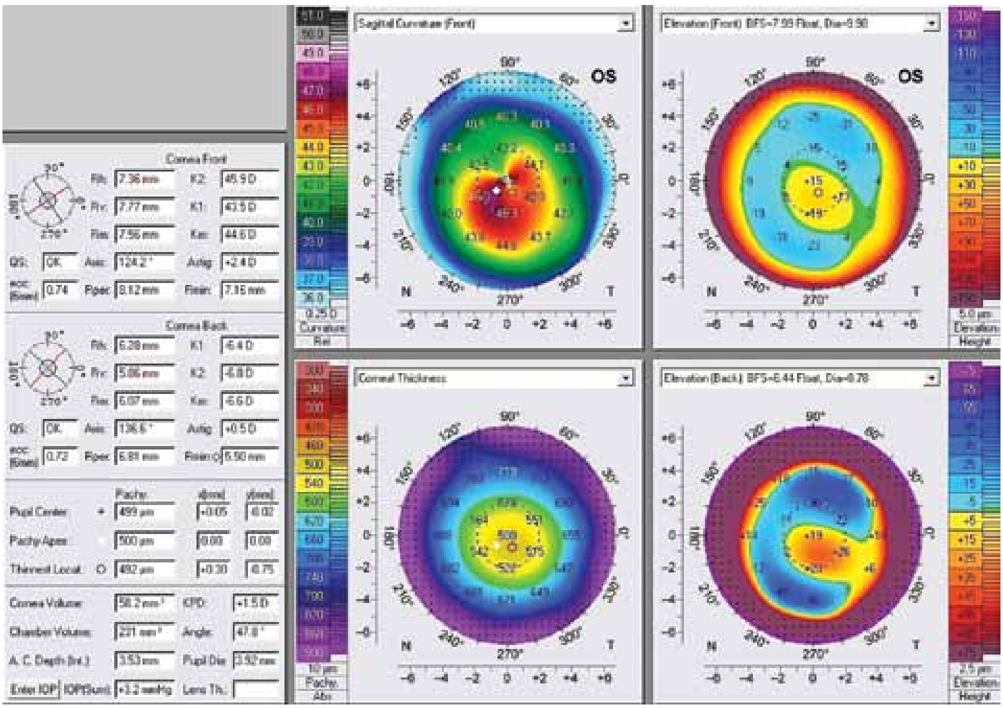

Fig. 9.8.20 The four composite maps of the left eye of patient's brother.

To decide, which WFGT should be performed (corneal vs. ocular), corneal and ocular wavefront should be measured to calculate the IWF and follow the decision tree shown in Fig. 5.47.

The right eye will be discussed as an example.

Figure 9.8.21 represents ocular wavefront of the right eye. In this figure, RMS related to HOAs = 0.56 µm (red ellipse), most of which is coma (red arrow) and the objective refractive error (green arrow) is consistent with the MR (see Table 9.8.1) except for axis of astigmatism. The patient was re-examined for axis and amount of astigmatism and the result was just the same as in Table 9.8.1.

Figure 9.8.22 is corneal wavefront of the right eye. In this Figure, the most significant HOA is coma. In comparison with ZC of coma in both figures, it is clear that HOAs are of corneal origin and IWF is almost = 0.

Therefore, SA with corneal WFGT profile is the option.

There is another option, that is to advise the patient to use glasses especially that his refractive error is small and stabile and there are no fatigue complaints and keep him under observation for the possibility of KC development. In case of any development or progression criteria (refer to chapter 8: ectasia progression), CXL can be performed either alone (since CXL alone may correct some of the refractive error) or with SA WFGT as mentioned before.

In case of CXL and SA in this case, the recommended correction will be as shown in Table 9.8.3.

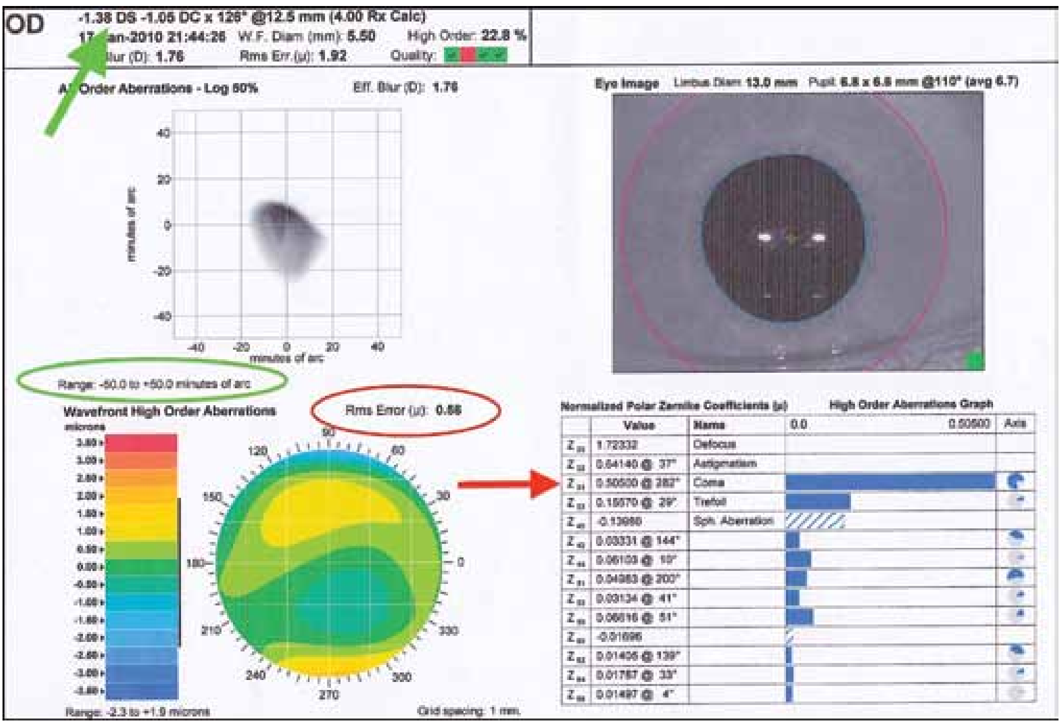

Fig. 9.8.21 Ocular wavefront of OD. The green arrow points at the objective refractive error. The green ellipse indicates the range of PSF. The red arrow points at coma, which is the major component of HOAs. The red ellipse indicates RMS related to HOAs.

Zernike	Micron	Diopter	Axis°	Aberration description
Z(2, 0)	0.501	-0.39	---	Defocus
Z(2, ±2)	0.432	-0.47	150	Astigmatism
Z(3, ±1)	0.723	0.56	68	Coma
Z(3, ±3)	0.182	0.14	73	Trefoil
Z(4, 0)	0.029	0.02	---	Spherical aberration
Z(4, ±2)	0.049	0.04	13	Secondary astigmatism
Z(4, ±4)	0.066	0.05	38	Quatrefoil
Z(5, ±1)	0.159	0.12	290	Secondary Coma
Z(5, ±3)	0.015	0.01	34	Secondary trefoil
Z(5, ±5)	0.043	0.03	9	Pentafoil
Z(6, 0)	0.028	0.02	---	Secondary Spherical
Z(6, ±2)	0.033	0.03	95	6th order astigmatism
Z(6, ±4)	0.013	0.01	5	6th order quatrefoil
Z(6, ±6)	0.012	0.01	46	Hexafoil

Fig. 9.8.22 Corneal wavefront of OD. The red arrow points at coma, which is the major component of HOAs.

TABLE 9.8.3 Recommended refraction for SA and CXL

	Sph	*Cyl*	*Axis*
OD	−0.75	−1	140
OS	−1	−0.75	25

3. **Quantification Step:** There is no need for calculations in this case since the amount of refractive error is small, the cornea is thick enough and the case is straight forward.

CASE 9

A 20-year-old male has a refractive error. He is complaining of fatigue after long near work with headache. He feels dissatisfied with and without his glasses. His refractive history shows different prescriptions in close check-ups indicating fluctuation in the refractive status.
His recent glasses and corresponding VA are shown in Table 9.9.1.

TABLE 9.9.1 Recent Glasses and Visual Acuity

	UDVA	*Sph*	*Cyl*	*Axis*	*CDVA (G)*
OD	0.4	–2	–2	95	0.8
OS	0.4	–2.5	–2.5	85	0.8

UDVA= uncorrected distance visual acuity; CDVA (G)= corrected distance visual acuity (by glasses)

His MR and corresponding VA are shown in Table 9.9.2.

TABLE 9.9.2 Manifest Refraction and Visual Acuity

	UDVA	*Sph*	*Cyl*	*Axis*	*CDVA (G)*
OD	0.4	–2.5	–2	95	0.9
OS	0.4	–3	–2.5	85	0.9

UDVA= uncorrected distance visual acuity; CDVA (G)= corrected distance visual acuity (by glasses)

His CR is shown in Table 9.9.3.

TABLE 9.9.3 Cycloplegic Refraction

	Sph	*Cyl*	*Axis*
OD	–0.5	–2.25	100
OS	–0.75	–2.75	80

Since, there is > 0.75 D difference between MR and CR, PMT should be performed.
PMT and corresponding VA are shown in Table 9.9.4.

TABLE 9.9.4 Post-medriatic Refraction and Visual Acuity

	UDVA	*Sph*	*Cyl*	*Axis*	*CDVA (G)*	*CDVA (G+PH)*
OD	0.4	–1.75	–2	95	0.9	1.0
OS	0.4	–2	–2.5	85	0.9	1.0

UDVA= uncorrected distance visual acuity; CDVA (G) = corrected distance visual acuity (by glasses); CDVA (G+PH) = corrected distance visual acuity (by glasses and Pin hole).

Figures 9.9.1 to 9.9.9 represent right eye tomography. Figures 9.9.10 to 9.9.18 represent left eye tomography.

1. **Qualification Step:**

   Right Eye:

   a. In a general look, it is an ATR astigmatism with some irregularity on the posterior elevation map (Fig. 9.9.1).

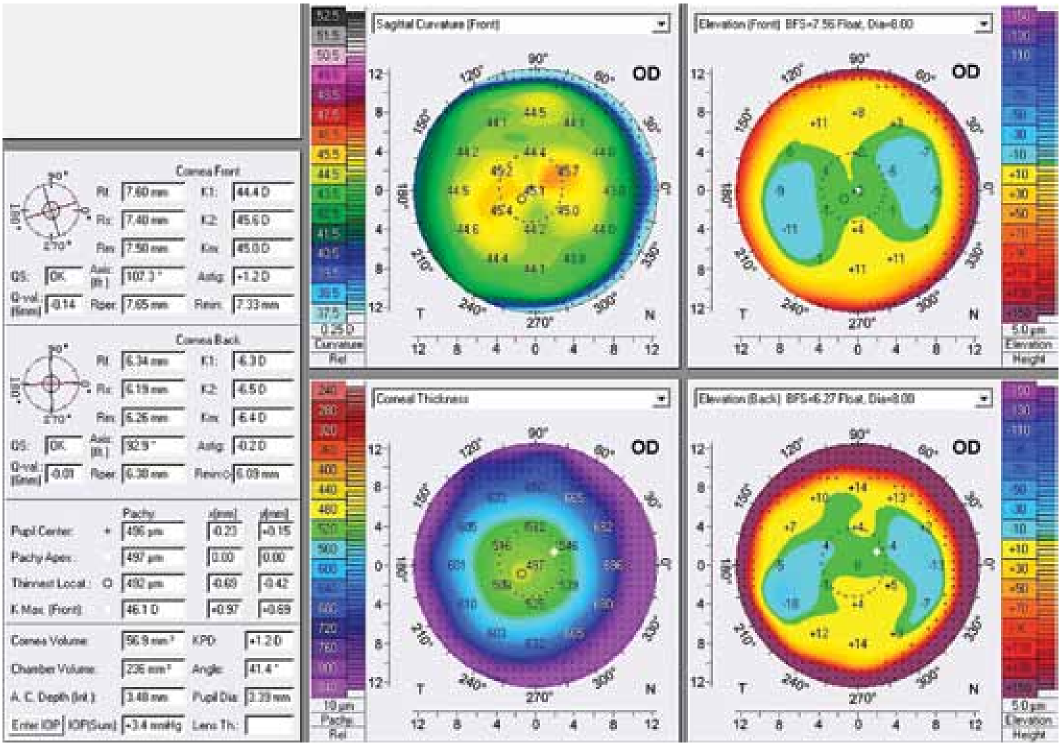

Fig. 9.9.1 OD. The four composite maps.

b. Studying single maps:
   i. The anterior sagittal curvature map (Fig. 9.9.2) shows horizontal SB indicating ATR astigmatism.
   ii. The anterior elevation map:
      1. In BFS mode (Fig. 9.9.3): horizontal sandy watch pattern.
      2. In the BFTE mode (Fig. 9.9.4): normal values within the central 5 mm circle.
   iii. The posterior elevation map:
      1. In BFS mode (Fig. 9.9.5): Tongue-like extension.
      2. In BFTE mode (Fig. 9.9.6): Normal values within the central 5 mm circle.
   iv. The pachymetry map (Fig. 9.9.7):
      Relatively thin cornea with temporal displacement of the thinnest location (white arrow). (See coordinates in Figs 9.9.1 and 9.9.9).
   v. Thickness profiles (Fig. 9.9.8) show normal slope with normal average (1.0).
c. Qualification of values (Fig. 9.9.9):
   i. QS is OK.
   ii. K readings including K-max are <48 D.
   iii. K-max-steep K is < 1 D.
   iv. Astigmatism is < 6 D.
   v. Thickness at the thinnest location is <500 µm (relatively thin cornea).
   vi. Pachy-Thinnest difference in thickness is <10 µm.
   vii. *Y*-coordinate of the thinnest location is < –500 µm.

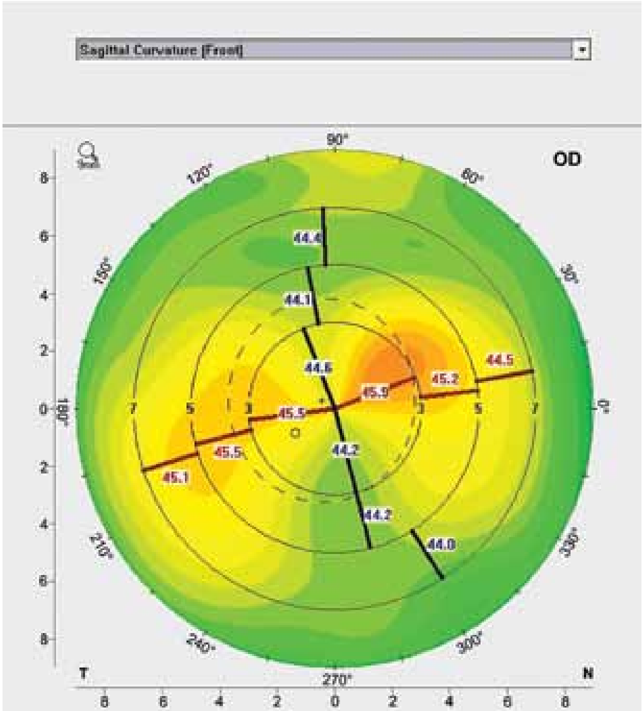

Fig. 9.9.2 OD. Anterior curvature sagital map. Horizontal SB indicating ATR astigmatism.

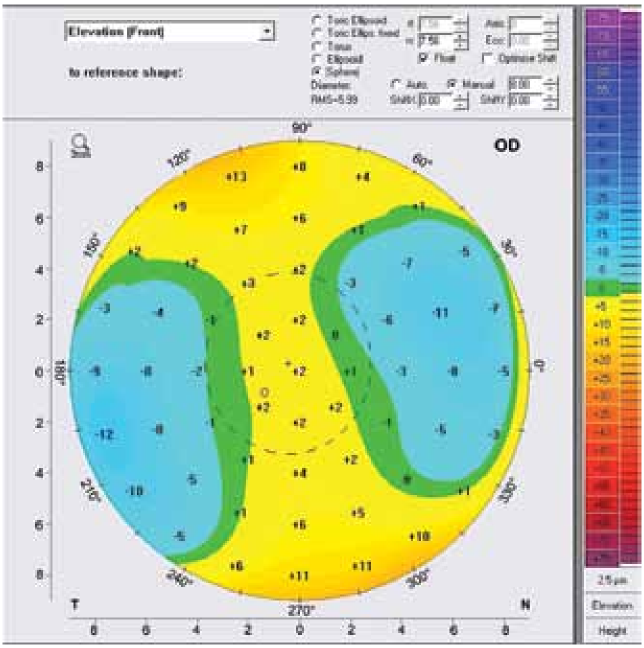

Fig. 9.9.3 OD. Anterior elevation map in BFS mode. Horizontal sandy watch pattern.

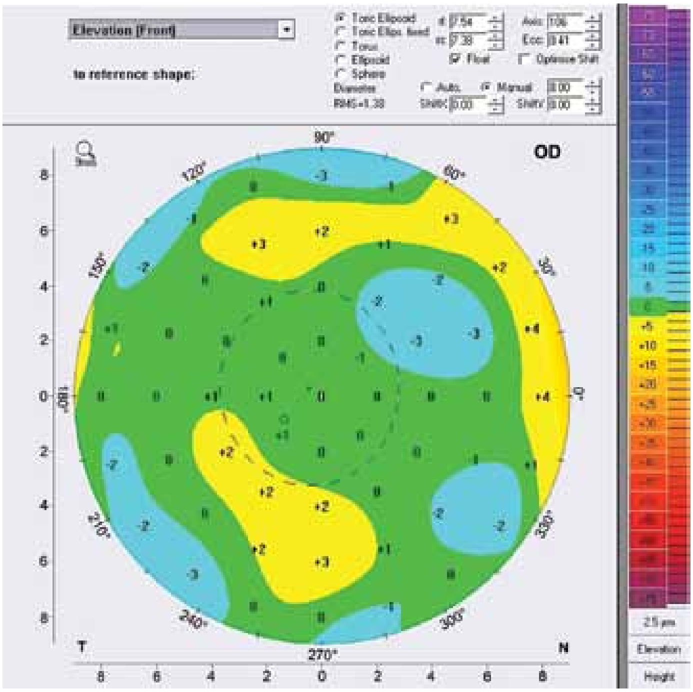

Fig. 9.9.4 OD. Anterior elevation map in BFTE mode.

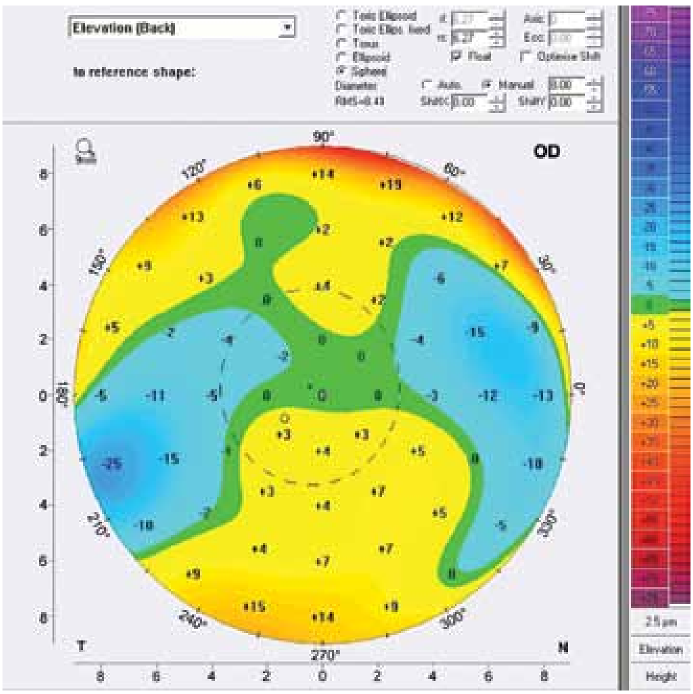

Fig. 9.9.5 OD. Posterior elevation map in BFS mode. Tongue-like extension.

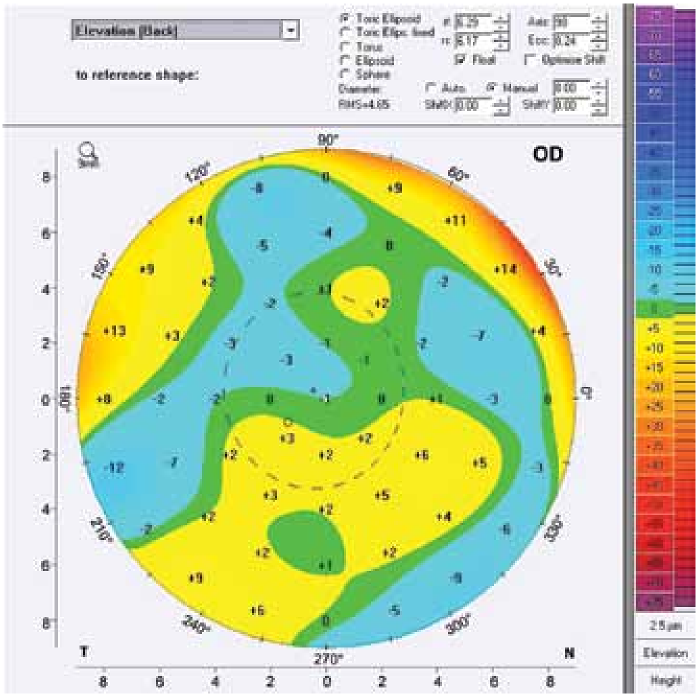

Fig. 9.9.6 OD. Posterior elevation map in the BFTE mode.

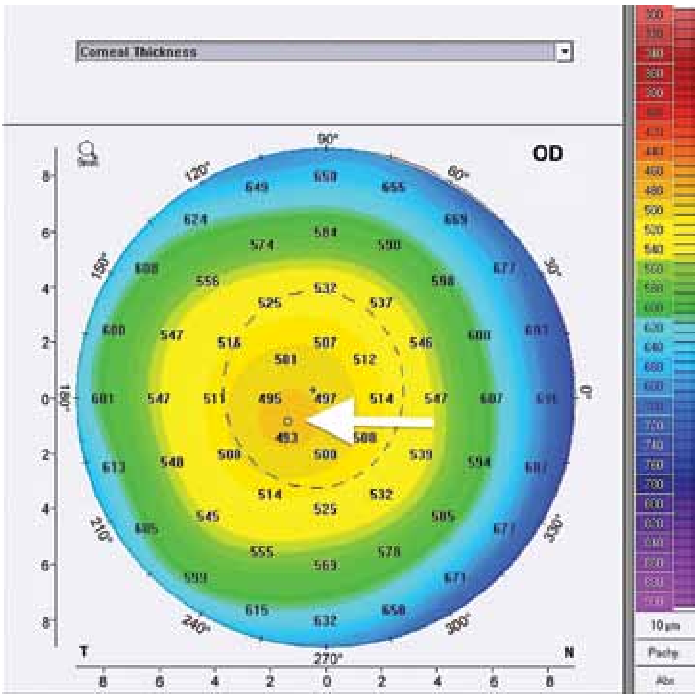

Fig. 9.9.7 OD. Pachymetry map. The white arrow points at the horizontally displaced thinnest location.

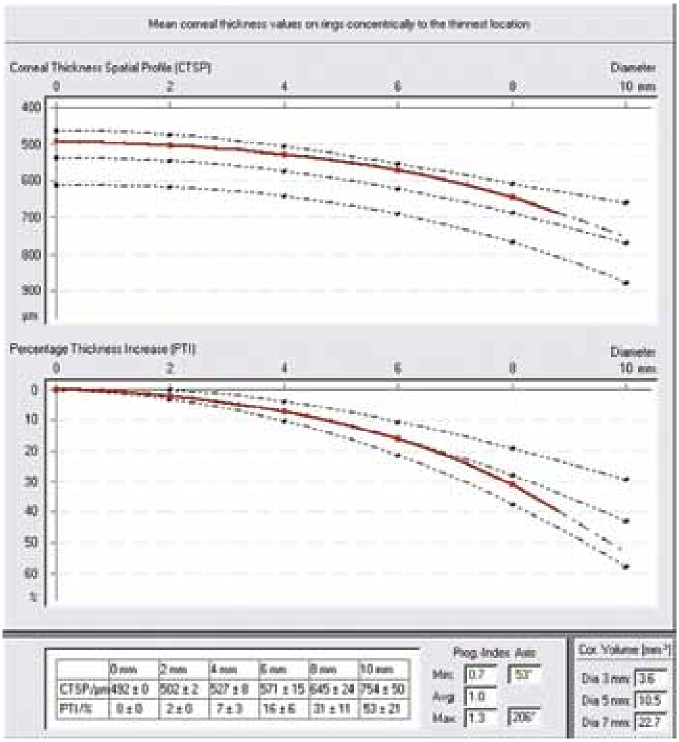

	0 mm	2 mm	4 mm	6 mm	8 mm	10 mm
CTSP/µm	492 ± 0	502 ± 2	527 ± 8	571 ± 15	645 ± 24	754 ± 50
PTI/%	0 ± 0	2 ± 0	7 ± 3	16 ± 6	31 ± 11	53 ± 21

Fig. 9.9.8 OD. Thickness profiles.

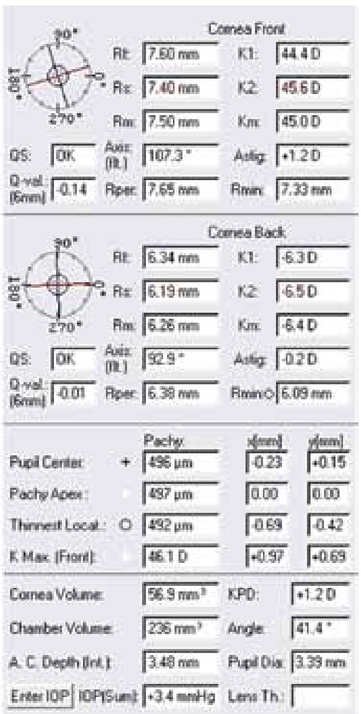

Fig. 9.9.9 OD. Corneal parameters.

viii. ACD, ACV and ACA are normal (3.48 mm and 236 mm^3 and 41.4°, respectively).
ix. Mesopic pupil diameter is 3.39 mm.
x. Pupil coordinates indicate slightly decentered pupil and significant angle Kappa.

Left Eye:

a. In a general look, it is an ATR astigmatism with some irregularity on the posterior elevation map (Fig. 9.9.10).
b. Studying single maps:
   i. The anterior sagittal curvature map (Fig. 9.9.11) shows horizontal SB indicating ATR astigmatism.
   ii. The anterior elevation map:
      1. In BFS mode (Fig. 9.9.12): Horizontal sandy watch pattern.
      2. In the BFTE mode (Fig. 9.9.13): Normal values within the central 5 mm circle.
   iii. The posterior elevation map:
      1. In BFS mode (Fig. 9.9.14): Tongue-like extension.
      2. In BFTE mode (Fig. 9.9.15): Normal values within the central 5 mm circle.
   iv. The pachymetry map (Fig. 9.9.16):
      Relatively thin cornea with dome shape and displaced thinnest location (white arrow), see coordinates in Figures 9.9.10 and 9.9.18.
   v. Thickness profiles (Fig. 9.9.17) show normal slope with normal average (1.0).

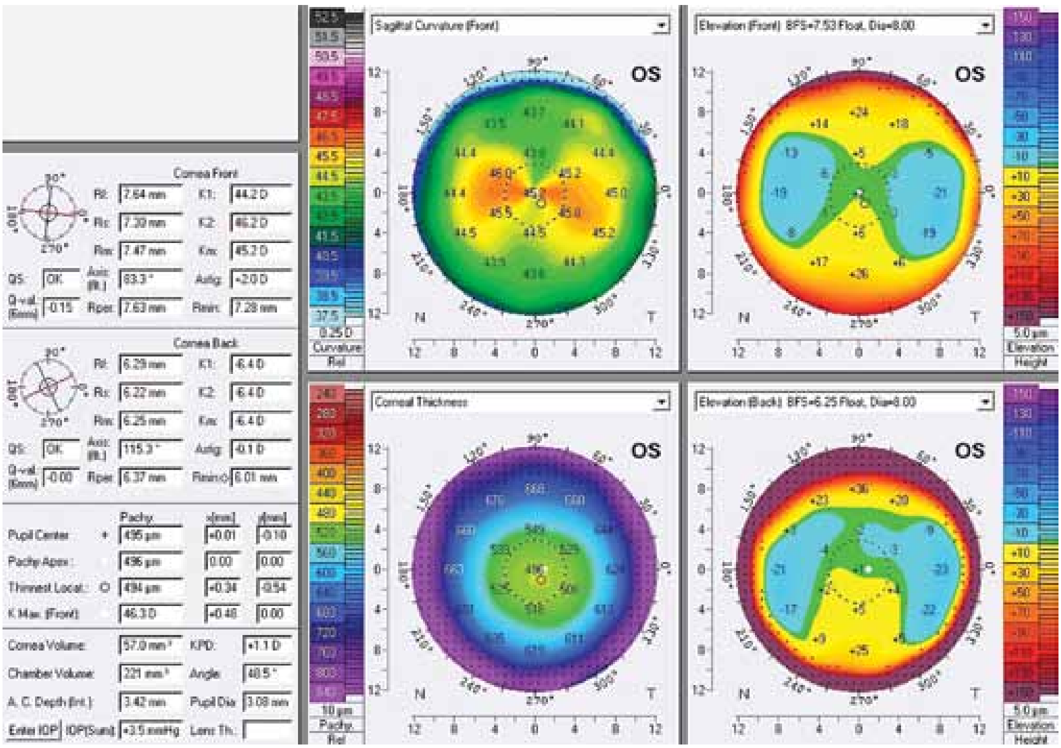

Fig. 9.9.10 OS. The four composite maps.

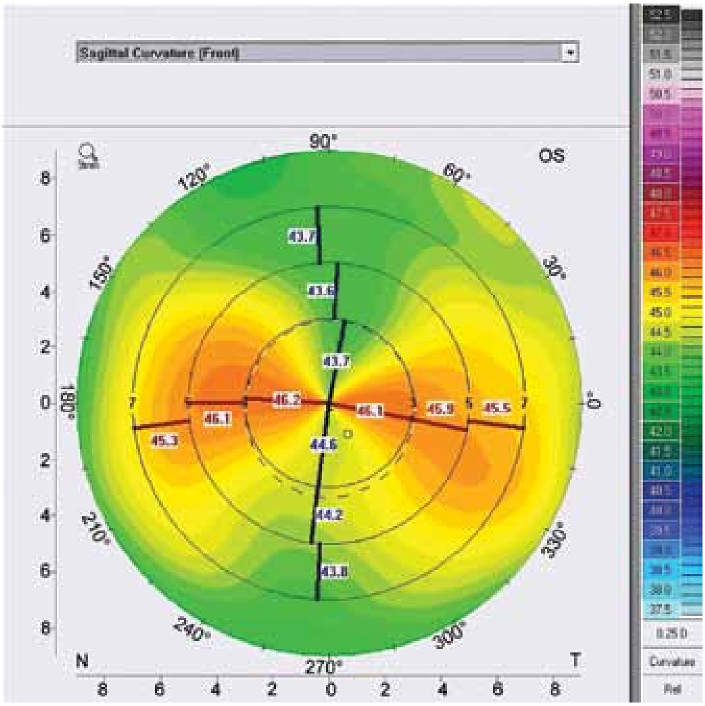

Fig. 9.9.11 OS. Anterior curvature sagital map. Horizontal SB indicating ATR astigmatism.

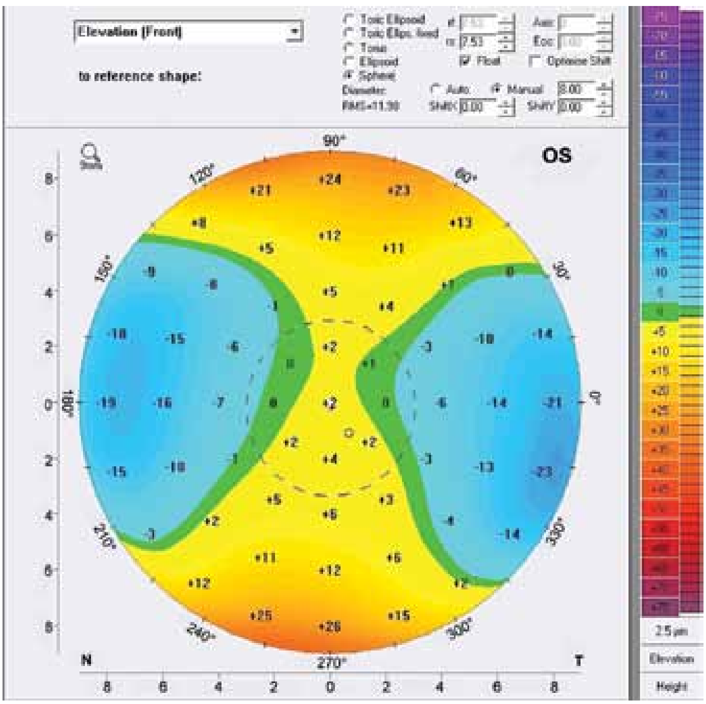

Fig. 9.9.12 OS. Anterior elevation map in BFS mode. Sandy watch pattern.

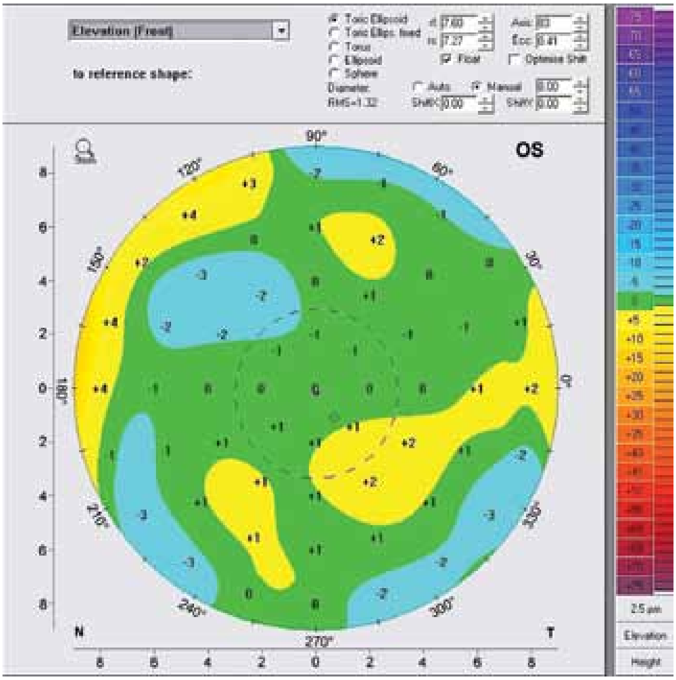

Fig. 9.9.13 OS. Anterior elevation map in BFTE mode.

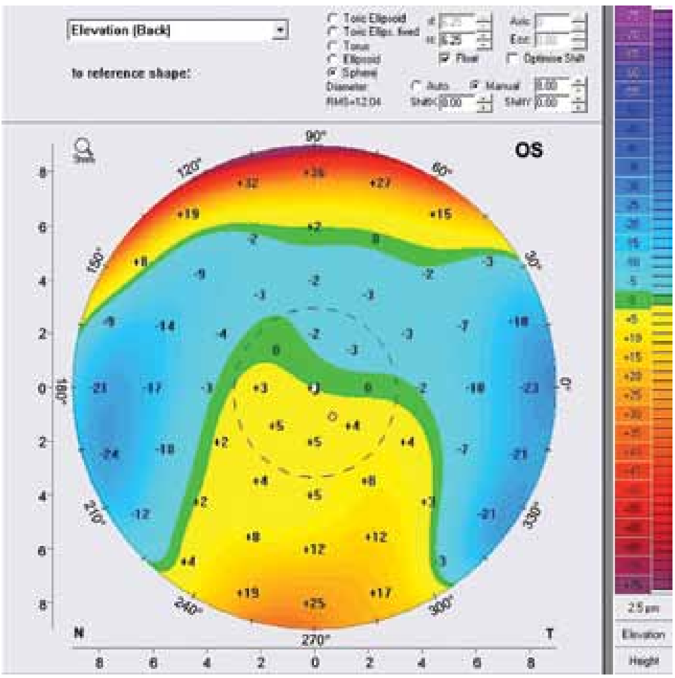

Fig. 9.9.14 OS. Posterior elevation map in BFS mode. Tongue-like extension.

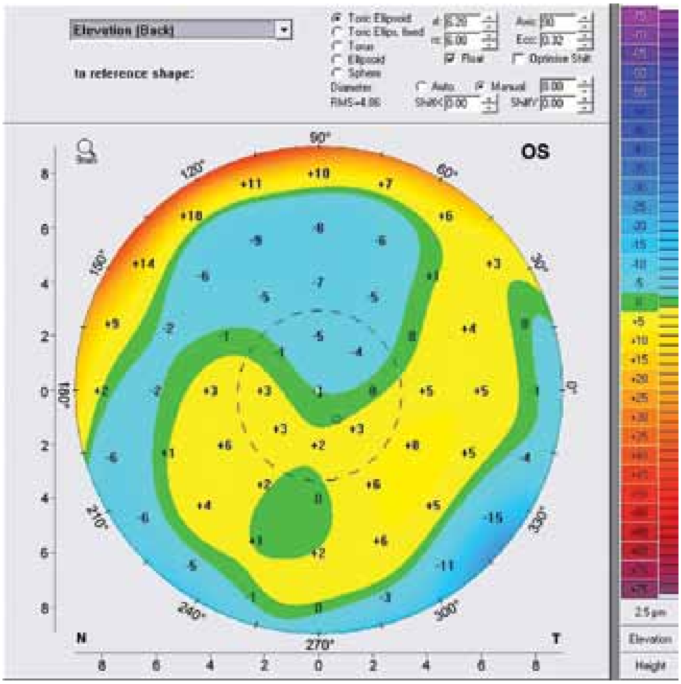

Fig. 9.9.15 OS. Posterior elevation map in BFTE mode.

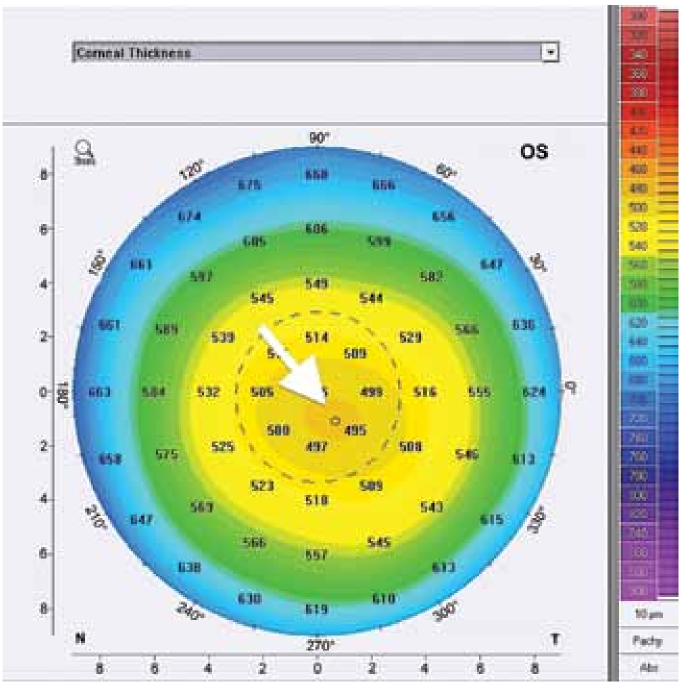

Fig. 9.9.16 OS. Pachymetry map. Relatively thin cornea with dome shape. The white arrow points at the displaced thinnest location.

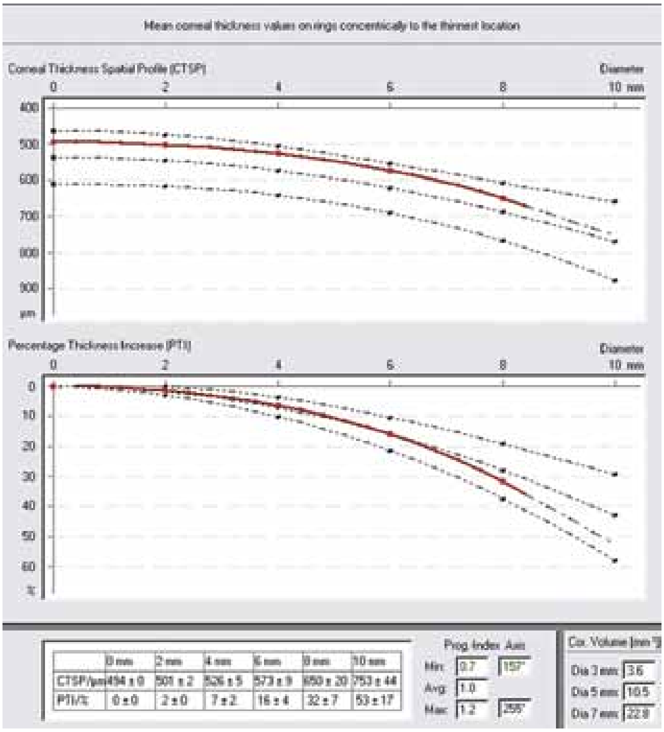

	0 mm	2 mm	4 mm	6 mm	8 mm	10 mm
CTSP/µm	494 ± 0	501 ± 2	526 ± 5	573 ± 9	650 ± 20	753 ± 44
PTI/%	0 ± 0	2 ± 0	7 ± 2	16 ± 4	32 ± 7	53 ± 17

Fig. 9.9.17 OS. Thickness profiles.

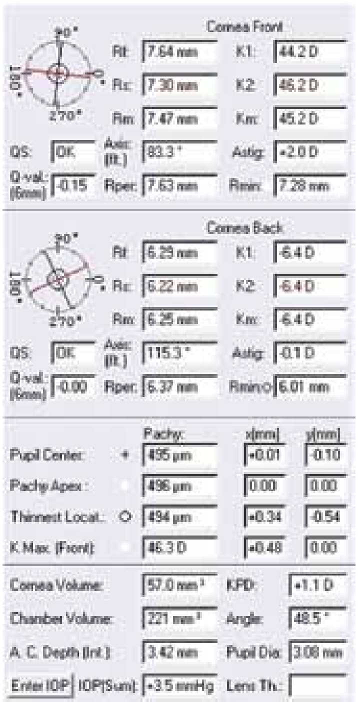

Fig. 9.9.18 OS. Corneal parameters.

c. Qualification of values (Fig. 9.9.9):
   i. QS is OK.
   ii. K readings including K-max are <48 D.
   iii. K-max-steep K is < 1 D.
   iv. Astigmatism is < 6 D.
   v. Thickness at the thinnest location is <500 µm (relatively thin cornea).
   vi. Pachy-Thinnest difference in thickness is <10 µm.
   vii. Y-coordinate of the thinnest location is > –500 µm (–540 µm).
   viii. ACD, ACV and ACA are normal (3.42 mm and 221 mm^3 and 48.5°, respectively).
   ix. Mesopic pupil diameter is 3.08 mm.

2. **Discussion Step:**

It is a case of ATR astigmatism. In this kind of astigmatism, accommodative spasm is very common. Accommodative spasm explains patient's complaints including fluctuation of refraction, fatigue and strain on near work, dissatisfaction with and without glasses and headache. Current glasses, MR, CR and PMT show that the patient is overcorrected due to accommodative spasm.

On the other hand, there is a disparity between TA and MA following probability 4; both are ATR and TA < MA; (see example 24, chapter 6).

Treating astigmatism in general and ATR astigmatism in particular improves reading function even in young individuals. At the same time, treating oblique and ATR astigmatisms frequently results in a subjective improvement out of proportion to any modest improvement in visual acuity.

The recommended refraction for treatment is shown in Table 9.9.5.

TABLE 9.9.5 Recommended Refraction

	Sph	*Cyl*	*Axis*
OD	–1	–2	95
OS	–1.25	–2.5	85

This recommended refraction is calculated as follows:

– The spherical component is the CS added –0.5 D for the cycloplegic effect.
– The cylindrical component is the MA.

Since the MA is > TA, treatment will create WTR astigmatism on the anterior corneal surface. The expected amount will be –0.75 D in the right eye and –0.5 D in the left eye. The patient will tolerate this, since it is WTR and < –1 D and the spherical equivalent will be 0. On the other hand, one may expect that accommodation spasm may recur after treatment causing manifest myopia; indeed this is rare since the ATR astigmatism has been eliminated. But the thing that the patient should know prior to surgery is that visual recovery may be slow.

The patient is young, this excludes RLE. The refractive error is small, this excludes PIOL implantation. PRT seems to be suitable, but there are the following risk factors:

– ATR astigmatism.
– Tongue-like extension on the posterior elevation maps.
– Suspected *Y* co-ordinate of the thinnest location in the left eye.
– The cornea is relatively thin.

– Sub-optimal CDVA even with pin hole test. In such cases, wavefront imaging should be done. Wavefront imaging was performed and found to be within normal limits (not available).

According to Randleman risk score system, this case is scored 3 in case of thin flap and RSB > 300 µm. Having this score, SA may be performed with caution.

In my opinion, even SA is risky unless accompanied with CXL. That is because the case is ATR astigmatism in a young patient although other abnormalities in corneal tomography are mild. Unfortunately, ORA was not available, otherwise a better idea could be taken about corneal biomechanics. However, family history of KC is very important and a detailed history taking for any systemic disease is mandatory.

In case of SA and CXL, a reduction of myopic correction by –0.5 to –0.75 D is necessary to compensate for the flattening effect of CXL. Therefore, the recommended refraction for treatment will be as shown in Table 9.9.6.

TABLE 9.9.6 Recommended Refraction for SA and CXL

	Sph	*Cyl*	*Axis*
OD	–0.5	–2	95
OS	–0.75	–2.5	85

Some surgeons may depend on refraction shown in Table 9.6.5 even with CXL since the patient is young and has good accommodation.

The case will not be quantified since the amount of refractive error is small and corneal parameters are suitable.

Finally, aspheric or aspheric-free profiles should be used in addition to decentration and compensation for cyclotorsion, since the astigmatism is > 1 D.

Index

Page numbers followed by '*f*' refer to figure and '*t*' refer to table